



ieaghg

EXTRACTION OF FORMATION WATER FROM CO₂ STORAGE

Report: 2012/12

November 2012

INTERNATIONAL ENERGY AGENCY

The International Energy Agency (IEA) was established in 1974 within the framework of the Organisation for Economic Co-operation and Development (OECD) to implement an international energy programme. The IEA fosters co-operation amongst its 28 member countries and the European Commission, and with the other countries, in order to increase energy security by improved efficiency of energy use, development of alternative energy sources and research, development and demonstration on matters of energy supply and use. This is achieved through a series of collaborative activities, organised under more than 40 Implementing Agreements. These agreements cover more than 200 individual items of research, development and demonstration. IEAGHG is one of these Implementing Agreements.

DISCLAIMER

This report was prepared as an account of the work sponsored by IEAGHG. The views and opinions of the authors expressed herein do not necessarily reflect those of the IEAGHG, its members, the International Energy Agency, the organisations listed below, nor any employee or persons acting on behalf of any of them. In addition, none of these make any warranty, express or implied, assumes any liability or responsibility for the accuracy, completeness or usefulness of any information, apparatus, product or process disclosed or represents that its use would not infringe privately owned rights, including any parties intellectual property rights. Reference herein to any commercial product, process, service or trade name, trade mark or manufacturer does not necessarily constitute or imply any endorsement, recommendation or any favouring of such products.

COPYRIGHT

Copyright © IEA Environmental Projects Ltd. (IEAGHG) 2012.

All rights reserved.

ACKNOWLEDGEMENTS AND CITATIONS

This report describes research sponsored by IEAGHG. This report was prepared by:
Energy & Environmental Research Center, University of North Dakota

The principal researchers were:

- Ryan J. Klapperich
- Robert M. Cowan
- Charles D. Gorecki
- Guoxiang Liu
- Jordan M. Bremer
- Yevhen I. Holubnyak
- Nicholas S. Kalenze
- Lisa S. Botnen
- Dayanand Saini
- Jonathan L. LaBonte
- Damion J. Knudsen
- Daniel J. Stepan
- Edward N. Steadman
- John A. Harju

To ensure the quality and technical integrity of the research undertaken by IEAGHG each study is managed by an appointed IEAGHG manager. The report is also reviewed by a panel of independent technical experts before its release.

The IEAGHG manager for this report was:

Millie Basava-Reddi

The Expert Reviewers for this report were:

- Pascal Audigane, BRGM
- Andy Cavanagh, Permedia
- Sam Holloway, BGS
- Michael Kuehn, GFZ
- Karsten Michael, CSIRO
- Lingli Wei, Shell
- Neil Wildgust, PTRC

The report should be cited in literature as follows:

‘IEAGHG, “Extraction of Formation Water from CO₂ Storage”, 2012-12, November 2012.’

Further information or copies of the report can be obtained by contacting IEAGHG at:

IEAGHG, Orchard Business Centre,
Stoke Orchard, Cheltenham,
GLOS., GL52 7RZ, UK

Tel: +44(0) 1242 680753 Fax: +44 (0)1242 680758

E-mail: mail@ieaghg.org Internet: www.ieaghg.org



EXTRACTION OF FORMATION WATER FROM CO₂ STORAGE

Background to the Study

Deep saline formations (DSF) constitute the largest potential global resource for the geological storage of CO₂ and are therefore crucial to the successful up-scaling of storage from pilot and demonstration projects to commercial operations. However, there are uncertainties relating to the capacity and injectivity of DSF, with particular concerns relating to the management of pressure and potential displacement of formation brines. Extraction of saline waters from storage formations provides a potential solution to pressure management; for example the proposed Gorgon storage project in Australia includes the provision of pressure relief boreholes.

The effect of pressurisation in a storage formation will depend largely on whether the system can be considered as open or closed. In a closed or semi-closed system, the pressure build-up will be determined by the boundary conditions, which include the shale permeability. Recent studies have shown that microdarcy scale shale permeability will allow brine displacement, while very low shale permeabilities on the nanodarcy to subnanodarcy scale will not. Part of the problem comes from the uncertainty in assessing brine displacement due to boundary condition uncertainty. It can be difficult to determine macroscopic scale permeability, even when samples have been obtained, due to problems with up scaling measurements as regional permeability effects also need to be taken into account (IEAGHG, 2010).

Pressure relief wells can compensate for increases in pressure caused by injection, though extraction rates will depend on site-specific factors e.g. geological structure, shale permeability and heterogeneity.

Heterogeneities in the storage formation may cause complexities in predicting flow rate and direction of injected CO₂. If an extraction well is placed along a path of high permeability, then the rate of flow towards the well would be high, resulting in unwanted CO₂ breakthrough. This may necessitate the plugging of the old well and the consequent drilling of a new pressure relief well, thereby increasing the potential cost of the project and possibly affecting the storage security. This possibility highlights the importance of a detailed site characterisation. Brine extraction could also play a part in plume management.

The plume may be managed both laterally and vertically, as the CO₂ will be forced to migrate towards the extraction wells. In the case of forced downward migration, the extraction wells will be towards the base of the storage formation. This will cause a larger vertical proportion of the formation to be used and the lateral extent and contact of the CO₂ plume with the caprock will be reduced. Both of these effects can increase storage security. This also means



that CO₂ plumes formed at adjacent or nearby injection wells would be less likely to interact with each other.

For large scale projects, there are likely to be multiple injection and pressure-relief wells. It is important to consider how they will interact with each other, as there will be an overlap of pressure footprints from each well.

The water extracted from the storage formations will need to be used or disposed of in some way, for example, at the proposed Gorgon project in Australia, the planned injection of the extracted brine will be into an overlying saline aquifer. Possibilities for future sites include disposal directly in the sea, which would be dependent on the composition of the brine; alternatively the water could be utilised for other industrial processes, such as the cooling process within power stations or use as geothermal energy or it could be desalinated and used either for irrigation or drinking water. The latter options would depend on the cost and demand of water as a resource.

The Energy & Environmental Research Center, in North Dakota, USA, was commissioned by IEAGHG to provide a thorough review of existing information and published research on the effects of brine extraction from CO₂ storage sites. The study also aims to highlight the current state of knowledge and / or gaps and recommend further research priorities on these topics.

Scope of Work

The main aim of the study would be to assess the global potential for extraction of formation waters as part of DSF storage projects. The study would comprise a comprehensive literature review, from published research and industrial analogues (e.g. brine disposal from petroleum and coal bed methane industries) to provide guidance on the following issues:

- Potential rates of brine extraction required for varying injection rates, across a typical range of DSF storage scenarios;
- Likely range in chemical composition of extracted brines;
- Options for disposal of brine, either surface or subsurface, and associated potential environmental impacts;
- Onshore and offshore considerations, including treatment required for different disposal options.
- Potential for utilisation of extracted brines, e.g. cooling water for power stations, geothermal energy, and assessment of associated environmental impacts;
- Potential for surface dissolution of CO₂ in extracted brine and re-injection into storage formations;
- Regulatory constraints, including for monitoring requirements, potential liability and water quality requirements for different uses.
- Potential economic implications for CO₂ storage of brine extraction and the various options for disposal/utilisation, to be illustrated by selected case studies.



The contractor was asked to refer to the following recent IEA GHG reports relevant to this study, to avoid obvious duplication of effort and to ensure that the reports issued by the programme provide a reasonably coherent output:

- Brine Displacement and Pressurisation (2010/15)
- Injection Strategies for CO₂ Storage Sites (2010/04)
- Impacts on Groundwater Resources (2011/11)

Findings of the Study

There is extensive industry experience in underground injection for EOR, gas storage and waste water injection, though only a limited amount in is DSF and the properties of the formations are not always detailed. Realistic and quantitative information about relevant characteristics of the subsurface is needed to assess feasibility, costs and risks associated with various options for water extraction in conjunction with CO₂ storage.

The approach taken in this report was to consider case studies with a wide range of geological, geographical and geopolitical conditions, which may impact the ability to implement an extracted water plan in conjunction with commercial scale storage projects. Relatively simple 3-D models were formed to test different injection and extraction scenarios and incorporate vital, heterogeneous reservoir properties, including structure, porosity, permeability, water quality, lithology, temperature, and pressure, which were obtained from published sources. When published data were insufficient to capture expected heterogeneity or did not appear in the literature, variogram ranges and property values were obtained from the revised AGD (Average Global database), which is comprised of information from hydrocarbon reservoir properties as a proxy for DSF characteristics. The AGD was compiled through use of existing US databases and an extensive literature review for other regions (IEAGHG, 2009).

Literature considering water disposal and usage was reviewed as well as those looking at likely salinity ranges. Direct water use options include geothermal energy recovery, for which there is no limits on TDS (total dissolved solids) or water chemistry, though there are practical limits based on scaling and corrosion potential. Another option is dissolution of CO₂ into the water and reinjection; this is discussed for the individual case studies. The water can also be treated and used as a beneficial supply of water; such as drinking water, agriculture, cooling water, boiler water and other industrial uses. If this is the case, it will need to be treated, which usually requires a pre-treatment option, to remove suspended solids, dissolved gases and non-aqueous- phase fluids, such as hydrocarbons, followed by desalination. The process used will depend on the salinity, content and quantity of water. These processes are detailed in the appendices of the report. The water quality needs to be relatively high to be used beneficially and these requirements are also detailed in the appendices. The salinity and end use will determine the best desalination technology for each case.



The case studies selected were Ketzin, (near Potsdam in Germany); Zama (Alberta, Canada); Gorgon (Barrow Island, Australia) and Teapot Dome (Wyoming, USA). These projects were selected to include a range of geological conditions and formation water quality.

For each case study a range of injection scenarios were considered as well as CO₂ surface dissolution, whereby CO₂ could be stored by dissolving it in extracted formation water and then injected into a geological formation.

The economic potential of the formation water from each case study site was evaluated with respect to its applicability for beneficial use. Cost estimates were provided for desalination due to a focus on beneficial use of the water. Other water treatment and disposal options were also outlined. The range of water quality represented by the four case studies is representative of a broad range of water quality that is likely to be found in deep saline formations. The type of purification process that can be applied depends on the quality of the formation water, which is taken into account for each case study.

Some of the case study sites are located in depleted oil or gas fields and, as such, are likely to contain varying concentrations of hydrocarbons, which may increase overall treatment costs and/or limit the potential for beneficial use. These sites function as analogues for similar and less well-characterised saline formations and therefore the presence of hydrocarbon constituents in extracted water were acknowledged, but ignored for the purpose of calculations.

Ketzin

This is a pilot scale CO₂ injection project into a deep saline formation in Germany and so far 59,000 tonnes have been injected into the Triassic Stuttgart Formation. This storage formation consists of a series of fluvial channels surrounded by floodplain deposits. The confining structure is the Ketzin-Roskow anticline. The formation water quality is the lowest of all the case studies and local demand is low due to the location of the Havel River.

This theoretical case study does not reflect actual injection operations as the site is limited to a maximum injection of <100, 000 tonnes, whereas the simulation uses an injection programme maximising injectivity and storage capacity aiming to inject 2Mt/yr for a 25 year period for each injection well. 16 cases (Table 1) were simulated to analyse different injection and extraction scenarios and assess differences in storage capacity and efficiency, as well as to define potential volumes of produced water for treatment or disposal.

Table 1: Case Scenarios and Resulting Storage Capacities for Ketzin

Scenario	Well Configuration	Gas Injection Rate/Well, kg/day	Water Production Rate/Well, m ³ /day	Boundary Conditions	Storage Capacity, megatonnes
Case 1	1 injector	451,000	*	Closed	4.12
Case 2 (base case)	1 injector	1,430,000	*	Semiclosed	13.0



Case 3	1 injector	1,980,000	*	Open	18.1
Case 4	1 injector 1 extractor	2,810,000	11,800,000	Semiclosed	25.7
Case 5	1 injector 1 extractor	3,000,000	12,500,000	Open	27.4
Case 6	2 injectors	3,550,000	*	Semiclosed	32.4
Case 7 (surface dissolution)	1 injector 1 extractor	*	3,060	Semiclosed	0.43
Case 8 (surface dissolution)	1 injector 1 extractor	*	3,090	Semiclosed	0.55
Case 9 (surface dissolution)	4 injectors 5 extractors	*	25,500	Semiclosed	2.61
Case 10 (surface dissolution)	4 injector 5 extractor	*	26,500	Semiclosed	2.88
Case 11	4 injectors	6,954,760	*	Semiclosed	63.3
Case 12	4 injectors 4 extractors	7,170,000	12,700	Semiclosed	65.4
Case 13	8 injectors	9,500,000	*	Semiclosed	86.7
Case 14	12 injectors	14,500,000	*	Semiclosed	132.0
Case 15	12 injectors 13 extractors	24,877,000	65,753	Semiclosed	226.7
Case 16	25 injectors	20,100,000	*	Semiclosed	183.8

Due to the structure, geological heterogeneity, and depositional environment at Ketzin, the modelling showed that it was difficult to obtain good connectivity between injector and producer pairs, resulting in poor improvements in plume control and storage capacity. This was evident by a higher storage capacity being obtained from two injectors rather than any scenario with an injector and producer. Simulations of increasing injectors and injector/extractor pairs show that upon reaching 25 injectors; a greater capacity is achieved through 12 injectors and 13 extractors. The reason for this is the pressure interference between injectors, which can be mitigated by extractor wells.

Surface dissolution was considered (cases 7 – 10), but due to high salinity of the formation water, large quantities of water would be required for CO₂ dissolution, leading to an extremely reduced storage capacity. Additional wells patterns were analysed to obtain an idea of how many wells would be needed to achieve 1Mt/yr. When considering 9 well patterns (4 injectors, 5 extractors) at 5 km intervals, 80-90 wells would be needed to store 1Mt/ yr, which would be prohibited by cost.

The formation water at Ketzin is high-salinity, with more than 200,000 ppm TDS (total dissolved solids) and not favourable for use as source water for beneficial use. The options that have been identified for handling this water include reinjection into a geological



formation or treatment with a zero liquid discharge (ZLD) method that results in a dry salt for disposal or beneficial use.

Based on the flow rate of 12,400m³/day (case 4 and 5) the water treatment was estimated to be \$8.02/m³ with the total capital cost of \$135 million. It is unlikely that this high price for treatment and/or purification of water would be accepted or viable, therefore, deep-water injection would be the most likely management strategy for extracted water. As the Stuttgart Formation is regionally extensive and generally underpressured, it is the most likely disposal target for the site.

Regarding regulations, it has been shown over the last few years that CCS faces obstacles in Germany. However, there are regulatory frameworks in place that allow brine injection to occur as part of other industrial activities. Therefore if CCS is able to take place, brine extraction and reinjection is not likely to be an issue.

Zama

This is a hydrocarbon bearing structure that has been the site of acid gas injection for the simultaneous purpose of EOR, H₂S disposal and CO₂ storage in north western Alberta, Canada. It is a carbonate pinnacle reef structure consisting of dolomite and surrounded and overlain by a very tight anhydrite (Muskeg Formation) that acts as a caprock. The pinnacle modelled is one of 700 similar hydrocarbon bearing structures in the Zama oil field. The formation water quality is low and there are other existing local water resources, though there is the possibility of using extracted water for oil and gas production activities.

7 different cases of simultaneous acid gas injection and formation water extraction (Table 2) were tested in predictive simulation runs.

Table 2: Case Scenarios and Resulting Storage Capacities for the Zama

Scenario	Well Configuration	Gas Injection Rate/Well, kg/day	Water Production Rate/Well, m ³ /day	Boundary Conditions	Storage Capacity, megatonnes
Case 1	1 Injector	310,680	N/A	Closed	0.05
Case 2	1 Injector 1 Extractor	310,680	516	Closed	0.47
Case 3	1 Injector 1 Extractor	310,680	516	Closed	0.62
Case 4	1 Injector 1 Extractor	310,680	429	Closed	0.68
Case 5	1 Injector 1 Extractor	310,680	397	Closed	0.69
Case 6	1 Injector 1 Extractor	621,359	1144	Closed	0.49
Case 7	1 Injector 2 Extractors	621,359	572	Closed	0.60



In the base case (case 1), acid gas was injected without the extraction of formation water. Simulation results indicate that a total of 50 Mt of acid gas could be injected before reservoir pressure reaches the maximum allowable pressure limit of 22,753 kPa. Case 4 appears to be the optimum scenario. In this case, an average volumetric ratio of nearly 1:1 between extracted water and injected gas was observed while injecting acid gas at a constant rate (0.113 Mt/year) for more than 5.5 years into a closed system. It also resulted in 13 times higher storage capacity compared to base case. With over 700 pinnacle reef structures in the Zama sub basin, a careful selection of eight pinnacle structures similar to the ones modelled may provide almost 0.91 Mt a year of storage capacity and a steady stream of extracted, low quality water.

Three options for water disposal investigated were, deep well injection into the overlying Slave Point Formation, treatment of extracted water using a multiple-step membrane desalination approach such as one involving nanofiltration followed by reverse osmosis treatment and lastly using extracted water as a source of geothermal energy.

The TDS of the waters range from 180,000 to 223,000 mg/L, with the lower value taken as the basis for evaluating treatment options. The flow rates used from the simulations were minimum, 3734 m³/day and maximum, 5261 m³/day. The capital costs for treating associated with the case studies at Zama ranged from \$5.25 million to \$60 million and the energy requirements 3.7 MW to 15.7 MW. It was therefore considered highly unlikely that treatment of the extracted water at Zama would be considered as a viable option. There is limited local population and it is a remote location, so no effort was made to identify water demands for Zama. The most likely management option is disposal into the overlying Slave Point Formation, a practice that is currently being carried out by oil and gas operators in the area.

Alberta currently has regulations dealing with brine extraction and injection related to the oil and gas industry and no issues were identified that would preclude injection of formation brines into the subsurface.

Gorgon

This is a planned future project for injection into a deep saline formation on Barrow Island off the west coast of Australia. The aim is to inject approximately 3.8 million tonnes a year through 8 injection wells with 4 production wells towards the west. Injection will be into the Dupuy Formation, a turbidite sequence at a depth of 2000m; the confining structure is a north–south trending double-plunging anticline. The formation water quality is of treatable quality, though there is low local demand.

Seven cases were simulated for the Gorgon test site using the planned eight injection wells and four extraction wells (Table 3).

Table 3: Case Scenarios and Resulting Storage Capacities for Gorgon

Scenario	Well Configuration	Gas Injection Rate/Well,	Water Production	Injection Period, yrs	Storage Capacity,
----------	--------------------	--------------------------	------------------	-----------------------	-------------------



		kg/day	Rate/Well, m ³ /day		megatonnes
Case 1	8 injectors	10,661,700	*	25	97.3
Case 2	8 injectors 4 extractors	10,661,700	215,120,000	25	97.5
Case 3	8 injectors	10,661,700	*	50	195
Case 4	8 injectors 4 extractors	10,661,700	334,919,000	50	196
Case 5	8 injectors 4 extractors	5,330,830	396,606,000	50	97.5
Case 6	8 injectors	60,400,000	*	25	551
Case 7	8 injectors 4 extractors	69,900,000	261,802,000	25	637

Based on the simulation results, water extraction at the Gorgon site appears to be most beneficial for pressure maintenance and plume control. Utilisation of the planned extraction wells achieved significant pressure reductions. Early breakthrough remains an issue and could require injectors to be shut in and more wells brought online. Capacity gains through water extraction are possible at the Gorgon site, although the amount of injection required to make those gains far exceeds the injection planned for the site.

Water handling scenarios considered for Gorgon were reinjection of extracted water into a geological formation (for pressure management in the natural gas field), ocean discharge, use as source water for reverse osmosis systems installed on Barrow island (ultimately for water supply on Barrow Island) and use as supply of water for mainland Australia communities.

Reinjection is considered to be the most likely scenario, though ocean discharge would be a low cost alternative, as the salinity is similar to seawater, TDS of 23,234 mg/L, as long as there are no hydrocarbons or radioactive material. The only other issue is the potential environmental impact of high temperature water, though it may be possible to cool it first if there is an issue. Water treatment is a high cost option, but may be an alternative to desalination of seawater, which is currently planned. The main cost is transportation, which becomes much greater when considering supplying the mainland.

If properly planned and implemented, use of extracted water could be considered as a source of feedwater for reverse osmosis production of purified water for operations at the Barrow Island site. Minimal transportation and infrastructure are required beyond current seawater desalination operations.

The current regulatory frameworks considered do not provide any serious constraints to brine disposal in Western Australia.

Teapot Dome

This is a demonstration site in Wyoming, situated next to a CO₂-EOR site (salt Creek). It is a stacked sedimentary sequence in an elongated anticline. The formation water is of high



quality and could have many uses as there are close by populated areas and agriculture; there may also be potential for geothermal production.

The Dakota/Lakota Formation was the primary target at Teapot Dome, which was examined through seven dynamic simulations (Table 4).

Table 4: Case Scenarios and Resulting Storage Capacities for Teapot Dome

Scenario	Well Configuration	Gas Injection Rate/Well, kg/day	Water Production Rate/Well, m ³ /day	Storage Capacity, megatonnes
Case 1	1 injector	565,128	*	5.2
Case 2	2 injectors	836,848	*	7.6
Case 3	1 injector 1 extractor	1,212,810	1657	11.1
Case 4	1 horiz. injector 1 horiz. extractor	2,090,498	6701	19.1
Case 5	2 horiz. injectors	1,953,238	*	17.8
Case 6 (surface dissolution)	1 horiz. injector 1 horiz. extractor	*	6346	0.56
Case 7 (surface dissolution)	1 injector 1 extractor	*	1599	0.15

Simulations also examined the potential for surface water saturation using extracted water followed by injection of the CO₂ saturated stream. Due to low salinity formation fluids, it was found that this technique could result in a capacity of 0.15 Mt over a 25-year period utilizing vertical wells (Case 7). This value was increased by utilizing horizontal wells, resulting in storage capacity of 0.56 megatonnes (Case 6). While these numbers are significantly less than free-phase injections, they are still potential candidates because of reductions in MVA cost and increased storage security. Using the single well pairs in Cases 6 and 7, it was determined that in order to reach an injection rate of one megatonne per year using surface dissolution, that approximately 170 vertical wells (85 injection–extraction well pairs) or approximately horizontal 44 wells (22 injection–extraction well pairs) would be required. Due to the large number of wells, it is unlikely that surface dissolution is a viable option.

Simulations at the Teapot Dome site indicate that water extraction can have an impact on storage capacity, reservoir pressure, and plume management. Utilisation of an injection extraction well pair resulted in increased storage capacity over the use of a single or pair of injection wells. Water extraction also strongly influenced reservoir pressures and plume migration. Although the overall size of the plume was not decreased with these simulations, eastward migration of the plume was reduced over the base case. The large plume was also



thinner and exerted less pressure on the overlying cap rock. It is expected that extraction could be designed to reduce overall plume size at this site as well.

Water management options considered for Teapot Dome included reinjection into a geological formation and desalination for use as a potable or agricultural water supply. Reinjection could take place into several overlying options at a minimal cost.

The TDS of the extracted water is 9263mg/L and contains some hydrocarbons, though this is discounted for cost calculations. Simulations of reverse osmosis based water treatment were performed and the purified water yield from the 10,000 mg/L TDS brine was estimated to be 83% at a feed pressure of 69 bar and a feed temperature of 40°C. The purified water was calculated to have a salinity of 260 mg/L with product brine salinity of 57,600 mg/L.

The range of water price ranges from \$0.97/m³ for the lowest extracted water flow rate (2600 m³/day) at the 1 million tonnes/year of CO₂ injection to \$0.74/m³ for the highest extracted water flow rate (59,600 m³/day) for the 8 million tonnes/year of CO₂ injection.

This was compared to local water rates, and the cost of treating the extracted water (assuming no cost for removal of hydrocarbons) is less than the standard base rate of water in this area but greater than the rate charged per unit of water above the monthly minimum.

While Wyoming does not currently have primacy to regulate carbon storage through the Class VI well program, the state does have primacy to regulate Class II – Oil and Gas-Related Injection Wells, including disposal wells. Therefore as long as conditions are met, brine injection is not thought to be an issue.

Expert Review Comments

Expert comments were received from 7 reviewers, representing industry and academia. The overall response was positive and highlighted a significant contribution to this area of storage research. Suggestions included making the report clearer on the aims of the project and improvement on the report structure, consistency with units and increased clarity on amount of increased capacity. There were also some inconsistencies in one of the case studies. This was all addressed in the final report.

Conclusions

Extracting water from a CO₂ storage reservoir was observed to have variable effects based on the specific nature of reservoir rock and reservoir boundary conditions, as well as operational factors such as injection/extraction management and placement of wells. While the assumption of achieving a 1:1 ratio of injected CO₂ to extracted water was generally appropriate, in some situations, the volume of water which must be removed from the reservoir was much higher in order to perform the desired pressure or plume management tasks. The most influential results were found in the closed reservoir test performed at Zama. In this situation, extracted volumes were approximately equal to injected volumes. In other



situations, it was found that the water extraction rate may be up to four times higher than the volume of injected CO₂.

Generally, the simulations conducted for this project illustrated that water extraction scenarios may be capable of increasing storage capacity by more than double. Site-specific factors affecting local injectivity resulted in the Teapot Dome site gaining more storage from an extraction/injection well pair and the Ketzin site storing more CO₂ with a pair of injection wells. Furthermore, optimising simulations to achieve pressure maintenance or plume management generally resulted in decreased reservoir storage capacity with a significant increase in the volume of extracted water.

It is unlikely that extracted water from storage locations in offshore or coastal area would be of beneficial use as potential cost savings of extracted water in place of seawater for desalination appears too small, even low salinities, 10,000 mg/L TDS.

In locations with formation waters with a high TDS, it is also unlikely that extracted water would be purified. While technologies exist to treat brines with the range of dissolved solids, the cost associated with treatment and implementation would likely be too high to justify. Treatment and beneficial use may be feasible under certain conditions: a combination of low-to-moderate extracted water quality, availability of inexpensive energy and sufficient local water demand. Of the case study sites, the best candidate for treatment and use of extracted water was the Teapot Dome site, where estimated treatment costs were comparable to that of local water supplies.

Surface dissolution involving the extraction of reservoir fluid, saturation, and subsequent reinjection is unlikely to be a viable option in most situations as the capacity of produced fluids to dissolve and carry CO₂ is too low. It is unlikely that this scenario will be able to compete with direct injection for storage of commercial-scale volumes of CO₂.

Existing regulations were not found that impose a barrier to the development of water extraction as part of reservoir management operations nor for the development of procuring additional water resources, provided the water quality is fit for the intended use. If extracted water is treated and utilised, effluent will be under regulations to adhere to wastewater treatment and handling.

Despite high costs and shortcomings encountered with extracting reservoir fluids for increasing reservoir capacity and/or management, it is important to consider these options for any specific storage site in an effort to:

- Optimise the injection scenario.
- Potentially alleviate costs through beneficial use.
- Reduce risk and MVA costs and increase reservoir efficiency by controlling plume migration.
- Manage pressure and injectivity.



Knowledge gaps and areas of additional and continued research were considered and the following list was thought necessary to address:

- Collect detailed water quality data for potential CO₂ storage targets, and develop a global database. This will aid in identifying targets with strong beneficial use potential and estimating the costs of water management strategies.
- Evaluate potential CO₂ capacity gains through additional site-specific research in order to increase known impacts of formation water extraction on CO₂ capacity.
- Evaluate additional strategies of CO₂ plume management using formation water extraction through detailed modelling and simulation activities. Evaluations of this type will help expand the knowledge of potential benefits of water extraction.
- Optimise injection simulation scenarios based on the distances between CO₂ injection and water extraction wells, using site-specific data, as opposed to optimizing the number of wells and/or their locations as was done in this study.
- Integrate additional chemical and physical phenomena, such as geochemical reactions and geothermal effects, into dynamic modelling simulators. Such integration will improve the comprehensive understanding of the storage–extraction system and provide more accurate estimations of storage potential and the utility of extracted formation water. This may be especially beneficial for evaluating cases of surface dissolution, where geochemical reactions are of a more immediate concern.
- Develop improved and more efficient methods of dissolving CO₂ directly into extracted water at the surface, as this would not currently be viable at most storage sites. This could lead to an increased utility of surface dissolution, and help more projects realize the potential benefits, such as reduced MVA costs.
- Develop efficient mechanisms to link potential sources of extracted formation water to potential users of treated extracted water. Once water is recognised as applicable for beneficial use, identify water supply shortages or bottlenecks in order to evaluate the economic benefit of the possible beneficial uses.
- Reduce the costs of extracted formation water treatment in order to increase the potential sources of extracted water that may be applied toward beneficial uses. Cost reductions may be found through improved technology, materials, or process efficiency.
- Conduct additional research to understand the economic benefits of formation water extraction on a site-specific basis. In particular, investigate how the benefit of increased storage capacity relates to the increased costs of the additional infrastructure required (additional wells, treatment facilities, etc.).
- Conduct additional research to evaluate the MVA cost savings associated with extracted water reservoir management versus the cost of the additional infrastructure required.
- Identify reservoir characteristics that may inherently enhance the effectiveness of formation water extraction strategies. This could lead to more effective usage of known and future storage targets.



- Develop formulaic methodology to estimate CO₂ storage capacity specific to the use of formation water extraction as a reservoir management strategy. This would allow for rapid assessment of the benefits of extraction on known and future CO₂ storage targets.

Recommendations

There is yet to be any large scale demonstration of this topic and most information is currently through modelling studies. It is recommended that IEAGHG continue to follow this topic and any updates, through future storage network meetings, namely the modelling network and by the study programme.

A future review of this topic would be useful as data is generated by future large scale demonstration projects.

EXTRACTION OF FORMATION WATER FROM CO₂ STORAGE

Final Report

(for the period of May 15, 2011, through June 30, 2012)

Prepared for:

Ludmilla Basava-Reddi

IEA Greenhouse Gas R&D Programme
The Orchard Business Centre
Stoke Orchard
Cheltenham, Gloucestershire GL52 7RZ
UNITED KINGDOM

Prepared by:

Ryan J. Klapperich
Robert M. Cowan
Charles D. Gorecki
Guoxiang Liu
Jordan M. Bremer
Yevhen I. Holubnyak
Nicholas S. Kalenze
Lisa S. Botnen
Dayanand Saini
Jonathan L. LaBonte
Damion J. Knudsen
Daniel J. Stepan
Edward N. Steadman
John A. Harju

Energy & Environmental Research Center
University of North Dakota
15 North 23rd Street, Stop 9018
Grand Forks, ND 58202-9018

DOE DISCLAIMER

This report was prepared as an account of work sponsored by an agency of the United States Government. Neither the United States Government, nor any agency thereof, nor any of their employees, makes any warranty, express or implied, or assumes any legal liability or responsibility for the accuracy, completeness, or usefulness of any information, apparatus, product, or process disclosed, or represents that its use would not infringe privately owned rights. Reference herein to any specific commercial product, process, or service by trade name, trademark, manufacturer, or otherwise does not necessarily constitute or imply its endorsement, recommendation, or favoring by the United States Government or any agency thereof. The views and opinions of authors expressed herein do not necessarily state or reflect those of the United States Government or any agency thereof.

EERC DISCLAIMER

LEGAL NOTICE This research report was prepared by the Energy & Environmental Research Center (EERC), an agency of the University of North Dakota, as an account of work sponsored by the U.S. Department of Energy and IEA Greenhouse Gas R&D Programme. Because of the research nature of the work performed, neither the EERC nor any of its employees makes any warranty, express or implied, or assumes any legal liability or responsibility for the accuracy, completeness, or usefulness of any information, apparatus, product, or process disclosed or represents that its use would not infringe privately owned rights. Reference herein to any specific commercial product, process, or service by trade name, trademark, manufacturer, or otherwise does not necessarily constitute or imply its endorsement or recommendation by the EERC.

EXTRACTION OF FORMATION WATER FROM CO₂ STORAGE

ABSTRACT

The Energy & Environmental Research Center (EERC) has conducted an analysis of formation water extraction from carbon dioxide (CO₂) storage reservoirs under joint sponsorship by the IEA Greenhouse Gas (IEAGHG) R&D Programme and the U.S. Department of Energy (DOE). The concept of extracting saline waters from reservoirs has been proposed as a means of managing storage formation pressures, increasing reservoir storage capacity, controlling CO₂ plumes, and controlling migration of displaced formation water. The practice may also provide water that can be put to a beneficial use such as the supply of potable water where treatment can be performed at reasonable cost.

The work included a survey of geologic and water quality conditions of deep saline aquifers (DSAs); selection of four case study sites representing a wide range of these geologic and water quality conditions; and a study of the impacts of formation water extraction on CO₂ storage and the potential for the beneficial use of extracted water at these sites. The four case study sites were the Ketzin site in Germany; the Zama Field in Canada; the Gorgon project area in Australia; and the Teapot Dome Field in the United States. Hypothetical reservoir-scale dynamic simulations were conducted to investigate the impact that formation water extraction could have on storage capacity and reservoir management and to determine effective water extraction rates for those purposes.

The results from the simulation studies show that the increase in CO₂ storage capacity achieved through the use of water extraction varies greatly based on site conditions. Additional benefits of water extraction in reservoir management included reduction of maximum reservoir pressures and plume management. In general, higher water extraction rates were required in order to provide better pressure and plume management. Analysis of surface dissolution, mixing CO₂ into extracted water prior to injection, reveal that surface dissolution would require removal (and reinjection) of very large volumes of water while providing only a small fraction of the CO₂ storage capacity that can be achieved through injection of supercritical CO₂.

Investigation of the potential for beneficial use of the extracted water revealed that most beneficial uses require water of significantly greater quality than is likely to be present in extracted water, meaning that desalination will be required. The cost of treating extracted water was estimated for reverse osmosis, brine concentrators, and brine crystallizers. In most cases, the cost of desalination will be too high to make this a viable option, and it should be expected that the extracted water will be disposed of through deep well injection.

Formation water extraction from CO₂ storage reservoirs is applicable for increasing storage capacity, reservoir pressure management, and plume control. Analysis of the resulting water quality and quantity, available treatment technologies, and potential transportation costs reveals there is likely to be limited potential for the beneficial use of extracted water from CCS facilities. Ideal circumstances of relatively high quality reservoir water and highly stressed or limited regional water resources will need to coexist before beneficial use of extracted water may be

considered. Additional work classifying the water quality of potential DSA storage targets is necessary before these conclusions can be revisited.

This subtask was funded through the EERC–DOE Joint Program on Research and Development for Fossil Energy-Related Resources Cooperative Agreement No. DE-FC26-08NT43291. Nonfederal funding was provided by the IEAGHG R&D Programme.

TABLE OF CONTENTS

LIST OF FIGURES	iii
LIST OF TABLES	v
EXECUTIVE SUMMARY	vii
INTRODUCTION	1
PROJECT APPROACH	3
BACKGROUND	3
Water Management Options.....	5
Direct Use	5
Beneficial Use as a Supply of Water	6
Water Management for Beneficial Use as Water Supply	7
Extracted-Water Quantity	7
Extracted-Water Quality	8
Quality for Beneficial Use.....	14
Applicability of Desalination Treatment Technologies to Various Waters	15
Global Desalination Capacity	15
Desalination Technology Trends	19
CASE STUDIES	20
Introduction	20
Modeling and Simulation	21
Evaluation of Water Management Options	23
Regulatory Concerns	23
CO ₂ Surface Dissolution	24
Ketzin Case Study	24
Site Characterization.....	24
Modeling.....	25
Case Study Simulation Results	28
Surface Dissolution.....	32
Evaluation of Water Management Options	34
Regulatory Concerns	34
Ketzin Summary	37
Zama Case Study.....	38
Site Characterization.....	38
Modeling.....	39

Continued . . .

TABLE OF CONTENTS (continued)

Case Study Simulation Results	39
Evaluation of Water Management Options	42
Regulatory Concerns	46
Zama Summary.....	47
Gorgon Case Study.....	47
Site Characterization.....	47
Modeling.....	48
Case Study Simulation Results	50
Evaluation of Water Management Options	55
Regulatory Concerns	61
Gorgon Summary.....	62
Teapot Dome Case Study	63
Site Characterization.....	63
Modeling.....	63
Case Study Simulation Results	66
Surface Dissolution.....	69
Evaluation of Water Management Options	69
Regulatory Concerns	75
Teapot Dome Summary	75
 CONCLUSIONS AND RECOMMENDATIONS	 76
CO ₂ Storage Benefit Derived from Water Extraction	77
Extracted Water Use.....	78
Surface Dissolution of CO ₂	78
Regulatory Situation Concerning Water Extraction.....	79
Recommendations	79
 REFERENCES	 80
 BENEFICIAL USE OPTIONS AND WATER QUALITY REQUIREMENTS	 Appendix A
 DESALINATION TECHNOLOGIES.....	 Appendix B
 KETZIN MODELING AND SIMULATIONS	 Appendix C
 ZAMA MODELING AND SIMULATIONS.....	 Appendix D
 GORGON MODELING AND SIMULATIONS	 Appendix E
 TEAPOT DOME MODELING AND SIMULATIONS	 Appendix F
 SURFACE DISSOLUTION MODELING AND SIMULATIONS	 Appendix G

LIST OF FIGURES

1	Emission reduction techniques.....	7
2	Saline groundwater well locations in the continental United States	11
3	Box plot for South Dakota saline formations.....	12
4	TDS distributions in formation waters of Colorado.....	13
5	TDS distributions in formation waters of Mississippi	13
6	TDS distributions in formation waters of North Dakota.....	14
7	Cumulative worldwide desalination capacity.....	15
8	Desalination feedwater source	16
9	Acceptable water quality ranges for water treatment technologies and resulting ranges of brine reject concentrations.....	20
10	Map depicting the location of the selected sites.....	21
11	Stuttgart formation structural map (left) and modeled surface produced from the data (right).....	26
12	Three-dimensional view of the Ketzin model showing the porosity attribute	26
13	Three-dimensional view of the Ketzin model showing the permeability attribute	27
14	Pressure map of Ketzin models after 25 years of injection for Cases 2 (top) and 4 (bottom).....	30
15	Outline of plume extent after 25 years of injection for Cases 2 and 4.....	31
16	Comparison of CO ₂ injection volumes utilizing multiple combinations of injection and extraction wells.....	33
17	Three-dimensional view of the Zama model showing the permeability attribute.....	38
18	Three-dimensional view of the Zama model showing the porosity attribute.....	39
19	Placement of acid gas injection well (named Gas Inj-1) in predictive simulations	41

Continued . . .

LIST OF FIGURES (continued)

20	Case 4, aerial view of injected gas plume at end of simulated injection period	42
21	Three-dimensional representation of the Gorgon reservoir model with location of injection and extraction wells	49
22	Cross section of the Gorgon reservoir model through the data well.....	49
23	Three-dimensional view of the Gorgon model showing the porosity attribute.....	50
24	Three-dimensional view of the Gorgon model showing the permeability attribute.....	51
25	Map of injection and extraction wells on Barrow Island with plume outlines of Cases 1 (base case) and 2 after 25 years of injection	53
26	Map of injection and extraction wells on Barrow Island with plume outlines of Cases 8 and 9 after 25 years of injection.....	53
27	Reservoir pressure after 25 years of injection for Cases 1 (top) and 2 (bottom) illustrating an appreciable pressure reduction	54
28	Plume distribution for Cases 4 and 5 demonstrating limited benefit from the reduction of the injection rate from 4 to 2 megatonnes per annum.....	55
29	Box and whisker plot for composition of Gorgon water.....	57
30	Salinity of Gorgon site water as a function of depth.....	58
31	Extracted-water production rates for Gorgon.....	59
32	Water cost versus purified water capacity for RO treatment of 20,000 mg/L TDS water ..	60
33	RO treatment costs for treating 10,000 mg/L TDS extracted water.....	60
34	Three-dimensional view of the Teapot Dome Dakota model showing the porosity attribute.....	64
35	Three-dimensional view of the Teapot Dome Dakota model showing the permeability attribute.....	65
36	Plume distribution of Teapot Dome Cases 3 and 4 illustrating the effects on plume size from the utilization of horizontal and vertical extraction wells.	68

LIST OF TABLES

1	Summary of Geothermal-Scale Formation Mechanisms and Mitigation Options	6
2	Salinity Values (TDS in mg/L) from AGD	10
3	Treatment Capacity Ranges for Popular Desalination Technologies Treating Brackish Water and/or Seawater	17
4	Selected Sites and Prominent Lithology Encountered in Target Storage Reservoirs	21
5	Ketzin Model Parameters	27
6	Case Scenarios and Resulting Storage Capacities for the Ketzin Site	29
7	Water Quality Values for Ketzin.....	35
8	Brine Crystallization Cost Analysis for Ketzin.....	36
9	Reservoir Properties for the Zama F Pool Pinnacle Reef.....	40
10	Cases Tested in Predictive Simulations for Zama.....	40
11	Extracted Water Flow Rates for Zama Based on a CO ₂ Injection Rate of 1 million tonnes/year	43
12	Water Quality for Zama	44
13	Cost and Energy-Use Analysis for Zama Extracted-Water Treatment	45
14	Unit Descriptions and Thicknesses from the Gorgon Site	48
15	Gorgon Model Parameters	48
16	Case Scenarios and Resulting Storage Capacities for Gorgon.....	52
17	Median TDS Sample Water Quality and Median Water Quality from All Samples	58
18	Unit Descriptions for the Teapot Dome Site	64

Continued . . .

LIST OF TABLES (continued)

19 Reservoir Properties for the Tensleep Formation Within the Teapot Dome Model 65

20 Reservoir Properties for the Dakota and Lakota Formations Within the Teapot Dome Model..... 66

21 Case Scenarios and Resulting Storage Capacities for Teapot Dome 67

22 Comparison of Water Parameters for Four Potential CO₂ Injection Sites 70

23 Simulated Extracted Water Flow Rates and Duration and Calculated Rate per million tonne/year of CO₂ Injection 72

24 Range of Water Flow Rates (m³ of water/day) for 1, 2, 4, and 8 Mt/yr CO₂ Injection..... 72

25 Range of Treated Water Flow Rates (m³ of water/day) for 1, 2, 4, and 8 Mt/yr CO₂ Injection..... 72

26 Range of Brine Concentrate Flow Rates (m³ of water/day) for 1, 2, 4, and 8 Mt/yr CO₂ Injection..... 72

27 Costs and Energy Use Estimates for Teapot Dome RO Reject Brine Treatment Options.. 74

EXTRACTION OF FORMATION WATER FROM CO₂ STORAGE

EXECUTIVE SUMMARY

Deep saline formations (DSFs) constitute the largest potential global resource for the geologic storage of carbon dioxide (CO₂). Their use is, in turn, crucial to the successful scale-up of storage from pilot and demonstration projects to commercial operations. However, questions related to the capacity and injectivity of DSFs remain, particularly the management of pressure and potential displacement of formation brines. Extraction of saline waters from CO₂ storage formations is a potential method to improve reservoir storage volume, manage CO₂ plume migration, reduce cap rock exposure to CO₂, manage storage reservoir pressure, and/or generate a new source of water for a variety of beneficial surface uses. Indirect benefits derived from the treatment and sale of the extracted water may also provide additional economic incentives or cost offsets for formation water extraction. Currently, extraction of formation water is not utilized for large-scale CO₂ storage projects such as Sleipner, Snohvit, and In Salah. Extraction has been included in the permitting plan for the proposed Gorgon project as an additional reservoir management tool.

In order to evaluate the implementation of extracted water on a commercial scale, evaluations were carried out by the Energy & Environmental Research Center (EERC) utilizing data from four existing and potential real-world storage projects. This report presents hypothetical injection scenarios to demonstrate the impact of formation water extraction at realistic locations. These sites are either being used for smaller CO₂ injection tests or are not currently being utilized for CO₂ storage. The sites, the Teapot Dome Field in the United States, Zama Field in Canada, the Gorgon site in Australia, and the Ketzin site in Germany, represent a range of geologic storage targets, reservoir water quality, injectivity, climates, populations, and water utilization opportunities. Geologic models were constructed on potential storage targets, encapsulating their geologic properties, structure, and heterogeneities based upon published data. A variety of CO₂ injection and formation water extraction scenarios were simulated to understand the nature between water extraction and its effects on CO₂ storage and plume behavior, including its effect in a closed system (Zama Field). Estimated rates of water extraction were derived from these simulations for analyzing their potential utilization at both industrial and domestic surface facilities. In addition, simulations were developed to test the possibility of mixing CO₂ with extracted water at the surface prior to injection.

The simulation results showed that the CO₂ storage capacity increased with the formation water extraction for all test sites. The volumetric ratio of CO₂ injection to water extraction was about 1:1 for most of the cases with pure CO₂ injection. This resulted in increased storage capacity for all sites, ranging from a 4% increase at Gorgon (where reservoir capacity vastly exceeded injection/extraction capability) to 1300% at Zama, (a closed system restricted by pressure limitations of the cap rock). Water extraction approximately doubled storage capacity at both Ketzin and Teapot Dome, 197% and 204%, respectively, where reservoir conditions limited injection rates. At Ketzin, it was found that a larger quantity of CO₂ could be injected (a 250% capacity increase) if the injector and extractor were utilized as injection wells. Additional simulations with up to 12 injectors and 13 extractors revealed that, with a larger quantity of

wells, water extraction could have a greater impact on potential storage than injecting through all wells. However, in the Teapot Dome site, the use of an injection/extractor pair was found to produce a larger storage capacity than two injectors. Because of the presence of a relatively thin injection zone, the simulations were repeated with horizontal wells, but the injection/extraction pair outperformed the two injection wells. Storage capacity was increased by 367% with the horizontal pair over the base case injection. As a result, it can be said that water extraction can significantly increase the available capacity of a reservoir, but because of the wide variety of geological and engineering variables involved in large-scale CO₂ storage, it may not be the most efficient use of resources in all cases.

Pressure and plume management were simulated at the Ketzin, Gorgon, and Teapot Dome sites. These practices resulted in a decrease of the ratio of CO₂ injected to water extracted of 1:2 to 1:4. Reservoir pressures could be reduced by 10% to 20%, and plume areas were increased by as much as 30% because of the interplay between natural plume migration and extraction influences. In the closed Zama Field, reservoir pressure could be maintained below acceptable limits using water extraction until the reservoir was nearly filled with CO₂. Thus water extraction appears to be a reasonable method of reservoir pressure and CO₂ plume management, especially in closed systems.

Simulations were developed for two of the case study sites to investigate and compare the utility of injection of CO₂ saturated water, and it was found to require much greater volumes of extracted water while only storing a small fraction of the CO₂ that could be injected as supercritical CO₂. It may be possible to use this approach for storage in more shallow saline formations where the pressure is subcritical for CO₂; however, with decreasing pressure comes decreasing solubility of CO₂, reducing the quantity of CO₂ which can be dissolved in the shallower saline formations. The associated technical challenges with maintaining CO₂ in solution through the changing pressure–temperature conditions from surface facilities to injection point and managing the potential scaling and corrosion possibilities further limit the economic utility of this practice.

It is generally expected that extracted water will be directly disposed of through deep well injection into overlying saline formations which are not deep enough for CO₂ storage. If conditions are identified for beneficial use of extracted water, several treatment technologies (primarily desalination) are commercially available. The type and cost of treatment will depend on the desired beneficial use and extracted water quality. Possible water treatment options include, but are not limited to, reverse osmosis and other membrane processes, mechanical vapor compression, and multistage flash distillation. Potential beneficial uses and the water quality required for each use are quite varied and range from agricultural and industrial uses to the production of drinking water. Potential synergies between water users and storage operations (e.g., water for cooling at the facility which provides CO₂ to the storage project) also exist. Options for the management of treatment reject products (e.g., concentrated brine) include injection disposal, brine concentrators, and brine crystallizers.

The quality of extracted waters from the case study sites, and indeed all potential storage formations, varies greatly from low-salinity waters (<10,000 ppm total dissolved solids [TDS]) to very high salinity waters (>200,000 ppm TDS). The possibility of treatment for beneficial use

is economically restricted to the lowest salinity waters because of the cost of desalinization. Economically viable waters were identified at Gorgon (10,000–20,000 ppm TDS) and Teapot Dome (10,000 ppm TDS), where treatment costs were estimated to range from US\$0.76/m³ to US\$0.88/m³ and US\$0.73/m³ to US\$1.06/m³, respectively. Input flow rates of extracted water are the greatest influence on these prices because of economies of scale. These figures are regionally competitive but do not include the costs of transportation which, in the Gorgon site, more than doubles the cost of the water. Treatment for beneficial use of water is unlikely at Ketzin and Zama because of high salinities, but extraction of the geothermal heat they contain or processing them in order to extract salts and minerals may be viable options. In these cases, the extracted water would be reinjected into another location in the same formation or another saline formations. The relatively high quality of water from the Gorgon site makes ocean disposal an option as well, in accordance with local regulations.

There do not appear to be any regulatory constraints for the extraction of formation water as a pressure maintenance technique for carbon capture and storage (CCS) projects in any of the jurisdictions reviewed. Regulations are not in place to specifically deal with brine injection related to CCS projects. Over the course of several decades, brines and other fluids associated with the production of oil and gas operations have been injected into wells in a variety of geologic settings throughout the world. Regulatory authorities and industry have developed best practice strategies and regulatory processes that have allowed for the safe disposal of brine into the deep subsurface. It is likely that these practices and regulations would also be applicable to CO₂ storage projects for the handling and disposal of extracted brines.

Formation water extraction from CO₂ storage reservoirs is applicable for increasing storage capacity, managing reservoir pressure, and controlling plume movement. At this point, the greatest potential appears limited to either closed systems or scenarios where a large number of injector producer pairs can be implemented to handle very large volumes of CO₂ and water. Analysis of the resulting water quality and quantity, available treatment technologies, and potential transportation costs reveals there is likely to be limited potential for the beneficial use of extracted water from CCS facilities. Although variable by location, the difference between the highest quality of water appropriate for CO₂ storage and the lowest quality of water economically viable for treatment and beneficial use is relatively small, ruling out a large majority of potential storage targets whose water quality exceeds those treatment limits. Ideal circumstances of relatively high quality reservoir water and highly stressed or limited regional water resources will need to coexist before beneficial use of extracted water should be considered. Additional work classifying the water quality of potential DSF storage targets is necessary before these conclusions can be revisited.

This subtask was funded through the EERC–U.S. Department of Energy (DOE) Joint Program on Research and Development for Fossil Energy-Related Resources Cooperative Agreement No. DE-FC26-08NT43291. Nonfederal funding was provided by IEA Greenhouse Gas R&D Programme.

EXTRACTION OF FORMATION WATER FROM CO₂ STORAGE

INTRODUCTION

Deep saline formations (DSFs) constitute the largest potential global resource for the geologic storage of carbon dioxide (CO₂). Their use is, in turn, crucial to the successful scale-up of storage from pilot and demonstration projects to commercial operations. However, questions remain related to the capacity and injectivity of DSFs, particularly the management of pressure and potential displacement of formation water. Extraction of saline waters from CO₂ storage formations is a potential method to improve reservoir storage volume, manage CO₂ plume migration, reduce cap rock exposure to CO₂, manage storage reservoir pressure, and/or generate a new source of water for a variety of surface uses (Court and others, 2010; Buscheck and others, 2010; Newmark and others, 2010). Indirect benefits derived from the treatment and sale of the extracted water may also provide additional economic incentives or cost offsets for formation water extraction. Currently, extraction of formation water is not utilized for large-scale CO₂ storage projects such as Sleipner, Snohvit, and In Salah. Extraction has been included in the permitting plan for the proposed Gorgon project as an additional reservoir management tool.

Monitoring and managing the formation pressure within a CO₂ storage formation are critical to carbon storage projects. This may be accomplished through the removal, or extraction, of formation water from the storage reservoir itself. Extraction of formation water will reduce the overall reservoir pressure, thereby increasing the potential CO₂ storage volume. The extraction scheme may also control the migration and development of the CO₂ plume. Both lateral and vertical migration of a CO₂ plume can be achieved through the use of water extraction wells (Buscheck and others, 2010).

Extraction of formation water for CO₂ plume and pressure management will have a direct impact on the scope and costs of monitoring, verification, and accounting (MVA) activities and provide immediate benefits to storage reservoir operators. Although the benefits of storage reservoir management are easily recognized, very few feasibility or economic analysis tools have been developed to examine the costs and benefits of treating extracted water for beneficial uses. The potential for beneficial use of extracted water may help offset some of the costs associated with developing new water resources for carbon capture and storage (CCS) technology (Gerdes and Nichols, 2009; Zhai and Rubin, 2010). Public and private sector water users may also benefit from an additional water source to augment existing supplies for a variety of water uses such as industrial process water or agriculture. This potential for additional supply from extracted water will become increasingly important, as globally available water resources continue to be strained by a variety of growth factors (Sandia National Laboratories, 2005).

The effect of pressurization in a storage formation will depend largely on whether the system can be considered open or closed. In a closed or semiclosed system, the pressure buildup will be determined by the boundary conditions, which include the confining unit's permeability. Uncertainty in characterizing appropriate reservoir boundary conditions contributes to the difficulty of predicting brine displacement. Determining macroscopic-scale permeability can be a difficult task, even when reservoir samples have been obtained, because of problems with up-

scaling measurements. Regional permeability effects also need to be taken into account (IEAGHG, 2010).

Another important concern is potential for CO₂ breakthrough into an extraction well. Heterogeneities in the storage formation may cause complexities in predicting flow rate and direction of injected CO₂ flow. If a formation water extraction well is placed along a path of high permeability, then the rate of flow toward the well could be high and may result in early CO₂ breakthrough. This may necessitate the plugging of the water extraction well and the consequent drilling of a new water extraction well, thereby increasing project cost.

Potential rates of water extraction from DSFs, with respect to CO₂ storage, are not well understood at this time. Extraction rates will depend on site-specific factors, e.g., geologic structure, confining layer permeability and heterogeneity, and local reservoir pressure relative to maximum potential reservoir pressure, as well as project design features such as the desired CO₂ injection rate. Additional challenges will be encountered when large-scale projects are considered where there are likely to be multiple injection and water extraction wells. It is important to consider how each well will interact with each other, as there may be an overlap of pressure footprints from each well. Thorough site characterization and modeling provide the primary counter to these reservoir management challenges.

When brought to the surface, the extracted water from the storage formations will need to be managed, through reuse, treatment, or reinjection. For the proposed Gorgon project in Australia, the planned management strategy is injection of the extracted formation water into an overlying saline formation (Flett and others, 2008). Another disposal option available to offshore operations is direct disposal into the sea. This action is dependent on the composition of the formation water and applicable local regulations. Alternatively, extracted water could be utilized for a variety of industrial processes, such as the cooling process within power stations or as a source of geothermal energy. Other possibilities include desalination of the extracted water, with subsequent beneficial use for either agriculture or as a source of drinking water. The latter options would depend on the cost of water treatment and on the demand and cost of local water resources. Not all extracted waters may be candidates for treatment and use because of the cost/benefit ratio of treating high-salinity extracted water. Available water treatment technologies must be assessed to evaluate their applicability to treatment of extracted formation water. In all cases, treatment will result in a residual brine or dry salt product that will require disposal. The potential rates of formation water extraction must be thoroughly understood before these challenges can be accurately addressed.

While the challenges of controlling the physical extraction of formation water and managing the extracted water once it is brought to the surface are numerous, the potential benefits to storage facilities also warrant further consideration. The ability to reduce upfront permitting and characterization costs by reducing the area of review (AOR – a predetermined area which undergoes extensive site characterization and within which injected CO₂ is expected to remain) and reducing the scope and scale of monitoring activities could make the potential of formation water extraction attractive for some CCS projects. The potential also exists to develop previously underutilized water resources that could supplement limited surface and subsurface water supplies in many parts of the world, providing immediate and tangible benefits to local and

regional stakeholders. This report details the potential for formation water extraction and provides recommendations for its utilization and management in future CO₂ storage projects.

PROJECT APPROACH

In order to evaluate the implementation of extracted water on a commercial scale, evaluations were carried out on existing and potential real-world storage projects. These sites represent a range of geologic storage targets, reservoir water quality, injectivity, climates, populations, and water utilization opportunities. Geologic models were constructed for each storage target, which were built using publicly available data to approximate each site's geologic properties, structure, and heterogeneities. This allowed for detailed simulation of a variety of CO₂ injection and formation water extraction scenarios to understand the dynamic nature of water extraction and its effects on CO₂ storage and plume behavior. Estimated rates of water extraction were derived from these simulations for analysis of their potential utilization at surface facilities, both industrial and domestic. In addition, simulations were developed to test the possibility of mixing CO₂ with extracted water at the surface prior to injection. These simulations also estimated rates and volumes of CO₂ storage and water extraction.

The potential for extracted water utilization was developed through the assessment of potential water treatment technologies applicable to the expected quality and rates of generation. Potential uses of the treated water were also identified. Case studies were developed for the modeled sites to evaluate the economic viability of supplying treated extracted water for some of these uses. Existing regulations were evaluated to identify CO₂ injection or wastewater disposal requirements which may impact the development and management of extracted-water production and treatment. From these various sources of information, recommendations were developed for the development of commercial-scale CO₂ storage and water extraction plans.

BACKGROUND

Extensive industry experience in underground injection for enhanced oil recovery (EOR), gas storage, and deep well waste injection demonstrates that injection into geologic environments is feasible using existing technology. However, only a limited number of saline formations are generally used for these purposes, and detailed documentation of the properties of DSFs are generally not compiled in an easy-to-access format. Realistic and quantitative information about the relevant characteristics of the subsurface is needed to assess feasibility, costs, and risks associated with various options for water extraction in conjunction with CO₂ storage.

As opposed to CO₂ EOR projects, which have production and injection wells, carbon storage in saline formations would not typically include any production or extraction wells. The degree to which CO₂ injection will increase formation pressure is a function of formation rock and fluid characteristics such as permeability, compressibility, salinity, initial formation pressure, and boundary conditions.

One way of mitigating concerns of overpressurization and interference from different projects or injection wells is to utilize formation water extraction wells as part of the storage scheme. Adding extraction wells could improve injectivity and reduce the number of injection wells required. It is not clear whether adding extraction wells will change the total number of injection wells required for a CO₂ storage project. In addition, the production of formation water requires surface facilities to dispose of or treat the water. If the total number of wells is constant with and without extraction, the additional surface facilities may make pressure management, through formation water extraction, an economically less attractive option. However, in some cases, formation water extraction wells may actually decrease the total number of wells necessary to achieve the target injection rates while staying below the required pressure limits, reducing overall costs.

Another primary concern for most MVA activities and injection permits is the development of a mobile, free-phase CO₂ plume (U.S. Environmental Protection Agency, 2011). The ultimate size, location, and migration pathways of the resulting plume must be adequately described prior to the start of any CO₂ storage project. The strategic placement of water extraction wells could influence the development of CO₂ plumes, most likely either drawing the plume toward a desired storage trap or discouraging migration from a desired location. A reduction in plume size is likely to reduce the monitoring costs associated with large-scale storage projects as costs associated with the number of monitoring wells, monitoring through seismic surveys, and surface-monitoring activities are reliant on the area to be observed. These reductions in cost may be enough to justify the added costs of drilling additional wells for extraction, although a variety of site-specific variables will factor into these costs.

Water extraction can also be utilized to increase the overall capacity of an injection target (Buscheck and others, 2010). Extraction wells may be used to increase the pore space available for storage in all directions. The greatest efficiencies may be achieved by extracting formation water from underneath the buoyant CO₂ plume, drawing it downward vertically, thereby making more efficient use of the available reservoir space (Buscheck and others, 2010). The potential storage gains will be controlled by reservoir temperature, pressure, heterogeneity (which will influence how CO₂ migrates toward extractors), structure, and other site-specific factors. Most DSFs targeted for storage are expected to be open systems, where formation fluids and increased pressures will be able to bleed off into the portions of the reservoir surrounding the storage target. This allows the reservoir to (eventually) return to initial pressure conditions during the postinjection phase. This is not possible in closed systems, such as isolated carbonate reef structures. The capacity of closed targets will be limited primarily by the difference between their initial pressure and the fracture pressure of the surrounding sealing formations. Reservoir pressure could be maintained below the fracture pressure for much longer time periods during the injection phase with the use of extraction wells, thereby greatly enhancing overall storage capacity. In this way, the cost of storage per tonne of CO₂ may be reduced by increasing the storage capacity of a given target.

Finally, treatment and utilization of extracted water for a beneficial surface use could be evaluated when considering extraction of formation water. The potential for beneficial use is largely dependent on the quality of the water present in the target formation, and the majority of storage targets are unlikely to contain economically treatable formation water. However, in

regions of the globe where available water resources are highly limited and storage formation water is of reasonable quality (perhaps below 50,000 ppm total dissolved solids [TDS]), treatment and use may be economically viable. Potential beneficial uses and treatment options are described in subsequent sections.

Water Management Options

Most DSFs contain waters with high salinity, which limits their applicability for beneficial use. Generally speaking, the costs of treatment increase rapidly with increasing TDS. It is expected by the authors that the vast majority of instances of storage in DSFs will not generate a viable stream of water for beneficial use. Instead, it is expected that the majority of water extracted will be directly disposed of into either another portion of the target formation or another disposal formation. In offshore locations, disposal may occur through direct discharge to the ocean in accordance with local wastewater disposal regulations. These are common and established industry practices for managing oil and gas produced water. Although there are numerous potential applications for extracted water, the actual opportunities for implementation are anticipated to be limited.

Direct use of the water may be achieved through geothermal energy recovery processes or an alternative injection strategy referred to here as surface dissolution of CO₂. Given the appropriate water quality, several water treatment options may be viable, consisting primarily of membrane and filtration processes and thermal processes. Once treated, this water may have applications ranging from industrial cooling or process feedwater, to a variety of agricultural uses, to a potable water supply. The water quality required for each beneficial use and the associated permitting requirements vary greatly. Potential synergies between water users and storage operations (e.g., water for cooling at the facility that provides CO₂ to the storage project) may also exist.

Direct Use (primary)

Water quality requirements for geothermal energy recovery are minimally restrictive. There is no limit on TDS or specific chemistry of water, but there are practical limits based on scaling and corrosion potential (Clark and others 2011). Scaling is typically controlled through the use of chemical additives injected downhole to keep scaling from forming in the well. Table 1 summarizes the major scale-forming mechanism and mitigation options for geothermal systems. Corrosion is typically controlled through selection of corrosion-resistant materials and the addition of chemical additives used for controlling corrosion.

Another potential direct-use option for extracted water is to dissolve the CO₂ directly into the saline water extracted from the storage target and subsequently reinject that CO₂-saturated fluid. This is referred to as the “surface dissolution approach” to carbon storage (Jain and Bryant, 2011; Burton and Bryant, 2009; Leonenko and Keith, 2008). The CO₂-saturated fluid is more dense than the existing formation fluid, which reduces the likelihood of buoyant flow and increases the chances of permanent, stable storage. The solubility of CO₂ in the formation

Table 1. Summary of Geothermal-Scale Formation Mechanisms and Mitigation Options (Clark and others, 2011)

Chemical Species	Drivers of Scale Formation	Mitigation Options
Metal Sulfide	↓ Temperature, ↑ pH, ↓ oxidation state, ↓ dissolved H ₂ S	Oxidation of geofluid; acidification of geofluid
Calcium Carbonate (calcite)	↑ Temperature, ↑ pH, ↓ dissolved CO ₂	Pressurization of geofluid in the wellbore; injection of specialized scale inhibitors
Silicon Dioxide (silica)	↓ Temperature, ↑ SiO ₂ concentration, pH close to neutral	Modification of system operating conditions to minimize oversaturation; modification of geofluid pH

fluid is dependent on the temperature, pressure, and salinity of the formation fluid. The viability of surface dissolution is evaluated as part of the case studies used in this report.

Beneficial Use as a Supply of Water (secondary)

There are challenges to management and treatment of extracted water, many of which are due to the varying composition of formation waters. The most common large-volume desalination technologies are the thermal processes: multistage flash distillation (MSF), multiple effect distillation (MED), and MED combined with thermal vapor compression (MED/TVC). The most common membrane systems are reverse osmosis (RO), nanofiltration (NF), and electrodialysis reversal (EDR). MSF, MED/TVC, and RO are the most widely applied methods for seawater desalination or treatment of other highly saline waters. NF is sometimes used as a pretreatment step prior to RO and thermal processes because it is effective at removing scale-forming ions.

Pretreatment is almost always required prior to desalination. The level of pretreatment required for the thermal methods is typically less than that required for the membrane methods. Pretreatment steps include removal of suspended solids (e.g., silt, organic or inorganic debris), nonaqueous-phase liquids (e.g., oil), dissolved gases (e.g., CO₂, N₂, O₂), and control of microbial growth (Veil and others, 2011). A wide range of chemical compositions of formation water could potentially be involved when CCS and desalination are joined. Moreover, compositions can vary within similar lithologies (i.e., both sulfate- and chloride-dominated compositions in sandstones) as well as within a single unit (i.e., two very different chemical compositions in a single formation), depending on the location within a formation. Treatment requires careful characterization of the feedwater and facility design to optimize a system for the specific input composition.

Water Management for Beneficial Use as Water Supply

Extracted-Water Quantity

As shown in Figure 1, the International Energy Agency (IEA) BLUE Map scenario for 2005–2050 indicates that 19% of the 48-Gt/year CO₂ emission reduction in 2050 needs to come from CCS (International Energy Agency, 2008). This means that, in the year 2050, there could be 9.12 Gt/year of CO₂ globally that needs to be injected for geologic storage (this is a conservative estimate as an additional 20%–25% of CO₂ could be generated by carbon capture processes and are not accounted for in these figures). The question then becomes, how much water extraction may be needed in order to assist in these efforts, and then how much of this water might be put to beneficial use?

If water extraction were used for all of the CCS and an assumption of 1 tonne of injected CO₂ (800 g/L density, ~about 100°C temperature, and 5000 kPa pressure) would displace 1.25 m³ of reservoir fluid, the extracted-water volume would be 11.4 Gm³/year (31.2 million m³/day) of water to replace the 9.12 Gt/year. This is probably close to the amount of source water currently used to produce purified water through desalination (International Desalination Association, 2011). 11.4 Gm³ water/year of water is equivalent to 40% of the global purified water production currently generated by desalination of seawater.

While much of the extracted water is likely to be too saline to be put to beneficial use, a significant amount will likely be of sufficiently low salinity (10,000 to 50,000 mg/L TDS) to economically treat and convert much of it to water of potable quality.

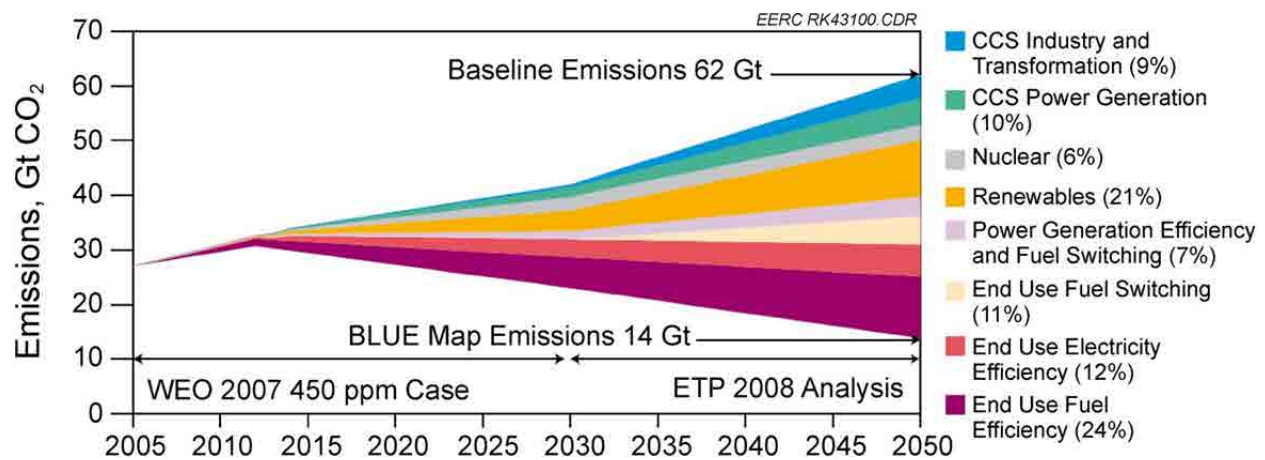


Figure 1. Emission reduction techniques (International Energy Agency, 2008).

It has been estimated that for a modern 1-GW (gigawatt) integrated gasification combined-cycle (IGCC) plant generating 7.5 million m³ CO₂/year, treating extracted formation fluid could provide 50% of the plant's operating water requirements, including cooling demand (Newmark and others, 2010). This estimate includes potential energy savings provided by the thermal and pressure energy present in the extracted fluid. Water requirements for cooling at power plants utilizing postcombustion carbon capture are higher than those for IGCC facilities. Phillips (2011) from the Electric Power Research Institute estimated 30% of the water requirements for a coal fired-power plant utilizing wet cooling could be supplied by water extracted at a 1:1 volume ratio (CO₂ density = 800 g/L) based on storage of the CO₂ captured. The water demand by both the IGCC and the supercritical boiler combustion systems could be decreased to levels below the extracted-water production volumes if dry cooling and, possibly, even hybrid cooling were used. This could then help the overall system provide power and water for a community.

Extracted-Water Quality

The quality of extracted waters will vary from low-salinity waters from former oil and gas reservoirs where hydrocarbons may be the main component of concern to very high salinity waters where beneficial use of the water is unlikely, but options for recovery of the geothermal heat, salts, and/or minerals may be considered.

Ideally, prior to formation water extraction, operators would obtain information concerning TDS, specific ions present, organics, radionuclides, pH, alkalinity, hardness, temperature, and other "common" water quality measures. Any potential for beneficial use for that water would be identified at this time as well. This information may or may not be present prior to site-specific investigation depending on data availability.

In many countries (United States, Canada, others), regulatory limits have been set for the lowest salinity waters that may be used for CCS. These restrictions have been placed to protect sources of water that may be used for potable water in the future. In the United States, waters with salt concentrations of less than 10,000 ppm are considered protected as potential sources of drinking water. Therefore, CO₂ storage in these aquifers will require special permits or exemptions. If the low-salinity groundwater is associated with oil or gas production, other water quality parameters (e.g., dissolved hydrocarbons) will likely prevent it from being considered as a potential source of potable water and ease the process of gaining permission to use it for CO₂ storage.

Extracted water will contain a variety of constituents that will need to be removed before the water could be put to beneficial use. The constituents of primary focus for this study are the dissolved inorganic ions, which constitute the salinity or TDS of the water. Most of the constituents that may be encountered are listed as follows:

- Dissolved gases – Removal of fixed gases (e.g., N₂, O₂) and CO₂ are common steps in pretreatment prior to desalination. Methane and other gaseous hydrocarbon removal may be necessary for some waters. Hydrogen sulfide removal as a gas may be desirable in some cases.

- Particulates – Sand, silt, and other particulate materials can be present in extracted water. Filtration of these materials is required prior to desalination.
- Hydrocarbons – Crude oil can potentially be present as dispersed, colloidal, emulsified, or suspended material, particularly where the target injection zone was an oil or gas reservoir. Recovery of useful product is desirable, and removal of residual is required prior to desalination.
- Dissolved organics – Dissolved organics may be present, particularly in water from formations containing oil and gas resources. Low levels of dissolved organics are not generally considered a problem for desalination, but removal of higher concentrations using physical, chemical, and/or biological processes may be necessary. If the extracted water is of sufficiently low salinity that desalination is not required, it is likely that treatment to remove dissolved organics will be required prior to disposal or use. Produced water literature contains significant coverage of this issue.
- Dissolved salts (typically measured as TDS) of particular concern including scale-forming components, toxic inorganics (e.g., arsenic, heavy metals, nitrates), and naturally occurring radioactive material (NORM) (e.g., radium, uranium) – It may be necessary or desirable to remove some of these compounds in pretreatment to provide for more reliable and lower-cost desalination. It may also be necessary to control the concentration of toxic inorganics and NORM in waste brine.

Salinity and chemical makeup of the dissolved species are highly dependent on the characteristics of the formation and cannot be simply inferred from geographic location or depth. While it will always be necessary to perform a detailed analysis of the water in a target formation before the potential for use of the extracted water can be fully realized, some information is available where oil and gas exploration and development have been most active.

As part of the IEAGHG project, development of storage coefficients for CO₂ storage in deep saline formations (IEAGHG, 2009), the Energy & Environmental Research Center (EERC) built the Average Global Database (AGD) for use in estimating CO₂ storage resource/capacity. The database contains 20,938 records from 23 countries. Table 2 includes a summary of the data from the AGD for all wells listed as having a depth of greater than 800 m for which a TDS value is also reported. Table 2 lists the number of entries for each country and, where possible, the mean, median, minimum, and maximum value point for each country. The database contains values that are predominantly from the United States, and simply evaluating the data by country provides a poor description of global water quality. What the database does indicate is that there is a need for collection and compilation of deep saline aquifer water quality data if global estimates are to be made of the potential for desalination of extracted water.

Groundwater data with detailed chemical analyses are even more difficult to find than those which contain a measure of TDS concentration. The most comprehensive database found is the NATCARB saline/water database (NATCARB, 2011), which covers the United States. Most

Table 2. Salinity Values (TDS in mg/L) from AGD

	United States	Australia	Germany	Canada	Brazil	China	Japan	Saudi Arabia
Number of Entries	1597	17	5	5	4	2	1	1
Mean	78,236	32,487	230,671	192,908	97,986	129,500	6100	137,000
Standard Deviation	69,686	44,436	4140	18,039	64,037	170,413		
Minimum	1	7000	224,928	178,948	55,533	9000		
Median	58,687	25,182	232,772	191,000	71,819			
Maximum	400,000	200,000	235,000	223,462	192,773	250,000		

of the saline data in the database, especially associated with deeper formations, comes from locations associated with oil and gas exploration and development. Figure 2 is a plot of all of the well locations in the NATCARB database. The database also contains some information for 36 wells in Alaska, but the current version (as of December 1, 2011) does not contain any information on the water chemistry for these wells.

The database is easily searched using online tools (www.natcarbviewer.org/brine/) for water quality information by state and county. These data can then be further evaluated based on a formation within the selected state or county and further segregated by formation within the selected geographic location. Box plots and Piper diagrams can then be produced. Figure 3 shows example box plots that can be made by the online plot tool. The samples produced are for South Dakota, which shows water from all formations in South Dakota (Figure 3). The TDS values for saline waters from South Dakota water range from very low at 1174 mg/L to very high at 322,733 mg/L. The median (7740 mg/L), first quartile (3080 mg/L), and third quartile (19,066 mg/L) values reveal that most of the water has salinities well below that of seawater. The information shown in Figure 3 reveals that these are sodium chloride- and sodium sulfate-dominated waters, mostly of moderate salinity, with pH near 7.5.

Ideally, an international database similar to the NATCARB database would be available for researchers, decision makers, and policymakers.

Harto (2011) and Wolery and others (2011) have analyzed a great deal of the NATCARB saline groundwater data and used a subset of the U.S. Geological Survey (USGS) Produced

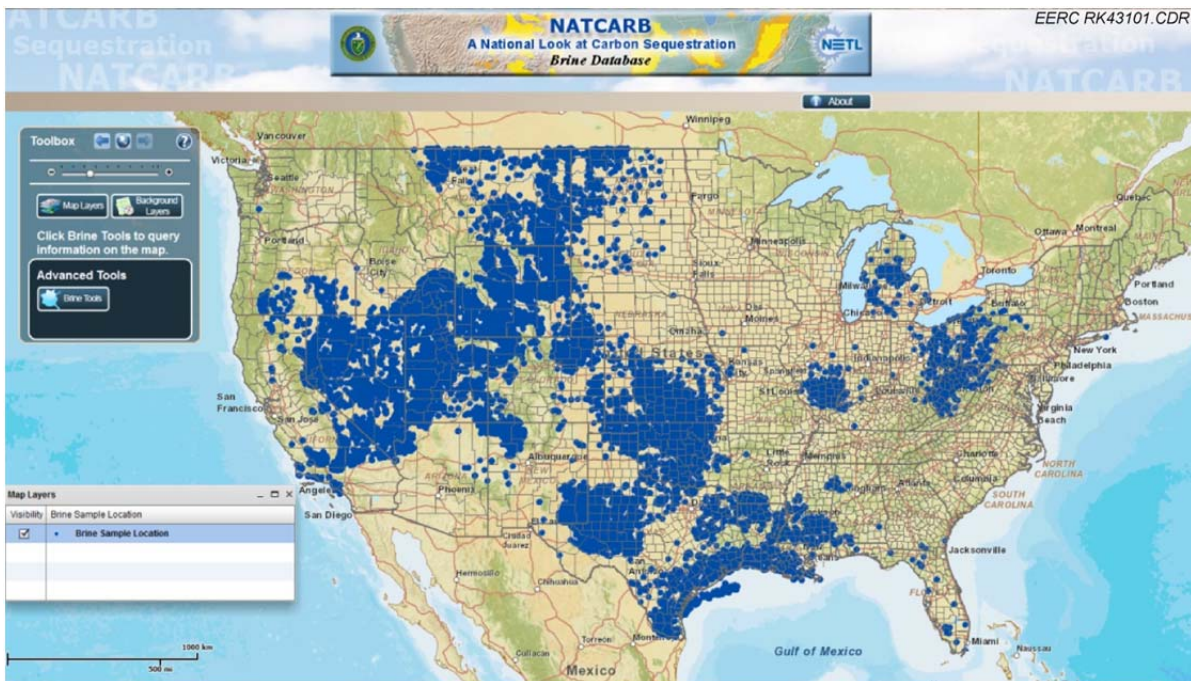


Figure 2. Saline groundwater well locations in the continental United States (NATCARB, 2011).

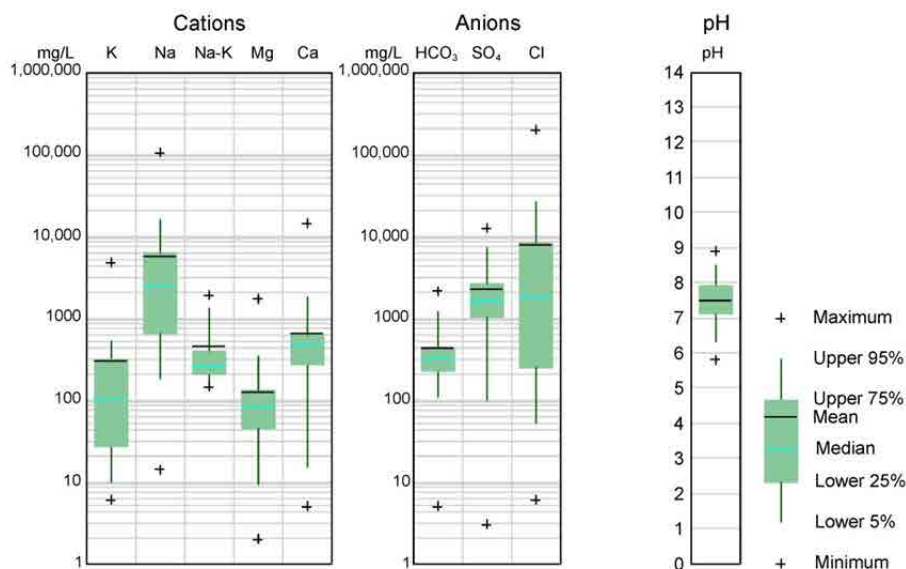


Figure 3. Box plot for South Dakota saline formations.

Waters Database (Breit, 2002) for compositions based on location dividing this information by U.S. Department of Energy (DOE) Regional Carbon Sequestration Partnership region (Harto, 2011) and by U.S. state (Wolery and others, 2011).

Wolery and others (2011) concluded that three types of saline formation waters seem to be common:

- NaCl-dominated waters with TDS ranges from approximately that of seawater (36,000 mg/L) up to ~350,000 mg/L TDS.
- Na–Ca–Cl-dominated waters with TDS generally above that of seawater up to ~400,000 mg/L TDS.
- Na–Cl–SO₄ “high-sulfate” waters (typically from basins in the Rocky Mountain region) with TDS ranging from less than 10,000 to ~110,000 mg/L.

They state further that HCO₃-rich formation waters related to Na–Cl–SO₄ formation waters mostly have low TDS values, <10,000 mg/L.

Their presentation of TDS range plots for three states, Colorado, Mississippi, and North Dakota, are illustrative (Figures 4–6). They present two plots for each state, with concentrations for a depth of >2625 and >7000 ft. They show that high-quality formation water is generally present in Colorado (Figure 4), with a slight trend of higher salinities with greater depth. Almost

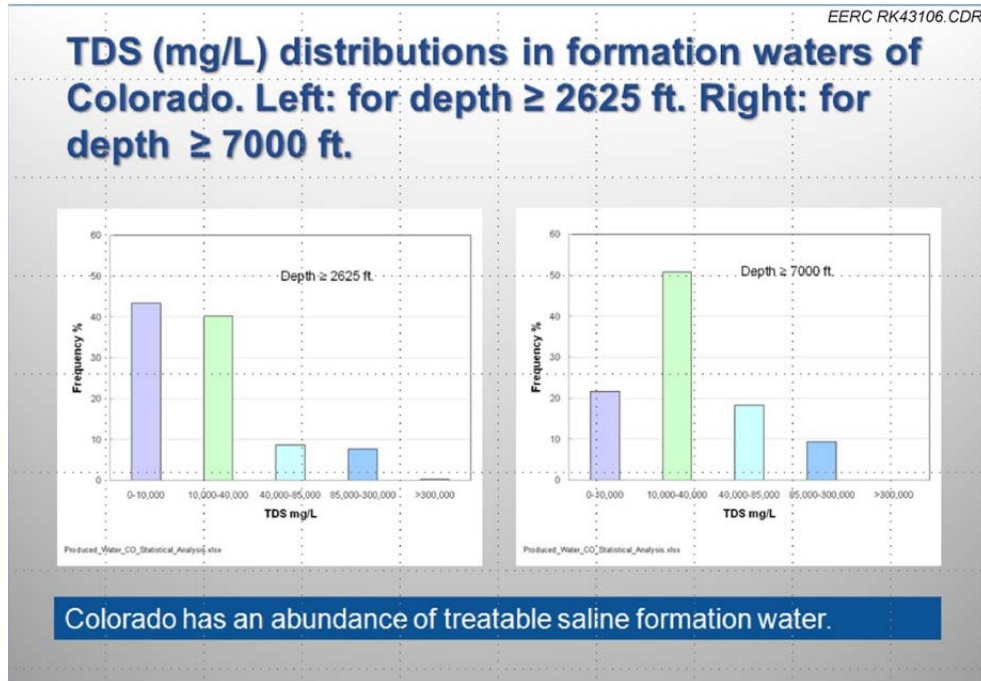


Figure 4. TDS distributions in formation waters of Colorado (Wolery and others, 2011).

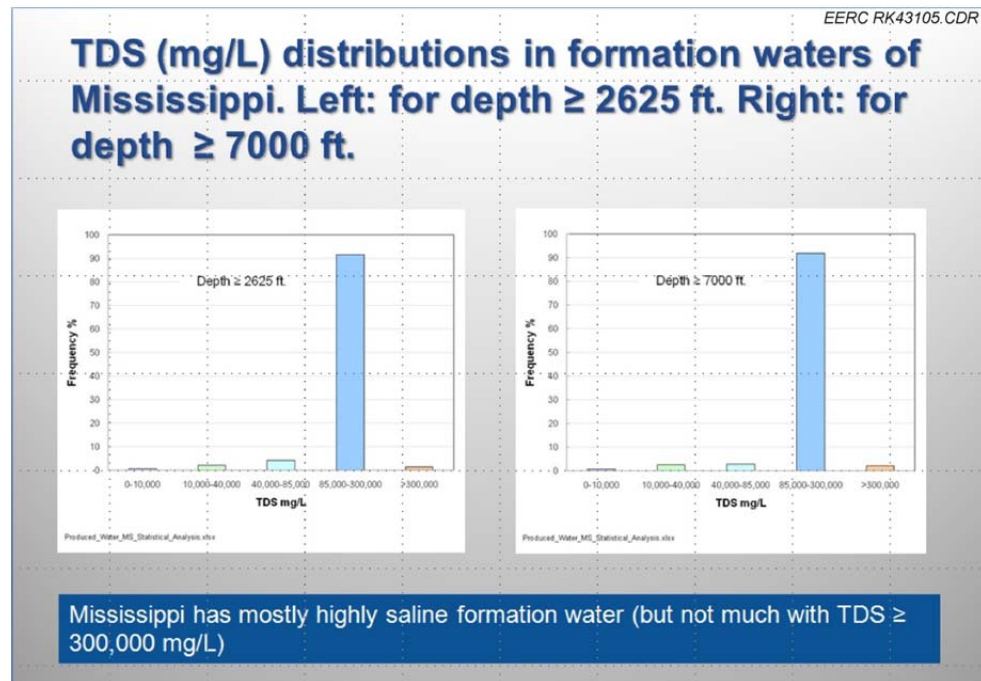


Figure 5. TDS distributions in formation waters of Mississippi (Wolery and others, 2011).

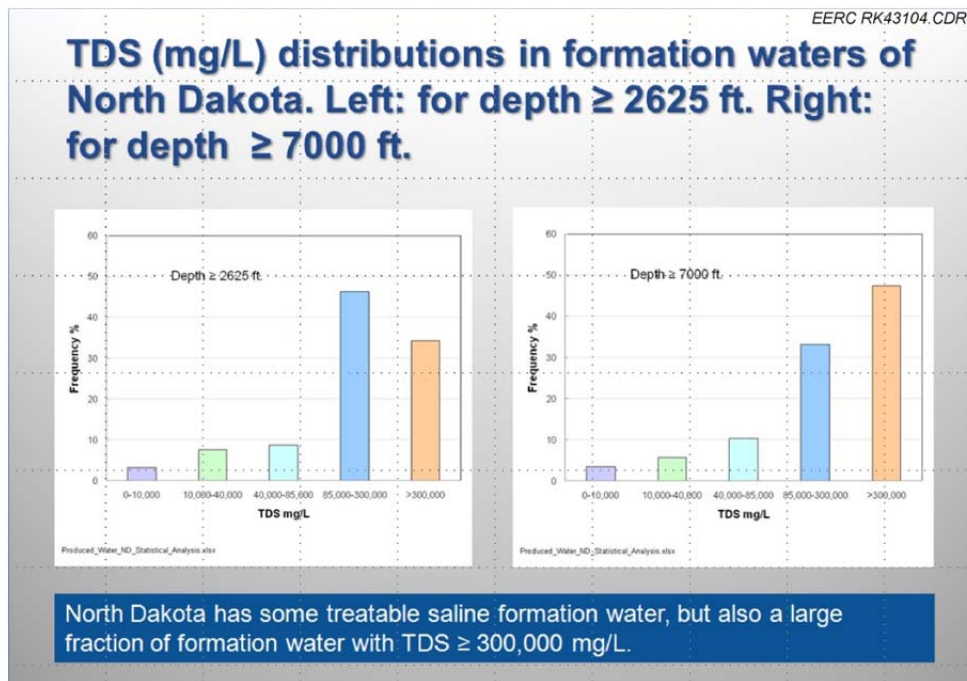


Figure 6. TDS distributions in formation waters of North Dakota (Wolery and others, 2011).

all of the formation water in Mississippi (Figure 5) falls in the TDS concentration range of 85,000 to 300,000 mg/L regardless of depth. A great deal of the formation water in North Dakota (Figure 6) has extremely high salinities ($>300,000$ mg/L) with an apparent increase in salinity with depth. If these results are any indication, depth cannot be used as local proxy for water quality when a potential target is evaluated for implementation of CO_2 storage with water extraction.

Quality for Beneficial Use

The water quality of CO_2 extracted formation water must be relatively high to be considered for beneficial use. These uses include geothermal heat recovery, various agricultural applications, industrial applications such as thermoelectric power facilities, and as a drinking water source. The quality of water required for each of these uses varies and, in some instances, has specific requirements. Detailed descriptions of the water quality requirements of various potential beneficial uses can be found in Appendix A. As the level of treatment required will vary both by the quality of the extracted water and the potential use, the economic viability of this resource is expected to vary highly by location.

Applicability of Desalination Treatment Technologies to Various Waters

Global Desalination Capacity

The International Desalination Association's IDA Desalination Yearbook 2011–2012 (International Desalination Association, 2011) indicates the global capacity for desalination grew to 77.4 million m³/day with 71.9 million m³/day of this currently online and 5.5 million m³/day of capacity under construction. Figure 7 illustrates that this capacity represents substantial growth over the last decade, which is anticipated to continue well into the next decade. The information in the figure also reveals that while the capacity of thermal desalination plants continues to grow at a steady pace, membrane-based capacity is expanding at an accelerated pace.

The total global desalination output comes from approximately 16,000 desalination plants, which vary in size from very small systems producing less than 0.365 million m³/year (1000 m³/day) of product water to very large systems producing up to 321.2 million m³/year (0.88 million m³/day) and one contracted to produce up to 374.1 million m³/year (1.025 million m³/day; International Desalination Association, 2011). The bulk of this capacity is for the production of a municipal supply. The bulk of the source water treated is seawater followed by brackish water, as illustrated in Figure 8.

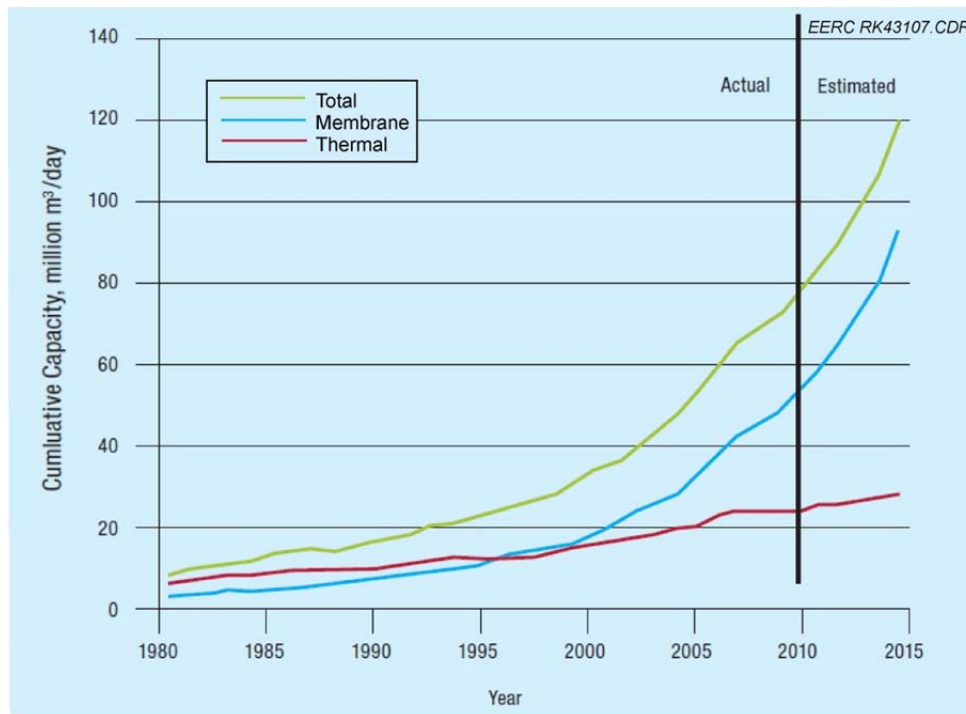
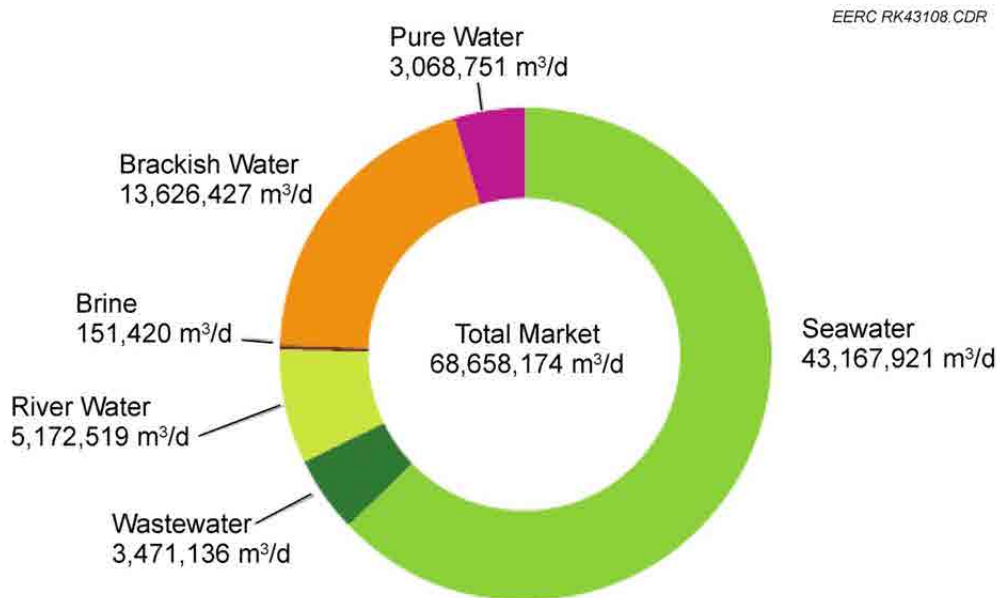


Figure 7. Cumulative worldwide desalination capacity (Birkett, 2011).

The largest capacity seawater desalination system currently running, Shoaiba 3 in Saudi Arabia, is a thermal system using waste heat from a 900-MW power plant to provide heat to a MSF desalination plant. The water is distributed through a pipeline network over 213 miles to deliver water to three major cities containing approximately 5 million people (Fraunhofer, 2011). The price of water from the system is contracted at \$0.77/m³ (GWI, 2005). The largest contracted plant under construction is the Ras Azzour project in Saudi Arabia. This is a hybrid MSF + RO system that will use waste heat from a power plant.

Membrane desalination facilities are 25 times smaller than thermal desalination facilities. The largest currently operating membrane desalination plant is the 127 million m³/year (0.348 million m³/day) seawater reverse osmosis (SWRO) plant in Hadera, Israel, which has been in operation since 2009 and delivers water at a cost of US\$0.57/m³ (IDE Technologies, 2011a). A similar plant in Ashkelon, Israel has been in operation since 2005 and is delivering 115 million m³/year (0.323 million m³/day) at a cost of US\$0.53/m³ (IDE Technologies, 2011b). The largest SWRO plant under construction is the Sorek Desalination Plant in Sorek, Israel, 15 km south of Tel Aviv, which will produce 150 million m³/yr (0.411 million m³/day) when it is finished in 2013 (IDE Technologies, 2011c). The anticipated water cost is ~US\$0.50/m³.

All of the very large desalination plants employ many parallel treatment trains of identical design, so while these very large systems provide a good indication of how large a volume of water can be processed in a single facility, they do not provide a good indication of the size of each treatment unit. Table 3 contains information concerning the largest sizes of individual units for each technology and the typical range of system size.



Source: GWI DesalData

Figure 8. Desalination feedwater source (DesalData.com, 2011).

Table 3. Treatment Capacity Ranges for Popular Desalination Technologies Treating Brackish Water and/or Seawater

	Multistage Flash Distillation (MSF)	Multieffect Distillation/Thermal Vapor Compression (MED/TVC)	Mechanical Vapor Compression (MVC)	Seawater Reverse Osmosis (SWRO)	Brackish Water Reverse Osmosis (BWRO)	Electrodialysis Reversal (EDR)	Nanofiltration (NF)
Feedwater Salinity, ppm	60,000– 70,000, ⁴ 30,000– 100,000 ³	>35,000 ¹	60,000 ² (desalination), much higher for MVC brine concentrator	>32,000 ¹ , 20,000 and above, ⁵ 1000–45,000 ³ (includes brackish), 18,000–45,000+ ⁶	<32,000, ¹ 1000– 20,000, ⁵ 500–3000 (brackish), ⁶ 3500– 18,000 (brackish to saline) ⁶	100–3000 ³	<1000 (desalination), much higher salinities when used for pretreatment
Product Water Salinity, ppm	<10 ^{3,7}	<10 ⁷	3, ⁸ <10 ⁷	<500, ^{1,3} 200–500 ⁷	<200 ¹	<10, ¹ <500 ³	Varies—see ion removal
% Recovery (water yield)	50, 35–45 (seawater) ⁷	40–65, 35–45 (seawater) ⁷	87, ^{2,9} 23–41 seawater, ⁷ as high as 95 for brine concentrator in zero liquid discharge applications	30 to 50, 30–60 ⁵	>80 (varies based on TDS), 60–85, ⁵ 50–90%	>90, ¹ 50–95 ⁷	90+, ⁵ 50–90 ⁷

¹ URS Australia, 2002.

² Stepan and others, 2010.

³ Fritzmann and others, 2007.

⁴ Yun and others, 2006.

⁵ Mickley, 2009.

⁶ WateReuse Association, 2011.

⁷ National Research Council, 2008.

⁸ Lokiec and Ophir, 2007.

⁹ Fountain/Quail Water Management, 2010.

¹⁰ Birkett, 2011.

¹¹ Veil, 2008.

¹² IDE Technologies, 2011a.

¹³ GE, 2009.

Table 3. Treatment Capacity Ranges for Popular Desalination Technologies Treating Brackish Water and/or Seawater (continued)

	Multistage Flash Distillation (MSF)	Multi Effect Distillation/Thermal Vapor Compression (MED/TVC)	Mechanical Vapor Compression (MVC)	Seawater Reverse Osmosis (SWRO)	Brackish Water Reverse Osmosis (BWRO)	Electrodialysis Reversal (EDR)	Nanofiltration (NF)
Electrical Energy Consumption, kWh/m ³	2.5–3, ¹⁰ 3–5 ^{3,7}	1.2–2, ¹⁰ 1.5–2.5 ⁷	8–15 ⁷	2.5–3, ¹⁰ 1.8–2.2 (RO process step only), ⁶ 2.8– 3.1 (total treatment energy) ⁶ – theoretical minimum about 1 kWh/m ³ – best practice 3 kWh/m, ³ 0.4–7, ³ 2.5– 7 ⁷	Lower than RO due to lower pressure, depends on salinity	1, ³ power consumption is directly related to number of ions moved across the membrane, approximately 0.53 kWh/m ³ per 1000 mg/L TDS removed ⁷	
Capital Costs, \$(m ³ /day product water		2.5–3.9 ¹		1.6–2.5 ¹	6–1.8 ¹	0.5–3.25 ¹	
System Capacity (range of plant sizes)	0.88 million m ³ /day	120 m ³ –0.8 million m ³ /day ¹³	16– 366 m ³ /day ^{2,9,11}	0.5–>0.376 million m ³ /day ^{1,4,12}	0.5–>0.376 million m ³ /day ⁴	90–200,000 m ³ /day ¹³	

¹ URS Australia, 2002.

² Stepan and others, 2010.

³ Fritzmann and others, 2007.

⁴ Yun and others, 2006.

⁵ Mickley, 2009.

⁶ WateReuse Association, 2011.

⁷ National Research Council, 2008.

⁸ Lokiec and Ophir, 2007.

⁹ Fountain/Quail Water Management, 2010.

¹⁰ Birkett, 2011.

¹¹ Veil, 2008.

¹² IDE Technologies, 2011a.

¹³ GE, 2009.

Desalination Technology Trends

Treatment of saline extracted waters up to concentrations as high as that in seawater is likely to be economically feasible, especially in areas of significant water demand and low freshwater availability. Globally, the market for desalination has risen dramatically over the past 20 years as the cost of desalination has come down. During this time, the cost of traditional water treatment has risen as has the cost of transporting freshwater long distances.

The primary reasons desalination costs have decreased include:

- Increased use of collocation of thermal desalination plants with power plants in order to use waste heat to drive water evaporation in thermal desalination processes. This has been especially important in the Middle East.
- Economies of scale and/or better optimization of the size of facilities.
- Energy recovery devices on RO systems.
- Improved membranes and membrane modules, in particular, larger membrane module diameters.
- Improved pretreatment options, especially with the increased use of nanofiltration as a pretreatment in RO systems.
- Increased use and optimization of hybrid systems.

Systems incorporating renewable energy as part of the desalination project have also been implemented. These types of projects are particularly popular in Australia (wind power) and Saudi Arabia (solar electric).

The three major high-volume water desalination technologies are RO, MSF, and MED. While several plants exist that use MED alone without employing another integrated desalination technology, effectively all recent MED facilities are hybrid plants that most commonly integrate the use of TVC with MED. Part of the reason these three systems, RO, MSF, and MED/TVC, are the most popular for high-volume applications is that they are all applicable to the use of seawater and higher concentration brackish water as the feedwater (Figure 9). The only other desalination system that has been commonly applied for high-volume applications at reasonable frequency is EDR. Application of EDR at high-production volumes is generally limited to desalination of low-concentration brackish waters. These systems are described in Appendix B.

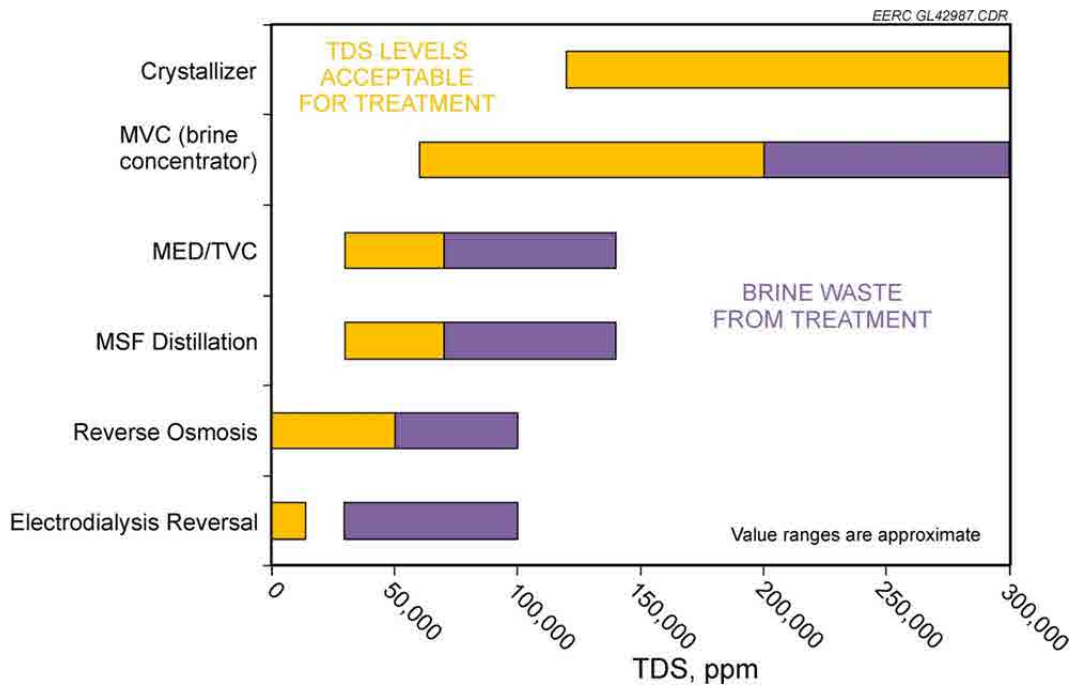


Figure 9. Acceptable water quality ranges for water treatment technologies and resulting ranges of brine reject concentrations (values generalized from Appendix B).

CASE STUDIES

Introduction

To achieve the goal of pairing extracted-water quantity and quality, treatment options, and potential CO₂ storage sites, four “idealized” real-world storage sites were identified and geologically modeled. These relatively simplistic 3-dimensional models were developed to simulate different injection and extraction scenarios and incorporate vital, heterogeneous reservoir properties, including structure, porosity, permeability, water quality, lithology, temperature, and pressure, which were obtained from published sources. When published data were insufficient to capture expected heterogeneity or did not appear in the literature, the properties, along with the ranges of variability, were obtained from the AGD (IEAGHG, 2009).

The AGD was constructed as a statistical data set with details from over 20,000 hydrocarbon reservoirs and saline formations resulting from an extensive literature review of worldwide (although primarily U.S. oil and gas) reservoirs. The data are separated by lithology and depositional environment and contain useful parameters used to populate heterogeneity and supplement property distribution. Exact uses of AGD data varied based on the site, with details presented in each site’s respective section.

Sites were identified and selected to represent currently operating or upcoming commercial-scale CCS projects with a variety of reservoir scenarios, climates, and water use demands. In all, four sites were selected which represent a range of geological, geophysical, and

climatic conditions (Table 4, Figure 10). Sites range in climate from arid (Gorgon) to temperate (Ketzin) with regional water supply ranging from stressed (Teapot Dome) to sufficient (Ketzin). Transportation of treated water ranged from manageable when located near population centers, industry, and agriculture (Ketzin), to challenging for the Gorgon site, with project infrastructure located on an offshore island and wildlife refuge. Transportation issues for Teapot Dome and Zama were in between, with Zama being more remote and isolated and the more challenging of the two. Finally, water quality ranges from nearly fresh at Teapot Dome to concentrated brine (>180,000 ppm) at Zama and Ketzin.

Modeling and Simulation

In order to generate the most accurate models possible, preference was given to sites with extensive previous characterization. Two of the selected sites (Zama and Teapot Dome) are depleted oil and gas reservoirs. The presence of hydrocarbons provides additional challenges both for fluid flow simulation and estimates of water treatment costs. However, the authors have chosen to use these sites as analogs for similar saline formations in lieu of adequately described formations. It is also important to note that, for a variety of reasons, assumptions were made regarding the geology of each case study site, resulting in heterogeneous models that are as much

Table 4. Selected Sites and Prominent Lithology Encountered in Target Storage Reservoirs

Site	Location	Depositional Environment
Ketzin	Central Germany	Fluvial
Gorgon	Offshore Western Australia	Clastic slope
Teapot Dome	Wyoming, western USA	Mixed; nearshore marine, Eolian, Deltaic
Zama	Northern Alberta, Canada	Carbonate reef



Figure 10. Map depicting the location of the selected sites.

inspired by their source material as they are representative of the actual case study sites. As a result, the reservoir data presented represent the data used to generate the results of this study but may not exactly match known or observed reservoir conditions in all cases.

The goal of the modeling and simulation efforts was to assess the applicability and potential uses of brine extraction in a variety of settings. The sites were chosen to reflect worldwide CCS projects with variable climate and water demands. Published and well-characterized CCS sites were preferred, as the technical information and site processes can be better understood and the necessary information exists to produce representative models of the sites. With cost-effective planning, the maximum CO₂ storage and water production were optimized based on the designed CO₂ injection rate of 1 million tonnes (1 megatonne) of CO₂/year.

A literature review of each site was conducted to gather pertinent geologic and reservoir data such as structure tops, well logs, and interpreted depositional environments. Modeling parameters and techniques were also collected and utilized, when available, to replicate previously constructed models. Structural models were populated with lithology, which was then used to model the additional heterogeneous properties throughout the modeled volume using Schlumberger Petrel™ software.

The Generalized Equation-of-State Model Compositional Reservoir Simulator (GEM) by the Computer Modelling Group (CMG, 2011 version) was used for all dynamics modeling and simulations. All scenarios/simulations were run under isothermal conditions with negligible geomechanical behaviours, limited by the maximum cap rock pressure for cap rocks of each respective site.

All of the geologic information and modeling parameters, including residual saturations, relative permeability curves, boundary conditions, and initial reservoir pressure for each site, were derived from published material. If specific data elements were not available from publications, the parameters were referenced from a similar reservoir type within the AGD database.

Evaluation of fluids and flow was limited to formation water, CO₂, and various compositions of CO₂ dissolved in the formation water. The properties of fluids in models for four sites were generated by the Phase Property Program, WinProp, one of the components of the CMG software package. The basic pressures and temperatures used in WinProp were the average values of the specific site. The solubility coefficients were determined and correlated based on the Li-Nghiem Method (Li and Nghiem, 1986). The fluid density and viscosity were correlated by the Rowe-Chou aqueous density correlation (Rowe and Chou, 1970) and Kestin aqueous viscosity correlation (Kestin and Shankland, 1984), respectively, for various pressures and temperatures along with depth of the models.

All of the wells in the models were tied to existing wells whenever possible, including the injection well for the Ketzin site in Germany (Kempka and others, 2010; Martens and others, 2011; Wiese, 2010a), the Zama field in Canada (Burke, 2009), and all proposed injection and production wells in the Gorgon site in Australia (Flett and others, 2008, 2009; CO2CRCTPL,

2008). If additional wells were required for a given scenario, their locations were suggested based on the hydraulic conductivity and geologic structure of the specific site. Well parameters such as radius and skin were also referenced to published data whenever possible. If such data were not available, the typical values of the well radius of 0.108 m and a skin of 0 were used for the simulations.

For CO₂ injection, a commercial-scale injection rate and period were assumed; that is, one million tonnes/year injection rate (2 million tonnes in the Gorgon study site), with a 25-year injection period to meet the maximum CO₂ storage and moderate water extraction period. The postinjection period for monitoring purposes was set at 75 years for a total modeling and simulation period of 100 years. The injection well was controlled by the injection rate and maximum bottomhole pressure (BHP) for all scenarios. If the pressure buildup was less than the maximum BHP constraint, the specified injection rate was utilized. Otherwise, injection rate was reduced to match the maximum BHP constraint. The maximum BHP for the specific site was determined by the static pressure at the depth of the well bottomhole with an extra 10% buffer.

Water extraction was carried out based on the minimum BHP and maximum production rate. The reasonable minimum BHP used for most of the scenarios was 2000 kPa. Water extraction was shut in at each extraction well at the end of the injection period or when CO₂ breakthrough occurred (>1000 m³/day).

Evaluation of Water Management Options

The economic potential of the formation water from each case study site was evaluated with respect to its applicability for beneficial use. Cost estimates are provided for desalination because of a focus on beneficial use of the water. Other water treatment and disposal options were also outlined. The range of water quality represented by the four case studies is representative of a broad range of water quality that is likely to be found in deep saline formations.

Most of the case study sites are located in depleted oil or gas fields and, as such, are likely to contain varying concentrations of hydrocarbons, which may increase overall treatment costs and/or limit the potential for beneficial use. As described earlier, these sites function as analogs for similar and less well-characterized saline formations. Thus the authors acknowledge the presence of hydrocarbon constituents in the extracted water but have chosen to ignore them for the purposes of these calculations.

Regulatory Concerns

While no jurisdiction to date has specific rules for brine disposal directly associated with carbon storage operations, many have rules and regulations in place that deal with brine disposal as it relates to other industrial activities. Given this information, one may be able to discern that brine disposal related to carbon storage is a feasible option for pressure management, and other purposes, in the storage reservoir.

Because of the evolving nature of regulatory frameworks at various levels of government as well as daily changes in legislative reporting, this document is intended to provide general guidance of rules and policies currently in existence and can be considered to be up to date as of November 2011, unless otherwise noted.

CO₂ Surface Dissolution

It has been proposed that CO₂ could be stored by dissolving it in extracted formation water and then injecting the solution into a geologic formation (Eke and others, 2011). This would result in an injected fluid that would be initially denser than the native formation fluid, substantially reducing the risks typically associated with injection of buoyant, free-phase CO₂. Prior to dynamic modeling, the potential effectiveness of this technique was evaluated by calculating the amount of CO₂ that could be dissolved into various waters over a range of temperatures and pressures. The CO₂ dissolution value at formation conditions is then compared to the amount of CO₂ that would occupy the same volume under the same pressure and temperature conditions. An evaluation of the effect of CO₂ interaction with formation minerals is also provided.

Geochemical thermodynamic equilibrium modeling was used to calculate the solubility of CO₂ in various waters over a wide range of temperatures and pressures. This approach calculates the most “stable” thermodynamic state for the system at infinite time conditions. Therefore, the calculated CO₂ dissolution should be considered to be the maximum possible (i.e., the most optimistic scenario).

Previous water analyses were selected (Trupp, 2011; Würdemann and others, 2010; Talman and Perkins, 2009; Milliken, 2007) and utilized as a basis for the calculations (Appendix G). The CO₂ dissolution was calculated over the pressure range of 50 to 300 bar at temperatures ranging from 40° to 140°C at surface and subsurface conditions for each of the case study sites.

Ketzin Case Study

Site Characterization

The Ketzin pilot site, led by the GFZ German Research Centre for Geosciences, is Europe’s longest-operating onshore CO₂ storage site with the aim of increasing the understanding of geologic storage of CO₂ in saline aquifers. Located near Berlin, the Ketzin pilot site has been developed since 2004 and comprises three wells to depths of 750 to 800 m and one shallow observation well, an injection facility, and permanently installed monitoring devices. Since June 30, 2008, CO₂ has been injected into a 630- to 650-m-deep sandstone unit in an anticlinal structure of the Northeast German Basin. After 44 months of injection (February 2012), about 59,000 tonnes of CO₂ has been stored without any safety issues.

An extensive monitoring program integrates geological, geophysical, and geochemical investigations for a comprehensive characterization of the reservoir and the CO₂ migration at various scales. The Ketzin project demonstrates safe CO₂ storage in a saline aquifer on a research

scale (Schilling and others, 2009; Würdemann and others, 2010; Martens and others, 2011). The Ketzin pilot site is a research and development project and limited by legal regulations to a maximum amount of stored CO₂ of <100,000 tonnes. Thus the presented Ketzin simulation results within this report are a theoretical case study not reflecting the real site conditions, e.g., with respect to the injection operation.

Ketzin lies on top of the Ketzin–Roskow Anticline, a double plunging structure trending northeast–southwest, approximately 12 × 43 km in size, with a maximum vertical closure of approximately 1000 m. The reservoir unit for the site is the Stuttgart Formation, which consists of a series of fluvial channels surrounded by low-reservoir-quality floodplain deposits. The site is relatively shallow, with the reservoir unit being approximately 650 m deep. Several separate modeling efforts have been produced over the course of the project that served as templates, parameters, and data sources for model production (Forster and others, 2006; Frykman and others, 2006; Kopp and others, 2006; Kempka and others, 2010). The city of Ketzin is located along the Havel River; therefore, it is expected that local demand for water is extremely low. At the same time, the reservoir contains the lowest-quality water of the four examined sites, severely limiting potential beneficial use.

Modeling

Wells, well logs, and Stuttgart Formation structure maps were incorporated for the injector and monitoring wells according to data presented in Norden and others (2010), including interpreted facies logs (Figure 11). The full structure was modeled, contrary to previous studies, as the smaller models were not adequate for accurately modeling a commercial-sized (~1 million tonnes/year for 25 years) injection without experiencing model edge effects (Appendix C).

Model workflow continued by populating channels according to inputs defined in Forster and others (2006) who collected fluvial analog data for the production of Ketzin geologic modeling. Object modeling processes, which distribute channel-shaped objects according to input parameters, were performed to define the channel facies throughout the defined unit. In addition to previous modeling parameters, dolomite lenses of small extent were also incorporated throughout the model as observed in petrophysical well logs in all three wells. It is understood that data availability is extremely scarce, and it is unlikely that channel parameters are definable, let alone understandable, across the entire structure through this simplistic operation, but these constraints do not limit this model in its representation of the Ketzin site (Figures 12 and 13).

Assigned facies were populated with reservoir properties according to values presented in Forster and others (2006) and Norden and others (2010), following geostatistical ranges from the AGD, as shown in Table 5. Fluid properties were populated according to default variograms with values from Würdemann and others (2010).

Several publications address the status of the Ketzin CO₂ storage and modeling activities (Schilling and others, 2009; Würdemann and others, 2010; Wiese and other, 2010a, b; Martens

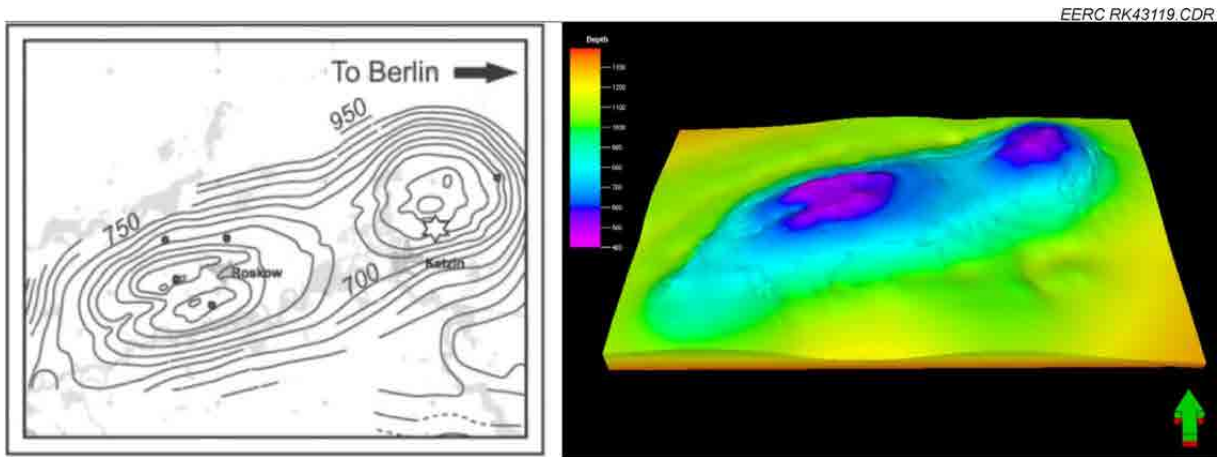


Figure 11. Stuttgart formation structural map (left) and modeled surface produced from the data (right). Topographic map is from Norden and others (2010).

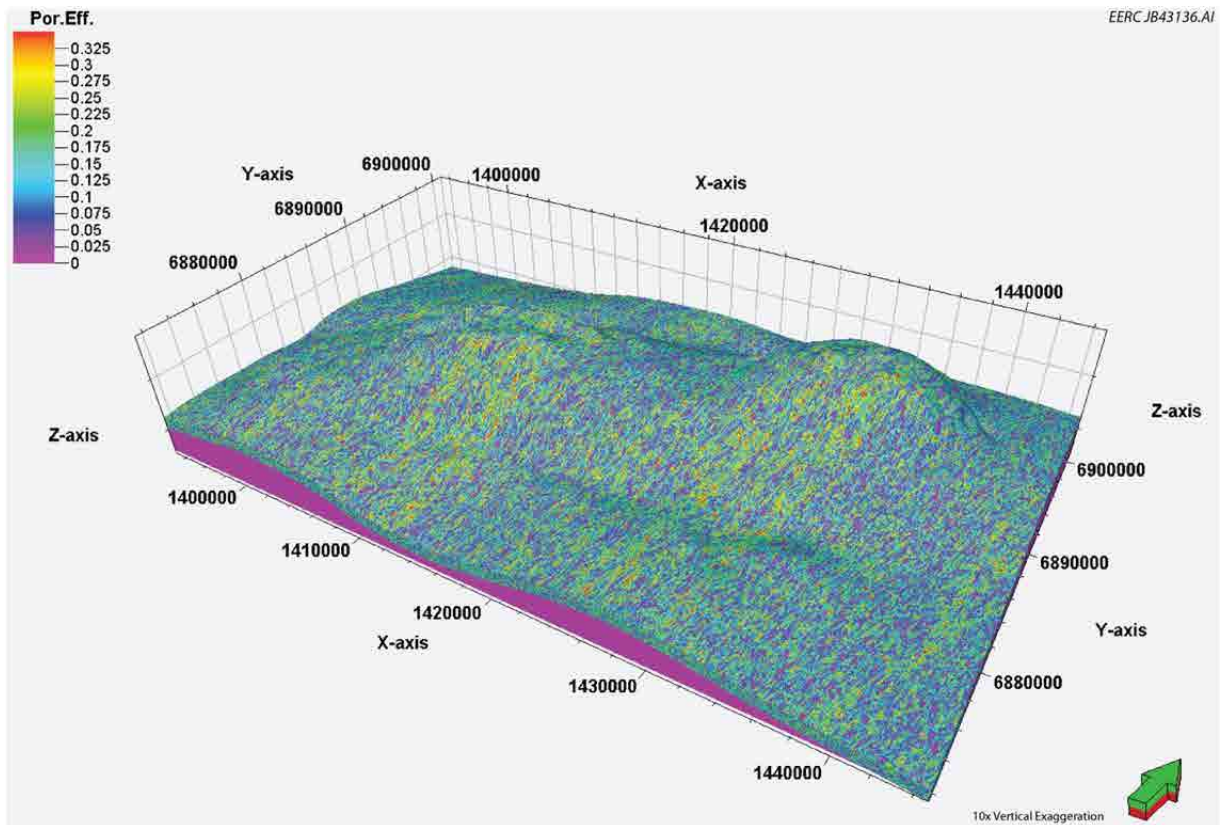


Figure 12. Three-dimensional view of the Ketzin model showing the porosity attribute. Cap rock units have been removed to show model structure, and a 10× vertical exaggeration has been applied.

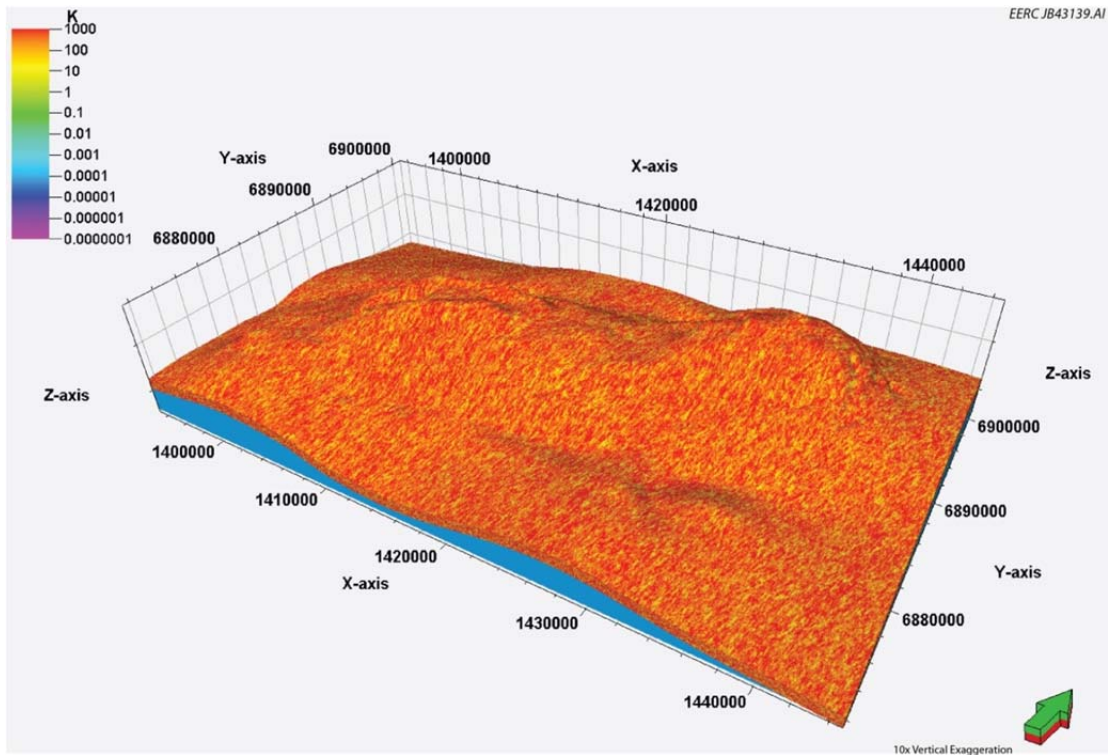


Figure 13. Three-dimensional view of the Ketzin model showing the permeability attribute. Cap rock units have been removed to show model structure, and a 10× vertical exaggeration has been applied.

Table 5. Ketzin Model Parameters

Property	Value	Source
Total Porosity	0.07%–0.51%, avg: 0.24%	Norden and others, 2010
Effective Porosity	0.00%–0.50%, avg: 0.12%	Norden and others, 2010
Permeability	0.03–3400 mD, avg: 232 mD	Norden and others, 2010
Thickness	80 m	Würdemann and others, 2010
Depth	~650 m	Würdemann and others, 2010
Pressure (average)*	9623.7 kPa	Würdemann and others, 2010
Temperature (average)	38°C	Prevedel and others, 2008
CO ₂ Density	643.91 kg/m ³	MIT, 2011
Variogram Range (long)	398	IEAGHG, 2009
Variogram Range (short)	108	IEAGHG, 2009
TDS	228.8–236.5 g/L	Würdemann and others, 2010**
Channel Orientation	15°–20°	Forster and others, 2006
Sinuosity Amplitude	100–250 m	Forster and others, 2006
Wavelength	5000–9000 m	Forster and others, 2006
Belt Width	100–1600 m	Forster and others, 2006
Channel Thickness	1–8 m	Forster and others, 2006

* Modeled reservoir pressure ranges from 4646 to 13,460 kPa.

** Water chemistry is the variation in four time-lapse samples, not absolute range.

and others, 2011). Most of the properties and parameters for the modeling and simulations and initial reservoir pressure were based on publications of the Ketzin project by the GFZ German Research Center and associated research projects (Lengler and others, 2010; Henniges and others, 2011; Fleury and others, 2010; Kempka and others, 2010; Wiese and others, 2010a,b; Würdemann and others, 2010; Martens and others, 2011). The well design parameters were cited based on the works of Prevedel and others (2009) and Wiese and others (2010). The location of injection well Ktzi-201 was located based on the work of Norden and others (2008). Water chemistry data were obtained from a report on water samples (Würdemann and others, 2010).

The model dimension used in this study was 29,317×51,370×915 m which extended the model from 5000 × 5000 × 400 m reported by Kempka and others (2010). The extended model tried to fit the commercial-scale potential of CO₂ storage around the structural dome in the top right of Figure 11. Detailed properties and parameters are listed in Table 5.

Case Study Simulation Results

A total of sixteen cases were simulated for the Ketzin site to analyze different scenarios of injection and water extraction in order to assess differences in storage capacity and efficiency, as well as to define potential volumes of produced water for treatment or disposal. An injection program was selected that maximized injectivity and ultimately storage capacity aimed to inject 2 megatonnes per year for a period of 25 years per single vertical injection well. Detailed results for the Ketzin simulation scenarios can be found in Appendix C.

The initial three cases examined Ketzin test site performance with one vertical injection well, under closed, semiclosed, and open boundary conditions, Cases 1, 2, and 3, respectively, with no water extraction. Case 1 was considered the most conservative case, storing approximately 4 million tonnes of CO₂. Case 3 was considered the most optimistic case, storing approximately 18 million tonnes of CO₂ over the 25-year injection period. These cases bound the realistic storage potential, given the modeling assumptions made for this study, and it was determined that a semiclosed system (Case 2) would be the best scenario to use as the base case. These boundary conditions were applied using super volume cells at the modeled edges containing identical attributes. The simulation resulted in 13 megatonnes of total storage capacity (Table 6). An additional simulation was conducted utilizing a second injection well (Case 6), which resulted in a total injected volume of over 32 megatonnes. This increase over the single injection well case was due to the presence of increased injectivity at the second well location and emphasizes the importance of well site selection in injection design.

The addition of a single vertical extraction well coupled with a single vertical injection well increased storage capacity to 25.7 and 27.4 megatonnes (Cases 4 and 5), approximately doubling the potential Case 2 capacity and demonstrating an approximately 1:1 ratio between water extraction and CO₂ injection. However, this gain was not as great as the storage capacity improvement achieved by utilizing the second well as a CO₂ injector (Case 6). This is likely a result of the strong structural control and local heterogeneity adversely affecting plume mobility and reducing the efficiency of water extraction. Furthermore, injectivity appears to be higher at the location of the second injection well resulting in even higher storage gains.

Table 6. Case Scenarios and Resulting Storage Capacities for the Ketzin Site

Scenario	Well Configuration	Gas Injection Rate/Well, kg/day	Water Production Rate/Well, m ³ /day	Boundary Conditions	Storage Capacity, megatonnes
Case 1	1 injector	451,000	NA*	Closed	4.12
Case 2 (base case)	1 injector	1,430,000	NA	Semiclosed	13.0
Case 3	1 injector	1,980,000	NA	Open	18.1
Case 4	1 injector 1 extractor	2,810,000	12,752	Semiclosed	25.7
Case 5	1 injector 1 extractor	3,000,000	13,580	Open	27.4
Case 6	2 injectors	3,550,000	NA	Semiclosed	32.4
Case 7 (surface dissolution)	1 injector 1 extractor	NA	3060	Semiclosed	0.43
Case 8 (surface dissolution)	1 injector 1 extractor	NA	3,090	Semiclosed	0.55
Case 9 (surface dissolution)	4 injectors 5 extractors	NA	25,500	Semiclosed	2.61
Case 10 (surface dissolution)	4 injectors 5 extractors	NA	26,500	Semiclosed	2.88
Case 11	4 injectors	6,954,760	NA	Semiclosed	63.3
Case 12	4 injectors 4 extractors	7,170,000	12,700	Semiclosed	65.4
Case 13	8 injectors	9,500,000	NA	Semiclosed	86.7
Case 14	12 injectors	14,500,000	NA	Semiclosed	132.0
Case 15	12 injectors 13 extractors	24,877,000	65,753	Semiclosed	226.7
Case 16	25 injectors	20,100,000	NA	Semiclosed	183.8

* Not applicable.

Reservoir pressure reductions of approximately 10% were observed in the central area of the injection plume as a result of water extraction in Case 4 (Figure 14). Along with a pressure reduction, the plume area increased by 32% as CO₂ was drawn south toward the downdip extraction well (Figure 15). Similar results of structurally dominated migration were observed in Case 5, where open model boundary conditions allowed for a greater injection rate.

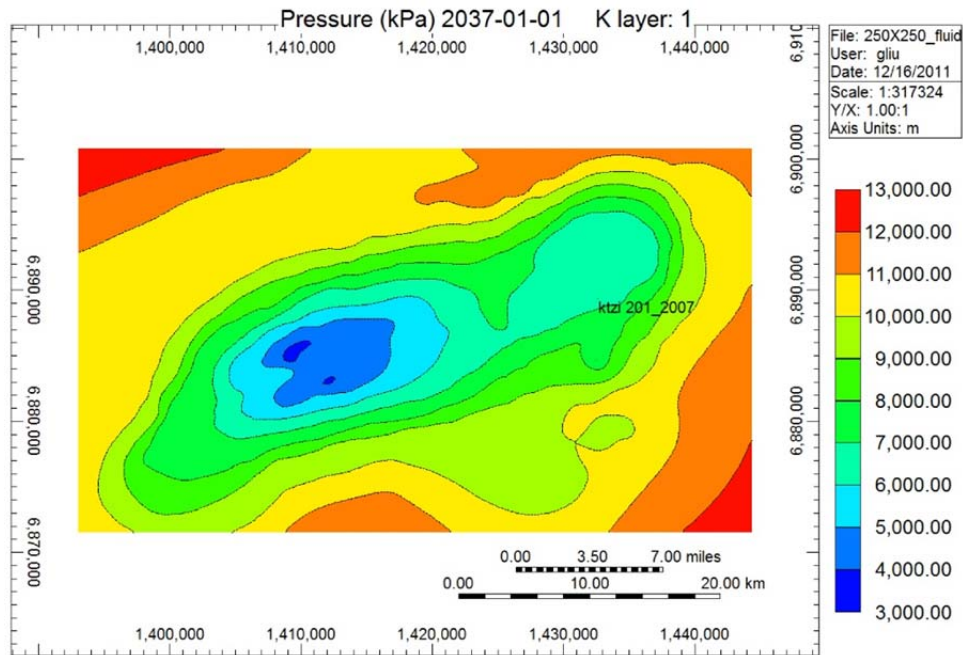
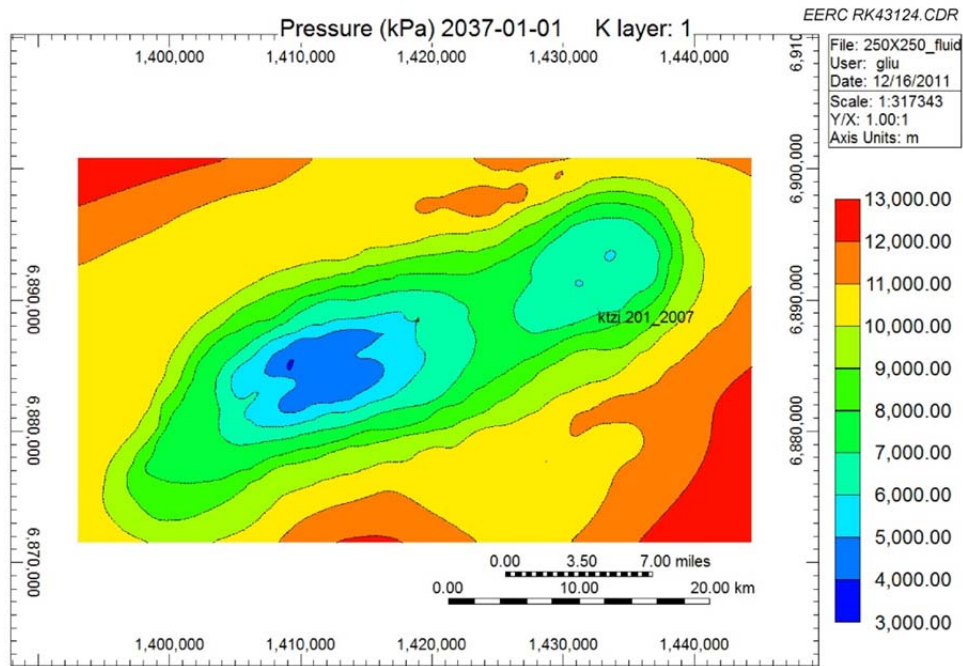


Figure 14. Pressure map of Ketzin models after 25 years of injection for Cases 2 (top) and 4 (bottom). A reduction in pressure is observed in Case 4.

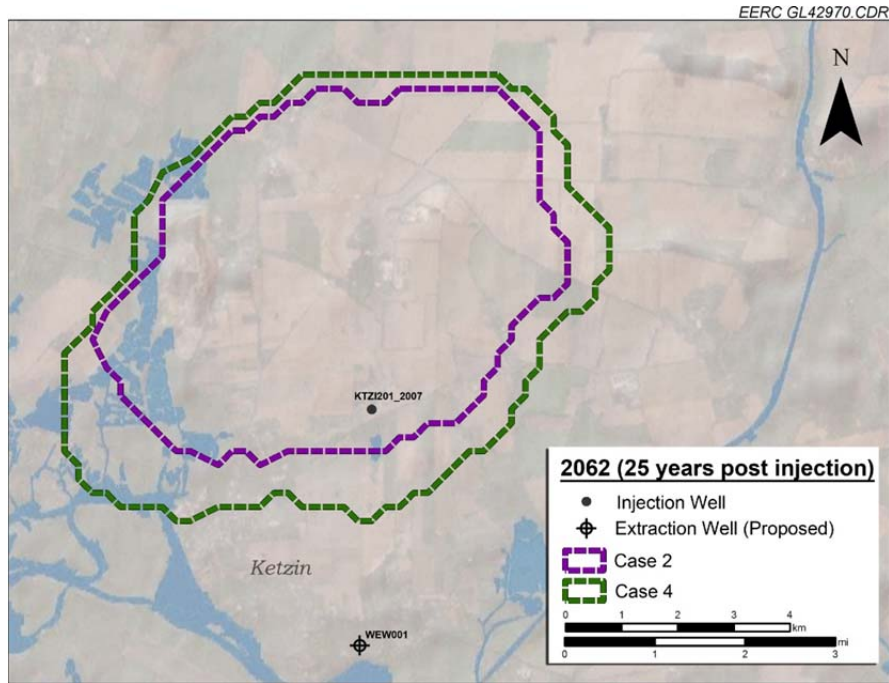


Figure 15. Outline of plume extent after 25 years of injection for Cases 2 and 4. The strong influence of geologic structure on CO₂ mobility results in limited influence of water extraction on the plume.

A second series of simulations was conducted to understand the point at which water extraction becomes more beneficial than simply increasing the number of supercritical CO₂ injection wells. This was done by simulating progressively larger numbers of injection wells and corresponding extraction well pairs (Appendix C). The resulting series of injections is reported in Cases 11–16. In Case 11, four vertical injection wells inject with no corresponding extraction, and result in the storage of 63.3 million tons of CO₂ over the life of the injection. The addition of more vertical injection wells with no extraction wells, represents a 95% increase in storage from Case 6 with two vertical injection wells, indicating that injection volumes are limited in this case by near wellbore effects rather than pressure interference between different injectors. When these same four injection wells are paired with four extraction wells (Case 12), the total storage increases only a few percent above Case 11 to 65.4 million tons of CO₂. This low amount of storage gain is likely due to the strong effects of heterogeneity and poor connectivity between injector and producer pairs. Careful pairing of injector and extraction well pairs could likely increase the storage gains, however in this storage scenario it is unlikely that pairing four injection wells with four extraction wells could increase the storage volumes more than simply turning all eight wells into injection wells. In Case 13, eight vertical injection wells, with no corresponding extraction wells, inject a total of 86.7 million tons of CO₂, or a 36% increase in storage capacity over Case 11 and a 32% increase over Case 12. This reduced effectiveness of adding injection wells appears to finally be from pressure interference between injectors and some loss of injectivity due to the utilization of less ideal reservoir locations, however the use of vertical injection wells, with no extraction wells, still is a better option for increasing storage capacity than injection/extraction well pairs (Case 12). In Case 14, twelve vertical injection wells

are utilized and result in the storage of 132 million tons of CO₂, representing an increase of 52% over Case 13 with eight injection wells. The good scale up in storage volumes from Case 13 to 14 is likely due to the increased spacing between injectors and the actual locations of the injection wells with respect to reservoir quality. With the addition of thirteen extraction wells, with twelve injection wells (Case 15), storage capacity is increased to 226.7 million tons of CO₂ or 71%. In Case 16, where all 25 wells are converted to injectors, 183.8 million tons of CO₂ are stored or a 39% increase over Case 14. Cases 15 and 16 illustrate how the use of extraction wells with injection wells can out performs all-wells-as-injectors. The effects of pressure interference between injectors is mitigated in this case by water extraction and results in a large increase in storage capacity.

As might be expected, the total storage capacity continues to increase more as the number of injection wells are increased, as opposed to adding injection/extraction well pairs (Figure 16). However, this trend is reversed by the last two cases, Cases 15 and 16, which utilize 12 injectors with 13 extractors and 25 injectors respectively. Here it is clearly seen that the combination of injection and extraction wells outperforms the all-wells-as-injectors case, where an additional 43 million tonnes, or 23%, is stored. It is likely that in this scenario, with this well spacing, the injection well pressure interference starts to dominate, and the use of extraction wells helps reduce the overall reservoir pressure, as well as, the interference between injectors. It is also important to note that the volume of water removed is much less than the injected volume of CO₂ for Cases 12 and 15. At these larger volumes, the 1:1 ratio no longer holds up. Although the additional cost of permitting and drilling 25 wells over two wells is likely to be prohibitive for the storage gained at the hypothetical Ketzin injection site, this test does demonstrate that water extraction may be used to substantially increase the CO₂ storage capacity available in a reservoir and may be necessary in a situation where the volume of CO₂ requiring storage exceeds the capacity of available reservoirs.

Surface Dissolution

The extraction, surface saturation with CO₂, and reinjection of reservoir fluids were also examined through hypothetical simulations at the Ketzin site (Cases 7 and 8). Because of the high salinity of the brine, large quantities of water were required, and even in the most vigorous situations, only 0.5 megatonnes was able to be injected through one injection well and one producing well scenario. To obtain an idea of the number of wells needed to achieve one million tonnes of CO₂ a year storage through surface dissolution, additional well patterns of injection and extraction well were analyzed. This consisted of a nine-well pattern (four injectors and five water extractors) and spaced at 5-km intervals. These patterns were compared by running just the injection wells, running the injection and extraction wells, and conducting injection through all the wells in the pattern. The increased number of wells generally resulted in increased dissolved CO₂ storage capacity, with the largest increase up to 2.9 million tonnes. This appears to be the upper limit for the simulated conditions, as additional wells do not show increased capacity.

Based on a single well pair and the nine-well pattern, storage volumes of 1 million tonnes a year would require 80–90 wells, half injectors and half extractor wells, spread across the entire geologic reservoir. This substantial increase in the number of wells makes the prospect of surface dissolution at the Ketzin site cost-prohibitive given the very limited quantity of CO₂ storage.

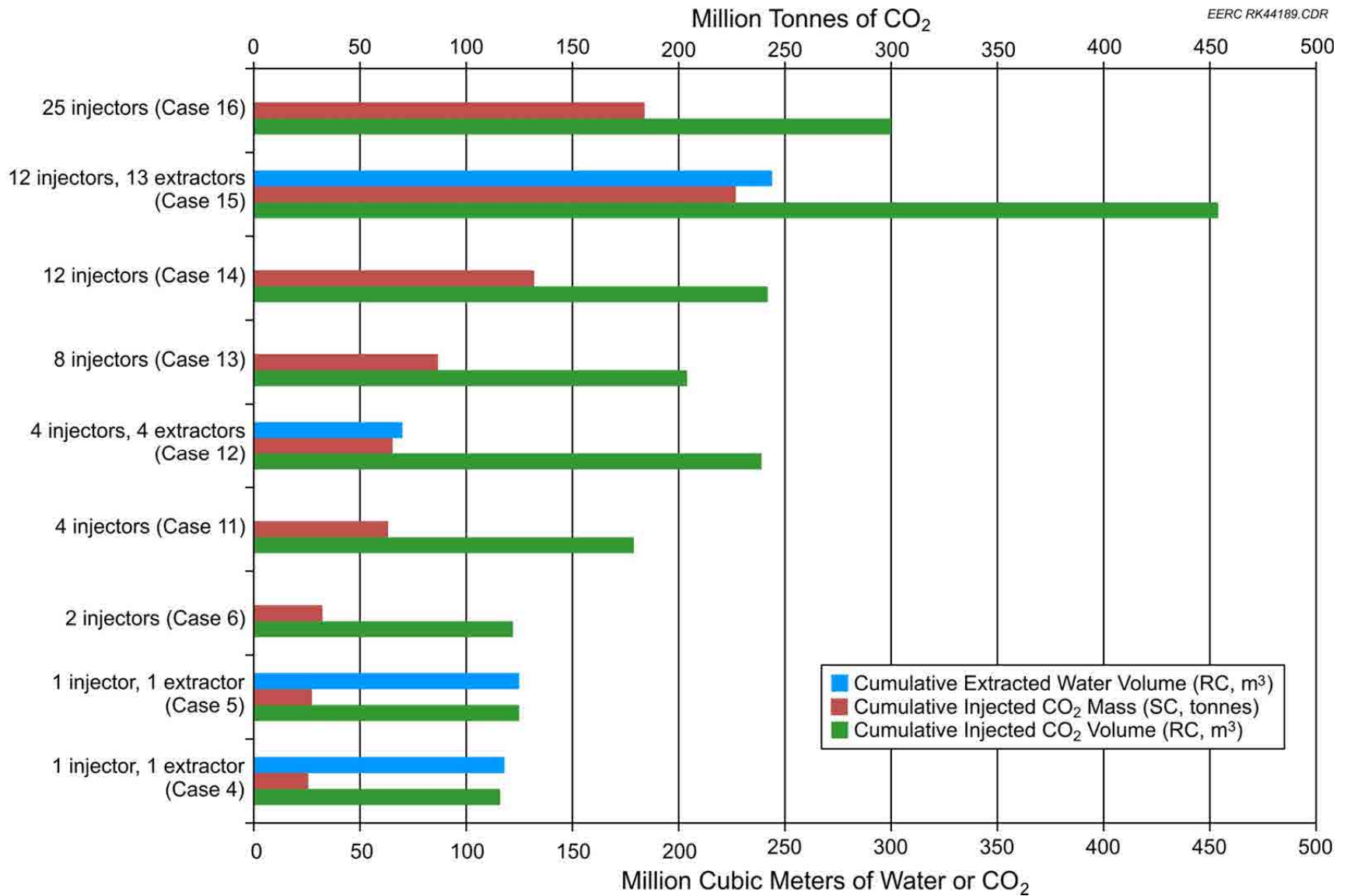


Figure 16. Comparison of CO₂ injection volumes utilizing multiple combinations of injection and extraction wells.

Because of the structure, geologic heterogeneity, and depositional environment at Ketzin, it was difficult to obtain good connectivity between injector and extractor pairs, resulting in poor improvements in plume control and storage capacity. This was evident by the highest storage capacity being obtained from two injectors rather than any scenario with an injector and extractor. Surface dissolution is not viewed as a viable option in the Ketzin case because of extremely high salinities, resulting in very low storage capacities, and local heterogeneities, resulting in poor communication between injection and extraction wells.

Evaluation of Water Management Options (with desalination cost estimates)

Water quality information from Ketzin is provided in Table 7. This high-salinity water is not favorable for use as source water for beneficial use. The options that have been identified for handling this water include:

1. Reinjection of the extracted water into a geologic formation.
2. Treatment with a zero liquid discharge (ZLD) method that results in a dry salt for disposal or beneficial use.

Scenario 1 is considered to be the most likely disposition for extracted water at Ketzin.

Scenario 2 was evaluated using capital cost and energy use estimates for crystallizer as provided in Mickley (2006). The flow rate of water extraction used for this estimate was 12,400 m³/day (3.38 MGD). This is the approximate extracted water flow rate found for Case 4 and 5 simulations when corrected to a CO₂ injection rate of 1 million tonne/year. The water treatment cost based on the volume of extracted water treated was estimated to be US\$8.02/m³. The water supply cost based on the volume of purified water produced was US\$8.92/m³, assuming a 90% yield of purified water. The total capital cost was estimated to be US\$135 million. Energy use rate was estimated to be 33.8 MW. The calculations used an electricity cost of US\$0.10/kWh. More details on the calculations are given in Table 8.

It is highly unlikely that this high price for treatment and/or purification of water would be accepted or viable; therefore, deep-well injection is the most likely management strategy for this extracted water. As the Stuttgart Formation is regionally extensive and generally underpressured, it is the most likely disposal target for the site.

Regulatory Concerns

In 2009, the European Parliament and the Council issued Directive 2009/31/EC stating that all member states must develop CCS regulations by June 2011. The Directive stipulates that CO₂ streams may only be injected into the ground once risk assessments have been completed and exploration and storage permits have been secured. The Directive also provides member states with guidance as to the operation and monitoring of CO₂ storage facilities (Energy in Germany, 2011).

Table 7. Water Quality Values for Ketzin

	Ketzin			
pH (surface, 25°C, 1 atm):	6.7	6.5	6.5	6.4
pH (in reservoir):	5.4	–	–	–
Element	mg/L	mg/L	mg/L	mg/L
Na	87,400	90,400	88,400	90,400
Ba	–	–	–	–
K	412	297	294	282
Ca	2092	2059	2133	2090
Mg	814	835	852	842
Mn	1	1	1	1
Fe	7	7	6	6
Li	2	2	2	2
NH ₄	18	19	19	19
Sr	–	–	–	–
Si	–	–	–	–
Mn	–	–	–	–
Cl	134,000	139,000	136,000	139,000
Br	42	45	47	45
SO ₄	4	4	4	4
HCO ₃	88	57	56	59
CO ₃	–	–	–	–
H ₂ SiO ₃	12	10	9	9
HBO ₂	36	36	36	36
H ₂ S	–	–	–	–
TDS (sum of elements)	224,928	232,772	227,859	232,795
TDS (listed)	228,800	236,400	231,500	236,500
TDS (formation)	230,263	–	–	–
TDS (surface, 25°C, 1 atm)	228,440	236,400	231,500	236,500
Mineral Precipitation	–	–	–	–
Calcite/Strontianate/Dolomite	1200	–	–	–
CaCl ₂	200	–	–	–
Surface Dissolution	–	–	–	–
CO ₂ dissolution (mol/L)	0.45	–	–	–
CO ₂ dissolution (g/L)	40	–	–	–
TDS increase from	228,440	–	–	–
to	241,814	–	–	–
pH from CO ₂ Dissolution from	6.7	–	–	–
to	3.3	–	–	–
Mineral Precipitation	–	–	–	–
Sulfate (anhydrite/gypsum)	500	–	–	–

Table 8. Brine Crystallization Cost Analysis for Ketzin

Cost and Energy Curves from Mickley (2006) in US\$	Ketzin
	Crystallizer
	Ketzin
Flow Rate (MGD)	3.28
Reject Level of Unit	NA
Concentrator Reject/Feed to Crystallizer (MGD) ¹	3.28
Feed to Crystallizer or Waste Brine Flow Rate (gpm) ¹	2240.4
Capital Cost of Installed Concentrator (\$)	–
Capital Cost of Installed Crystallizer (\$)	3.00E+06
Energy Usage for Concentrator (kW)	–
Energy Usage for Crystallizer (kW)	750
Cost of Electricity (\$/kWh)	0.1
Annualized Capital Cost of Concentrator, \$/yr	–
Annualized Capital Cost of Crystallizer, \$/yr	150,000
Annual Energy Cost of Concentrator, \$/yr	–
Annual Energy Cost of Crystallizer, \$/yr	657,000
Total Annual Cost for One Unit (\$)	807,000
Number of Crystallizer Units	45
Number of Concentrator Units	–
Brine Input, m ³ /day	12,400
Cost/m ³ of Water Treated	\$8.02
Product Water Flow Rate, m ³ /day (90% yield)	11,160
Cost/m ³ of Purified Water Produced	\$8.92
Total Capital Cost, \$	1.35E+08
Total Energy Use Rate, MW	33.8

¹U.S. unit required for cost curves.

In accordance with CCS Directive Article 18, liability for damage to the environment should be regulated by Environmental Liability Directive 2004/35/EC regarding the prevention and mitigation of environmental damage. Liability for climate damage that results from leakages will be regulated by Emissions Trading Directive 2003/87/EC, which covers storage sites and mandates that emission trading allowances be surrendered for any leaked emissions. All other liabilities will be handled at the national level. The Directive mandates that the operator of a storage facility maintains responsibility for the site until it is handed over to a member state's competent authority (Energy in Germany, 2011).

The fact that, to date, no specific legal regime for CCS exists in Germany does not mean that the area is not regulated. For example, the mining authority of the state of Brandenburg, Landersamt für Bergbau, Geologic und Ruhstoffe Brandenburg, granted a mining permit to operate at Ketzin to Verbundnetz Gas AG (VNG AG) (Forster and others, 2006).

The applicable legal regime for CO₂ storage currently depends on how and where the CO₂ is to be stored. National and local water law applies to the extent aquifers are affected. Mining law may apply where CO₂ storage takes place in the context of oil and gas production or use of brine caverns. However, German mining law was not drafted with CO₂ storage in mind, as CO₂ injection into the earth is not a traditional mining activity. Therefore, the application of the mining law regime to CCS provides some challenges. For lack of a better legal basis, exploratory work for potential CCS storage in salt caverns in the state of Brandenburg currently relies on the mining law regime for brine exploration (Energy in Germany, 2011).

During the sixteenth legislative period of the German Parliament (2005–2009), a bill on CCS regulation was drafted in response to the EU Directive and introduced in April 2009. The draft was not enacted into law and, therefore, lapsed at the end of the legislative session. The German legislative bodies have yet to reach a compromise on various CCS bills introduced.

Ketzin Summary

The Ketzin pilot-scale injection site served as an excellent test bed for hypothetical large-scale CO₂ injection and formation water extraction scenarios. The site is well characterized because of the extensive work conducted for the pilot project. The site presents a large structural trap ideal for CO₂ storage. Simulations showed the opportunity to double storage potential by utilizing formation water extraction, although even greater gains could be achieved by simply using additional wells for CO₂ injection. This was the case until the number of wells was increased to 25, where in this scenario, the use of injection/extraction well pairs finally outperformed all-wells-as-injectors cases. This indicates that even in very good storage reservoirs, such as those at the Ketzin Site, the use of injection/extraction well pairs can increase the storage capacity and reduce overall plume size in cases where extremely large volumes of CO₂ need to be stored, especially if good connectivity can be achieved between injection and extraction pairs.

The formation water quality is of the lowest of the investigated sites, averaging in excess of 200,000 ppm TDS. This limited the possibilities of both surface dissolution of CO₂ prior to injection and beneficial use of extracted formation water. Both practices were found to be cost-prohibitive at this site.

It has been shown over the last few years that CCS faces obstacles in Germany. However, regulatory frameworks are in place that have allowed for demonstration projects to transpire and brine injection to occur as part of other industrial activities.

Zama Case Study

Site Characterization

The Zama Keg River F oil pool is one of several oil pools discovered in the Zama oil field in northwestern Alberta, Canada. It has been the site of acid gas (approximately 70% CO₂ + 30% H₂S) injection for the simultaneous purpose of EOR, H₂S disposal, and CO₂ storage. The Zama Keg River F oil pool is one of over 700 hydrocarbon-bearing geologic structures in the Zama subbasin located in northwestern Alberta, Canada. These geological structures, known as pinnacle reefs, produce oil from the Middle Devonian Keg River Formation at an average depth of 1500 m below ground surface. A generalized stratigraphic section of the Zama subbasin is shown in Appendix D.

The Zama subbasin has over 700 pinnacles of an average areal extent of 0.16 km² (0.06 mi²) at the base and roughly 122 m (400 ft) high (Burke, 2009). The reefs typically consist of variably dolomitized carbonate and are surrounded and overlain by very tight anhydrite Muskeg Formation that acts as a cap rock, effectively forming a closed system. A large variation in both porosity and permeability is observed in the heterogeneous pinnacles with a decrease in both properties towards the reef tops (Figures 17 and 18). The principal rock types include various carbonate lithologies, including wackestone, packstone, floatstone, and rudstone with varying degrees of alteration due to secondary leaching and dolomitization. Porosity type varies from intercrystalline to microfracture (Burke, 2009).

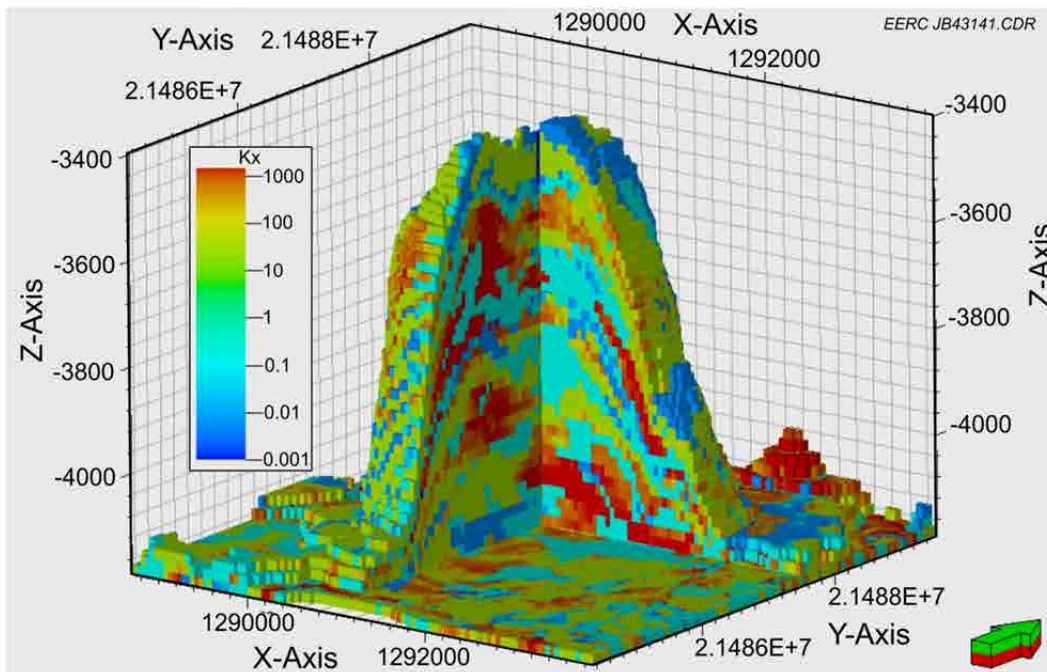


Figure 17. Three-dimensional view of the Zama model showing the permeability attribute. Cap rock units have been removed to show model structure, and a 5× vertical exaggeration has been applied. A cutaway view is shown to better illustrate internal reef heterogeneity.

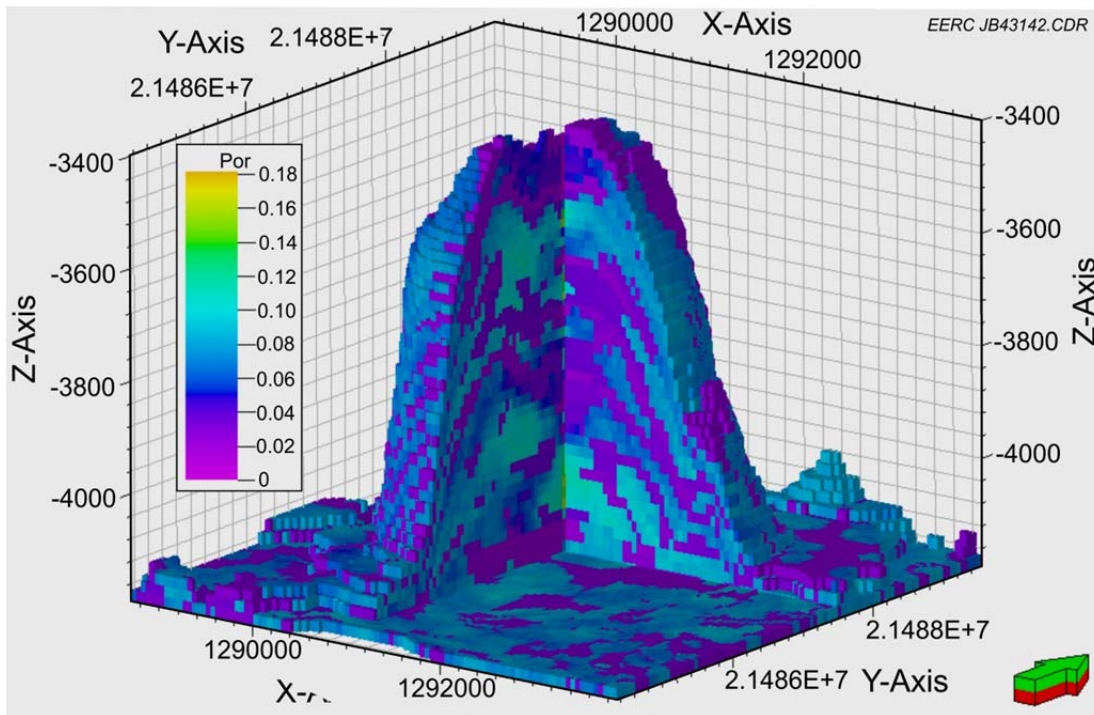


Figure 18. Three-dimensional view of the Zama model showing the porosity attribute. Cap rock units have been removed to show model structure, and a 5× vertical exaggeration has been applied. A cutaway view is shown to better illustrate internal reef heterogeneity.

Water use and integration at the Zama site are challenging because of the remoteness of the site, the presence of local water resources, and low reservoir water quality. Possible consumers of extracted water are the oil and gas operators in the region.

Modeling

Core-calibrated multiminereral petrophysics were performed on well logs, and borehole image logs were used to more accurately identify the different facies and determine each facies’ properties along the wellbores. Seismic attribute data interpretations were used to identify the reef versus nonreef facies to aid in the distribution of the facies in the reservoir (Table 9). These properties were then spatially distributed throughout the reservoir using a combination of multiple-point statistics and object modeling workflows to produce equiprobable reef facies, structure, and volumetric realizations.

Case Study Simulation Results

Seven different cases of simultaneous acid gas injection and formation water extraction (Table 10) along with a base case (Case 1, gas injection only) were tested in predictive simulation runs at Zama. These cases include acid gas injection through an injector well placed in a selected high-permeability oil-producing zone situated in the top portion of the structure

Table 9. Reservoir Properties for the Zama F Pool Pinnacle Reef

Property	Value	Source
Effective Porosity	0.03%–17%	Log-derived
Permeability	0.001 to 2127 mD	Log-derived
Thickness	240 m	Burke, 2009
Depth (structure top)	1427 m	Burke, 2009
Temperature	71.1°C	Operator communication
Pressure	14,450 kPa	Operator communication
CO ₂ Density	653.43 kg/m ³	MIT, 2011
TDS	180,000 ppm	Operator communication

Table 10. Cases Tested in Predictive Simulations for Zama

Case	Well Configuration	Gas Injection Rate/Well, kg/day	Water		Boundary Conditions	Storage Capacity, megatonnes
			Injection Rate/Well, m ³ /day	Production Rate/Well, m ³ /day		
Case 1	One injector	310,680	NA		Closed	0.05
Case 2	One injector	310,680	516		Closed	0.47
Case 3	One injector One extractor	310,680	516		Closed	0.62
Case 4	One injector One extractor	310,680	429		Closed	0.68
Case 5	One injector One extractor	310,680	397		Closed	0.69
Case 6	One injector One extractor	621,359	1144		Closed	0.49
Case 7	One injector Two extractors	621,359	572		Closed	0.60

(Figure 19). Two different gas injection rates of 310,680 and 621,359 kg/day were tested. These rates are equivalent to 0.113 and 0.227 megatonnes a year, respectively. Formation water was extracted by placing water injection wells at selected locations in available high-permeability streaks in the bottom portion of the reef structure (Figure 19). In view of significantly high formation water salinity, solubility of acid gas in water was neglected while running predictive simulations (Appendix D).

In the base case, acid gas was injected without the extraction of formation water. Simulation results indicate that a total of 50,000 tonnes (0.05 megatonnes) of acid gas could be injected before reservoir pressure would reach the maximum allowable pressure limit of 22,753 kPa. Use of an extraction well in Cases 2–6 resulted in a total storage capacity ranging from 0.47 megatonnes to 0.69 megatonnes. In Case 2, gas breakthrough occurred after 3 years

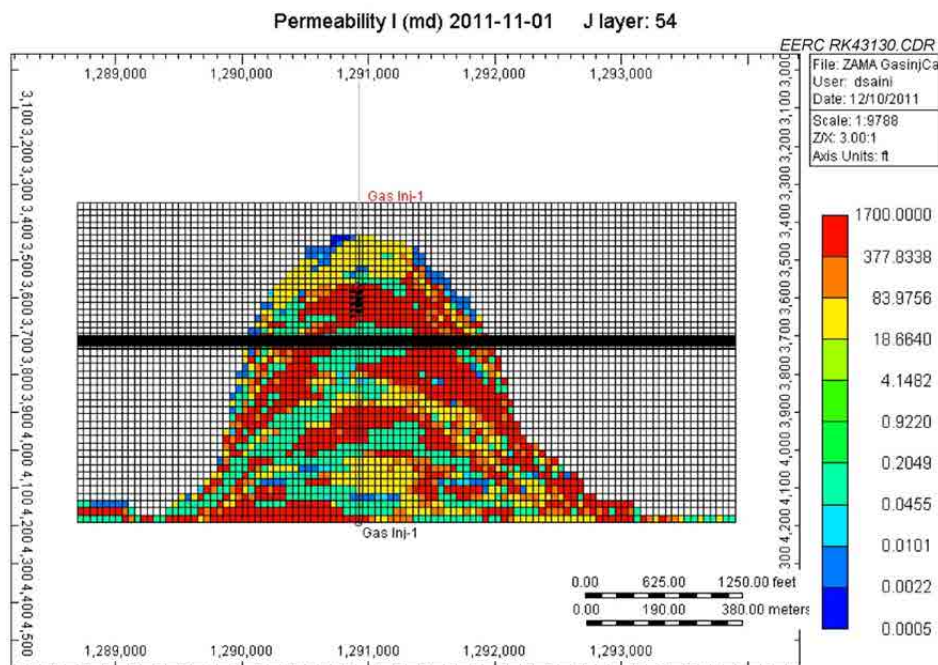


Figure 19. Placement of acid gas injection well (named Gas Inj-1) in predictive simulations.

and 5 months of water extraction. In this case, nine times more acid gas was stored in the reservoir compared to the base case. However, an optimized extraction well location, gas injection, and water extraction rates could delay gas breakthrough, resulting in additional storage capacity gain and lengthened supplies of extracted water. In Cases 3–5, the extraction well was placed at a different location compared to Case 2. In Case 3, where gas injection and water extraction rates were similar to Case 2, gas breakthrough occurred after 4 years and 5 months. During this period, a total of 0.47 megatonnes acid gas was stored while 0.87 million cubic meters of formation water was extracted.

Optimization efforts were carried out by reducing the rate of water extraction. In Case 4, a reservoir condition volumetric ratio of approximately 1:1.2 between extracted water and injected acid gas was observed. Additional modifications resulted in minimal improvement over this figure (Appendix D). Cases 6 and 7 represent attempts to increase rates of both injection and water extraction. However, because of the heterogeneous nature of reservoir and higher injection/extraction rates, early CO₂ breakthrough was observed in both cases, limiting the total CO₂ that could be stored in the reef structure.

Based on the results of predictive simulations for the Zama scenarios, Case 4 appears to be the optimum scenario. In this case, an average volumetric ratio of nearly 1:1 between extracted water and injected gas was observed while acid gas was injected at a constant rate (0.113 megatonnes/year) for more than 5.5 years into a closed system. It also resulted in a 13 times higher storage capacity compared to the base case (Figure 20). With over 700 pinnacle

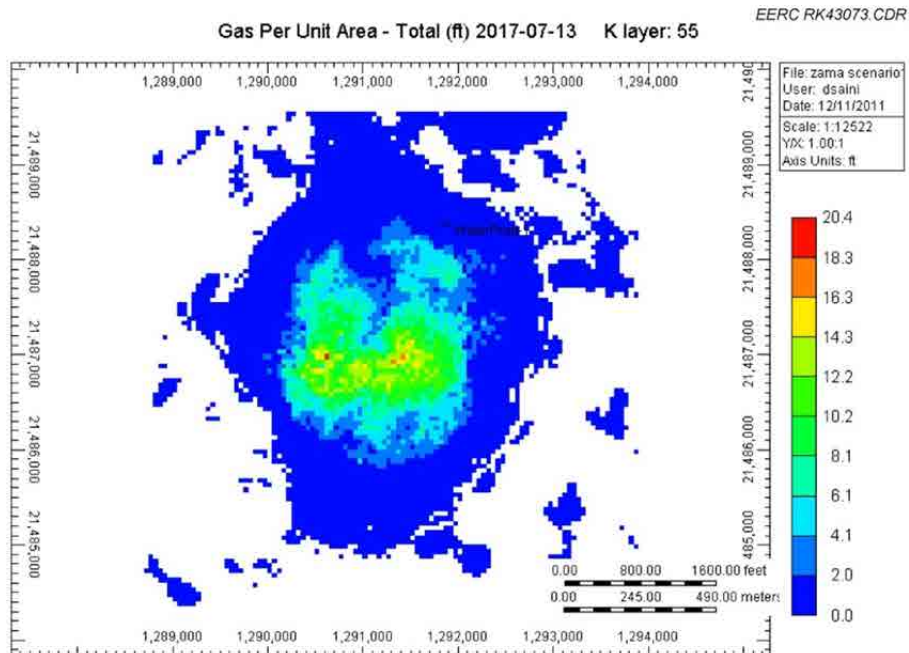


Figure 20. Case 4, aerial view of injected gas plume at end of simulated injection period.

reef structures in the Zama subbasin, a careful selection of 36 pinnacles, each storing 690,000 tons of CO₂ similar to the ones modeled (Appendix D), may provide 1 million tonnes a year of storage capacity and a steady stream of extracted water, albeit at low quality.

Evaluation of Water Management Options (with desalination cost estimates)

Flow rates for extracted water at Zama are provided in Table 11. The flow rates are based on the injection of 1 million m³/year of CO₂ with a 1:1 ratio of water extraction. It is assumed that several similar pinnacle reefs in the Zama Field would need to be utilized to attain these rates based on the simulation case studies.

In the Zama Case Study, two options were investigated, including:

1. Deep well injection into the overlying Slave Point Formation.
2. Treatment of Zama extracted water using a multistep brine concentrator and crystallizer.

Information on water quality for Zama is given in Table 12. The TDS of the waters range from 180,000 to 223,000 mg/L, with the lower value taken as the basis for evaluating treatment options. Cost analysis for treating Zama extracted water was carried out for Option 2.

Table 11. Extracted Water Flow Rates for Zama Based on a CO₂ Injection Rate of 1 million tonnes/year*

	Extracted Water Flow Rate at CO ₂ Injection of 1 Mt/year*	
	m ³ /year	MGD
Case 3	4566	1.21
Case 4	3734	0.99
Case 6	5040	1.33
Case 7	5261	1.39

* Million tonnes/year.

Cost analysis for treatment and/or production of purified water from extracted water at Zama was performed using capital cost and energy use estimates for brine concentrators and crystallizers as provided in Mickley (2006). Two flow rates of extracted water were used. These were the minimum (3734 m³/day) and the maximum (5261 m³/day) flow rates observed from the case study simulations. A brine concentration of 180,000 mg/L was used for the calculations.

Three treatment scenarios were assessed:

1. Treatment of the extracted water in a brine concentrator yielding a concentrated brine containing 250,000 mg/L TDS that would require disposal. The water removed from the brine was considered to be purified water that was acceptable for use.
2. Treatment of the extracted water in a crystallizer yielding a dry salt that would require disposal. A 90% yield of useful purified water was assumed.
3. Treatment of the extracted water in a brine concentrator yielding a concentrated brine containing 250,000 mg/L TDS that is then treated in a crystallizer yielding a dry salt that would require disposal. The purified water produced was taken to be the water removed in the brine concentrator and 90% of the flow delivered to the crystallizer.

The cost of disposing of concentrated brine and/or dry salts was not included in the analysis.

Table 13 contains the details of the cost and energy-use analysis. The capital costs for extracted water treatment associated with the case studies at Zama ranged from US\$5.25 million to US\$60 million. The energy requirements ranged from 3.7 to 15.7 MW. The costs were found to be only weakly dependent on the flow rate of the extracted water over the range of flow rates considered. While the annual cost of treating the extracted water using a brine concentrator was found to be only US\$2.57/m³ to US\$2.58/m³, the annual cost of treatment using a crystallizer was between US\$8.29/m³ and US\$8.41/m³. The same capital and energy costs, when considered on the basis of the amount of purified water, worked out to be very similar for all cases, having a range of US\$9.12 to US\$9.34/m³. The amount of purified water obtained using the brine

Table 12. Water Quality for Zama (not including hydrocarbons)

	Zama				
pH, surface, 25°C, 1 atm:	7.2	6	5.9	6.5	–
pH, in reservoir:	5.4				
Element	mg/L	mg/L	mg/L	mg/L	mg/L
Na	65,223	77,800	68,700	73,400	78,100
Ba					
K	314				
Ca	9800	9820	9750	7450	18,100
Mg	2400	2300	8070	2800	7100
Mn	–	–	–	–	–
Fe	–	–	–	–	–
Li	–	–	–	–	–
NH ₄	–	–	–	–	–
Sr	–	–	–	–	–
Si	–	–	–	–	–
Mn	–	–	–	–	–
Cl	100,000	100,000	94,000	89,000	120,000
Br	–	–	–	–	–
SO ₄	1450	1000	4100	6200	84
HCO ₃	810	80	6500	98	78
CO ₃	–	–	–	–	–
H ₂ SiO ₃	12	–	–	–	–
HBO ₂	–	–	–	–	–
H ₂ S	–	–	–	–	–
TDS (sum of elements)	180,009	191,000	191,120	178,948	223,462
TDS (listed)	180,016	–	–	–	–
TDS (formation)	180,163	–	–	–	–
TDS (surface)	177,111	–	–	–	–
Mineral Precipitation					
Calcite/Strontionate/Dolomite	500	–	–	–	–
CaCl ₂	300	–	–	–	–
Surface Dissolution					
CO ₂ dissolution, mol/L	1.5	–	–	–	–
CO ₂ dissolution, kg/m ³	66	–	–	–	–
TDS Increase from	180,009	–	–	–	–
To	210,031	–	–	–	–
pH from CO ₂ Dissolution from	7.2	–	–	–	–
To	3.2	–	–	–	–
Mineral Precipitation		–	–	–	–
Sulfate, anhydrite/gypsum	500	–	–	–	–

Table 13. Cost¹ and Energy-Use Analysis for Zama Extracted-Water Treatment

Enter Variable Values	Brine Concentrator		Zama (extracted water) Crystallizer Only		Combined Treatment	
	Zama – 1a	Zama – 2a	Zama – 1b	Zama – 2b	Zama – 3	Zama – 4
Flow Rate, MGD	0.99	1.39	0.99	1.39	0.99	1.39
Reject Level of Unit	72%	72%	NA	NA	72%	72%
Make Calculation						
Concentrator Reject/Feed to Crystallizer, MGD ²			0.99	1.39	0.71	1.00
Feed to Crystallizer or Waste Brine Flow Rate, gpm ²			684.5	964.5	494.7	694.6
Find Costs and Energies from Figures						
Capital Cost of Installed Concentrator, \$ millions	5.25	8.00			5.25	8.00
Capital Cost of Installed Crystallizer, \$ millions			3.00	3.00	3.00	3.00
Energy Usage for Concentrator, kW	3700	5200			3700	5200
Energy Usage for Crystallizer, kW			750	750	750	750
Estimate Energy Cost						
Cost of Electricity, \$/kWh	0.10	0.10	0.10	0.10	0.10	0.10
Annual Costs						
Annualized Capital Cost of Concentrator, \$/yr	0.26	0.40			0.26	0.40
Annualized Capital Cost of Crystallizer, \$/yr			0.15	0.15	0.15	0.15
Annual Energy Cost of Concentrator, \$/yr	3,241,200	4,555,200			3.24	0.46
Annual Energy Cost of Crystallizer, \$/yr			0.66	0.66	0.66	0.66
Total Annual Cost for One Unit, \$ millions						
Number of Crystallizer Units			14	20	10	14
Number of Concentrator Units	1	1			1	1
Brine Input, m ³ /day	3734	5261	3734	5261	3734	5261
Cost/m ³ of Water Treated	\$2.57	\$2.58	\$8.29	\$8.41	\$8.49	\$8.46
Product Water Flow Rate, m ³ /day	1046	1473	3361	4735	3465	4882
Cost/m ³ of Water Produced	\$9.18	\$9.22	\$9.21	\$9.34	\$9.15	\$9.12
Total Capital Cost, \$ millions	5.25	8.00	4.20	6.00	3.53	5.00
Total Energy Use Rate, MW	3.7	5.2	10.5	15.0	11.2	15.7

¹ Cost in US\$.

² U.S. units required for cost curves by Mickley (2006).

concentrator was so low that the cost based on amount of water purified was 3.57 times the cost based on the amount of extracted water treated.

Based on these costs, it is highly unlikely that treatment of the extracted water at Zama would be considered as a viable option. Because of the limited local population and remote location, no effort was made to identify water demands for Zama. The most likely management option is disposal into the overlying Slave Point Formation, a practice that is currently being carried out by oil and gas operators in the area.

Regulatory Concerns

Alberta is an oil- and gas-producing province and, as such, regulators and citizens are familiar with activities occurring in the subsurface. The provincial government of Alberta has committed Can\$2 billion to fund CCS projects (Alberta Energy, 2011). Additionally, the province has implemented several pieces of legislation that promote the effective and safe use of CCS technologies. As in other oil- and gas-producing jurisdictions, many aspects of CCS projects are covered by Alberta's existing oil and gas regulations. This could include underground extraction and injection of brine as a pressure management technique in a CO₂ storage reservoir.

The Alberta Energy Resources Conservation Board currently regulates injection and disposal wells in the province. Directive 051 contains all the well classification, completions, logging, monitoring, and testing requirements for these types of wells. Procedures to protect the subsurface environment are also included.

Directive 051 identifies the information that needs to be submitted in support of an application for approval to inject or dispose of certain fluids, as well as operating and monitoring procedures. The primary purpose of this information is to ensure wellbore integrity during injection or disposal operations. In all cases, the location and purpose of the well must first be approved as a part of a specific scheme approval as required by Oil and Gas Conservation Act (OGCA) and the Oil and Gas Conservation Regulations (OGCR), or the Oil Sands Conservation Act (OSCA) (Energy Resources Conservation Board, 2011).

Directive 051 specifies cementing and casing requirements that must provide for hydraulic isolation of the injection zone as well as isolation of usable groundwater from aquifer cross flow of the injected fluid, regardless of the fluid being disposed. Initial logging requirements and subsequent logging requirements are also included to evaluate the hydraulic isolation of the injection zone and casing integrity. Additionally, operating parameters, which include a discussion on wellhead and annular pressures, are included in the Directive.

Given the provinces' current regulatory structure, no issues were identified that would preclude injection of extracted water into the subsurface.

Zama Summary

The pinnacle reef structures of the Zama subbasin provided an excellent opportunity to evaluate hypothetical CO₂ injection and formation water extraction in a closed system. The reef structures are well characterized as some of them contain oil and are under development for EOR. Although each individual structure is small, the field contains over 700 similar structures and the theoretical storage capacity to support a commercial scale injection project. Because of the closed nature of the reservoirs, water extraction was found to have the most dramatic impact at this site, resulting in a maximum of a 13-fold increase in potential storage for a single reef structure. Based on these simulations, it was determined that 36 pinnacle reefs could support a 25-year, 1-million-ton/year CO₂ storage project.

The formation water quality is very low at this site, averaging in excess of 180,000 ppm TDS. This limited the possibilities of beneficial use of extracted formation water. Thus the most likely management option would be injection into the overlying Slave Point formation.

Alberta has implemented a variety of regulations related to potential CCS activities and ongoing extraction of hydrocarbons and disposal of reservoir fluids. There do not appear to be any substantial regulatory barriers to the development of large-scale storage and formation water extraction projects at this time.

Gorgon Case Study

Site Characterization

The Gorgon project is a joint venture to inject and store separated CO₂ from gas produced from the Greater Gorgon Area managed by the Chevron, ExxonMobil, and Royal Dutch Shell oil companies. Tokyo Gas, Osaka Gas, and Chubu Electric are also involved with the project (MIT, 2011). The injection target is the Dupuy Formation, a clastic turbidite sequence 2000 m below the surface infrastructure on Barrow Island off the west coast of Australia. The project aims to inject approximately 3.8 million tonnes a year through eight injection wells, with four water production wells located to the west of the site (Flett and others, 2008). The project has undergone development and characterization and is expected to begin injection in 2014 (MIT, 2011).

Infrastructure will be located on Barrow Island and includes multiple injection wells as well as water extraction wells for pressure management. Barrow Island is largely uninhabited, resulting in low local water demand, despite treatable levels of dissolved solids. The island is located atop a large (25 × 38 km), north-south-trending double-plunging anticline. The injection target is 200–500 meters thick, comprising sandstones and siltstones deposited as turbidite and debris flows, which discharged onto the Australian slope and were later uplifted. Four major subunits have been defined, with lithology presented in Table 14. Data are scarce for the site for both modeling workflow and reservoir data, with basic results from modeling efforts reported by Flett and others (2008). In order to develop the hypothetical injection plan for this study, additional data, including well logs from an exploratory well, were incorporated from Brantjes (2008).

Table 14. Unit Descriptions and Thicknesses from the Gorgon Site

Subunit	Lithology (from Brantjes, 2008)	Thickness
Basal Dupuy	Siderite cemented fine-grained sandstone. Poor quality.	95 m
Lower Dupuy	Fine-grained sandstone/siltstone to shale. Fair quality.	190 m
Upper Massive Sand	Medium-grained sandstone. High quality.	140 m
Upper Dupuy	Bioturbated siltstone. Poor quality.	111 m

Modeling

Well locations and the structure on top of the Upper Massive Sand unit of the Dupuy Formation were used as baseline data according to Flett and others (2008) (Appendix E). As insufficient well logs or structure maps for additional subunits were present, constant unit thickness was defined from unit boundaries on well logs from Brantjes (2008) as shown in Table 15. The model size used by Flett and others (2008) was found to be sufficient to contain the 3.3–3.8-million-tonnes/year injection without reaching the model boundaries (Figure 21).

Because of the poor reservoir quality encountered in downhole logs, facies were not assigned for the Basal Dupuy, and the unit is considered to behave as a lower seal. The Lower Dupuy was assigned facies using truncated Gaussian simulation, using parameters and techniques suggested by Flett and others (2008), who stated that reservoir quality degrades from high on the north end to silty then shaley moving south (Figure 22). The Upper Massive Sand and Upper Dupuy zones were modeled using Petrel’s object modeling processes for fan-type deposits with thicknesses and prevalence suggested by Flett and others (2008) and Brantjes (2008) and shown in Table 15. Facies were populated with porosity and permeability properties according to AGD variograms for clastic slope/basin environments and porosity, effective porosity, and permeability values from Brantjes (2008) (Figures 23 and 24).

Water chemistry was assigned and populated throughout the model from data provided by personnel from Chevron (Trupp, 2011).

Table 15. Gorgon Model Parameters

Property	Value	Source
Total Porosity	0%–31%	Brantjes, 2008
Effective Porosity	0%–25.3%	Brantjes, 2008
Permeability	0–272 mD	Brantjes, 2008
Depth (top of Upper Dupuy)	2245 m	Flett and others, 2008
Pressure (average)	25,165 kPa	Flett and others, 2008
Temperature (average)	161°C	Colombo and others, 2010
CO ₂ Density	528.1 kg/m ³	MIT, 2011
Variogram Range (long)	1346	IEAGHG, 2009
Variogram Range (short)	367	IEAGHG, 2009
TDS	7096–28,615 ppm	Trupp, 2011

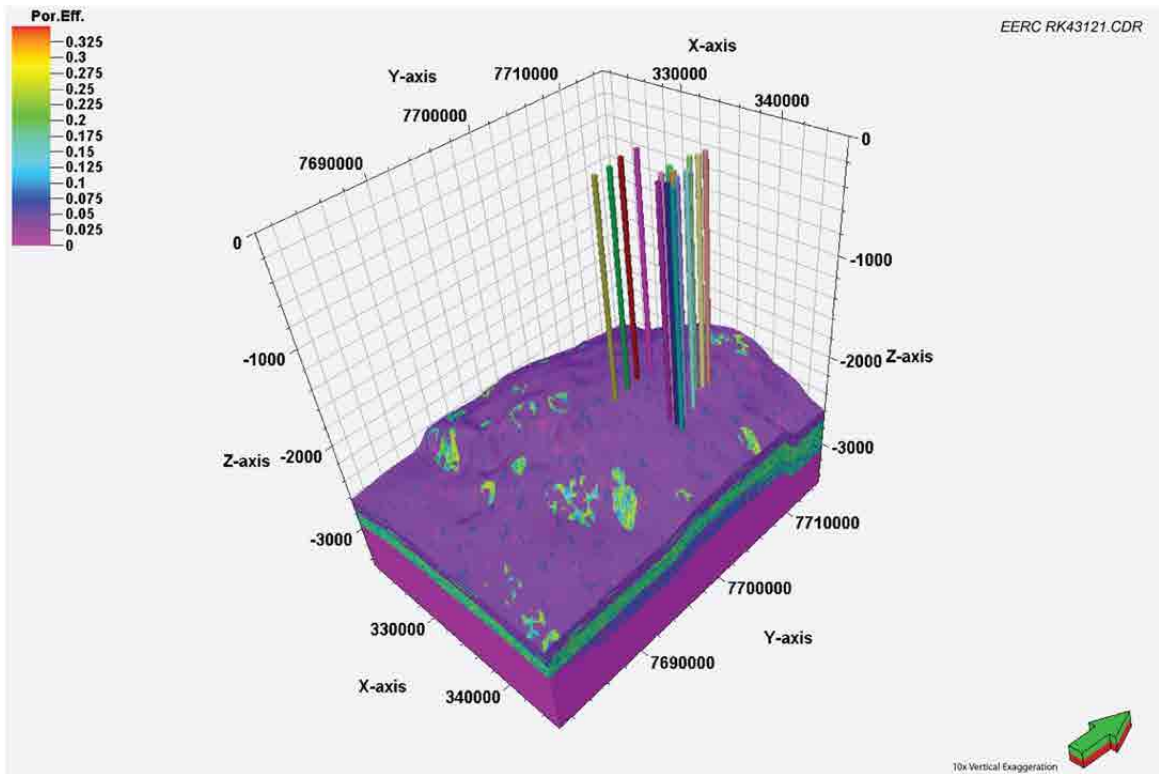


Figure 21. Three-dimensional representation of the Gorgon reservoir model with location of injection and extraction wells.

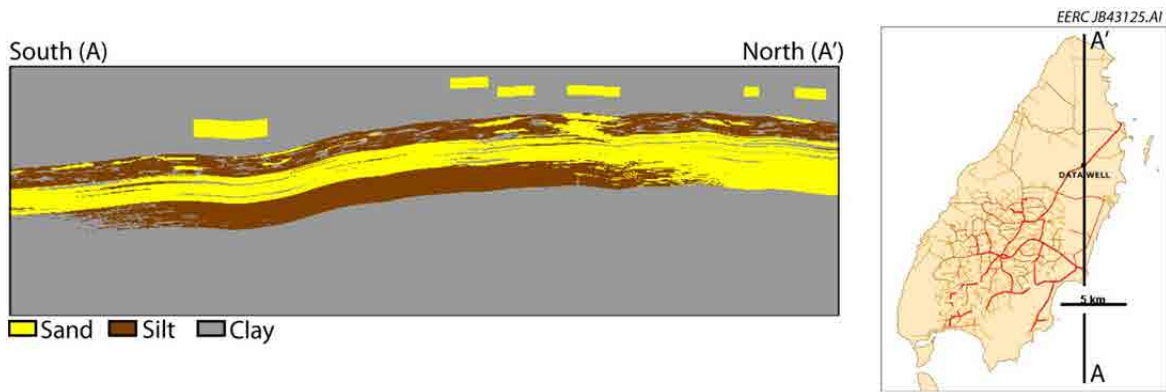


Figure 22. Cross section of the Gorgon reservoir model through the data well. Index map modified from Flett and others (2008).

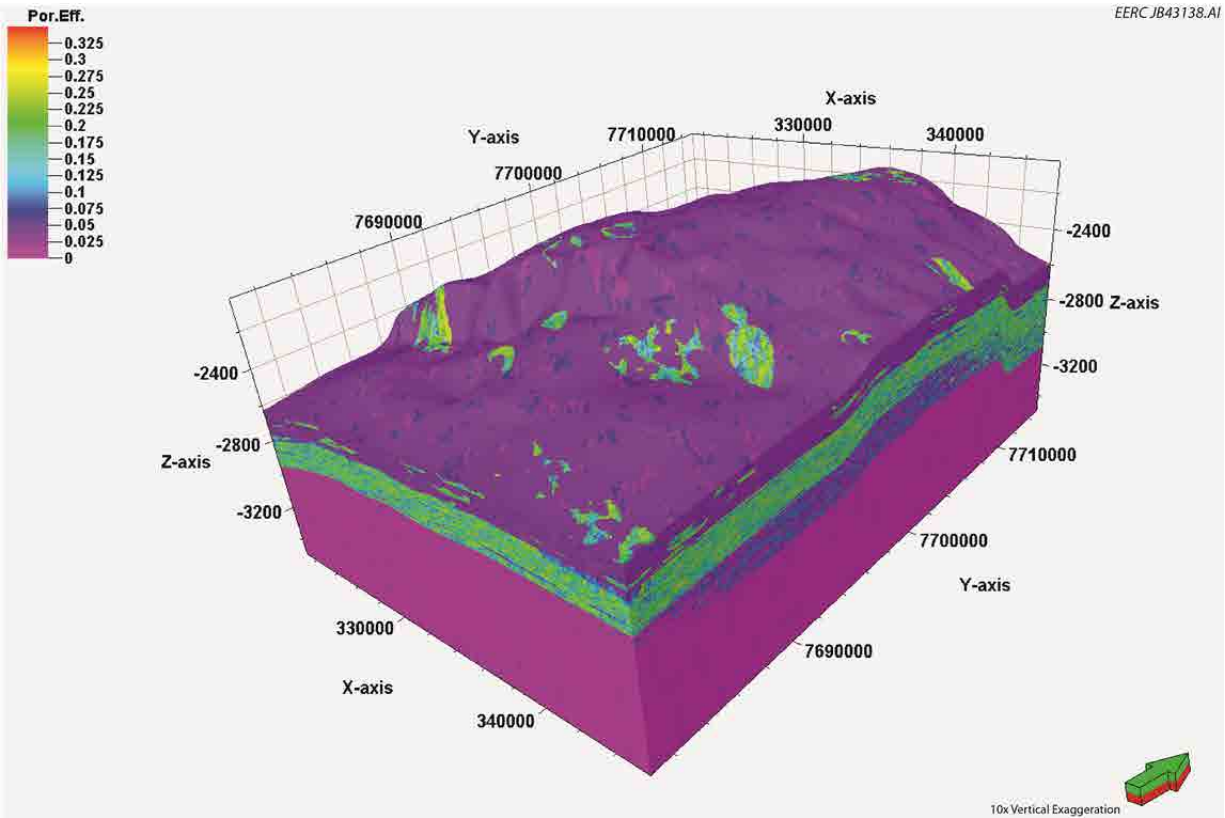


Figure 23. Three-dimensional view of the Gorgon model showing the porosity attribute. Cap rock units have been removed to show model structure, and a 10× vertical exaggeration has been applied.

Reports and publications by CO2CRC Technologies (CO2CRCTPL, 2008, 2009; Flett and others, 2009) provided overall information on the Gorgon site. Most of the properties and parameters including saturations, relative permeability curves, boundary conditions, and initial reservoir pressure for modeling and simulations were based on publications (Brantjes, 2008; Flett and others, 2004, 2006, 2008, 2009; Schembre-McCabe and others, 2008). Specially, the proposed location of the injection and production wells followed in the study of Flett and others (2008). The other detailed properties and parameters are listed in Table 15.

Case Study Simulation Results

Seven hypothetical cases were simulated for the Gorgon test site using the planned eight injection wells and four extraction wells. The base scenario will inject 0.5 megatonnes per annum through each well, totaling 4 megatonnes per annum for an investigational period of 25 and 50 years. This injection plan results in total volumes of 100 and 200 megatonnes for the respective time periods. The primary purpose of extraction at the Gorgon site is to manage reservoir pressures. The effects of extraction on capacity were minimal, as the reservoir has excellent injectivity and capacity, meaning the upper limit of injection was not achieved through these simulations. All simulations were run with semiclosed boundary conditions.

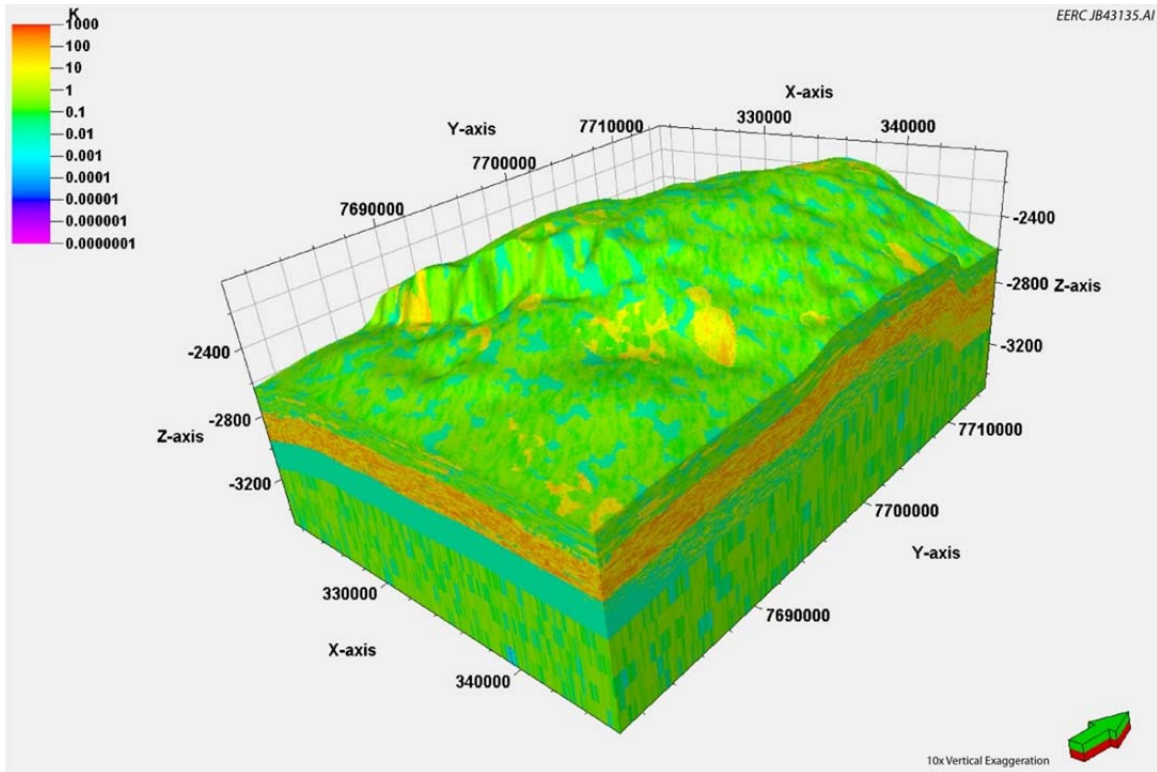


Figure 24. Three-dimensional view of the Gorgon model showing the permeability attribute. Cap rock units have been removed to show model structure, and a 10× vertical exaggeration has been applied.

The base case simulations injected CO₂ in all eight injection wells and did not utilize the extraction wells, resulting in storage capacity of 97 megatonnes for a 25-year injection (Case 1) and 195 megatonnes for a 50-year injection (Case 3) (Table 16). The base case simulations were able to accomplish these target injection volumes without any water production, although slight increases in storage capacity were observed when water was extracted (Cases 2 and 4). A third scenario sought to maximize the injection rate, bumping it up over seven times the yearly injection rate to 3.75 megatonnes per year per well for 25 years (Cases 8 and 9). Because of the higher injection rates, pressure increases near the injection wells were expected to cause issues that may be alleviated by water extraction. Simulations under this scenario resulted in storage capacities of 551 megatonnes for the modeled reservoir, which increased to 637 megatonnes with water extraction, an increase of 16%.

Optimal reservoir conditions resulted in the generation of very large volumes of extracted water. Ratios of approximately 1:1 water to CO₂ were readily achieved in Cases 2 and 4 and increased to 4:1 in Case 9, although this resulted in early breakthrough at the extractors, meaning only one extractor was active for the entire injection phase (Appendix E).

The difference in plume size was relatively small between Cases 1 and 2 (Figure 25), differing by a negligible percentage. The size difference between Cases 8 and 9 was a notable

Table 16. Case Scenarios and Resulting Storage Capacities for Gorgon

Scenario*	Well Configuration	Gas	Water	Injection Period, yr	Storage Capacity, megatonnes
		Injection Rate/Well, kg/day	Production Rate/Well, m ³ /day		
Case 1 (base case)	8 injectors	10,661,700	NA	25	97.3
Case 2	8 injectors 4 extractors	10,661,700	215,120,000	25	97.5
Case 3	8 injectors	10,661,700	NA	50	195
Case 4	8 injectors 4 extractors	10,661,700	334,919,000	50	196
Case 5	8 injectors 4 extractors	5,330,830	396,606,000	50	97.5
Case 8	8 injectors	60,400,000	NA	25	551
Case 9	8 injectors 4 extractors	69,900,000	261,802,000	25	637

* Cases 6 and 7 were omitted from the report because of duplicative results.

10.1% (Figure 26). However, pressure management through water extraction proved very consistent as pressures were reduced by approximately 20% between both Cases 1 and 2 and (Figure 27) Cases 3 and 4. This reduced pressure signal remained present throughout the 100-year simulation period in all extraction cases (Appendix E). This demonstrates a significant plume management benefit to the operator. In Case 5, injection rates were reduced by half while higher extraction rates were maintained for Case 4 to test the opportunity for increased pressure reduction and plume control; however, the excellent nature of the reservoir resulted in only small gains in pressure and plume distribution (Figure 28).

Based on the simulation results, water extraction at the Gorgon site appears to be most beneficial for pressure maintenance and, potentially, plume control as well. Utilization of the planned extraction wells achieved significant pressure reductions. Early breakthrough remains an issue and could require extractors to be shut in and more wells brought online. Capacity gains through water extraction are possible at the Gorgon site, although the amount of injection required to make those gains far exceeds the injection planned for the site.

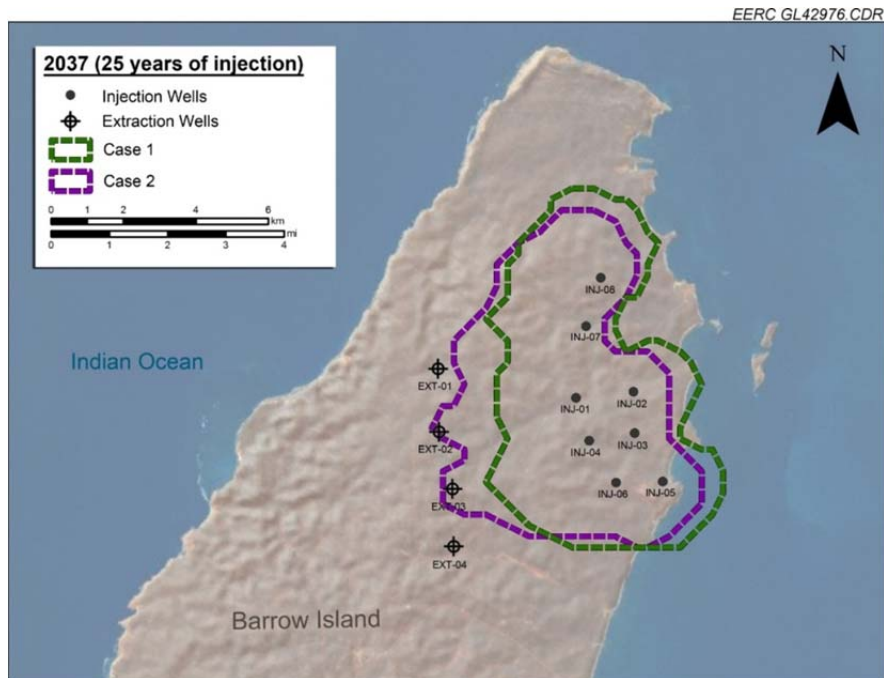


Figure 25. Map of injection and extraction wells on Barrow Island with plume outlines of Cases 1 (base case) and 2 after 25 years of injection. The effect on plume distribution as well as simulated CO₂ breakthrough is illustrated.

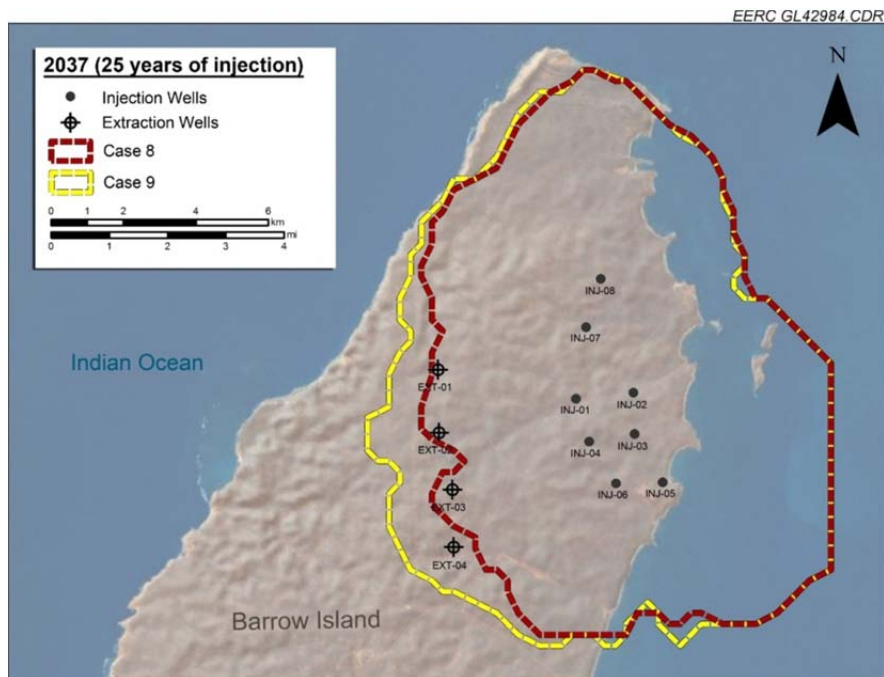


Figure 26. Map of injection and extraction wells on Barrow Island with plume outlines of Cases 8 and 9 after 25 years of injection. The effect on plume distribution is illustrated as well.

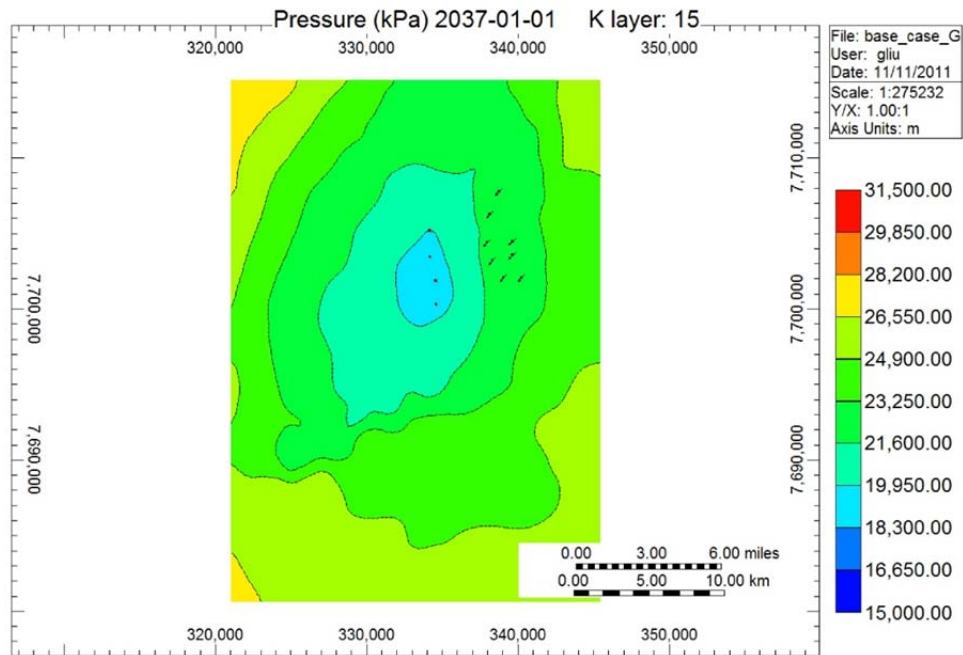
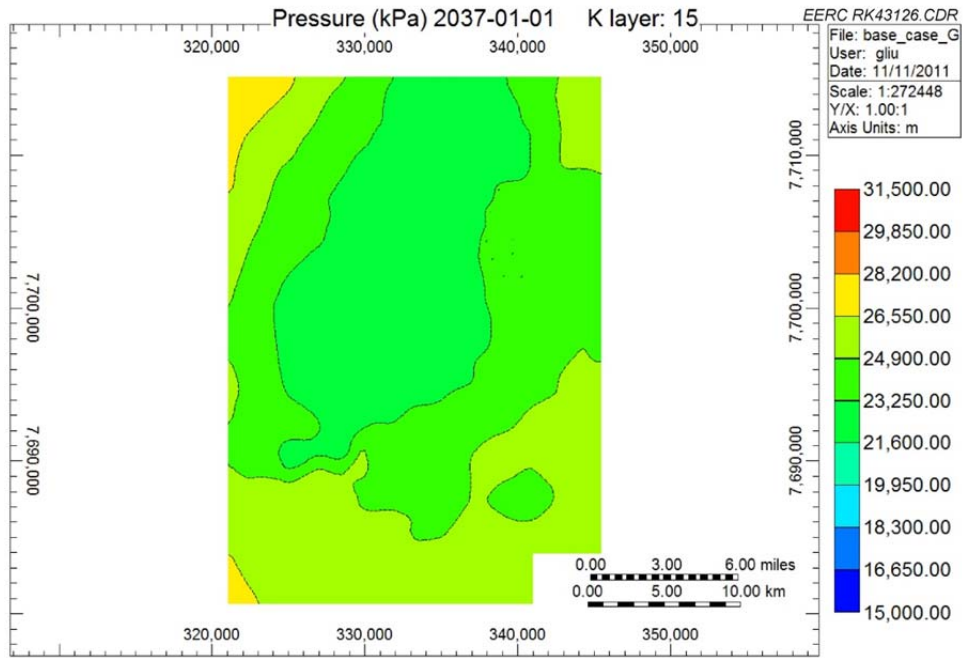


Figure 27. Reservoir pressure after 25 years of injection for Cases 1 (top) and 2 (bottom) illustrating an appreciable pressure reduction.

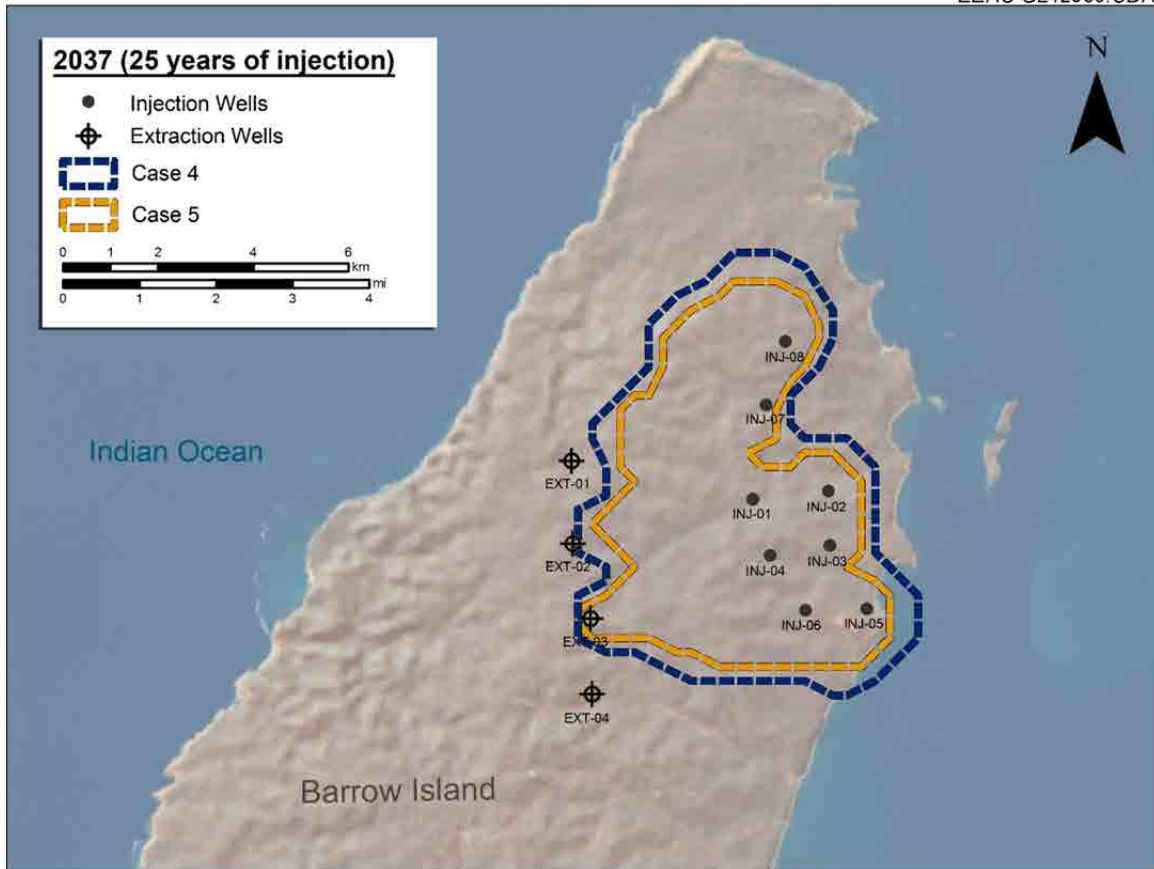


Figure 28. Plume distribution for Cases 4 and 5 demonstrating limited benefit from the reduction of the injection rate from 4 to 2 megatonnes per annum.

Evaluation of Water Management Options (with desalination cost estimates)

Four potential water-handling scenarios have been considered for the extracted water at Gorgon:

1. ReInjection of the extracted water into a geologic formation (for pressure management in the natural gas field)
2. Ocean discharge
3. Use as source water for RO systems installed on Barrow Island (ultimately for water supply on Barrow Island)
4. Use as supply of water for mainland Australia communities

Scenario 1 is considered to be the most likely disposition for extracted water at Gorgon because it will require minimal handling of the water and it will serve as a benefit to the natural gas production project in the Gorgon or Jansz Fields for pressure maintenance purposes.

Scenario 2 is a low-cost option, especially if the extracted water does not contain hydrocarbons or naturally occurring radioactive materials that would necessitate significant treatment prior to disposal. The salinity of the extracted water is, at most, the same as the local seawater so discharge should not be an issue. There is some question concerning the potential environmental impact for discharge of the extracted water at high temperature and what processing can be done to decrease this impact. It may be acceptable to minimize environmental impact by use of dilution diffusers, or it may be necessary to remove heat with thermal recovery units or in some other manner.

Scenario 3 is a high-cost option, but it provides potential cost savings over the use of seawater as the source water for RO-based desalination on Barrow Island, provided the cost of transporting the source water is kept to a minimum to reduce the cost of providing purified water. In this case, the lower salinity of the extracted water would provide for higher RO processing yields and lower purified water production costs than those achieved with seawater as the source water. Details on this analysis are given later in this section.

Scenario 4 is a very high-cost option because the cost of transporting water long distances is prohibitively expensive, especially when the communities that might be interested in the water can access seawater for desalination without the need to transport it over long distances. Even if the extracted water were of potable water salinity, the transport of water over the distances in question might make it more expensive than locally produced desalinated seawater. Some details concerning distances needed for water transport from Barrow Island to communities on the mainland and water needs of those communities are provided in the following text.

Distance of Barrow Island to Mainland Australia, Karratha, and Cape Preston

Barrow Island is approximately 65 km from mainland Australia. The closest large communities on the mainland include Cape Preston and Karratha, which are about 85 and 150 km from Barrow Island, respectively. Transport of water this distance is likely to be prohibitively expensive because of the cost of installing the pipeline. Bruno Oreste Bellettini Cedeño (2009) estimated the cost of installing a subseawater pipeline at US\$1.320 million/km (\$2.1 million/mile). This cost is likely high given the fact that he was designing a very large diameter pipe but it is similar to a commonly estimated pipeline cost of US\$625/meter (\$1 million/mile). Assuming that these are reasonable first estimates, the cost of installing a pipe to transport water from Barrow Island to Karratha would be US\$93 million to US\$198 million. Even if 31,000 m³/day of water were produced and transported through the pipeline for 25 years, this water would be at a cost of \$0.33 to \$0.70/m³ solely for installation of the pipeline alone. Transportation costs were estimated in DEEP 4.0 (IAEA, 2011) using the default settings with a 150-km pipeline. The estimate for the 31,000 m³/day condition was a transportation cost of 0.88 US\$/m³. Transportation costs per unit of water increase with a decrease in amount of water moved.

Water Quality and Flow Rate of Gorgon Extracted Water

Water quality data were available from the literature for 14 samples collected at the Gorgon case study site (Trupp, 2011). A box and whisker plot of the water composition is given as Figure 29. It was recognized that the salinity and pH of these samples decreased with depth, as shown in Figure 30. The water extraction simulations performed as part of this project removed water from depths between 1800 and 2300 meters, so it was desirable to use a lower TDS value for the extracted water. Unfortunately, it appears that a lack of reporting of carbonate and bicarbonate ion concentrations is, at least in part, the reason for the lower salinity of the four samples taken at depths of greater than 2150 meters. Because of this, the water quality for a representative sample with a lower pH was selected to represent the anticipated water chemistry for the extracted water.

Table 17 provides the mean and median water quality values for the 14 samples and the water quality data for the sample selected as representative. The TDS of this sample was 20,610 mg/L, close to the mean TDS of 23,234 mg/L and the median TDS of 26,189 mg/L, of all the samples.

Figure 31 provides the total extracted-water flow rates for the model conditions that included water extraction for the Gorgon case study. Appendix D provides the extracted water flow rate plots for each of the four extraction wells for each of these cases. None of the cases provided for a steady water extraction rate for the entire period of CO₂ injection. Constant water flow rates are the best situation for the beneficial use of the water. Figure 31 also shows the

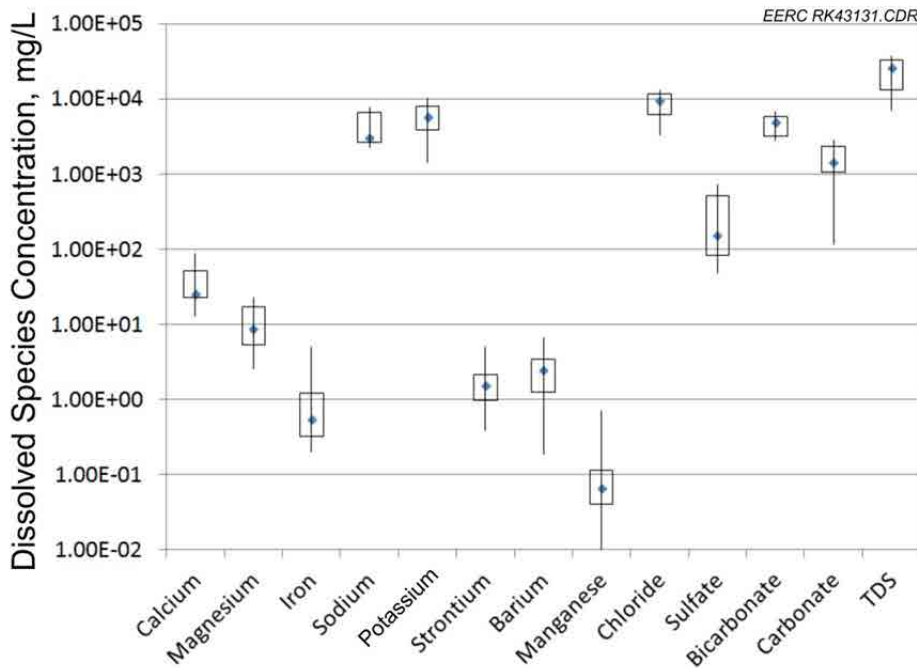


Figure 29. Box and whisker plot for composition of Gorgon water. Point indicates median, box shows first and third quartile (25% and 75%), whisker shows minimum to maximum.

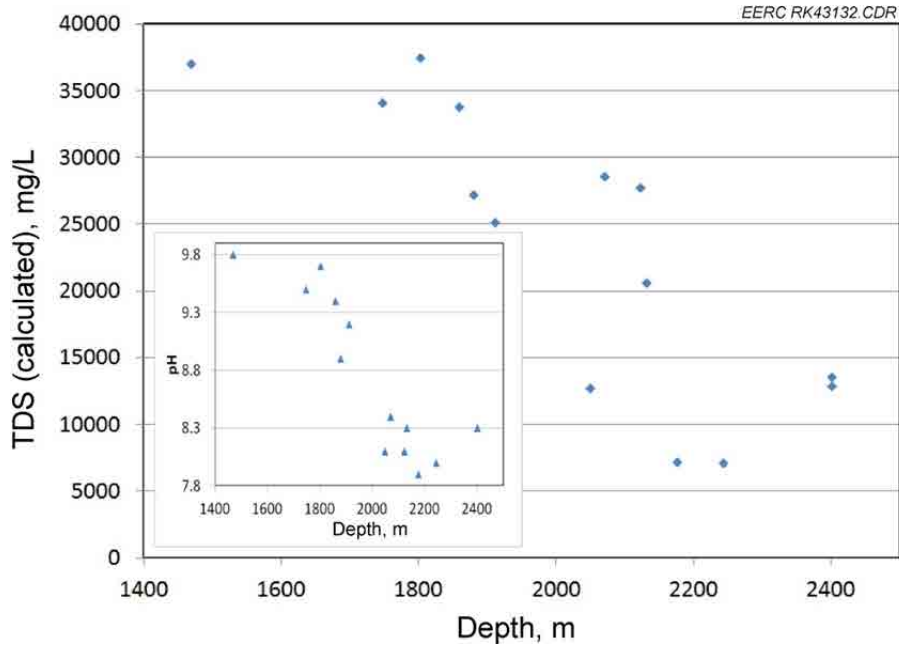


Figure 30. Salinity of Gorgon site water as a function of depth. Inset shows that pH measured at surface also decreases with depth.

Table 17. Median TDS Sample Water Quality and Median Water Quality from All Samples

Constituent	Unit	Mean	Median	Selected Sample (MPSR 2108)
Ca	mg/L	37.9	25.5	61
Mg	mg/L	10.8	8.75	5.20
Fe	mg/L	1.15	0.55	0.32
Na	mg/L	4418	3095	2890
K	mg/L	5644	5695	6120
Sr	mg/L	2.05	1.55	1.90
Ba	mg/L	2.57	2.50	3.60
Mn	mg/L	0.14	0.07	0.05
Cl	mg/L	8666	9490	8231
SO ₄	mg/L	287	152	106
HCO ₃	mg/L	4717	4976	3191
CO ₃	mg/L	1593	1417	
pH	pH units	8.71	8.35	8.30
Resistivity, at 25°C	ohm-m	0.39	0.31	0.35
TDS (calculated)	mg/L	23,234	26,189	20,610
Density, at 25°C	g/cm ³	1.02	1.02	1.01
Refractive Index, at 25°C		1.34	1.34	1.34

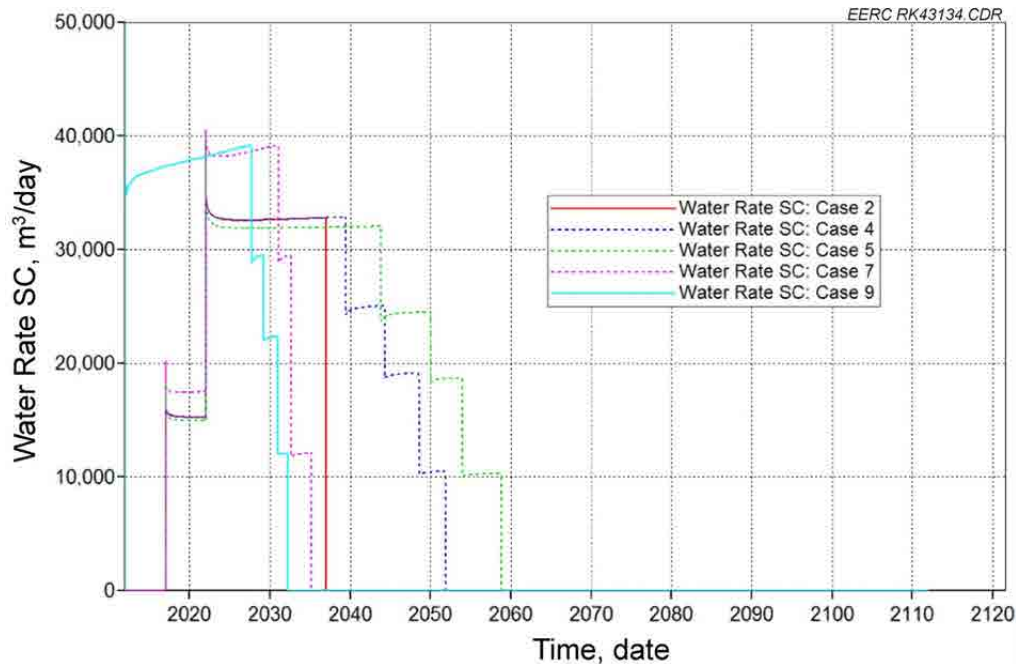


Figure 31. Extracted-water production rates for Gorgon.

minimum and maximum extracted water volume and the duration of production for each case. These values represent the water treatment facility size that would be needed for each case, but it would be best from a water supply standpoint as well as a facilities design and cost basis if more steady water extraction rates could be obtained. This can be achieved at a CO₂ storage site like Gorgon by placing new CO₂ injection wells and water extraction wells into the formation at appropriate locations and times.

Figure 32 shows the range of extracted water flow rates can be seen to vary between about 10,000 and 40,000 m³/day. At a salinity of 20,000 mg/L and an RO feedwater delivery pressure of 69 bar, this should provide a purified water yield of 67% for a purified water flow rate of approximately 7000 to 27,000 m³/day. The 7000 m³/day matches the seawater RO desalination capacity being constructed at Barrow Island (Osmoflow, 2010). Seawater in that part of the world has a salinity of approximately 35,000 mg/L TDS (NOAA, 2011). Therefore, the use of the extracted water may be a better option than using seawater at this site.

A comparison was performed using the default settings in the International Atomic Energy Agency DEEP 4.0 (IAEA, 2011) model for producing this 20,000 m³/day of water using waters with salinities of 35,000 (seawater), 20,000, and 10,000 mg/L TDS. Sensitivity analysis on the cost was performed to provide the cost for production volumes from 7000 to 31,000 m³/day. Figure 33 shows the cost of the purified water as a function of the source water salinity as calculated using the default parameters of the IAEA DEEP 4.0 model with source water temperature set at 40°C and an RO process feed pressure of 69 bar. The yield of product water per unit of source water depends on the source water salinity, with costs being less for

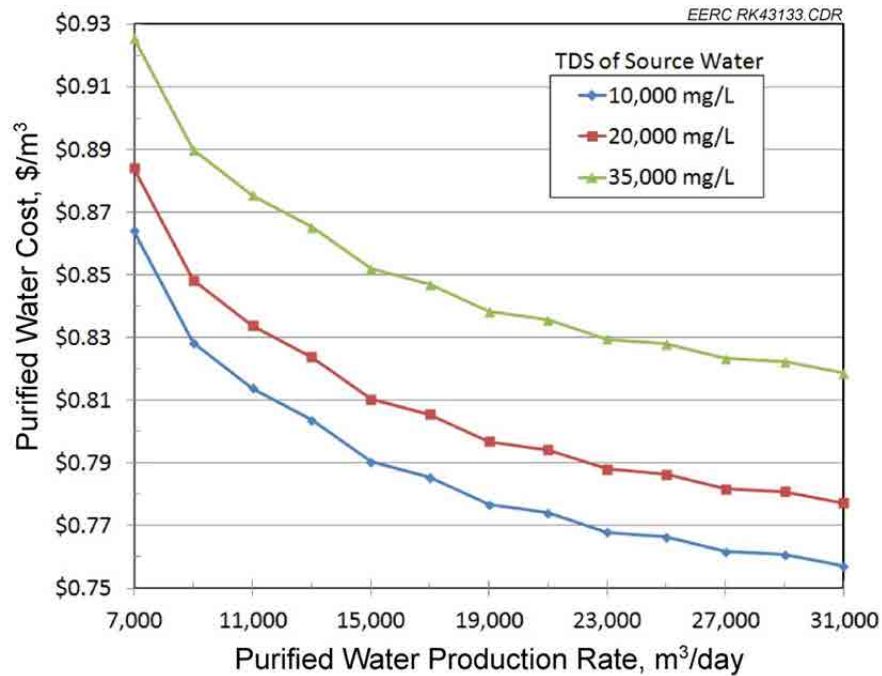


Figure 32. Water cost versus purified water capacity for RO treatment of 20,000 mg/L TDS water (calculated using default parameters for IAEA DEEP 4.0).

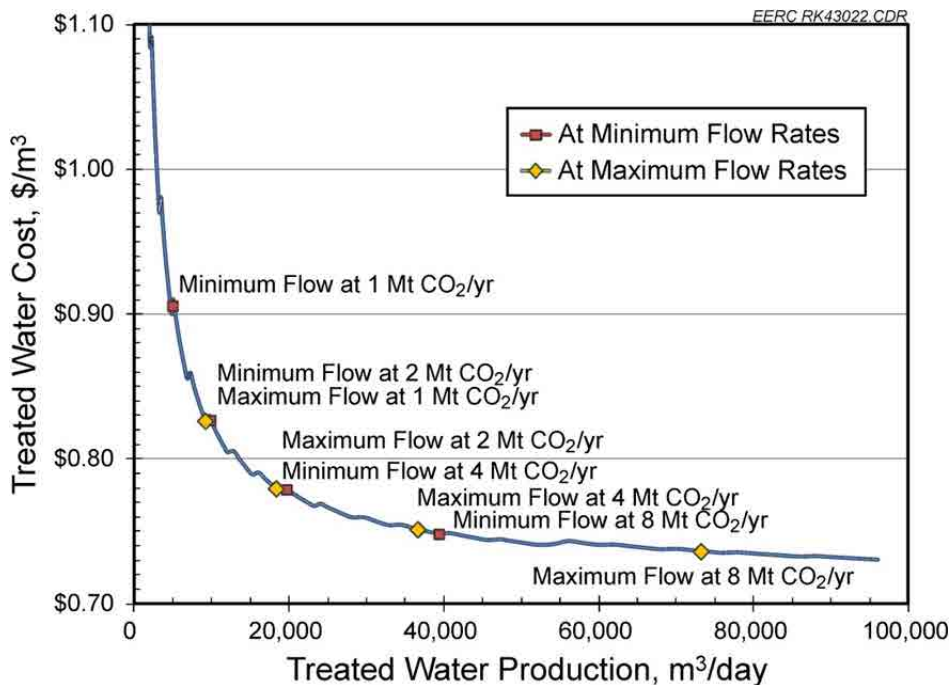


Figure 33. RO treatment costs for treating 10,000 mg/L TDS extracted water. Estimated for a large range of flow rates using DEEP 4.0. Red (minimum flow rate) and yellow (maximum flow rate) points indicate the cost at extracted water flow rates associated with 1, 2, 4, and 8 Mt/year CO₂ injection scenarios.

production of water from lower-salinity feed water. The values shown in Figure 33 suggest that replacing seawater with the 20,000 mg/L extracted water for production of 7000 m³/day of purified water, the amount planned for Barrow Island, would result in a 4.5% (4.2 cents/m³) drop in the cost of producing that water. If the extracted water had a salinity of 10,000 mg/L TDS, the price drop at 7000 m³/day of production capacity would be 6.7% (6.2 cents/m³). This decreased processing cost would also be accompanied by a decrease in the amount of waste brine that requires disposal because there is a large change in treated water yield with salinity. The treated water yields were 42%, 67%, and 83%, respectively, for the 35,000, 20,000, and 10,000 mg/L TDS cases. The waste brine concentrations were 103,750, 93,800, and 58,824 mg/L TDS, respectively, for the 35,000, 20,000, and 10,000 mg/L TDS source water cases. With ocean disposal of the waste brine, the disposal cost of the different amounts of waste brine is likely not a significant factor.

If properly planned and implemented, the use of extracted water could be considered as a source of feedwater for RO production of purified water for operations at the Barrow Island site. Minimal transportation and infrastructure are required beyond current seawater desalination operations.

Regulatory Concerns

Similar to Alberta, Western Australia has a developed oil and gas industry. While the Australian Government has jurisdiction over Commonwealth waters (extending from 3 nautical miles offshore to the edge of Australia's continental shelf), the states and territories have jurisdiction over onshore areas and coastal waters (up to 3 nautical miles). The development of legislative and regulatory systems in each jurisdiction is a matter for the jurisdiction concerned.

For saline groundwater (brine) extraction from a deep aquifer system, reinjection into another system with similar groundwater quality may be possible. Geothermal projects commonly extract "hot" saline groundwater from a deep aquifer system, harvest the energy associated with the groundwater and then reinject into a shallower system. This is also similar to issues that arise during hydrocarbon exploration and drilling, which operates under the Petroleum Act administered by the Australian Department of Minerals and Petroleum (DMP). Project developers must provide an Environment Plan for its drilling and injection programs in accordance with the Offshore Petroleum and Greenhouse Gas Storage (Environment) Regulations 2009.

Additionally, the disposal of dewatered effluent into marine environments is common when the construction activity is adjacent to the marine environment. In these situations, conditions of effluent quality and sediment load are determined in discussions with the Department of Environment and Conservation (Leonhard, 2011).

There are regulations that control offshore petroleum activities managed by the DMP that may include reinjection:

- The DMP would be the lead organization for regulations and guidelines for geothermal development (including disposal/reinjection).

- The DMP manages the operation and environmental impacts associated with hydrocarbon exploration and development projects, including brine disposal.
- The Western Australia Department of Environment and Conservation would be the lead organization for guidelines and conditions for the disposal of dewatered effluent.

The Gorgon Joint Venture (GJV: Chevron, ExxonMobil and Shell) CCS project is regulated under the Barrow Island Act 2003, the only legislation in Western Australia that currently allows for CCS. Under the current injection project approval, the State government has not provided the GJV with postclosure indemnity. This matter will need to first be considered and endorsed by Parliament through a variation to the Barrow Island Act (Western Australia Department of State Development [DSD], 2011).

It is anticipated that the GJV will be injecting CO₂ for up to 60 years or more. For at least 15 years after the cessation of gas production, the GJV will be required to manage and monitor the injection site. An indemnity would only be provided to the GJV once it has satisfied both governments that the site can be closed. The GJV is responsible for all costs associated with the project up to the point of closure (Western Australia DSD, 2011).

There is a precedent nationally for the provision of postclosure liabilities for CO₂ injection projects. In late 2008, the Commonwealth Offshore Petroleum and Greenhouse Gas Storage Act 2006 passed. This legislation allows for the Commonwealth government to take on liability postclosure for CCS projects in the offshore Commonwealth jurisdiction (Western Australia DSD, 2011).

The current regulatory frameworks described here do not provide any serious constraints to brine disposal in Western Australia.

Gorgon Summary

The Gorgon case study site consists of a large clastic reservoir comprising layered turbidite sequences which have excellent properties for injection and CO₂ storage. As the site is being developed for a large-scale CO₂ storage project, reservoir data were available to aid in development of the hypothetical injection scenarios developed for this study. Simulations revealed that the addition of water extraction is likely to have only a nominal effect of increasing storage in this reservoir. The reservoir has a native storage capacity that far exceeds even the 25-year, 3.8-million-tonne/year injection project proposed here. Water extraction was found to be useful as a tool for pressure management and plume control at this site, although additional simulations could provide additional optimization over what was presented here.

The formation water quality at the Gorgon site is reasonably high, at approximately 25,000 ppm TDS. This presented the opportunity to develop a treatment plan for water extraction utilizing desalination technology similar to that used to treat ocean water. The remoteness of Barrow Island means that any transportation of treated extracted water to onshore municipalities or other locations would be cost-prohibitive. Instead, it is proposed that the extracted water could

be treated for use at the surface facilities installed on Barrow Island in place of treatment of seawater.

There do not appear to be any significant regulatory barriers to development of a large-scale CO₂ injection project with formation water extraction at the Gorgon site.

Teapot Dome Case Study

Site Characterization

Teapot Dome, also known as Naval Petroleum Reserve 3 (NPR-3) or the Rocky Mountain Oilfield Testing Center (RMOTC), is a demonstration site near Casper, Wyoming. Teapot Dome is a stacked sedimentary sequence on the western flank of the Powder River Basin present as an elongated anticline and is adjacent to the Salt Creek Anticline, a commercial oil field currently undergoing CO₂ EOR. Over 1300 wells penetrate the structure at the Teapot Dome, which has historic production within the Tensleep and Frontier sandstones and reserves in the Muddy sandstone. Additionally, saline aquifers are located in both clastic and carbonate beds including the Dakota/Lakota and Madison Formations. Descriptions of these units are provided in Table 18. Produced water from oil field activities at Teapot Dome is of extremely high quality and has many uses in the semiarid Powder River Basin. Additionally, the field is located near populated locations and agriculture, and the potential may exist for geothermal energy production.

Simulation efforts were focused on the Dakota and Lakota Formations for this site, although it is recognized that utilizing several formations in the stratigraphic section is optimal for storing large volumes of CO₂ (Appendix F). Because of historic hydrocarbon production, characterization of the site has resulted in large volumes of data, and the field continues to operate as a demonstration and experimental site, as oil production has declined to unprofitable levels. Recent activity at the site involves hydrothermal energy generation from the deeper units; however, interest in CO₂ EOR is present because of successful CO₂ EOR ongoing in the adjacent Salt Creek Field since 2003, where 6583 tonnes of CO₂ a day is injected, totaling 6.6 million tonnes as of February 2010 (ZERO, 2011).

Modeling

A data set of Teapot Dome information including well locations, picked formation tops, and well logs was available in CD format from the Rocky Mountain Oilfield Testing Center (2007). Formation tops were used to form a high-resolution structural model of each horizon. Unfortunately, characterization information yielded from literature review was not conducive to direct application in modeling, and full-scale petrophysical interpretation of the site is beyond the scope of this project. A limited amount of data collection has been processed by Milliken (2007) regarding geothermal resources and water quality, and a historical perspective and field overview were performed by Curry (1977). Because of the lack of petrophysical data at Teapot Dome, modeling was performed using the AGD variogram ranges from interpreted depositional environments with reported or derived rock properties collected through core analysis, including

Table 18. Unit Descriptions for the Teapot Dome Site

Formation	Interpreted Lithology
Frontier	Interbedded sandstones and shales, Deltaic
Muddy	Sandstone body, shallow shelf
Dakota	Sandstone bodies, shallow shelf
Tensleep	Interbedded sandstone and dolomite, sandstones primarily Eolian
Madison	Variable reservoir quality, shallow shelf

porosity and permeability (Figures 34 and 35). For formations without site-specific water quality data, values were acquired from the RMOTC. Properties for specific units are reported in Tables 19 and 20.

Most of the properties and parameters for modeling and simulations were based on publications (Curry, 1977; Doll and others, 1995; LeBeau, 1996; Gaviria, 2005; Friedmann and Stamp, 2006; Smith, 2008; Chiaramonte, 2008; Klusman, 2009). The injection and production

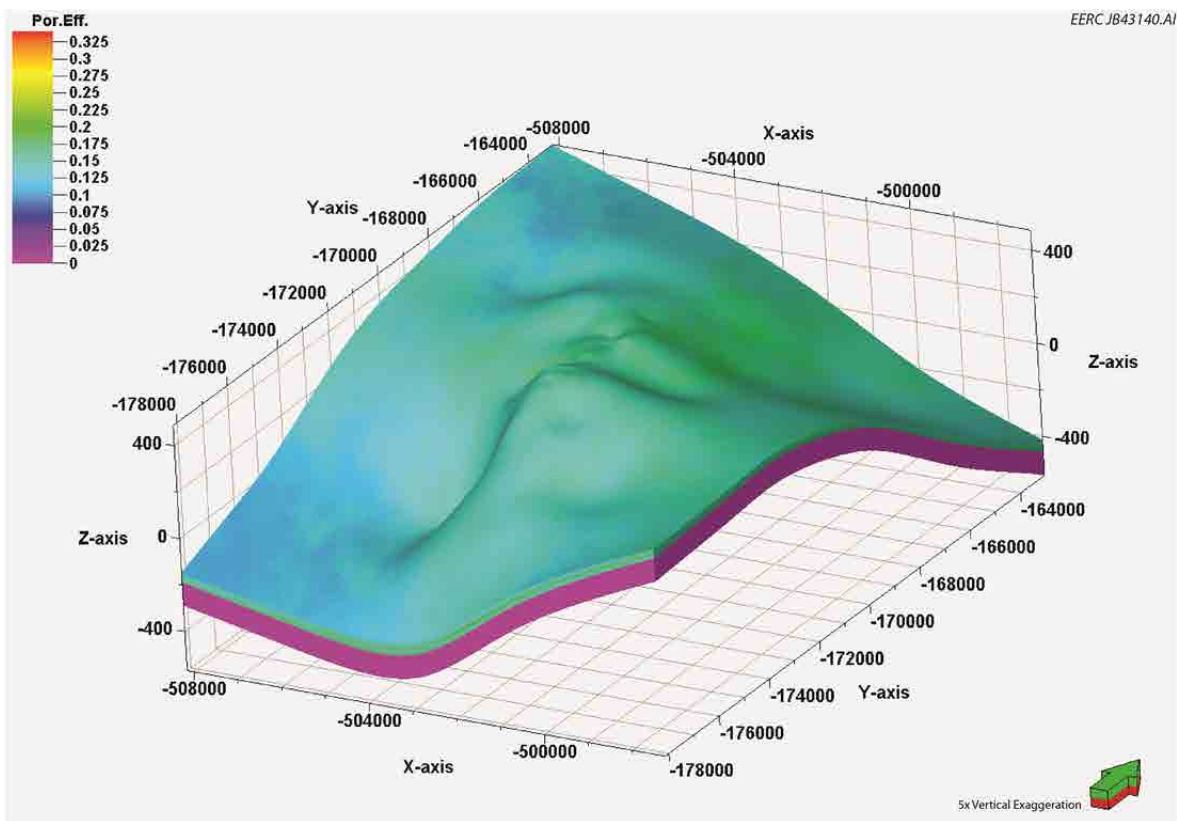


Figure 34. Three-dimensional view of the Teapot Dome Dakota model showing the porosity attribute. Cap rock units have been removed to show model structure, and a 5× vertical exaggeration has been applied.

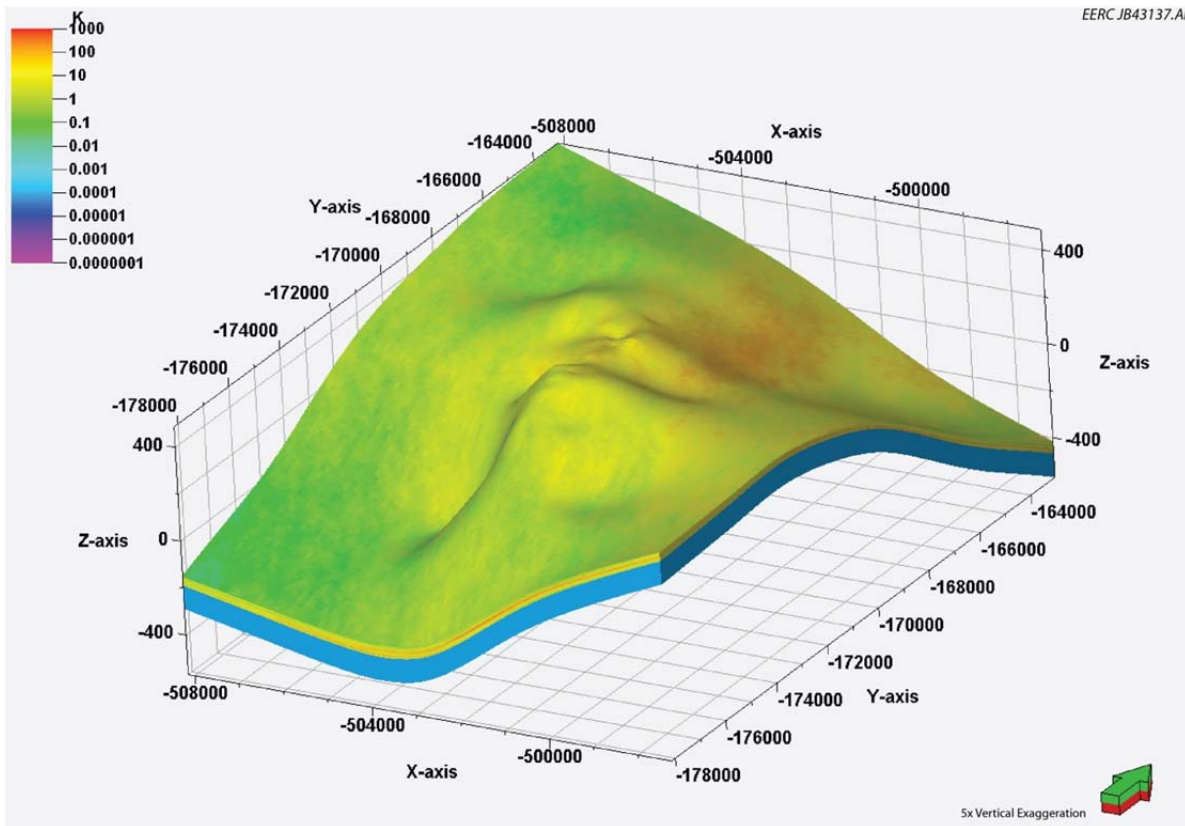


Figure 35. Three-dimensional view of the Teapot Dome Dakota model showing the permeability attribute. Cap rock units have been removed to show model structure, and a 5× vertical exaggeration has been applied.

Table 19. Reservoir Properties for the Tensleep Formation Within the Teapot Dome Model

Property	Value	Source
Effective Porosity	3.7%–16.7%	Curry, 1977
Permeability	1–591 mD	Curry, 1977
Thickness (average)	75 m	RMOTC, 2007
Depth (structure top)	1900 m	RMOTC, 2007
Temperature (average)	93.3°C	Milliken, 2007
Pressure (average)	17,200 kPa	*
CO ₂ Density	425.48 kg/m ³	MIT, 2011
Variogram Range (long)	529	IEAGHG, 2009
Variogram Range (short)	144	IEAGHG, 2009
TDS	2900–3200 ppm	RMOTC, 2011

* From gradients based on data from Curry (1977).

Table 20. Reservoir Properties for the Dakota and Lakota Formations Within the Teapot Dome Model

Property	Value	Source
Effective Porosity	0%–25.3%	IEAGHG, 2009
Permeability	0.4–319 mD	IEAGHG, 2009
Thickness	40 m	RMOTC, 2007
Depth (structure top)	1450 m	RMOTC, 2007
Temperature	65.5°C	*
Pressure	~11,000 kPa	*
CO ₂ Density	163.23 kg/m ³	MIT, 2011
Variogram Range (long)	6792	IEAGHG, 2009
Variogram Range (short)	1852	IEAGHG, 2009
TDS	9500 ppm	RMOTC, 2011

* From gradients based on data from Milliken (2007).

wells used in the models were a combination of existing wells in the field and hypothetical wells based on the geologic structure and geology for these scenarios.

Case Study Simulation Results

The Dakota/Lakota Formation was the primary target for hypothetical large-scale injection at Teapot Dome, which consisted of seven dynamic simulations which investigated a base case and various extracted water scenarios (Table 21). A base injection target of 1 megatonne per year was used for the site, which would be injected through one injection well. Downhole pressure constraints would limit this high value with the expectation that extracted water might aid in pressure management, and boundary conditions were considered semiclosed using high-volume super cells at model borders. The baseline simulation (Case 1) without extracted water resulted in a total storage capacity of 5.2 megatonnes for the site over 25 years, which is significantly lower than the injection target.

Case 2 was run using two CO₂ injection wells to look at injection scale-up and resulted in 7.6 megatonnes of CO₂ storage for the site over 25 years, resulting in an approximately 50% increase in storage capacity. This poor scale-up is likely due to a combination of poor reservoir quality and pressure interference between the closely spaced injectors. In Case 3, one of the injectors was replaced by a water extraction well and resulted in a storage capacity of 11.1 megatonnes, more than doubling the single injection well results. Further, these results indicate that, in these cases, an injection–extraction well pair makes more efficient use of the reservoir pore space than utilizing two injection wells.

An alternative for increasing storage capacity is using horizontal wells in place of vertical wells. In Case 4, two 1-km-long horizontal wells were utilized: one for injection and one for water extraction. This case resulted in 19.1 megatonnes of storage capacity, nearly doubling the capacity of using a vertical well pair. In addition to increasing the storage capacity, the plume

Table 21. Case Scenarios and Resulting Storage Capacities for Teapot Dome

Scenario	Well Configuration	Gas Injection Rate/Well, kg/day	Water Production Rate/Well, m ³ /day	Storage Capacity, megatonnes
Case 1 (base case)	1 injector	565,128	NA	5.2
Case 2	2 injectors	836,848	NA	7.6
Case 3	1 injector 1 extractor	1,212,810	1657	11.1
Case 4	1 horiz. injector 1 horiz. extractor	2,090,498	6701	19.1
Case 5	2 horiz. injectors	1,953,238	N/A	17.8
Case 6 (surface dissolution)	1 horiz. injector 1 horiz. extractor	N/A	6346	0.56
Case 7 (surface dissolution)	1 injector 1 extractor	N/A	1599	0.15

size increased by 44% from Case 3 to Case 4 (Figure 36) with an associated drop in overall reservoir pressure (Appendix F). For comparison, Case 5 was run with two 1-km-long horizontal injection wells instead of an injector–extractor pair and resulted in 17.8 megatonnes of storage capacity over the 25-year injection period, which was about 7% less storage. The results from these five cases indicate that storage capacity can be further improved by utilizing injection–extraction pairs rather than by adding more injectors.

Simulations also examined the potential for surface water saturation using extracted water followed by injection of the CO₂ saturated stream. Because of the low salinity of fluids at Teapot Dome, it was found that this technique could result in a capacity of 0.15 megatonnes over a 25-year period utilizing vertical wells (Case 7). This value was increased by utilizing horizontal wells, resulting in storage capacity of 0.56 megatonnes (Case 6). While these numbers are significantly less than free-phase injections, they are still potential candidates because of reductions in MVA cost and increased storage security. Using the single well pairs in Cases 6 and 7, it was determined that in order to reach an injection rate of 1 megatonne a year using surface dissolution, approximately 170 wells (85 injection–extraction vertical well pairs) or approximately 44 wells (22 injection–extraction horizontal well pairs) would be required using vertical or horizontal wells, respectively. Because of the large number of wells required, even with reduced MVA costs, it is unlikely that surface dissolution is a viable option at the Teapot Dome site.

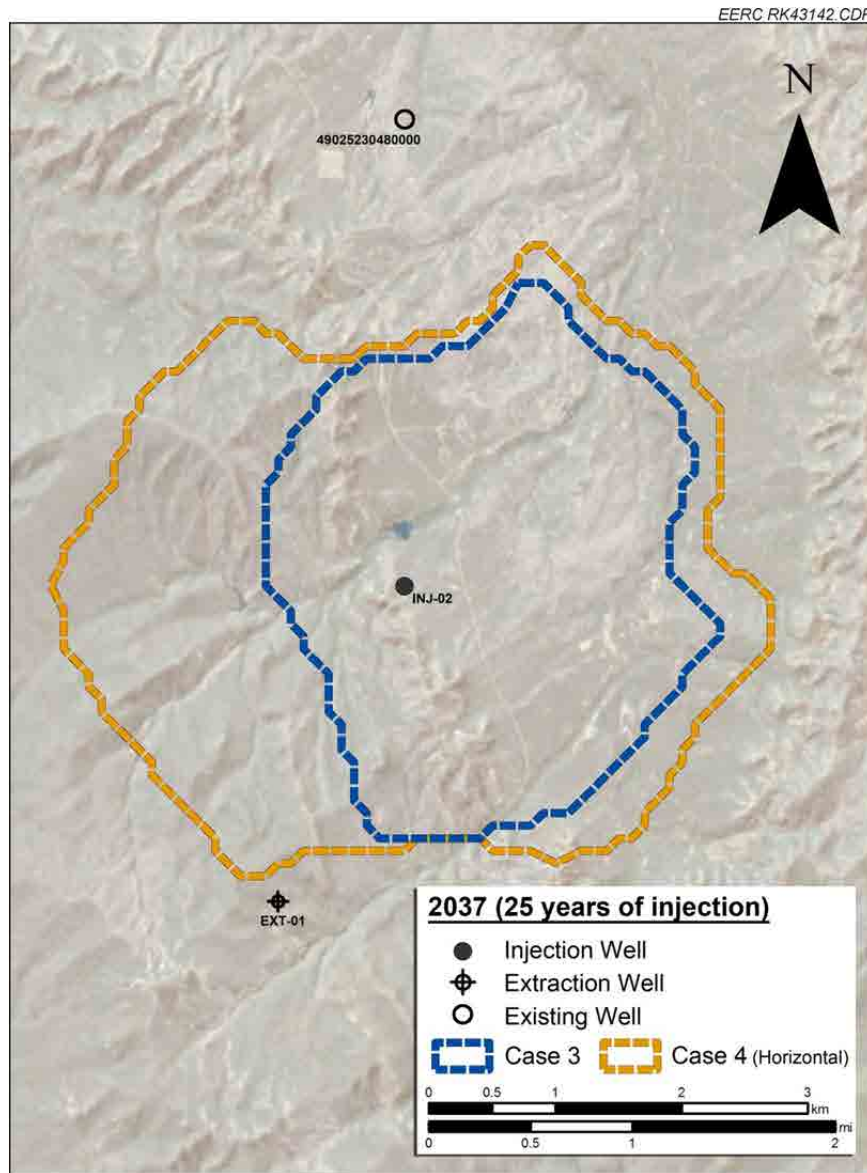


Figure 36. Plume distribution of Teapot Dome Cases 3 and 4 illustrating the effects on plume size from the utilization of horizontal and vertical extraction wells.

Simulations at the Teapot Dome site indicate that water extraction can have an impact on carbon storage capacity, reservoir pressure, and plume management. Utilization of an injection extraction well pair resulted in increased storage capacity over the use of a single injection well or pair of injection wells. Water extraction also strongly influenced reservoir pressures and plume migration. Although the overall size of the plume was not decreased with these simulations, eastward migration of the plume was reduced over the base case. The large plume was also thinner and exerted less pressure on the overlying cap rock. It is expected that extraction could be designed to reduce overall plume size at this site as well.

Surface Dissolution

Operational concerns for surface dissolution are not trivial. Dissolution of CO₂ into water at high pressure would require the use of high-pressure equipment made of corrosion-resistant materials. These materials must be resistant to both wet CO₂ and high-salinity waters. Other operational concerns are associated with water production/extraction from the reservoir for on-surface dissolution. In the course of handling the water, it will be passed through a range of pressures and temperatures which will allow for the release of dissolved gases, the precipitation of dissolved solids, and the formation of scales. Scale and precipitate formation potentials were calculated for each water and are presented in Table 22 along with the rest of the summarized CO₂ dissolution results. Only the low-salinity Teapot Dome water showed no potential for scale formation either in the production wellbore or in the formation. Scale formation in the production wellbore is an issue commonly of concern in oil and gas production and even in some water production wells. The most common approach used to overcome wellbore scale and corrosion problems is the use of chemical corrosion and scale inhibitors.

Table 22 compares formation water parameters for four sites: Gorgon, Ketzin, Zama, and Teapot Dome. For Ketzin and Zama, the model estimates that mineral precipitation or scaling might occur in the wellbore at certain pressure and temperature conditions. During the CO₂ dissolution in produced water at the surface, the precipitation of sulfate minerals and desalination might become a concern. In addition, highly saline waters/brines, such as those from Ketzin and Zama, are highly corrosive to wellbore steels, pipelines, and other equipment.

Dissolution of CO₂ into formation water that has been pumped to the surface does not appear to be a viable method of storing CO₂. The amount of CO₂ that can be dissolved is a fraction of the amount of supercritical CO₂ that can be stored in the same volume. It may be possible to use this approach for storage in more shallow formations where the pressure is subcritical for CO₂; however, with decreasing pressure comes decreasing solubility of CO₂; thus less CO₂ can be dissolved into the shallower saline waters.

Risk minimization is essential in the CO₂ capture and storage industry; any issues associated with wellbore and equipment integrity must be rigorously addressed, possibly at great expense. The corrosiveness of the acidic CO₂-containing brine stream could require the use of expensive alloys rather than carbon or even stainless steel, or at the very least, the use of corrosion inhibitors and/or coatings. Mineral precipitation, scaling, or desalination could cause significant operational issues. Assuming that all of the safety and operational concerns could be cost-effectively addressed, application of this approach would probably be limited to sites with lower salinity and higher-pH waters.

Evaluation of Water Management Options (with desalination cost estimates)

Extracted water management options for Teapot Dome include:

1. Reinjection of the extracted water into a geological formation.

Table 22. Comparison of Water Parameters for Four Potential CO₂ Injection Sites

	Gorgon		Ketzin	Zama	Teapot Dome Inj 1 ¹
	High Salinity	Low Salinity			
Temperature Used for Surface Dissolution, °C	120	140	40	60	100
Pressure Used for Surface Dissolution, bar	200	250	50	150	200
CO ₂ Density ² at Limit Pressure, kg/m ³	390	429	116	562	461
pH (surface, 25°C, 1 atm)	9.7		6.7	7.2	7.93
pH (in reservoir)	7.2		5.4	5.4	6.4
pH (after dissolution without minerals)	5.2		3.3	3.3	3.6
pH (after dissolution with minerals)	6.4		5.2	4	5.1
TDS (formation)	39,311	7096	230,263	180,163	3400
TDS (surface, 25°C, 1 atm)	35,671		228,440	177,111	3200
Surface CO ₂ Dissolution, kg/m ³	79.6	92.4	16.0	8.33	92.2
Subsurface Dissolution, kg/m ³	181	187	41.4	8.55	98.7
Water Production Mineral Precipitation Wellbore Scaling Prediction					
Chrysotile, mg/L	80		None	None	None
Calcite/Strontianate/Dolomite, mg/L	2		1200	500	None
CaCl ₂ , mg/L	None		200	300	None
Water Injection Mineral Precipitation Wellbore Scaling Prediction					
Sulfate (anhydrite/gypsum), mg/L	None		500	500	None

¹ Injection Well 1 = Well 490252304800.

² CO₂ density calculated using Styrjek and Vera (1986).

2. Desalination for use as a potable or agricultural water supply with:
 - a. Disposal of brine from desalination by deep well injection.
 - b. Further treatment of the brine using ZLD methods, such as brine concentration and/or crystallization.

Reinjection of extracted water could occur into any of several overlying formations at the Teapot Dome site. Furthermore, disposal wells currently operate in the area, so the first option is considered the most cost-effective option for this report.

Water Quality at Teapot Dome

Several saline reservoirs are present at the Teapot Dome site. The one selected for water extraction in all of the scenarios studied is the Dakota Formation, which has a salinity of 9260 mg/L at a temperature of 72.8°C (163°F) (Rocky Mountain Oilfield Testing Center, 2009). Hydrocarbons are present in this water, but it is assumed that produced waters would be relatively clean through decades of production or that hydrocarbons would be economically removed prior to water use. Furthermore, a salinity of 10,000 mg/L will be used for the desalination calculations.

The rate of water extracted for the simulations at Teapot Dome varied between approximately 1700 m³/day for Cases 3 where the duration of water extraction was the full 25 years of the injection period to values near 7000 m³/day for Case 5 where water extraction was stopped after 7 years because of CO₂ breakthrough. These water extraction rates were converted to the observed rate of water extraction per megatonnes/year of CO₂ injected (Table 23).

These flow rates were used to develop a table of flow rates for the two cases for CO₂ injection rates of 1, 2, 4, and 8 million tonnes/year based on the assumption that a large CO₂ storage project might be possible at Teapot Dome. The saline source water flow rates are given in Table 24.

Simulations of RO-based water treatment were performed using DEEP 4.0 from the IAEA. The purified water yield from the 10,000 mg/L TDS brine was estimated to be 83% at a feed pressure of 69 bar and a feed temperature of 40°C. The purified water was calculated to have a salinity of 260 mg/L with the product brine having a salinity of 57,600 mg/L. The product water and brine flow rates are given in Tables 25 and 26, respectively.

Figure 33 shows the calculated water cost based on RO treatment versus the product water flow rate. The points for the purified water cost at minimum and maximum flow for 1, 2, 4, and 8 million tonnes/year of CO₂ injection are labeled on the plot. The range of water price ranges from \$0.97/m³ for the lowest extracted water flow rate (2600 m³/day) at the 1 million tonne/year of CO₂ injection to \$0.74/m³ for the highest extracted water flow rate (59,600 m³/day) for the 8 million tonnes/year of CO₂ injection.

Table 23. Simulated Extracted Water Flow Rates and Duration and Calculated Rate per million tonne/year of CO₂ Injection

Case	Injection Target Zone	Water Flow Design, standard conditions, m ³ /day	Water Flow Design, MGD	Water Design Period, years	Water Flow per m ³ /day at one million tonnes CO ₂ /yr
Case 3	Dakota	1687	0.45	25	3811
Case 4	Dakota	6845	1.81	7.1	8971

Table 24. Range of Water Flow Rates (m³ of water/day) for 1, 2, 4, and 8 Mt/yr CO₂ Injection

Case	1 Mt/yr	2 Mt/yr	4 Mt/yr	8 Mt/yr
3	3811	7622	15,423	30,486
4	8971	17,942	35,885	71,769

Table 25. Range of Treated Water Flow Rates (m³ of water/day) for 1, 2, 4, and 8 Mt/yr CO₂ Injection

Case	1 Mt/yr	2 Mt/yr	4 Mt/yr	8 Mt/yr
3	3163	6326	12,652	25,304
4	7446	14,892	29,784	59,568

Table 26. Range of Brine Concentrate Flow Rates (m³ of water/day) for 1, 2, 4, and 8 Mt/yr CO₂ Injection

Case	1 Mt/yr	2 Mt/yr	4 Mt/yr	8 Mt/yr
3	648	1296	2591	5183
4	1525	3050	6100	12,201

Local estimates of water supply costs were acquired for comparison. The public water supply in this region of Wyoming comes from the Central Wyoming Regional Water System (CWRWS). The City of Casper Water Utility is a major member of the CWRWS and most of the water provided by the system comes from the Casper area, including the North Platte River and well fields near the North Platte River. The capacity of the treatment plant that used river water as the raw water source is 87,000 to 94,600 m³/d (23 to 25 MGD). The well field production capacity is 45,000 to 53,000 m³/d (12 to 14 MGD). The city of Casper, Wyoming, has a city population of 55,316 with a total metro population of 75,450. Assuming a generalized 100 gallons/person/day water usage rate, the total municipal water use for the Casper area would

be 28,600 m³/day (7000 MGD). Monthly rates for the Casper Water Utility for 2011 are (City of Casper, 2011) as follows:

- Water (inside city limits):
 - \$7.05 for the first 5.68 m³ (1500 gallons) consumed (minimum monthly fee) (\$1.24/m³)
 - \$3.17 for every 3.79 m³ (1000 gallons) of water consumed thereafter (\$0.56/m³)
- Water (outside city limits):
 - \$8.45 for the first 5.68 m³ (1500 gallons) consumed (minimum monthly fee) (\$1.49/m³)
 - \$4.11 for every 3.79 m³ (1000 gallons) consumed thereafter (\$0.72/m³)

The estimated cost of treating the extracted Dakota aquifer water (assuming no cost for removal of hydrocarbons) is less than the standard base rate of water in this area but greater than the rate charged per unit of water above the monthly minimum of 5.68 m³ (1500 gallons), which is 0.19 m³/day (50 gallons/day).

Brine Treatment

Two RO reject brine treatment scenarios were considered. One involved recovery of additional water from the 55,600 mg/L RO reject brine using a brine concentrator. The second involved the use of a brine concentrator followed by treatment of the 250,000 mg/L TDS brine concentrator reject in a crystallizer. Costs associated with the disposal of waste brine and/or solid wastes are not included. The analysis was performed using capital cost and energy use estimates provided in Mickley (2006). The RO reject brine flow rates considered are those for the minimum and maximum extracted water flow rates (648 to 1525 m³/day) associated with a 1-million-tonne/year CO₂ injection. Table 27 provides the details from the cost and energy use analysis. The capital cost for the low-flow conditions were estimated to be \$2.10 million and \$4.35 million for the brine concentrator only and combined brine concentrator/crystallizer situations, respectively. The similar situations for the high-flow-rate cases had capital costs of \$3.5 million and \$9.5 million. The low-flow conditions require 0.6 MW of power for the brine concentrator and 1.0 MW of power for the combined brine concentrator plus crystallizer. For the high flow rate of extracted water, the power requirements are 1.45 and 2.95 MW.

Costs per unit of water treated and per unit of purified water produced were estimated to be slightly higher for the higher-flow conditions, but the difference is small enough to be considered negligible. The lowest cost of water treatment was \$2.67/m³, which was for the low flow with use of only the brine concentrator. The higher water treatment cost was \$5.50/m³ for the high-flow combined treatment system. The range of costs based on purified water production was \$3.42/m³ to \$5.61/m³.

Given the probable high availability of deep well injection disposal resources in the Teapot Dome region, it is unlikely that the extra effort would be made to recover only an additional 15% to 20% more purified water when the per unit cost of obtaining that extra water is 2.84 to 5.38 times the water obtained from the RO process.

Table 27. Costs and Energy Use Estimates for Teapot Dome RO Reject Brine Treatment Options

	Teapot Dome (RO reject brine)			
	Brine Concentrator Only		Combined Treatment	
	Teapot Dome-1	Teapot Dome-2	Teapot Dome-1	Teapot Dome-2
Flow Rate, MGD	0.17	0.40	0.17	0.40
Reject Level of Unit	22%	22%	22%	22%
Concentrator Reject/Feed to Crystallizer, MGD ²			0.04	0.09
Feed to Crystallizer or Waste Brine Flow Rate, gpm ²			26.1	61.5
Capital Cost of Installed Concentrator, \$ million	210E+06	3.50E+06	2.10E+06	3.50E+06
Capital Cost of Installed Crystallizer, \$ million			2.10E+06	3.50E+06
Energy Usage for Concentrator, kW	600	1450	600	1450
Energy Usage for Crystallizer, kW			370	750
Cost of Electricity, \$/kWh	0.10	0.10	0.10	0.10
Annualized Capital Cost of Concentrator, \$	1,050,000	175,000	105,000	175,000
Annualized Capital Cost of Crystallizer, \$			112,500	150,000
Annual Energy Cost of Concentrator, \$ million	525,600	1,270,200	112,500	150,000
Annual Energy Cost of Crystallizer, \$ million			525,600	1,270,200
Total Annual Cost for One Unit, \$ million	630,600	1,445,200	1,067,220	2,252,200
Number of Concentrator Units	1	1	1	1
Number of Crystallizer Units			1	2
Brine Input, m ³ /day	493	2,036	493	2036
Cost/m ³ of Water Treated	\$2.35	\$2.39	\$4.24	\$4.32
Product Water Flow Rate, m ³ /day	385	1588	482	1991
Cost/m ³ of Water Produced	\$3.01	\$3.07	\$4.34	\$4.42
Total Capital Cost, \$ million	1.45	4.00	3.35	6.40
Total Energy Use Rate, MW	0.4	1.8	0.7	3.3

¹ Costs are in US\$.² US units required for cost curves by Mickley (2006).

Regulatory Concerns

Again, similar to Alberta and Western Australia, Wyoming produces oil and gas; therefore, the regulators as well as the general public are accustomed to dealing with subsurface issues. Wyoming has passed legislation that requires the development of rules and procedures to accommodate carbon storage projects. Those rules were promulgated by the Wyoming Department of Environmental Quality in November 2010. However, in December 2010, the U.S. Environmental Protection Agency (EPA) finalized the requirements for a new well class (Class VI) under the authority of the Safe Drinking Water Act's Underground Injection Control (UIC) Program. The rule establishes federal requirements for the underground injection of CO₂ for the purpose of long-term underground storage, or geologic storage. In the final rule, EPA gave states a deadline of September 6, 2011, to apply for primary enforcement responsibility, or primacy, over Class VI wells. No states met this deadline; therefore, as of September 7, 2011, EPA will directly implement the Class VI Program nationally. As a result, in order to permit a CO₂ geologic storage project, potential owners or operators of a CO₂ geologic storage well will need to submit a permit application to the appropriate EPA regional office (Region 8 for Wyoming). Direct federal implementation of the Class VI program will remain in effect until such time that a state-submitted primary enforcement responsibility (primacy) application is approved by EPA.

While the Class VI rule does not regulate reservoir pressure maintenance options, it does provide evidence that the United States is looking to carbon storage as an option to mitigate greenhouse gas emissions.

While Wyoming does not currently have primacy to regulate carbon storage through the Class VI well program, the state does have primacy to regulate Class II – Oil- and Gas-Related Injection Wells. This includes disposal wells. In order to obtain a permit for brine disposal via underground injection, certain conditions must be met. An injection application must include maps of existing and proposed wells, information on the injection formation, casing and testing program, injection water source and makeup, operating parameters, and an analysis of the mechanical integrity of wells within the radius of investigation. Public notice is also required (Wyoming Oil and Gas Conservation Commission, 2011).

Teapot Dome Summary

The Teapot Dome case study site contains sandstone and limestone reservoirs with high-quality formation water and excellent properties for large-scale CO₂ injection and storage. A long history of oil production from the region means reservoir data were available to help develop the hypothetical CO₂ storage scenarios. Simulations evaluated both the potential of injection with water extraction and injection of CO₂ saturated formation water. Storage capacity was nearly doubled with the addition of a water extraction well for both the vertical and horizontal well pair configurations. The injection–extraction well pairs also outpaced the two injection well pairs in both the vertical and horizontal well simulations, although only by a small margin. Injection of dissolved CO₂ was shown to be possible at this site, but not effective for the large volume of CO₂ set as the simulation goal for this report.

Water extraction was also found to be useful as a tool for pressure management and plume control at this site, although the simulations were not optimized for this purpose and it is likely that additional pressure reduction and plume migration influence could be achieved.

The formation water quality is reported to be below 10,000 ppm TDS, so all treatment cost calculations were conducted assuming this figure. Treatment costs for desalination of this formation water were found to be competitive with local water supplies and could be improved if flow rates were eventually scaled up to the equivalent of injecting 4 million tonnes of CO₂ per year. While sustainability concerns need to be addressed, the dry local climate and increasing local industrial activity make the beneficial use of extracted water at the Teapot Dome site a viable and realistic opportunity should such a project ever be undertaken.

There do not appear to be any significant regulatory barriers to development of a large-scale CO₂ injection project with formation water extraction at the Teapot Dome site, as a wide variety of water injection and extraction projects are currently carried out for various domestic and commercial purposes.

CONCLUSIONS AND RECOMMENDATIONS

The case study sites were selected to represent a wide range of geological, geographical, and geopolitical conditions which may impact the ability to implement an extracted water plan in conjunction with commercial-scale CO₂ storage projects. In most cases, data necessary to build 3-dimensional, representative, heterogeneous geologic models were available from the literature, although some data ranges were supplemented from the AGD. The Zama site was included specifically as an example of a closed system to contrast with the other sites. Although the single pinnacle structure modeled is too small by itself to accommodate commercial-scale storage, the presence of nearly 700 structures of similar size and characteristics allows for estimations to be readily scaled up to commercial levels. Dynamic simulations were carried out on each of the modeled reservoirs to test the applicability and influence of water extraction on storage capacity, plume management, and extracted-water generation. Additional runs were used to investigate the potential application of surface dissolution prior to injection under reservoir conditions.

Water extraction rates were set with a goal of producing a volume of water equal to the volume of CO₂ that was injected. This is especially important in closed reservoirs such as Zama, as it removes the existing fluids and creates additional space for injected CO₂ to inhabit, rather than relying on the less effective compressibility dynamic. In open systems, the extracted water can be used for pressure maintenance and plume management as well (in the case of Gorgon) or to otherwise enhance operations. This process may also reduce MVA costs as well as increase overall site security.

It was determined that water extraction does not necessarily increase the amount of injected CO₂ that may be stored. In some cases, it was observed that formation water extraction wells yielded significantly less storage capacity and efficiency than simply adding a second injection well. This is due largely to the inefficiencies in flow through the heterogeneous reservoirs.

Generally speaking, the most effective extraction scenarios increased the potential storage from 0 to nearly 1300%, although in every simulated case, it was found that additional injection wells were able to increase injectivity (and, therefore, capacity) as well. The greatest capacity gains were observed in the closed system (Zama) where capacity was increased 13-fold. While 1:1 ratios of water extracted to CO₂ injected could be achieved, in the majority of the cases, this ratio was higher, as much as 4:1.

The influence of water extraction on the migration of pressure and free-phase CO₂ plumes was observed in each of the open-system sites. However, this influence was moderated by other factors such as geologic structure and local reservoir heterogeneities. The utilization of water extraction for the purposes of reservoir management are best applied to reservoirs with low-structural control.

Relatively steady rates of water extraction could be achieved through various changes in injection–extraction rates and well placement, but this typically resulted in smaller total storage volumes. However, the need to prioritize steady rates of water extraction is only high priority when treatment and beneficial use of the water can be developed.

CO₂ Storage Benefit Derived from Water Extraction

Extracting water from a CO₂ storage reservoir was observed to have variable effects based on the specific nature of reservoir rock and reservoir boundary conditions, as well as operational factors such as injection/extraction management and placement of wells. The assumption of achieving a 1:1 ratio of injected CO₂ to extracted water was generally appropriate for increasing CO₂ storage capacity. However, in order to perform pressure or plume management tasks, the volume of water which must be removed from the reservoir was found to be four or more times greater in some cases.

As a tool for increasing storage capacity, formation water extraction was generally found to be effective, although each hypothetical case study site reacted differently to its implementation. The most dramatic results were found in the closed reservoir simulations from the Zama site, where storage capacity could be increased by nearly 1300% in a single pinnacle reef structure with proper well placement. Although individually small, capable of holding approximately 690,000 tonnes of CO₂, the Zama Field has hundreds of similar structures, which could be developed in the same way to meet the 1-million-tonne/yr injection goal. The site with the least capacity impact resulting from water extraction was the Gorgon site. Injectivity at this site is such that the hypothetical injection simulations were far below the volumes required to fill the reservoir and necessitate formation water extraction. However, even though water extraction had essentially no impact on potential storage capacity, it was still found to influence plume behavior and pressure propagation in such a way as to be useful for plume management.

Simulations of hypothetical injections at the Ketzin and Teapot sites showed potential CO₂ storage capacity increases of approximately double (197% and 204%, respectively) from formation water extraction. In each of these cases, capacity and the relative influence on plume behavior could be enhanced by modifying the injection scheme. The Ketzin simulations initially showed that two CO₂ injection wells outperformed an injection extraction pair. However, it was

found that if the number of wells were substantially increased to a 25-spot well pattern, the combination of 12 injection and 13 extraction wells outperformed 25 injection wells by 123% and did so while removing approximately half as much water (by volume) as CO₂ injected. At the Teapot Dome site, it was found that use of horizontal well pairs could further increase the impact of water extraction and increase the CO₂ storage capacity. Overall capacity was increased by 367% over the base case single vertical injection well and thus represents an additional 163% increase over the injection extraction pair. In both these cases, optimizing simulations to achieve pressure maintenance or plume management generally resulted in decreased reservoir storage capacity with a significant increase in the volume of extracted water. The results of these four case studies illustrate the wide range of results that may be possible and that geologic and reservoir engineering factors may both have a large influence on the final results. It can also be said that if it is feasible to utilize a large number of injection and extraction wells, overall storage may be increased by a large margin, even in high-quality storage reservoirs.

Extracted Water Use

The treatment of extracted water for beneficial use is technically achievable. Treatment technologies and systems exist or can be designed to manage the volumes and rates of extracted water that may be derived from storage activities. However, it is highly unlikely that any extracted water would be put to beneficial use for CO₂ storage locations that are offshore or in coastal areas. The potential cost savings for use of an extracted water in place of seawater for desalination appears to be too small, even for a salinity as low as 10,000 mg/L TDS, to justify use of the extracted in place of the seawater. Use of the extracted water would likely place greater uncertainties on supply, as ocean sources would be more reliable and longer-term than CO₂ storage projects.

In higher TDS locations, it is also unlikely that extracted water would be purified. While technologies exist to treat brines with the encountered range of dissolved solids, the cost associated with treatment and implementation would likely be too high to justify. Treatment and beneficial use may be feasible under certain conditions: likely a combination of low-to-moderate extracted water quality, availability of inexpensive energy, and sufficient local water demand. Of the case study sites, the best candidate for treatment and use of extracted water was the Teapot Dome site, where estimated treatment costs were comparable to that of local water supplies. While an uninterrupted sustainable supply is required for municipal supplies, extracted water could be a supplemental supply, particularly during periods of prolonged drought.

Surface Dissolution of CO₂

Surface dissolution involving the extraction of reservoir fluid, saturation with CO₂, and subsequent reinjection is unlikely to be a viable option in most situations as the capacity of produced fluids to dissolve and carry CO₂ is too low. It is unlikely that this scenario will ever be able to compete with direct injection for storage of commercial-scale volumes of CO₂.

Regulatory Situation Concerning Water Extraction

Existing regulations were not found that impose barriers to the development of water extraction as part of reservoir management operations nor for the development of procuring additional water resources. While regulations are not in place to specifically deal with brine injection related to CCS projects, disposal of brine solutions is occurring all over the world in relation to other industrial practices. The oil and gas industry has developed and successfully implemented operational practices to handle the disposal of large volumes of brine safely and effectively. Over the course of several decades, brines and other fluids associated with the production of oil and gas operations have been injected into wells in a variety of geologic settings throughout the world. Regulatory authorities and industry have developed best management practices and regulatory processes that have allowed for the safe disposal of brine into the deep subsurface. It would seem these practices and regulations would not pose a significant threat to the development of CO₂ storage projects managed with extracted water.

Recommendations

Several areas of additional and continued research should be addressed to forward the utility extracting formation water in conjunction with CO₂ storage projects. They are as follows:

- Collect detailed water quality data for potential CO₂ storage targets, and develop a global database. This will aid in identifying targets with strong beneficial use potential and estimating the costs of water management strategies.
- Evaluate potential CO₂ capacity gains through additional site-specific research in order to increase known impacts of formation water extraction on CO₂ capacity.
- Evaluate additional strategies of CO₂ plume management using formation water extraction through detailed modeling and simulation activities. Evaluations of this type will help expand the knowledge of potential benefits of water extraction.
- Optimize injection simulation scenarios based on the distances between CO₂ injection and water extraction wells, using site-specific data, as opposed to optimizing the number of wells and/or their locations as was done in this study.
- Integrate additional chemical and physical phenomena, such as geochemical reactions and geothermal effects, into dynamic modeling simulators. Such integration will improve the comprehensive understanding of the storage–extraction system and provide more accurate estimations of storage potential and the utility of extracted formation water. This may be especially beneficial for evaluating cases of surface dissolution, where geochemical reactions are of a more immediate concern.
- Develop improved and more efficient methods of dissolving CO₂ directly into extracted water at the surface. This could lead to an increased utility of surface dissolution and help more projects realize the potential benefits, such as reduced MVA costs.

- Develop efficient mechanisms to link potential sources of extracted formation water to potential users of treated extracted water. Once water is recognized as applicable for beneficial use, identify water supply shortages or bottlenecks in order to evaluate the economic benefit of the possible beneficial uses.
- Reduce the costs of extracted formation water treatment in order to increase the potential sources of extracted water that may be applied toward beneficial uses. Cost reductions may be found through improved technology, materials, or process efficiency.
- Conduct additional research to understand the economic benefits of formation water extraction on a site-specific basis. In particular, investigate how the benefit of increased storage capacity relates to the increased costs of the additional infrastructure required (additional wells, treatment facilities, etc.).
- Conduct additional research to evaluate the MVA cost savings associated with extracted water reservoir management versus the cost of the additional infrastructure required.
- Identify reservoir characteristics that may inherently enhance the effectiveness of formation water extraction strategies. This could lead to more effective usage of known and future storage targets.
- Develop formulaic methodology to estimate CO₂ storage capacity specific to the use of formation water extraction as a reservoir management strategy. This would allow for rapid assessment of the benefits of extraction on known and future CO₂ storage targets.

REFERENCES

- Alberta Energy, 2011, www.energy.alberta.ca/Initiatives/1438.asp (accessed November 2011).
- Birkett, J., 2011, Desalination at a glance: International Desalination Association. www.idadesal.org/pdf/IDA%20guide_webonly.pdf (accessed November 2011).
- Brantjes, J., 2008, Formation evaluation for CO₂ disposal: SPWLA 49th Annual Logging Symposium, Edinburgh, Scotland, May 25–28.
- Breit, G.N., 2002, Produced waters database: United States Geological Survey. <http://energy.cr.usgs.gov/prov/prodwat/index.htm> (accessed June 2011).
- Burke, L., 2009, PCOR Project—Apache Zama F pool acid gas EOR & CO₂ storage: Report prepared by RPS Energy Canada for the Energy & Environmental Research Center, September.
- Burton, M., and Bryant, S.L., 2009, Eliminating buoyant migration of sequestered CO₂ through surface dissolution—implementation costs and technical challenges: SPE Reserv. Eval. Eng., v. 12, p. 399–407.

- Buscheck, T.A., Sun, Y., Wolery, T.J., Bourcier, W., Tompson, A.F.B., Jones, E.D., Friedmann, S.J., and Aines, R.D., 2010, Combining brine extraction, desalination, and residual-brine with CO₂ storage in saline formations—implications for pressure management, capacity, and risk mitigation: Energy Procedia. www4.eventsinteractive.com/iea/viewpdf.asp?id=270025&file=\\DCFILE01\EP11%24\Eventwin\Pool\office27\docs\pdf\ghgt10Final00414.pdf (accessed June 2011).
- Cedeño, B.O.B., 2009, Economic valuation of two technologies to import water—a case study of Morocco: UNESCO-IHE Institute for Water Education, Delft, the Netherlands. www.eldis.org/vfile/upload/1/Document/0907/Economic_valuation_of_two_technologies_to_import_water_A_case_study_of_Morocco.pdf (accessed December 2011).
- Chiaramonte, L., 2008, Geomechanical characterization and reservoir simulation of a CO₂ sequestration project in a mature oil field, Teapot Dome, WY: Ph.D. Dissertation, Stanford University.
- City of Casper, 2011, City of Casper water utility 2011 rates (monthly): www.casperwy.gov/WaterBillingRates/tabid/281/Default.aspx. (accessed November 2011).
- Clark, C.E., Harto, C.B., Sullivan, J.L., and Wang, M.Q., 2011, Water use in the development and operation of geothermal power plants: Argonne National Laboratory, www1.eere.energy.gov/geothermal/pdfs/geothermal_water_use.pdf (accessed January 2011).
- CO2CRCTPL (CO2CRC Technologies Pty Ltd), 2008, A technical appraisal of the feasibility for CO₂ sequestering operations for the Gorgon Gas Field development proposal—Phase III: technical report, CO2CRC Technologies Pty Ltd, www.dmp.wa.gov.au/documents/Executive_Summary_from_Gorgon_DueDilligence_08_1028.pdf.
- CO2CRCTPL (CO2CRC Technologies Pty Ltd), 2009, A technical appraisal of the feasibility for CO₂ sequestering operations for the Gorgon gas field development proposal—Phase IV: Technical Report, CO2CRC Technologies Pty Ltd, August, www.dmp.wa.gov.au/documents/ExecSumIV.doc.
- Colombo, L., Cursan, M., Dell'Orto, L., Piccinelli, C., and Riboldi, L., 2010, Gorgon natural gas project: Norwegian University of Science and Technology, TPG 4140 Natural gas, November 2010.
- Court, B., Celia, M.A., Nordbotten, J.M., and Elliot, T.R., 2010, Active and integrated management of water resources throughout CO₂ capture and sequestration operations: Energy Procedia. www4.eventsinteractive.com/iea/viewpdf.asp?id=270025&file=\\DCFILE01\EP11\Eventwin\Pool\office27\docs\pdf\ghgt10Final00103.pdf (accessed June 2011).
- Curry, W.H., 1977, Teapot Dome—past, present, and future: American Association of Petroleum Geologists Bulletin, v. 61, no. 5.
- DesalData.com, 2011, Defining desalination: www.desaldata.com/desalination-markets-2010 (accessed November 2011).

- Doll, T.E., Luers, D.K., Strong, G.R., Schult, R.K., Sarathi, P.S. Olsen, D.K. and Hendricks, M.L., 1995, An update of steam injection operations at Naval Petroleum Reserve No. 3, Teapot Dome field, Wyoming—A shallow heterogeneous light oil reservoir: International Heavy Oil Symposium, Calgary, Alberta, Canada, Society of Petroleum Engineers Paper 30286, p. 1–20.
- Eke, P.E., Naylor, M., Haszeldine, S., and Curtis, A., 2011, CO₂/brine surface dissolution and injection—CO₂ storage enhancement: SPE Proj Fac & Const, v. 6, no. 1, p. 41–53.
- Energy in Germany, 2011, www.germanenergyblog.de/?page_id=3061 (accessed December 2011).
- Energy Resources Conservation Board, 2011: www.ercb.ca/portal/server.pt/gateway/PTARGS_0_0_323_253_0_43/http%3B/ercbContent/publishedcontent/publish/ercb_home/industry_zone/rules__regulations__requirements/directives/directive051 (accessed November 2011).
- Flett, M., Brantjes, J., Gurton, R., McKenna, J., Tankersley, T., and Trupp, M., 2009, Subsurface development of CO₂ disposal for the Gorgon Project: Energy Procedia, v. 1, Issue 1, February, p. 3031–3038.
- Flett, M., Beacher, G., Brantjes, J., Burt, A., Dauth, C., Koelmeyer, F., Lawrence, R., Leigh, S., McKenna, J., Gurton, R., Robinson IV, W., and Tankersley, T., 2008, Gorgon project—subsurface evaluation of carbon dioxide disposal under Barrow Island: SPE Asia Pacific Oil and Gas Conference, SPE 116372, Perth, Australia, October 20–22.
- Flett, M., Gurton, R., and Weir, G., 2006, Heterogeneous saline formations for carbon dioxide disposal—impact of varying heterogeneity on containment and trapping: Journal of Petroleum Science and Engineering, v. 57, nos. 1–2, 2010, p. 106–118.
- Flett, M., Gurton, R., and Taggart, T., 2004, The function of gas–water relative permeability hysteresis in the sequestration of carbon dioxide in saline formations: SPE paper 88485, Presented at the 2004 SPE Asia-Pacific oil and gas conference and exhibition, Perth, Australia, October 18–20.
- Fleury, M., Gautier, S., Gland, N., and Boulin, P., Petrophysical measurements for CO₂ storage—Application to the Ketzin site: The Society of Core Analysts, SCA News SCA2010-06, v. 22, no. 2.
- Forster, A., Norden, B., Zinck-Jorgensen, K., Frykman, P., Kulenkampff, J., Spangenberg, E., Friedmann, S.J., and Stamp, V.W., 2006, Teapot Dome—characterization of a CO₂-enhanced oil recovery and storage site in eastern Wyoming: Environmental Geosciences, v. 13, p. 181–199.
- Fountain/Quail Water Management, 2010, Aqua Pure: www.aqua-pure.com (accessed 2010).
- Fraunhofer, 2011, Shoaiba phase III—drinking water supply in Saudi Arabia: www.iosb.fraunhofer.de/servlet/is/15010/SHOAIBA-III-Saudi-Arabia.pdf.pdf?command

- =downloadContent&filename=SHOAIBA-III-Saudi-Arabia.pdf.pdf (accessed December 2011).
- Friedmann, S.J., and Stamp, V.W., 2006, Teapot Dome—characterization of a CO₂-enhanced oil recovery and storage site in eastern Wyoming: *Environmental Geosciences*, v. 13, p. 181–199.
- Fritzmann, C., Lowenberg, J., Wintgens, T., and Melin, T., 2007, State-of-the-art of reverse osmosis desalination: *Desalination*, v. 216, nos. 1–3, p. 1–76.
- Frykman, P., Zink-Jorgensen, K., Bech, N., Norden, B., Forster, A., and Larsen, M., 2006, Site characterization of fluvial, incised-valley deposits, *in* *Proceedings, CO2SC Symposium*, Lawrence Berkeley National Laboratory.
- Gaviria, G.R., 2005, Reservoir simulation of CO₂ sequestration and enhanced oil recovery in Tensleep Formation, Teapot Dome field: Master's thesis, Texas A&M University.
- GE, 2009, GE empowers Barcelona community with water quality solutions: General Electric Company. www.gewater.com/pdf/Case%20Studies_Cust/Americas/English/CS1298EN.pdf (accessed December 2011).
- Gerdes, K., and Nichols, C., 2009, Water requirements for existing and emerging thermoelectric plant technologies: DOE/NETL-402/080108. www.netl.doe.gov/energy-analyses/pubs/WaterRequirements.pdf (accessed May 2010).
- GWI, 2005, ACWA Power offers sole bid for Shoaiba: *Global Water Intelligence*, v. 6, no. 3. www.globalwaterintel.com/archive/6/3/general/acwa-power-offers-sole-bid-for-shoaiba.html (accessed December 2011).
- Harto, C.B., 2011, Extracting water from carbon sequestration projects: NETL CO₂ Storage and Water Projects WebEx, November 1, 2011.
- Henniges, J., Liebscher, A., Bannach, A., Brandt, W., Hurter, S., Köhler, S., and Möller, F., 2011, CO₂SINK Group, and two-phase fluid conditions with inverted density profile in observation wells at the CO₂ storage site at Ketzin (Germany): *Energy Procedia*, v. 4, p. 6085–6090.
- IAEA, 2011, International Atomic Energy Agency, Desalination Economic Evaluation Program (DEEP), Version 4.0, February 2011: <http://www.iaea.org/NuclearPower/Desalination/> (accessed December 2011).
- International Desalination Association, 2011, IDA desalination yearbook 2011–2012: www.desalyearbook.com/market-profile/11-global-capacity (accessed November 2011).
- IDE Technologies Ltd., 2011a, Hadera—127 million m³/year—the world's largest SWRO desalination plant: www.ide-tech.com/files/990b0fa01310a9c82f841f2183e9ebcb/page/2009/10/Hadera%20Success%20Story.pdf (accessed November 2011).

- IDE Technologies Ltd., 2011b, Ashkelon—118 million m³/year—GWI's SWRO desalination plant of the year 2006: www.ide-tech.com/files/990b0fa01310a9c82f841f2183e9ebcb/page/2009/10/Ashkelon%20Success%20Story.pdf (accessed November 2011).
- IDE Technologies Ltd., 2011c, Construction of Sorek—the world's largest sea water reverse osmosis desalination plant: www.ide-tech.com/news/construction-sorek-%E2%80%93-worlds-largest-sea-water-reverse-osmosis-desalination-plant) (accessed November 2011).
- International Energy Agency, 2008, Energy technology perspectives—executive summary: www.iea.org/techno/etp/ETP_2008_Exec_Sum_English.pdf (accessed December 2011).
- IEAGHG (IEA Greenhouse Gas R&D Programme), 2010, Pressurization and brine displacement issues for deep saline formations CO₂ storage: 2010/15, November.
- IEAGHG (IEA Greenhouse Gas R&D Programme), 2009, Development of storage coefficients for CO₂ storage in deep saline formations: 2009/13, October.
- Jain, L., and Bryant, S.L., 2011, Optimal design of injection/extraction wells for the surface dissolution of CO₂ storage strategy: *Energy Procedia*, v. 4, p. 4299–4306.
- Kempka, T., Kuhn, M., Class, H., Frykman, P., Kopp, A., Nielsen, C.M., and Probst, P., 2010, Modelling of CO₂ arrival time at Ketzin—Part I: *Elsevier International Journal of Greenhouse Gas Control*, v. 4, p. 1007–1015.
- Kestin, J. and Shankland, I.R., 1984, Viscosity of aqueous NaCl solutions in the temperature range 25–200 °C and in the pressure range 0.1–30 MPa: *International Journal of Thermophysics*, v. 5, no. 3, p. 241–263.
- Klusman, R.W., 2009, Simulation of light hydrocarbon migration in a stacked petroleum reservoir at Teapot Dome, Wyoming, with pressurization during carbon dioxide sequestration, in M. Grobe, J. C. Pashin, and R. L. Dodge, eds., *Carbon dioxide sequestration in geological media—state of the science: AAPG Studies in Geology*, v. 59, p. 571–586.
- Kopp, A., Bielinski, A., Ebigbo, A., Class, H., and Helmig, R., 2006, Numerical investigation of temperature effects during the injection of carbon dioxide into brine aquifers: GHGT 8. www.co2sink.org/publications/GHGT8_IWS_UniStuttgart.pdf (accessed June 2011).
- LeBeau, J., 1996, Preliminary geological characterization of the Dakota Formation, Naval Petroleum Reserve 3, Midwest, Wyoming, RMOTC/Halliburton multilateral test, October 1996: *Rocky Mountain Oilfield Technology Center Internal Report*, 25 p. plus appendices.
- Lengler, U., De Lucia, M., and Kühn, M., 2010, The impact of heterogeneity on the distribution of CO₂—numerical simulation of CO₂ storage at Ketzin: *International Journal of Greenhouse Gas Control*, v. 4, no. 6, p. 1016–1025.

- Leonenko, Y., and Keith, D.W., 2008, Reservoir engineering to accelerate the dissolution of CO₂ stored in aquifers: *Environ. Sci. Technol.*, v. 42, p. 2742–2747.
- Leonhard, L., October 2011, personal communication with Lazarus Leonhard, Senior Hydrogeologist, Midwest Gascoyne Region, Department of Water, Western Australia.
- Li, Y.-K. and Nghiem, L.X., 1986, Phase equilibria of oil, gas and water/brine mixtures from a cubic equation of State and Henry's Law: *Can. J. Chem. Eng.*, v. 64.
- Lokiec, F., and Ophir, A., 2007, The mechanical vapor compression—38 years of experience: IDA World Congress, Maspalomas, Gran Canaria, Spain, October 21–26, 2007. www.ide-tech.com/files/990b0fa01310a9c82f841f2183e9ebcb/newsevent/2009/10/MVC%2038%20years%20of%20experience.pdf (accessed December 2011).
- Martens, S., Liebscher, A., Möller, F., Würdemann, H., Schilling, F., and Kühn, M., 2010, Ketzin Group, Progress report on the first european on-shore CO₂ storage site at Ketzin (Germany)—second year of injection: *Energy Procedia*, v. 4, p. 3246–3253.
- MIT (Massachusetts Institute of Technology), 2011, Gorgon fact sheet: carbon dioxide capture and storage project: <http://sequestration.mit.edu/tools/projects/gorgon.html>, date modified: November 23, 2011 (accessed November 2011).
- Mickley, M., 2009, Treatment of concentrate: U.S. Department of the Interior, Bureau of Reclamation, Technical Service Center, Water Treatment Engineering and Research Group, Denver.
- Mickley, M., 2006, Membrane concentrate disposal: practices and regulation (2nd ed.): U.S. Department of the Interior, Bureau of Reclamation, Technical Service Center, Water Treatment Engineering and Research Group, April: www.usbr.gov/pmts/water/media/pdfs/report123.pdf (accessed December 2011).
- Milliken, M., 2007, Geothermal resources at Naval Petroleum Reserve 3 (NPR-3) Wyoming, *in* Proceedings, Thirty-Second Workshop on Geothermal Reservoir Engineering Stanford University: Stanford, California, January 22–24, 2007, <http://pete.stanford.edu/ERE/pdf/IGAstandard/SGW/2007/millike.pdf>.
- NATCARB, 2011, Brine database: <http://www.natcarbviewer.org/brine/> (accessed December 2011).
- National Research Council, 2008, Desalination, a national perspective: Committee on Advancing Desalination Technology, National Research Council, National Academies Press. www.nap.edu/catalog/12184.html.
- Newmark, R.L., Friedmann, S.J., and Carroll, S.A., 2010, Water challenges for geologic carbon capture and sequestration: *Environmental Management*, February.

- NOAA, 2011, World ocean atlas 2009: www.nodc.noaa.gov/OC5/WOA09F/pr_woa09f.html (accessed December 2011).
- Norden, B., Förster, A., Vu-Hoang, D., Marcelis, F., Springer, N., and Le Nir, I., 2010, Lithological and petrophysical core-log interpretation in CO₂SINK, the European CO₂ onshore research storage and verification project: SPE Res Eval & Eng, v. 13, no. 2, p. 179–192.
- Norden, B., Förster, A., Vu-Hoang, D., Marcelis, F., Springer, N., and Le Nir, I., 2008, Lithological and petrophysical core-log interpretation in CO₂SINK, the European CO₂ onshore research storage and verification project: SPE 115247, SPE Asia Pacific Oil and Gas Conference and Exhibition, Perth, Australia, October 20–22.
- Osmoflow, 2010, Osmoflo providing desalination to Gorgon Project: www.osmoflo.com/library/Gorgon%20Update%20Sept%202010.pdf (accessed December 2011).
- Phillips, J., 2011, Water use impacts of CO₂ capture, *in* Shi, J., 2011, RFI informational webcast: Electric Power Research Institute (EPRI). http://mydocs.epri.com/docs/publicmeetingmaterials/1102/PublicWebcast/RFI_Webcast_Recording_Details_2011-03-02.pdf accessed May 2011.
- Prevedel, B., Wohlgemuth, L., Henninges, J., Krüger, K.C., Norden, A., and Förster, A., 2008, The CO₂ sink boreholes for geological CO₂-storage testing: Scientific Drilling, no. 6, p. 32–37.
- Prevedel, B., Wohlgemuth, L., Legarth, B., Henninges, J., Schütt, H., Schmidt-Hattenberger, C., Norden, B., Förster, A., and Hurter, S., 2009, The CO₂SINK boreholes for geological CO₂-storage testing: Energy Procedia, v. 1, no. 1, p. 2087–2094.
- Rocky Mountain Oilfield Testing Center (RMOTC), 2011, Reservoir data—Rocky Mountain Oilfield Testing Center (RMOTC)—NPR-3/Teapot Dome: U.S. Department of Energy.
- Rocky Mountain Oilfield Testing Center (RMOTC), 2007, NPR-3 well data set: U.S. Department of Energy.
- Rowe, A.M. and Chou, J.C.S., 1970, Pressure–volume–temperature–concentration relation of aqueous NaCl solutions, J. Chem. Eng. Data, v. 15, no. 1, 1970, p. 61–66.
- Sandia National Laboratories, 2005, Addressing our global water future: Center for Strategic and International Studies, Washington D.C., September. 134 p. http://csis.org/files/media/csis/pubs/050928_gwf.pdf (accessed June 2011).
- Schembre-McCabe, J.M., Kamath, J., Gurton, R., Mechanistic studies of CO₂ sequestration, International Petroleum Technology Conference, IPTC 11391, Dubai, UAE, December 4–6, 2008.

- Schilling, F., Borm, G., Würdemann, H., Möller, F., and Kühn, M., 2009, CO₂ SINK Group, Status report on the first European on-shore CO₂ storage site at Ketzin (Germany): *Energy Procedia*, v. 1, no. 1, p. 2029–2035.
- Smith, V., 2008, Modeling natural fracture networks—establishing the round work for flow simulation at Teapot Dome, Wyoming: Master's thesis, West Virginia University.
- Stepan, D.S., Shockey, R.E., Kurz, B.A., Kalenze, N.S., Cowan, R.M., Ziman, J.J., and Harju, J.A., 2010, Bakken water opportunities assessment—Phase 1: University of North Dakota Energy and Environmental Research Center, Northern Great Plains Water Consortium, April 2010.
- Talman, S., and Perkins, E., 2009, Geochemical modeling of acid gas injection with reference to the Zama 08-33-115-6W6 Well: March 2009 Report for Carbon Energy Management, Alberta Research Council, Edmonton, Alberta.
- Trupp, M., 2011, e-mail message to authors, July 17.
- URS Australia, 2002, Economic and technical assessment of desalination in Australia—with particular reference to national action plan priority regions: Agriculture, Fisheries & Forestry – Australia, 2 September 2002. www.environment.gov.au/water/publications/urban/pubs/desalination-full-report.pdf (accessed November 2011).
- U.S. Environmental Protection Agency, 2011, Secondary drinking water regulations—guidance for nuisance chemicals: <http://water.epa.gov/drink/contaminants/secondarystandards.cfm> (accessed December 2011).
- Veil, J.A., 2008, Thermal distillation technology for management of produced water and frac flowback water: Argonne National Laboratory Water Technology Brief 2008-1, U.S. Department of Energy Office of Fossil Energy, National Energy Technology Laboratory.
- Veil, J.A., Harto, C.B., and McNemar, A.T., 2011, Management of water extracted from carbon sequestration projects—parallels to produced water management: Paper presented at Society of Petroleum Engineers SPE Americas E and P Health, Safety, Security, and Environmental Conference, March 21–23, SPE 140994.
- WateReuse Association, 2011, Seawater desalination power consumption white paper: www.watereuse.org/sites/default/files/u8/Power_consumption_white_paper.pdf (accessed November 2011).
- Western Australia Department of State Development, 2011, www.dsd.wa.gov.au/7599.aspx#7605, (accessed November 2011).
- Wiese, B., Böhner, J., Enachescu, C., Würdemann, H., Zimmermann, G., 2010a, Hydraulic characterisation of the Stuttgart formation at the pilot test site for CO₂ storage, Ketzin, Germany: *International Journal of Greenhouse Gas Control*, v. 4, no. 6, p. 960–971.

- Wiese, B., Nimtz, M., Klatt, M., and Kühn, M., 2010b, Sensitivities of injection rates for single well CO₂ injection into saline aquifers: *Chemie der Erde – Geochemistry*, v. 70, no. 3, p. 165–172.
- Wolery, T.J., Bourcier, W.L., and Aines, R.D., 2011, Brine treatment: NETL CO₂ Storage and Water Projects WebEx, November 1, 2011.
- Würdemann, H., Möller, F., Kühn, M., Heidug, W., Christensen, N., Borm, G., and Schilling, F., 2010, The CO₂SINK Group, CO₂SINK—from site characterisation and risk assessment to monitoring and verification—one year of operational experience with the field laboratory for CO₂ storage at Ketzin, Germany: *International Journal of Greenhouse Gas Control*, v. 4, no. 6, p. 938–951.
- Wyoming Oil and Gas Conservation Commission, 2011, <http://wogcc.state.wy.us/rules-statutes.cfm?Skip='Y> (accessed November 2011).
- Yun, T.I., Gabelich, C.J., Cox, M.R., Mofidi, A.A., and Lesan, R., 2006, Reducing costs for large-scale desalting plants using large-diameter, reverse osmosis membranes: *Desalination*, v. 189, p. 141–154.
- ZERO, Zero Emission Resource Organisation, 2011, Salt Creek EOR: www.zeroco2.no/projects/salt-creek-eor, Last modified: July 19, 2011 (accessed November 2011).
- Zhai, H. and Rubin, E.S., 2010, Carbon capture effects on water use at pulverized coal power plants: *Energy Procedia*, [www.cmu.edu/epp/iecm/rubin/PDF%20files/2010/GHGT- 10_Zhai 20and%20Rubin-%20CCS%20water%20use.pdf](http://www.cmu.edu/epp/iecm/rubin/PDF%20files/2010/GHGT-10_Zhai20and%20Rubin-%20CCS%20water%20use.pdf) (accessed June 2011).

APPENDIX A

BENEFICIAL USE OPTIONS AND WATER QUALITY REQUIREMENTS

BENEFICIAL USE OPTIONS AND WATER QUALITY REQUIREMENTS

The quality of water required for beneficial use of the extracted water varies based on the intended use of that water, which will influence the level of treatment. Beneficial uses include use of the heat in the extracted water as a source of energy through geothermal energy recovery, use of the water directly with minimal treatment such as in its use as cooling water makeup, and a wide variety of uses which typically will require treatment using desalination technologies. Following is information on a variety of the potential uses and their water quality requirements.

DRINKING WATER

In order to ensure the safety of drinking water, regulatory agencies set standards for its quality. Some of these standards are mandatory requirements, i.e., primary standards; some are recommended, or nonmandatory, values, i.e., secondary standards. The primary standards are set to protect the public against consumption of drinking water contaminants that present a risk to human health. The secondary standards are established as guidelines to assist public water systems in managing their drinking water for aesthetic considerations.

In the United States, the primary drinking water standards regulate microorganisms, disinfectants, disinfectant by-products, several inorganic chemicals (mostly heavy metals, nitrate, and nitrite), many organic chemicals (mostly solvents and pesticides), and radionuclides. The secondary drinking water regulations include the recommendation for lower concentrations of some of the inorganic compounds listed in the primary regulations, and it is here that limits are set on color, odor, corrosivity, pH, and total dissolved solids (TDS) (Table A-1). This means that while the U.S. Environmental Protection Agency (EPA) sets a secondary standard of TDS of 500 mg/L, this is a recommended limit, not an absolute one. EPA does not enforce the secondary standards. This means that a community can choose to accept water at a higher TDS if it so chooses.

The World Health Organization has concluded that water containing TDS at concentrations below 1000 mg/L is generally acceptable to consumers (World Health Organization, 2003). However, concentrations of TDS in public water supplies in some areas of the United States are often well above 500 mg/L and even well above 1000 mg/L. An informal survey was performed by accessing water reports available online. One U.S. city with particularly high TDS levels in its potable water is Midland, Texas. The values reported as the average TDS for the period 2005–2009 (Midland, 2009) was 1890 mg/L and for 2010 was 1990 mg/L (Midland, 2010).

Australia has similar regulatory guidelines for drinking water based on health and aesthetics (National Health and Medical Research Council, 2011). As in the United States, there is no set limit for TDS based on health. The aesthetic limit is given as 600 mg/L, and further comments are provided indicating the aesthetic limit is based on taste and appearance:

- <600 mg/L is regarded as good-quality drinking water.
- 600–900 mg/L is regarded as fair quality.
- 900–1200 mg/L is regarded as poor quality.
- >1200 mg/L is regarded as unacceptable.

Table A-1. EPA Secondary Maximum Contaminant Levels* (U.S. Environmental Protection Agency, 2011)

Contaminant	Secondary MCL	Noticeable Effects above the Secondary MCL
Aluminum	0.05 to 0.2 mg/L**	Colored water
Chloride	250 mg/L	Salty taste
Color	15 color units	Visible tint
Copper	1.0 mg/L	Metallic taste, blue-green staining
Corrosivity	Noncorrosive	Metallic taste, corroded pipes/ fixtures staining
Fluoride	2.0 mg/L	Tooth discoloration
Foaming Agents	0.5 mg/L	Frothy, cloudy; bitter taste; odor
Iron	0.3 mg/L	Rusty color, sediment, metallic taste, reddish or orange staining
Manganese	0.05 mg/L	Black to brown color, black staining, bitter metallic taste
Odor	3 TON (threshold odor number)	“Rotten-egg,” musty or chemical smell
pH	6.5–8.5	<i>Low pH</i> : bitter metallic taste, corrosion <i>high pH</i> : slippery feel, soda taste, deposits
Silver	0.1 mg/L	Skin discoloration, graying of the white part of the eye
Sulfate	250 mg/L	Salty taste
TDS	500 mg/L	Hardness, deposits, colored water, staining, salty taste
Zinc	5 mg/L	Metallic taste

* Maximum contaminant levels = MCLs.

** mg/L is milligrams of substance per liter of water.

COOLING WATER MAKEUP

Generally it is desirable to have relatively high quality water for use as the supply of makeup water for recirculated cooling water operations, but it is possible to use water with relatively high TDS provided that scaling and corrosion problems are controlled. The issues then become the economics of using water, which will allow for only a small number of cycles of concentration, and how to handle a concentrated waste brine. The quality of water needed for a cooling water supply to the cooling towers is addressed in considerable detail by Maulbetsch and DiFilippo (2006). They included consideration of fresh, brackish, saline, and reclaimed water as the cooling water supply for 500-MW nominal gas-fired combined-cycle power plants. Freshwater use was assumed to allow for ten cycles of concentration with disposal back to the environment or a municipal treatment facility. Reclaimed (treated municipal effluent) water was assumed to be good for five cycles of concentration with disposal of the water back to the municipal treatment facility; reclaimed water use with further treatment of the blowdown using an evaporator/crystallizer was employed to provide ten to 12 cycles of concentration and zero liquid discharge (ZLD; the low silica concentration of reclaimed water was important for achieving the highest cycles of concentration). Brackish water with TDS between 2000 and 5000 mg/L could be used to provide five to ten cycles of concentration with the cooling water

blowdown treated using high-efficiency reverse osmosis (HERO) and crystallizers for ZLD. Saline water (>5000 mg/L TDS) could be used in a manner similar to the brackish waters with maximum cycles of concentration as high as 5 to 8 and ZLD.

A more recent report by the same authors concentrated on the use of seawater-fed cooling towers (Maulbetsch and DiFilippo, 2010). That report details design, operation, and cost concerns for operation of cooling towers with saline or brackish water and lists several concerns that limit the cycles of concentration that can be achieved. These are mainly limitations on the maximum concentration of dissolved species that can be present in the discharged water. Specifically, they indicate limitations on the concentrations of toxic species that can be discharged (e.g., arsenic, copper, mercury, silver, zinc) and a limitation on the concentration of TDS that can be discharged to a municipal treatment plant (listed as 50,000 to 70,000 ppm). These limitations will significantly reduce the acceptable cycles of concentration that can be used where the water is discharged to the ocean (typically the limit is a toxic metal concentration) or a municipal treatment plant. The increased cycles of concentration can only be achieved then if further treatment of the blowdown water is performed as was suggested in Maulbetsch and DiFilippo (2006). However, in their more recent (2010) document, they conclude that:

“Treatment, volume reduction, or on site disposal of the blowdown stream would be prohibitively expensive. For towers operating on seawater makeup at two cycles of concentration, the blowdown rates are very high—on the order of 10 gpm per MW, or 5000 gpm for a 500 MW steam plant. The cost of evaporation ponds, even if the plant were located in an area with a high net annual evaporation rate, would be extremely high—on the order of a few hundred million dollars. The cost of evaporator/crystallizer systems, frequently used on zero discharge plants but at far lower input rates, would be equally unacceptable. (p. 22)”

Although this suggests treatment costs are too high in general to allow for further treatment of the blowdown, there are facilities where cooling water will be used in a ZLD scenario. These are likely to be where hybrid cooling is used in order to gain greater efficiencies than can be achieved with dry cooling. In these cases, the water use rates will be much lower than for a 100% wet-cooling design but will allow for much greater cooling efficiency and a lower likelihood of the need to decrease plant output during seasonally hot days. Together, the lower water use rate and higher efficiency will make the use of ZLD cooling much more economically feasible (Duke, 2007).

BOILER WATER

It is desirable to use water of the highest quality as boiler feed water in order to avoid the negative effects of scale and corrosion. Lenntech (2011) provides two tables summarizing the water quality characteristics for boilers as recommended by APAVE (2011; Association des Propriétaires d'Appareils à Vapeur et Electriques [French: Association of Steam and Electric Apparatus Owners]) and American Boiler Manufacturers Association (ABMA). The ABMA table is given here as Table A-2. According to Banks Engineering (2011), ABMA recommends

Table A-2. Acceptable Water Quality Characteristics for Use in a Boiler

Drum Pressure, psig	Range TDS ¹ Boiler Water, ppm	Range Total Alkalinity ^{2,3}	Suspended Solids Boiler Water, ppm	Range TDS ^{2,4} Steam, ppm (max. expected value)
0–300	700–3500	140–700	15	0.2–1.0
301–450	600–3000	120–600	10	0.2–1.0
451–600	500–2500	100–500	8	0.2–1.0
601–750	200–1000	40–200	3	0.1–0.5
751–900	150–750	30–150	2	0.1–0.5
901–1000	125–625	25–125	1	
1001–1800	100	Note ⁵	1	0.1
1801–2350	50	Note ⁵	Not Applicable	0.1
2351–2600	25	Note ⁵	Not Applicable	0.05
2601–2900	15	Note ⁵	Not Applicable	0.05

¹ Actual values within the range reflect the TDS in the feedwater. Higher values are for high solids; lower values are for low solids in the feedwater.

² Actual values within the range are directly proportional to the actual value of TDS of boiler water. Higher values are for high solids; lower values are for low solids in the boiler water.

³ Expressed as equivalent calcium carbonate in ppm.

⁴ These values are exclusive of silica.

⁵ Dictated by boiler water treatment.

the water quality characteristics listed in Table A-2 in order to ensure high-quality steam (American Boiler Manufacturers Association, 2011). The information in the table reveals that the higher the boiler operating pressure (i.e., the higher the steam temperature), the purer the water should be that is used to feed the boiler.

AGRICULTURE

Irrigation

Assuming organic content is not of concern for water being considered for use in irrigation, the salt-related water quality requirements most critical with respect to use for irrigation are salinity and sodium adsorption ratio (SAR). Alkalinity, pH, nitrate, and other water quality parameters are not unimportant, but salinity and SAR are of primary importance. If the salinity and SAR characteristics are within acceptable limits, it is likely that the water will be acceptable for use at relatively low cost even if other parameters need to be adjusted to more favorable values.

Salinity is a problem because of its effect on plants. The higher the salinity, the lower the water activity and the more difficult it becomes for the plant to extract water from the environment for use.

Sodium or, more accurately, the SAR (ratio of sodium to calcium and magnesium) is a problem because of its effects on soils. Irrigation with high-SAR water will lead to breakdown of the soil structure. The soil becomes hard, compact, and relatively impervious to water penetration and loses its water-holding capacity.

Table A-3 provides information on acceptable values of salinity for irrigation waters. The information in the table is a rough guide, as salinity limits are dependent on the plants being grown, the drainage conditions, and the irrigation management approach taken. In general, salinities below 525 ppm TDS will be acceptable without special efforts being made unless the crop is particularly sensitive. Most of these cite the work of Ayers and Westcot (1994), which contains significant detail on crop sensitivities to salinity and information on best practices for irrigation in order to minimize negative impacts on crop yields and soil fertility.

Table A-4 provides guidelines concerning permissible SAR values for irrigation water as a function of soil type. These acceptable SAR values will also depend on the ratio of irrigation water used to rainfall and the total salinity of the water. The limit on the acceptable SAR with respect to its effect on infiltration rate (the speed at which water enters a soil) is a function of salinity. Very low salinity waters will cause problems with infiltration rates even at SAR values approaching zero. Higher SAR values are permissible with higher salinities (Ayers and Westcot,

Table A-3. Acceptability of Water Salinities for Irrigation (after Bauder and others, 2011; Fipps, 2003)

Limitations on Use	EC, ¹ mS/cm (25°C)	TDS, mg/L
None	0.25–0.75	175–525
Some ²	0.75–1.5	525–1050
Moderate ³	1.5–3.0	1050–2100
Severe ³	>3.0	>2100

¹Electrical conductivity.

²Leaching is required, particularly higher in this range.

³Very good drainage is needed, sensitive plants may have difficulty at germination.

Table A-4. Permissible SAR of Irrigation Water (Environment Australia, 2000a)

Clay, Content, %	Soil Texture	Permissible Irrigation Water SAR				
		Clay Mineralogy Expressed as CCR ^a (mmole/kg)				
		<0.35	0.35–0.55	0.55–0.75	0.75–0.95	>0.95
<15	Sand, sandy loam	>20	>20	>20	>20	>20
15–25	Loam, silty loam	20	11	10	10	8
25–35	Clay loam	13	11	8	5	6
35–45	Light clay	11	8	5	5	5
45–55	Medium clay	10	5	5	5	5
55–65	Medium-heavy clay	5	5	5	4	4
65–75	Heavy clay	–	4	4	4	4
75–85	Heavy clay	–	–	4	5	5

^a CCR – cation exchange capacity/clay ratio.

1994). Therefore, if desalination is used to treat extracted water destined for irrigation, it may be necessary to blend the treated water with some other source water to adjust the salinity, particularly if thermal methods are used for desalination. It may also be necessary to adjust the SAR, especially if the water will be used to irrigate more SAR-sensitive soils.

LIVESTOCK DRINKING WATER

The quality of water acceptable to livestock is similar, in general, to the quality of water acceptable to humans. It should not contain unacceptable concentrations of potential toxicants; it should be microbially acceptable so as not to risk the spread of disease, and it should have an acceptable taste and odor. Like humans, livestock will consume pleasant-tasting but unsafe water while avoiding consumption of unpleasant-tasting water of acceptable quality if both are available. Extensive coverage of livestock water quality issues is readily available in fact sheets and other publications from cooperative extension services and various national departments of agriculture. A widely referenced table from that work which provides guidance concerning the effect of salinity of drinking water on livestock is given here as Table A-5. More detailed information from the Australian and New Zealand Environment and Conservation Council and the Agricultural and Resource Management Council of Australia and New Zealand lists salinities acceptable to different animals. This table reveals that the limit on TDS for poultry is between 3000 and 4000 mg/L, while that for sheep can be as high as 10,000 to 13,000 mg/L if they are grazing on lush green feed.

Table A-5. Effect of Salinity of Drinking Water on Livestock and Poultry (National Research Council, 1974; Pfof and others, 2001)

Soluble Salt, mg per L	Effect
<1000	Low level of salinity; presents no serious burden to any class of livestock or poultry.
1000 to 2999	Satisfactory for all classes of livestock and poultry; may cause temporary, mild diarrhea in livestock and water droppings in poultry at higher levels; no effect on health or performance.
3000 to 4999	Satisfactory for livestock; may cause temporary diarrhea or be refused by animals not accustomed to it; poor water for poultry causing watery feces and, at high levels, increased mortality and decreased growth (especially in turkeys).
5000 to 6999	Reasonable safety for dairy and beef cattle, sheep, swine, and horses; avoid use for pregnant or lactating animals; not acceptable for poultry as it causes decreased growth and production or increased mortality.
7000 to 10,000	Unfit for poultry and swine; risk in using for pregnant or lactating cows, horses, and sheep, or the young of these species, or animals subjected to heavy heat stress or water loss; use should be avoided, although older ruminants, horses, poultry, and swine may subsist for long periods under conditions of low stress.
>10,000	Risks are great; cannot be recommended for use under any conditions.

Table A-6 provides average consumption volumes required for livestock as given in Environment Australia (2000a). It must also be recognized that the volume of water required by livestock depends on their diet, the ambient temperature and humidity, and the stage of life. Table A-6 provides average daily consumption and peak daily consumption. Peak consumption rates will occur when the livestock are consuming a diet containing low-water-content feeds and when living at higher ambient temperatures and decreased ambient humidity.

Cement and Concrete Production

Water quality limits for cement and concrete production are covered in detail in a report by Cement, Concrete and Aggregates Australia (2007). The document is focused on the use of reclaimed water for use in mixing cement and concrete, so it deals with contaminants that may be present in water reclaimed from industrial and municipal wastewater as well as groundwater and bore water. Direct use of sewage is also considered. Table A-7 lists the negative effects that various classes of impurities can have on the properties of concrete. Greater details given in other tables in this document indicate a generally suggested limit on TDS of <2000 ppm and a suggested limit for total impurities to somewhere between 5000 and 10,000 ppm. Testing should be done whenever a water of lower purity will be used, especially if any of the suggested limits are exceeded. One particular limit that would be very relevant to the potential use of water extracted from saline reservoirs is that for chloride ions. These limits are fairly strict,

Table A-6. Stock Water Requirements (Environment Australia, 2000b)

Type of Livestock	Average Daily Consumption, liters/head	Peak Daily Consumption, liters/head
Sheep		
Nursing Ewes on Dry Feed	9	11.5
Mature Sheep on Dry Pastures	7	8.5
Mature Sheep on Green Pastures	3.2	4.5
Fattening Lambs on Dry Pasture	2.2	3
Fattening Lambs on Green Pasture	1.1	
Cattle		
Dairy Cows in Milk	70	85
Dairy Cows, dry	45	60
Beef Cattle	45	60
Calves	22	30
Horses		
Working	55	70
Grazing	35	45
Pigs		
Brood Sows	22	30
Mature Pigs	11	15
Poultry		
	(liters/100 birds)	(liters/100 birds)
Laying Hens	32	40
Nonlaying Hens	18	23
Turkeys	55	70

Table A-7. Effects of Impurities in Mixing Water on Some Properties of Concrete

Impurity	Effect
Oil, Fat, or Detergents	Air entraining possible
Calcium Chloride and Some Other Calcium Salts	Probability of set acceleration
Sugar, Salt or Zinc, Lead, and a Range of Other Inorganic and Organic Materials	Probability of set retardation
Chloride Ions	Strong probability of steel corrosion

depending on the type and use of the concrete. Both ASTM International C94 and EN 1008 require chloride concentrations below 500 ppm for prestressed concrete and grout and/or bridge decks and below 1000 ppm for reinforced concrete. EN 1008 allows Cl⁻ content as high as 4500 ppm without reinforcement.

Other Industries

Desalting Handbook for Planners (U.S. Department of the Interior, 2003) contains a useful overview of water quality requirements for a variety of industries. In general, the requirements for industry are similar to or more restrictive than those for municipal water supplies.

REFERENCES

- American Boiler Manufacturers Association, 2011: www.abma.com/ (accessed December 2011).
- APAVE, 2011, www.apave.com/en/international.html (accessed December 2011).
- Ayers, R.S., and Westcot, D.W., 1994, Water quality of agriculture: FAO Irrigation and Drainage Paper, 29 Rev. 1. www.fao.org/docrep/003/t0234e/t0234E00.htm (accessed October 2011).
- Banks Engineering, 2011, Boiler water treatment considerations: www.banksengineering.com/blrwater.htm (accessed December 2011).
- Bauder, T., Waskom R., Sutherland, P., and Davis, J., Irrigation water quality criteria: Colorado State University, Fact Sheet No. 0.506. www.ext.colostate.edu/pubs/crops/00506.pdf (accessed November 2011).
- Cement Concrete and Aggregates Australia, 2007, Use of recycled water in concrete production: www.concrete.net.au/publications/pdf/RecycledWater.pdf.
- Duke, D., 2007, ZLD—new silica based inhibitor chemistry permits cost-effective water conservation for HVAC and industrial cooling towers: The International Water Conference 68th Annual Meeting, Orlando, Florida, IWC Report 07-11, 10 p. www.water-cti.com/pdf/IWC_07-11_Report.pdf.

- Environment Australia, 2000a, Australian and New Zealand guidelines for fresh and marine water quality: volume 3—primary industries—rationale and background information—section 9.2 Water quality for irrigation and general use: Australian and New Zealand Environment and Conservation Council, Agriculture and Resource Management Council of Australia and New Zealand. www.mincos.gov.au/__data/assets/pdf_file/0018/316143/gfmwq-guidelines-vol3-9-2.pdf (accessed December 2011).
- Environment Australia (2000b) Australian and New Zealand guidelines for fresh and marine water quality: volume 3—primary industries—section 9.3 Livestock drinking water guidelines: Australian and New Zealand Environment and Conservation Council, Agriculture and Resource Management Council of Australia and New Zealand. www.mincos.gov.au/__data/assets/pdf_file/0019/316144/gfmwq-guidelines-vol3-9-3.pdf.
- Fipps, G., 2003, Irrigation water quality standards and salinity management: Texas Cooperative Extension, Document B-1667. <http://lubbock.tamu.edu/irrigate/documents/2074410-B1667.pdf>.
- Lenntech, 2011, Characteristics of boiler feed water: www.lenntech.com/applications/process/boiler/boiler-feedwater-characteristics.htm (accessed 2011).
- Maulbetsch, J.S., and DiFilippo, M.N., 2010, Performance, cost and environmental effects of saltwater cooling towers: California Energy Commission, PIER Energy-Related Environmental Research Program. CEC-500-2008-043. www.energy.ca.gov/2008publications/CEC-500-2008-043/CEC-500-2008-043.PDF.
- Maulbetsch, J.S., and DiFilippo, M.N., 2006, Cost and value of water use at combined-cycle power plants: California Energy Commission, PIER Energy-Related Environmental Research Program. CEC-500-2006-034. www.energy.ca.gov/2006publications/CEC-500-2006-034/CEC-500-2006-034.PDF.
- Midland, 2010, Water quality report: www.midlandtexas.gov/departments/utilities/pdf/WaterRpt2010.pdf (accessed November 2011).
- Midland, 2009, Water quality report: www.midlandtexas.gov/departments/utilities/pdf/WaterRpt2009.pdf (accessed November 2011).
- National Health and Medical Research Council, 2011, Australian drinking water guidelines: www.nhmrc.gov.au/_files_nhmrc/publications/attachments/eh52_aust_drinking_water_guidelines_111130.pdf.
- National Research Council, 1974, Nutrients and toxic substances in water for livestock and poultry: Washington, DC, National Academy Press.
- Pfost and others, 2001, Water quality for livestock drinking: MU Extension, University of Missouri-Columbia. <http://extension.missouri.edu/p/EQ381> and <http://extension.missouri.edu/explorepdf/envqual/eq0381.pdf>.

U.S. Department of the Interior, 2003, Desalting handbook for planners: Report No. 72, 310 p. Available online at www.usbr.gov/pmts/water/media/pdfs/report072.pdf (accessed December 2011).

U.S. Environmental Protection Agency, 2011, Secondary drinking water regulations—guidance for nuisance chemicals: <http://water.epa.gov/drink/contaminants/secondarystandards.cfm> (accessed December 2011).

World Health Organization, 2003, Total dissolved solids in drinking-water: www.who.int/water_sanitation_health/dwq/chemicals/tds.pdf (accessed December 2011).

APPENDIX B

DESALINATION TECHNOLOGIES

DESALINATION TECHNOLOGIES

This appendix contains descriptions of the desalination technologies applicable to high volumes of feedwater. These include multistage flash distillation (MSF), multieffect distillation (MEF), hybrid multieffect distillation with thermal vapor compression (MEF/TVC), reverse osmosis (RO), nanofiltration (NF), membrane softening (MS), electrodialysis, and electrodialysis reversal. Technologies applicable to management of high-salinity formation water and brine treatment reject water are also described. Operational parameters can be found in Table B-1.

THERMAL PROCESSES: MSF, MED, AND MED/TVC

The thermal desalination processes MSF, MED, and MED/TVC use the application of a vacuum to allow for evaporation of water at temperatures low enough to allow for the use of waste heat as the energy source for evaporation and to avoid calcium sulfate scale formation. Because of their ability to use waste heat to supply a significant amount of the energy needed for the overall process (electricity is also needed to power pumps and other equipment), these processes are most popular when built in combination with a thermal electrical power plant.

Multistage Flash Distillation

MSF is illustrated in Figures B-1 and B-2. Following the system from left to right: steam is supplied to the brine heater on the left. Typically, this is waste heat steam from the outlet of a low-pressure turbine. The temperature of each progressive stage is lower, flowing from left to right. Vacuum is applied to each stage to promote flash evaporation from the brine with increasing vacuum (decreasing pressure) applied to each stage from left to right. Product water is condensed and collected from each stage. When the process is used for seawater desalination, the seawater is used as both the cooling water supply and as the source of water for desalination. In the once-through configuration (Figure B-1) all of the seawater undergoes full pretreatment and passes through all of the condensers. In the brine recirculation configuration (Figure B-2), there is a decoupling of the use of the seawater for cooling and as the source water. This design allows for more efficient operation throughout all seasons of the year and decreases the amount of seawater which must undergo full pretreatment for use as source water.

Because seawater is used for cooling and as the source water for MSF, it may seem unlikely that this technology could find use in the treatment of extracted water. However, it may be possible to use MSF for desalination of extracted water. Extracted water treatment with MSF could take advantage of waste heat from a power plant and/or the geothermal energy present in high-temperature extracted water. A low-water-consumption cooling system like dry or hybrid cooling could be used place of seawater.

Table B-1. Treatment Capacity Ranges for Popular Desalination Technologies Treating Brackish Water and/or Seawater

	Multistage Flash Distillation (MSF)	Multieffect Distillation/Thermal Vapor Compression (MED/TVC)	Mechanical Vapor Compression (MVC)	Seawater Reverse Osmosis (SWRO)	Brackish Water Reverse Osmosis (BWRO)	Electrodialysis Reversal (EDR)	Nanofiltration (NF)
Feedwater Salinity (ppm)	60,000– 70,000, ⁴ 30,000– 100,000 ³	>35,000 ¹	60,000 ² (desalination), much higher for MVC brine concentrator	>32,000, ¹ 20,000 and above, ⁵ 1000–45,000 ³ (includes brackish), 18,000–45,000+ ⁶	<32,000, ¹ 1000– 20,000, ⁵ 500–3000 (brackish), ⁶ 3500– 18,000 (brackish to saline) ⁶	100–3000 ³	<1000 (desalination), much higher salinities when used for pretreatment varies—see ion removal
Product Water Salinity (ppm)	<10 ^{3,7}	<10 ⁷	3 ¹⁰ , <10 ⁷	<500, ^{1,3} 200–500 ⁷	<200 ¹	<10 ¹ , <500 ³	
% Recovery (water yield)	50, 35–45 (seawater) ⁷	40–65, 35–45 (seawater) ⁷	87, ^{8,2} 23–41 seawater, ⁷ as high as 95 for brine concentrator in zero liquid discharge (ZLD) applications	30 to 50, 30–60 ⁵	>80 (varies based on TDS), 60–85, ⁵ 50–90%	>90, ¹ 50–95 ⁷	90+, ⁵ 50–90 ⁷
% ion removal	99.9+	99.9+	99.9+	99–99.5	99–99.5 ⁷	50–90 ⁷	50–98 removal of divalent ions; 20–75 removal of monovalent ions ⁷

¹ URS Australia, 2002.
² Stepan and others, 2010.
³ Fritzmann and others, 2007.
⁴ Yun and Others, 2006.
⁵ Mickley, 2009.
⁶ WateReuse Association, 2011.
⁷ National Research Council, 2008.
⁸ Fountain/Quail Water Management, 2011.

⁹ Birkett, 2011.
¹⁰ Lokiec and Ophir, 2007.
¹¹ NanoH2O, 2011.
¹² SIDEM, 2011a (also lists largest SWRO/MED Hybrid plant at 0.4546 million m³/day).
¹³ Veil, 2008.
¹⁴ IDE Technologies, 2011a.
¹⁵ GE, 2009.
¹⁶ Cooley and others, 2006.

B-2

Continued . . .

Table B-1. Treatment Capacity Ranges for Popular Desalination Technologies Treating Brackish Water and/or Seawater (continued)

	Multistage Flash Distillation (MSF)	Multieffect Distillation/Thermal Vapor Compression (MED/TVC)	Mechanical Vapor Compression (MVC)	Seawater Reverse Osmosis (SWRO)	Brackish Water Reverse Osmosis (BWRO)	Electrodialysis Reversal (EDR)	Nanofiltration (NF)
Maximum Concentrate Salinity (ppm)	Typically ~2X feed salinity	Typically ~2X feed salinity	Typically ~2X feed salinity for desalination, 250,000 to 300,000 for brine concentrator	~70,000 ⁵ , can be as high as 100,000	~70,000 ⁵	Can be very high if desired	~12,000 (assume 97% recovery and 70% TDS rejection) ⁵
Individual Unit Size (large)	>98,000 m ³ /day ⁹	76,000 m ³ /day ⁹	3000 m ³ /day ^{9,10}	52 m ³ /day ¹¹	52 m ³ /day ¹¹		Similar to RO
System Capacity (range of plant sizes)	0.88 million m ³ /day	120 m ³ –0.8 million m ³ /day ¹²	16–366m ³ /day ^{8,2,13}	0.5–>0.376 million m ³ /day, ^{1,4,14}	0.5 ->0.376 million m ³ /day ⁴	90–200,000 m ³ /day ¹⁵	
Size of Typical Plant Installation	10,000–35,000 m ³ /d, ¹⁶	1000–10,000 m ³ /d (MED), ¹⁶	250–2000 m ³ /d, ¹⁶	< 20,000 m ³ /day ⁷	<20,000 ⁷	<12,000 ⁷	
Operating Temperature (°C)	<76,000 m ³ /d ⁷	<36,000 m ³ /d ⁷	<3000 m ³ /d ⁷	<45 ⁷	<45 ⁷	<43	<45
Typical Feed Pressure	Low pressure	Low pressure	Low pressure	55–65 bar, ³ 44.8–82.7 bar ⁶	10–15 bar, ³ 3.4–10.3 bar for 500 to 3500 ppm TDS and 10.3–44.8 got 3500–18,000 mg/L TDS)	Low pressure	Up to 10 bar

B-3

¹ URS Australia, 2002.

² Stepan and others, 2010.

³ Fritzmman and others, 2007.

⁴ Yun and Others, 2006.

⁵ Mickley, 2009.

⁶ WateReuse Association, 2011.

⁷ National Research Council, 2008.

⁸ Fountain/Quail Water Management, 2011.

⁹ Birkett, 2011.

¹⁰ Lokiec and Ophir, 2007.

¹¹ NanoH2O, 2011.

¹² SIDEM, 2011a (also lists largest SWRO/MED Hybrid plant at 0.4546 million m³/day).

¹³ Veil, 2008.

¹⁴ IDE Technologies, 2011a.

¹⁵ GE, 2009.

¹⁶ Cooley and others, 2006.

Continued . . .

Table B-1. Treatment Capacity Ranges for Popular Desalination Technologies Treating Brackish Water and/or Seawater (continued)

	Multistage Flash Distillation (MSF)	Multieffect Distillation/Thermal Vapor Compression (MED/TVC)	Mechanical Vapor Compression (MVC)	Seawater Reverse Osmosis (SWRO)	Brackish Water Reverse Osmosis (BWRO)	Electrodialysis Reversal (EDR)	Nanofiltration (NF)
Energy Form	Steam (heat) ⁷	Steam (heat and pressure) ⁷	Mechanical (electrical energy) ⁷	Mechanical (electrical) energy ⁷	Mechanical (electrical) energy	Electrical energy	Mechanical (electrical) energy
Thermal Energy Consumption (kWh/m ³)	12 ³ [-69.4–91.7] ⁷	[-40.3–108.3] ⁷	Heat used waste heat off compressor	NA ⁷	NA ⁷		
Electrical Energy Consumption (kWh/m ³)	2.5–3, ⁹ 3–5 ^{3,7}	1.2–2, ⁹ 1.5–2.5 ⁷	8–15 ⁷	2.5–3a, 1.8–2.2 (RO process step only), ⁶ 2.8–3.1 (total treatment energy) ⁶ – Theoretical minimum about 1 kWh/m ³ – best practice 3 kWh/m ³ , 0.4–7, ³ 2.5–7 ⁷	Lower than RO due to lower pressure, depends on salinity	1, ³ power consumption is directly related to number of ions moved across the membrane, approximately 0.53 kWh/m ³ per 1000 mg/L TDS removed ⁷	
Capital Costs (\$/(m ³ /day product water))		2.5–3.9 ¹		1.6–2.5 ¹	6–1.8 ¹	0.5–3.25 ¹	
Operating and Maintenance Costs (\$/m ³)		0.55–0.95 with waste heat, 1.80–2.80 without waste heat ¹		1.89–2.20 ¹	0.65–1.50 ¹	1.00–2.80 ¹	

B-4

¹ URS Australia, 2002.

² Stepan and others, 2010.

³ Fritzmann and others, 2007.

⁴ Yun and Others, 2006.

⁵ Mickley, 2009.

⁶ WaterReuse Association, 2011.

⁷ National Research Council, 2008.

⁸ Fountain/Quail Water Management, 2011.

⁹ Birkett, 2011.

¹⁰ Lokiec and Ophir, 2007.

¹¹ NanoH2O, 2011.

¹² SIDEM, 2011a (also lists largest SWRO/MED Hybrid plant at 0.4546 million m³/day).

¹³ Veil, 2008.

¹⁴ IDE Technologies, 2011a.

¹⁵ GE, 2009.

¹⁶ Cooley and others, 2006.

Continued . . .

Table B-1. Treatment Capacity Ranges for Popular Desalination Technologies Treating Brackish Water and/or Seawater (continued)

	Multistage Flash Distillation (MSF)	Multieffect Distillation/Thermal Vapor Compression (MED/TVC)	Mechanical Vapor Compression (MVC)	Seawater Reverse Osmosis (SWRO)	Brackish Water Reverse Osmosis (BWRO)	Electrodialysis Reversal (EDR)	Nanofiltration (NF)
Typical Production Cost (\$/m ³)			0.65 to 0.90 (2005) ³	0.53 to 0.83 ³	0.20 to 0.30 ³		
Pretreatment Requirements (seawater)	Low ⁷	Low	Very Low	High ⁷	High ⁷	Medium ⁷	
Reliability	Very high ⁷	Very high ⁷	High ⁷	Moderate ⁷	Moderate	Moderate	Moderate

¹ URS Australia, 2002.

² Stepan and others, 2010.

³ Fritzmann and others, 2007.

⁴ Yun and Others, 2006.

⁵ Mickley, 2009.

⁶ WateReuse Association, 2011.

⁷ National Research Council, 2008.

⁸ Fountain/Quail Water Management, 2011.

⁹ Birkett, 2011.

¹⁰ Lokiec and Ophir, 2007.

¹¹ NanoH2O, 2011.

¹² SIDEM, 2011a (also lists largest SWRO/MED Hybrid plant at 0.4546 million m³/day).

¹³ Veil, 2008.

¹⁴ IDE Technologies, 2011a.

¹⁵ GE, 2009.

¹⁶ Cooley and others, 2006.

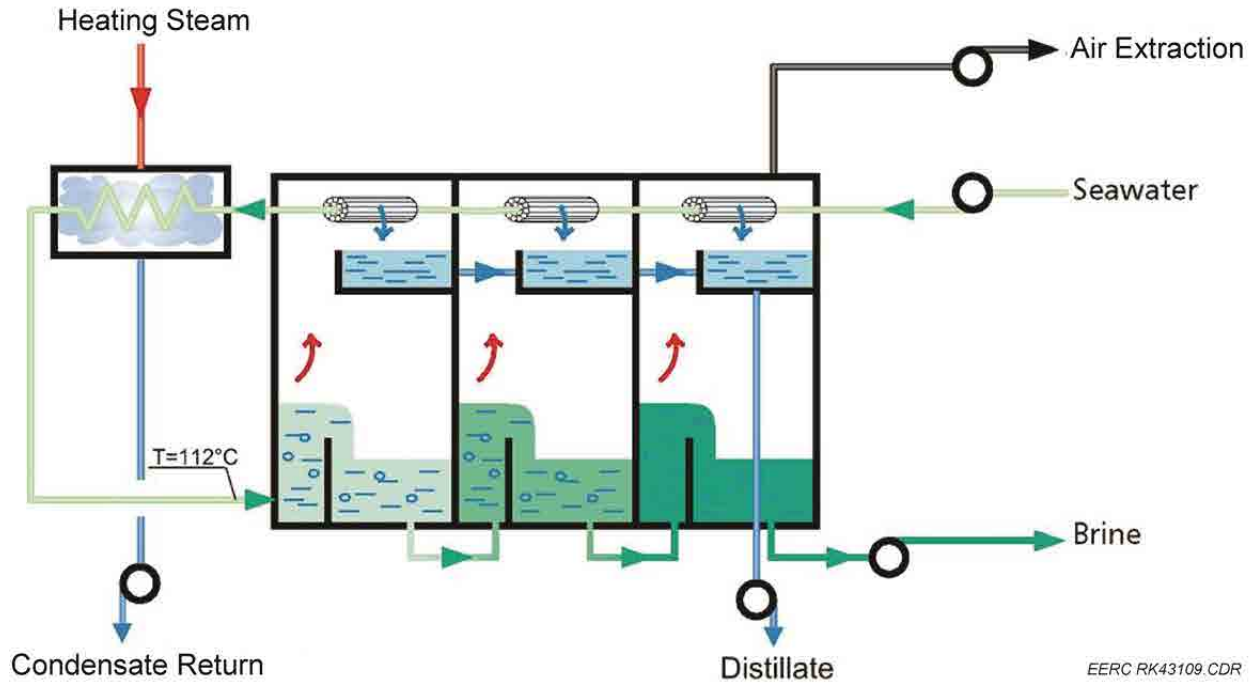


Figure B-1. Multistage flash “once-through” desalination process (SIDEM, 2011b).

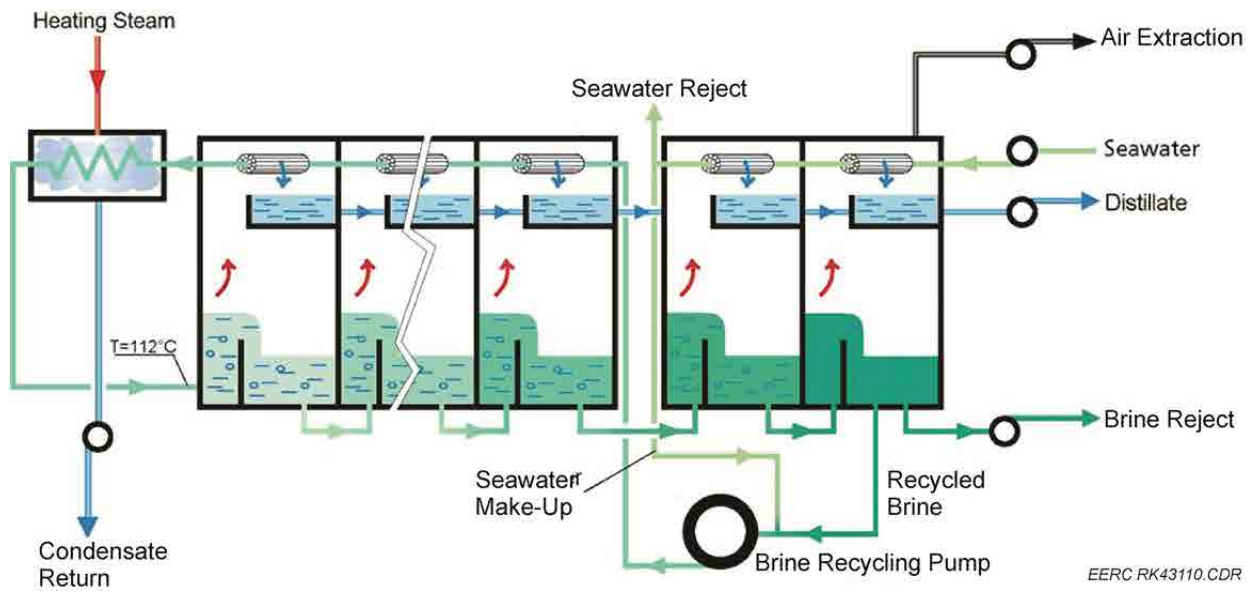


Figure B-2. Multistage flash process with brine recycling (SIDEM, 2011b).

Multieffect Distillation

An MED system utilizes a series of evaporation steps where evaporation of water from a film of liquid on one heat exchanger tube or plate is coupled with condensation of water vapor on the opposite side. The evaporation and condensation occur at nearly identical temperatures because higher pressure is applied to the steam on the condensation side while lower pressure is applied on the evaporation side. Each of these coupled sections is known as an effect. Figure B-3 shows an illustration of a single effect of a mechanical vapor compression system, where a mechanical compressor is used to compress the vapor formed on one side of the effect in order to have it condense on the other side. In an MED desalination system, several consecutive effects are maintained at decreasing temperature and pressure. As shown in Figure B-4, steam (e.g., from the outlet of a low-pressure turbine) is used to supply heat to produce water vapor from the source water. This water vapor is passed to the highest temperature effect, where it is condensed and used to produce water vapor that is condensed in the next effect. An external source of cooling (typically seawater when MED is used for seawater desalination) is used to supply the final condenser which condenses the water vapor from the final effect. This final cooling step establishes the lowest temperature and thus lowest pressure for a simple MED (Figure B-4). The air extraction vacuum pump illustrated is used to remove noncondensable gases that leak into the system or enter as dissolved gases that come out of solution during treatment. MED systems can be operated with saturated steam at pressures as low as 0.3 bar (absolute) as the source of heat (SIDEM, 2011c). Note that 0.3 bar saturated steam has a temperature of 69°C. This is a much

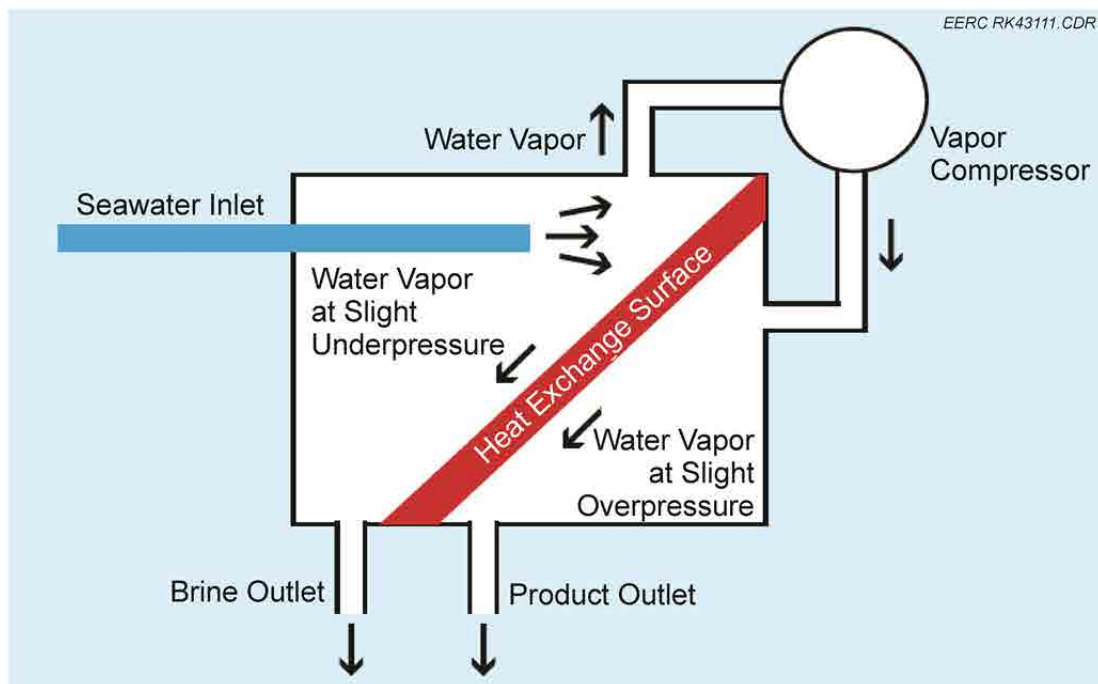


Figure B-3. Mechanical vapor compression (MVC) (Birkett, 2011).

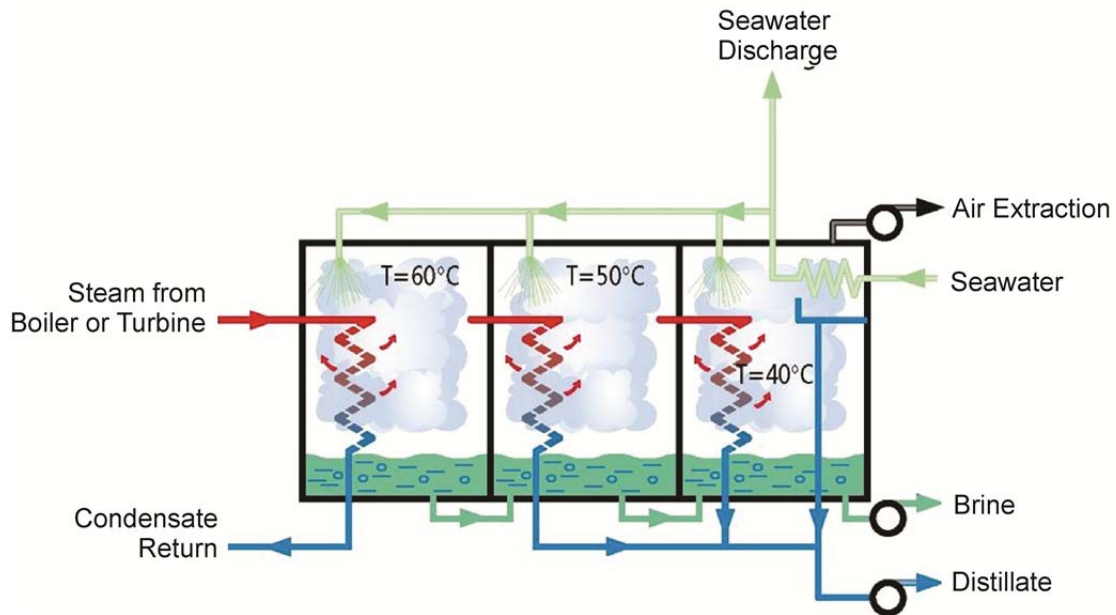


Figure B-4. Multiple effect distillation process (SIDEM, 2011c).

lower grade heat than can be used for MSF, and it allows for operation at much lower temperatures, which decreased the capital cost by allowing the use of lower-cost heat exchange materials (Birkett, 2011).

MED/TVC

In the hybrid MED/TVC system, a thermocompressor is used to take advantage of the higher amounts of water, which can be evaporated and condensed as product when a higher-pressure steam supply (above 2 bar absolute [SIDEM, 2011d]) is available. As illustrated in Figure B-5, the steam is supplied to a thermocompressor, which is used to draw a vacuum on the final effect stage. This recycles the latent heat of the recycled vapor leading to higher gain output ratios (GORs). SIDEM (2011d) refers to a MED/TVC system in the French West Indies with a GOR of 17; i.e., it produces 17 kg of distilled water for every kg of 30 bar steam supplied. Note that 30 bar saturated steam has a temperature of 234°C.

As with MSF, there may be some potential for MED and MED/TVC systems to be used for extracted water treatment, particularly if waste heat from collocated power plants or geothermal energy in the extracted water is used as a source of heat for the process. It will probably be necessary for cooling to be supplied by low-water-consumption systems in order to make it logical to use this system to treat inland saline waters.

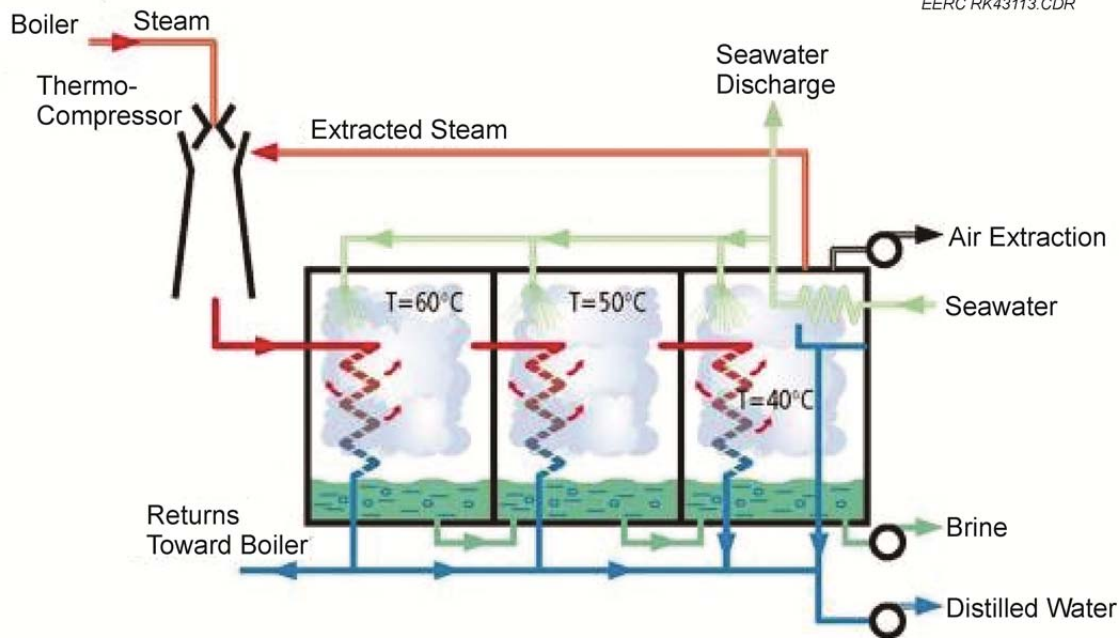


Figure B-5. MED/TVC (SIDEM, 2011d).

MEMBRANE PROCESSES: REVERSE OSMOSIS, NANOFILTRATION, MEMBRANE SOFTENING, AND ELECTRODIALYSIS REVERSAL

The membrane desalination processes RO, NF, and membrane softening (MS) use pressure to force water through membranes that selectively reject dissolved ions and other dissolved species that remain in a reject stream. NF and MS membranes strongly reject multivalent ions but are still fairly permeable to monovalent ions such as sodium and chloride. Depending on conditions, they can achieve >99% removal of the multivalent ions and up to 50% of the monovalent ions. RO membranes can reject almost all ions at rates exceeding 99%, depending on the membrane used and the supply pressure.

Electrical energy is used to run pumps used to supply the pressure for membrane desalination. With RO systems, the pressures used are very high (1200 psi for a typical seawater RO [SWRO] system). This means the waste brine exits the RO modules at very high pressures and, therefore, contains a significant amount of recoverable energy. For this reason, energy recovery units are used in all modern RO systems of any significant size in order to help minimize the energy cost of operating the system. NF and MS are performed at lower pressures than RO systems. They are typically used as a pretreatment before RO or thermal desalination. Energy recovery units are not used for NF or MS.

EDR is a membrane desalination system in which an electrical current is used to drive the removal of ions from the source water. In EDR, the salts being removed move across the membrane rather than the water. EDR systems are typically used for lower-concentration brines.

Reverse Osmosis

While MSF, MED, and MED/TVC may have some potential for use in extracted water treatment, it is almost certain the RO systems will be used to treat extracted water, especially in situations where the extracted water has salinities below that of seawater (i.e., brackish water salinities).

RO can be viewed as a pressurized mechanical filtration process, but in reality, it is a more complex process in which water is forced at high pressure through a porous membrane while most dissolved species in the water are retained in the waste brine, which is a concentrated aqueous solution of the remaining water and all dissolved species that do not pass through the membrane. In other words, impurities within the source water are retained on the pressurized side of the membrane, and (nearly) pure water passes through the membrane to the other side. Systems that use RO can treat organic and inorganic chemicals, including salts (National Research Council, 2008). Particulate matter and microorganisms will not pass through an RO membrane, but these are removed in pretreatment steps prior to the RO membrane in order to increase flux, reliability, and lifetime of the membrane modules. Some pesticides and low-molecular-weight organics can pass through RO membranes (National Research Council, 2008).

RO treatment requires substantial energy input, and energy requirements increase with the salinity of the source water, the purity of the product water, and the percent recovery as purified water (i.e., increasing salinity of the waste brine). Reduction in membrane pore size to provide higher-quality product water will require higher pressure drops across the membrane.

Fouling of RO membranes, which can be caused by a variety of factors such as microbial growth, chemical precipitation, and filtration of particulates, can lead to short membrane life, decreased production rates (low flux), and the need for frequent cleaning of the membrane modules. These problems are avoided through the use of pretreatment to remove particulates, adjusting the chemistry of the water (e.g., through acid addition and/or upstream removal of scale-forming ions) to ensure precipitation or scaling does not occur, and disinfection (e.g., chlorination, ozonation) of the water upstream of the RO membranes (Interstate Oil and Gas Compact Commission and ALL Consulting, 2006). Effective pretreatment and good cleaning policies and procedures prevent the need for premature module replacement.

RO units are commonly configured as spiral wound modules that contain a set of flat sheet membranes separated by spacer material. One flow path parallels the axis of the module and allows for flow of source water in and waste brine out of the ends of the module. The other flow path allows the product water that has passed through the membrane to flow into the central core of the module and out to the product collection piping. Figure B-6 illustrates the assembly and flow paths of a spiral wound RO module.

The cost of RO desalination has dropped dramatically over time because of improvement in membranes, module design, module size, and improvements in the overall treatment system. Better pretreatment and membrane maintenance procedures have helped, but one of the main reasons for substantial reductions in costs has been the incorporation of energy recovery devices

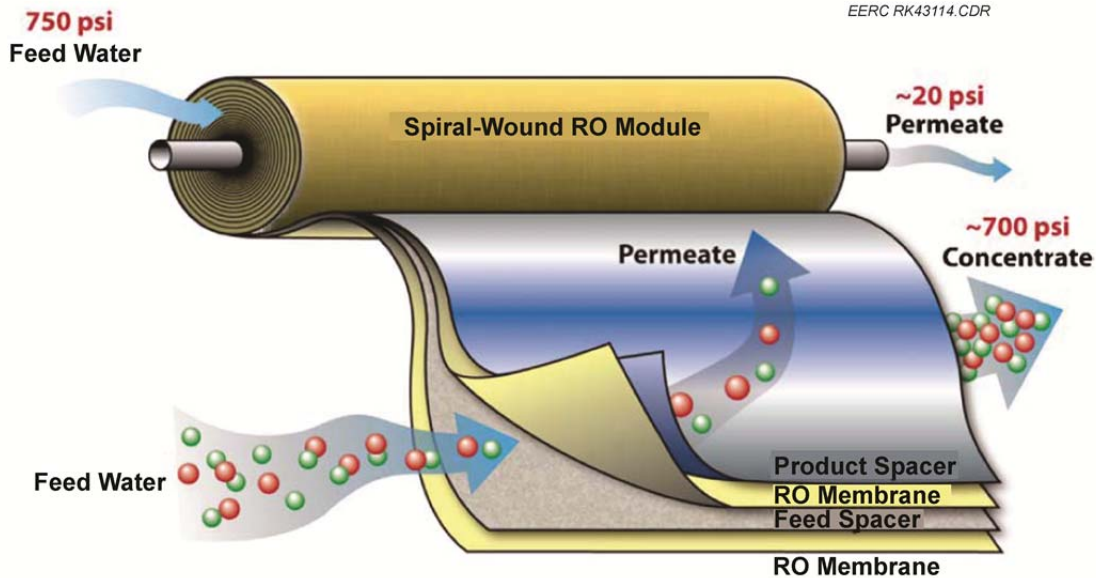


Figure B-6. Schematic of RO membrane geometry. Example pressures of feed, concentrate, and permeate are shown to illustrate relative pressures during conventional treatment of seawater (Bourcier and others, 2011).

into the RO systems (Birkett, 2011). Energy recovery devices recover the energy during the depressurization of the waste brine. Bourcier and others (2011) suggest that the energy required for RO treatment of extracted water will be different than that for seawater desalination because of differences in the source water pressure and the required waste brine pressure. How much difference this energy requirement will make will be highly site-specific and will also depend on the waste brine management approach. Bourcier and others (2011) suggest that some extracted water situations will supply the source water at sufficient pressure so as to not require pressurization. This would save on energy costs for pumping the feedwater, but if the waste brine is disposed through deep well injection into a pressurized formation, it prevents the use of an energy recovery unit and may require coupling to increase its pressure for injection. The potential applications will be highly site-specific.

Other Membrane Filtration Processes Microfiltration, Ultrafiltration, and NF

The membrane treatment technologies microfiltration (MF), ultrafiltration (UF), and NF use membranes that have larger pore sizes than those used for RO. While RO is capable of removing dissolved matter (salts) from the produced wastewater stream, depending on the desired water quality, pretreatment of the feedwater may be an important step. Mastouri and Nadim (2010) document that MF and UF are applied in wastewater treatment (though not very frequently), while NF is rarely applied. UF is sometimes combined with biological treatment membrane bioreactor applications. Examples of membrane treatment applications and qualities of these applications are compared in Tables B-2 and B-3. The values in Table B-3 reveal the fact that UF membranes provide no removal of ions, NF membranes provide some removal of

Table B-2. Applications of Advanced Membrane Filtration Technologies (Arthur and others, 2005)

Membrane Filtration	Separation Specifications	Applications/Removal
Microfiltration	>100,000 daltons 10–0.1µm	Bacteria, viruses, suspended solids, etc.
Ultrafiltration	10,000 to 100,000 daltons 0.05–5 E-3 µm	Proteins, starch, viruses, colloid silica, organics, dyes, fats, paint solids, etc.
Nanofiltration	1,000 to 100,000 daltons 5 E-3 – 5 E-4 µm	Starch, sugar, pesticides, herbicides, divalent ions, organics, biochemical oxygen demand (BOD), chemical oxygen demand (COD), detergents, etc.
Reverse Osmosis	Salts and lower molecular weight cutoff 1 E-4 – 1 E-5 µm	Metal ions, acids, sugars, aqueous salts, dyes, natural resins, monovalent salts, BOD, COD, ions etc.
Gas Liquid Membrane	CO ₂ , H ₂ S	Decarbonation, hydrogen sulfide removal

Table B-3. Pilot Water Treatment Plant Results (GE, 2001)

Constituent	Feed	UF Permeate	NF Permeate	RO Permeate
Sodium, ppm	9610	9610	5250	144
Calcium, ppm	715	715	163	5
Magnesium, ppm	412	412	115	2
Potassium, ppm	174	174	77	2
Ammonium, ppm	110	110	68	2
Chloride, ppm	8010	8010	4710	114
Sulfate, ppm	1090	1090	Nondetectable	Nondetectable
Oil, ppm	10–50	<1	Nondetectable	Nondetectable
Recovery, %	–	90–95	90–95	80–90

monovalent ions but substantial removal of divalent ions. For this reason, NF membranes are increasingly used for membrane softening of drinking waters and as a pretreatment step for desalination via RO and thermal desalination.

Electrodialysis and Electrodialysis Reversal

In electrodialysis and EDR, an electrical current is used to drive the removal of ions from the source water through ion-exchange membranes into a waste brine. Unlike the other membrane desalination techniques, which drive the water through the membrane leaving the residual brine on the same side as the source water, in EDR the salts move across the membrane forming the waste brine on the opposite side. Because the electrical current is used as the driving force to move the ions across the membrane, the power requirements for EDR are essentially proportional to the number of ions moved. For this reason EDR systems are typically used for lower-concentration brines (National Research Council, 2008).

HIGH SALINITY AND DESALINATION REJECT BRINE MANAGEMENT

The primary methods of dealing with reject brines from desalination include discharge to surface waters (ocean disposal), discharge to wastewater treatment plants with offshore outfalls (ocean disposal with dilution prior to discharge), deep well injection (geologic disposal), evaporation ponds (El-Naas, 2011). None of these methods provides for further recovery of water from the brine. Methods of water brine management that result in production of a dry salt that can be disposed of in a landfill, used as road salt, or used as a feed stock for chemical production are commonly classified as ZLD (Mickley, 2006). These technologies allow for full recovery of water from waste brines produced by the major membrane and thermal desalination processes and are also applicable to the treatment of high concentration source brines. Mickley (2006) also lists the use of thermal brine concentrator processes that are capable of recovering water from RO reject brines but which result in extremely high concentration brines rather than dried salts. A brief description of these brine concentrator and ZLD methods is provided here.

Brine Concentration Methods

Multiple Effect Evaporators

Multiple effect evaporators that are similar to MED can be used to treat saline waters to concentrations much higher than the typical RO waste brine concentrations (Mickley, 2006).

Vapor Compression Evaporator Systems (brine concentrators)

Vapor compression evaporators are multiple effect MVC systems where an electrically driven compressor is used to raise the pressure and saturation temperature of the evaporated vapor so that it may be used as a source of heating steam. This allows recirculation of the latent heat of the vapor for evaporation of more water instead of rejection of this heat to cooling water. Scaling problems are avoided through the use of a seeded slurry process which provides for precipitation of scale-forming minerals in a controlled manner in a safe location in the process rather than on heat-transfer surfaces. Brine concentrators are available in sizes from 10 to 700 gpm of feedwater. Most are single-effect vertical tube, falling film designs. Product water quality is high, <10 mg/L TDS, and concentrated brine salinity can be as high as 250,000 mg/L TDS.

Mickley (2006) provides capital cost curves for smaller (skid-mounted, 20 to 100 and 100 to 200 gpm) and larger (0.3 to 1 million gallons/day [MGD]) brine concentrators and indicates that electric power consumption costs fall in the range of 60 to 100 kWh/1000 gal of feedwater.

Zero Liquid Discharge – Dry Salt Product Methods

Crystallizers

A forced-circulation vapor compression crystallizer produces a small flow of concentrated brine that contains highly soluble salts such as calcium chloride, but most of the salts are removed as wet solids (Figure B-7). Crystallizers can be directly used for treatment of RO discharge brines but are usually fed the more concentrated brine that comes from a brine concentrator.

Crystallizers are available in sizes from 2 to 50 gpm. Smaller systems generally use steam as the heat supply. Larger systems commonly use heat from electrically driven vapor compressors. Where steam is used, it is typically of higher quality (higher temperature, higher pressure) than that needed for thermal systems used for seawater desalination.

Mickley (2006) provides capital cost curves for small (2–12 gpm) and large (5–50 gpm) crystallizers and reports power consumption costs for crystallizers as 200 to 250 kWh/1000 gal of feedwater.

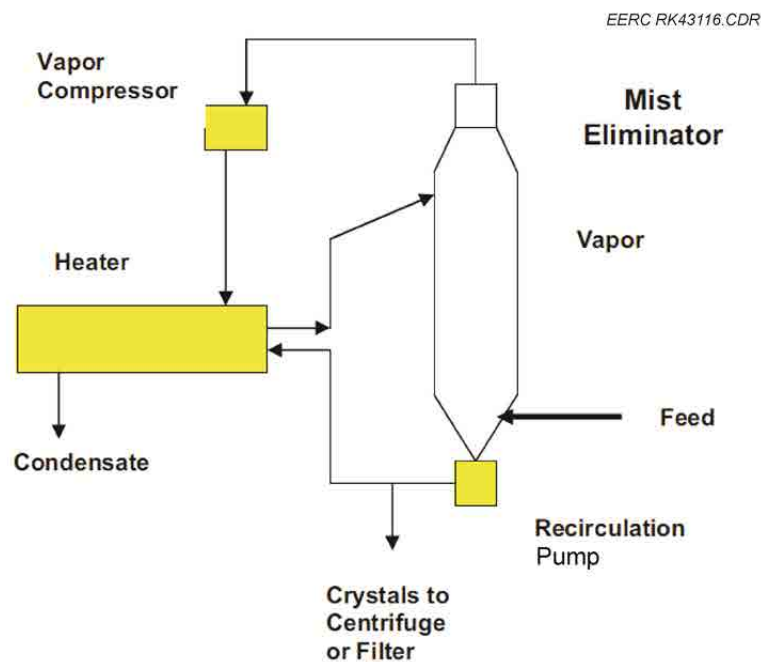


Figure B-7. Schematic diagram of forced-circulation vapor compression crystallizer process flow (Mickley, 2006).

Spray Dryers

Figure B-8 is a schematic for a spray dryer ZLD system. The discharge from this system is water vapor diluted in air so, as shown, this is a brine management rather than a water recovery system. The goal is to make a dry solid. Spray dryers are generally considered to be more economical for smaller flows than crystallizers. When treating RO brine concentrate, they can be used with or without an upstream brine concentrator.

Mickley (2006) provides capital cost curves for brine concentrators and indicates that electric power consumption costs fall in the range of 60 to 100 kWh/1000 gal of feedwater. Where natural gas or fuel oil is used for spray dryers, Mickley (2006) suggests using 0.7 Btu/gpm of feedwater flow.

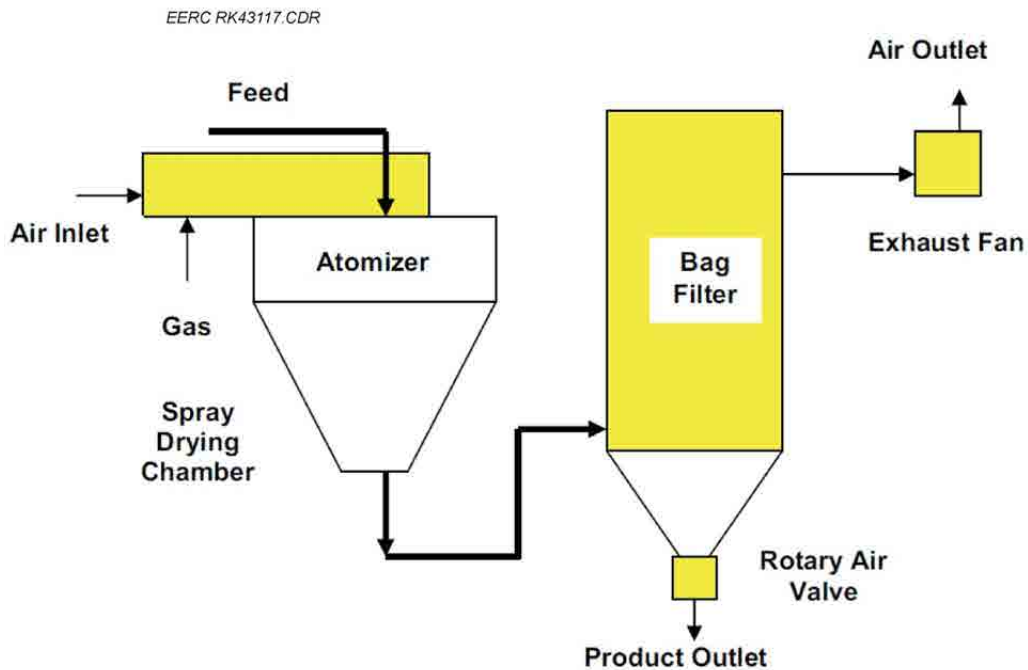


Figure B-8. Schematic diagram of a typical spray dryer (Mickley, 2006).

REFERENCES

- Arthur J., Langhus B., and Patel C., 2005, Technical summary of oil and gas produced water treatment technologies: ALL Consulting, LLC.
- Birkett, J., 2011, Desalination at a glance: International Desalination Association. www.idadesal.org/pdf/IDA%20guide_webonly.pdf (accessed November 2011).
- Bourcier W., Wolery, T., and Aines, R., 2011, Use of formation fluids produced at carbon capture sites for power plant cooling: Carbon Capture and Sequestration Conference.

- Cooley, H, Gleick, P., and Wolff, G., 2006, Desalination, with a grain of salt—a California perspective—Appendix A: Desalination technologies: Pacific Institute for Studies in Development, Environment, and Security. Oakland, California. www.pacinst.org/reports/desalination/appendix_A.pdf.
- El-Naas, M.H., 2011, Reject brine management, *in* Schoor, M., ed., Desalination, trends and technologies: Rijeka, Croatia, InTech. www.intechopen.com/books/show/title/desalination-trends-and-technologies (accessed November 2011).
- Fountain/Quail Water Management, 2010, Aqua Pure: www.aqua-pure.com (accessed 2010).
- Fritzmann, C., Lowenberg, J., Wintgens, T., and Melin, T., 2007, State-of-the-art of reverse osmosis desalination: Desalination, v. 216, nos. 1–3, p. 1–76.
- GE, 2009, GE empowers Barcelona community with water quality solutions: General Electric Company. www.gewater.com/pdf/Case%20Studies_Cust/Americas/English/CS1298EN.pdf (accessed December 2011).
- GE Infrastructure Water & Process Technologies (GE), 2001, Produced water pilot study.
- IDE Technologies Ltd., 2011a, Hadera—127 million m³/year—the world’s largest SWRO desalination plant: www.ide-tech.com/files/990b0fa01310a9c82f841f2183e9ebcb/page/2009/10/Hadera%20Success%20Story.pdf (accessed November 2011).
- Interstate Oil and Gas Compact Commission (IOGCC) and ALL Consulting, 2006, A guide to practical management of produced water from onshore oil and gas operations in the United States: Prepared for the U.S. Department of Energy National Energy Technology Laboratory.
- Lokiec, F., and Ophir, A., 2007, The mechanical vapor compression—38 years of experience: IDA World Congress, Maspalomas, Gran Canaria, Spain October 21–26, 2007. www.ide-tech.com/files/990b0fa01310a9c82f841f2183e9ebcb/newsevent/2009/10/MVC%2038%20years%20of%20experience.pdf (accessed December 2011).
- Mastouri, R., and Nadim, F., 2010, A time to review the produced water treatment technologies, a time to look forward for new management policies, integrated petroleum environmental consortium: Presented at 17th Annual International Petroleum & Biofuels Environmental Conference, San Antonio, Texas, August 30 – September 2. <http://ipecc.utulsa.edu/Conf2010/Powerpoint%20presentations%20and%20papers%20received/Mastouri.pdf> (accessed July 2011).
- Mickley, M., 2006, Membrane concentrate disposal—practices and regulation (2nd ed.): U.S. Department of the Interior, Bureau of Reclamation, Technical Service Center, Water Treatment Engineering and Research Group, April: www.usbr.gov/pmts/water/media/pdfs/report123.pdf (accessed December 2011).

- NanoH₂O, 2011, NanoH₂O delivers the most productive and energy efficient seawater reverse osmosis membrane to the desalination marketplace: www.nanoh2o.com/company/news/2011/45 (accessed December 2011).
- National Research Council, 2008, Desalination, a national perspective: Committee on Advancing Desalination Technology, National Research Council, National Academies Press. www.nap.edu/catalog/12184.html.
- SIDEM, 2011a, Desalination solutions for your drinking & process water needs: SIDEM Veolia. www.sidem-desalination.com/lib/sidem/reference/15473,Sidem-Flyer-Nov09.pdf (accessed December 2011).
- SIDEM, 2011b, Multiple stage flash processes: Veolia Water Solutions & Technologies. www.sidem-desalination.com/en/process/MSF/ (accessed December 2011).
- SIDEM, 2011c, Multiple effect distillation process: Veolia Water Solutions & Technologies. www.sidem-desalination.com/en/process/MED/Process/ (accessed December 2011).
- SIDEM, 2011d, MED/TVC: Veolia Water Solutions & Technologies. www.sidem-desalination.com/en/process/MED/MED-TVC/ (accessed December 2011).
- Stepan, D.S., Shockey, R.E., Kurz, B.A., Kalenze, N.S., Cowan, R.M., Ziman, J.J., and Harju, J.A., 2010, Bakken water opportunities assessment—Phase 1: University of North Dakota Energy and Environmental Research Center, Northern Great Plains Water Consortium, April 2010.
- URS Australia, 2002, Economic and technical assessment of desalination in Australia—with particular reference to national action plan priority regions: Agriculture, Fisheries & Forestry – Australia, 2 September 2002. www.environment.gov.au/water/publications/urban/pubs/desalination-full-report.pdf (accessed November 2011).
- Veil, J.A., 2008, Thermal distillation technology for management of produced water and frac flowback water: Argonne National Laboratory Water Technology Brief 2008-1, U.S. Department of Energy Office of Fossil Energy, National Energy Technology Laboratory.
- WaterReuse Association, 2011, Seawater desalination power consumption white paper: www.watereuse.org/sites/default/files/u8/Power_consumption_white_paper.pdf (accessed November 2011).
- Yun, T.I., Gabelich, C.J., Cox, M.R., Mofidi, A.A., and Lesan, R., 2006, Reducing costs for large-scale desalting plants using large-diameter, reverse osmosis membranes: Desalination, v. 189, p. 141–154.

APPENDIX C

KETZIN MODELING AND SIMULATIONS

KETZIN MODELING AND SIMULATIONS

DYNAMICS MODELING AND SIMULATIONS

In this case study, a total of 16 scenarios were designed to address the relationships between CO₂ storage and water extraction with varying injection and extraction strategies (Table C-1). Cases 1 through 3 were developed to test the effects of different model boundary conditions on simulation results, specifically, closed, semiclosed, and open. The closed boundary, tested with Case 1, significantly limited the storage capacity of the model (Figure C-1). Therefore, open and semiclosed boundary conditions were used as settings for the remaining simulations. Moreover, the case with open boundaries shows only a slight increase in capacity over that of the semiclosed setting used in Cases 4 and 5. This is due to the strong influence the dome structure of the Ketzin site has over the movement of CO₂ within the reservoir. The structure sufficiently trapped a large portion of the free-phase CO₂ and reduced the effects from open boundary simulations on CO₂ injectivity. When water extraction is considered, the total injected CO₂ volumes are double compared to the results without any water extraction. The extraction wells were set to remove approximately the same volume of water as the volume of injected CO₂. This opened up additional pore space for the CO₂ to occupy.

All of the detailed results of total injected CO₂, well rates and bottomhole pressures (BHPs), CO₂ plumes, and pressure distributions over time are shown in Figures C-1 to C-67, ordered by simulation case. These results are presented as plots, 3-D views, areal views, and cross sections. Figures C-68 through C-73 show surficial map-based views of plume extents.

Generally, surficially dissolved CO₂ brine injection (Table C-2) shows significantly less CO₂ storage capacity compared with the free-phase injections, especially considering the natural efficiency of the structure at the Ketzin site. The main reason is the reduced mobility of the CO₂ saturated aqueous phase (as opposed to the free-phase CO₂) in the reservoir, resulting in pressure buildups that limit injection rates. To overcome this limitation, Cases 9 and 10 were run with an increased number of extraction and injection wells, utilizing a nine-spot pattern of injection and extraction (Figures C-52 and C-53). The results of these cases indicate that the total volume of injected CO₂ was increased by five times over a single well pair (one injector and extractor). However, this volume was still only 22% of the volume of free-phase CO₂ injected in the base case (Case 2). Cases 9 and 10 also show the influence of well location and structure on CO₂ storage capacity.

To further investigate the effects of water extraction via multiple-well patterns on storage capacity, 8-spot and 25-spot patterns were simulated. For each pattern, three scenarios were designed: 1) injectors only, no water extraction, 2) injectors and extractors, and 3) implying all wells as injectors (Table C-3). The well locations were located atop the Ketzin dome structure and employed the same injection wells used in the previous simulations in addition to new wells on a 3-km spacing (Figures C-74 and C-75). The simulation results show that the storage capacity substantially increases with water extraction (Table C-3 and Figure C-14; found in main body of report). For example, for the 8-spot pattern, the storage capacity increased by about 34% compared to the case of four injection wells with no production, while the storage capacity increases 88% for the 25-spot pattern for the similar comparisons. The cases using all wells as injectors for both patterns do not perform as well as those with water extraction, although the storage capacity increases by approximately 10% (Figures C-76 and C-77). Images of these

simulations of CO₂ plumes and pressure distributions over time are found in Figures C-78 to C-101, ordered by simulation case. These results are presented as 3-D CO₂ plumes and areal pressure plots.

Table C-1. Detailed Properties of the Simulation Cases Investigated

Variable	Unit	Case 1	Case 2	Case 3	Case 4	Case 5	Case 6
Injection Rate/Well	Mt/year	2	2	2	2	2	2
Injection Period	years	25	25	25	25	25	25
Actual Injection Rate	kg/day	4.51E+05	1.43E+06	1.98E+06	2.81E+06	3.00E+06	3.55E+06
Cumulative Injected CO ₂	SC, ^a tonnes	4.12E+06	1.30E+07	1.81E+07	2.57E+07	2.74E+07	3.24E+07
Cumulative Injected CO ₂	RC, ^b m ³	1.76E+07	5.82E+07	8.13E+07	1.16E+08	1.25E+08	1.22E+08
Number of Injection Wells		1	1	1	1	1	2
Extraction Wells		No	No	No	Yes	Yes	No
Extraction Well Location		N/A	N/A	N/A	1	1	N/A
Cumulative Extracted Water	RC, m ³	N/A	N/A	N/A	1.18E+08	1.25E+08	N/A
Average Daily Extraction Rate	SC, m ³ /day	N/A	N/A	N/A	1.28E+04	1.36E+04	N/A
Average Extraction Period	years	N/A	N/A	N/A	25.00	25.00	N/A
Highest Injection BHP	kPa	7400	7400	7400	7400	7400	7400 and 8250
Lowest Production BHP	kPa	N/A	N/A	N/A	2000	2000	N/A
Boundary Conditions		Closed	Volumed	Opened	Volumed	Opened	Volumed

^a Standard conditions (25°C, 0.999 bar).

^b Reservoir conditions (variable with depth, average of 25°C, 67 bar).

Table C-2. Detailed Properties of the Simulation Cases Utilizing Surface Dissolution

Variable	Unit	Case 7	Case 8	Case 9	Case 10
Injection Solvent	moles/kg	0.35	0.45	0.45	0.45
Injection Period	years	25	25	25	25
Cumulative Injected CO ₂	SC, tonnes	4.30E+05	5.55E+05	2.61E+06	2.88E+06
Number of Injection Wells		1	1	4+5 producers	4+5 producers
Extraction Wells		Yes (recycled)	Yes (recycled)	Yes (recycled)	Yes (recycled)
Extraction Well Location		1	1	1	2
Cumulative Extracted Water	RC, m ³	2.80E+07	2.82E+07	2.32E+08	2.41E+08
Average Daily Extraction Rate	SC, m ³ /day	3.06E+03	3.09E+03	2.55E+04	2.65E+04
Average Extraction Period	years	25	25	25	25
Highest Injection BHP	kPa	12500	12500	Various	Various
Lowest Production BHP	kPa	2000	2000	2000	2000
Boundary Conditions		Volumed	Volumed	Volumed	Volumed

Table C-3. Detailed Properties of the Simulation Cases Investigated

Variable	Unit	Case 11	Case 12	Case 13	Case 14	Case 15	Case 16
Injection Rate/Well	Mt/year	2	2	2	2	2	2
Injection Period	years	25	25	25	25	25	25
Actual Injection Rate	kg/day	6.95E+06	7.17E+06	9.50E+06	1.45E+07	2.49E+07	2.01E+07
Cumulative Injected CO ₂	SC, tonnes	6.33E+07	6.54E+07	8.67E+07	1.32E+08	2.27E+08	1.84E+08
Cumulative Injected CO ₂	RC, m ³	1.79E+08	2.39E+08	2.04E+08	2.42E+08	4.54E+08	3.00E+08
Number of Injection Wells		4	4	8	12	12	25
Extraction Wells		No	Yes (4)	No	No	Yes (13)	No
Cumulative Extracted Water	RC, m ³	N/A	7.03E+07	N/A	N/A	2.44E+08	N/A
Average Daily Extraction Rate	SC, m ³ /day	N/A	1.27E+04	N/A	N/A	6.58E+04	N/A
Average Extraction Period	years	N/A	14.92	N/A	N/A	10.00	N/A
Highest Injection BHP*	kPa	Various	Various	Various	Various	Various	7400
Lowest Production BHP	kPa	N/A	2000	N/A	N/A	2000	N/A
Boundary Conditions		Semiclosed	Semiclosed	Semiclosed	Semiclosed	Semiclosed	Semiclosed

* BHP pressure depends on the injection well location.

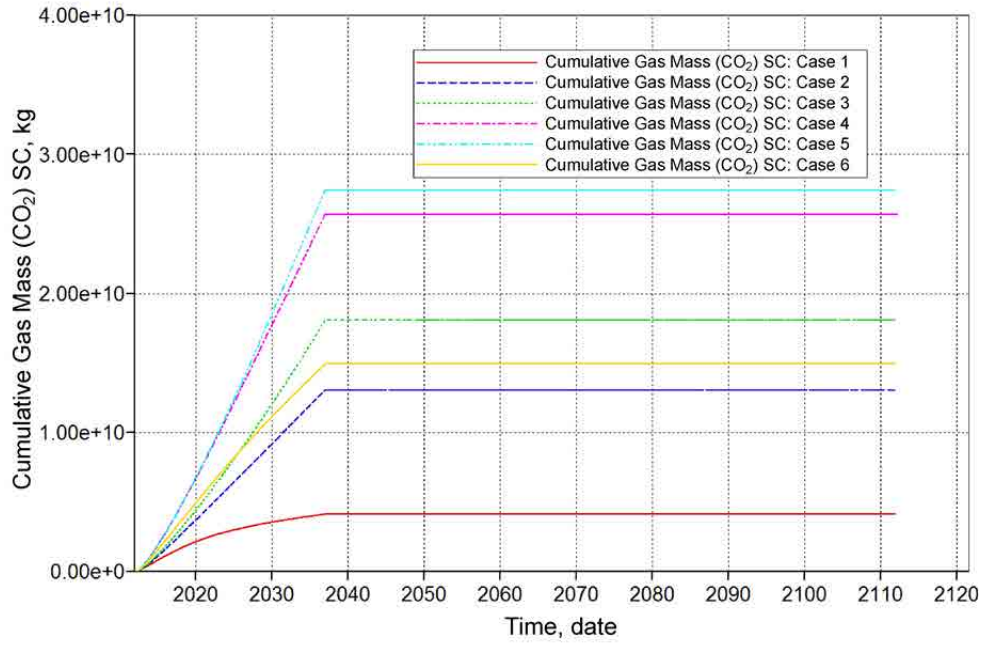


Figure C-1. Total injected CO₂ for Cases 1–6.

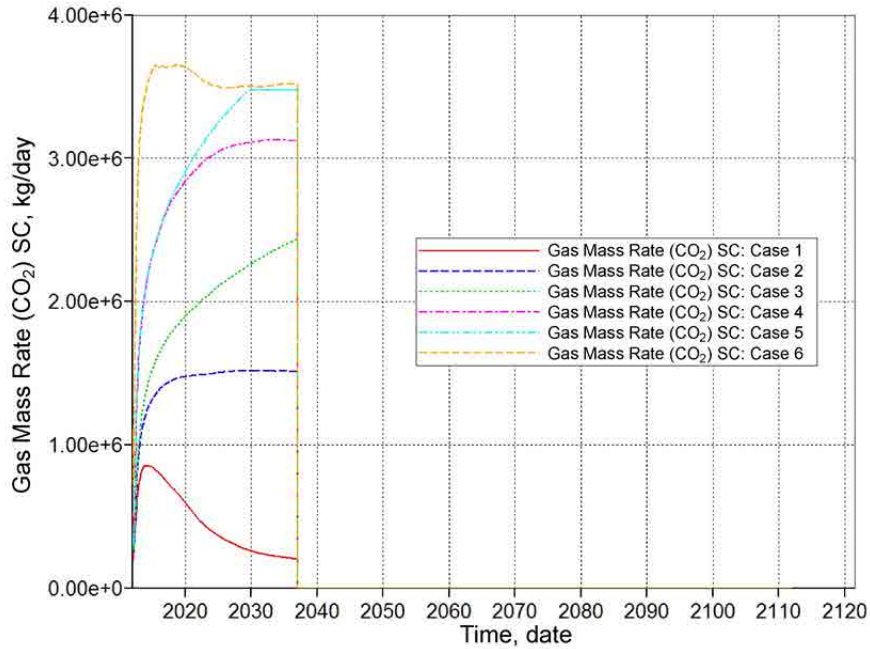


Figure C-2. CO₂ injection rates for Cases 1–6.

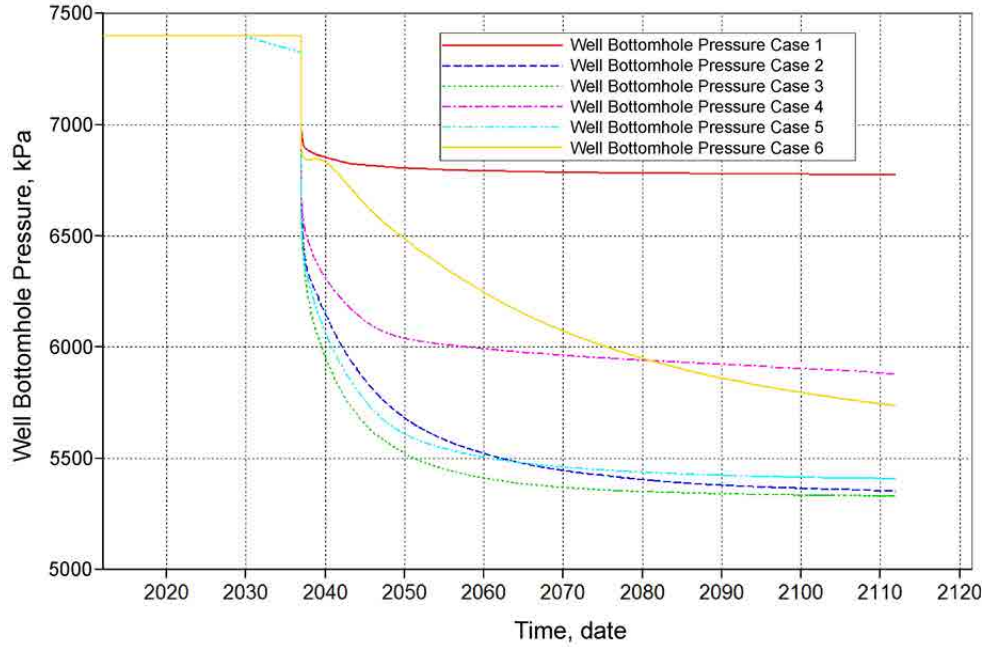


Figure C-3. Injection well BHPs for Cases 1–6.

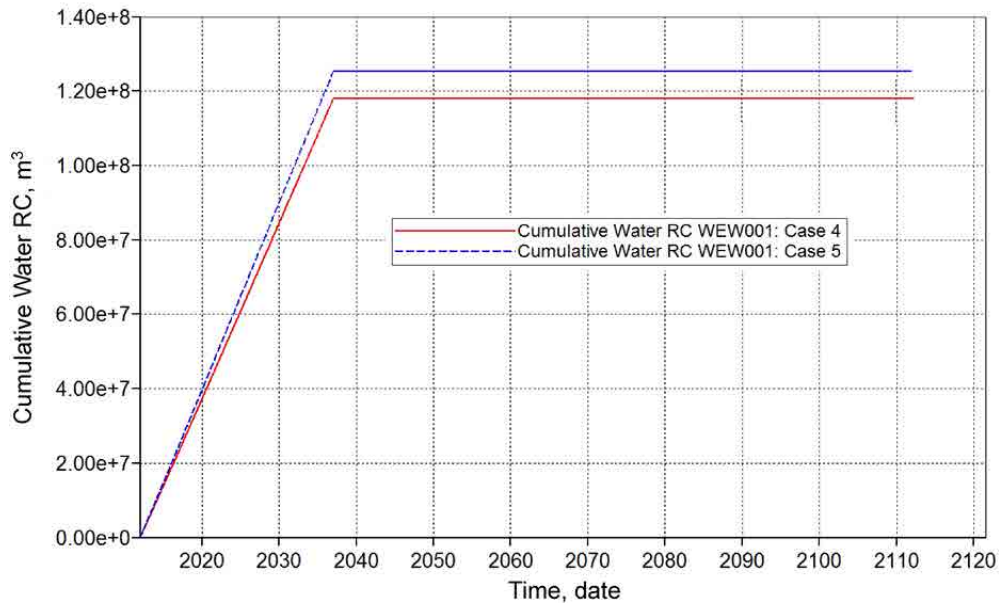


Figure C-4. Total produced water for Cases 4 and 5.

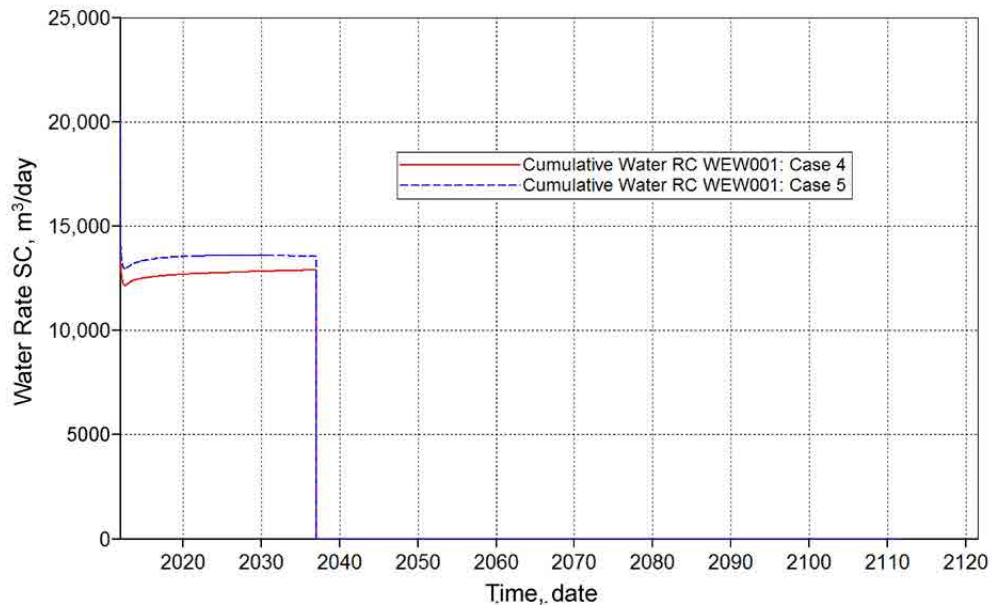


Figure C-5. Production rate for Cases 4 and 5.

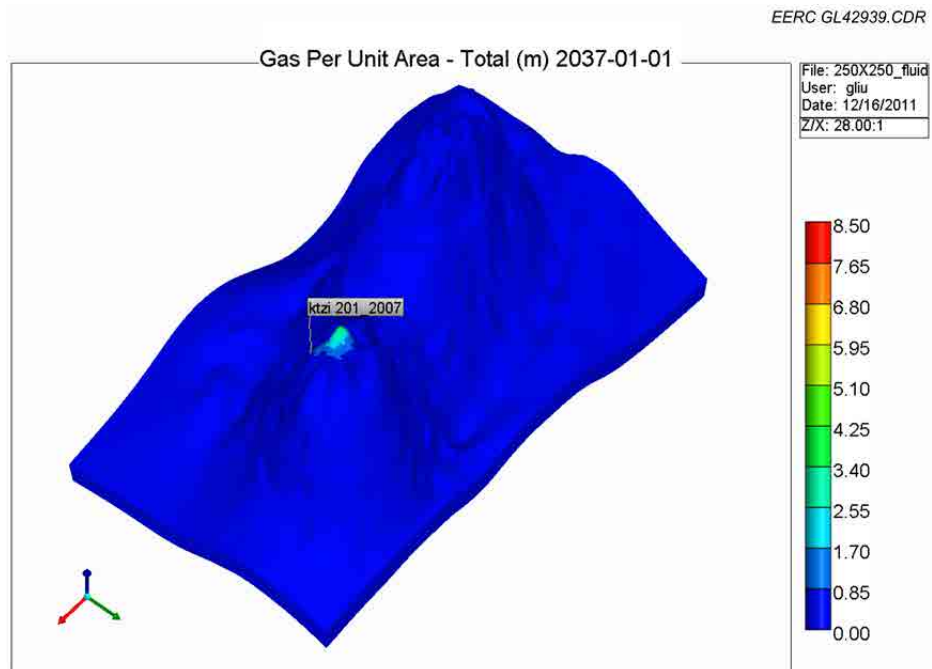


Figure C-6. 3-D view of Case 1: CO₂ plume migration for 25 years from beginning of injection.

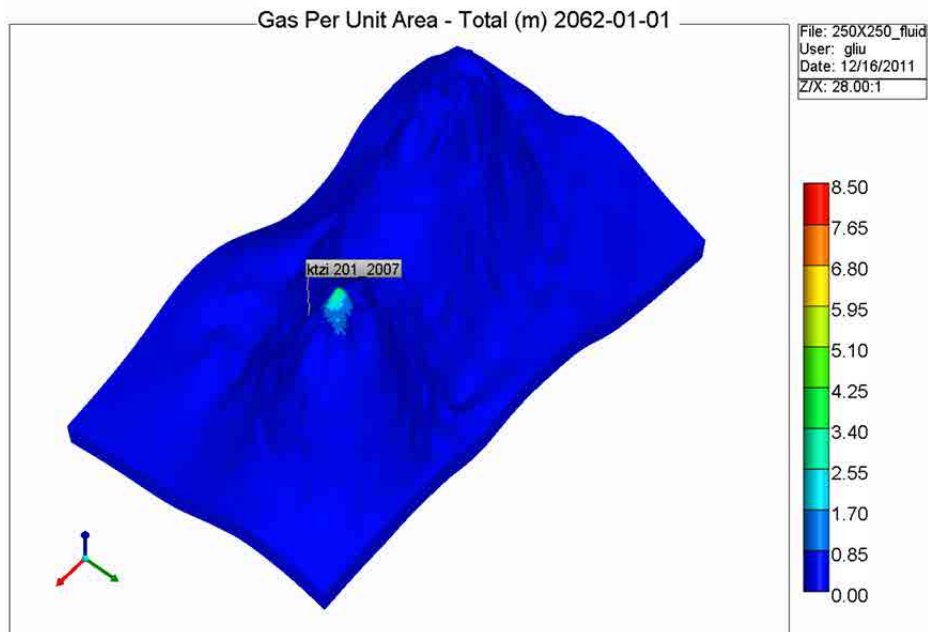


Figure C-7. 3-D view of Case 1: CO₂ plume migration for 50 years from beginning of injection.

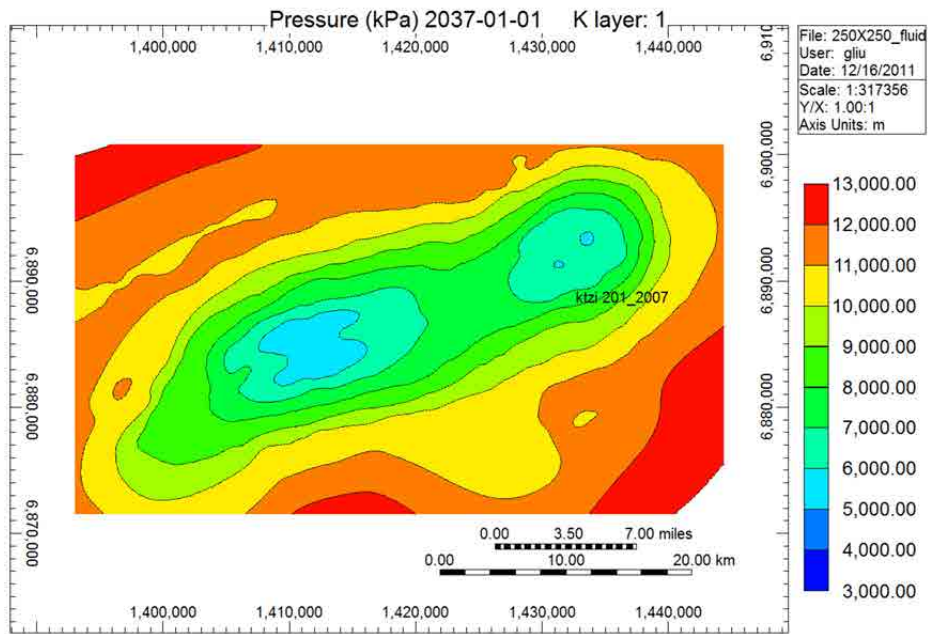


Figure C-8. Areal view of Case 1: pressure distributions for 25 years from beginning of injection.

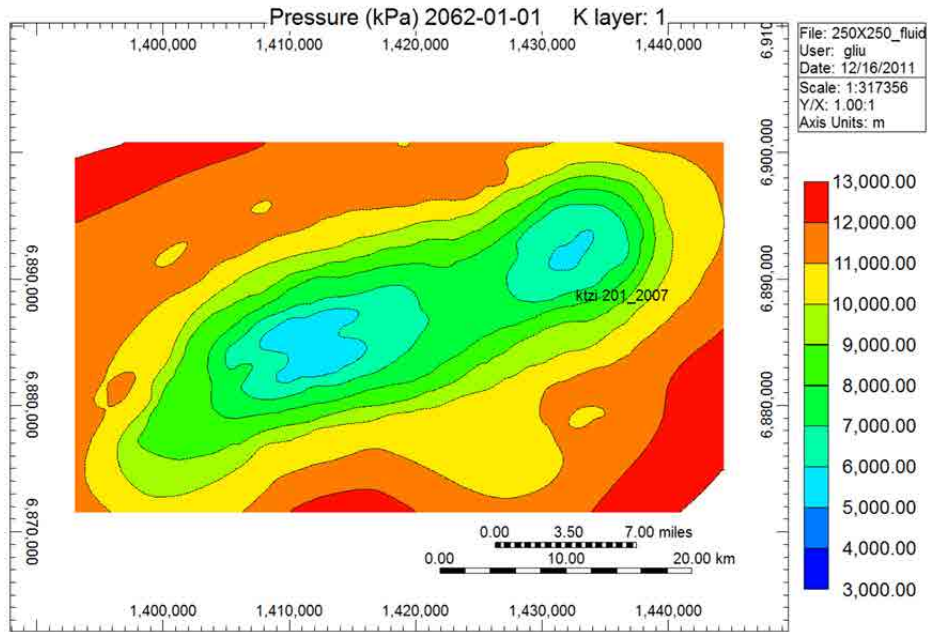


Figure C-9. Areal view of Case 1: pressure distributions for 50 years from beginning of injection.

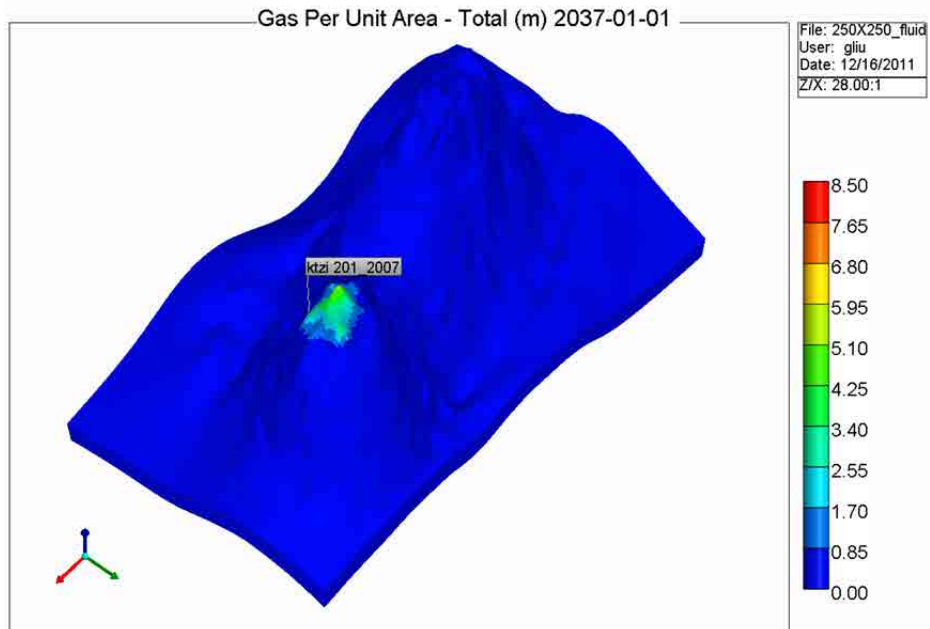


Figure C-10. 3-D view of Case 2: CO₂ plume migration for 25 years from beginning of injection.

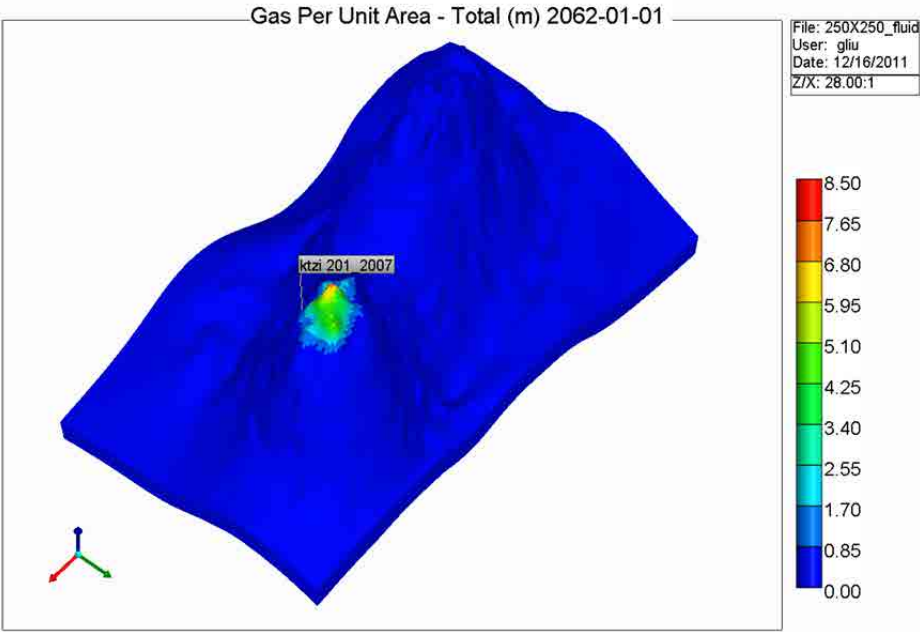


Figure C-11. 3-D view of Case 2: CO₂ plume migration for 50 years from beginning of injection.

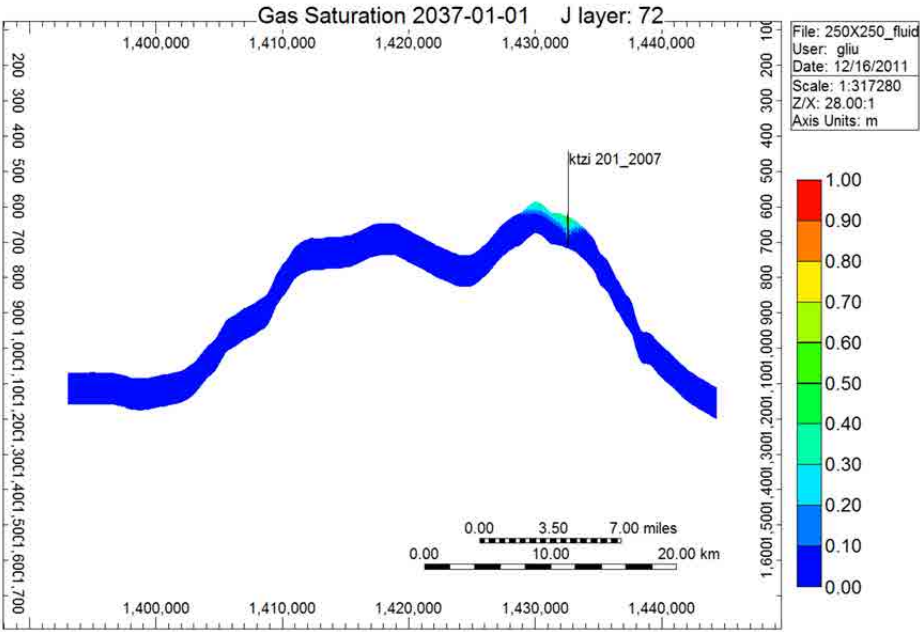


Figure C-12. Cross-sectional view of Case 2: CO₂ plume migration for 25 years from beginning of injection.

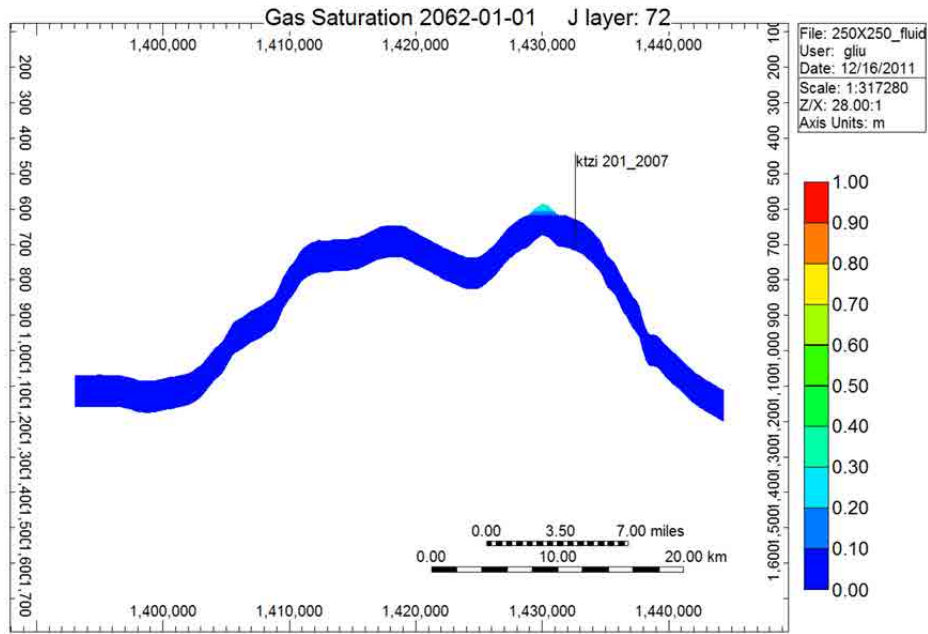


Figure C-13. Cross-sectional view of Case 1: CO₂ plume migration for 50 years from beginning of injection.

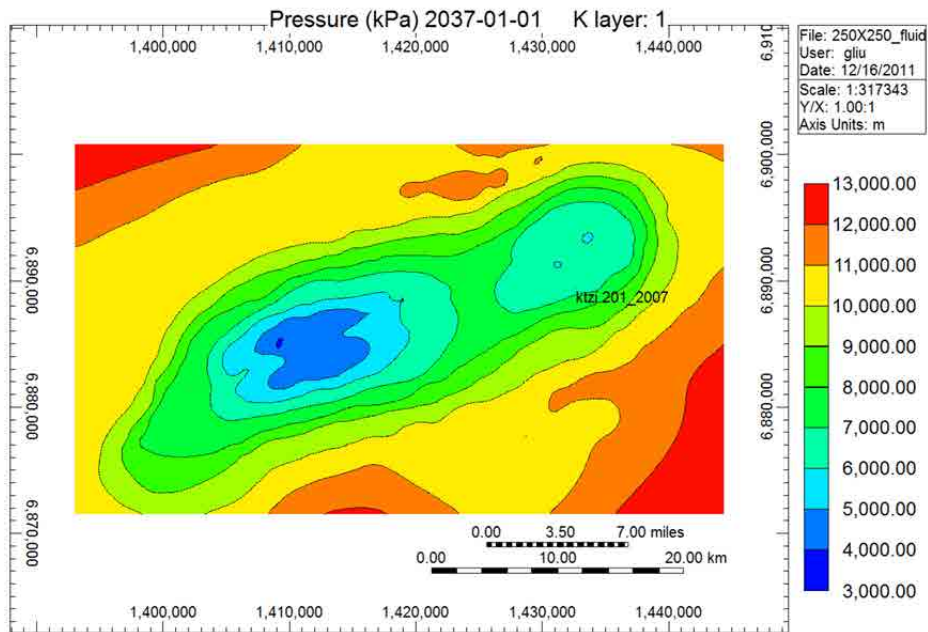


Figure C-14. Areal view of Case 2: pressure distributions for 25 years from beginning of injection.

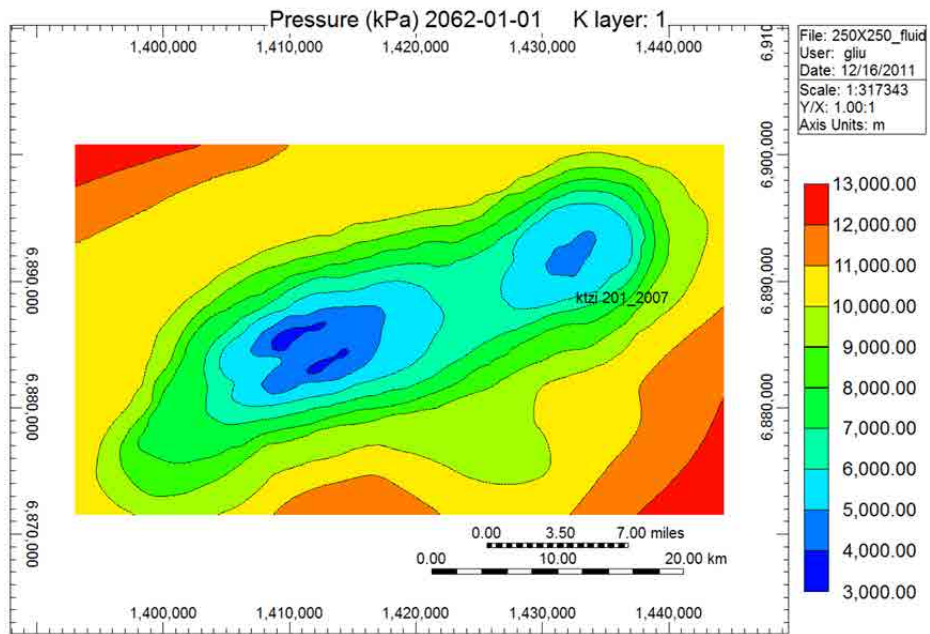


Figure C-15. Areal view of Case 2: pressure distributions for 50 years from beginning of injection.

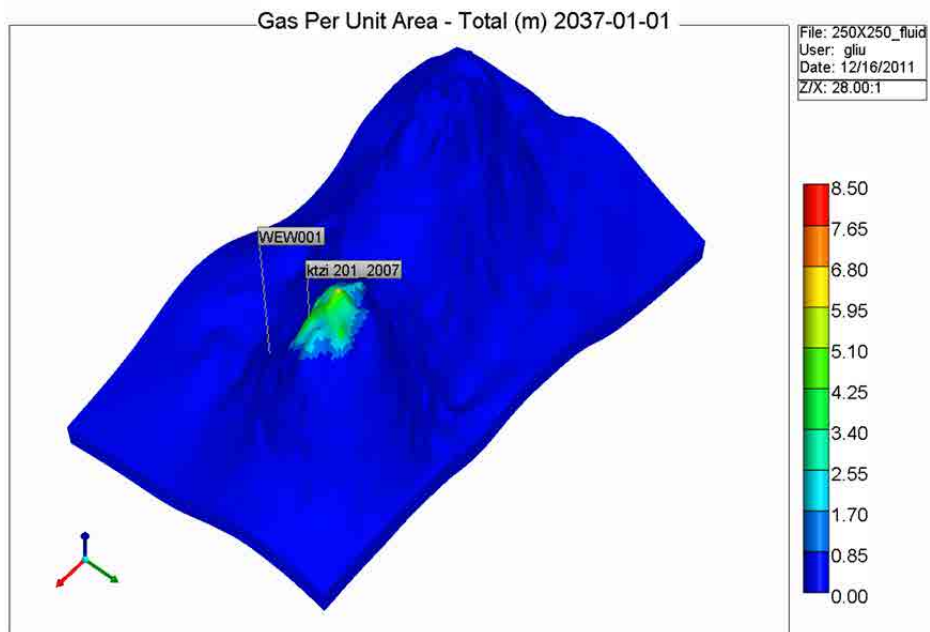


Figure C-16. 3-D view of Case 3: CO₂ plume migration for 25 years from beginning of injection.

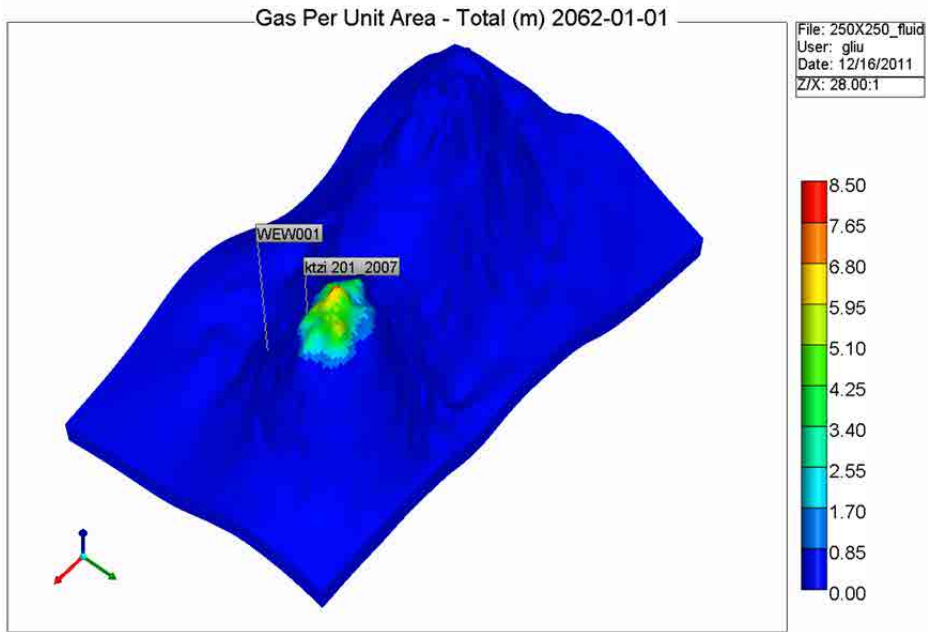


Figure C-17. 3-D view of Case 3: CO₂ plume migration for 50 years from beginning of injection.

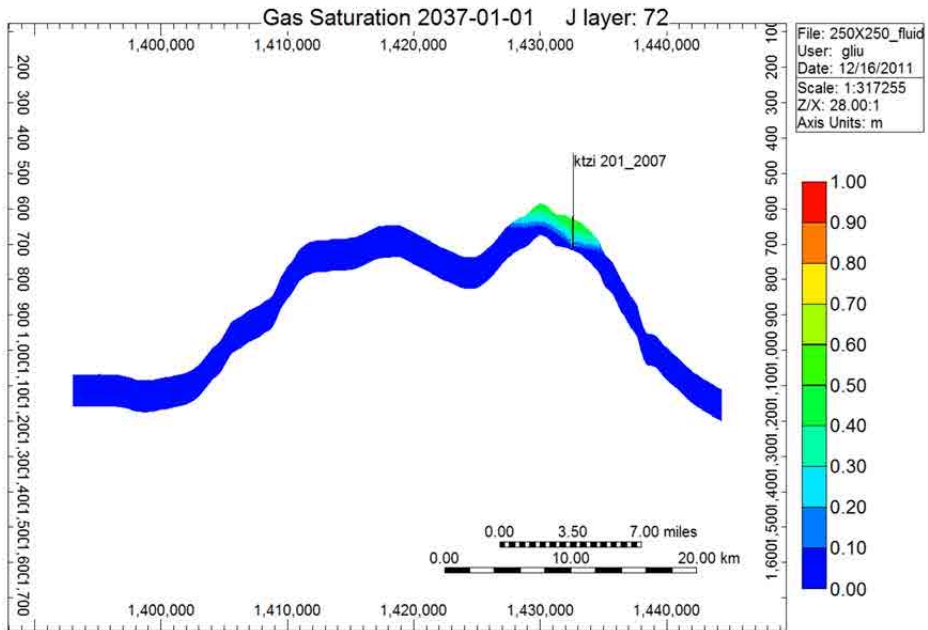


Figure C-18. Cross-sectional view of Case 3: CO₂ plume migration for 25 years from beginning of injection.

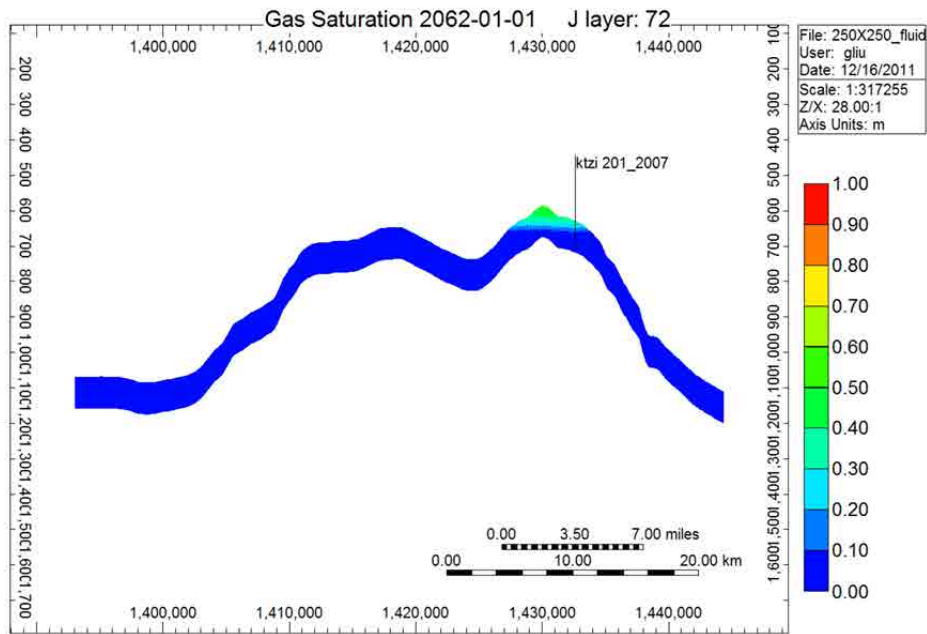


Figure C-19. Cross-sectional view of Case 3: CO₂ plume migration for 50 years from beginning of injection.

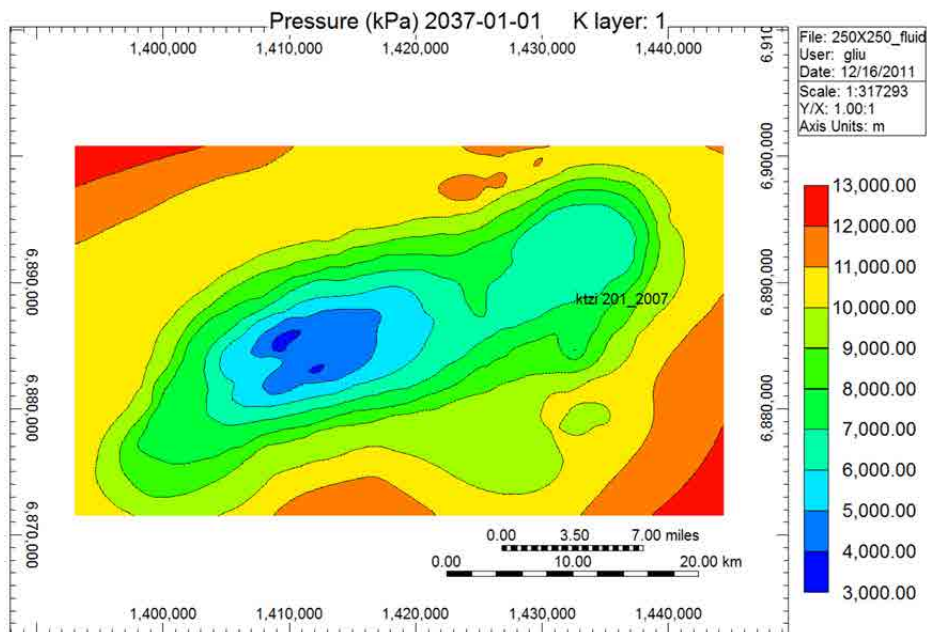


Figure C-20. Areal view of Case 3: pressure distributions for 25 years from beginning of injection.

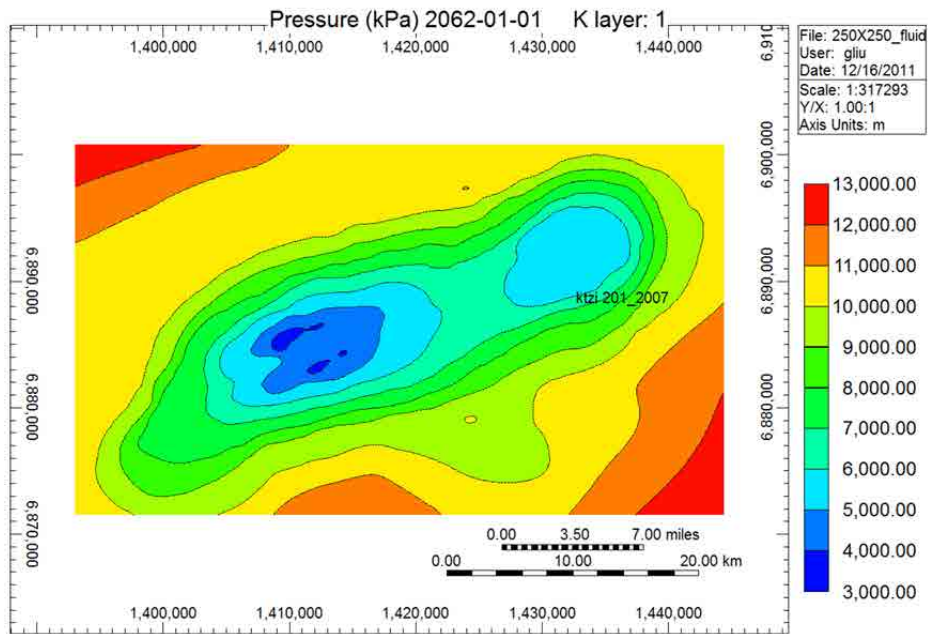


Figure C-21. Areal view of Case 3: pressure distributions for 50 years from beginning of injection.

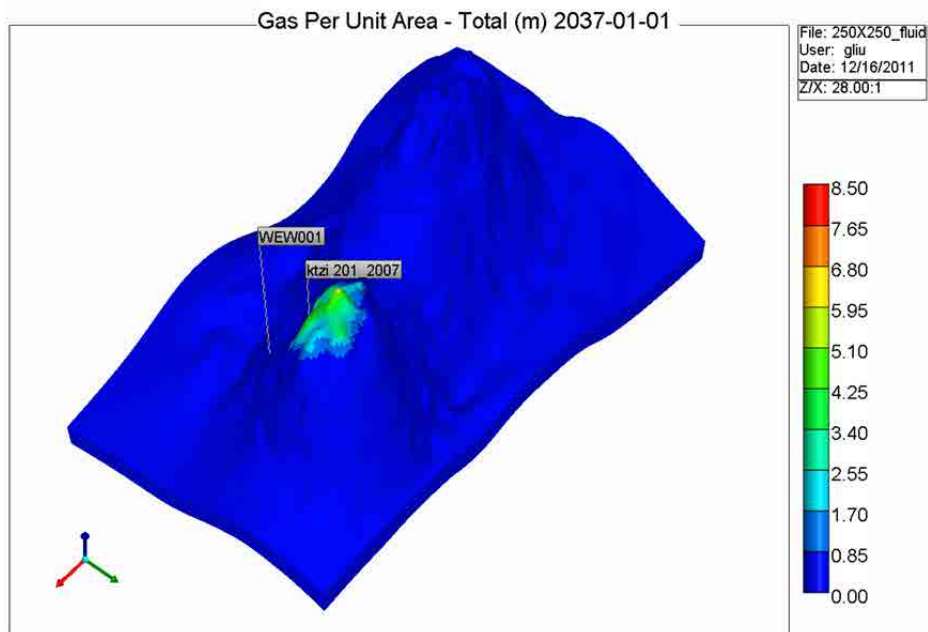


Figure C-22. 3-D view of Case 4: CO₂ plume migration for 25 years from beginning of injection.

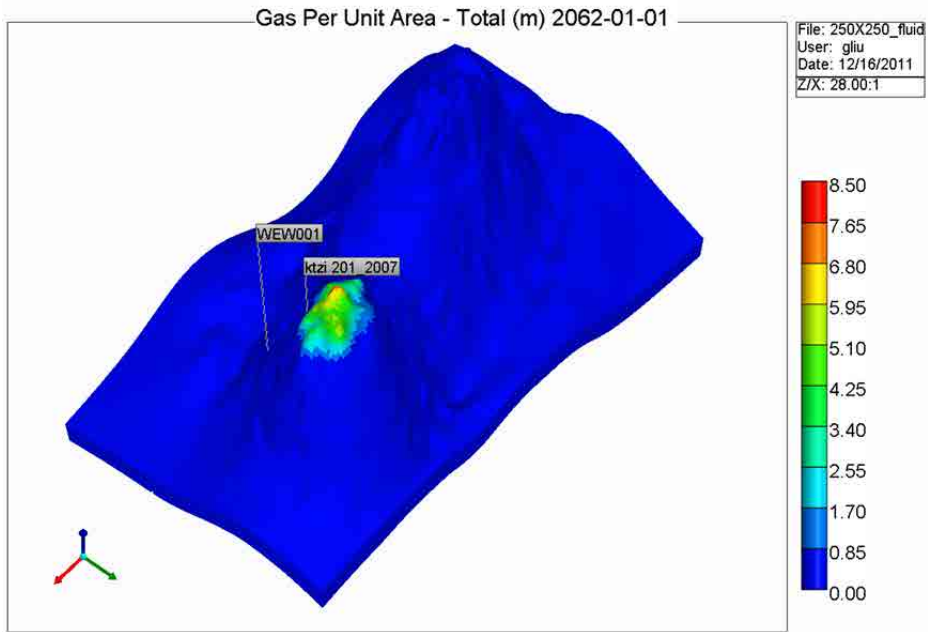


Figure C-23. 3-D view of Case 4: CO₂ plume migration for 50 years from beginning of injection.

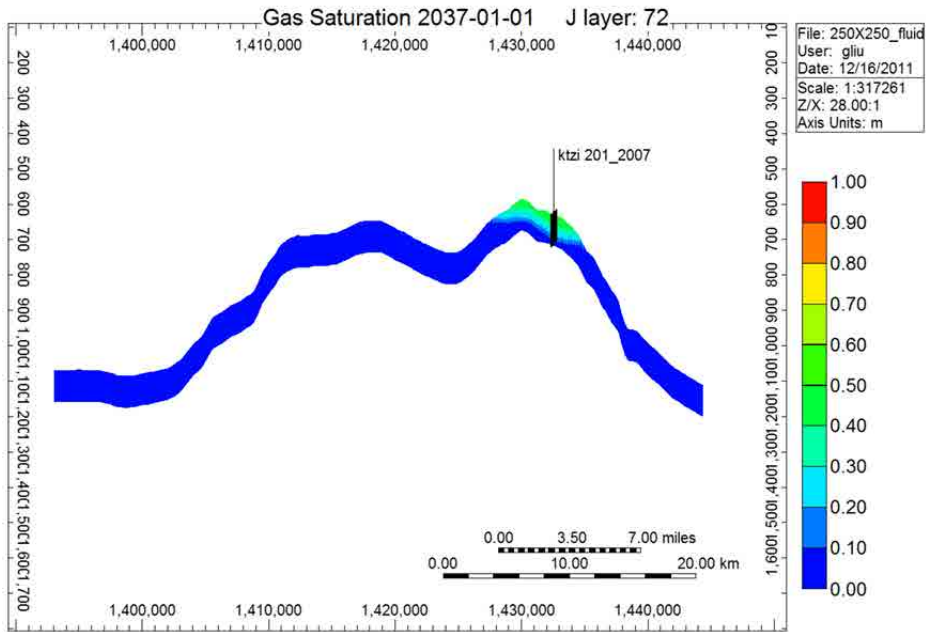


Figure C-24. Cross-sectional view of Case 4: CO₂ plume migration for 25 years from beginning of injection.

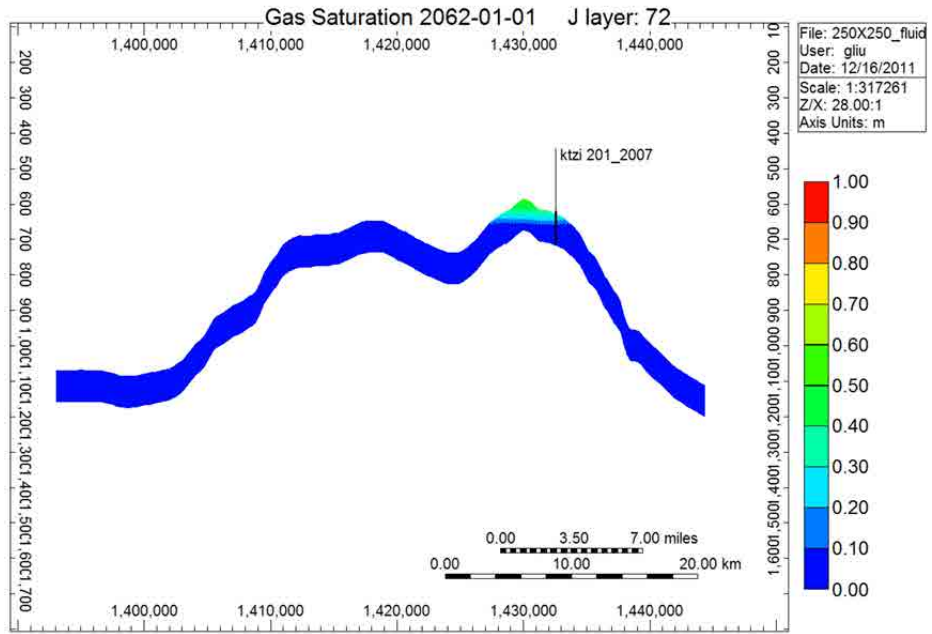


Figure C-25. Cross-sectional view of Case 4: CO₂ plume migration for 50 years from beginning of injection.

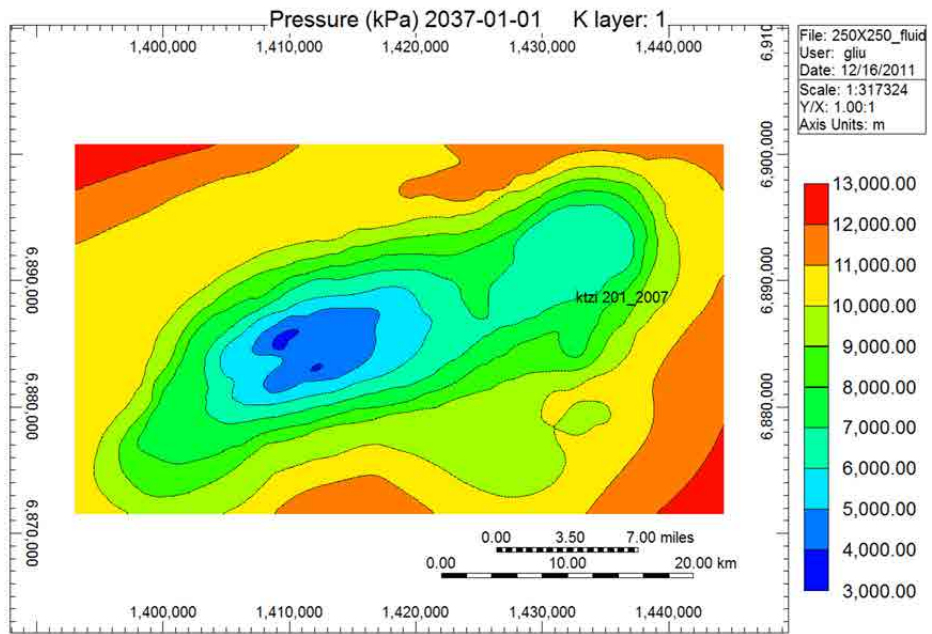


Figure C-26. Areal view of Case 4: pressure distributions for 25 years from beginning of injection.

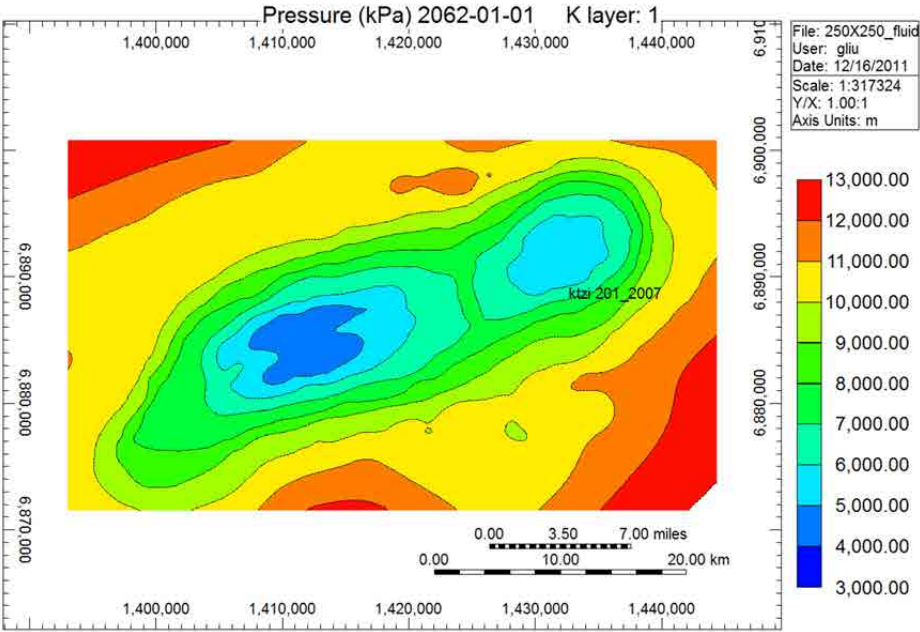


Figure C-27. Areal view of Case 4: pressure distributions for 50 years from beginning of injection.

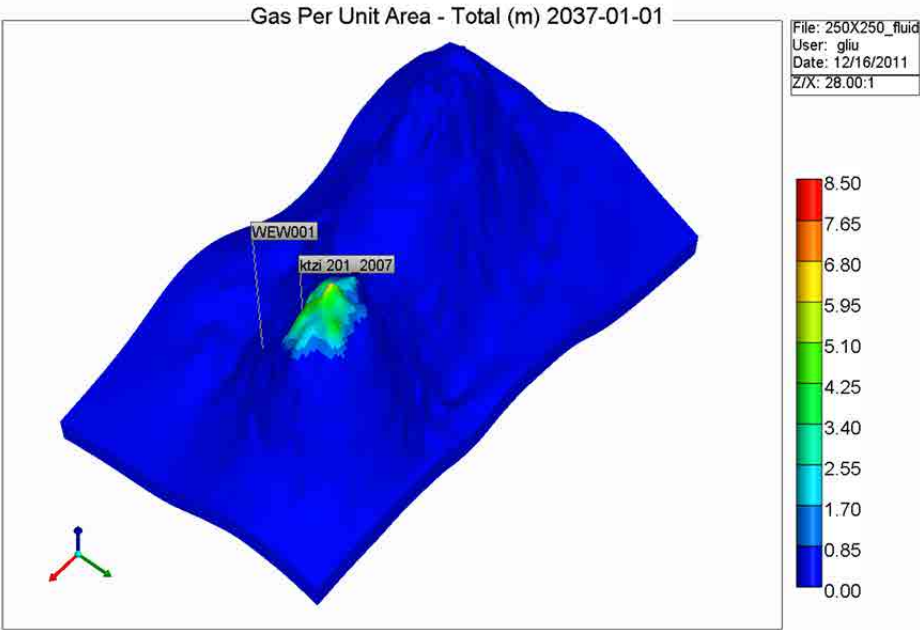


Figure C-28. 3-D view of Case 5: CO₂ plume migration for 25 years from beginning of injection.

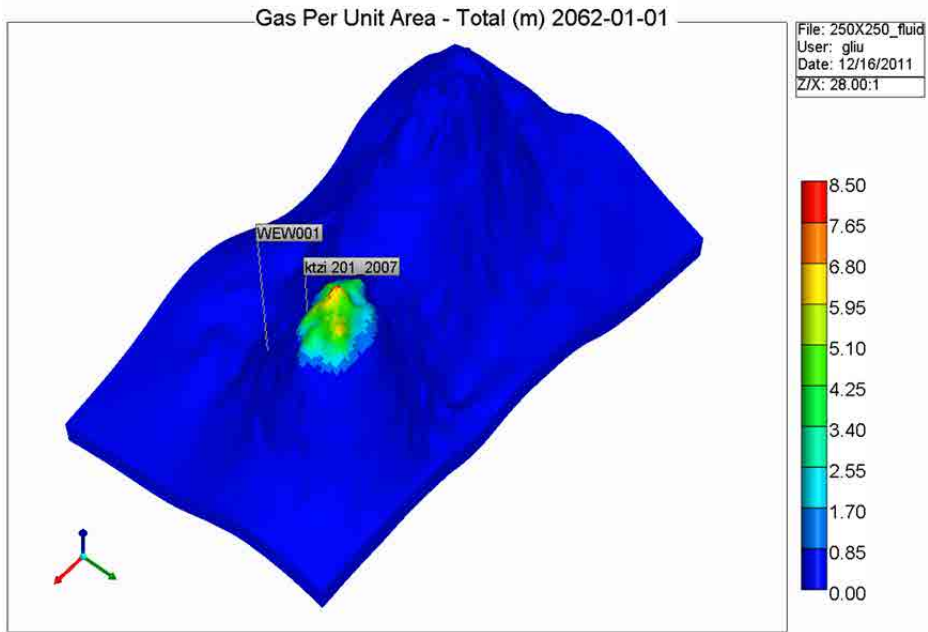


Figure C-29. 3-D view of Case 5: CO₂ plume migration for 50 years from beginning of injection.

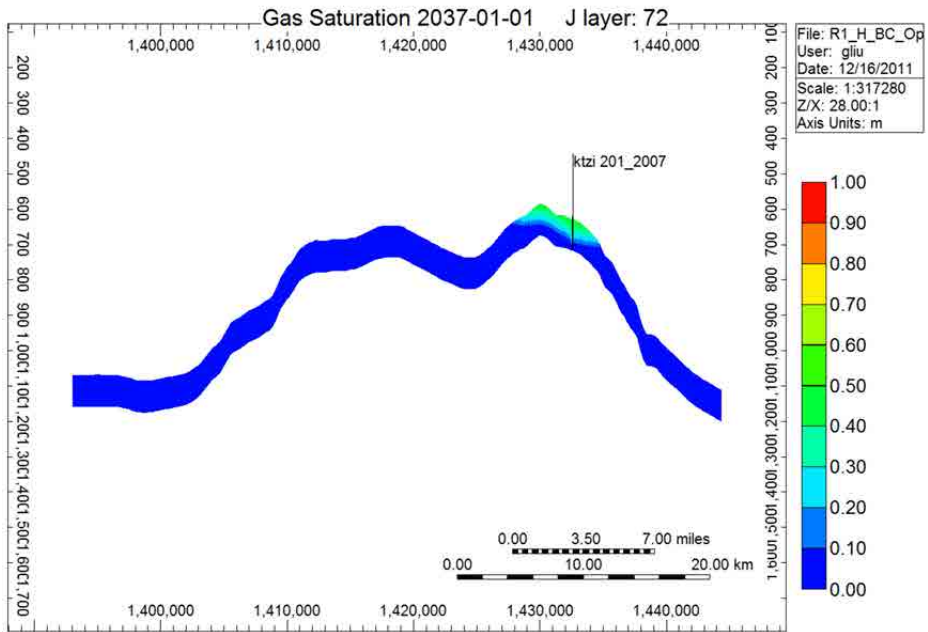


Figure C-30. Cross-sectional view of Case 5: CO₂ plume migration for 25 years from beginning of injection.

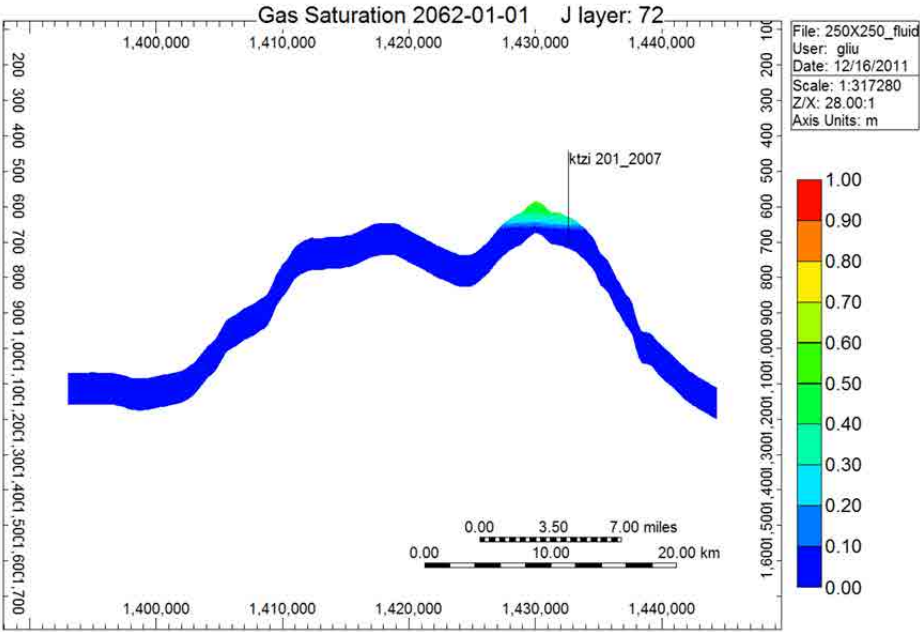


Figure C-31. Cross-sectional view of Case 5: CO₂ plume migration for 50 years from beginning of injection.

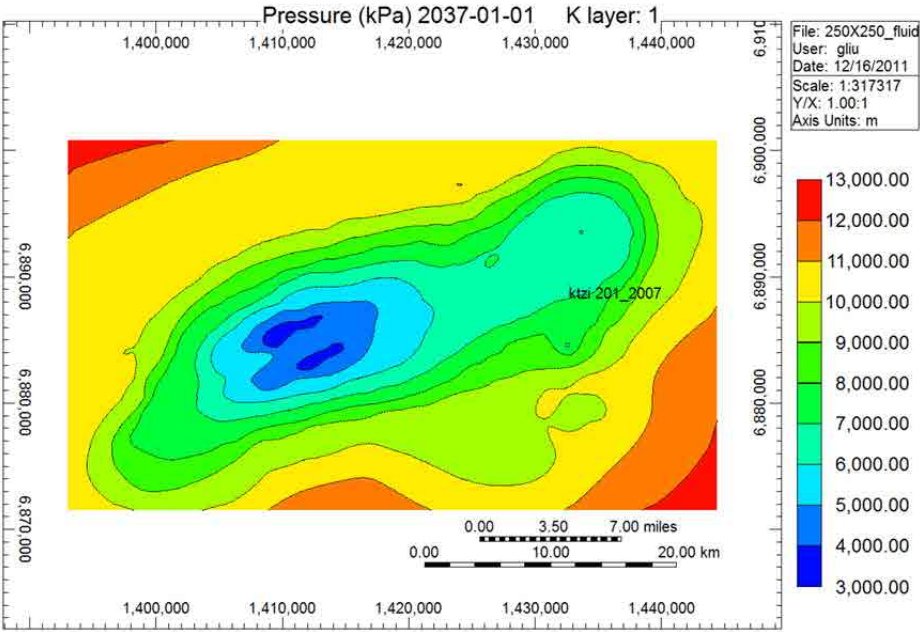


Figure C-32. Areal view of Case 5: pressure distributions for 25 years from beginning of injection.

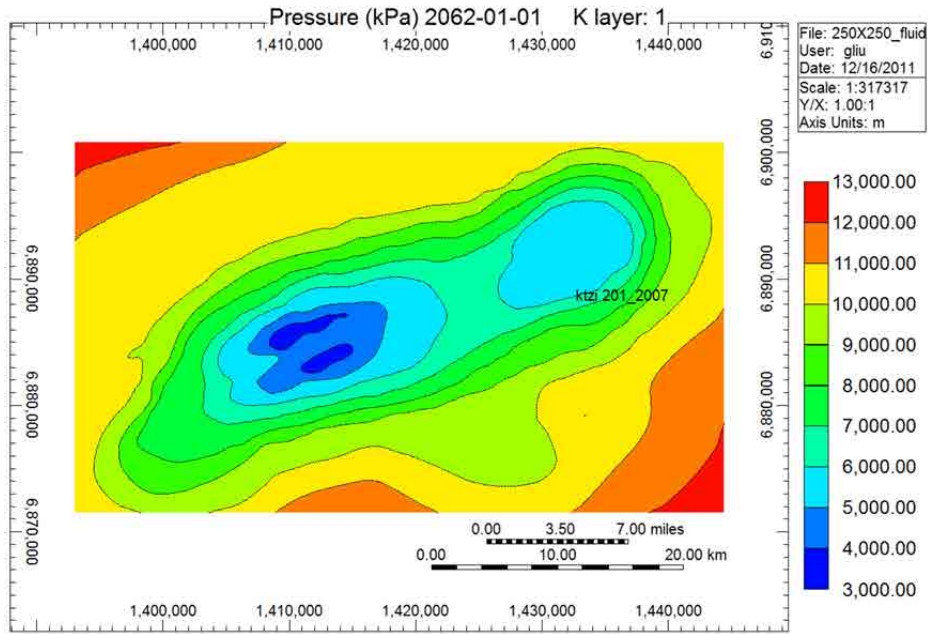


Figure C-33. Areal view of Case 5: pressure distributions for 50 years from beginning of injection.

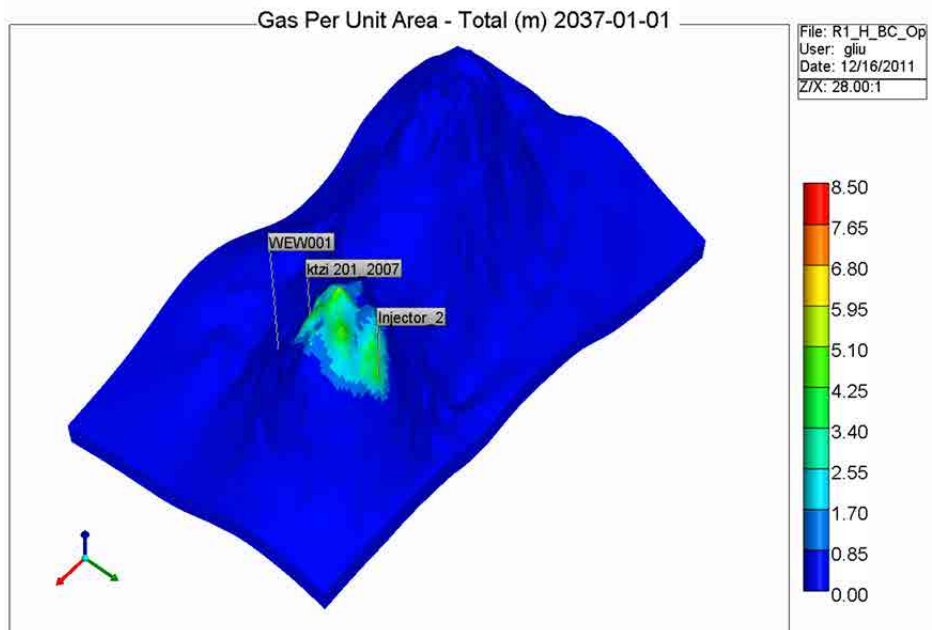


Figure C-34. 3-D view of Case 6: CO₂ plume migration for 25 years from beginning of injection.

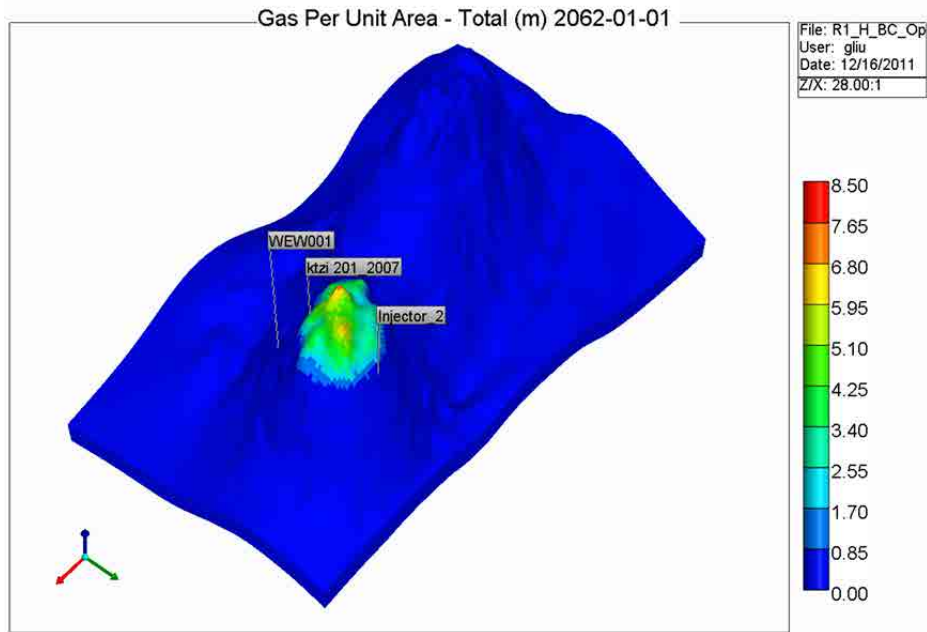


Figure C-35. 3-D view of Case 6: CO₂ plume migration for 50 years from beginning of injection.

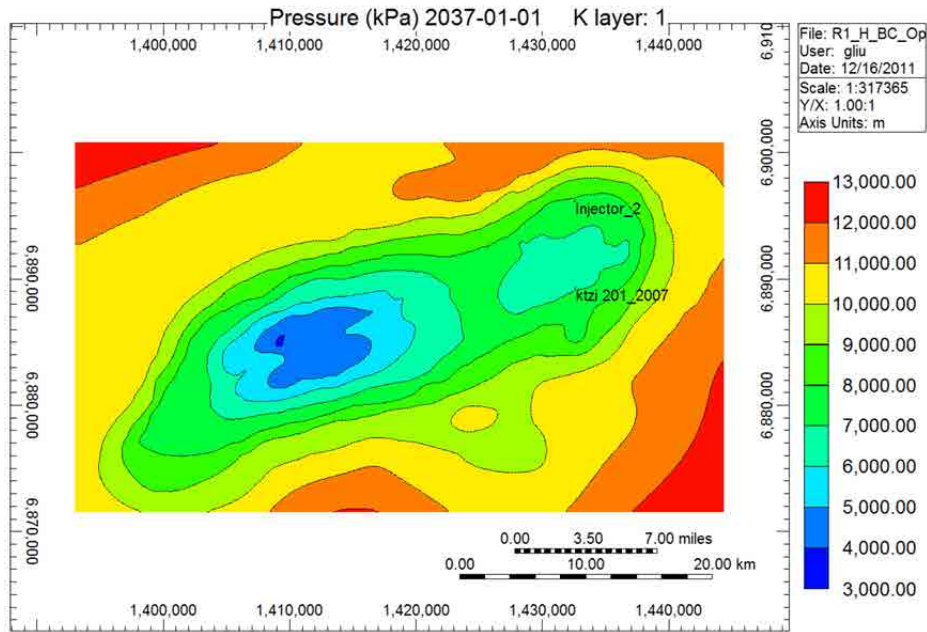


Figure C-36. Areal view of Case 6: pressure distributions for 25 years from beginning of injection.

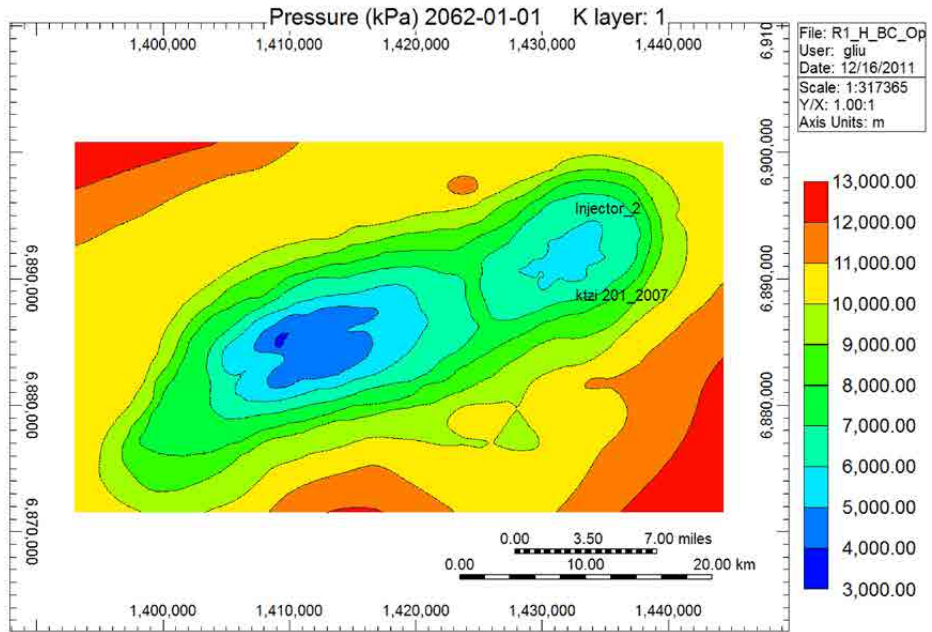


Figure C-37. Areal view of Case 6: pressure distributions for 50 years from beginning of injection.

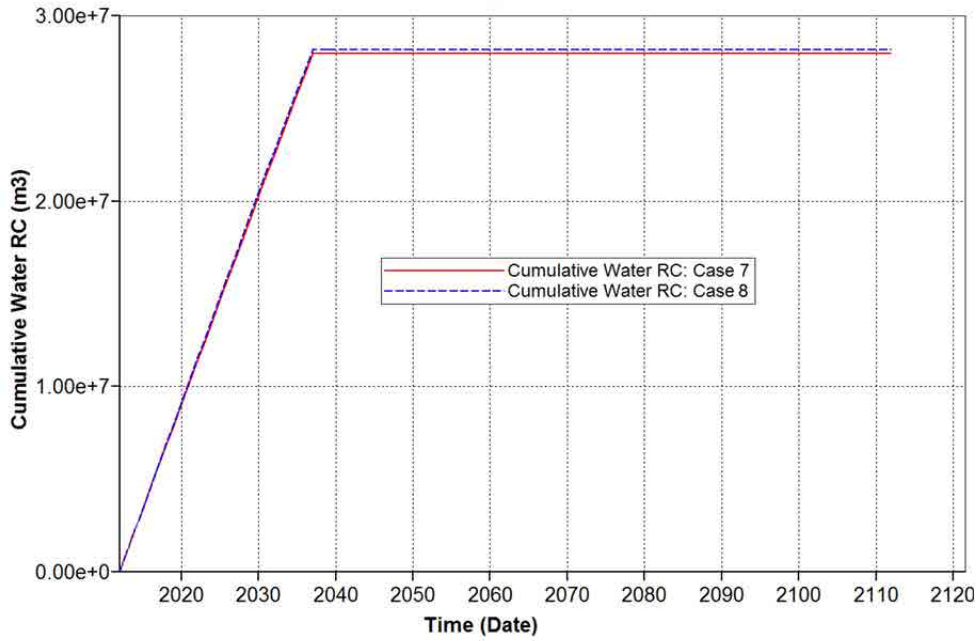


Figure C-38. Total produced water for Cases 7 and 8.

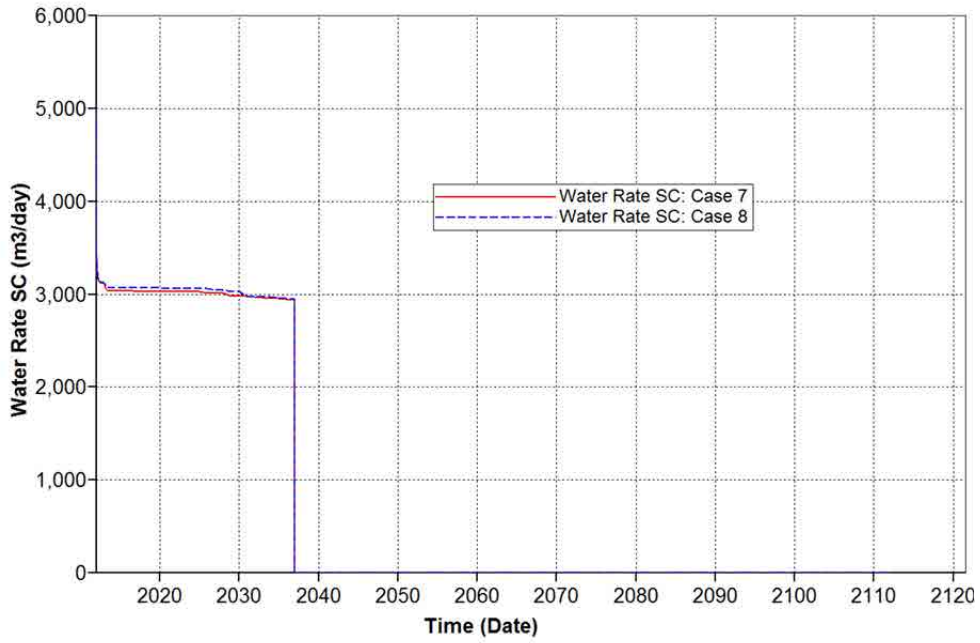


Figure C-39. Water production rate for Cases 7 and 8.

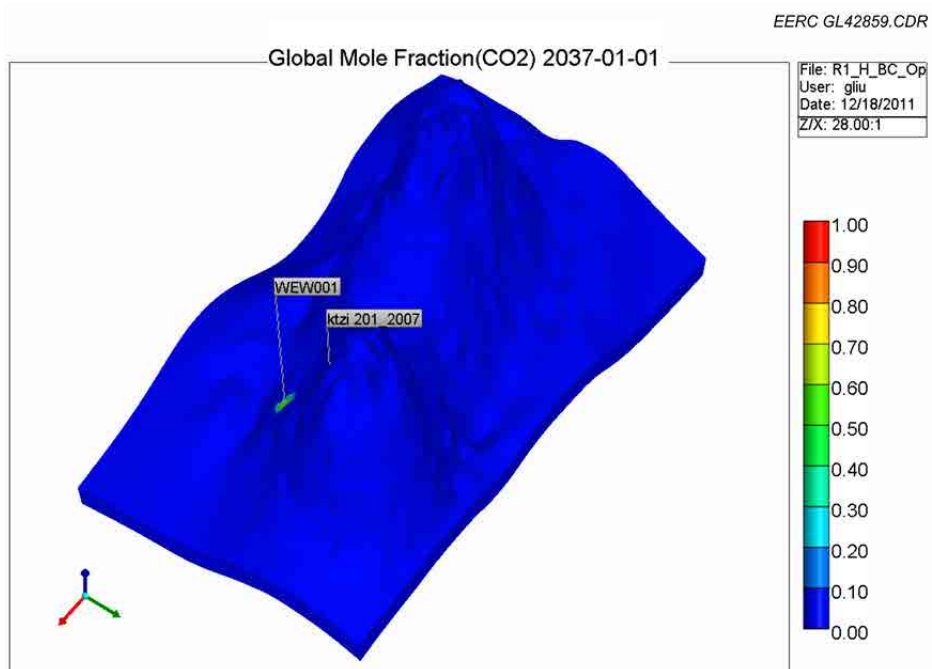


Figure C-40. 3-D view of Case 7: CO₂ plume migration for 25 years from beginning of injection.

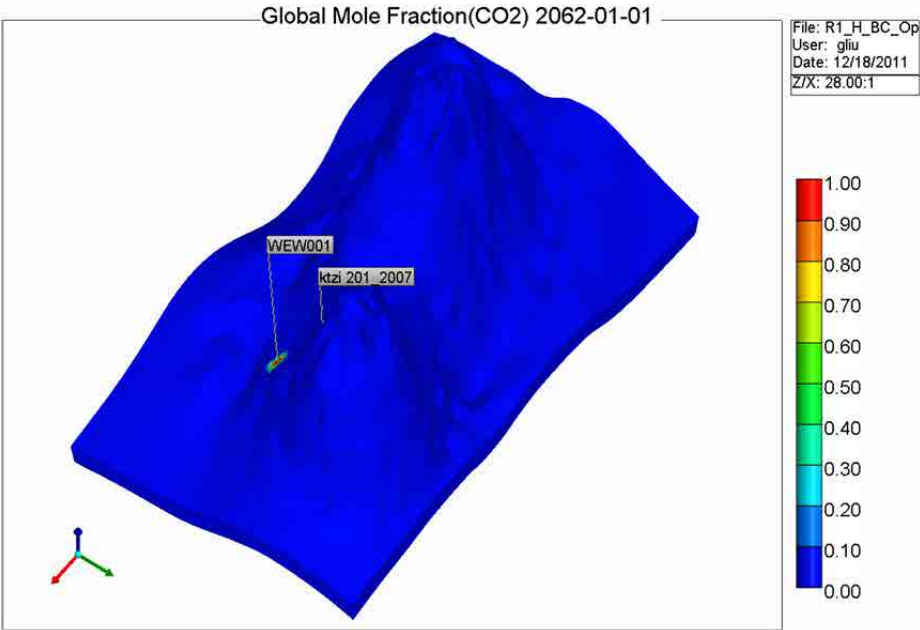


Figure C-41. 3-D view of Case 7: CO₂ plume migration for 50 years from beginning of injection.

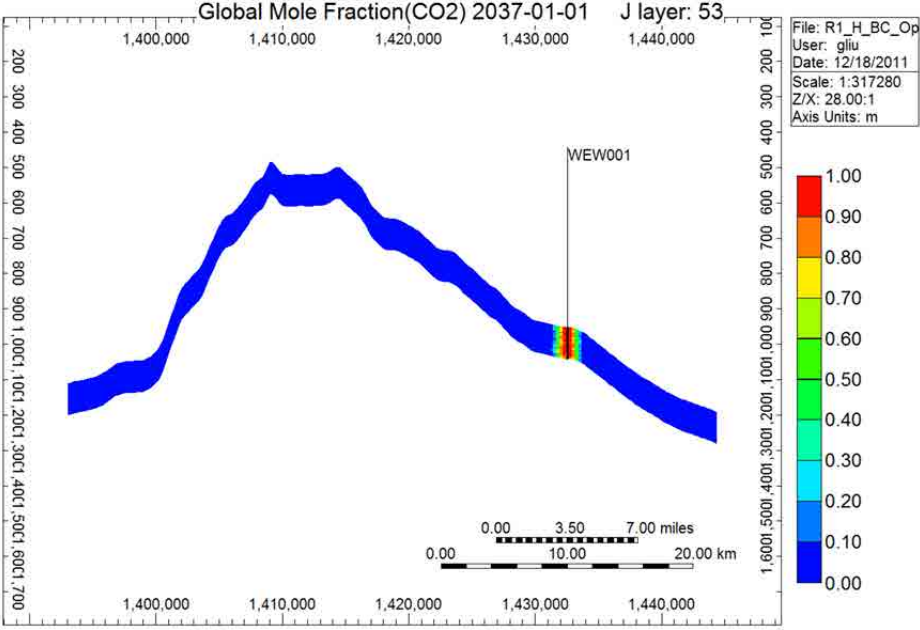


Figure C-42. Cross-sectional view of Case 7: CO₂ plume migration for 25 years from beginning of injection.

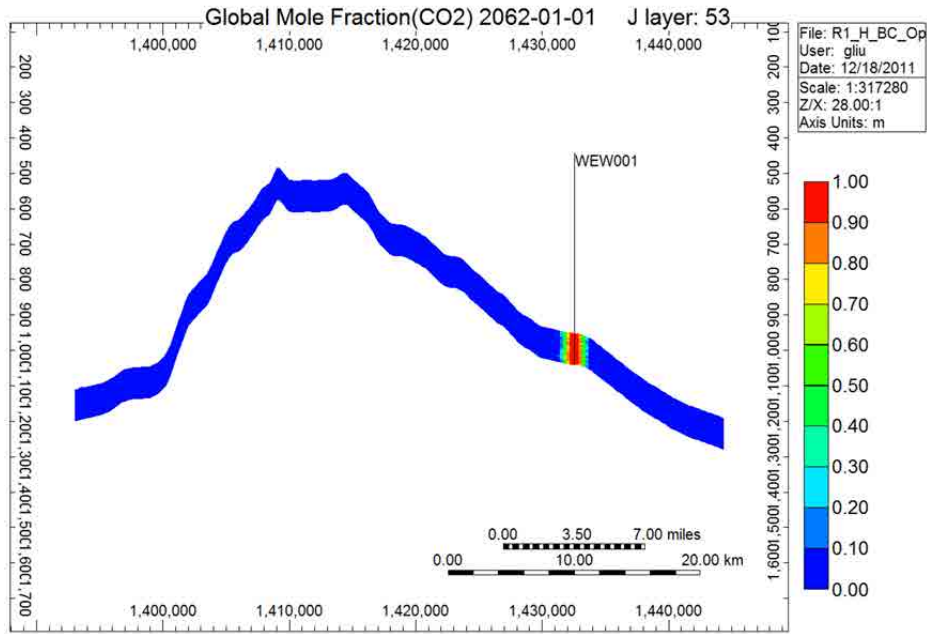


Figure C-43. Cross-sectional view of Case 7: CO₂ plume migration for 50 years from beginning of injection.

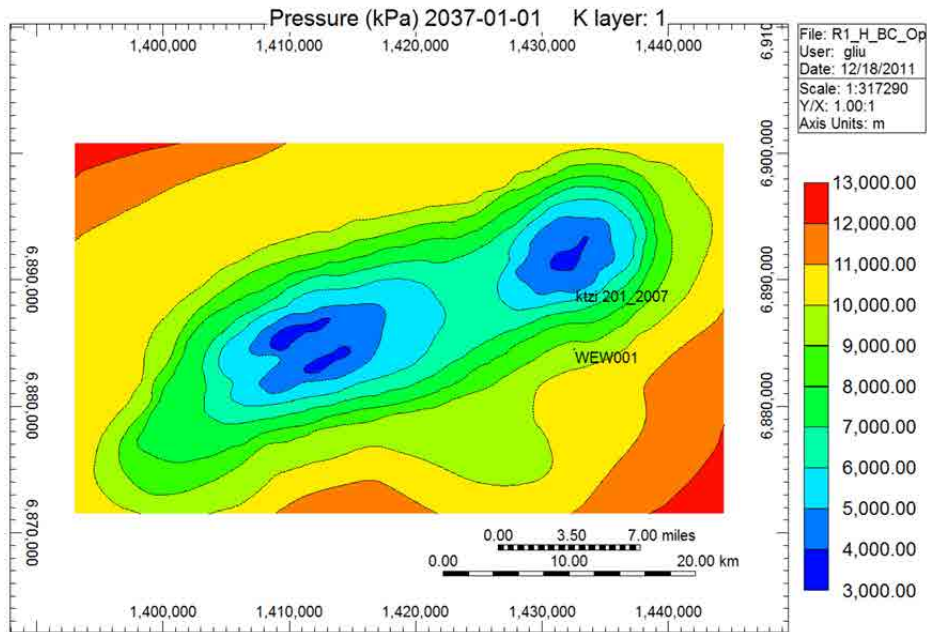


Figure C-44. Areal view of Case 7: pressure distributions for 25 years from beginning of injection.

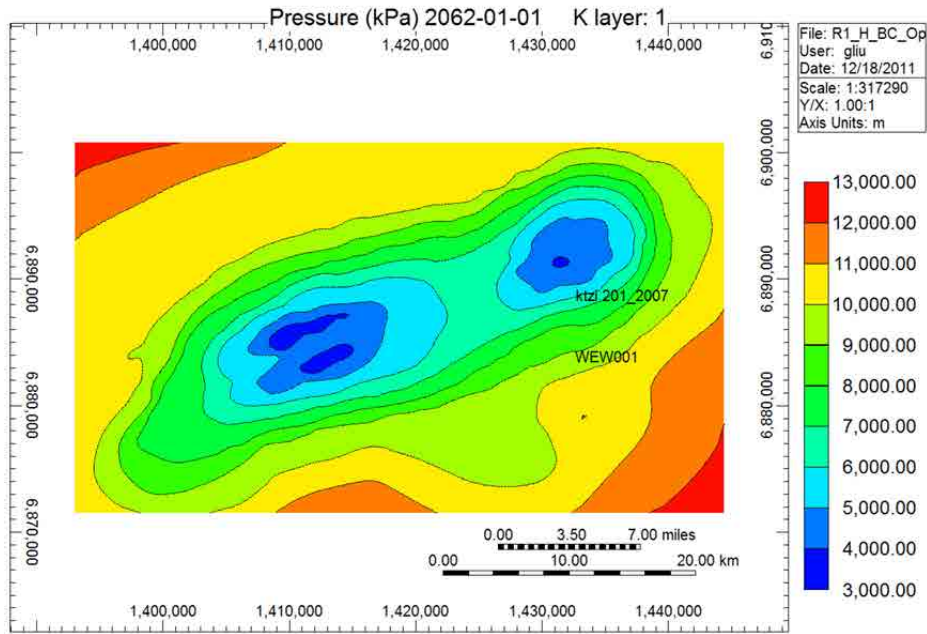


Figure C-45. Areal view of Case 7: pressure distributions for 50 years from beginning of injection.

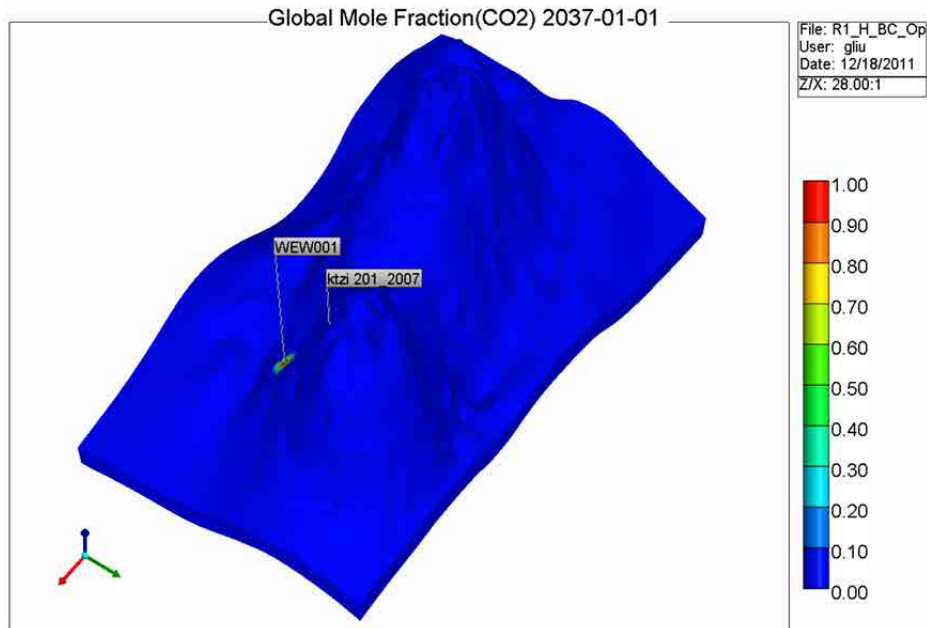


Figure C-46. 3-D view of Case 8: CO₂ plume migration for 25 years from beginning of injection.

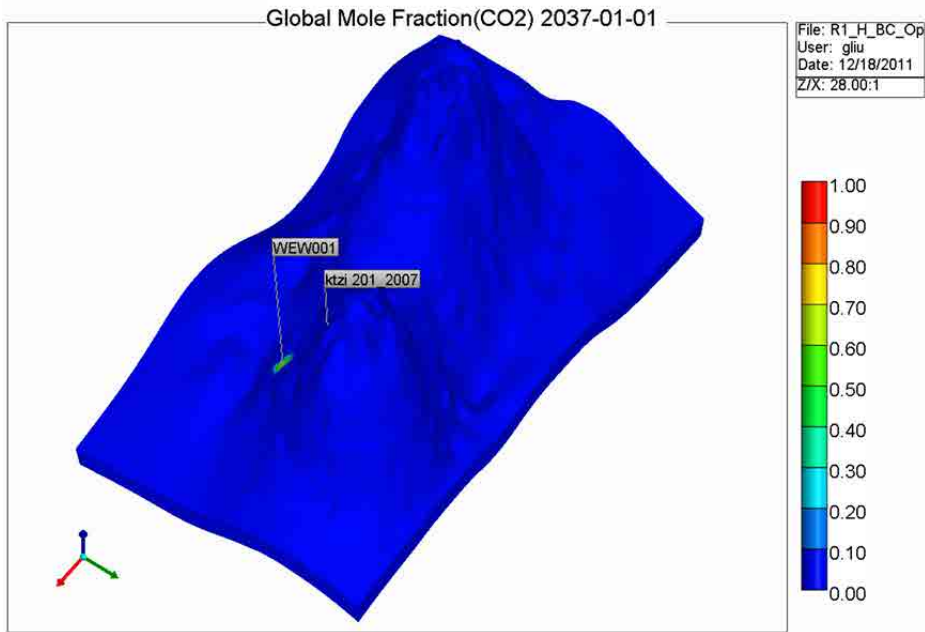


Figure C-47. 3-D view of Case 8: CO₂ plume migration for 50 years from beginning of injection.

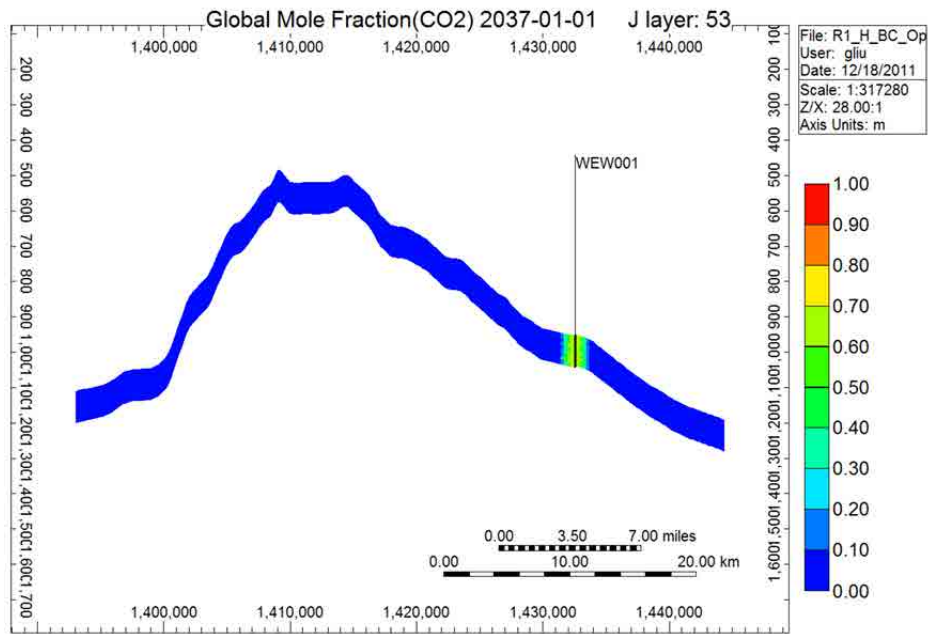


Figure C-48. Cross-sectional view of Case 8: CO₂ plume migration for 25 years from beginning of injection.

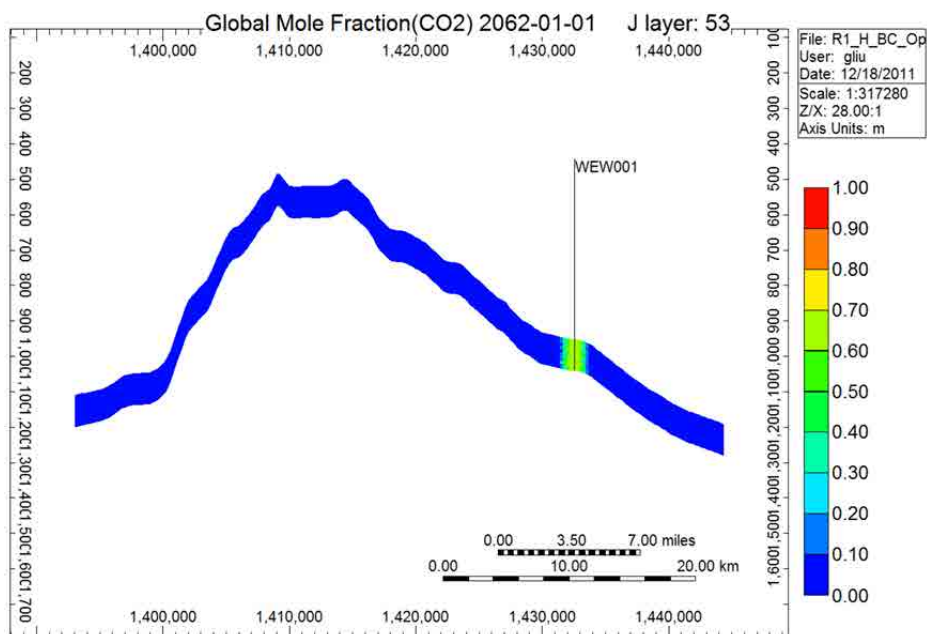


Figure C-49. Cross-sectional view of Case 8: CO₂ plume migration for 50 years from beginning of injection.

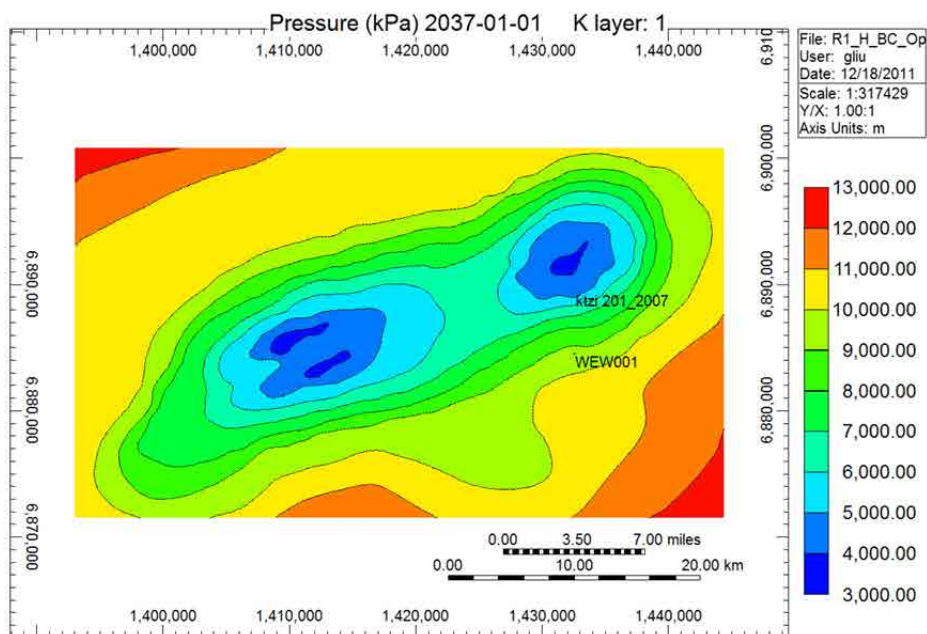


Figure C-50. Areal view of Case 8: pressure distributions for 25 years from beginning of injection.

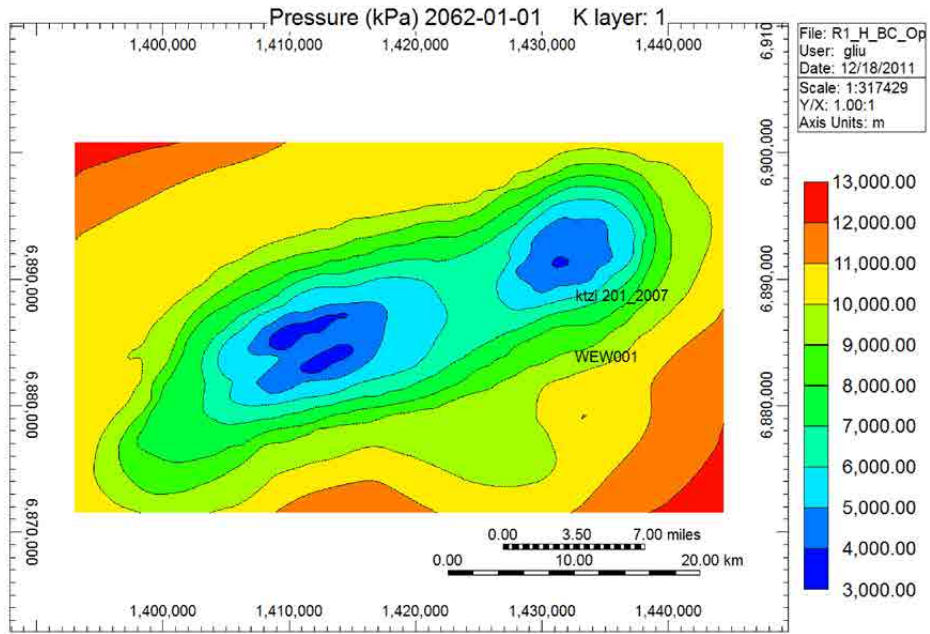


Figure C-51. Areal view of Case 8: pressure distributions for 50 years from beginning of injection.

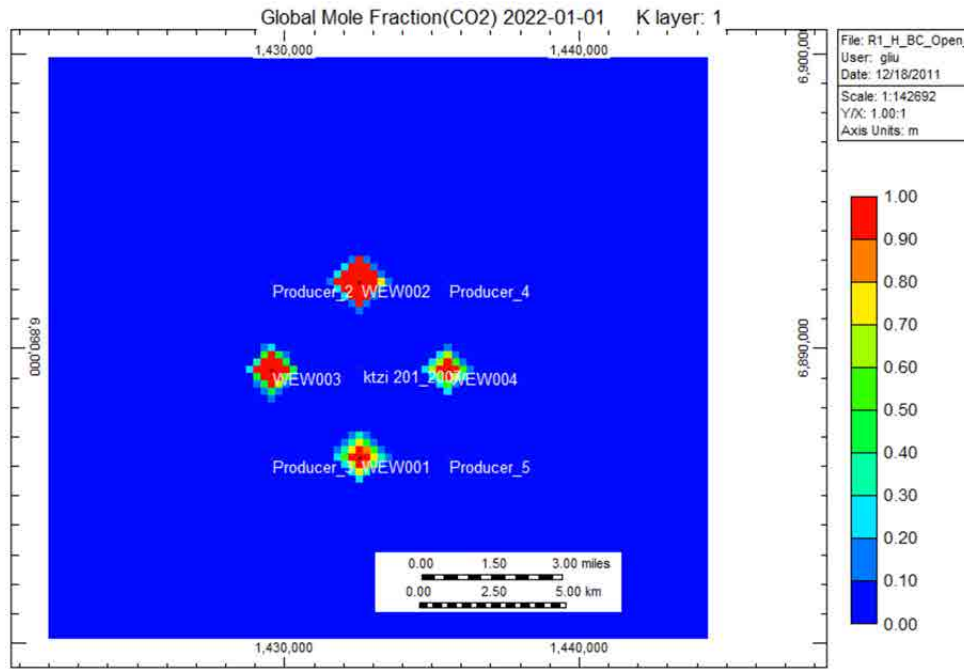


Figure C-52. Case 9 nine-spot pattern well locations.

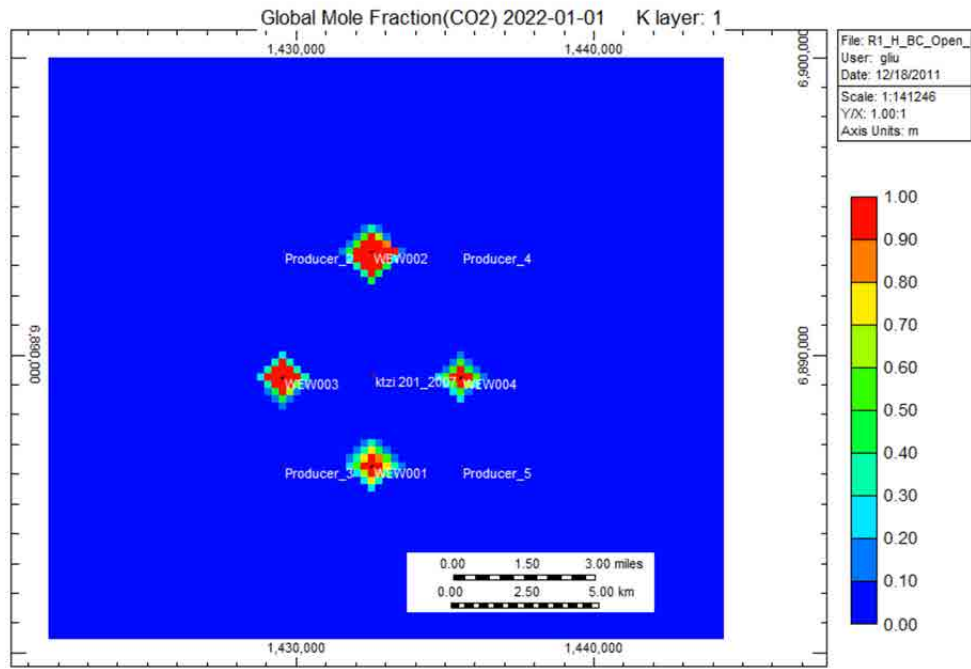


Figure C-53. Case 10 nine-spot pattern well locations.

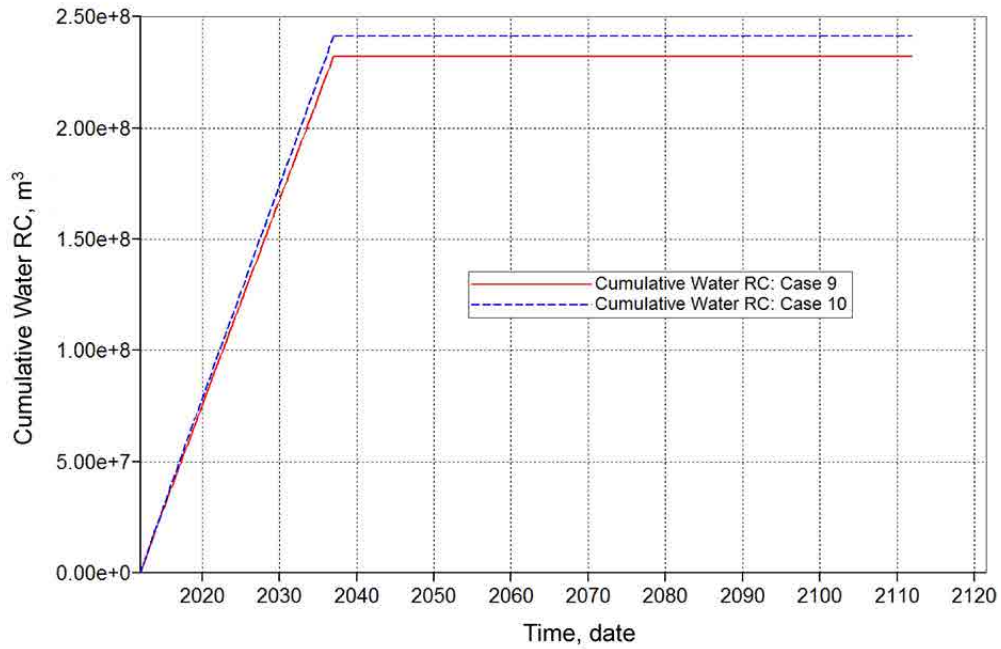


Figure C-54. Total produced water for Cases 9 and 10.

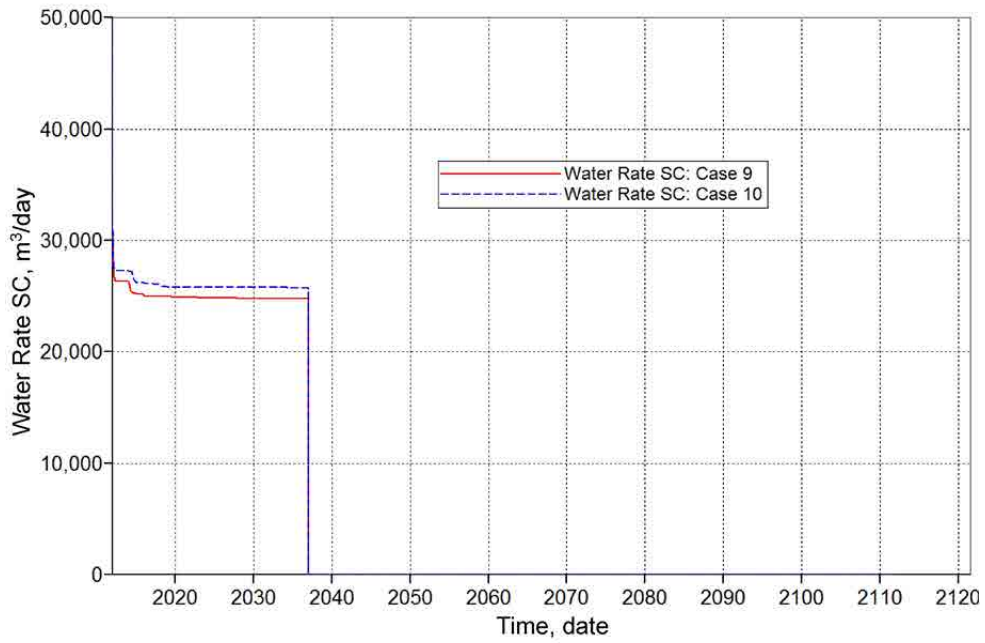


Figure C-55. Water production rate for Cases 9 and 10.

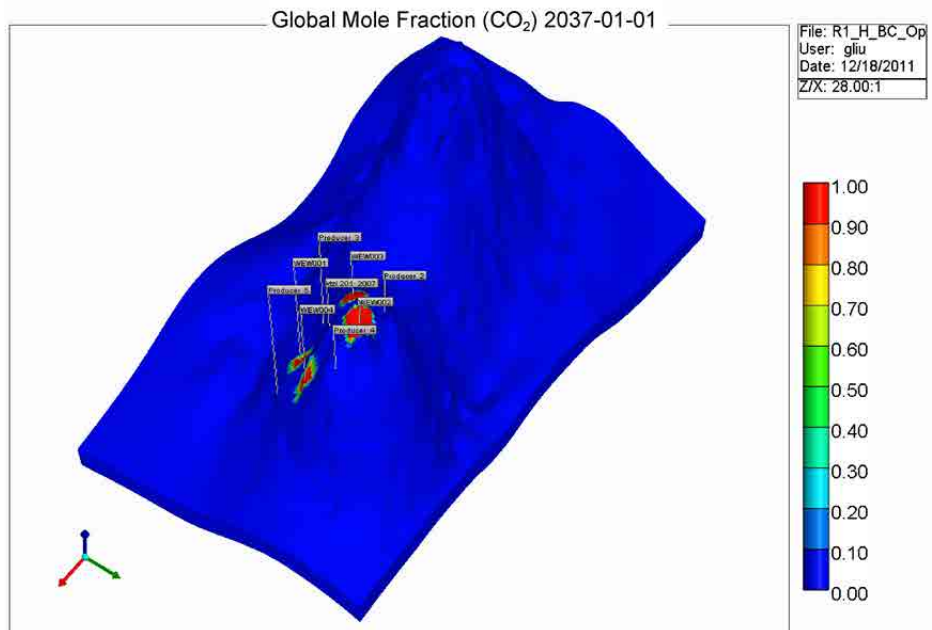


Figure C-56. 3-D view of Case 9: CO₂ plume migration for 25 years from beginning of injection.

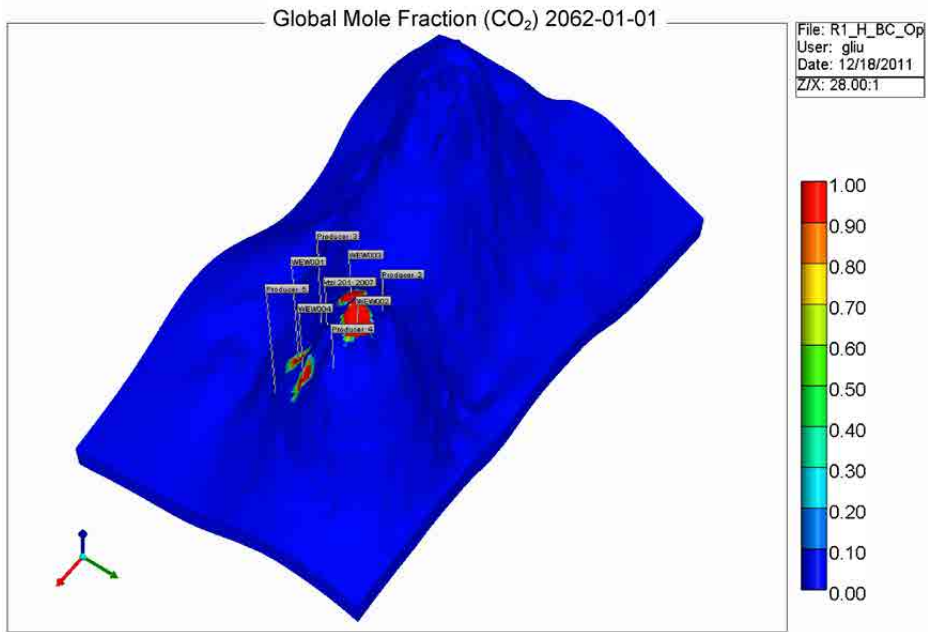


Figure C-57. 3-D view of Case 9: CO₂ plume migration for 50 years from beginning of injection.

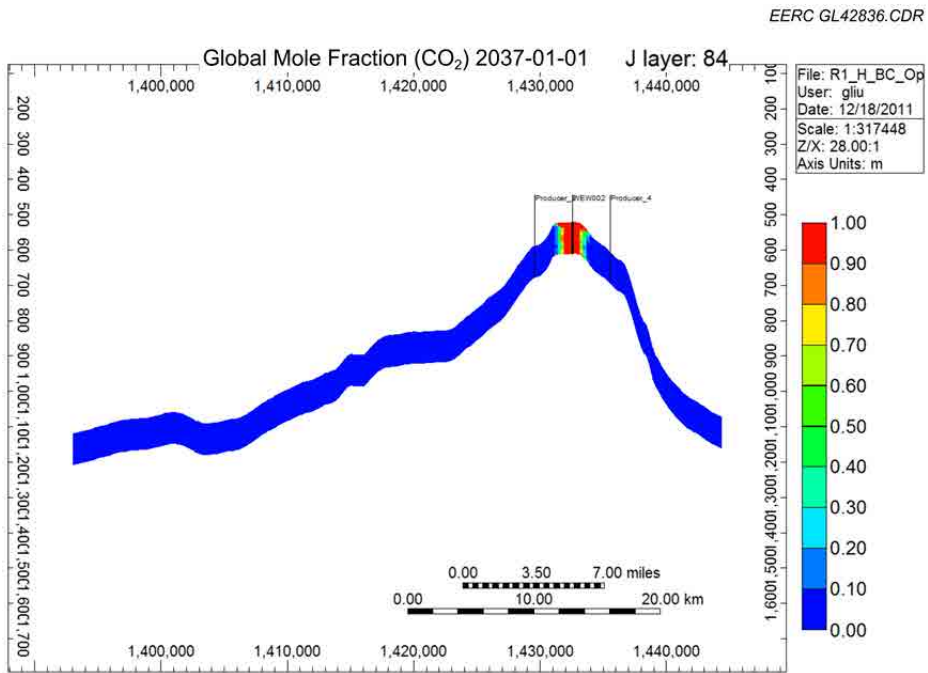


Figure C-58. Cross-sectional view of Case 9: CO₂ plume migration for 25 years from beginning of injection.

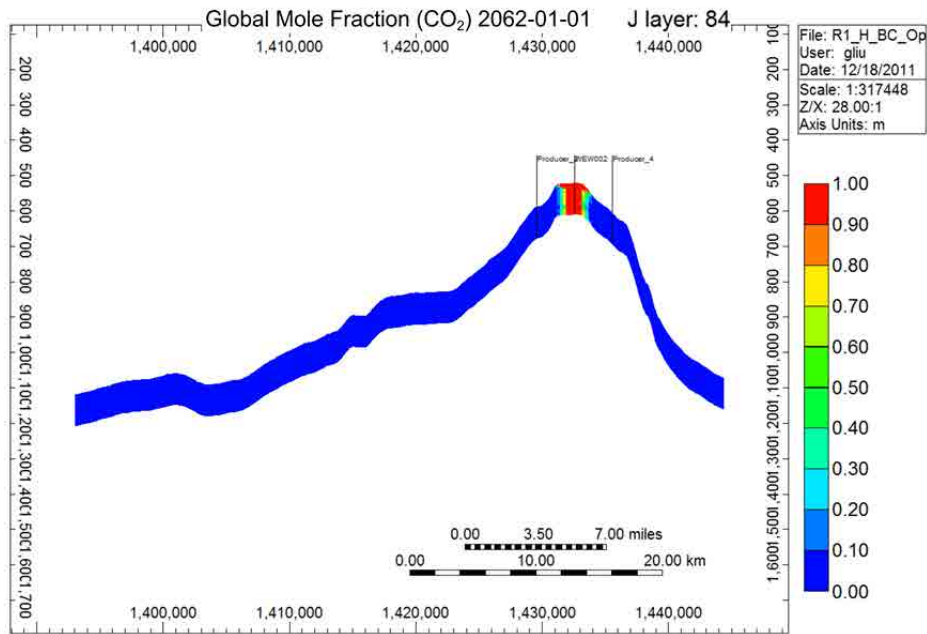


Figure C-59. Cross-sectional view of Case 9: CO₂ plume migration for 50 years from beginning of injection.

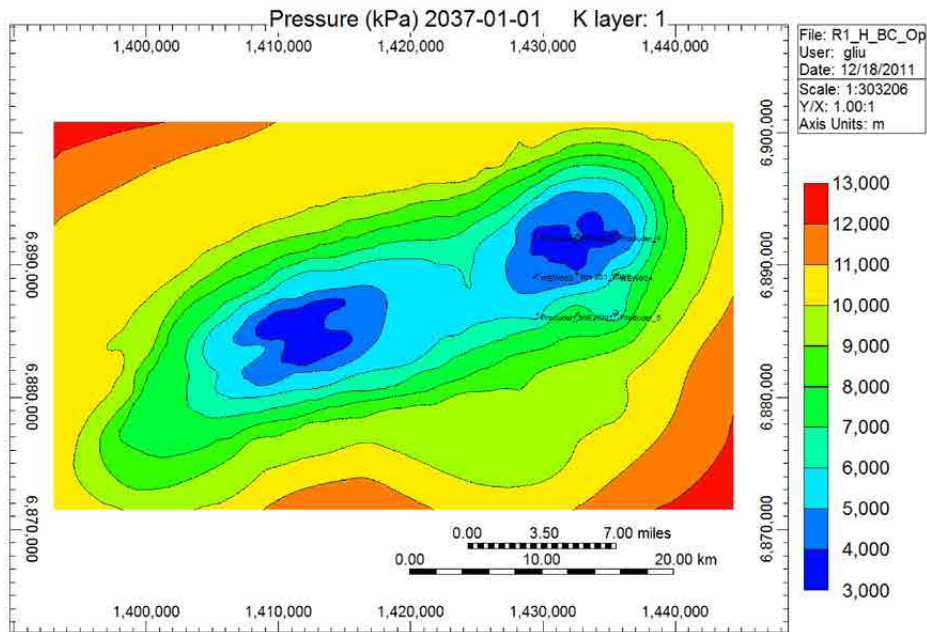


Figure C-60. Areal view of Case 9: pressure distributions for 25 years from beginning of injection.

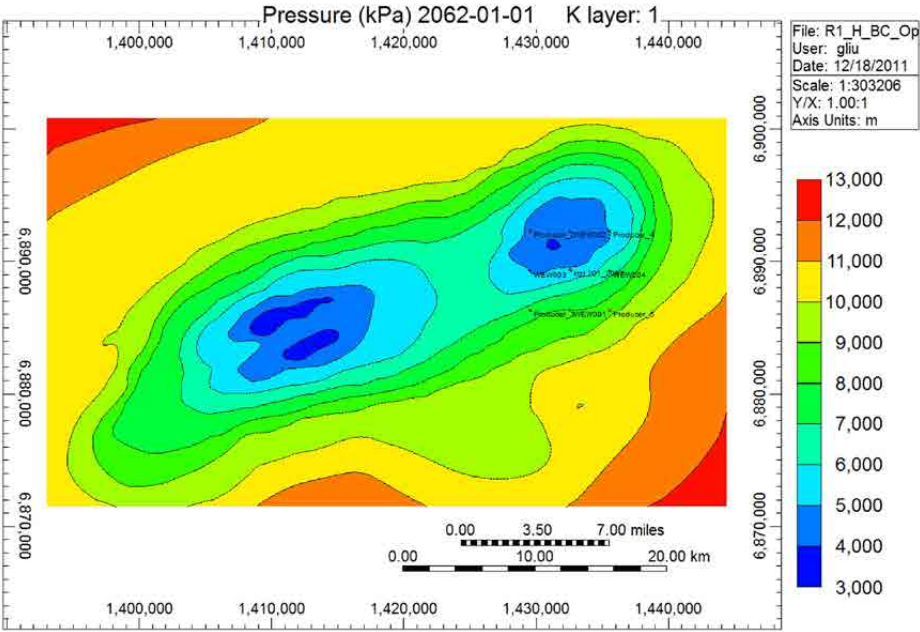


Figure C-61. Areal view of Case 9: pressure distributions for 50 years from beginning of injection.

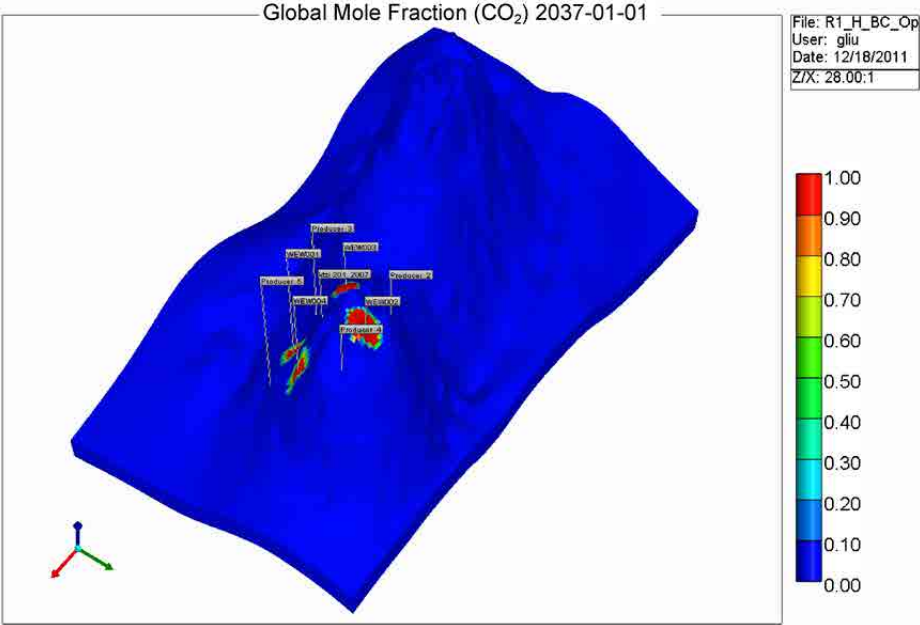


Figure C-62. 3-D view of Case 10: CO₂ plume migration for 25 years from beginning of injection.

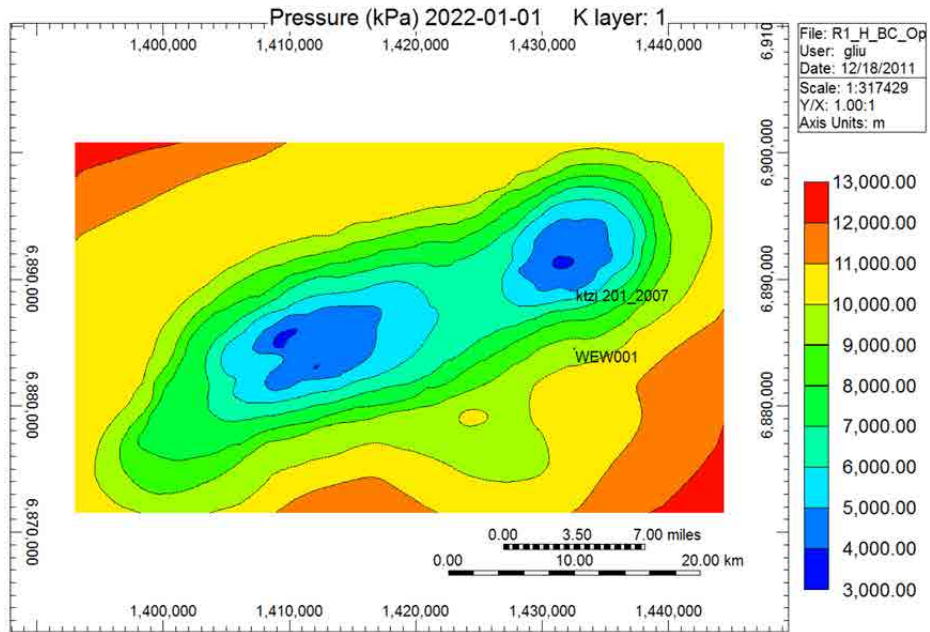


Figure C-63. 3-D view of Case 10: CO₂ plume migration for 50 years from beginning of injection.

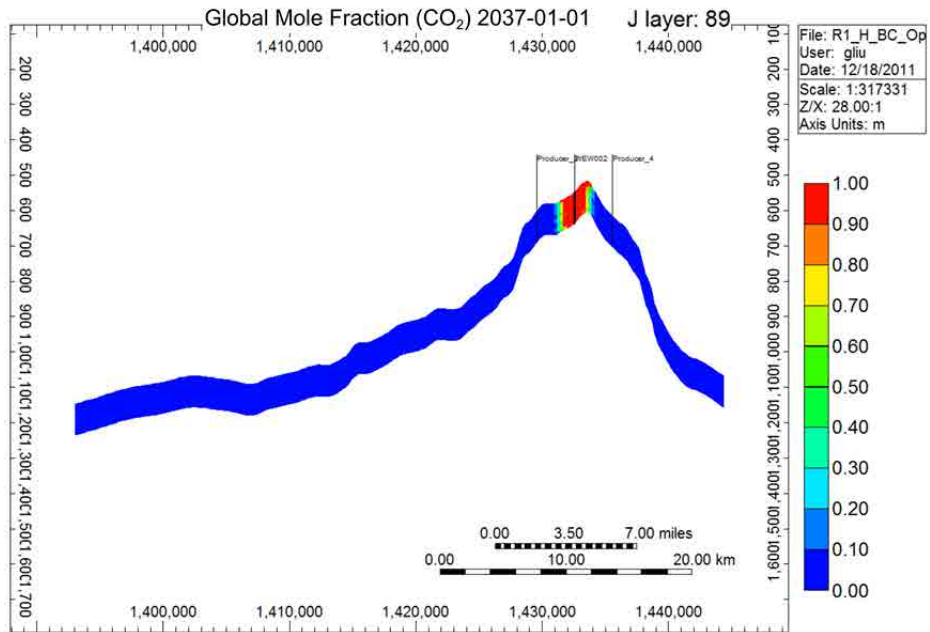


Figure C-64. Cross-sectional view of Case 10: CO₂ plume migration for 25 years from beginning of injection.

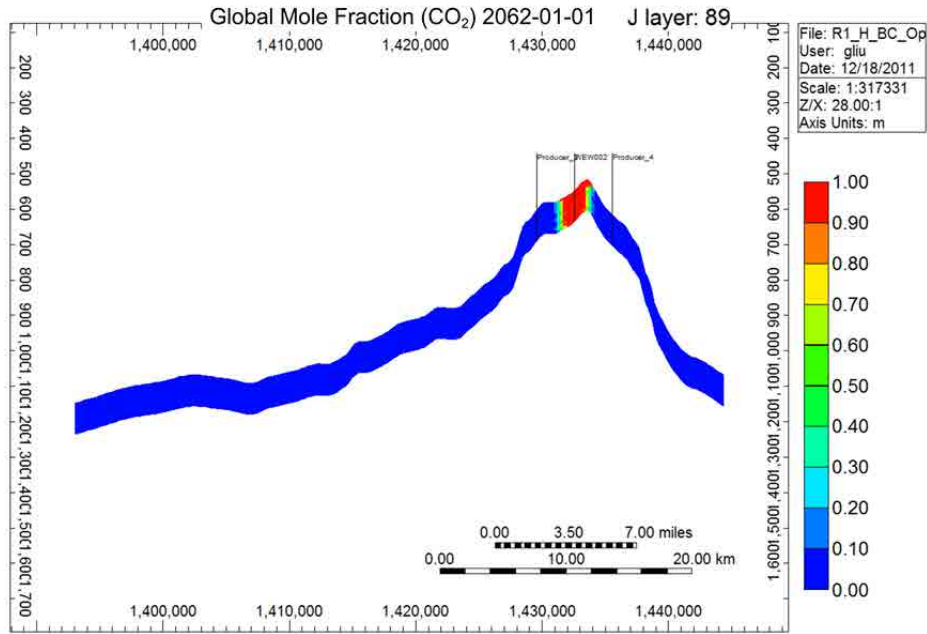


Figure C-65. Cross-sectional view of Case 10: CO₂ plume migration for 50 years from beginning of injection.

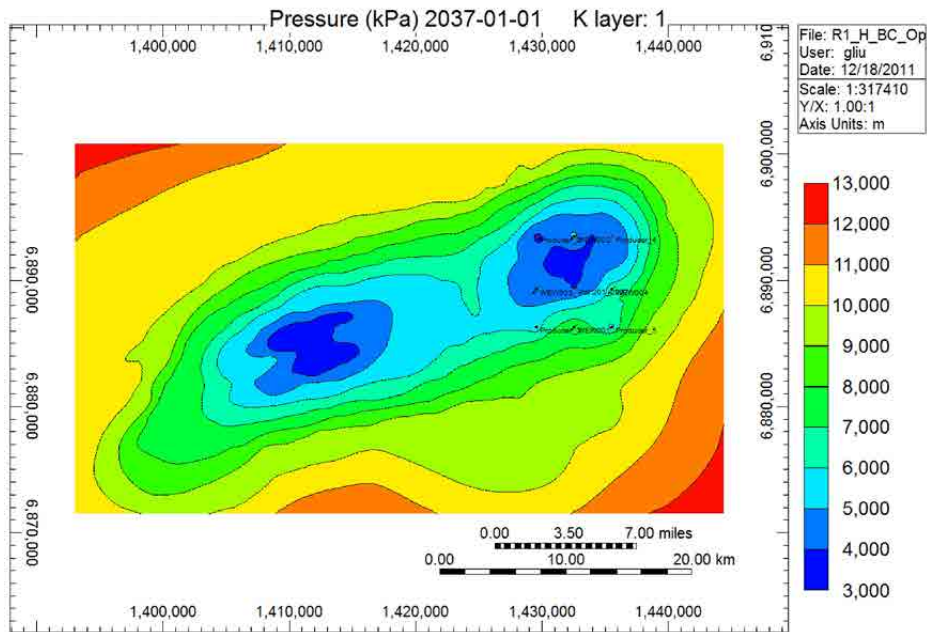


Figure C-66. Areal view of Case 10: pressure distributions for 25 years from beginning of injection.

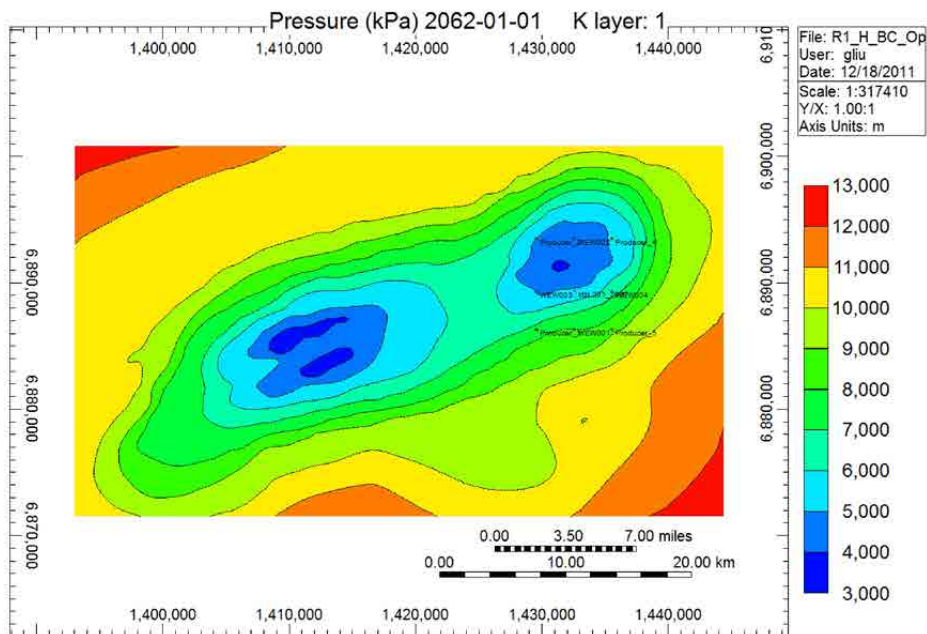


Figure C-67. Areal view of Case 10: pressure distributions for 50 years from beginning of injection.

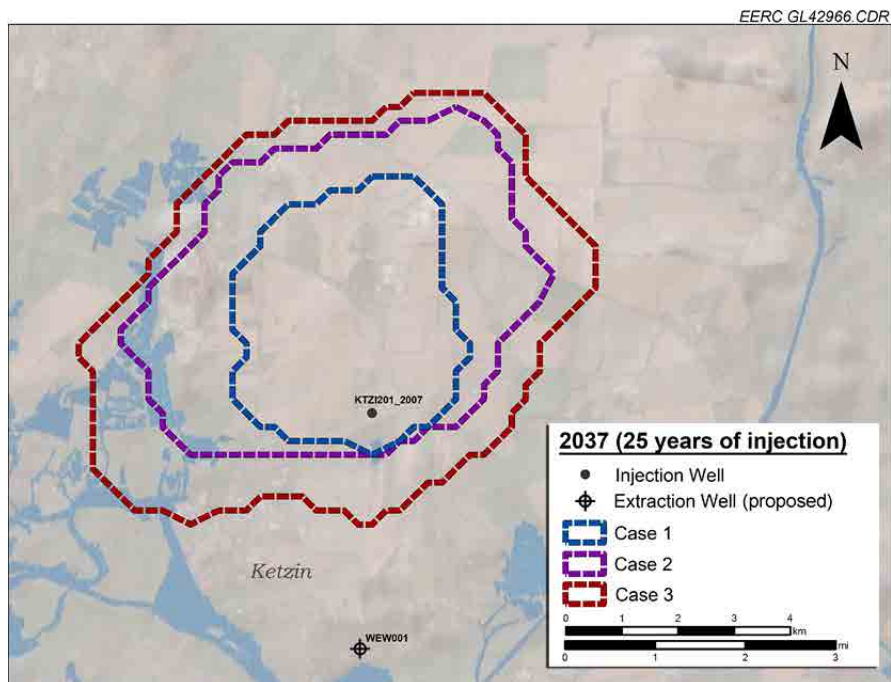


Figure C-68. Surface map view showing the plume extents generated by Cases 1, 2, and 3 after 25 years.

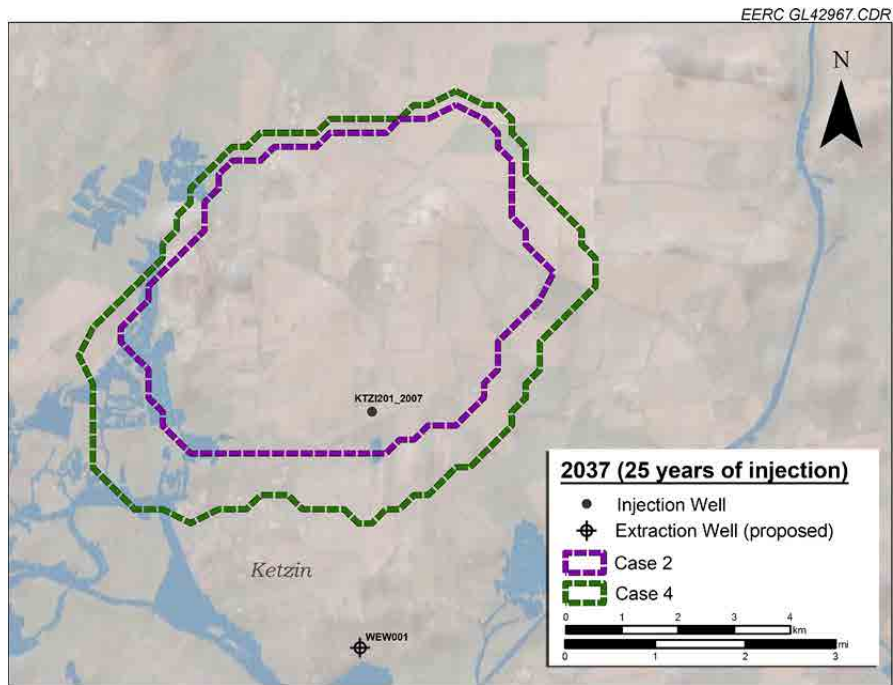


Figure C-69. Surface map view showing the plume extents generated by Cases 2 and 4 after 25 years.

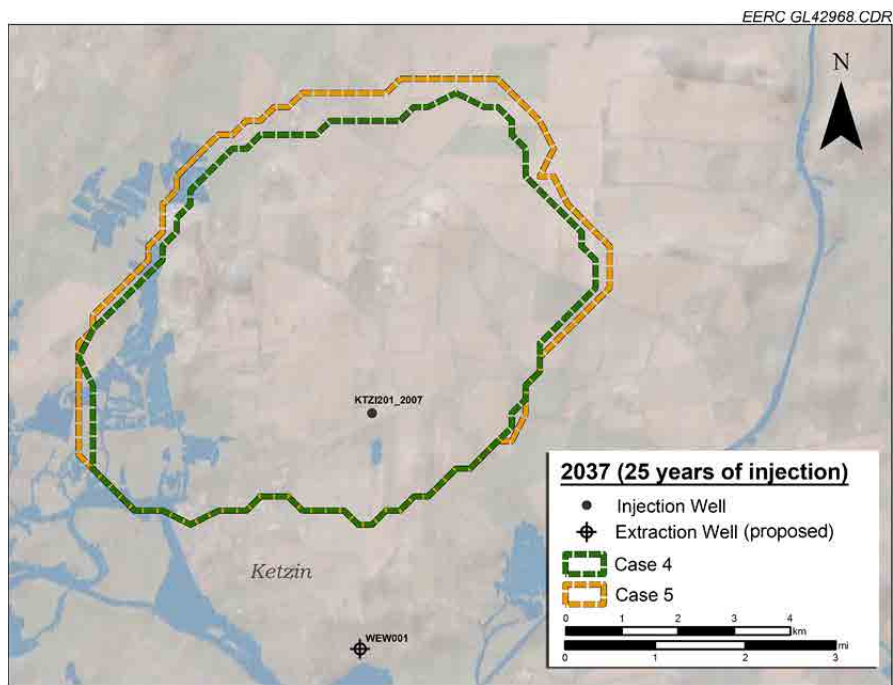


Figure C-70. Surface map view showing the plume extents generated by Cases 4 and 5 after 25 years.

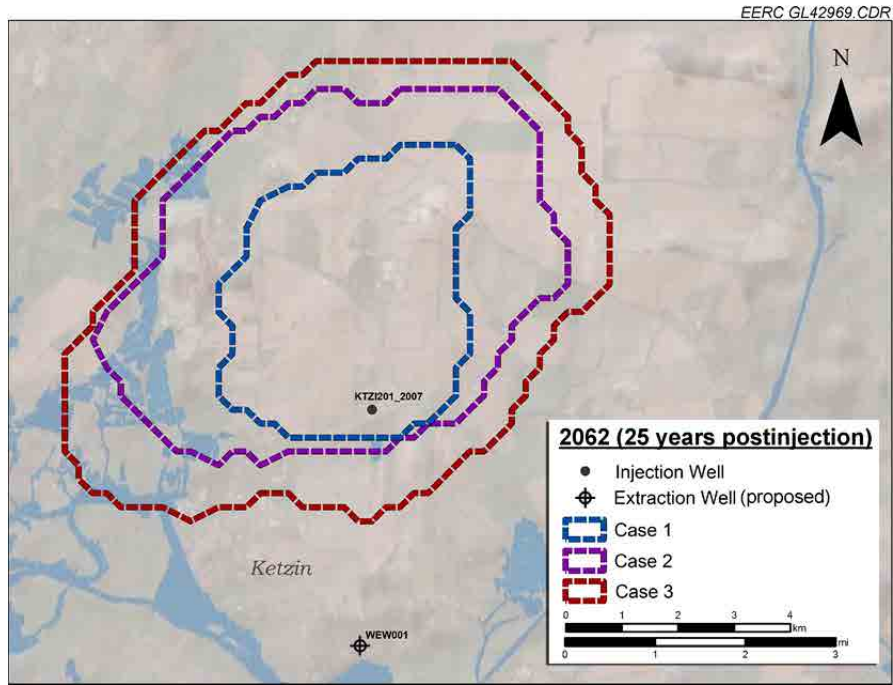


Figure C-71. Surface map view showing the plume extents generated by Cases 1, 2, and 3 after 50 years.

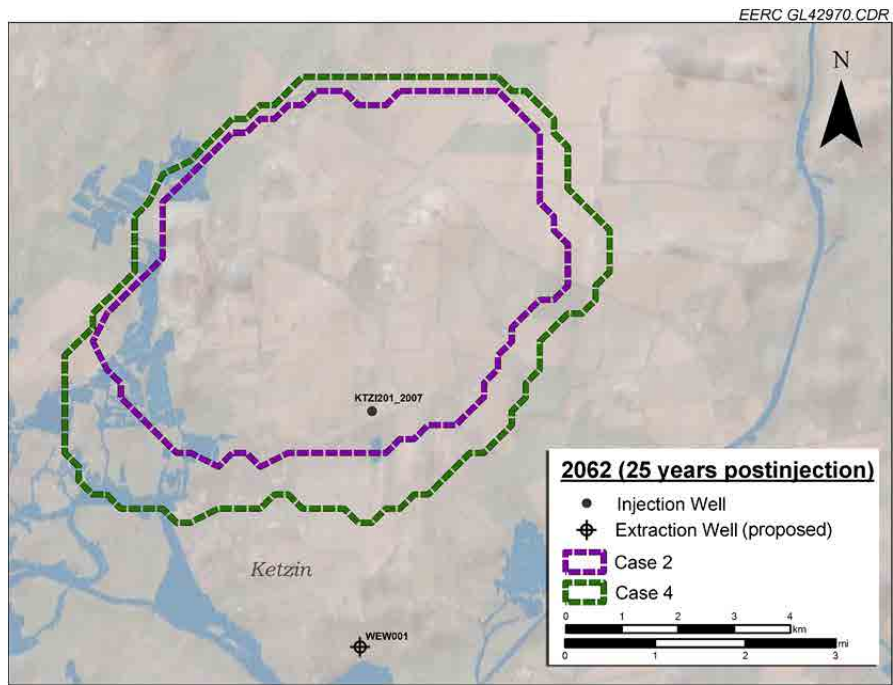


Figure C-72. Surface map view showing the plume extents generated by Cases 2 and 4 after 50 years.

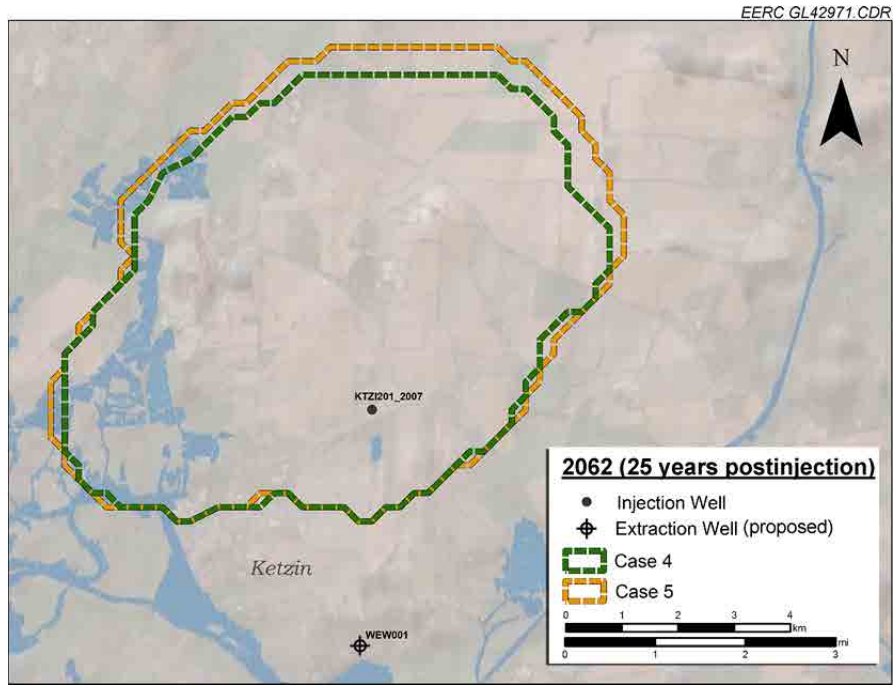


Figure C-73. Surface map view showing the plume extents generated by Cases 4 and 5 after 50 years.

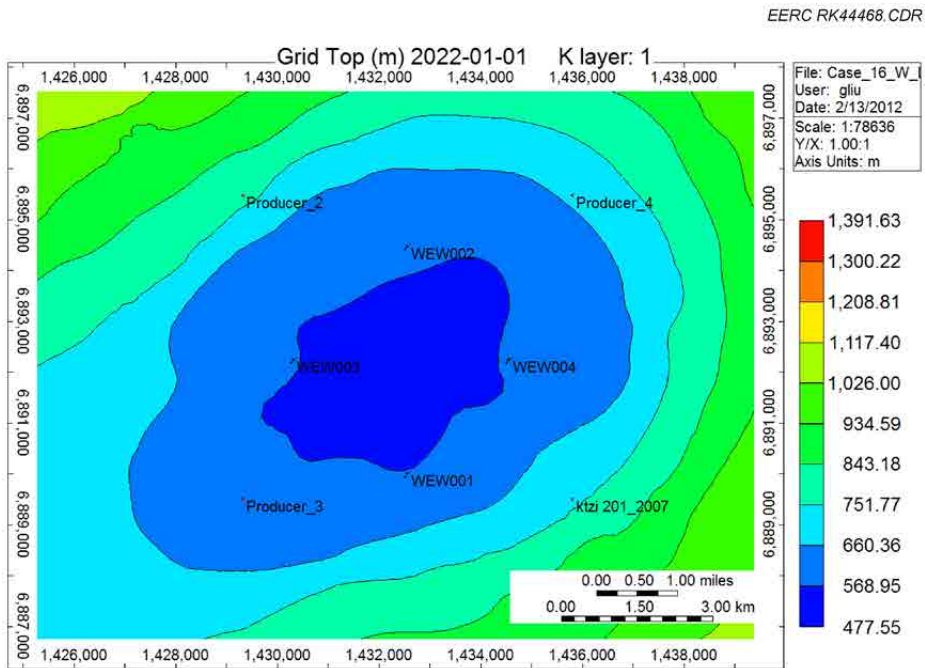


Figure C-74. Well locations of eight-spot pattern, used for Cases 11–13 (note: location of Ktzi 201_2007 for reference).

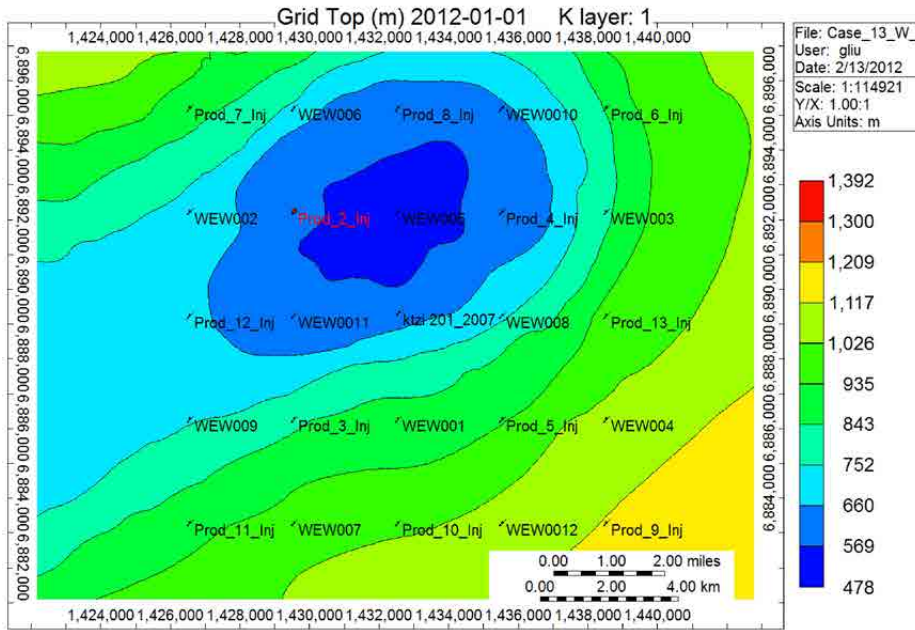


Figure C-75. Well locations of 25-spot pattern, Cases 14–16 (Note: location of Ktzi 201_2007 for reference).

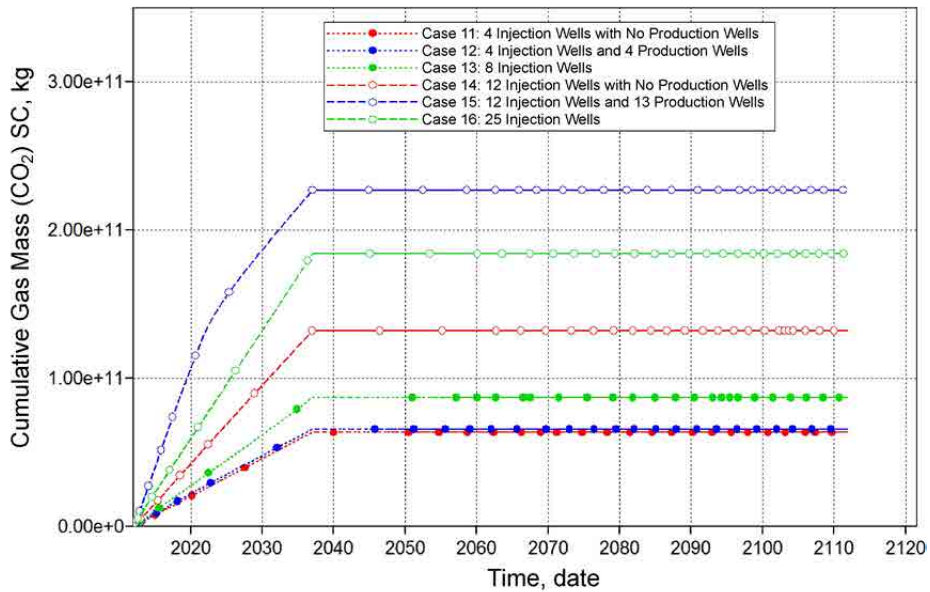


Figure C-76. Total injected CO₂ for Cases 11–16.

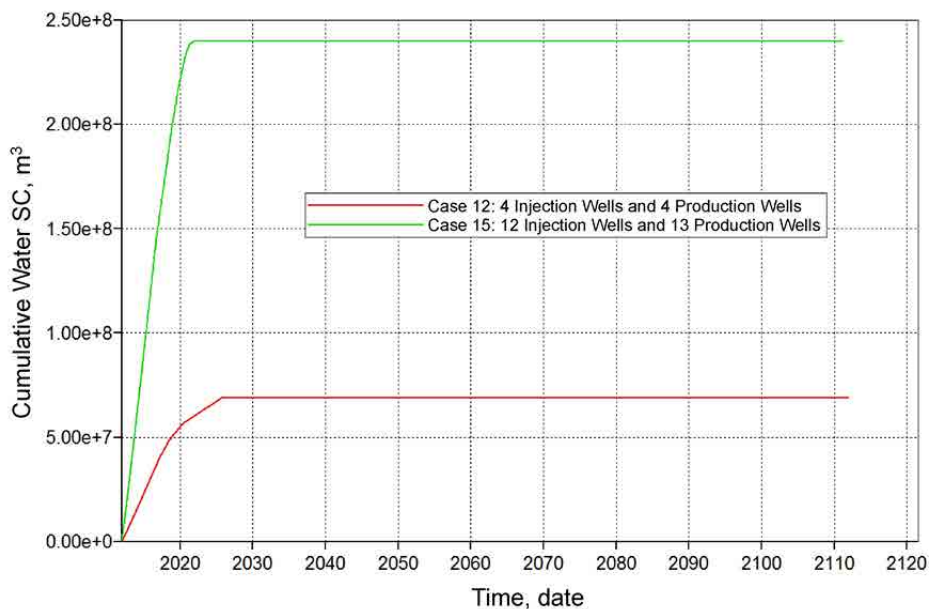


Figure C-77. Total produced water for Cases 12 and 15.

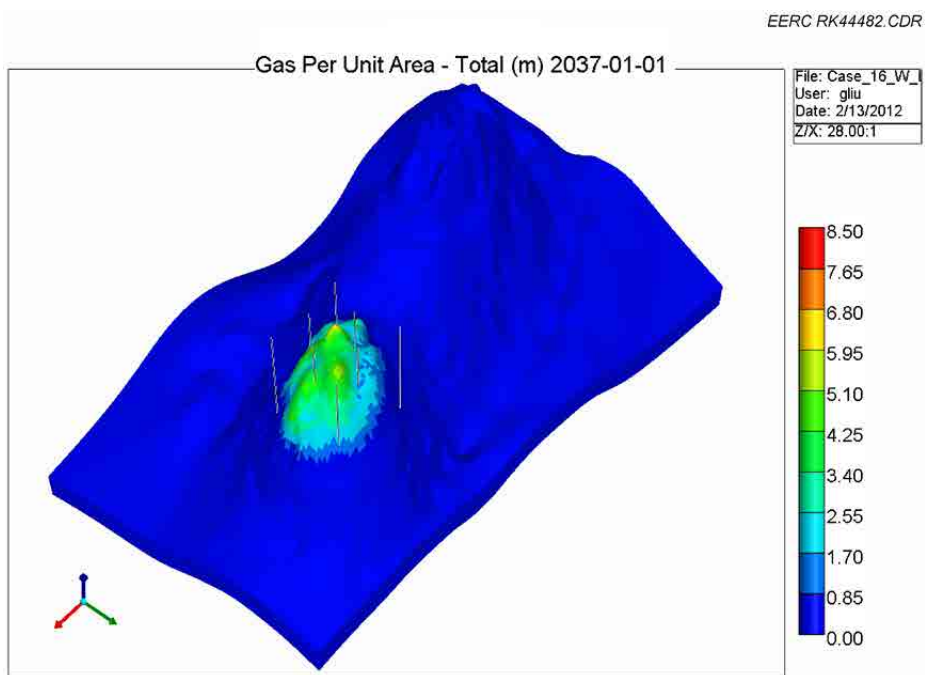


Figure C-78. 3-D view of Case 11: CO₂ plume migration for 25 years from beginning of injection.

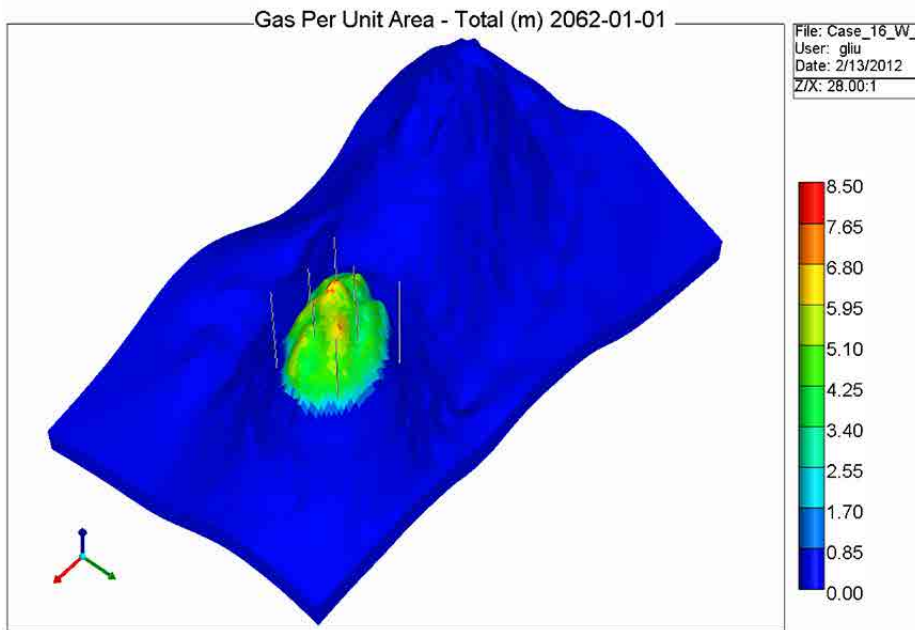


Figure C-79. 3-D view of Case 11: CO₂ plume migration for 50 years from beginning of injection.

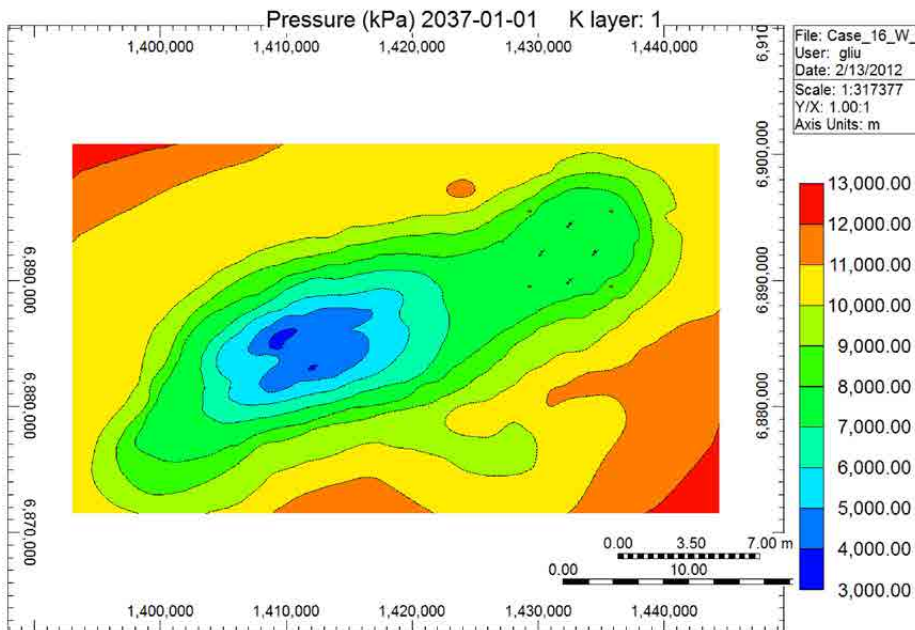


Figure C-80. Areal view of Case 11: pressure distributions for 25 years from beginning of injection.

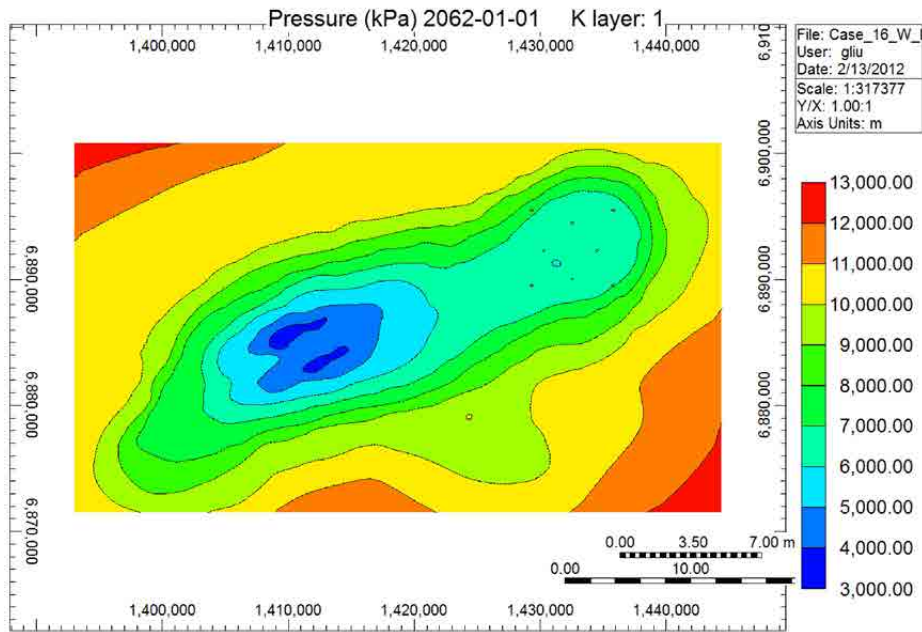


Figure C-81. Areal view of Case 11: pressure distributions for 50 years from beginning of injection.

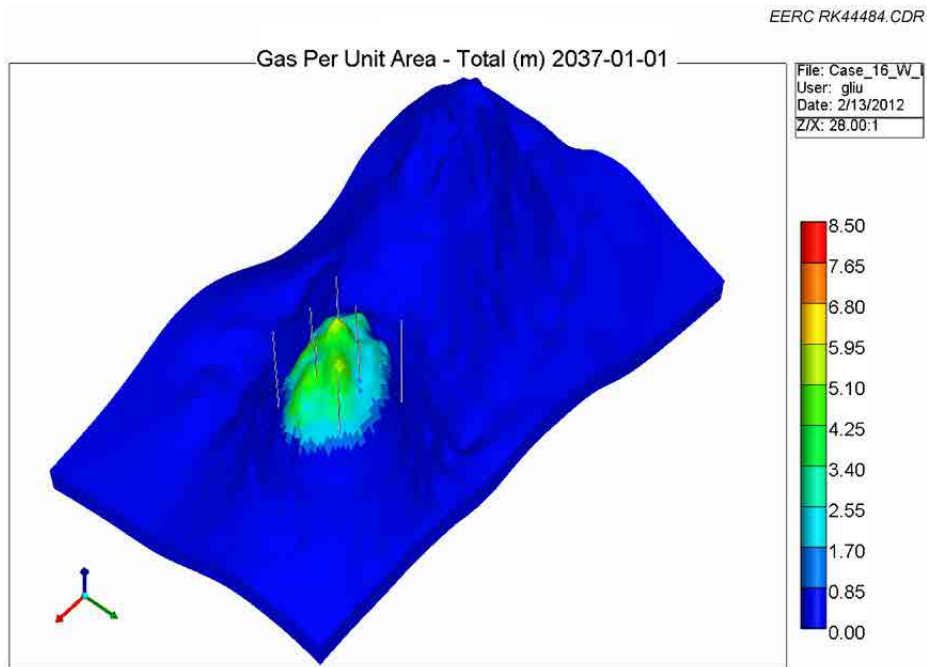


Figure C-82. 3-D view of Case 12: CO₂ plume migration for 25 years from beginning of injection.

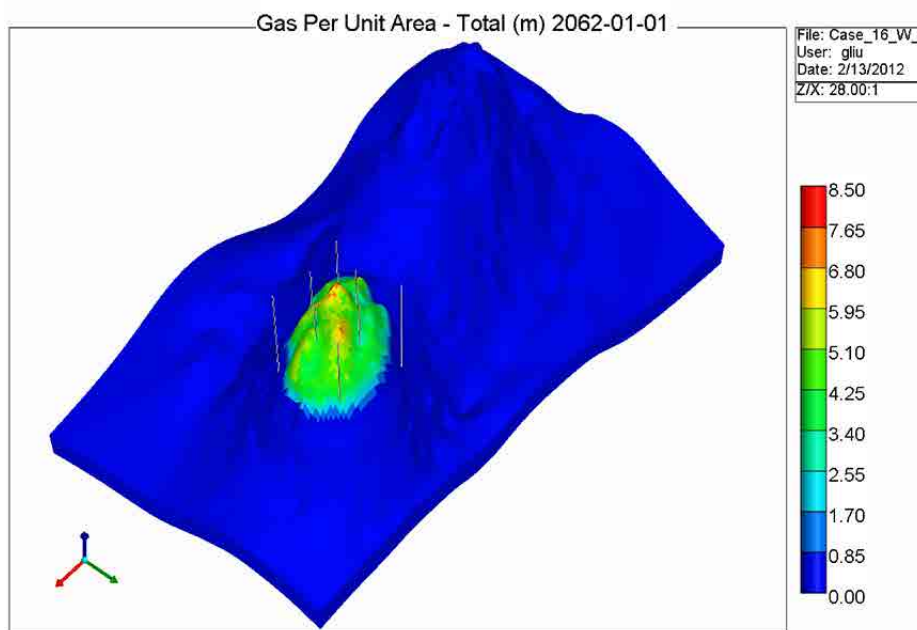


Figure C-83. 3-D view of Case 12: CO₂ plume migration for 50 years from beginning of injection.

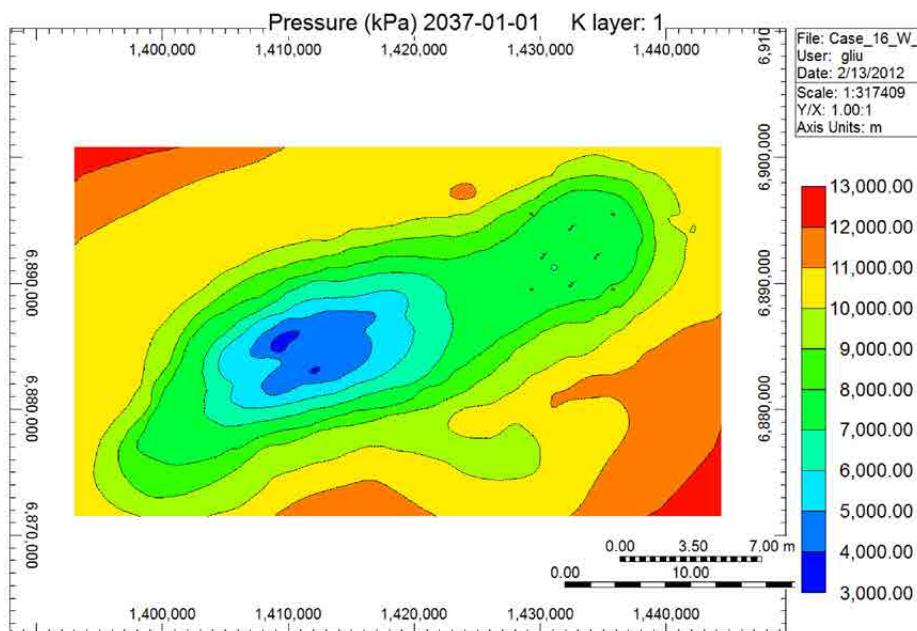


Figure C-84. Areal view of Case 12: pressure distributions for 25 years from beginning of injection.

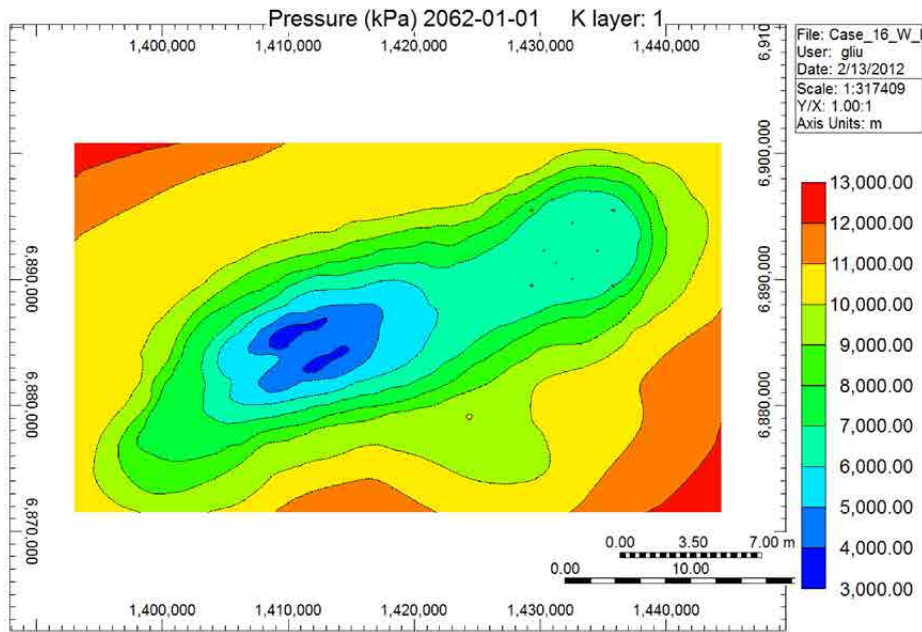


Figure C-85. Areal view of Case 12: pressure distributions for 50 years from beginning of injection.

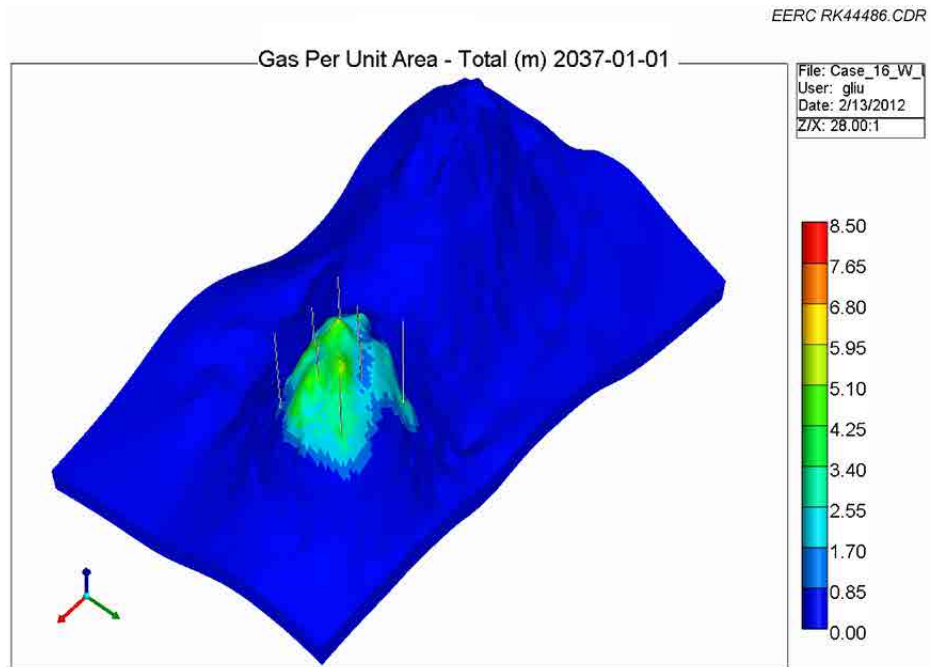


Figure C-86. 3-D view of Case 13: CO₂ plume migration for 25 years from beginning of injection.

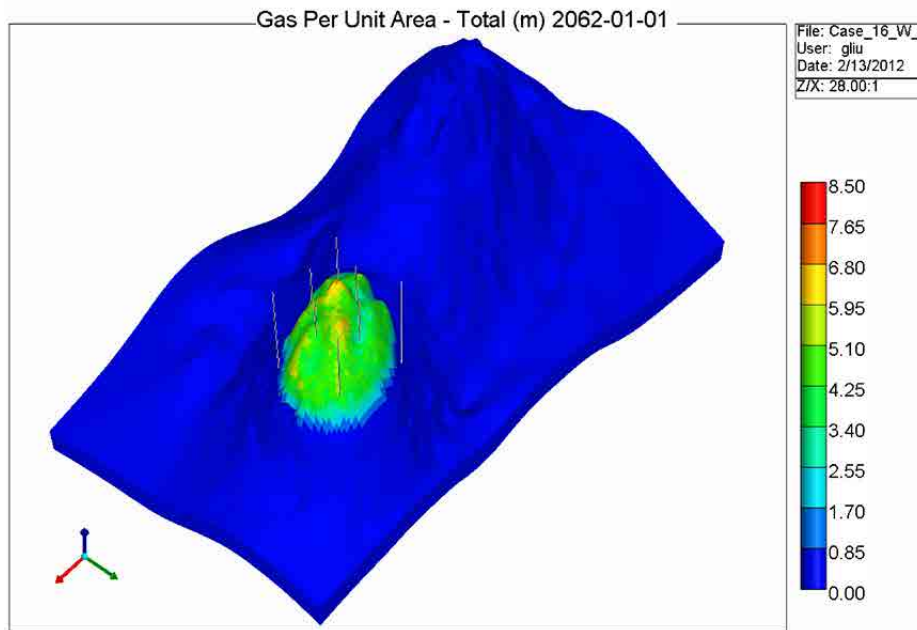


Figure C-87. 3-D view of Case 13: CO₂ plume migration for 50 years from beginning of injection.

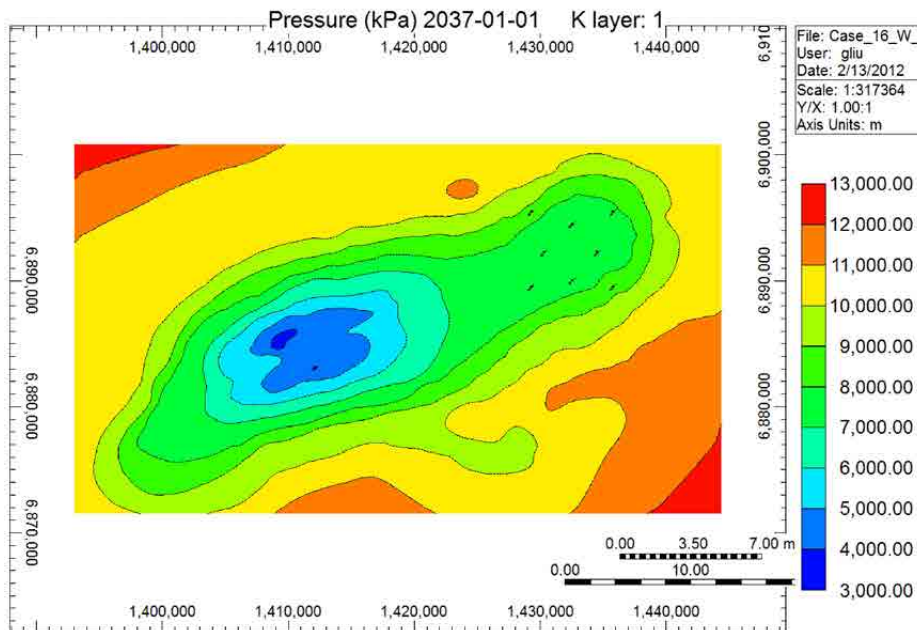


Figure C-88. Areal view of Case 13: pressure distributions for 25 years from beginning of injection.

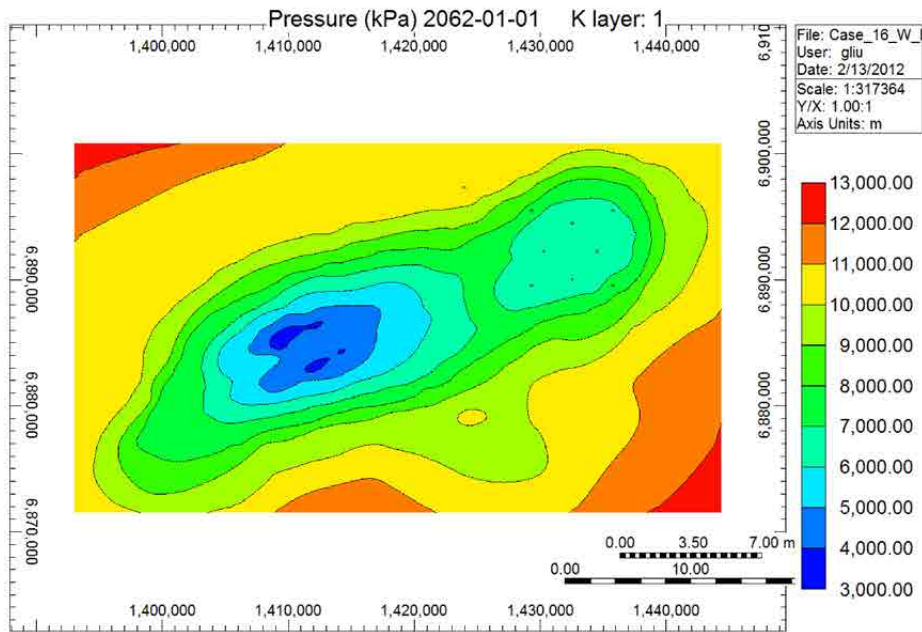


Figure C-89. Areal view of Case 13: pressure distributions for 50 years from beginning of injection.

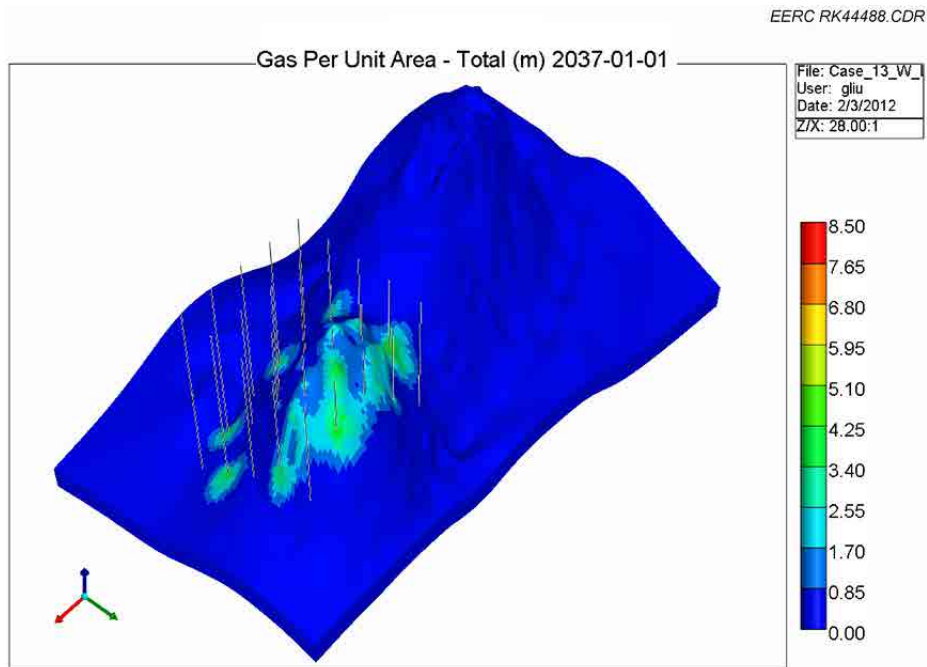


Figure C-90. 3-D view of Case 14: CO₂ plume migration for 25 years from beginning of injection.

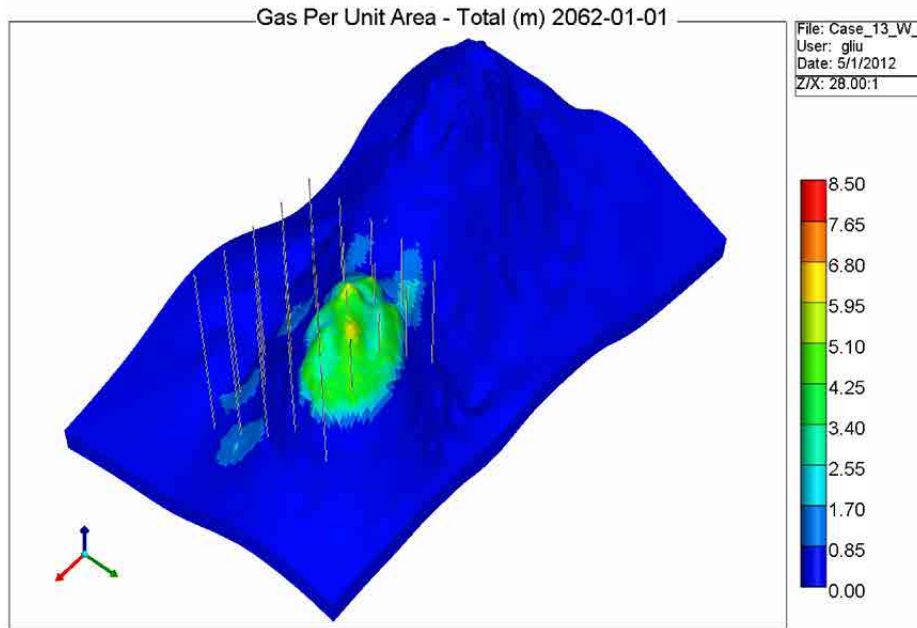


Figure C-91. 3-D view of Case 14: CO₂ plume migration for 50 years from beginning of injection.

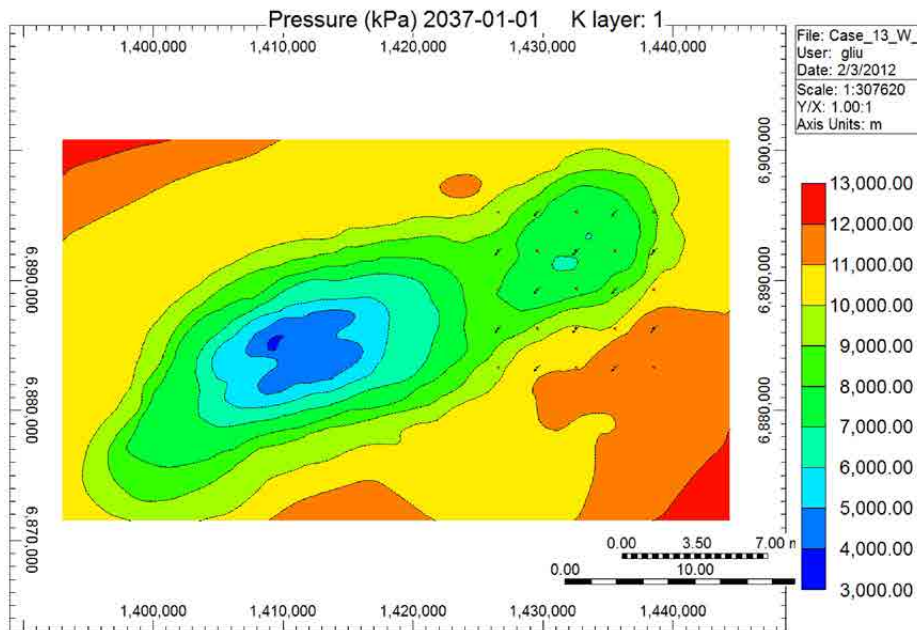


Figure C-92. Areal view of Case 14: pressure distributions for 25 years from beginning of injection.

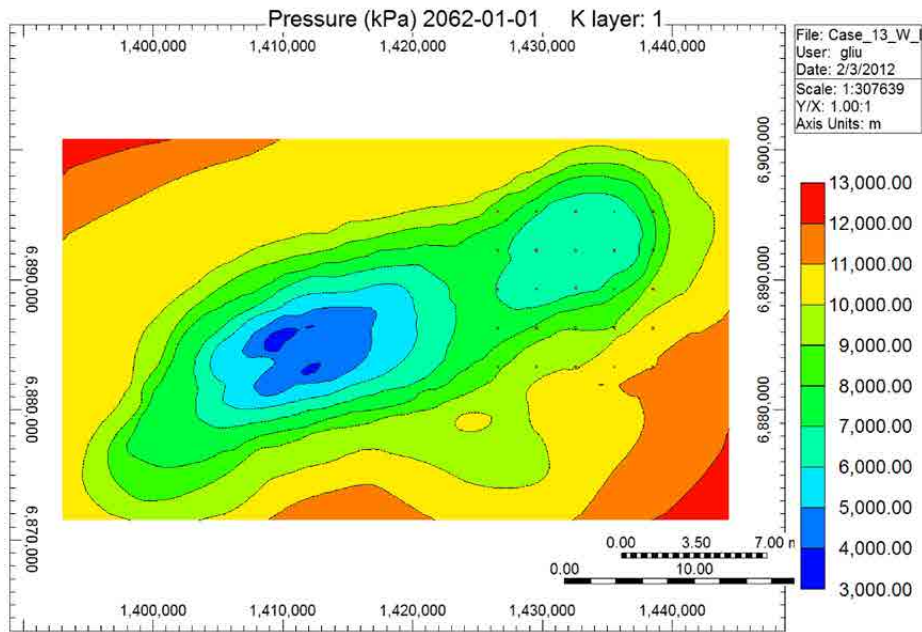


Figure C-93. Areal view of Case 14: pressure distributions for 50 years from beginning of injection.

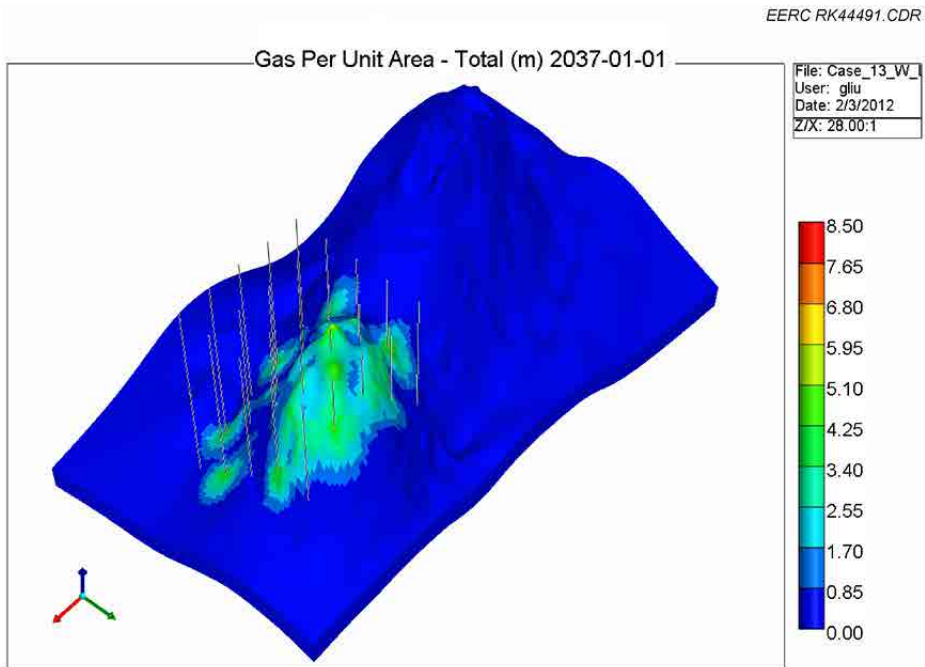


Figure C-94. 3-D view of Case 15: CO₂ plume migration for 25 years from beginning of injection.

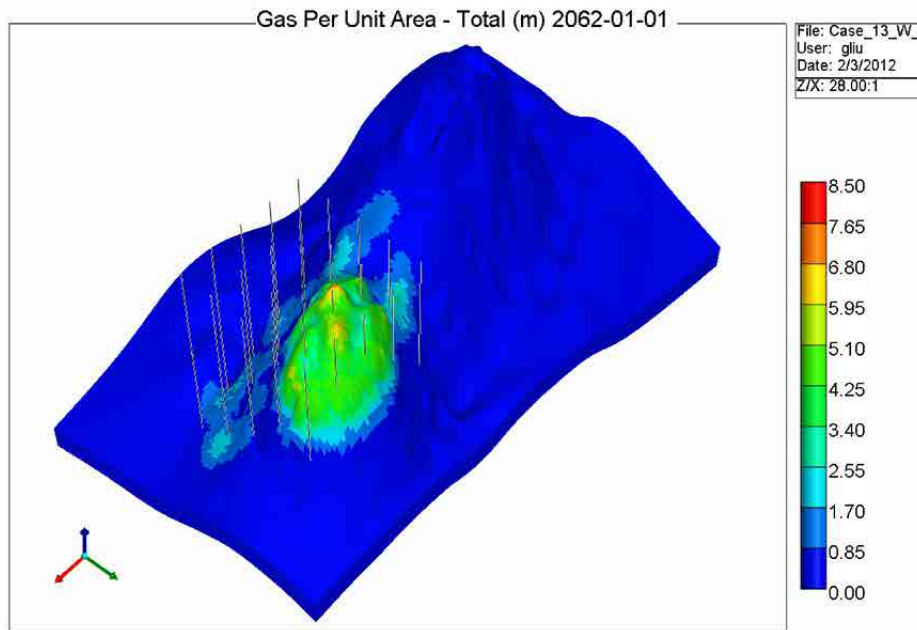


Figure C-95. 3-D view of Case 15: CO₂ plume migration for 50 years from beginning of injection.

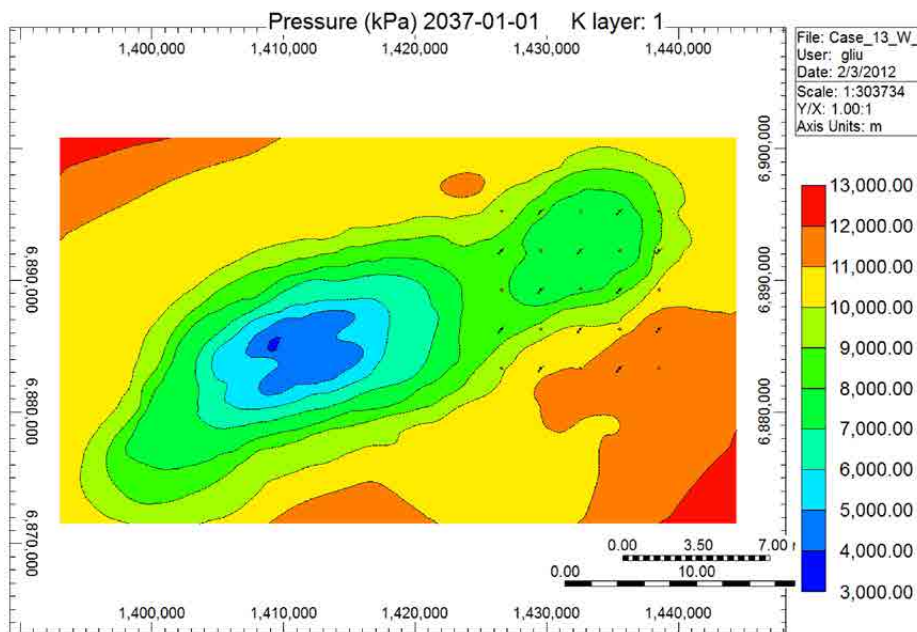


Figure C-96. Areal view of Case 15: pressure distributions for 25 years from beginning of injection.

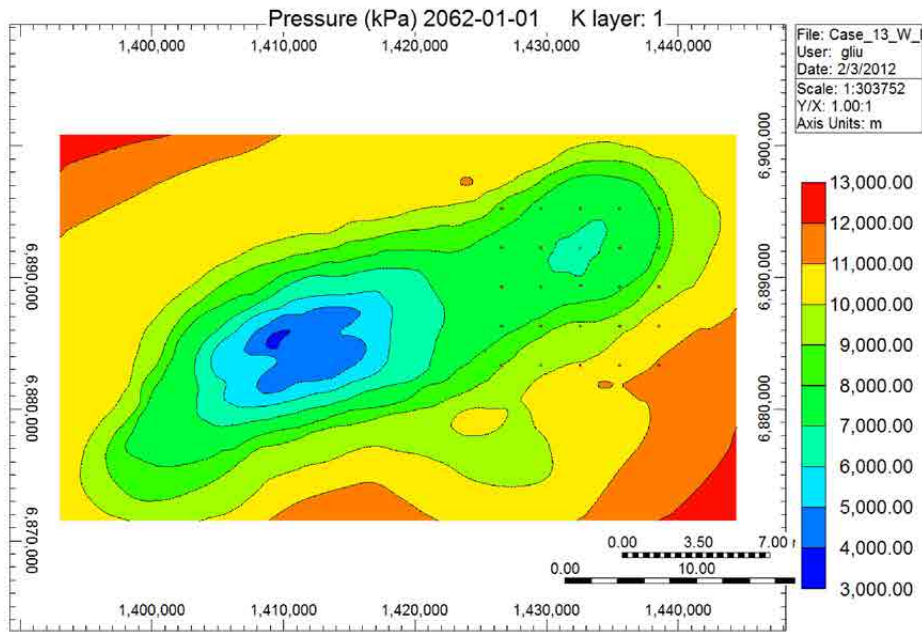


Figure C-97. Areal view of Case 15: pressure distributions for 50 years from beginning of injection.

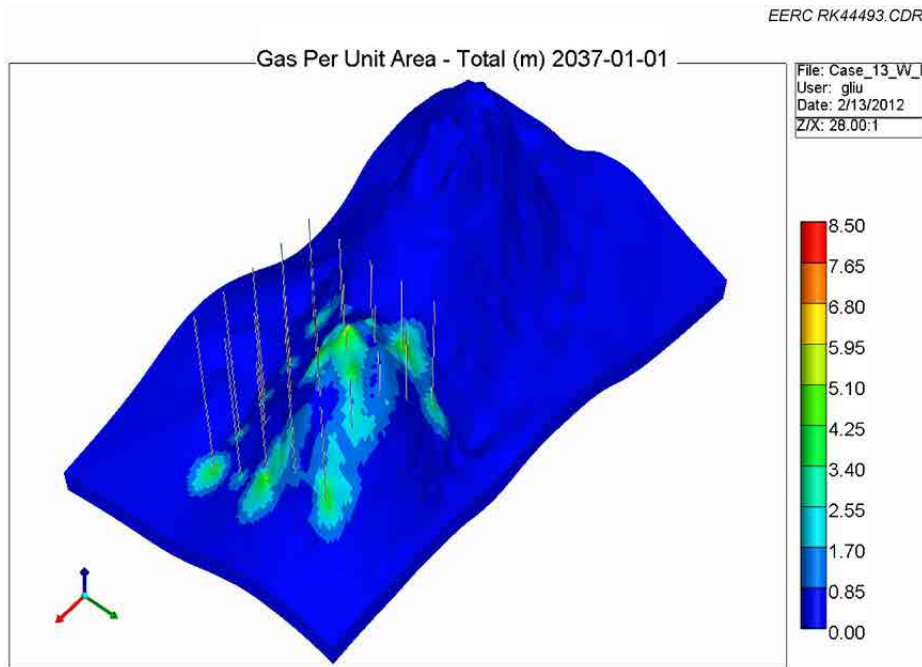


Figure C-98. 3-D view of Case 16: CO₂ plume migration for 25 years from beginning of injection.

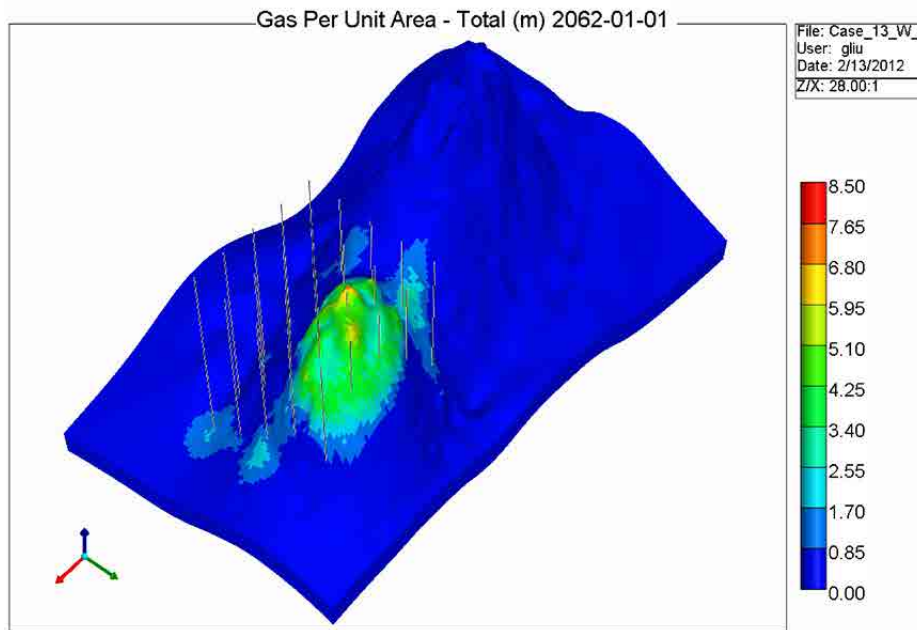


Figure C-99. 3-D view of Case 16: CO₂ plume migration for 50 years from beginning of injection.

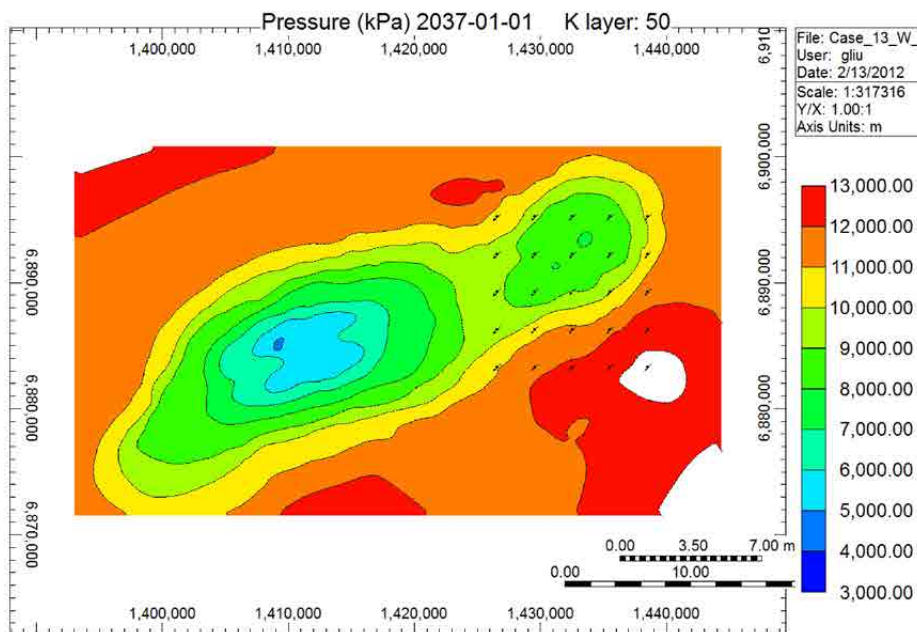


Figure C-100. Areal view of Case 16: pressure distributions for 25 years from beginning of injection.

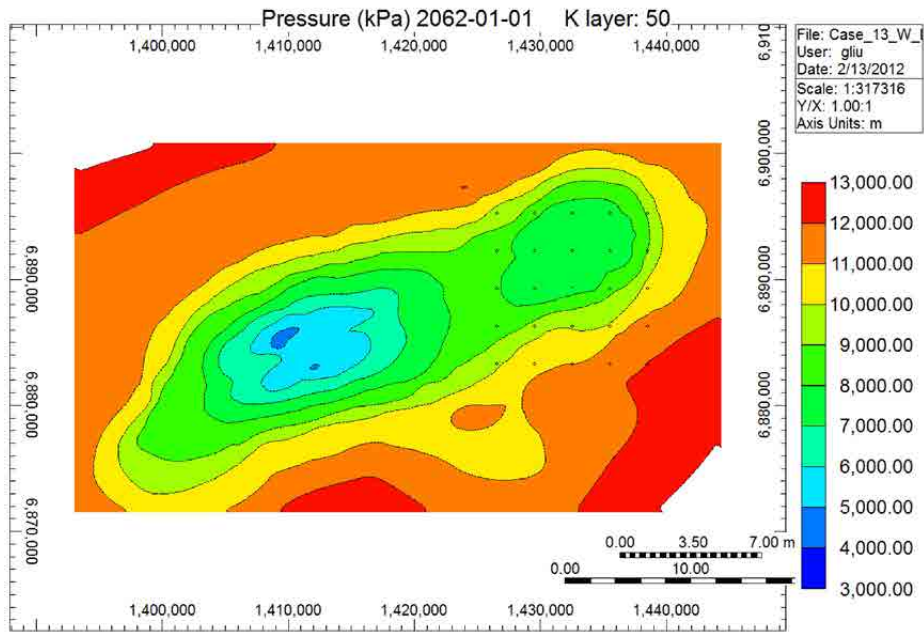


Figure C-101. Areal view of Case 16: pressure distributions for 50 years from beginning of injection.

APPENDIX D

ZAMA MODELING AND SIMULATIONS

ZAMA MODELING AND SIMULATIONS

The Zama Keg River F oil pool is one of the several oil pools discovered in the Zama oil field in northwestern Alberta, Canada (Figure D-1). It has been the site of acid gas (approximately 70% CO₂+ 30% H₂S) injection for the simultaneous purposes of enhanced oil recovery (EOR), H₂S disposal, and CO₂ storage. The Zama study site is unique in this study as it a closed system with detailed production history. Its current operation as a carbon capture and storage–EOR project afforded the opportunity for detailed characterization and simulation.

The Zama Keg River F oil pool is one of the several hydrocarbon-bearing geologic structures in the Zama subbasin located in northwestern Canada. These geological structures, known as pinnacle reefs, produce oil from the Middle Devonian Keg River Formation at an average depth of 5000 ft (1524 m) below ground surface. A generalized stratigraphic section of the Zama subbasin is shown in Figure D-2.

The presence of an anhydrite layer between the Zama and Keg River Formations acts as a nonflow barrier between the two formations. Another low-permeability and low-porosity anhydrite layer is also present at the oil–water contact, which has also affected the flow of reservoir fluids within the reservoir. However, the lateral extent of these anhydrite layers is not known.



Figure D-1. Location of the Zama oil field in Northwest Alberta (well locations are where the Keg River Formation was penetrated).

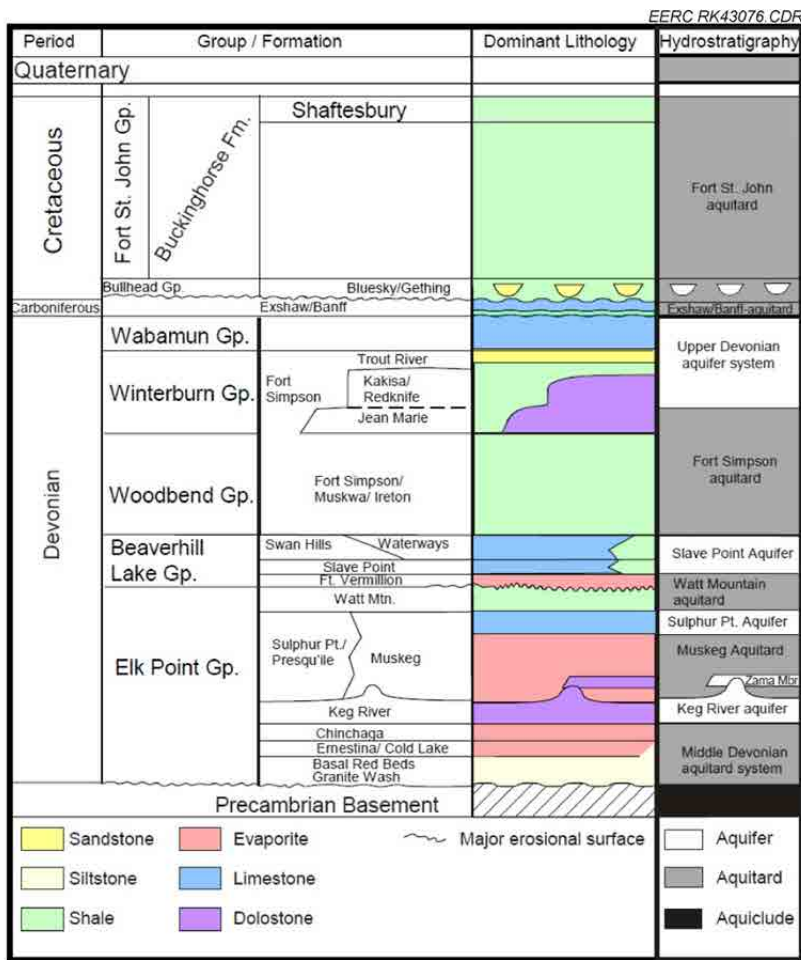


Figure D-2. The generalized stratigraphic column of Zama subbasin (Buschkuehle and others, 2007).

The static model consists of oil productive zone (Zama and Keg River Formations) at the top portion of the reef and lower Keg River aquifer (below oil/water contact). The static geologic model contains 6,16,512 (104 × 104 × 57) cells. The cells are of size 50 × 50 ft (15.2 m × 15.2 m) in I and J directions with varying thickness (K direction) ranging from 3 ft (0.91 m) to 19 ft (5.8 m). One of the realizations of the constructed static geological model was then exported to the CMG–GEM reservoir simulator and was used in the dynamic simulations performed in this study.

The availability of detailed production histories allowed for a preliminary history match of the dynamic model for cumulative oil, gas, and water production and pressure matching. This exercise was done to have a representative distribution of reservoir fluids and material balance prior to brine extraction/pressure relief modeling.

Figures D-3–D-5 show the distribution of porosity and horizontal and vertical permeabilities in the dynamic model. The overlying upper Muskeg Formation modeled in the static geologic model is not incorporated in dynamic model.

Six different cases of simultaneous acid gas injection and formation water extraction (Table D-1) along with a base case (gas injection only) were tested in predictive simulation runs. These cases included acid gas injection through an injector well (Gas Inj-1) placed in a selected high-permeability zone of oil productive area situated in the top portion of the structure. Two different gas injection rates of 310,680 kg a day (0.113 megatonnes a year) and 621,359 kg a day (0.227 megatonnes a year) were tested. Formation water (salinity ~180,000 ppm) was extracted by placing water injection wells at select locations in available high-permeability streaks in the bottom portion of the water zone. In view of the significantly high formation water salinity, the solubility of acid gas in water was neglected while running predictive simulations. The placement locations of the acid gas injection well (location X) and water production wells (location Y, location Z, and location Z1) used in the different prediction simulations are shown in Figures D-6 and D-7.

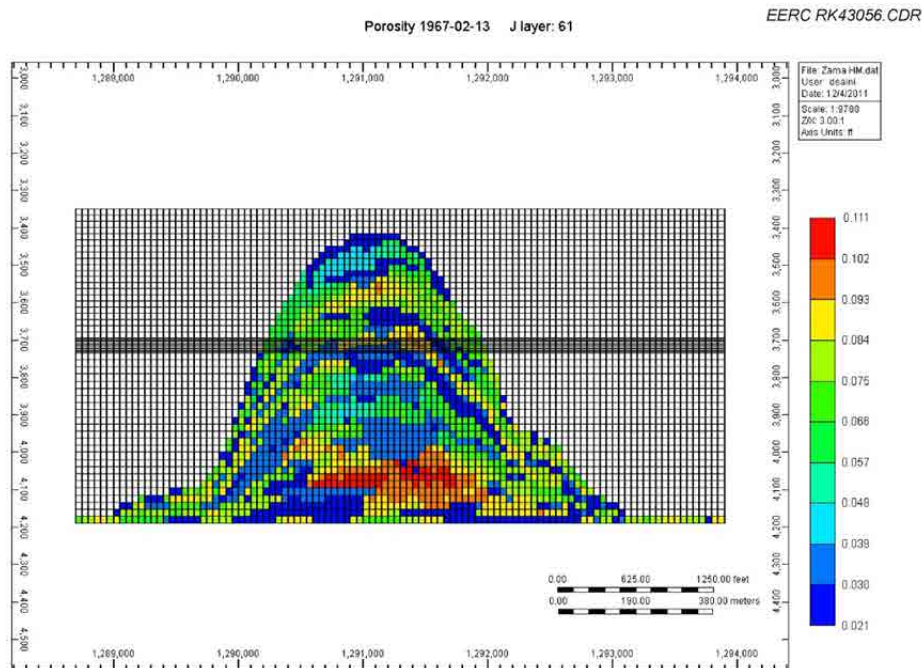


Figure D-3. Example of porosity distribution in the dynamic model.

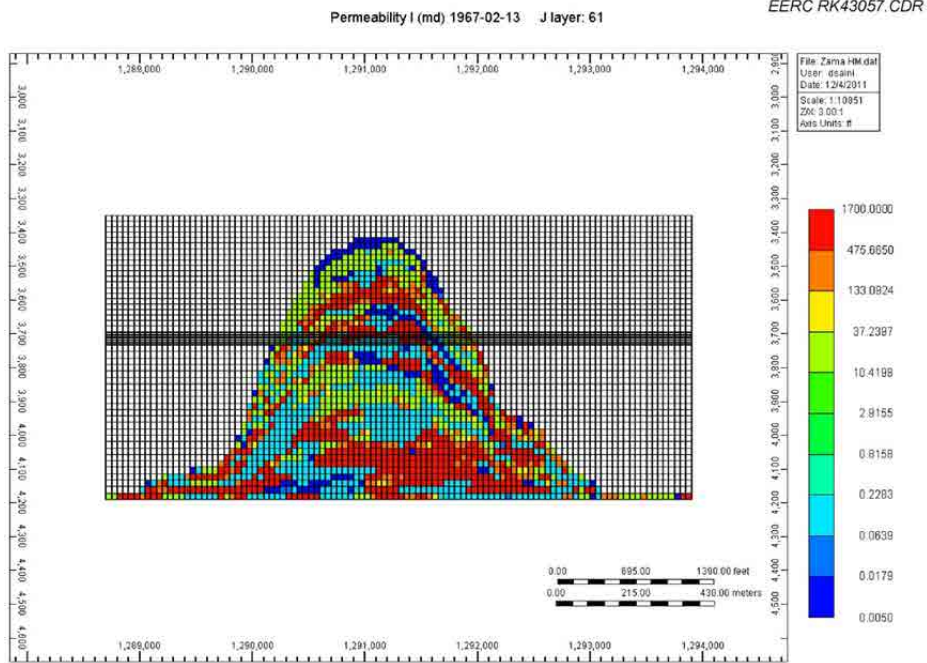


Figure D-4. Example of horizontal permeability distribution in the dynamic model.

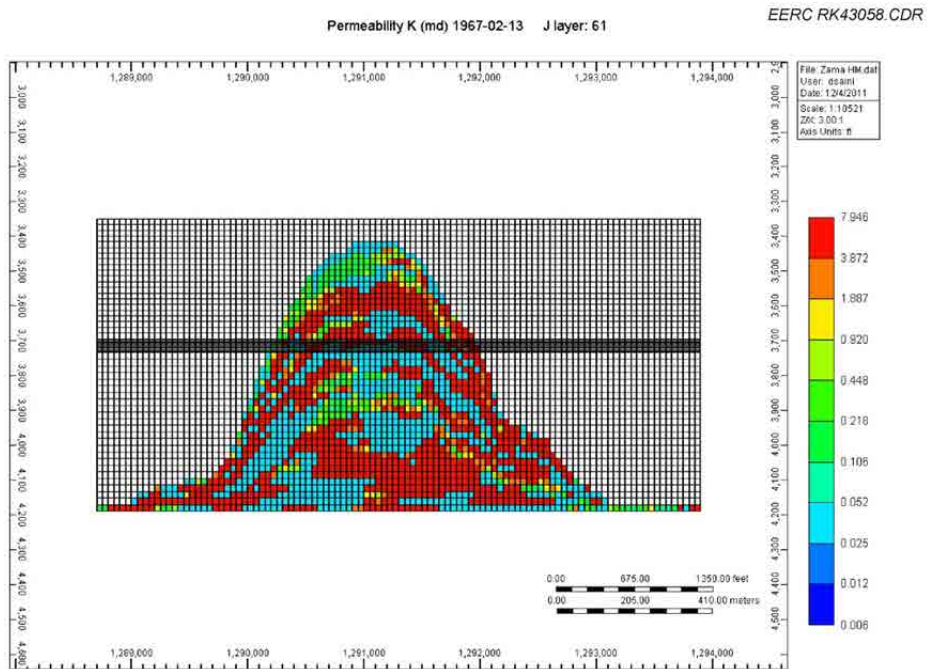


Figure D-5. Example of vertical permeability distribution in the dynamic model.

Table D-1. Cases Tested in Predictive Simulations

Case	Well Configuration	Gas Injection Rate/Well SC, ¹ kg/day	Water Production Rate/Well, SC, ¹ m ³ /day
Base Case	Gas Inj-1 (Location X)	310,680	N/A
Case 1	Gas Inj-1 (Location X) WaterProd-1 (Location Y)	310,680	516
Case 2	Gas Inj-1 (Location X) WaterProd-1 (Location Z)	310,680	516
Case 2A	Gas Inj-1 (Location X) WaterProd-1 (Location Z)	310,680	429
Case 2B	Gas Inj-1 (Location X) WaterProd-1 (Location Z)	Variable (310,680 to 277,599)	397
Case 3	Gas Inj-1 (Location X) WaterProd-1 (Location Z)	621,359	1144
Case 4	Gas Inj-1 (Location X) WaterProd-1 (Location Z) WaterProd-2 (Location Z1)	621,359	572

¹ Standard conditions (15.5°C, 101.25 kPa).

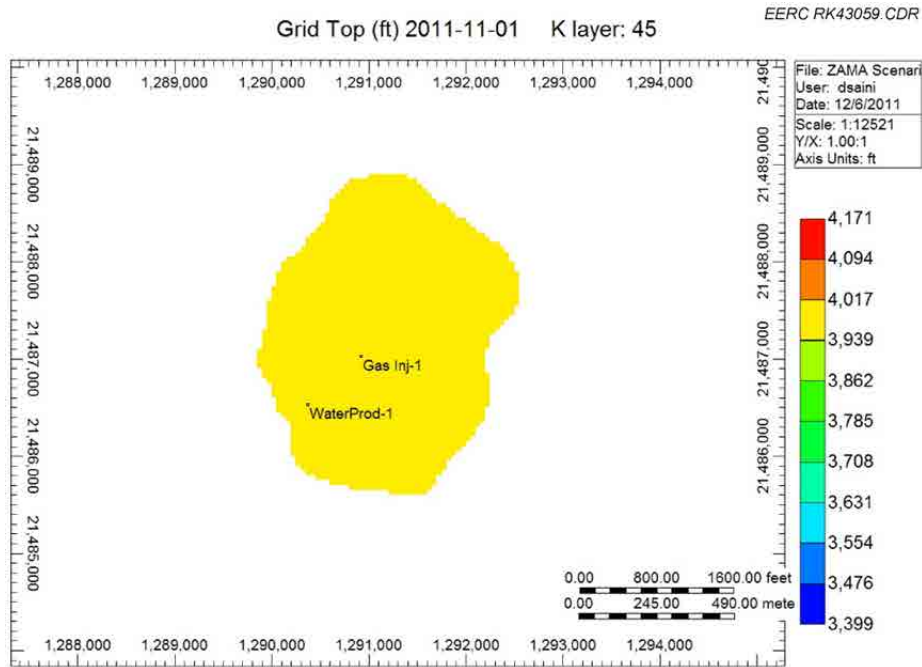


Figure D-6. Well locations for Gas Inj-1 (Location X), WaterProd-1 (Location Y) in Case 1.

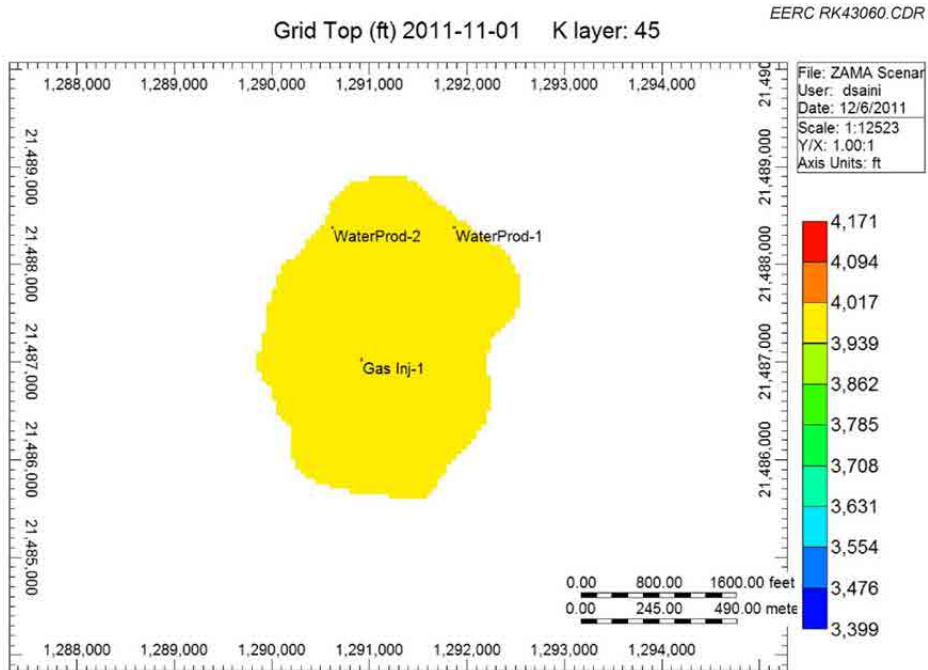


Figure D-7: Well locations for Gas Inj-1 (Location X), WaterProd-1 (Location Z), and WaterProd-2 (Location Z1). Locations X and Z were utilized for Cases 2, 2A, 2B, and 3 while WaterProd-2 (Location Z1) was used for Case 4.

The detailed results obtained in different simulation cases are given in Table D-2 and shown in Figure D-8–D-19. The examples of areal and cross-sectional views of gas saturation are presented in Figures D-20 and D-21.

REFERENCES

1. Buchkuehle, M., Haug, K., Michael, K., and Berhane, M., 2007, Regional-scale geology and hydrogeology of acid-gas enhanced oil recovery in the Zama oil field in northwestern Alberta: Alberta Energy and Utilities Board, Alberta Geological Survey, Canada, June.

Table D-2. Predictive Simulation Results of Formation Brine Extraction/Pressure Management Modeling, Zama Keg River F Pool

Variable	Unit	Base Case	Case 1	Case 2	Case 2A	Case 2B	Case 3	Case 4
Number of Injection Wells		1	1	1	1	1	1	1
Target Injection Rate/Well	megatonnes/year	0.113	0.113	0.113	0.113	0.113	0.227	0.227
Maximum Injection BHP ¹	kPa	22,753	22,753	22,753	22,753	22,753	22,753	22,753
Number of Extraction Wells		Not present	1	1	1	1	1	2
Lowest Production BHP	kPa	N/A	2068	2068	2068	2068	2068	2068
Well Configuration		Gas Inj-1 (Location X)	Gas Inj-1 (Location X) WaterProd-1 (Location Y)	Gas Inj-1 (Location X) WaterProd-1 (Location Z)	Gas Inj-1 (Location X) WaterProd-1 (Location Z) WaterProd-2 (Location Z1)			
Imposed Constraint for Additional Storage Capacity Gain Through Water Extraction		Average reservoir pressure = maximum allowable pressure limit	Shut in water production well once injected gas breakthrough occurs at water extraction well	Shut in water production well once injected gas breakthrough occurs at water extraction well	Shut in water production well once injected gas breakthrough occurs at water extraction well	Shut in water production well once injected gas breakthrough occurs at water extraction well	Shut in water production well once injected gas breakthrough occurs at water extraction well	Shut in water production well once injected gas breakthrough occurs at water extraction well
Injection Period until Target Injection Rate Is Maintained	years	1 year and 6 months	4 years and 1 month	5 years and 6 month	6 years	3 years and 5 months	2 years and 2 months	2 years and 8 months

¹ Bottomhole pressure.

² Standard conditions (15.5°C, 101.25 kPa).

³ Reservoir conditions (variable pressure ranging from 4000 kPa to 22,753 kPa, 71°C).

Continued . . .

Table D-2. Predictive Simulation Results of Formation Brine Extraction/Pressure Management Modeling, Zama Keg River F Pool (continued)

Variable	Unit	Base Case	Case 1	Case 2	Case 2A	Case 2B	Case 3	Case 4
Acid Gas Injection Rate/Well at Surface Conditions Prior to Violation of Imposed Constraint	kg/day	310,680 to 0	310,680	310,680	310,680	Variable (310,680 to 277,599)	621,359	621,359
Production Period until Imposed Constraint is Violated	years	–	3 years and 2 months	4 years and 5 months	5 years and 9 months	6 years and 4 months	1 year and 8 months	1 year and 10 months
Cumulative Gas Injected until Imposed Constraint is Violated	SC, ² megatonnes	0.05	0.36	0.50	0.65	0.69	0.38	0.43
Cumulative Acid Gas Injected	SC, ² megatonnes	0.05	0.47	0.62	0.68	0.69	0.49	0.60
Cumulative Acid Gas Injected	RC, ³ m ³	–	8.05+05	1.08E+06	1.05E+06	1.04E+06	8.48E+05	1.02E+06
Cumulative Extracted Water	RC, ³ m ³	–	6.20E+05	8.47E+05	9.08E+05	9.36E+05	7.20E+05	8.37E+05
Ratio of Acid Gas Injected to Extracted Water at Reservoir Conditions		–	1.30:1	1.28:1	1.16:1	1.11:1	1.18:1	1.22:1
Daily Water Extraction Rate/Well	SC, ¹ m ³ /day	N/A	516	516	429	397	1,144	572
Boundary Conditions		Closed	Closed	Closed	Closed	Closed	Closed	Closed

D-8

¹ Bottomhole pressure.

² Standard conditions (15.5°C, 101.25 kPa).

³ Reservoir conditions (variable pressure ranging from 4000 kPa to 22,753 kPa, 71°C).

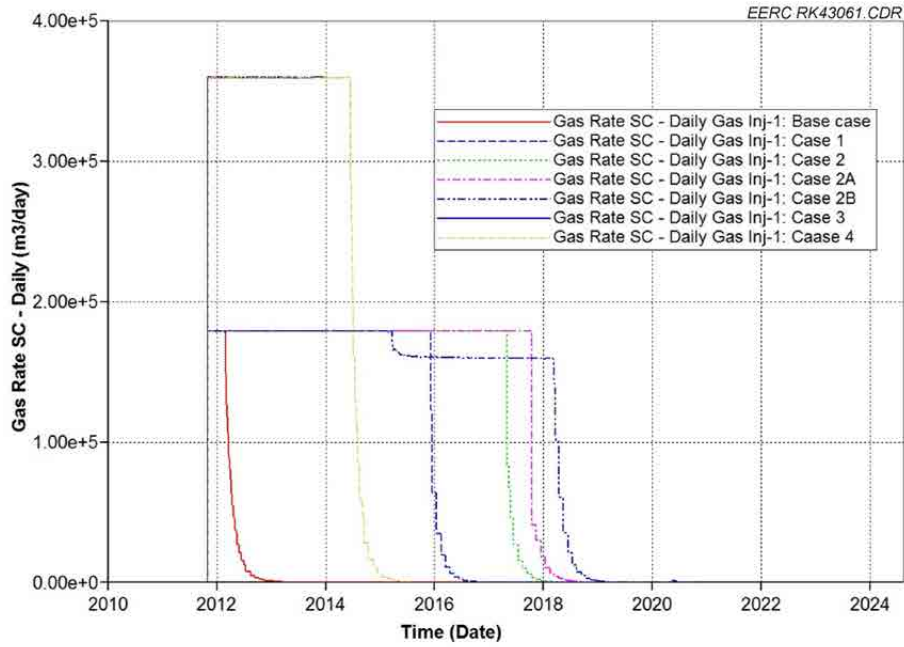


Figure D-8. Acid gas injection rates.

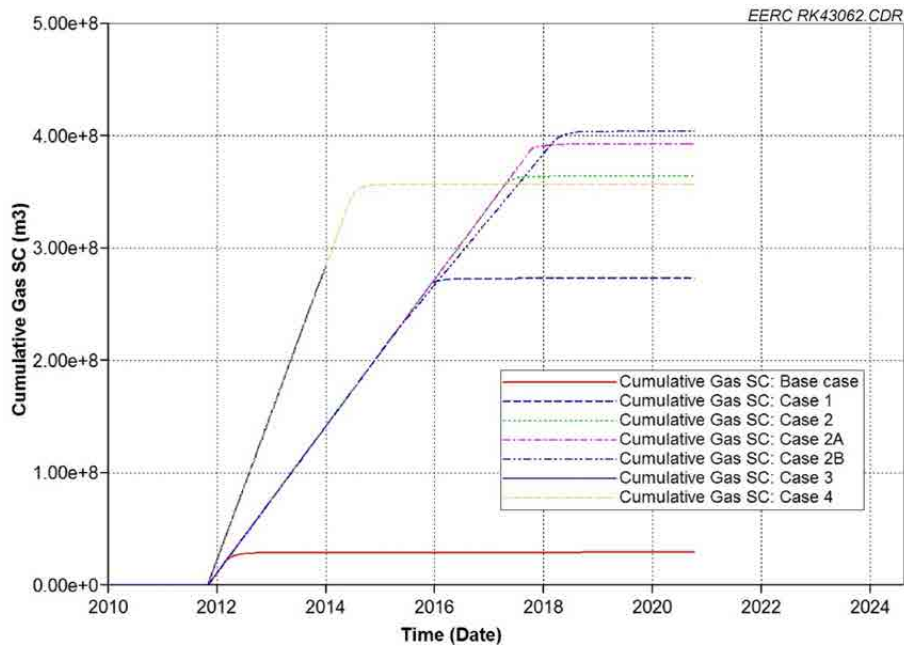


Figure D-9. Cumulative acid gas injected.

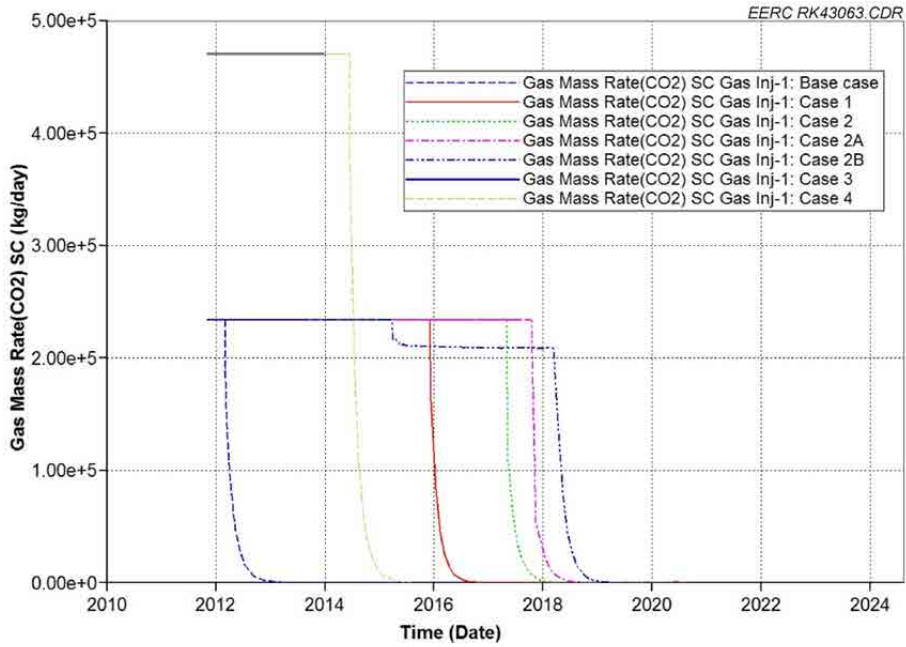


Figure D-10. CO₂ injection rates.

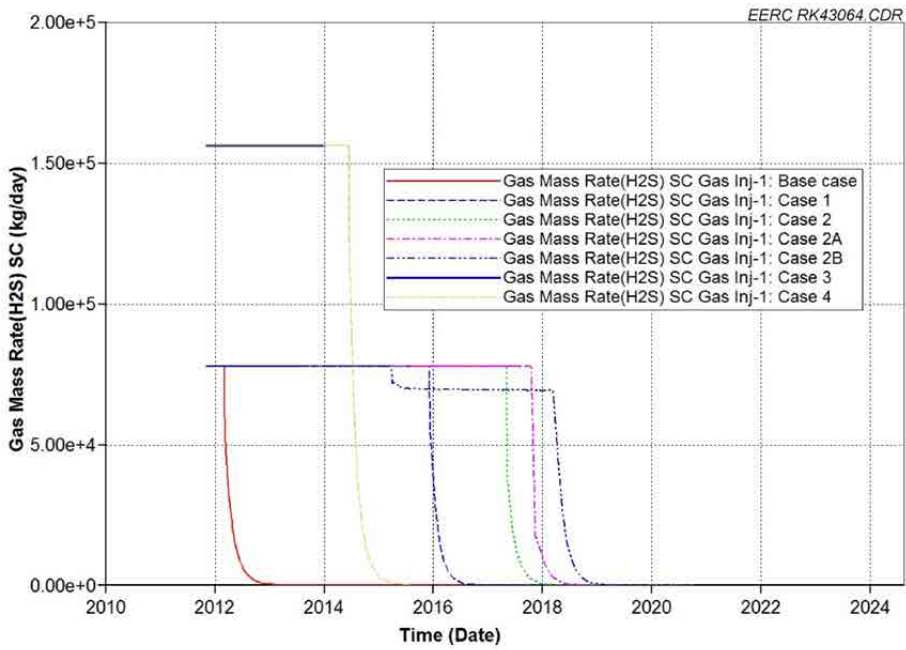


Figure D-11. H₂S injection rates.

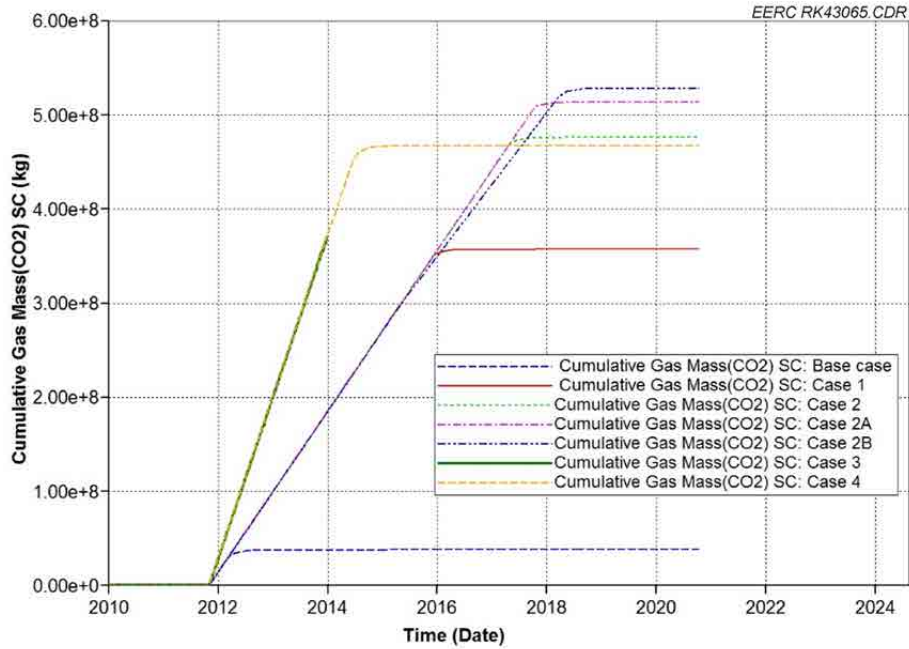


Figure D-12. Cumulative CO₂ injected.

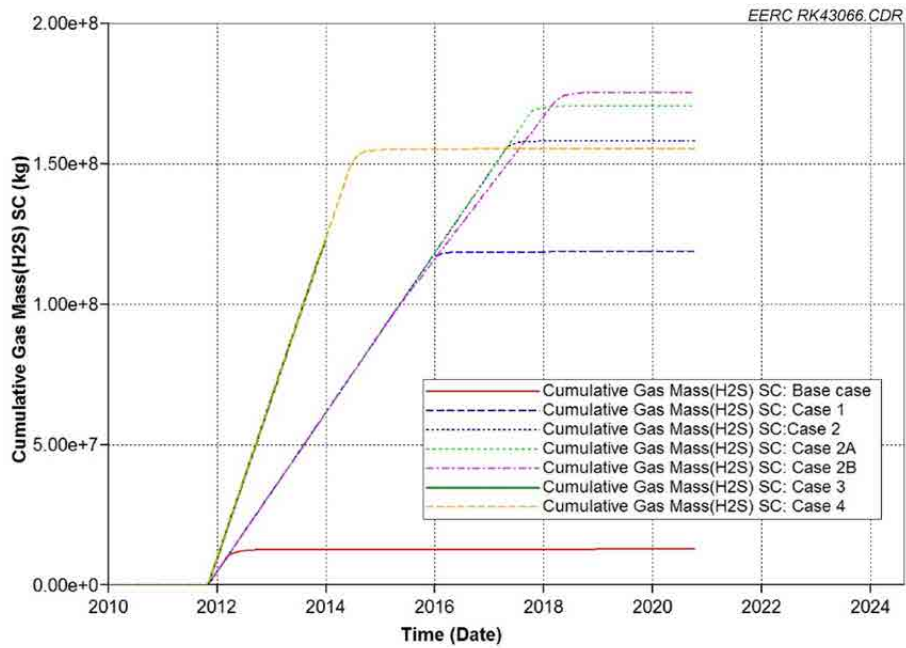


Figure D-13. Cumulative H₂S injected.

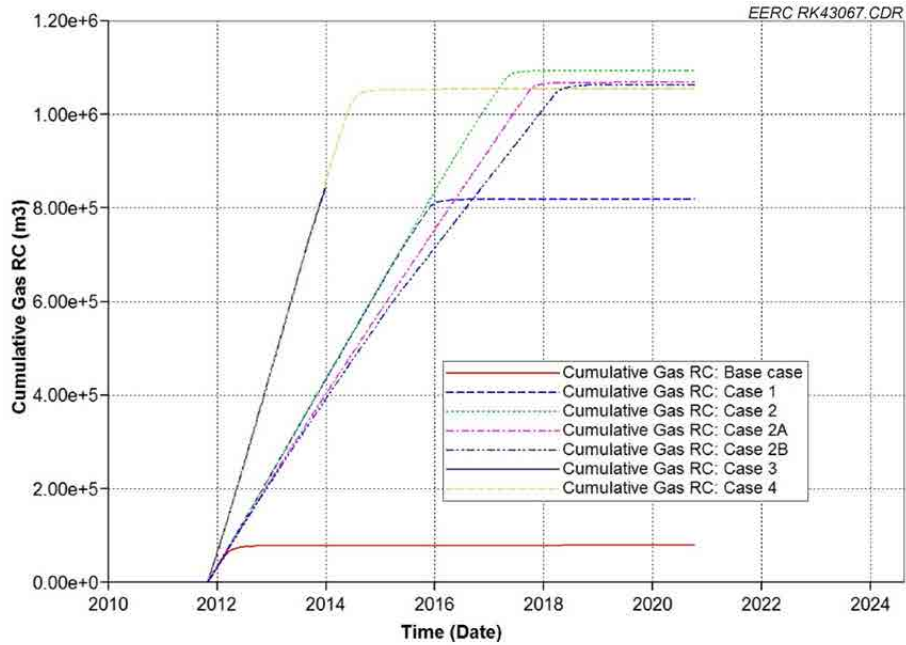


Figure D-14. Cumulative acid gas injected (reservoir conditions).

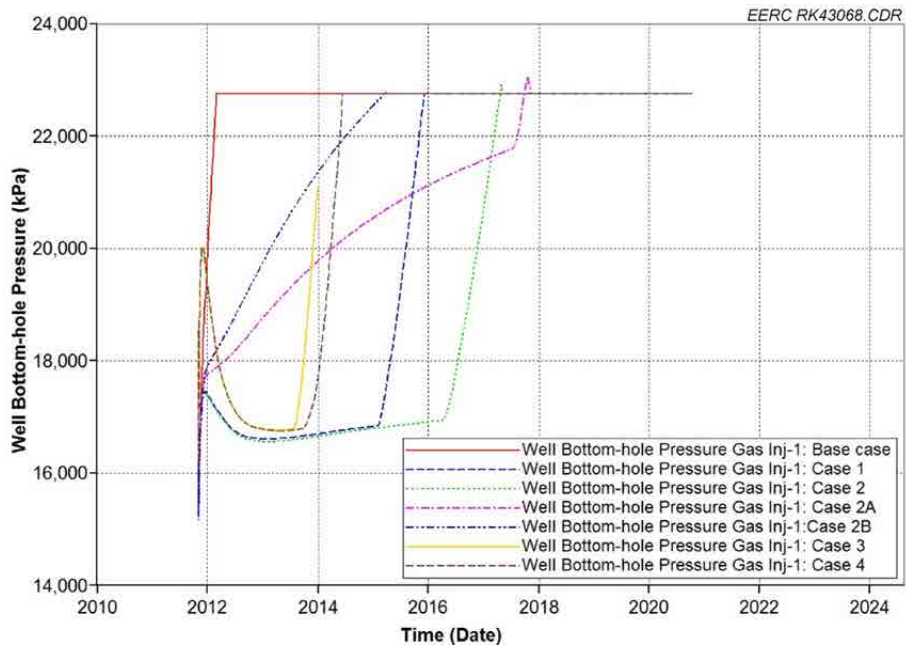


Figure D-15. Injection well BHPs.

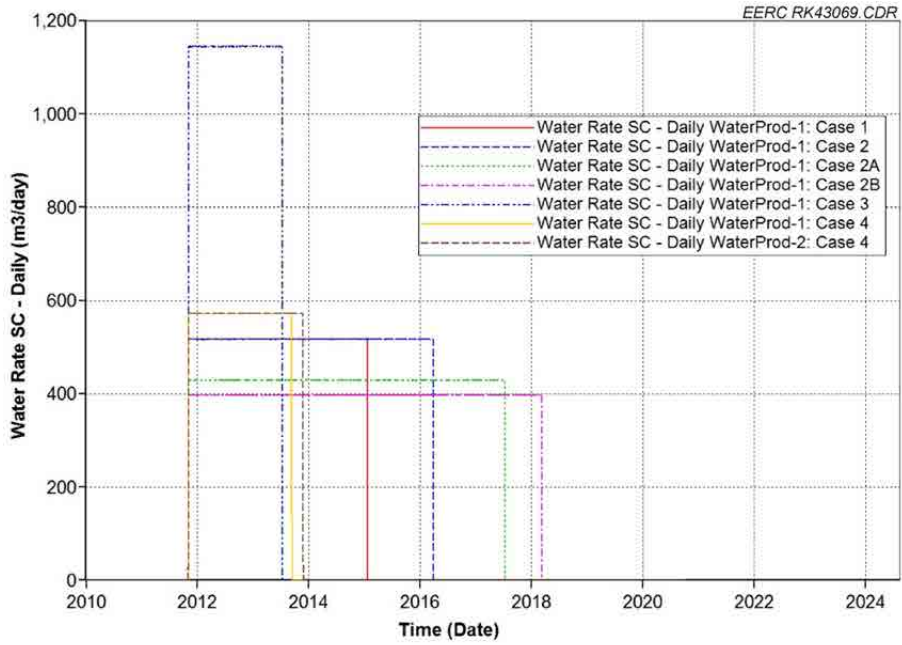


Figure D-16. Water extraction rates.

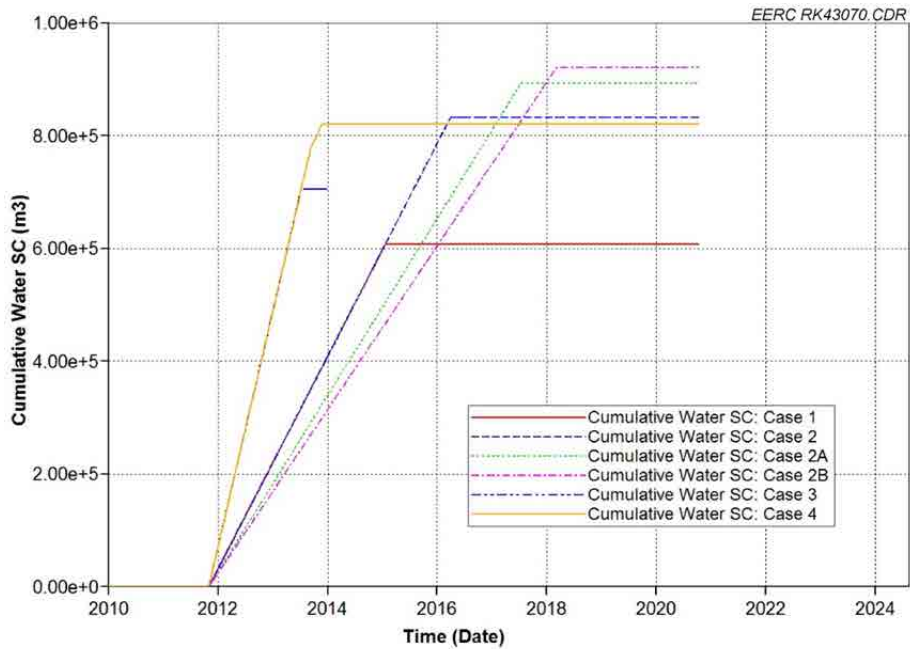


Figure D-17. Cumulative water extracted.

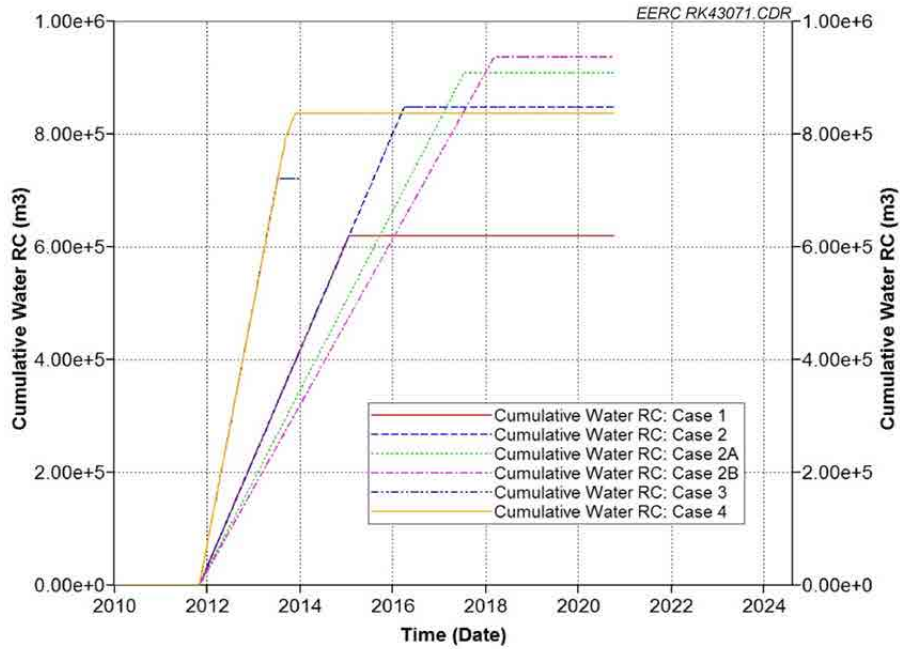


Figure D-18. Cumulative water extracted (reservoir conditions).

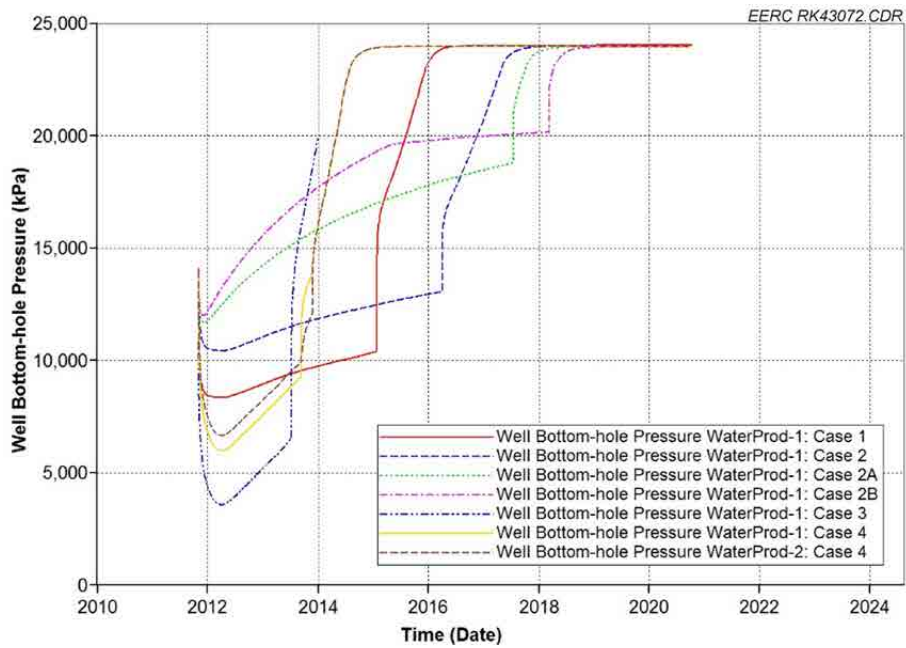


Figure D-19. Extraction well BHPs.

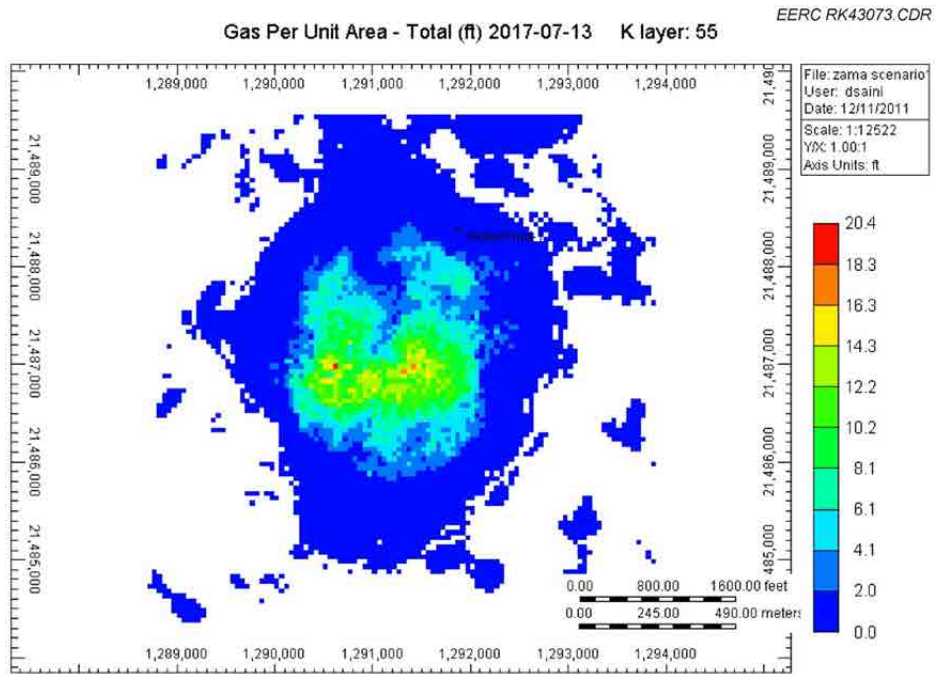


Figure D-20. Case 2A: Areal view of injected gas plume at gas breakthrough.

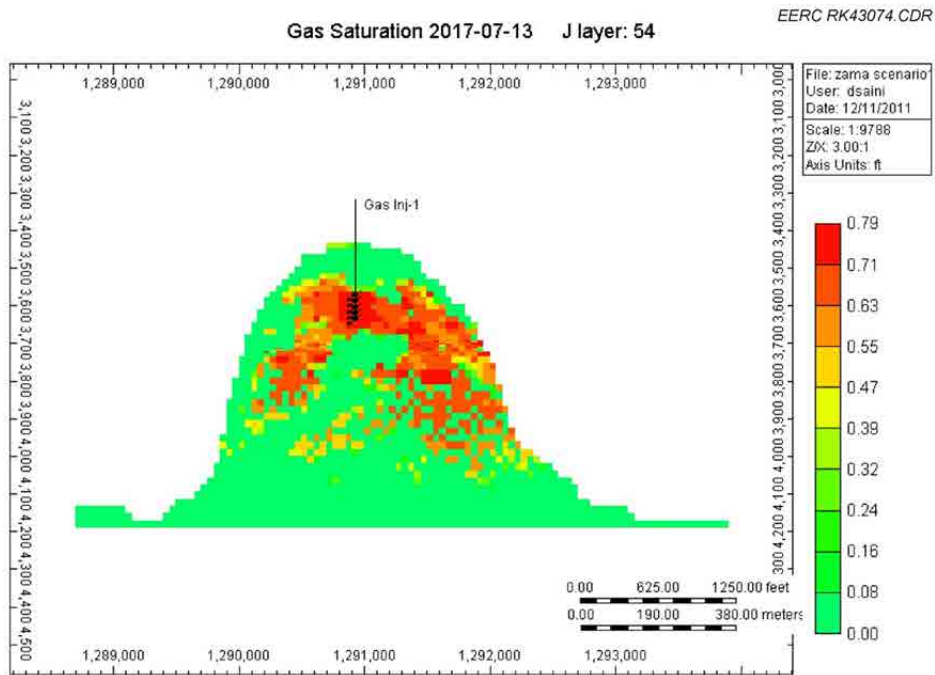


Figure D-21. Case 2A: Cross-sectional view of gas saturation at gas breakthrough.

APPENDIX E

GORGON MODELING AND SIMULATIONS

GORGON MODELING AND SIMULATIONS

DYNAMICS MODELING AND SIMULATIONS

In this case study, there are a total of seven scenarios for identifying the differences in CO₂ storage behavior by applying various injection and extraction strategies (Table E-1) based on the target formations and well locations designed for the Gorgon Project (Flett and others, 2008). The permeability of the target formation is shown by a 3-D view and vertical (north–south) cross section in Figures E-1 and E-2. The locations of the eight injection wells and four production wells are marked in Figures E-3 and E-4. All of the eight injectors were opened for CO₂ injection from the beginning of simulation activities. After 5-years, two water extraction wells will come online, with the remaining extraction wells coming online at a later time, depending on the scenario.

In the first five cases, all injectors are loaded at a rate of one-half million tons a year. The results show that the rate can be met for all of these cases even without water extraction. This is the reason why the results of the pairs (Cases 1 and 2 and Cases 3 and 4) are very similar for the total volume of injected CO₂ regardless of water extraction and injection period. An interesting observation is that extraction rates were higher for the cases with the lower injection rates (1/4 million tonnes per year) than the faster injections. This phenomenon is due to higher demand from extractors because of a longer distance between the injected plume and the extraction well.

Cases 8 and 9 are designed to identify the maximum CO₂ storage capacity with an unrealistically high injection rate of 3.75 Mt/year. The capacity in this scenario was found to be around 55 Mt without water extraction and 64 Mt with water extraction. However, because the injection rate ends up to be higher in Case 9, the period of CO₂ breakthrough becomes shorter, ultimately resulting in a total extracted water volume that is not much higher than cases with lower injection rates, such as Case 2. The results also show that the total volume of injected CO₂ is five to six times higher than Case 5, which had the slower injection rate of half a Mt/year for the eight injection wells. If four water extraction wells are used, the ratio of the total injected CO₂ increases to six to seven times.

All of the detailed results of total injected CO₂, well rates and bottomhole pressures (BHPs), CO₂ plumes, and pressure distributions over time are shown in Figures E-1 through E-116 ordered by simulation case. These results are presented as plots, 3-D views, areal views, and cross sections. Surface maps showing the plume extents for each case are shown in Figures E-117 through E-128.

REFERENCE

Flett, M., Beacher, G., Brantjes, J., Burt, A., Dauth, C., Koelmeyer, F., Lawrence, R., Leigh, S., McKenna, J., and Robinson W., 2008, Gorgon project—subsurface evaluation of carbon dioxide disposal under Barrow Island: SPE Asia Pacific Oil and Gas Conference and Exhibition, Perth, Australia, October 20–22, 2008.

Table E-1. Detailed Properties of the Simulation Cases Investigated^a

Variable	Unit	Case 1	Case 2	Case 3	Case 4	Case 5	Case 8	Case 9
Target Injection Rate/Well	Mt/year	0.5	0.5	0.5	0.5	0.25	3.75	3.75
Actual Injection Rate	kg/day	1.07E+07	1.07E+07	1.07E+07	1.07E+07	5.33E+06	6.04E+07	6.99E+07
Injection Period	Years	25	25	50	50	50	25	25
Cumulative Injected CO ₂	SC, ^b tonnes	9.73E+07	9.75E+07	1.95E+08	1.96E+08	9.75E+07	5.51E+08	6.37E+08
Cumulative Injected CO ₂	RC, ^c m ³	1.79E+08	1.84E+08	3.59E+08	3.67E+08	1.89E+08	8.99E+08	1.05E+09
Number of Injection Wells		8	8	8	8	8	8	8
Extraction Wells Present		No	4 added over time	No	4 added over time	4 added over time	No	4
Extraction Well Location		N/A	Various	N/A	Various	Various	N/A	Various
Cumulative Extracted Water	RC ² , m ³	N/A	2.15E+08	N/A	3.35E+08	3.97E+08	N/A	2.62E+08
Average Daily Extraction Rate	SC ¹ , m ³ /day	N/A	2.27E+04	N/A	2.21E+04	2.23E+04	N/A	3.40E+04
Average Extraction Period	Years	N/A	25.00	N/A	39.90	46.90	N/A	20.30
Highest Injection BHP	kPa	N/A	Various	N/A	Various	Various	N/A	Various
Lowest Production BHP	kPa	N/A	2000	N/A	2000	2000	N/A	2000
Boundary Conditions		Volumed	Volumed	Volumed	Volumed	Volumed	Volumed	Volumed

^a Cases 6 and 7 were omitted from the report because of duplicative results.

^b Standard conditions (25°C, 0.999 bar).

^c Reservoir conditions (Variable with depth, average of 255°C, 0.986 bar).

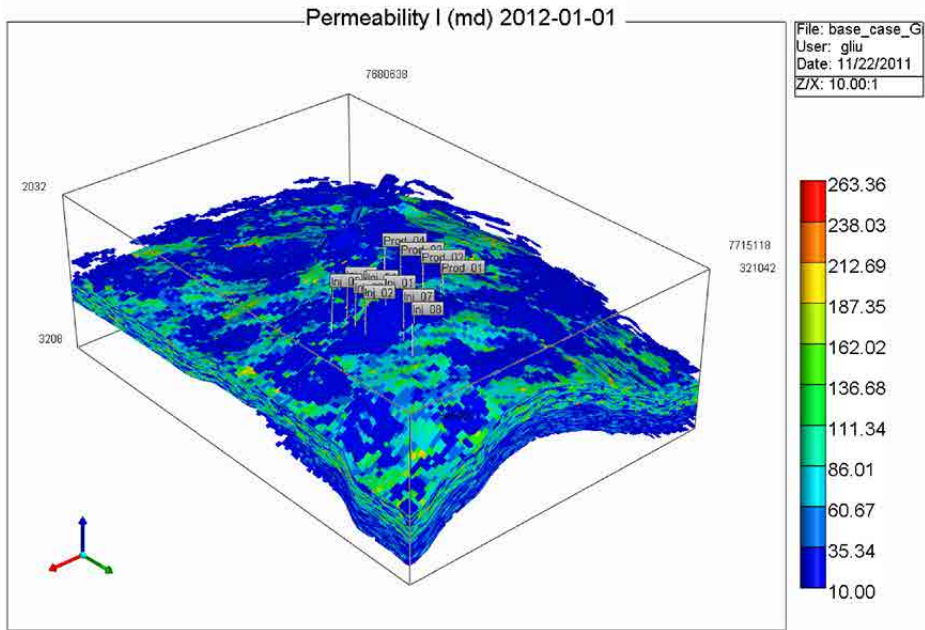


Figure E-1. 3-D view of the permeability of the target formations for CO₂ storage.

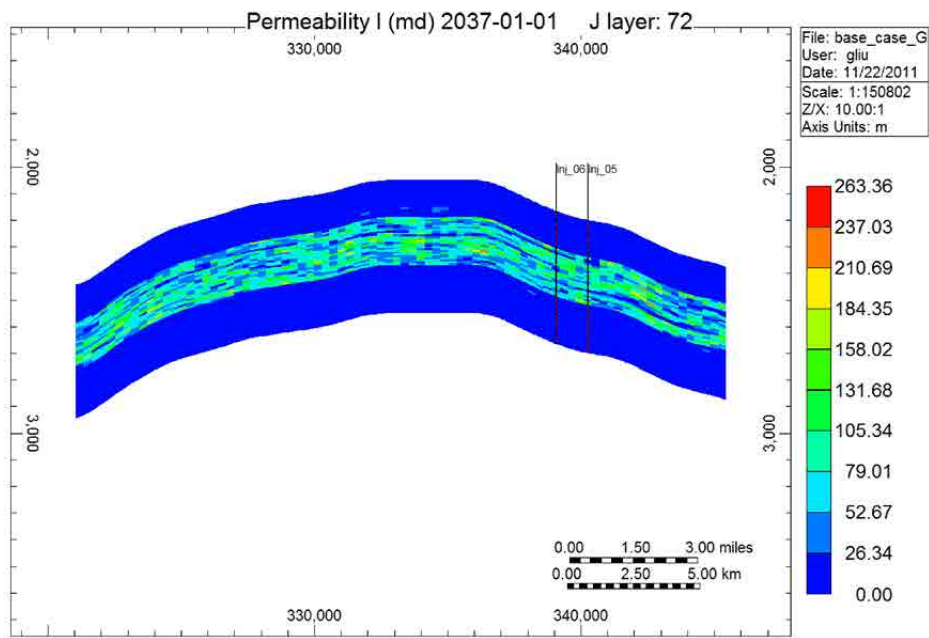


Figure E-2. Vertical view of the permeability of the target formations for CO₂ storage.

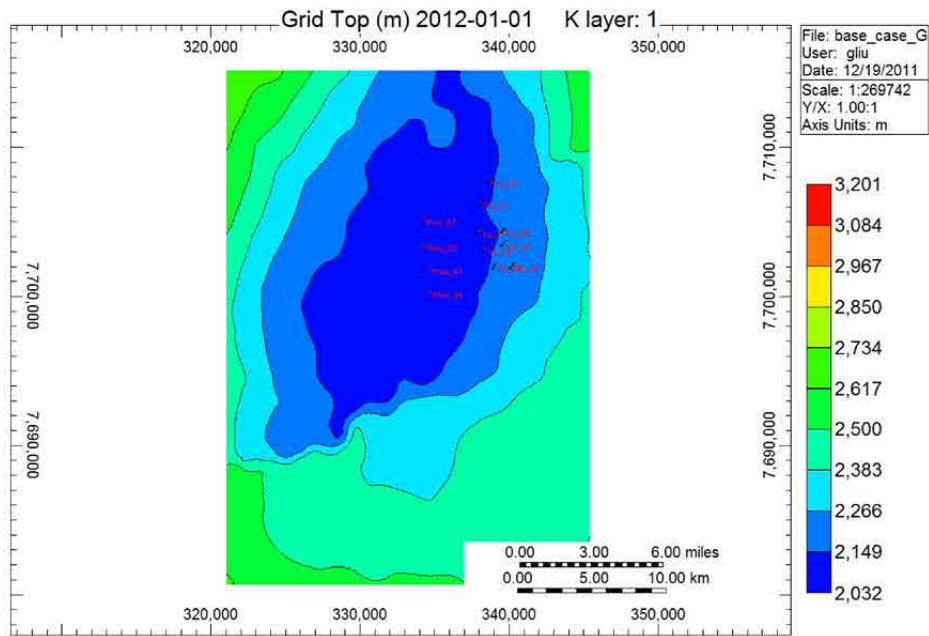


Figure E-3. Locations of injection and production wells.

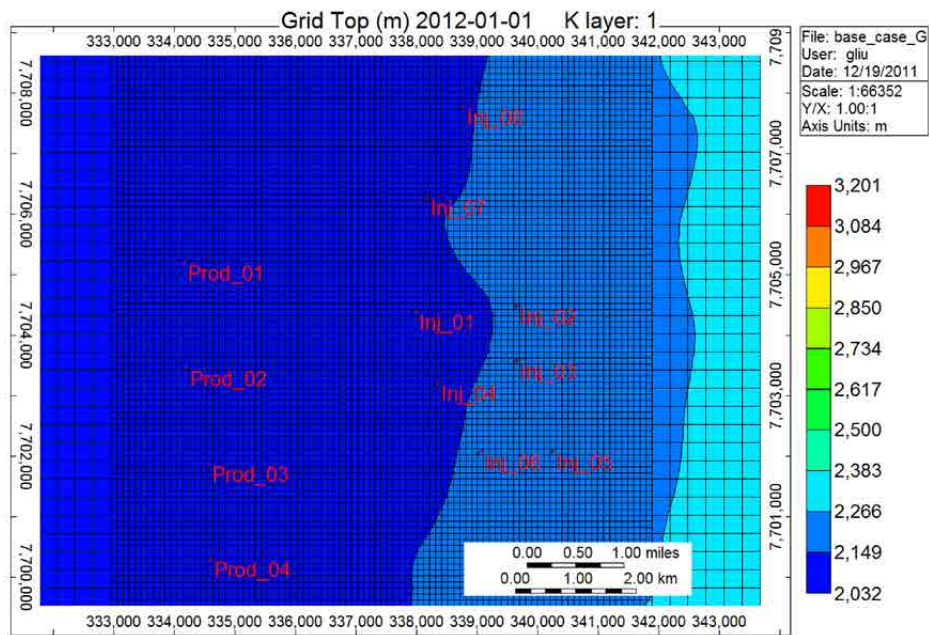


Figure E-4. Closed view of the locations of injection and production wells.

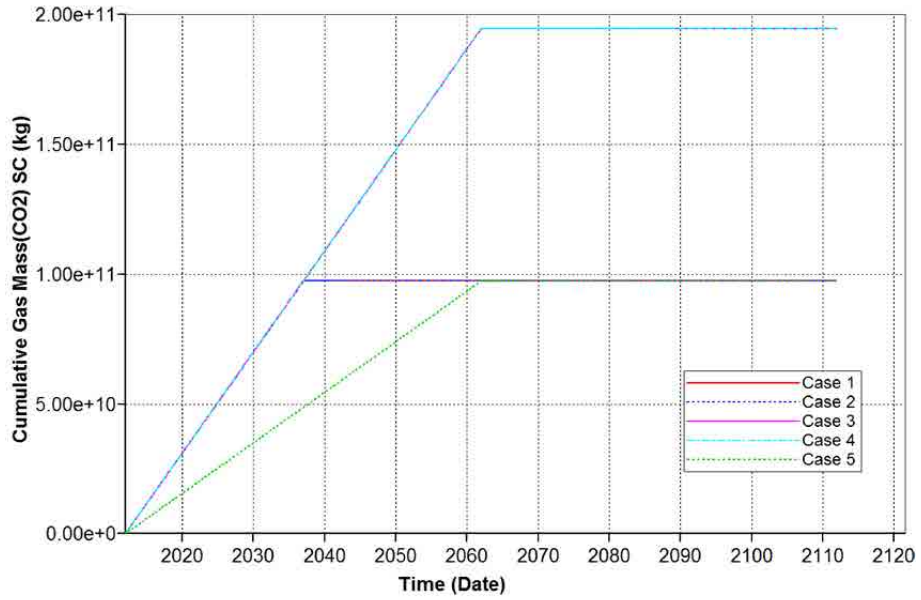


Figure E-5. Total injected CO₂ for Cases 1–5.

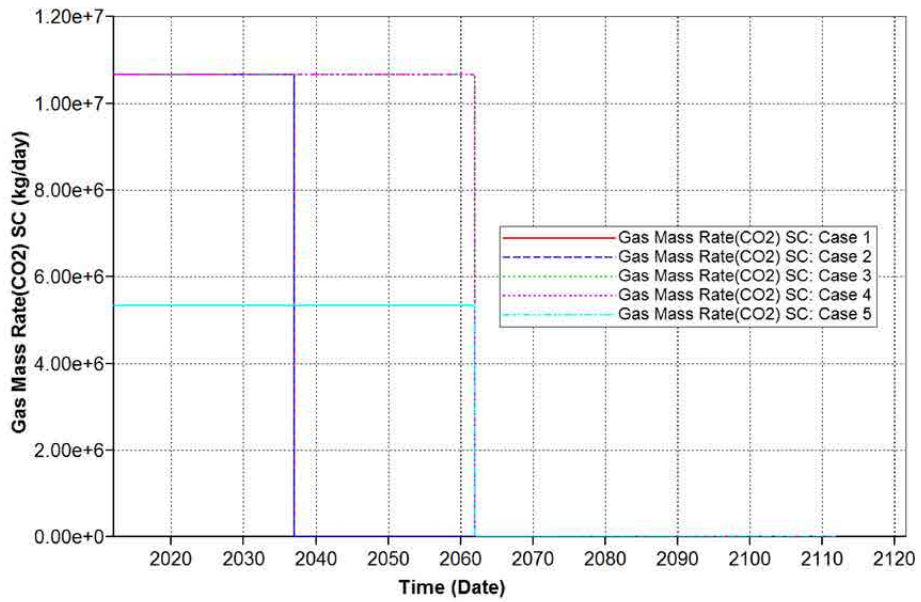


Figure E-6. CO₂ injection rates for Cases 1–5.

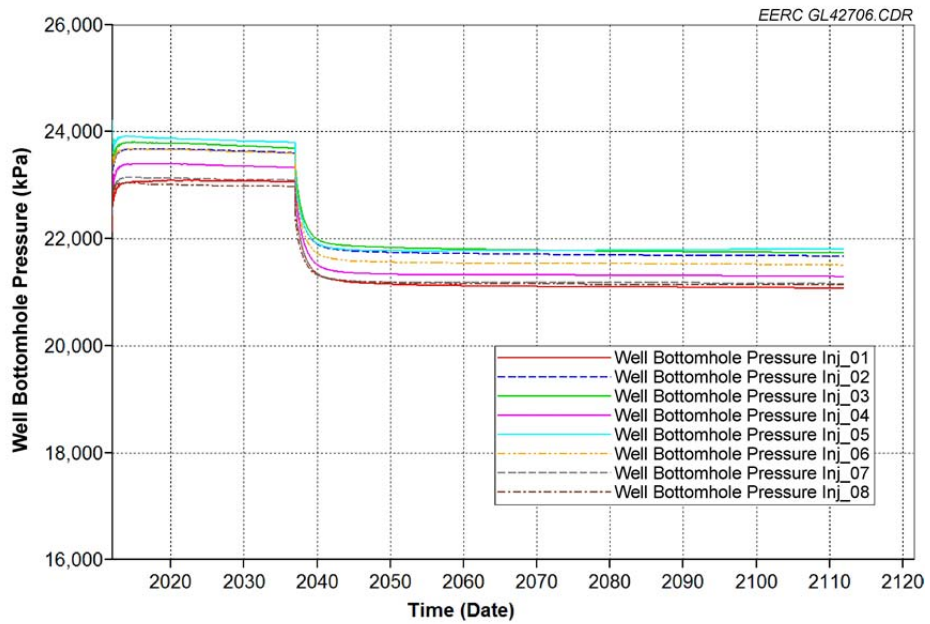


Figure E-7. Case 1 injection well BHPs.

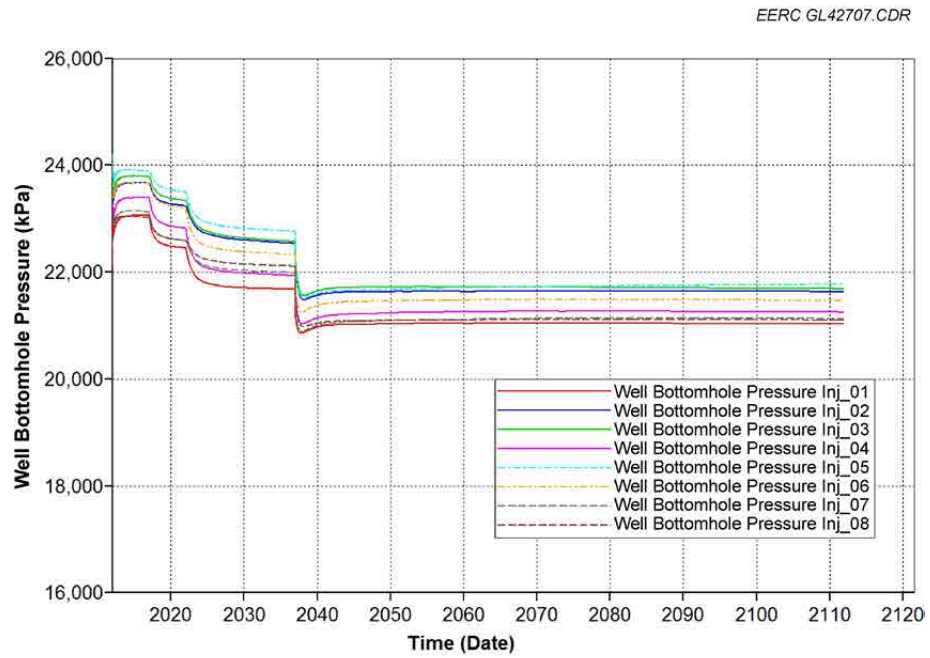


Figure E-8. Case 2 injection well BHPs.

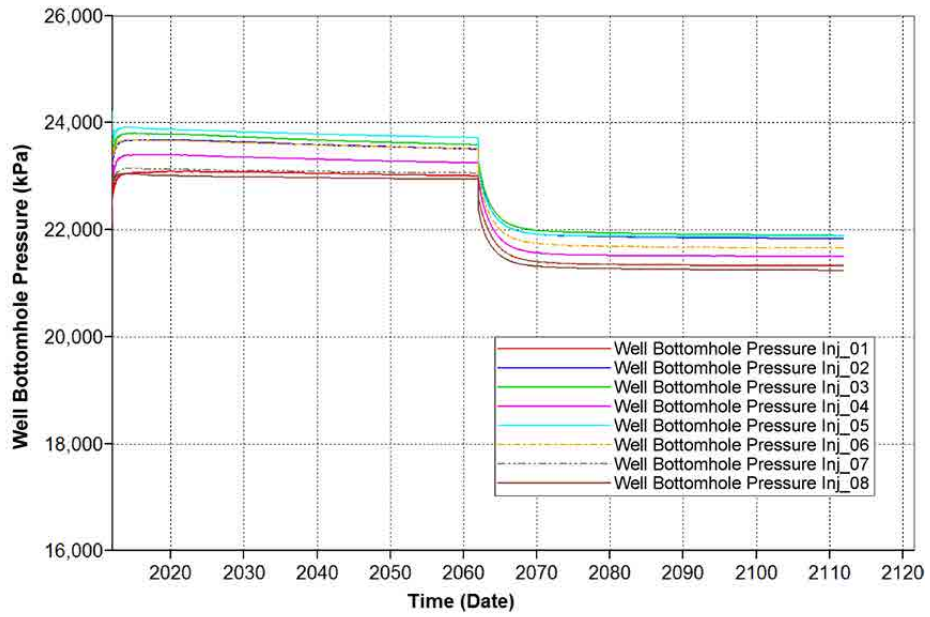


Figure E-9. Case 3 injection well BHPs.

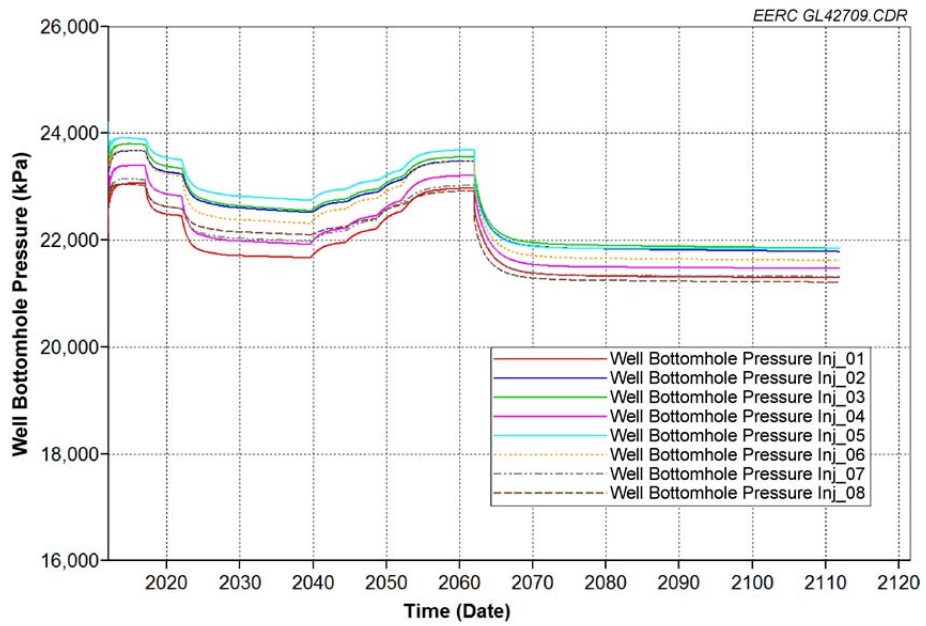


Figure E-10. Case 4 injection well BHPs.

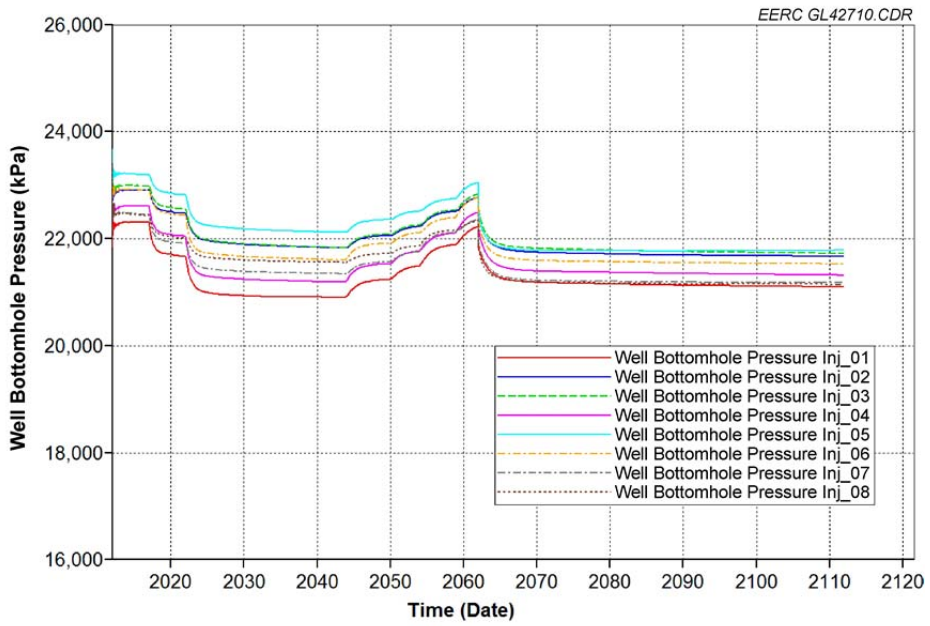


Figure E-11. Case 5 injection well BHPs.

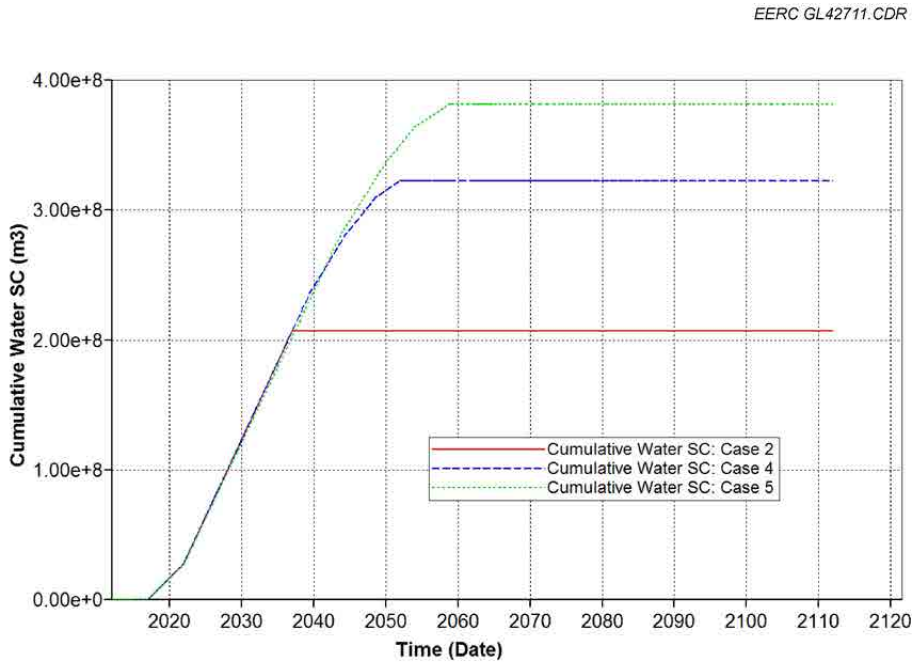


Figure E-12. Total produced water for Cases 2, 4, and 5.

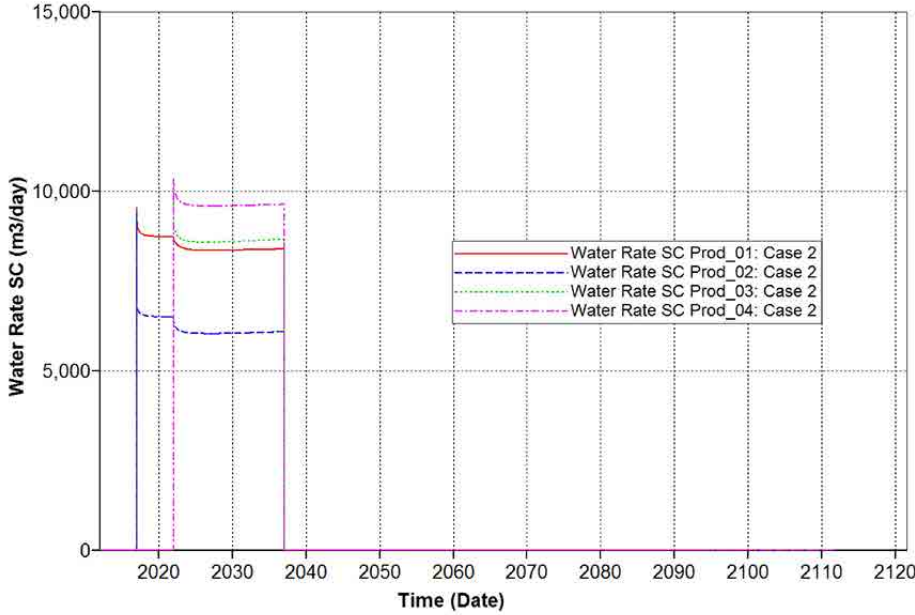


Figure E-13. Case 2 water production rates.

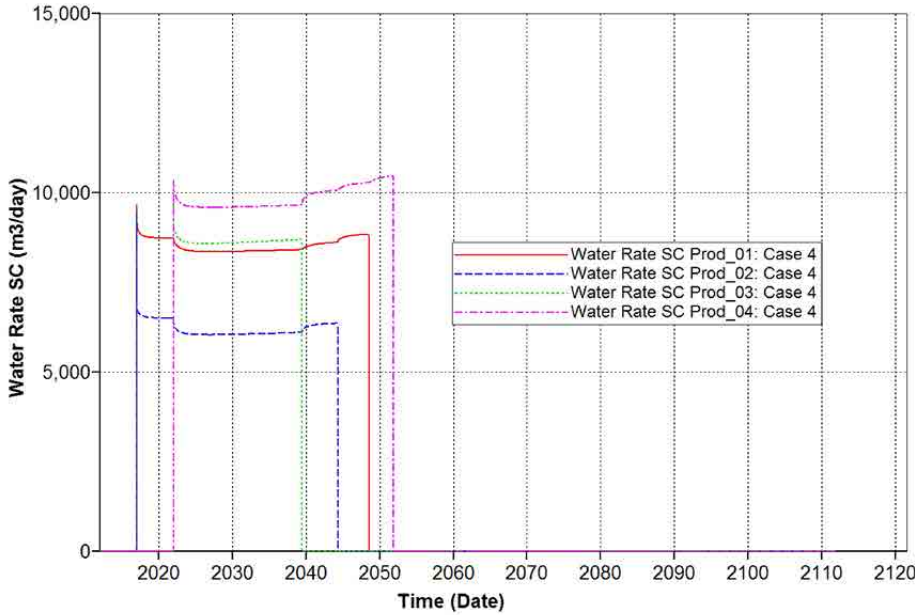


Figure E-14. Case 4 water production rates.

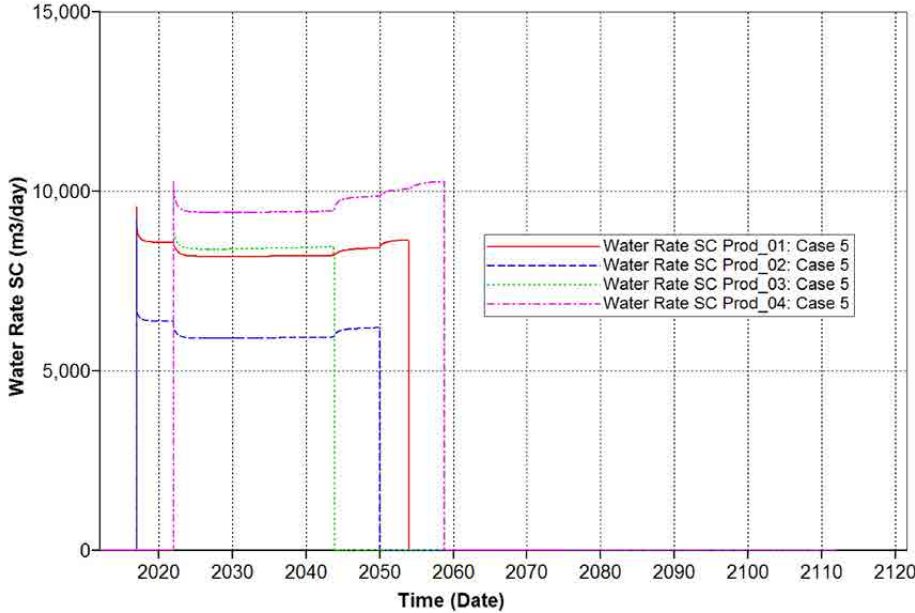


Figure E-15. Case 5 water production rates.

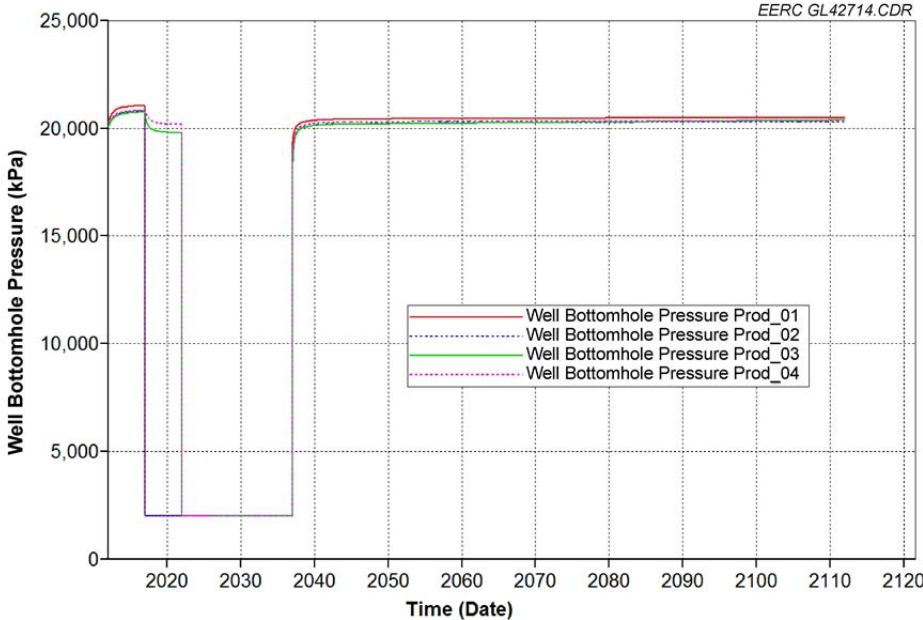


Figure E-16. Case 2 water production well BHPs.

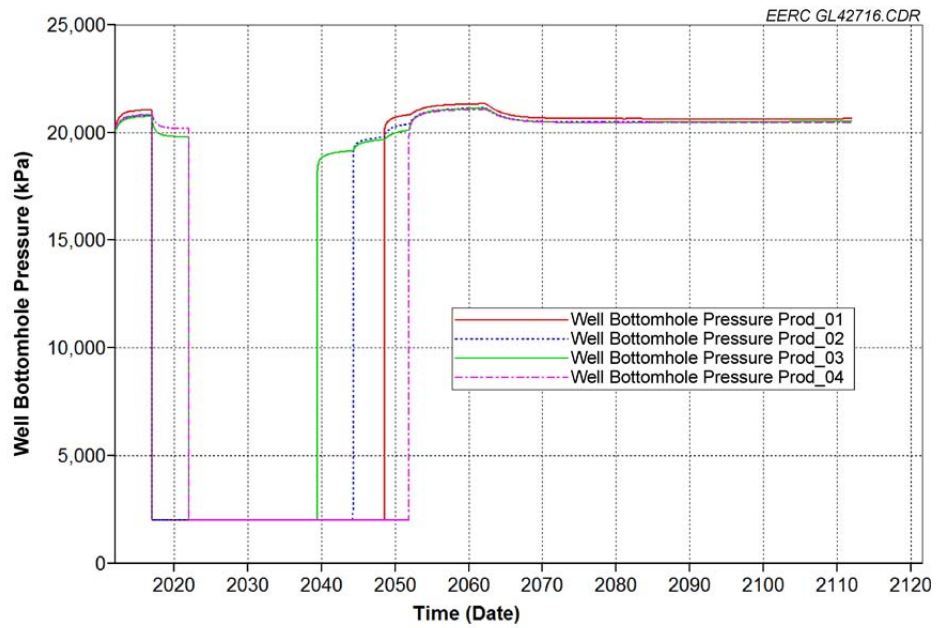


Figure E-17. Case 4 water production well BHPs.

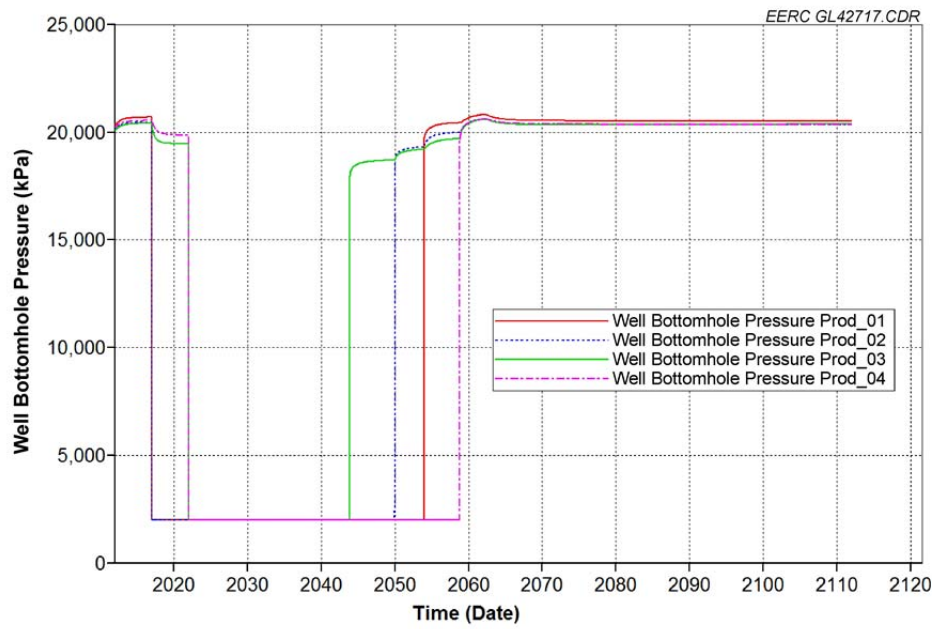


Figure E-18. Case 5 water production well BHPs.

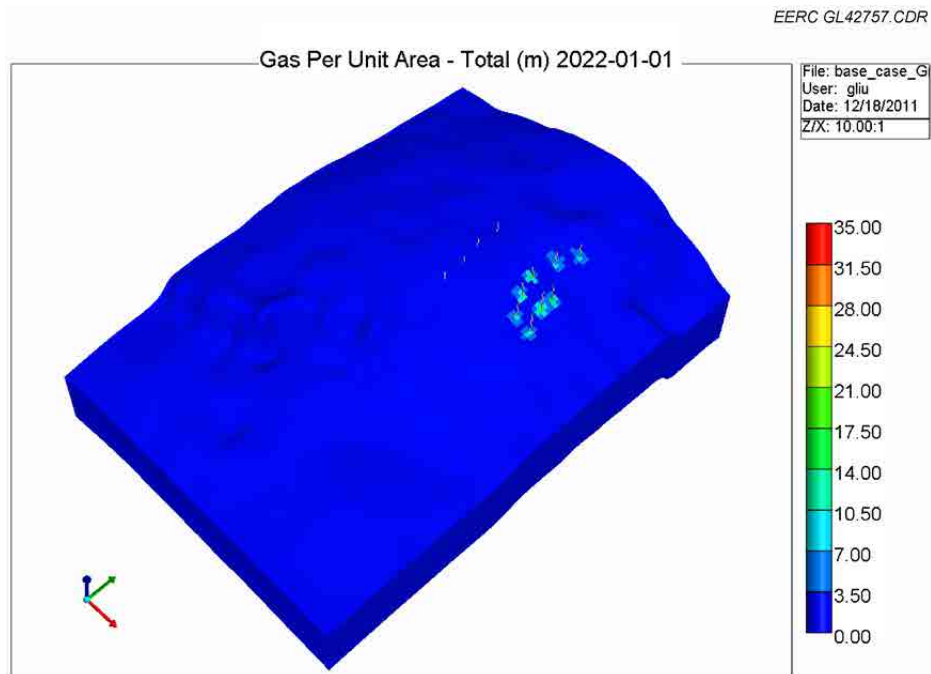


Figure E-19. 3-D view of Case 1: CO₂ plume migration for 10 years from beginning of injection.

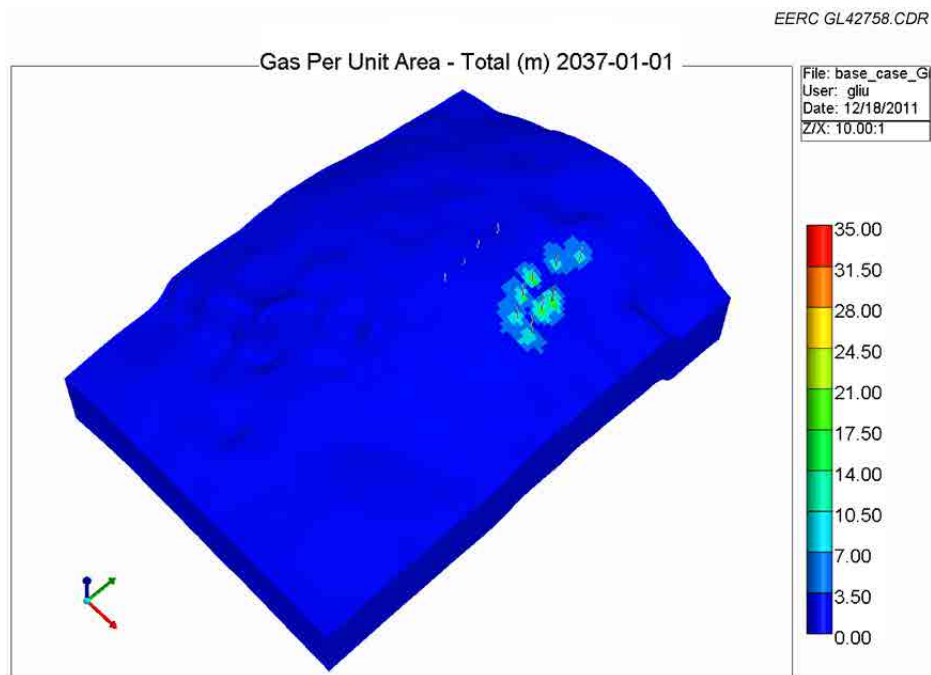


Figure E-20. 3-D view of Case 1: CO₂ plume migration for 25 years from beginning of injection.

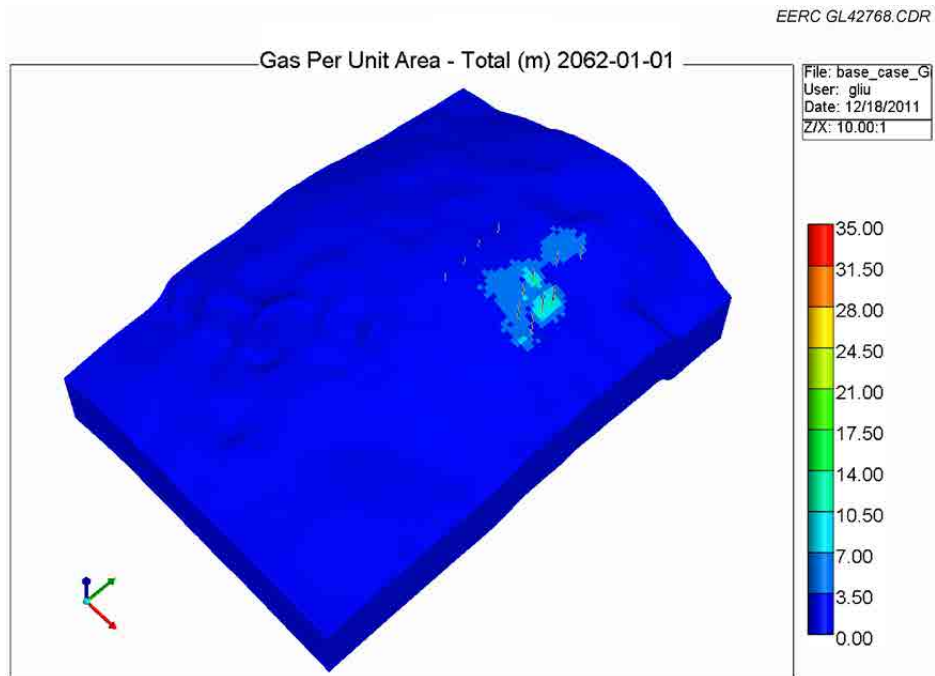


Figure E-21. 3-D view of Case 1: CO₂ plume migration for 50 years from beginning of injection.

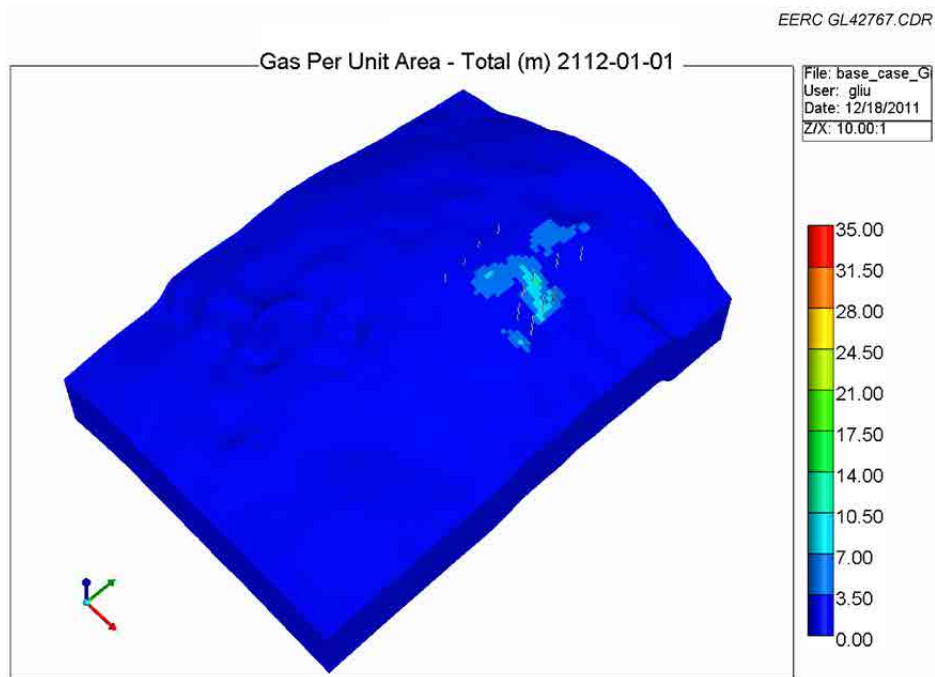


Figure E-22. 3-D view of Case 1: CO₂ plume migration for 100 years from beginning of injection.

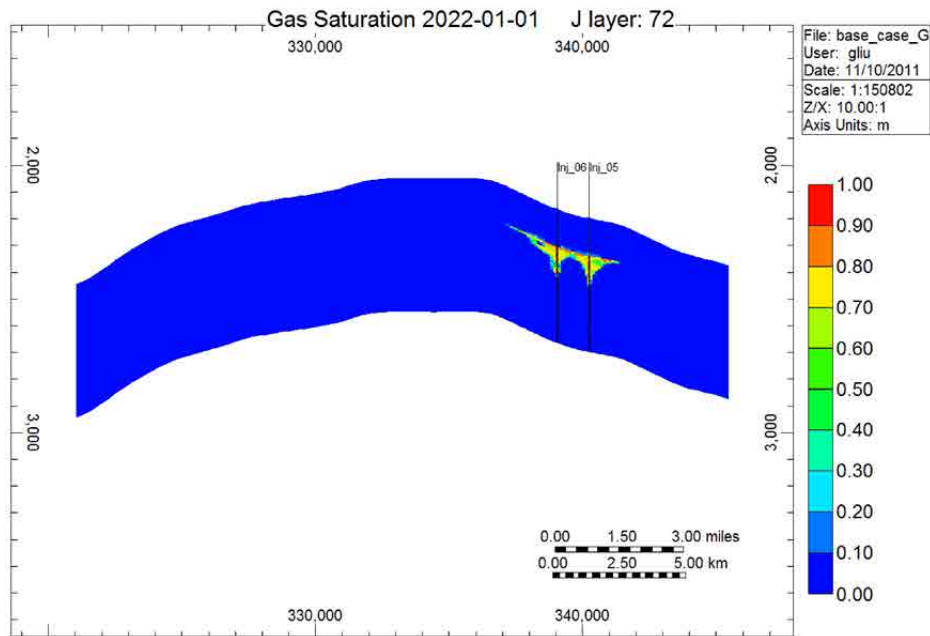


Figure E-23. Cross-sectional view of Case 1: CO₂ plume migration for 10 years from beginning of injection.

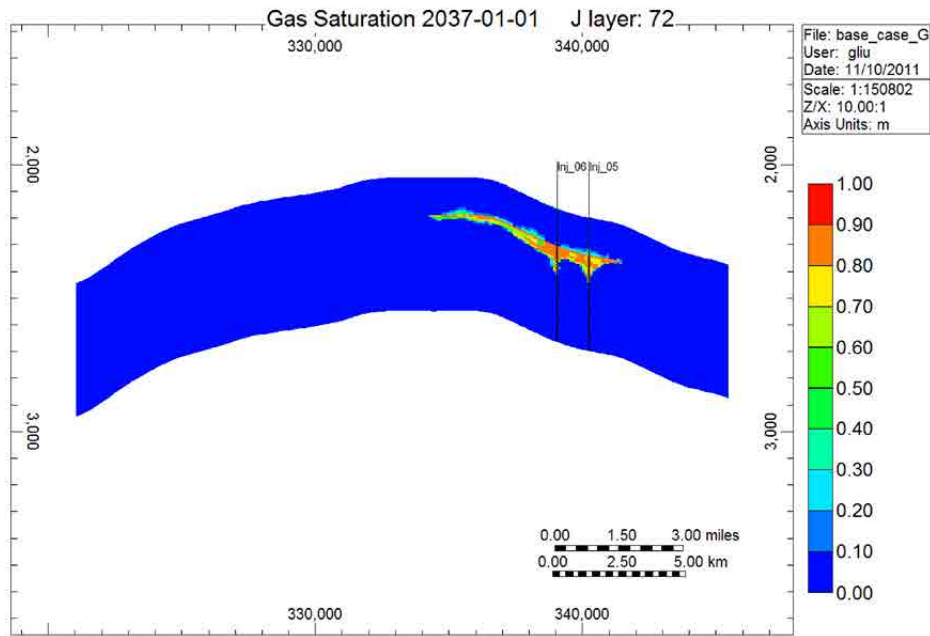


Figure E-24. Cross-sectional view of Case 1: CO₂ plume migration for 25 years from beginning of injection.

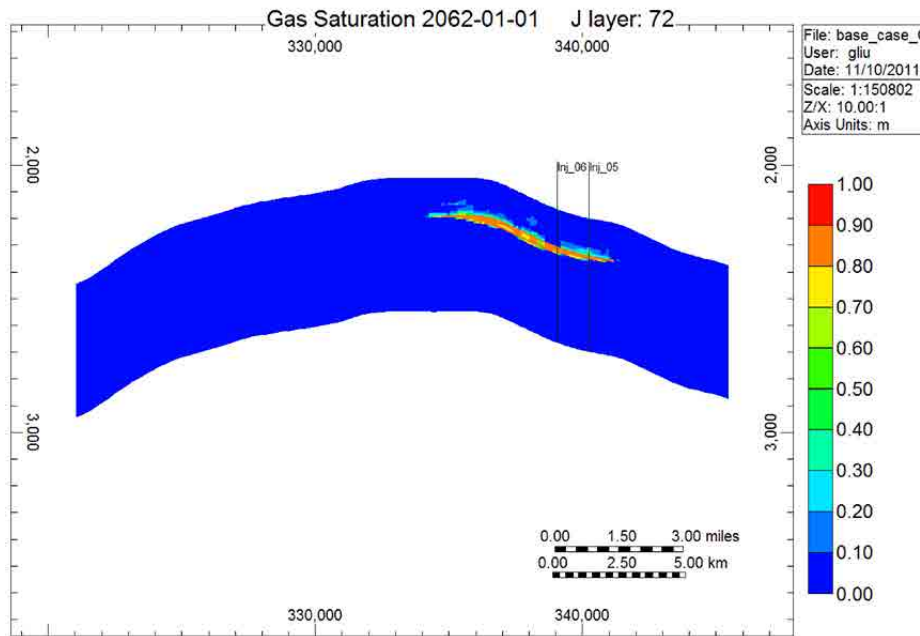


Figure E-25. Cross-sectional view of Case 1: CO₂ plume migration for 50 years from beginning of injection.

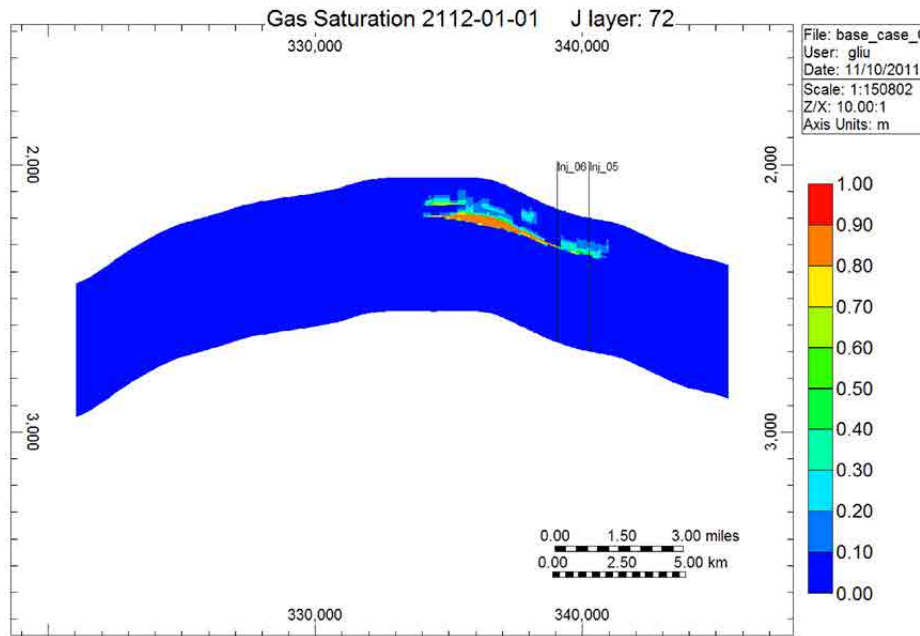


Figure E-26. Cross-sectional view of Case 1: CO₂ plume migration for 100 years from beginning of injection.

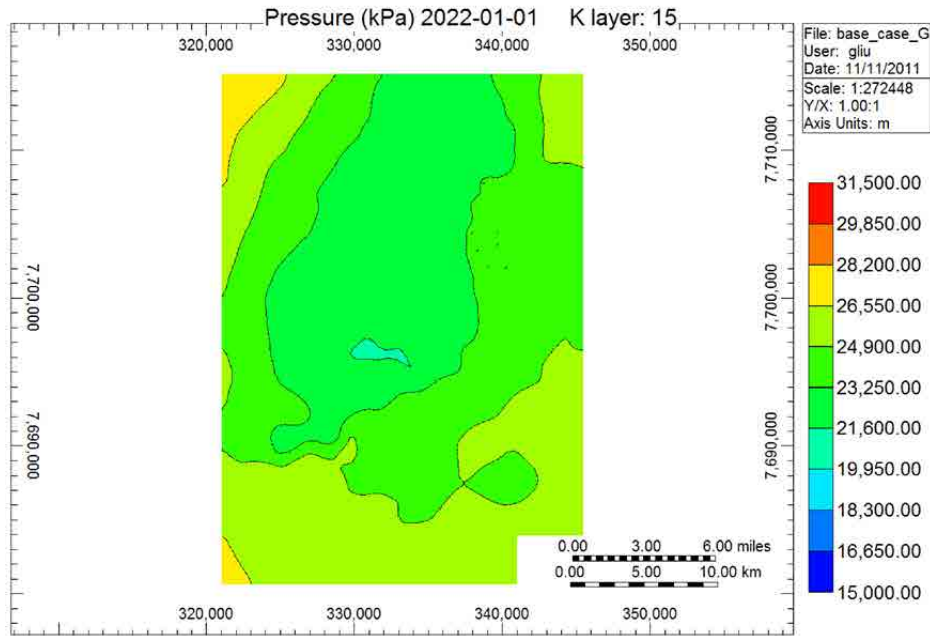


Figure E-27. Areal view of Case 1: pressure distributions for 10 years from beginning of injection.

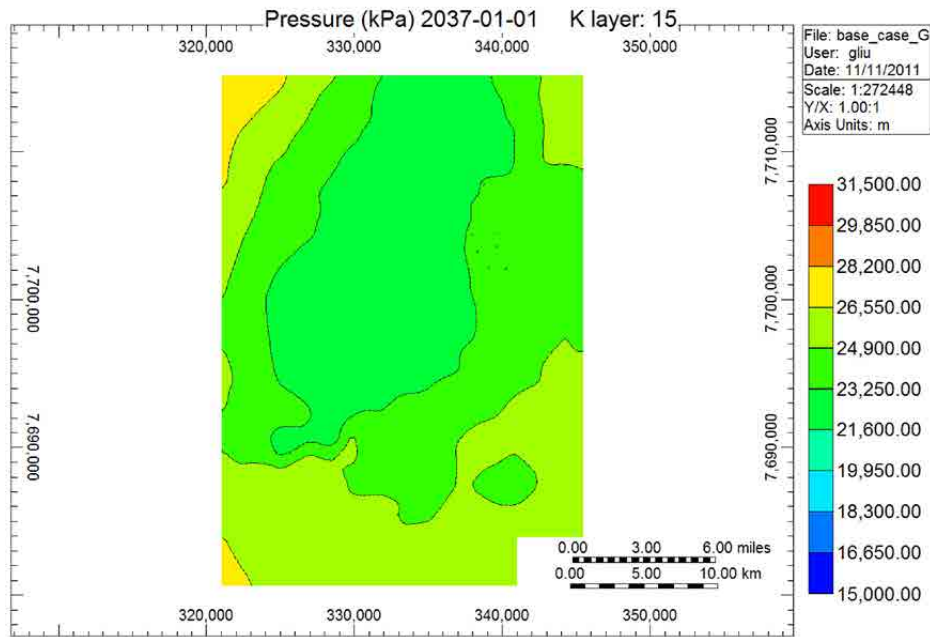


Figure E-28. Areal view of Case 1: pressure distributions for 25 years from beginning of injection.

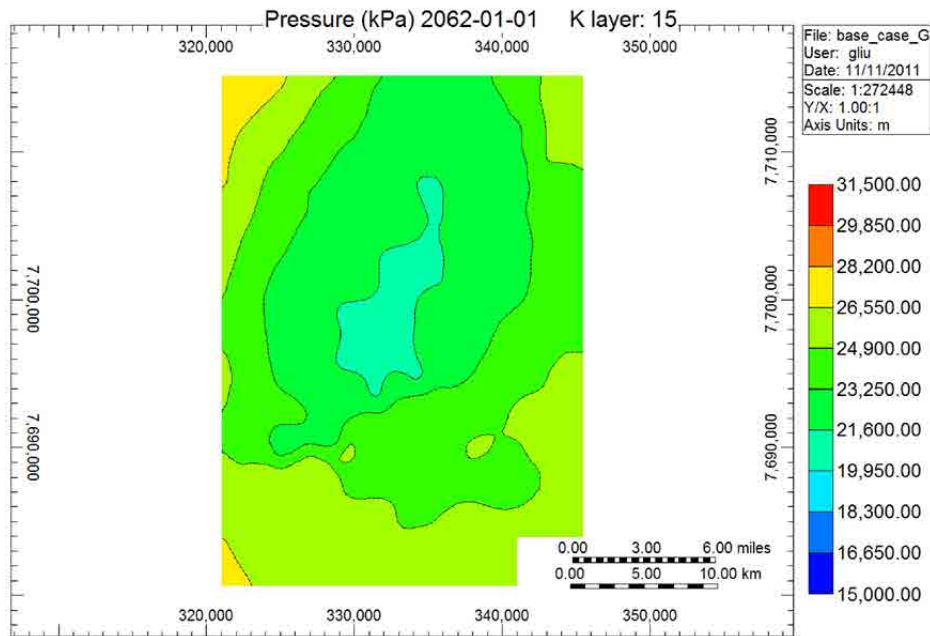


Figure E-29. Areal view of Case 1: pressure distributions for 50 years from beginning of injection.

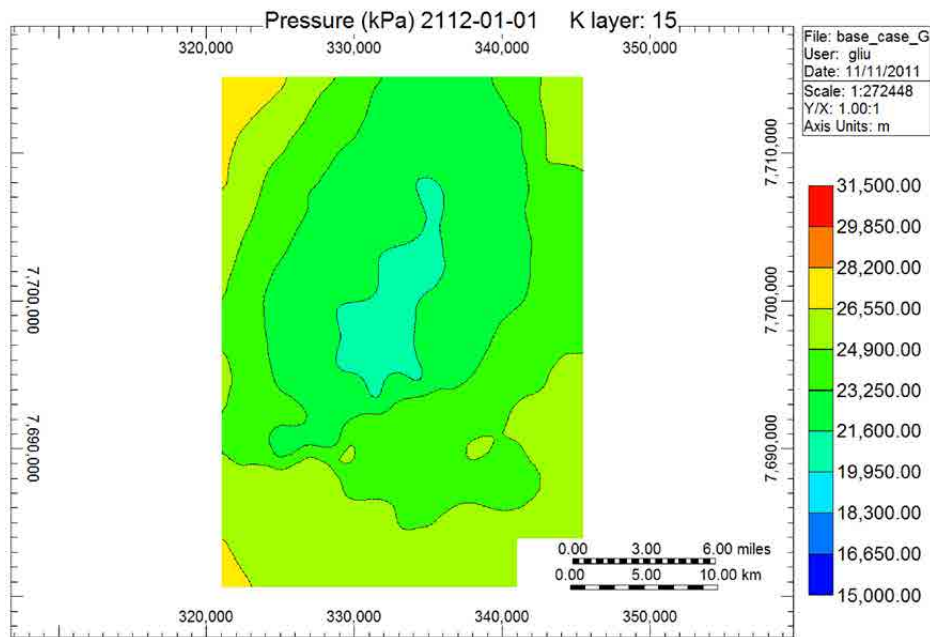


Figure E-30. Areal view of Case 1: pressure distributions for 100 years from beginning of injection.

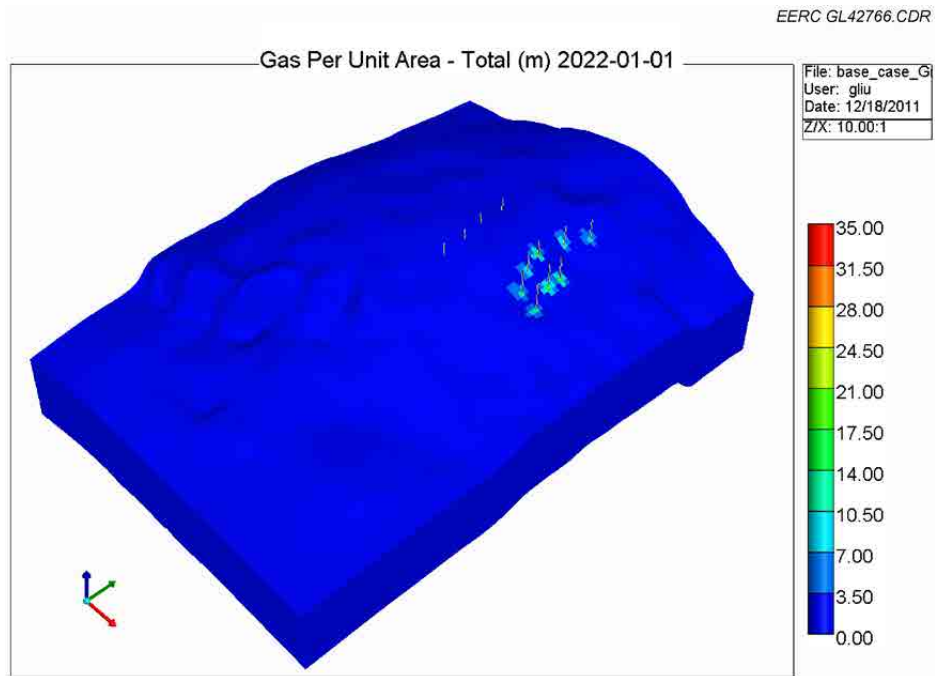


Figure E-31. 3-D view of Case 2: CO₂ plume migration for 10 years from beginning of injection.

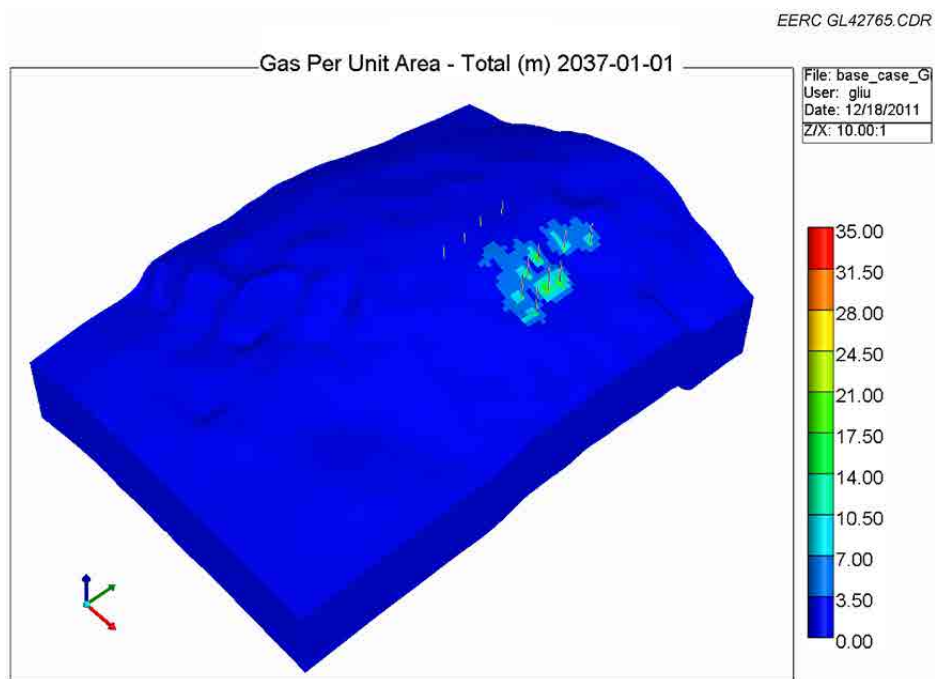


Figure E-32. 3-D view of Case 2: CO₂ plume migration for 25 years from beginning of injection.

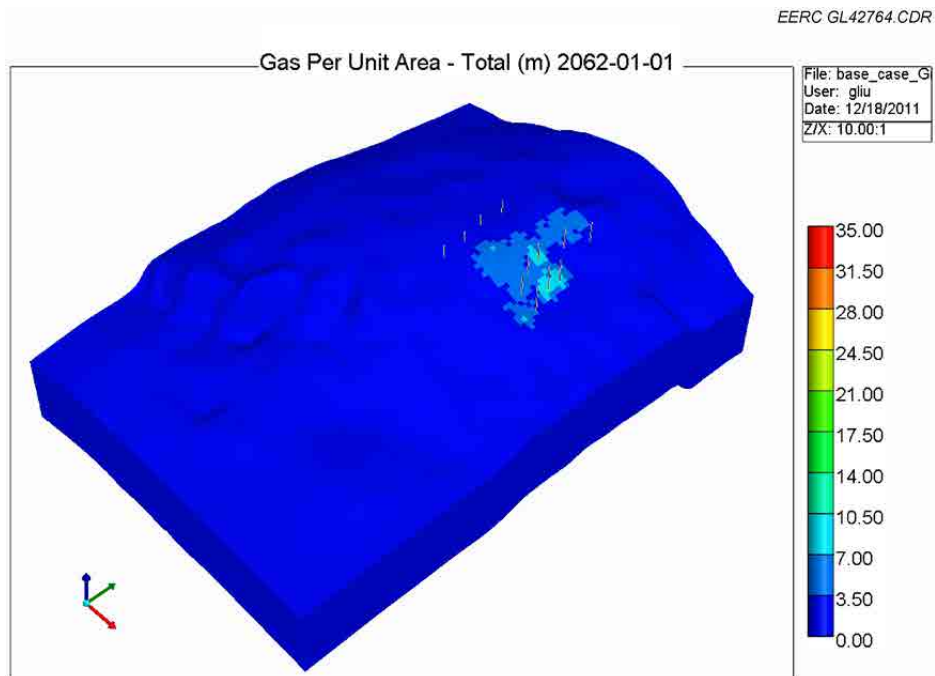


Figure E-33. 3-D view of Case 2: CO₂ plume migration for 50 years from beginning of injection.

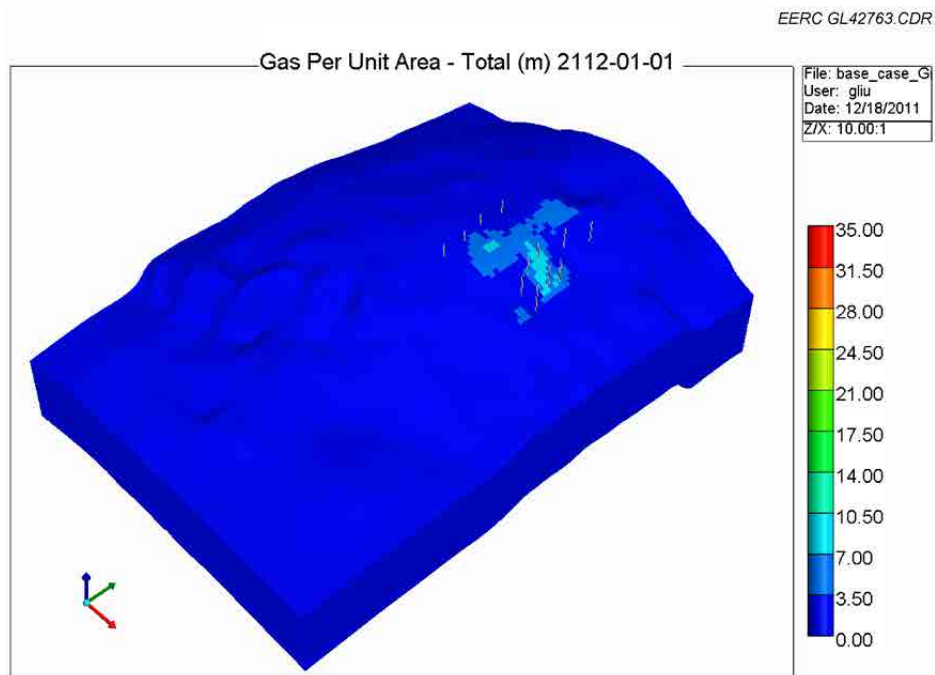


Figure E-34. 3-D view of Case 2: CO₂ plume migration for 100 years from beginning of injection.

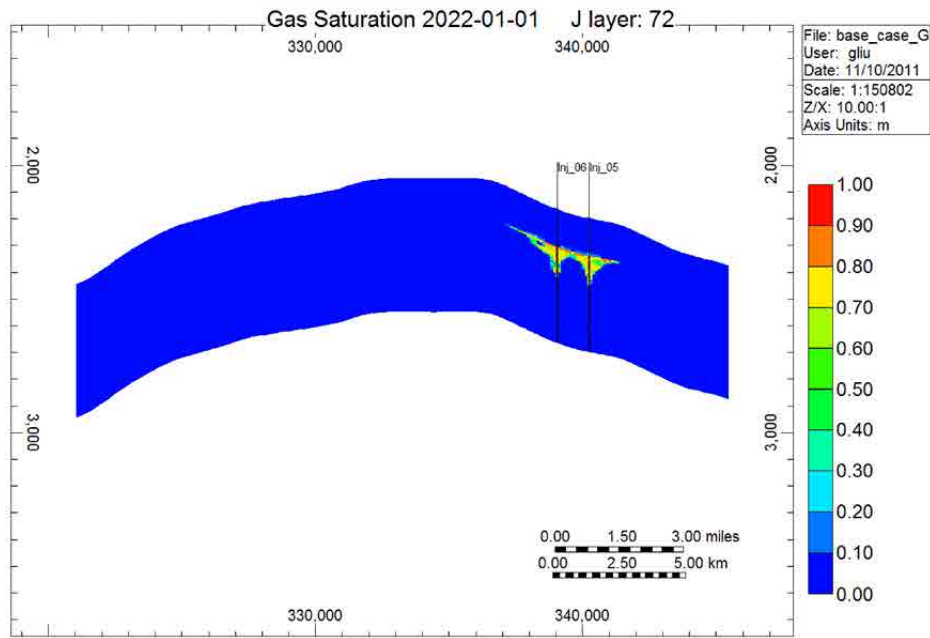


Figure E-35. Cross-sectional view of Case 2: CO₂ plume migration for 10 years from beginning of injection.

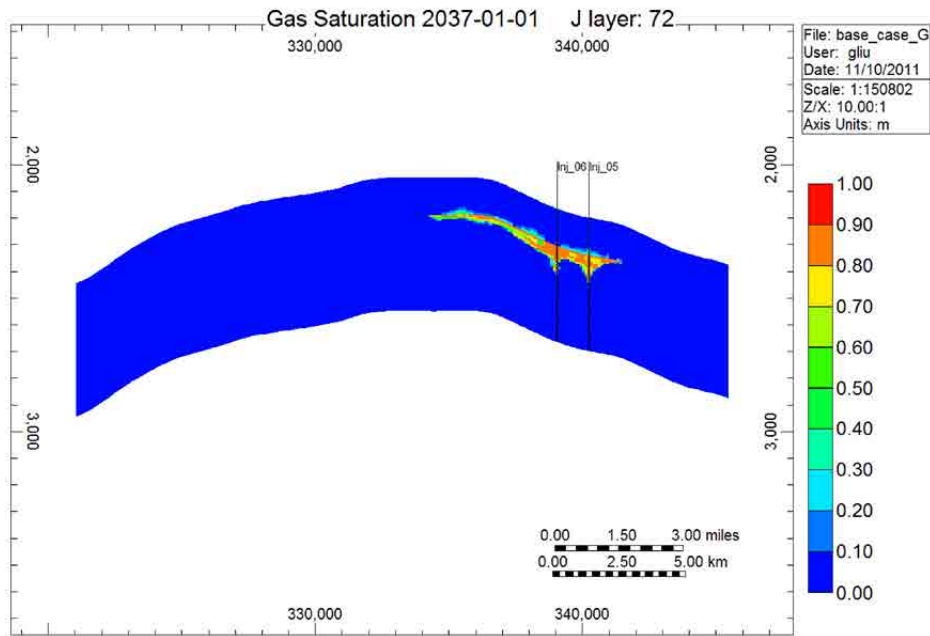


Figure E-36. Cross-sectional view of Case 2: CO₂ plume migration for 25 years from beginning of injection.

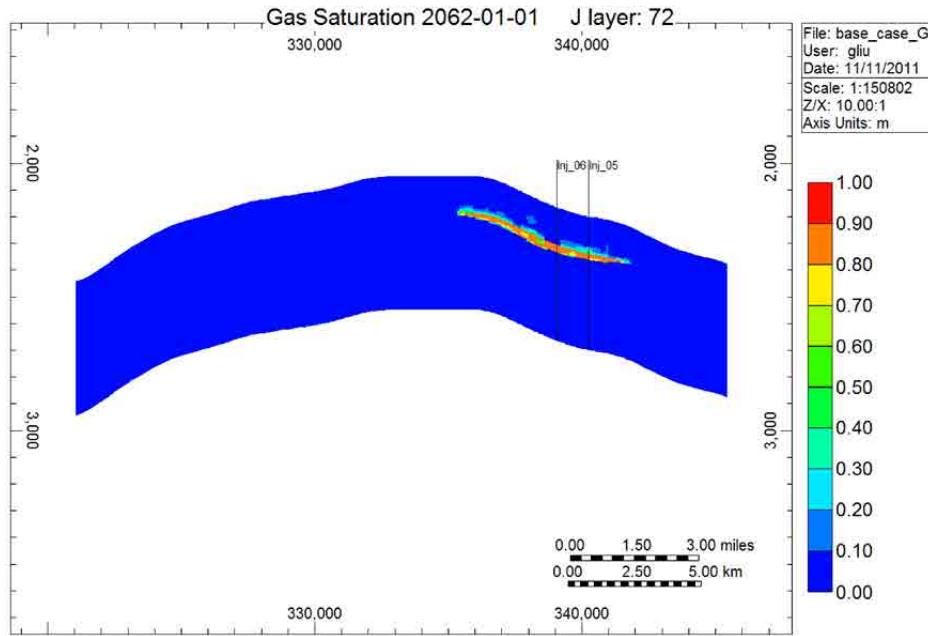


Figure E-37. Cross-sectional view of Case 1: CO₂ plume migration for 50 years from beginning of injection.

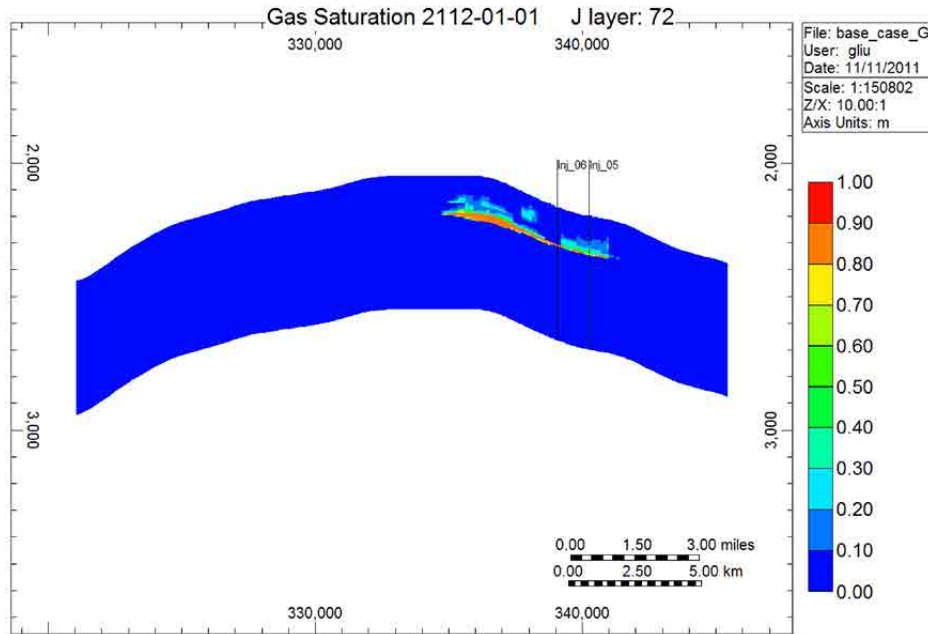


Figure E-38. Cross-sectional view of Case 1: CO₂ plume migration for 100 years from beginning of injection.

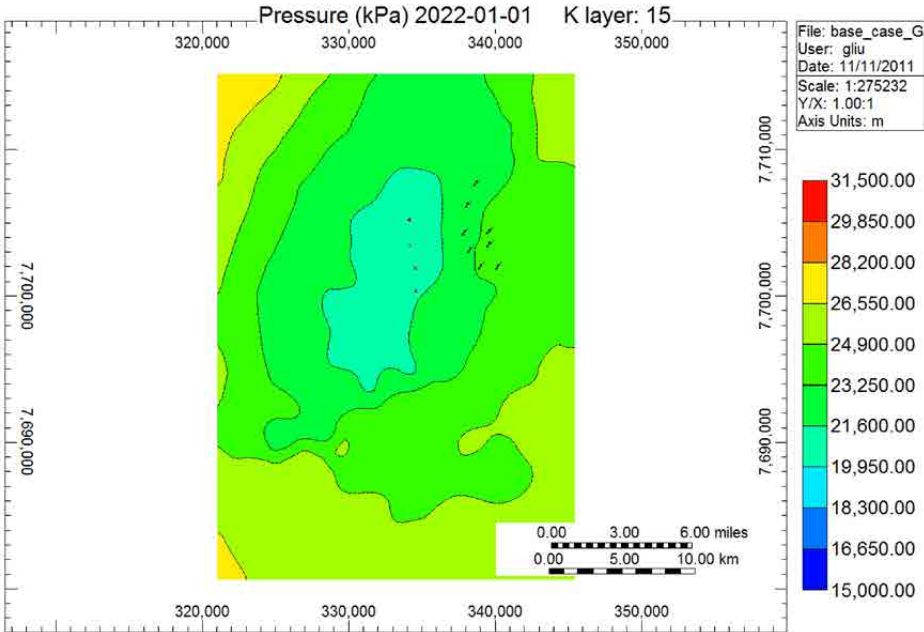


Figure E-39. Areal view of Case 2: pressure distributions for 10 years from beginning of injection.

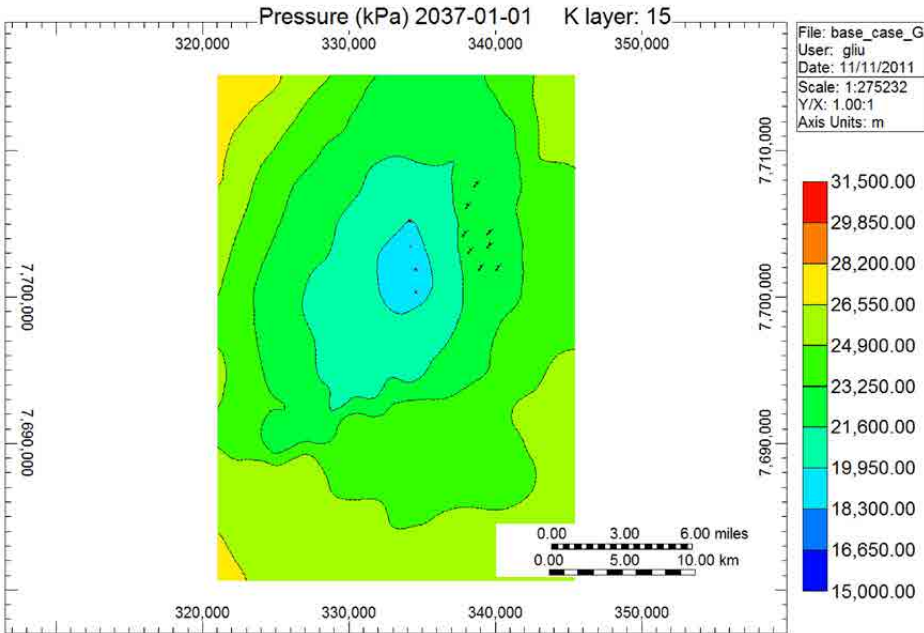


Figure E-40. Areal view of Case 2: pressure distributions for 25 years from beginning of injection.

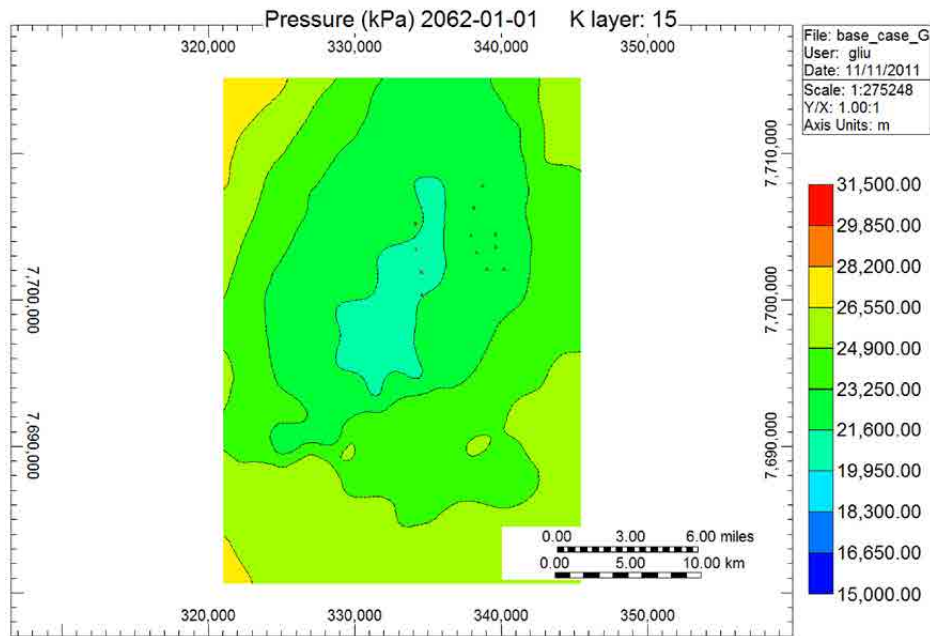


Figure E-41. Areal view of Case 2: pressure distributions for 50 years from beginning of injection.

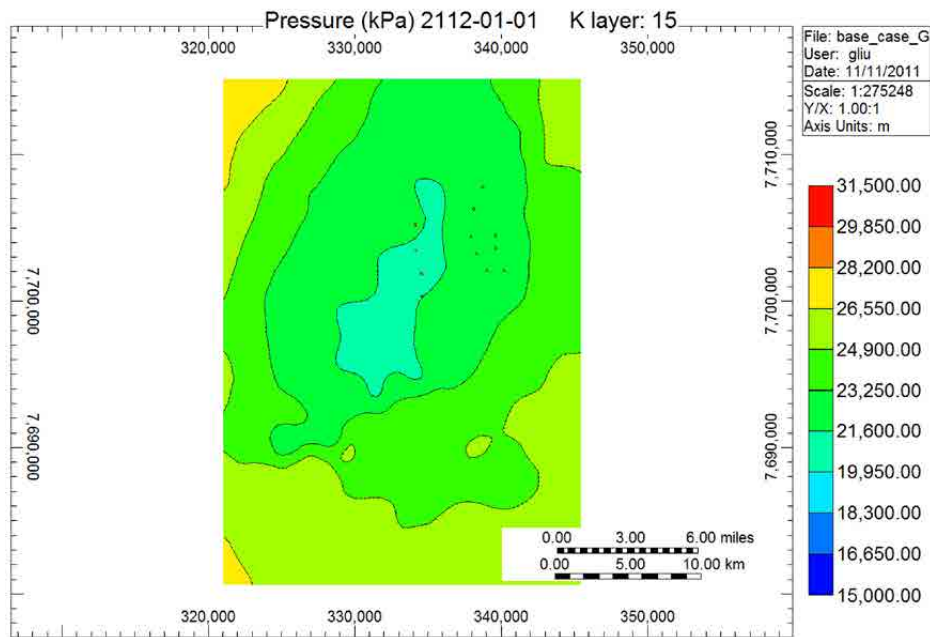


Figure E-42. Areal view of Case 2: pressure distributions for 100 years from beginning of injection.

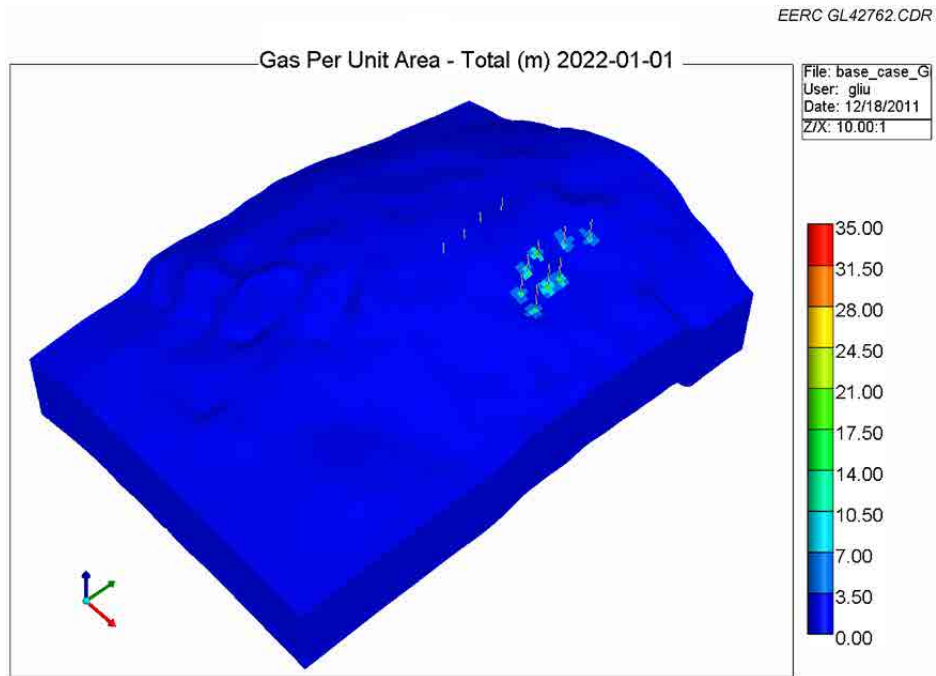


Figure E-43. 3-D view of Case 3: CO₂ plume migration for 10 years from beginning of injection.

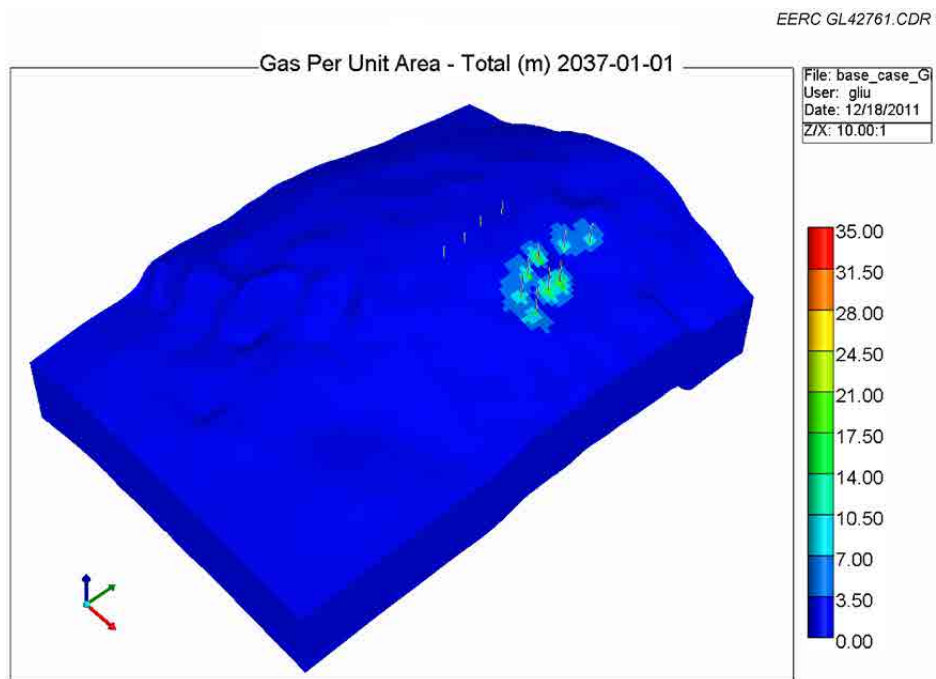


Figure E-44. 3-D view of Case 3: CO₂ plume migration for 25 years from beginning of injection.

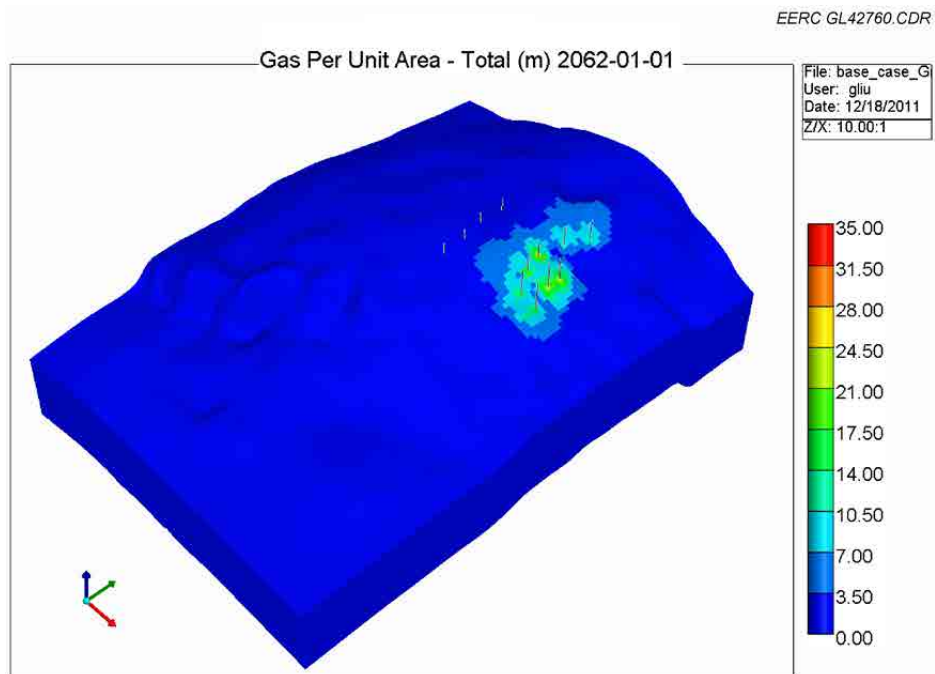


Figure E-45. 3-D view of Case 3: CO₂ plume migration for 50 years from beginning of injection.

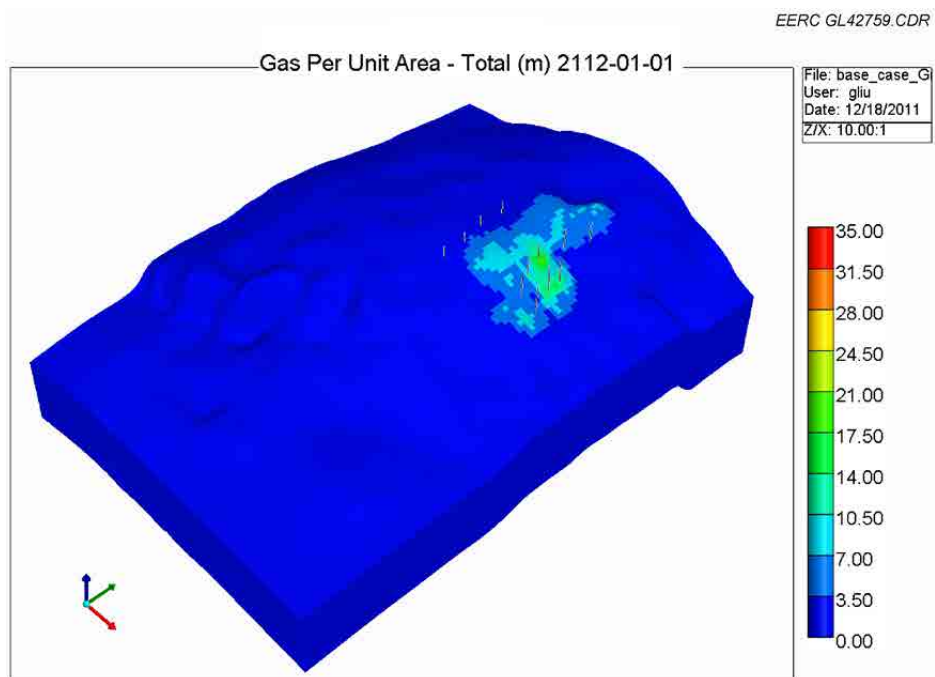


Figure E-46. 3-D view of Case 3: CO₂ plume migration for 100 years from beginning of injection.

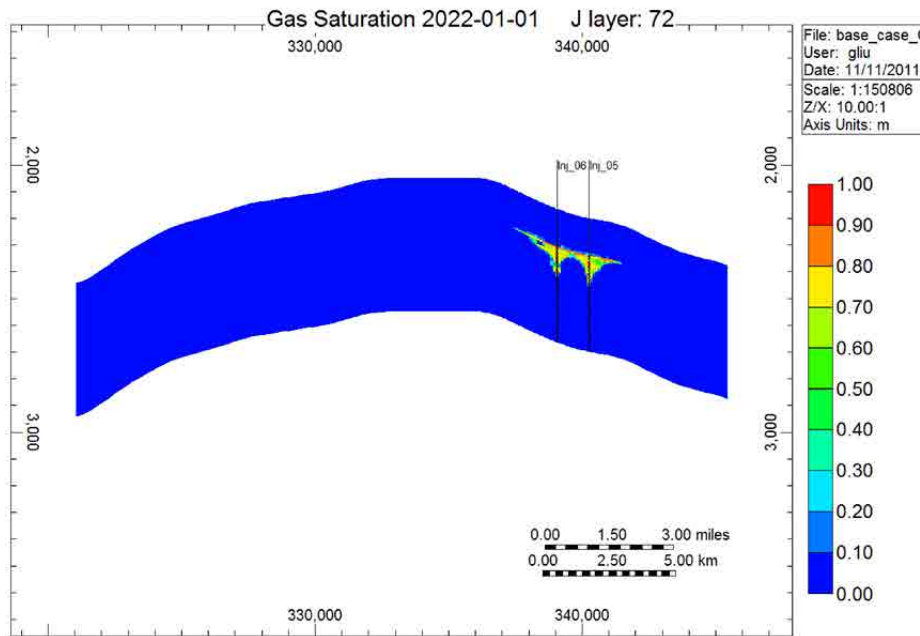


Figure E-47. Cross-sectional view of Case 3: CO₂ plume migration for 10 years from beginning of injection.

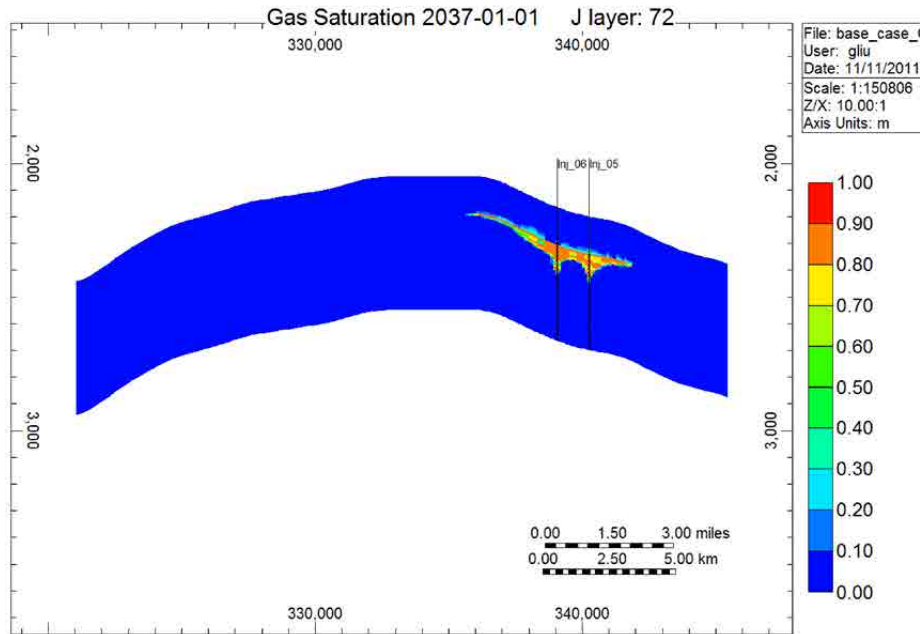


Figure E-48. Cross-sectional view of Case 3: CO₂ plume migration for 25 years from beginning of injection.

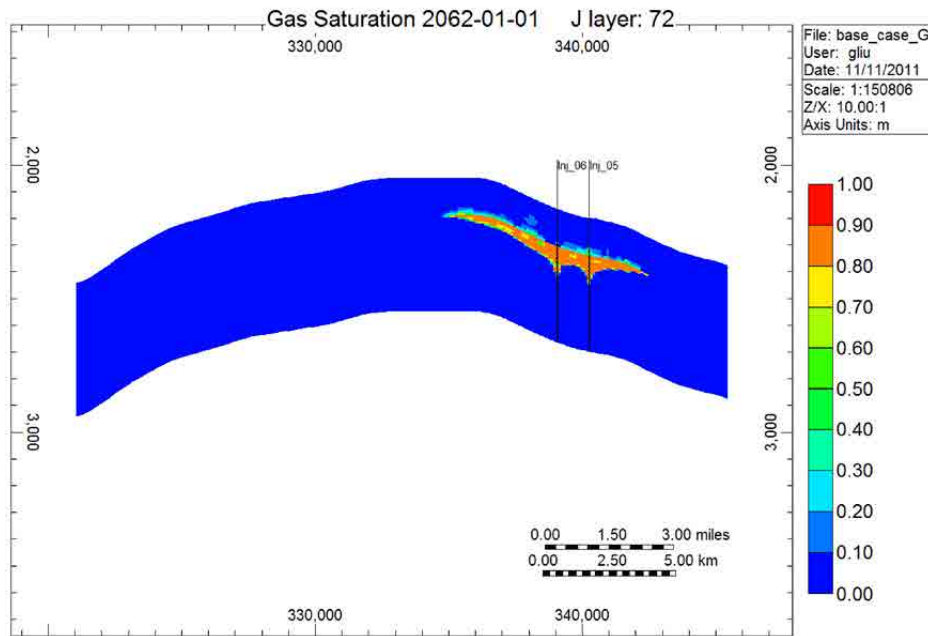


Figure E-49. Cross-sectional view of Case 3: CO₂ plume migration for 50 years from beginning of injection.

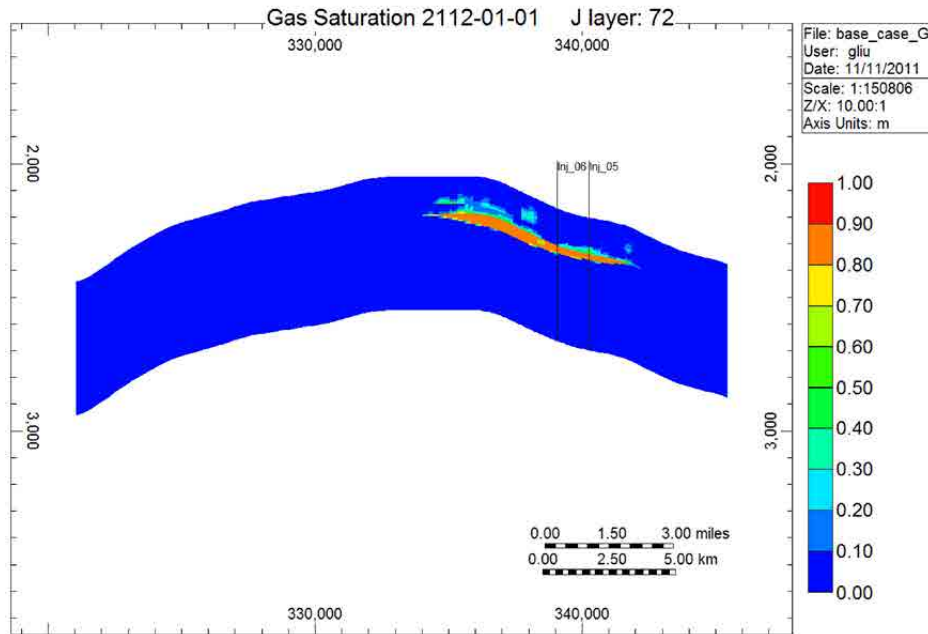


Figure E-50. Cross-sectional view of Case 3: CO₂ plume migration for 100 years from beginning of injection.

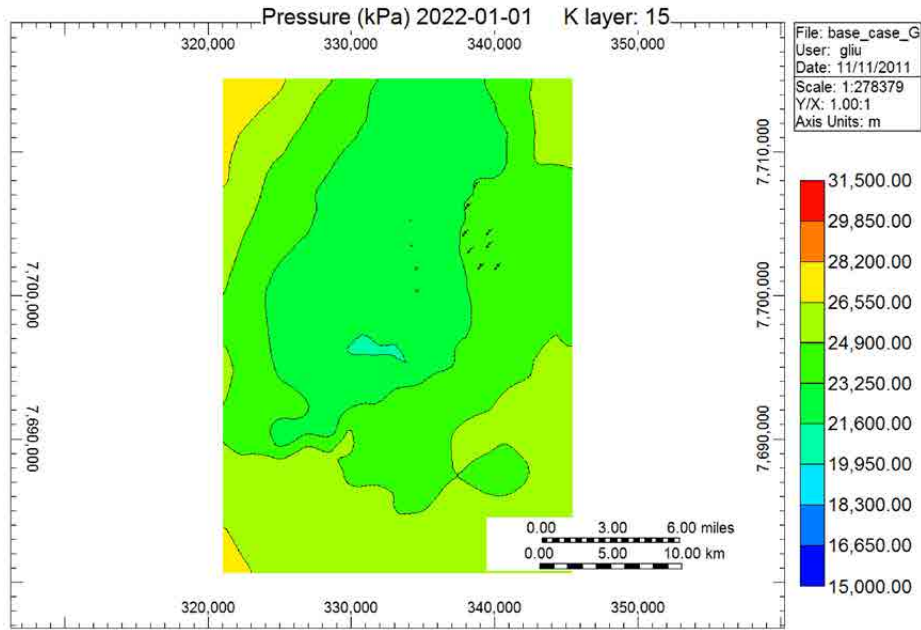


Figure E-51. Areal view of Case 3: pressure distributions for 10 years from beginning of injection.

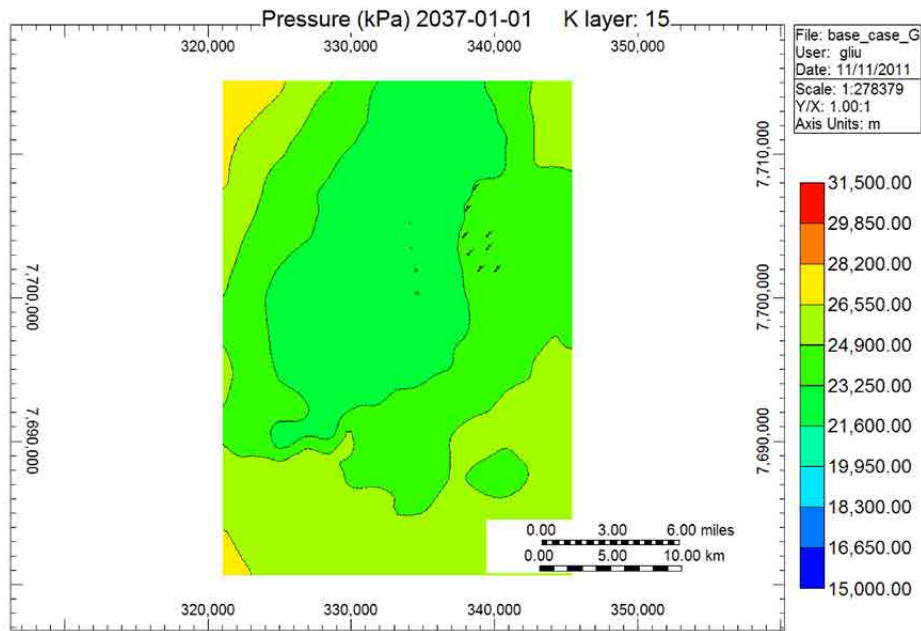


Figure E-52. Areal view of Case 3: pressure distributions for 25 years from beginning of injection.

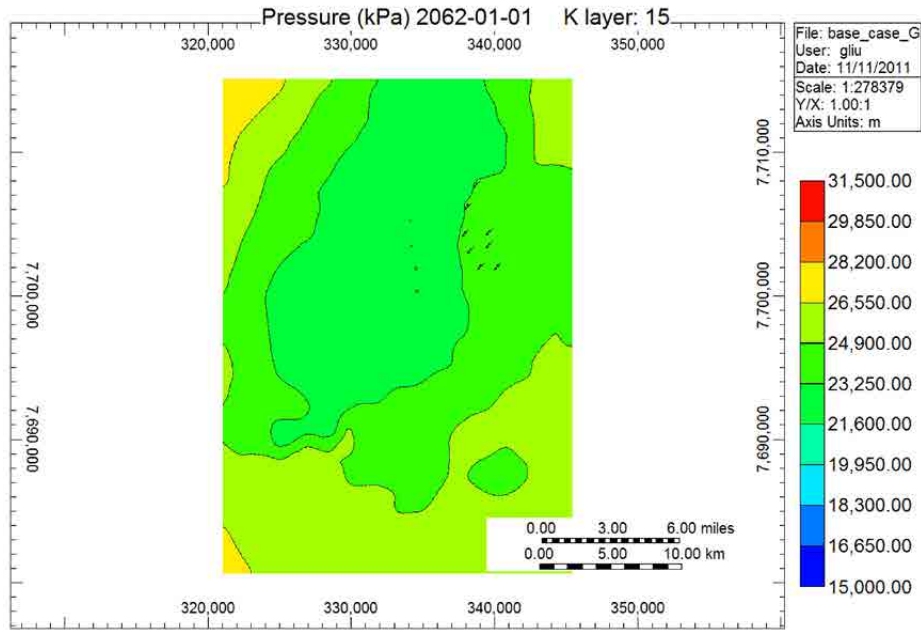


Figure E-53. Areal view of Case 3: pressure distributions for 50 years from beginning of injection.

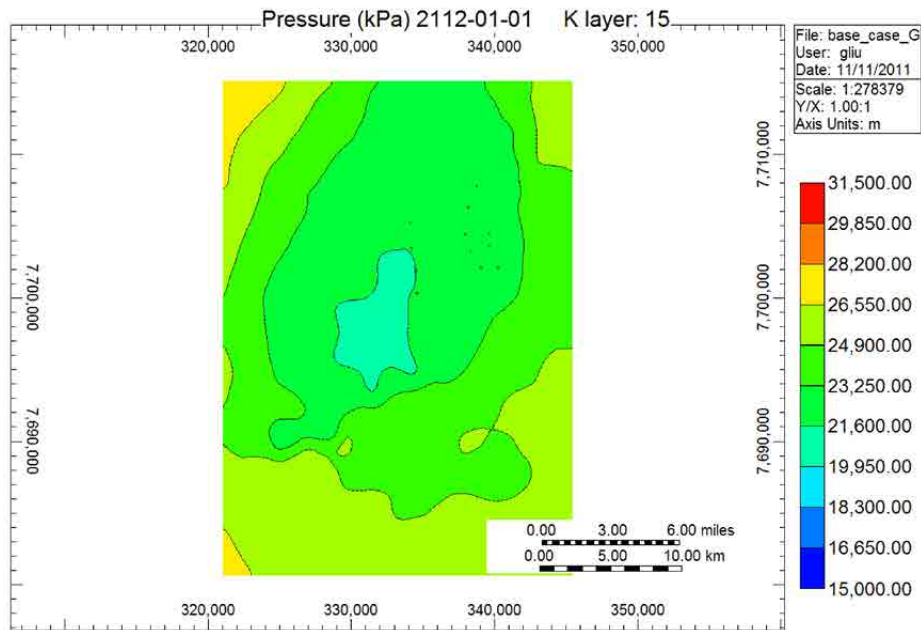


Figure E-54. Areal view of Case 3: pressure distributions for 100 years from beginning of injection.

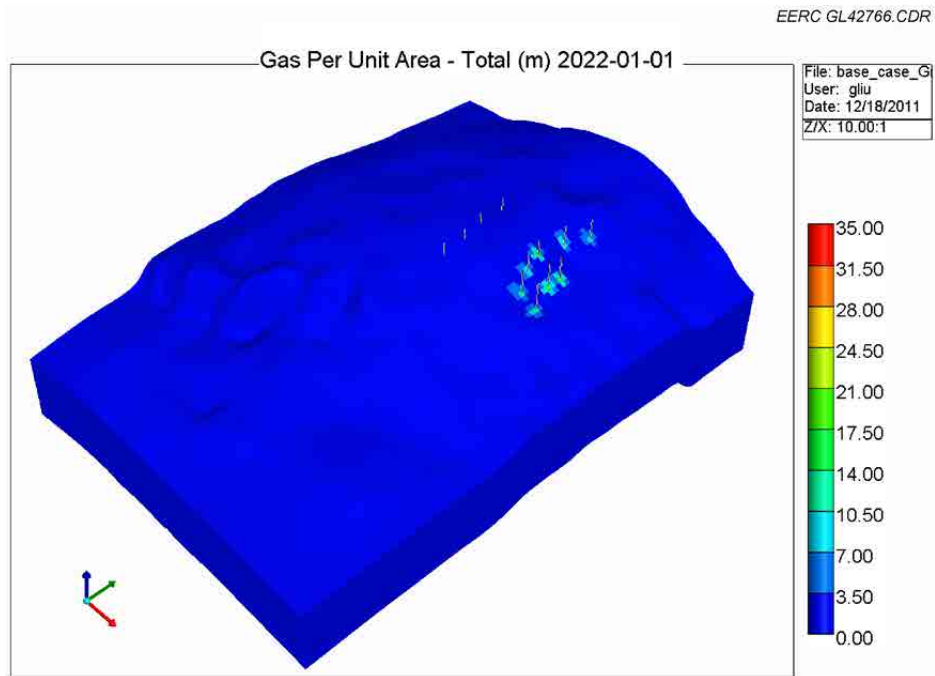


Figure E-55. 3-D view of Case 4: CO₂ plume migration for 10 years from beginning of injection.

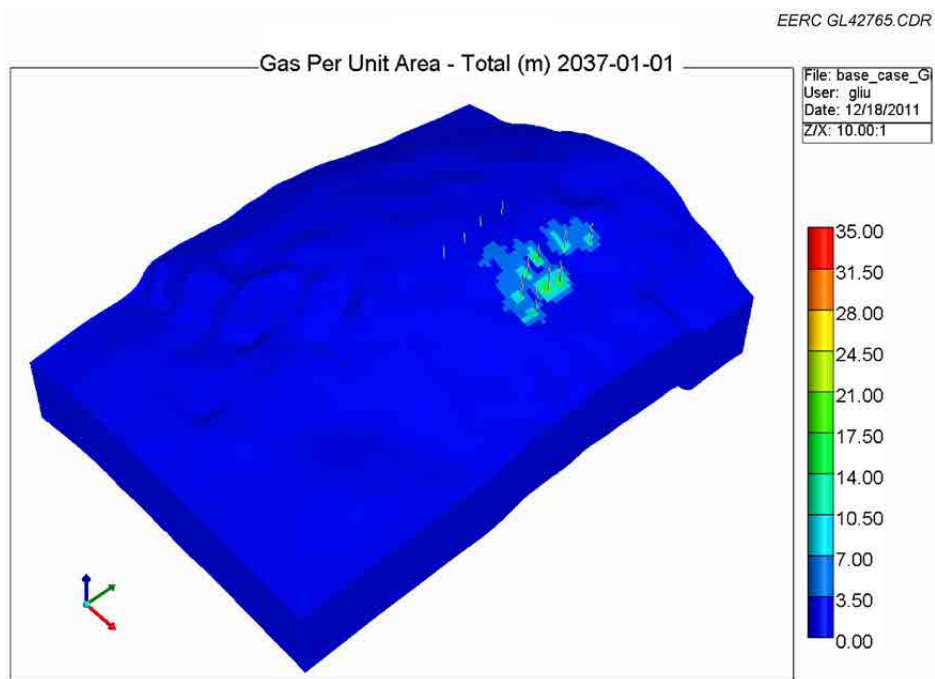


Figure E-56. 3-D view of Case 4: CO₂ plume migration for 25 years from beginning of injection.

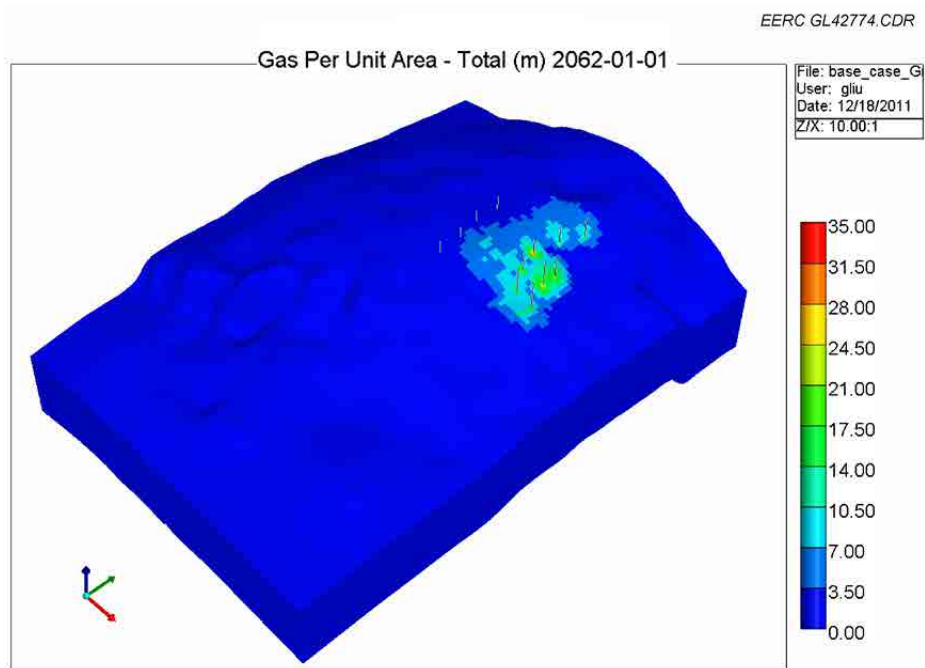


Figure E-57. 3-D view of Case 4: CO₂ plume migration for 50 years from beginning of injection.

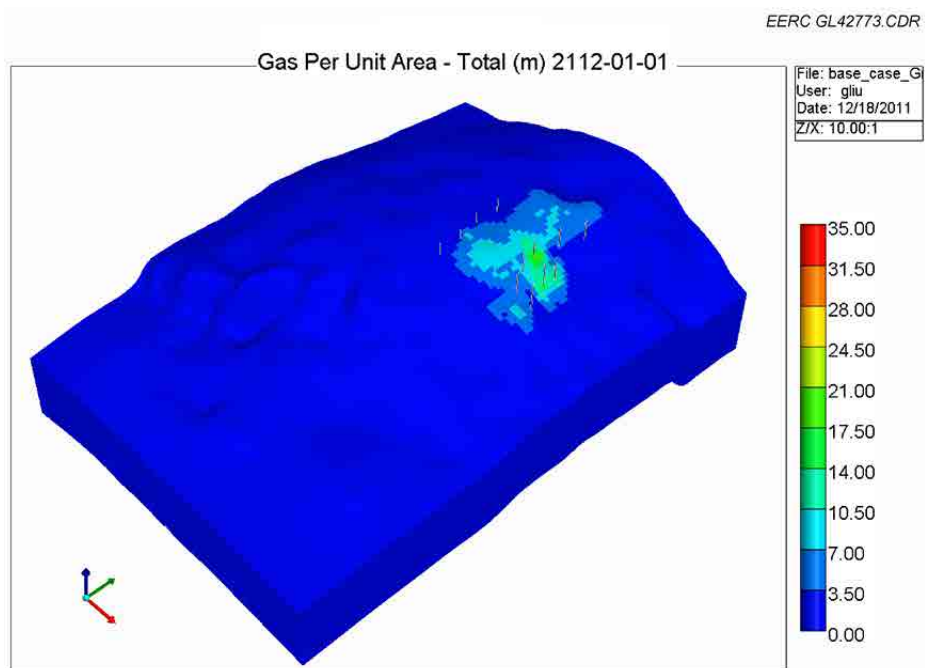


Figure E-58. 3-D view of Case 4: CO₂ plume migration for 100 years from beginning of injection.

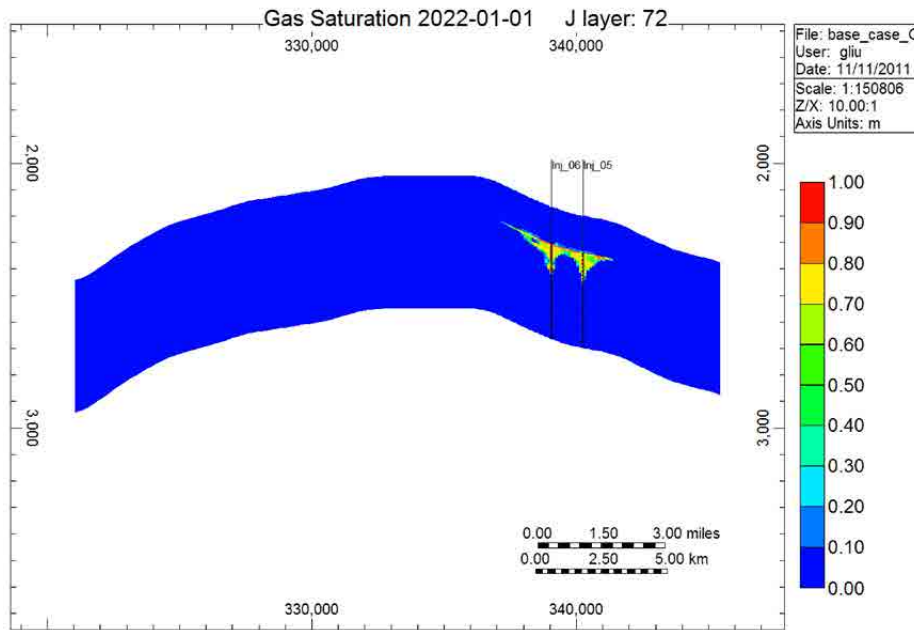


Figure E-59. Cross-sectional view of Case 4: CO₂ plume migration for 10 years from beginning of injection.

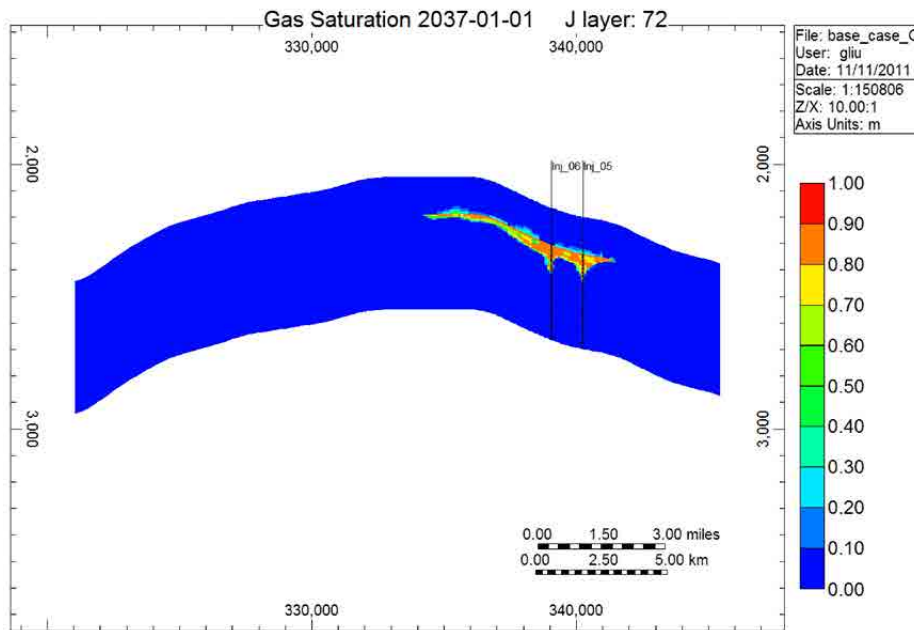


Figure E-60. Cross-sectional view of Case 4: CO₂ plume migration for 25 years from beginning of injection.

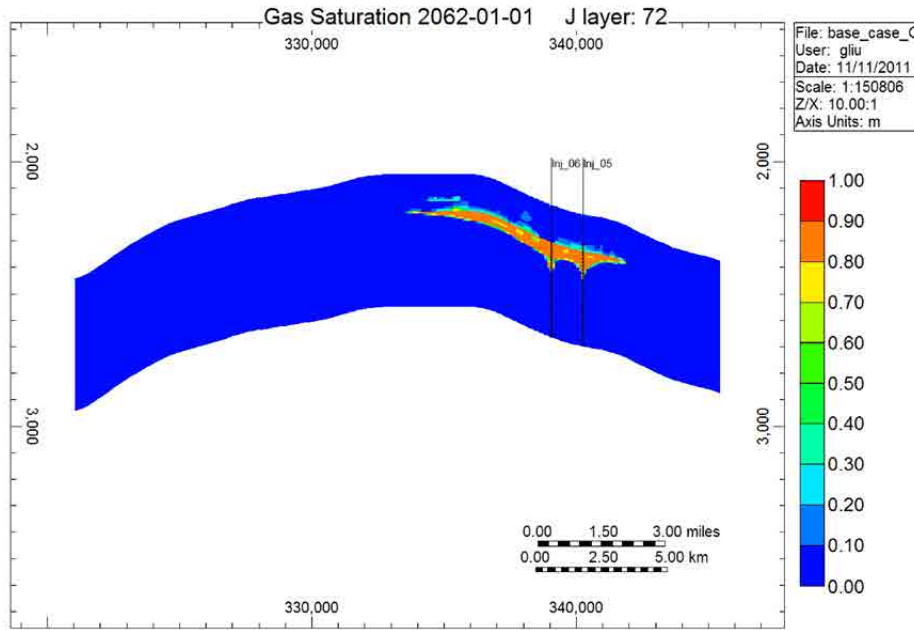


Figure E-61. Cross-sectional view of Case 4: CO₂ plume migration for 50 years from beginning of injection.

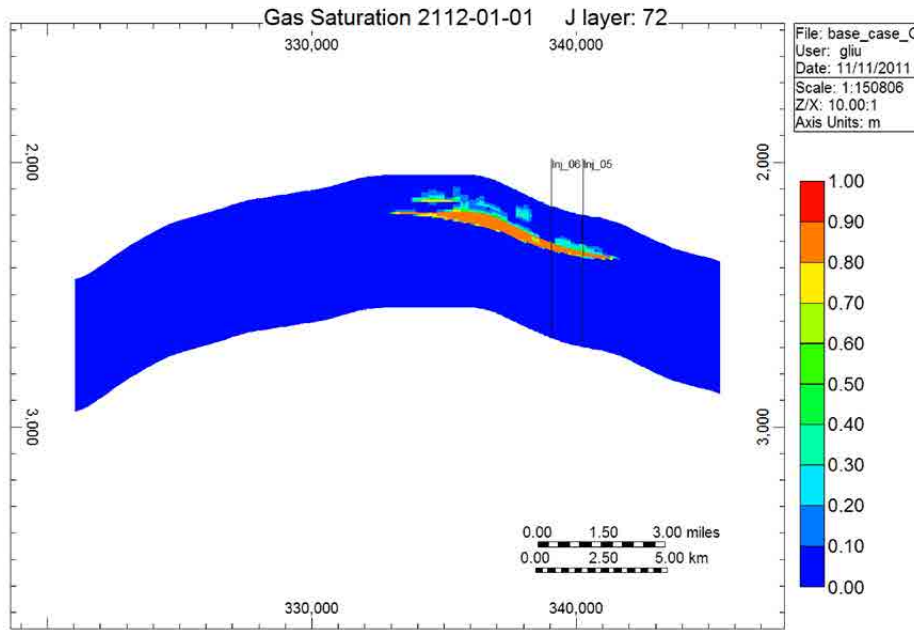


Figure E-62. Cross-sectional view of Case 4: CO₂ plume migration for 100 years from beginning of injection.

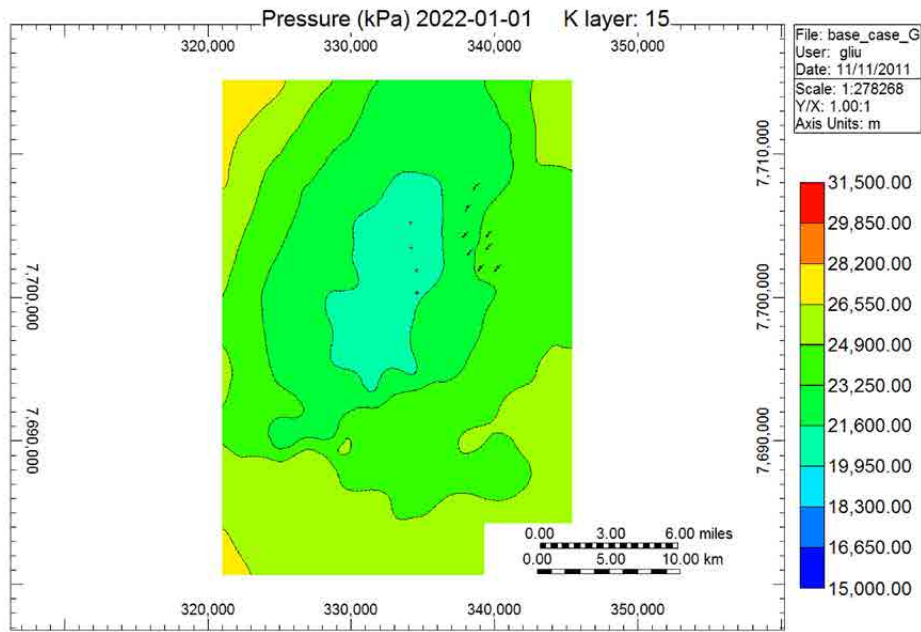


Figure E-63. Areal view of Case 4: pressure distributions for 10 years from beginning of injection.

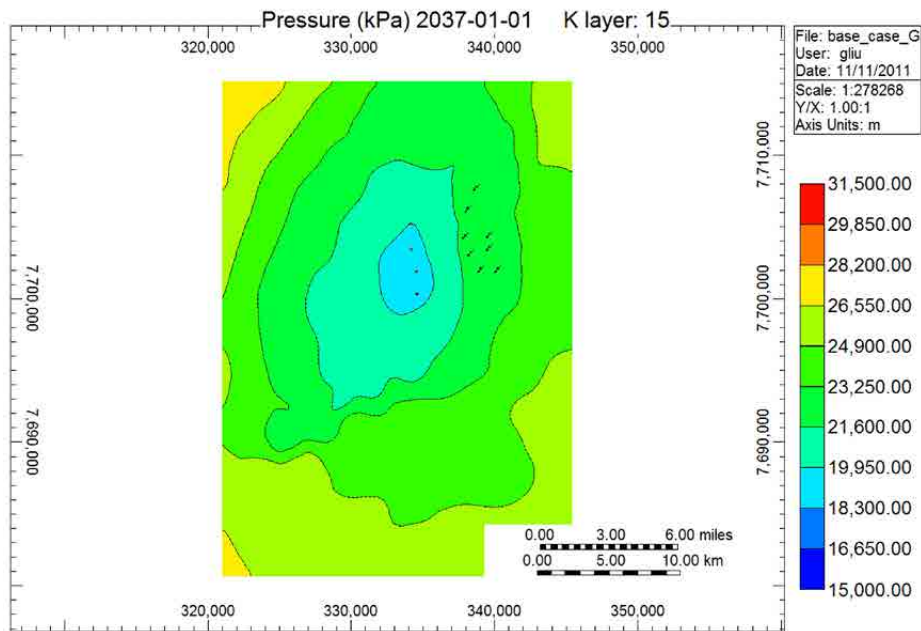


Figure E-64. Areal view of Case 4: pressure distributions for 25 years from beginning of injection.

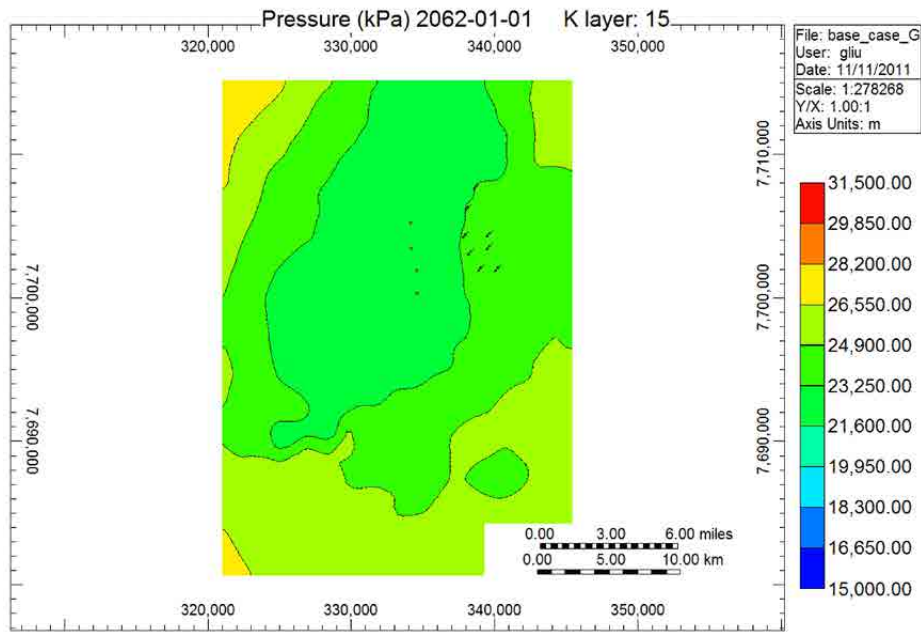


Figure E-65. Areal view of Case 4: pressure distributions for 50 years from beginning of injection.

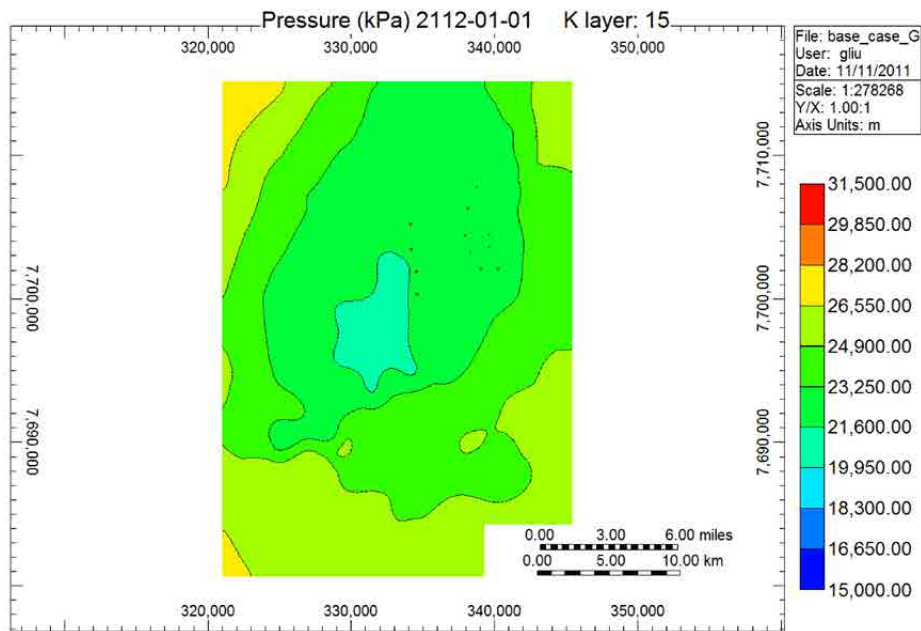


Figure E-66. Areal view of Case 4: pressure distributions for 100 years from beginning of injection.

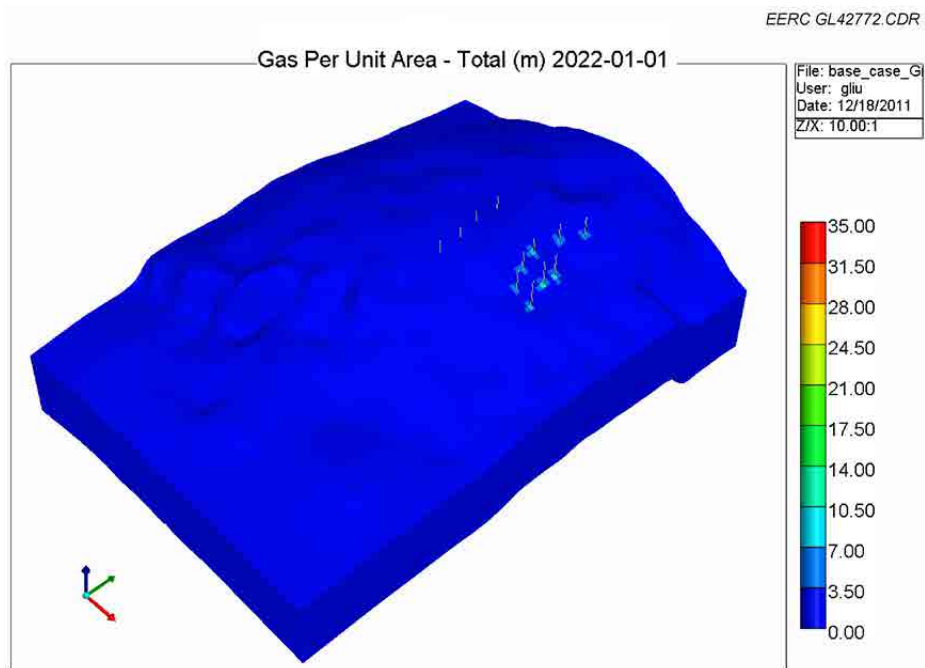


Figure E-67. 3-D view of Case 5: CO₂ plume migration for 10 years from beginning of injection.

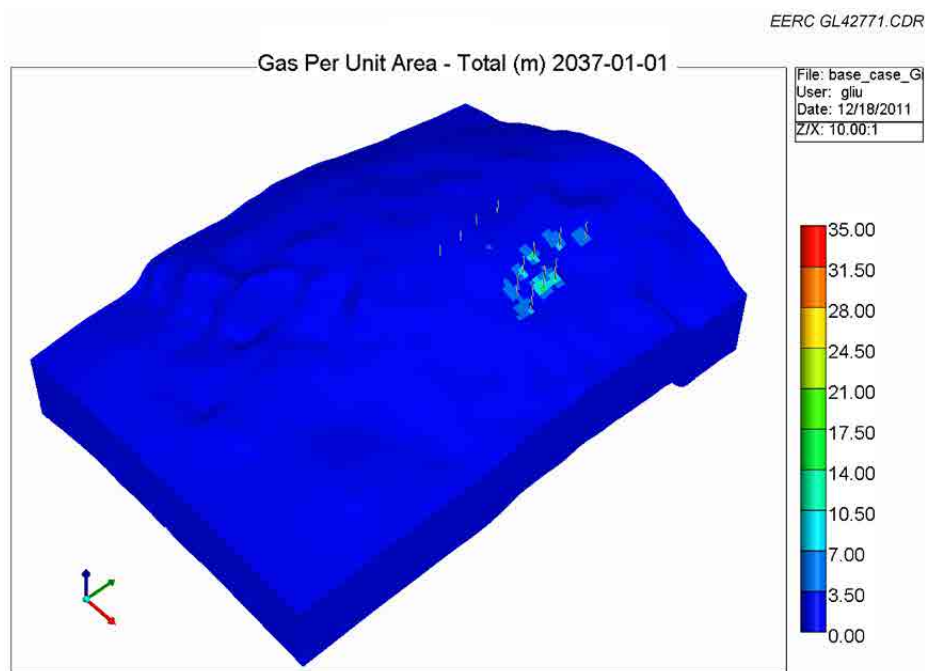


Figure E-68. 3-D view of Case 5: CO₂ plume migration for 25 years from beginning of injection.

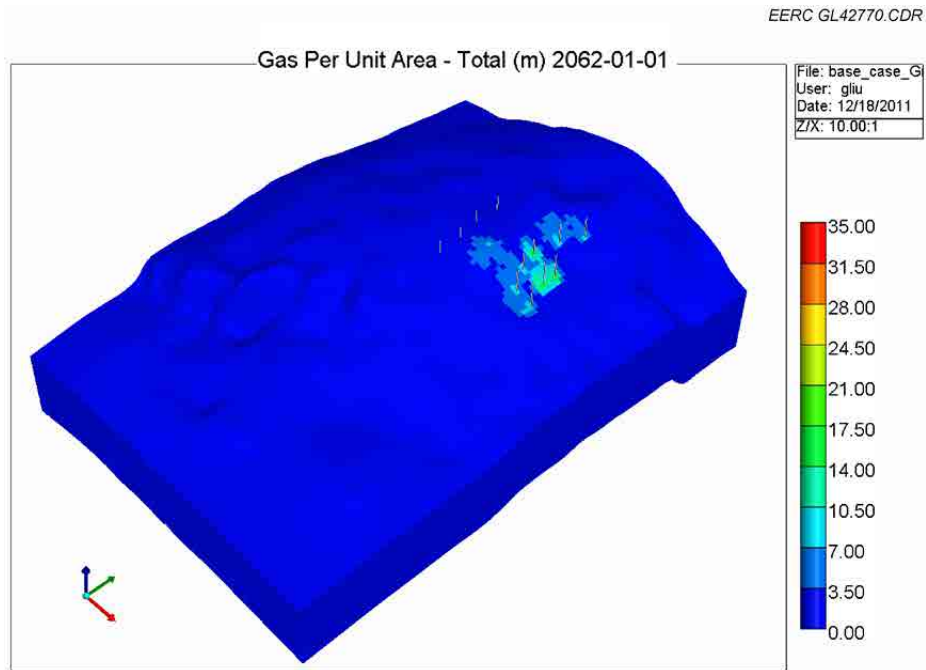


Figure E-69. 3-D view of Case 5: CO₂ plume migration for 50 years from beginning of injection.

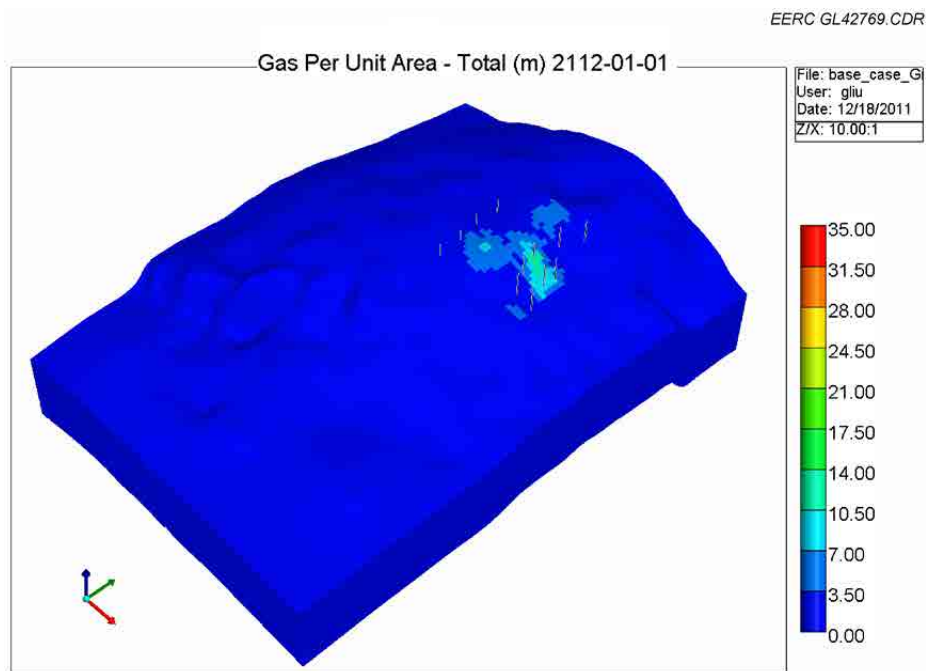


Figure E-70. 3-D view of Case 5: CO₂ plume migration for 100 years from beginning of injection.

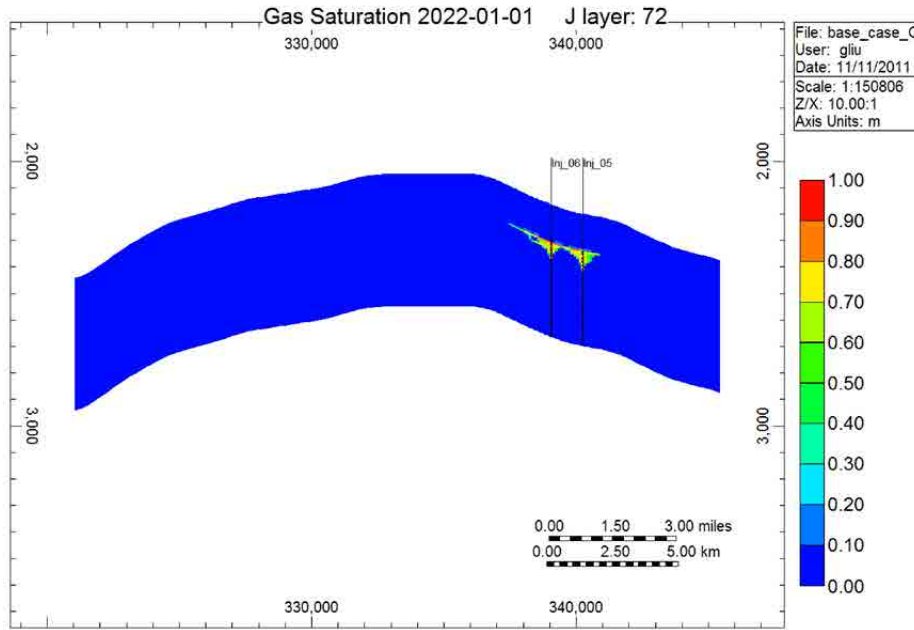


Figure E-71. Cross-sectional view of Case 5: CO₂ plume migration for 10 years from beginning of injection.

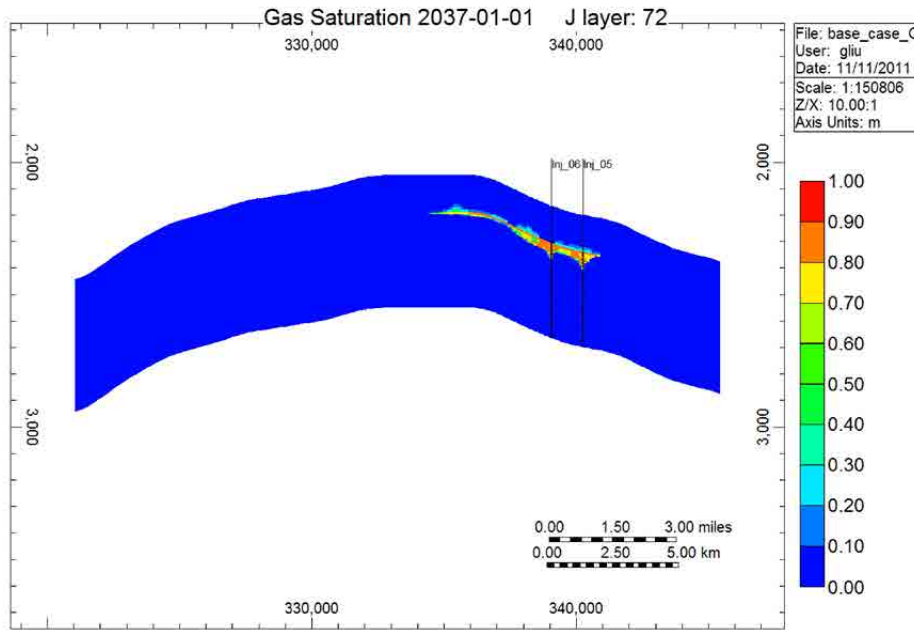


Figure E-72. Cross-sectional view of Case 5: CO₂ plume migration for 25 years from beginning of injection.

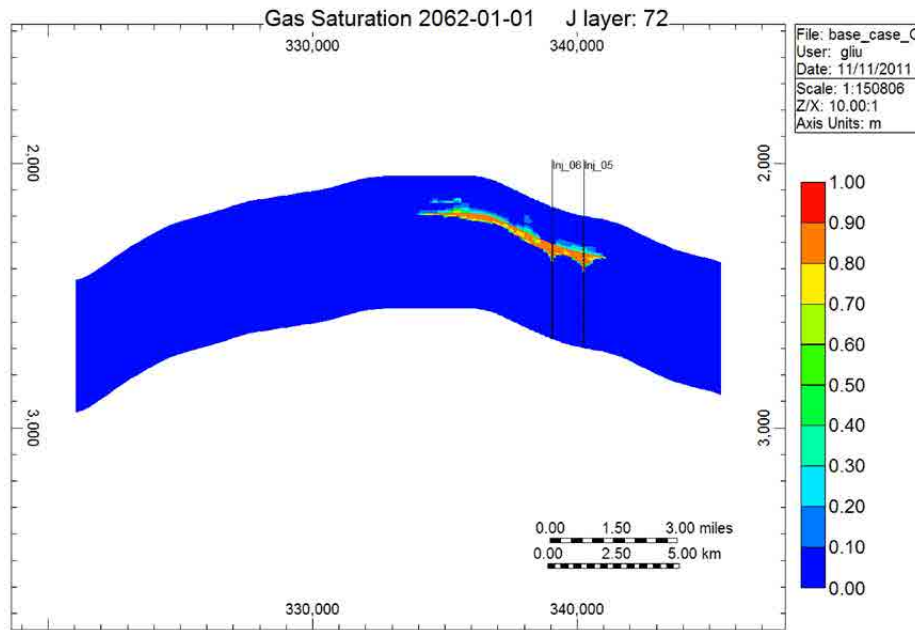


Figure E-73. Cross-sectional view of Case 5: CO₂ plume migration for 50 years from beginning of injection.

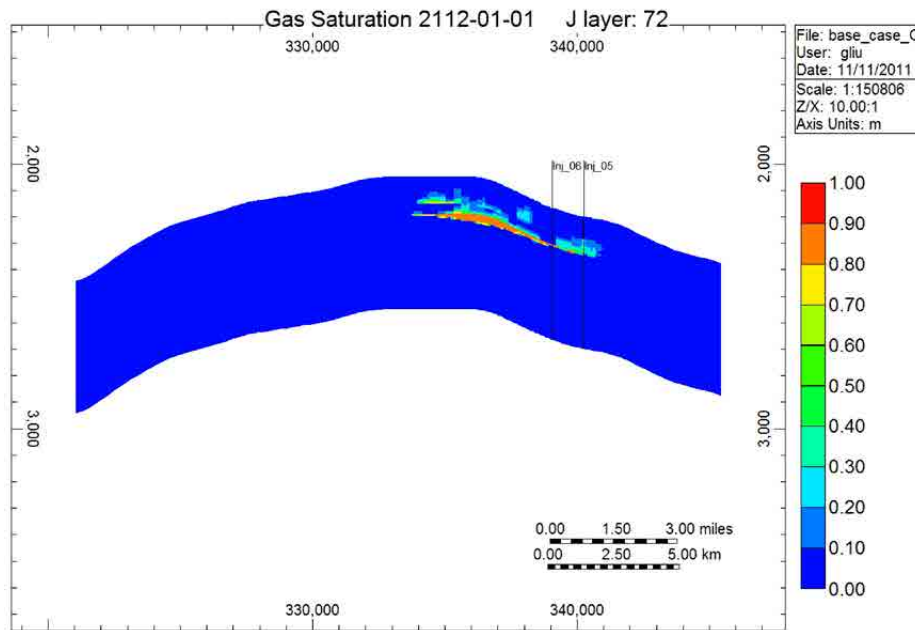


Figure E-74. Cross-sectional view of Case 5: CO₂ plume migration for 100 years from beginning of injection.

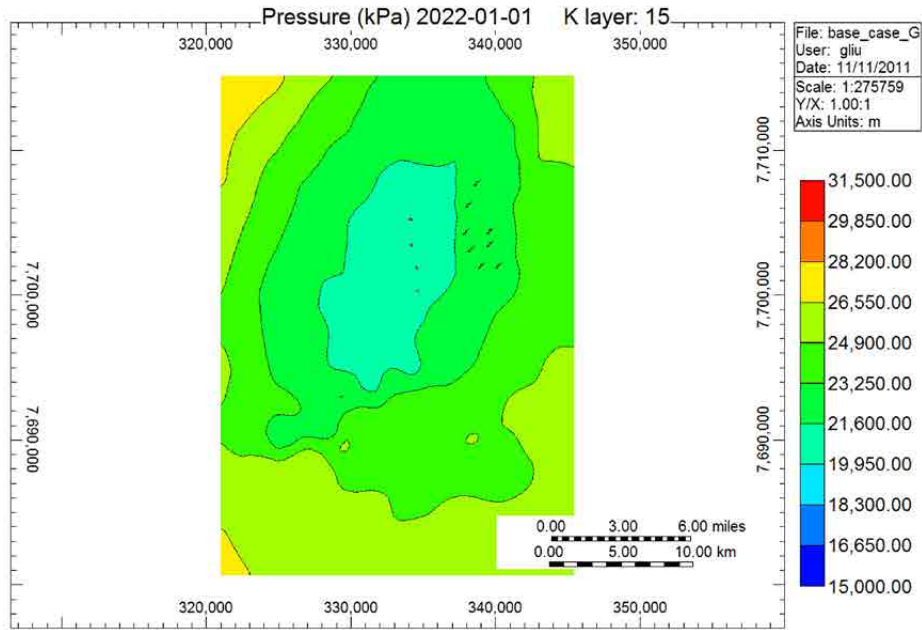


Figure E-75. Areal view of Case 5: pressure distributions for 10 years from beginning of injection.

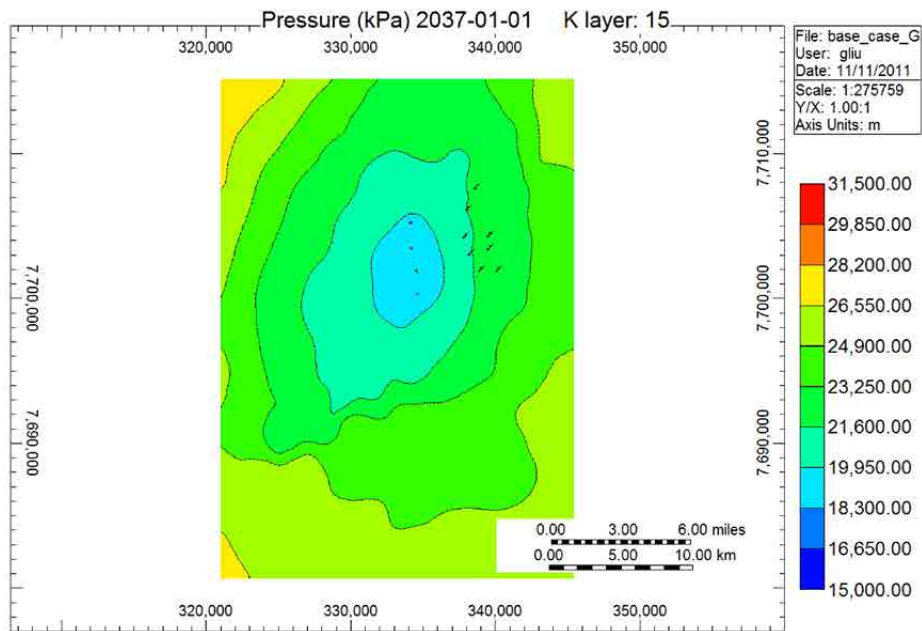


Figure E-76. Areal view of Case 5: pressure distributions for 25 years from beginning of injection.

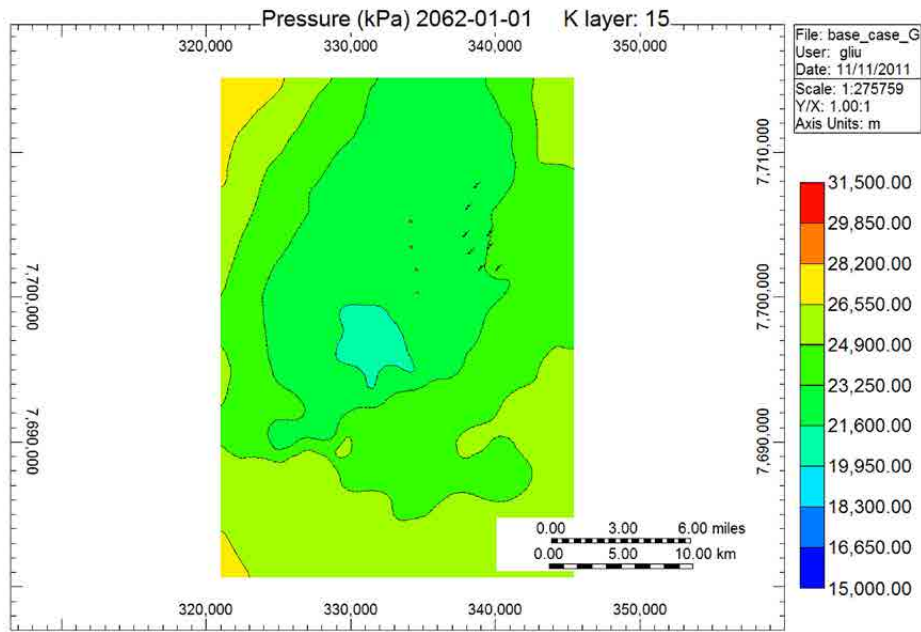


Figure E-77. Areal view of Case 5: pressure distributions for 50 years from beginning of injection.

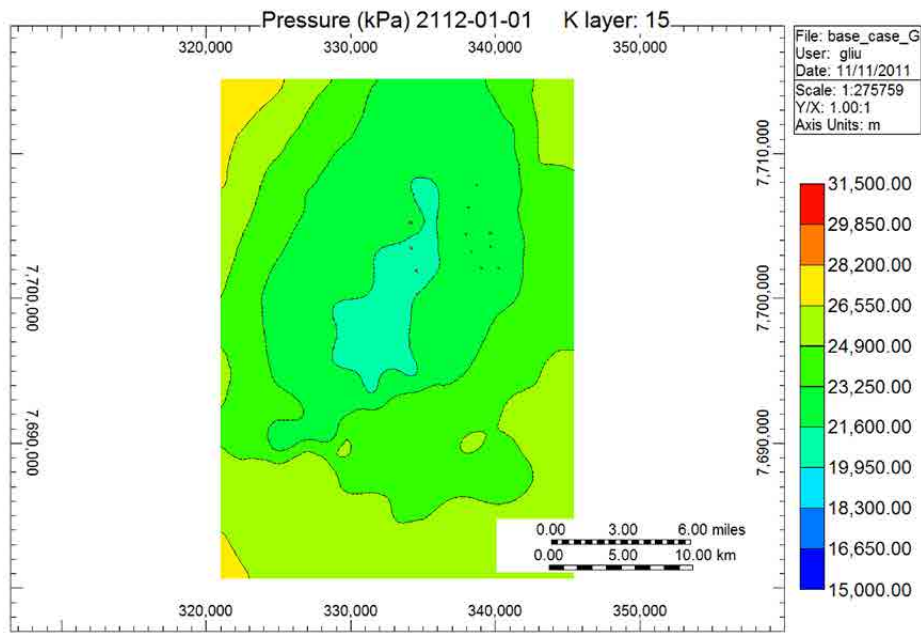


Figure E-78. Areal view of Case 5: pressure distributions for 100 years from beginning of injection.

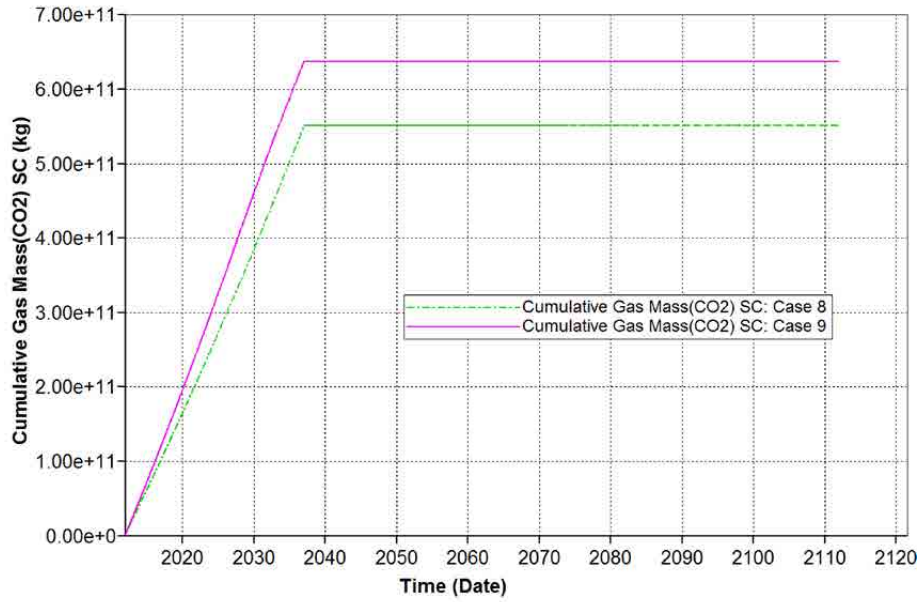


Figure E-79. Total injected CO₂ for Cases 6–9.

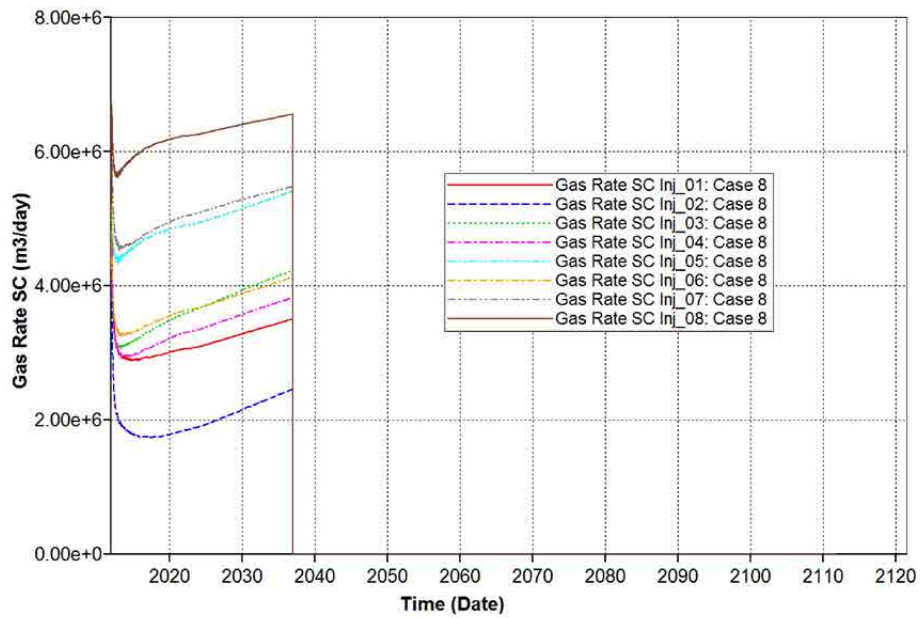


Figure E-80. Case 8 CO₂ injection rates.

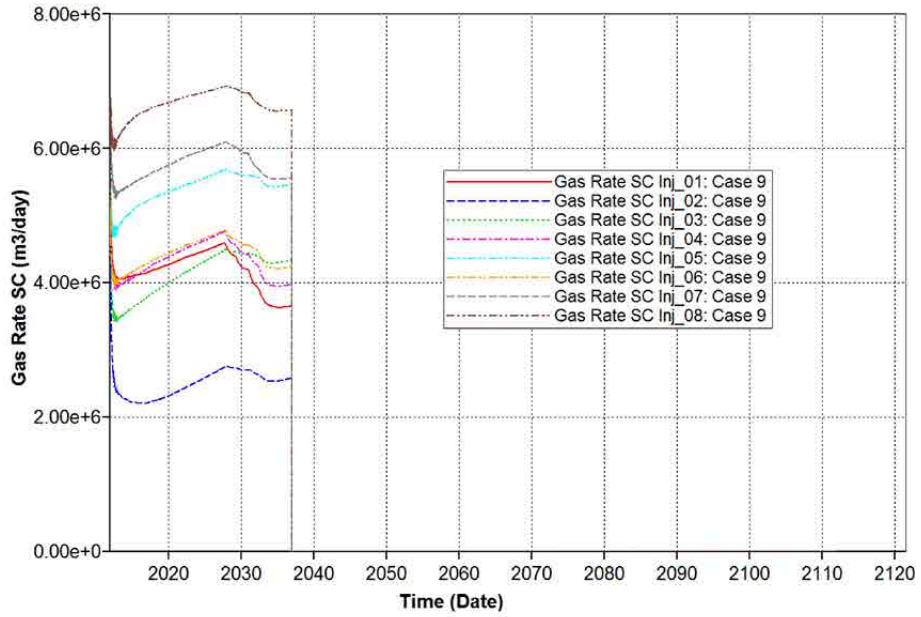


Figure E-81. Case 9 CO₂ injection rates.

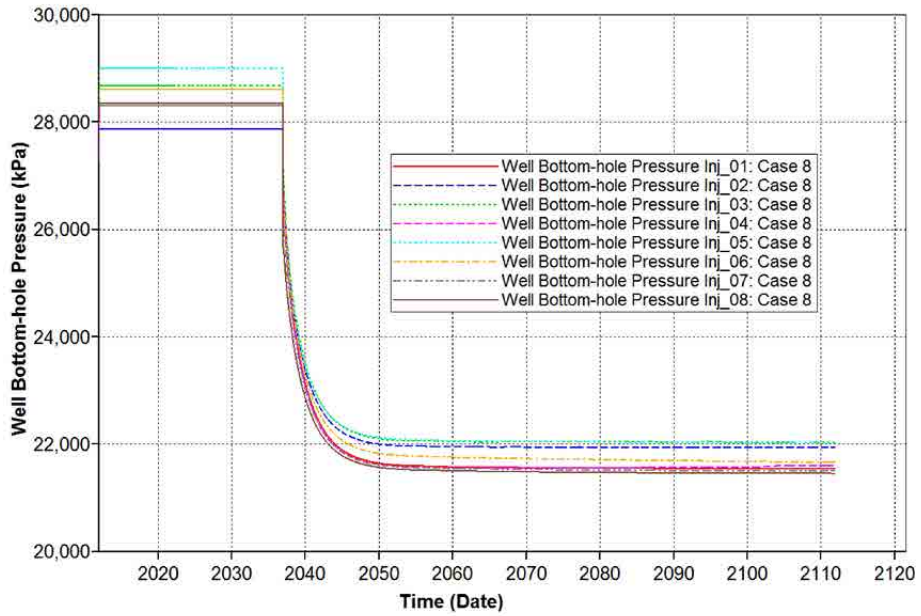


Figure E-82. Case 8 injection well BHPs.

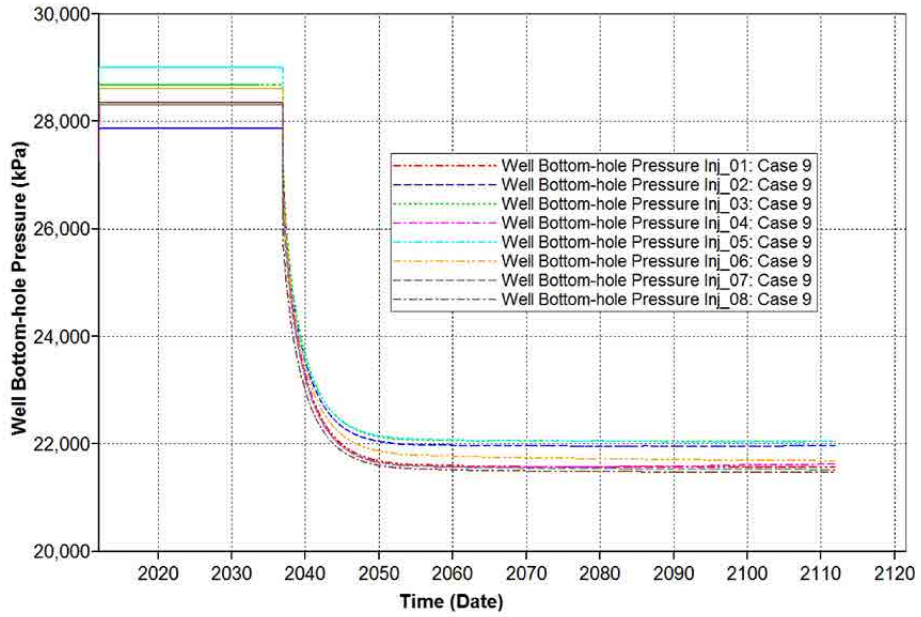


Figure E-83. Case 9 injection well BHPs.

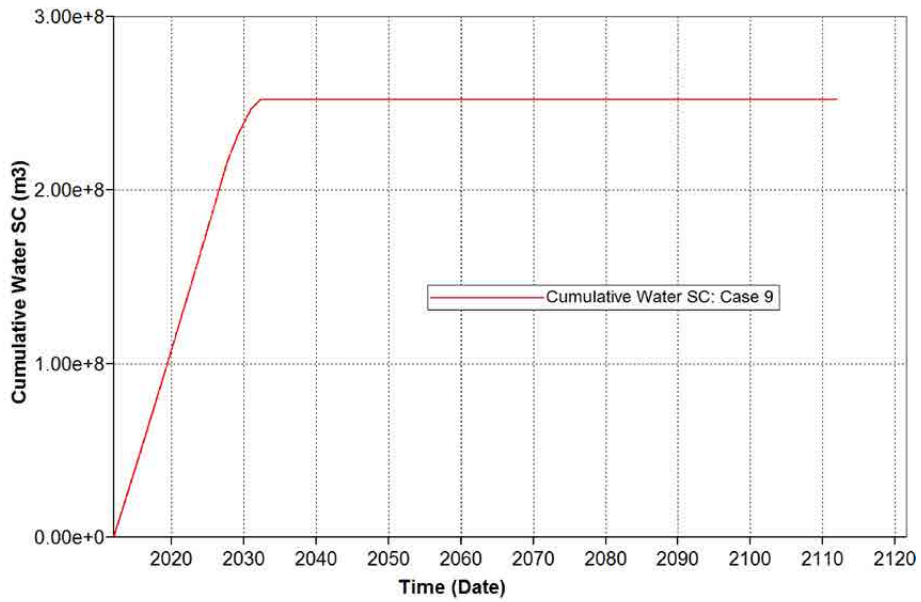


Figure E-84. Total produced water for Cases 7 and 9.

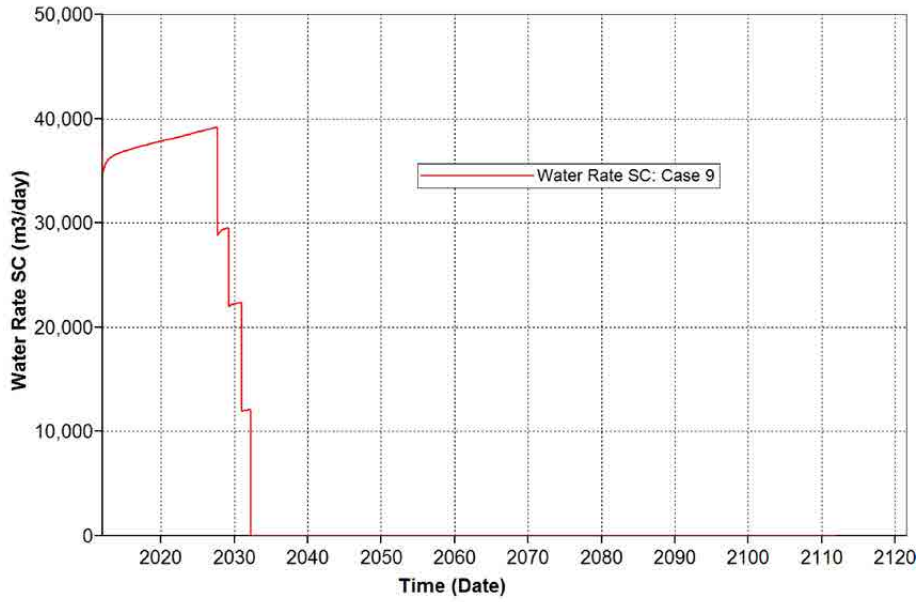


Figure E-85. Water production rate for Cases 7 and 9.

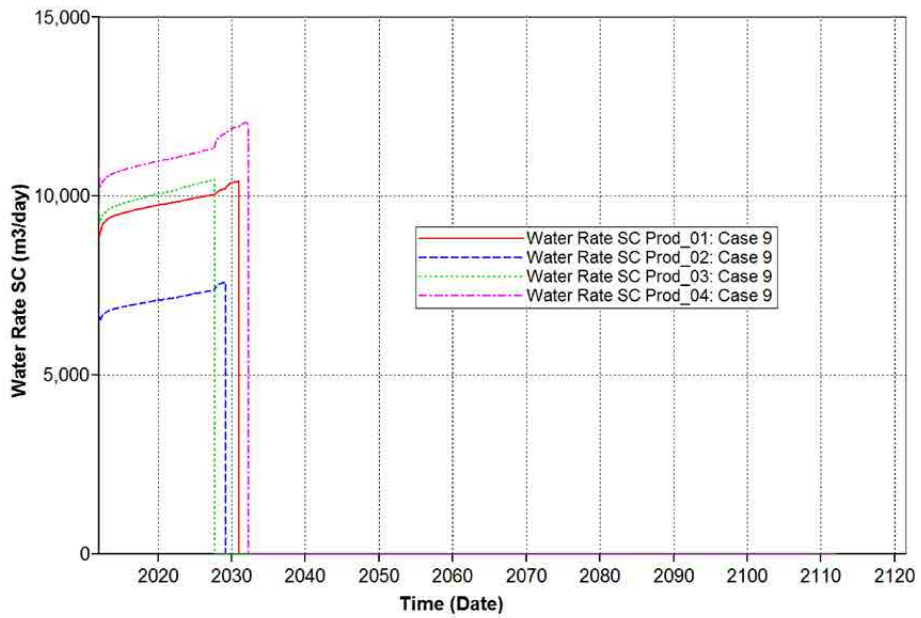


Figure E-86. Case 9 water production rate.

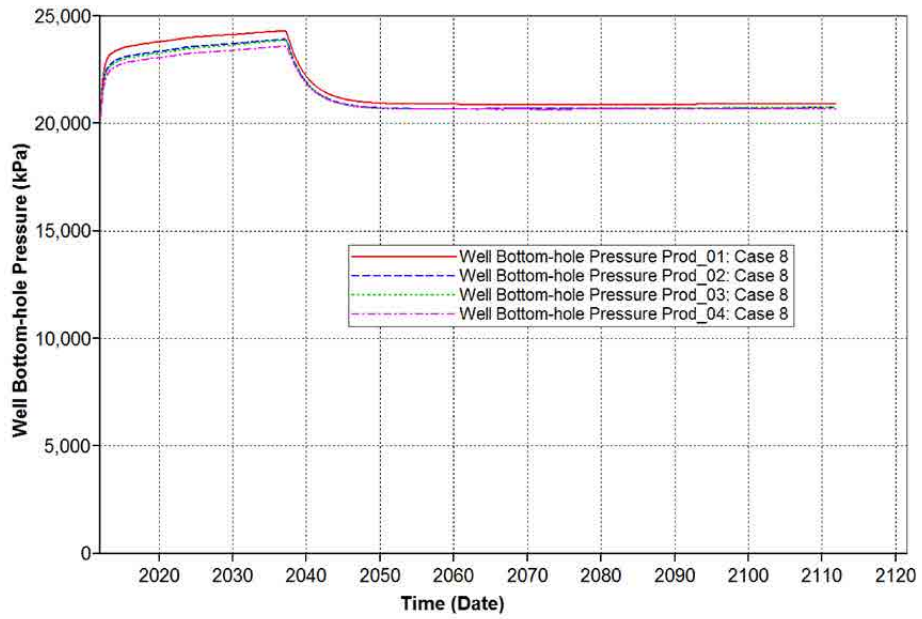


Figure E-87. Case 8 production well BHPs.

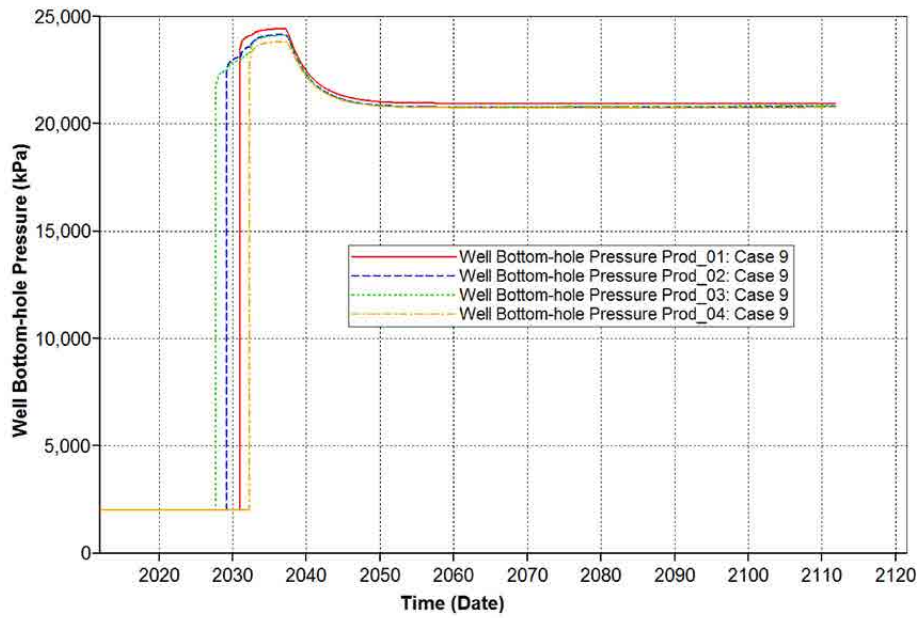


Figure E-88. Case 9 production well BHPs.

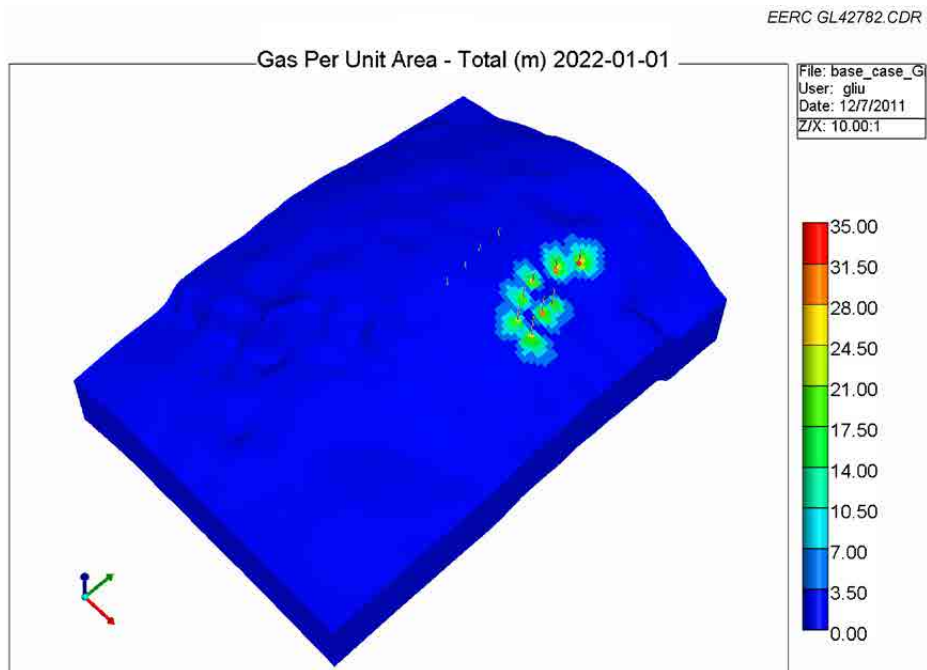


Figure E-89. 3-D view of Case 8: CO₂ plume migration for 10 years from beginning of injection.

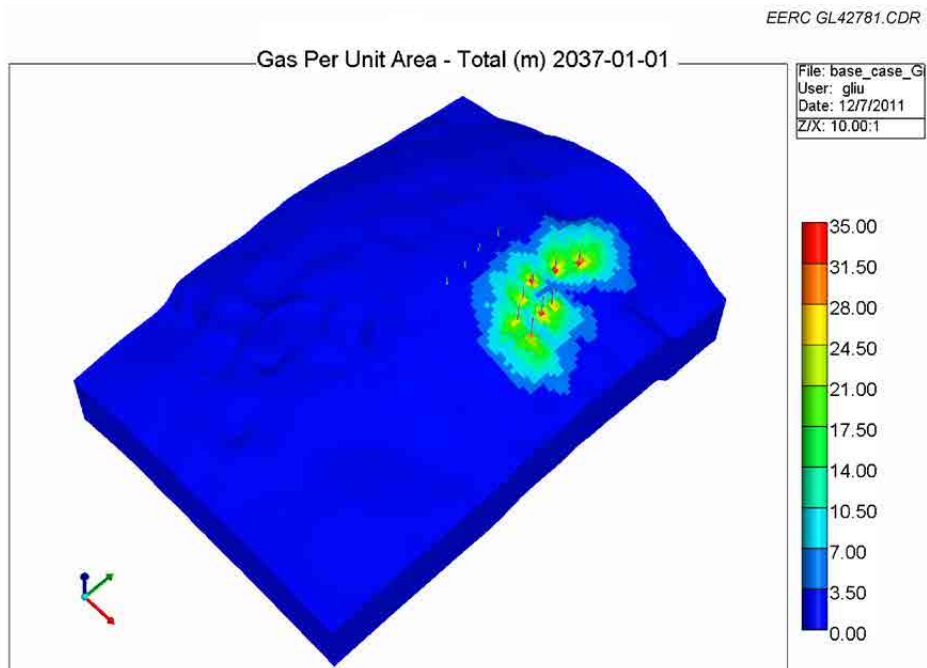


Figure E-90. 3-D view of Case 8: CO₂ plume migration for 25 years from beginning of injection.

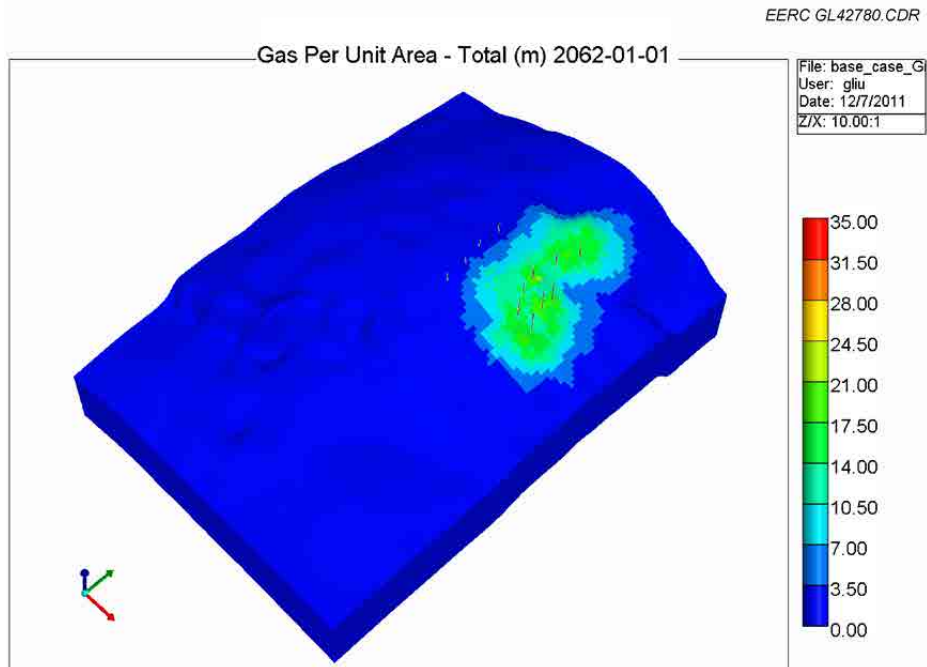


Figure E-91. 3-D view of Case 8: CO₂ plume migration for 50 years from beginning of injection.

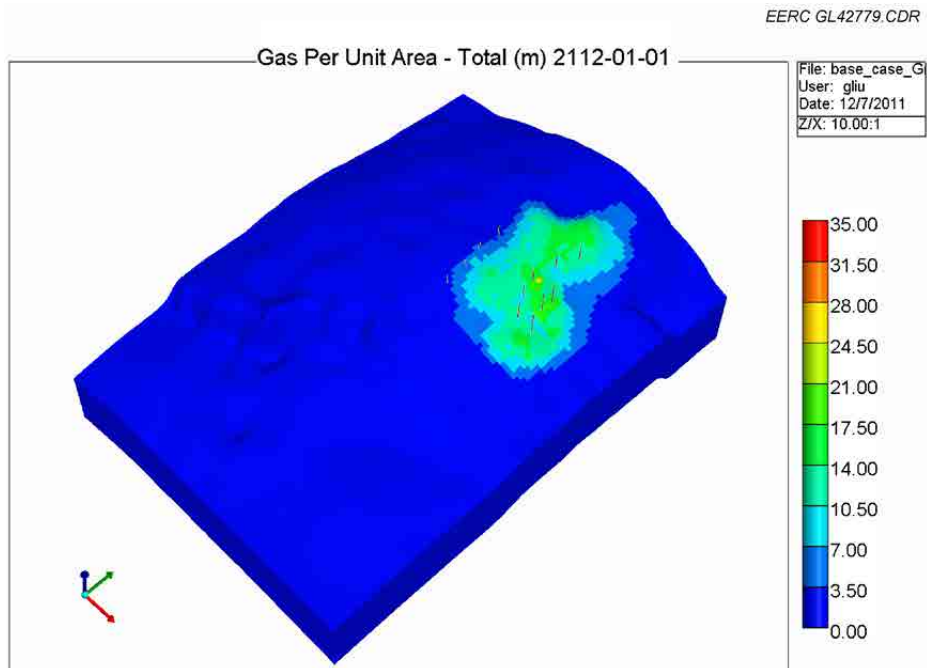


Figure E-92. 3-D view of Case 8: CO₂ plume migration for 100 years from beginning of injection.

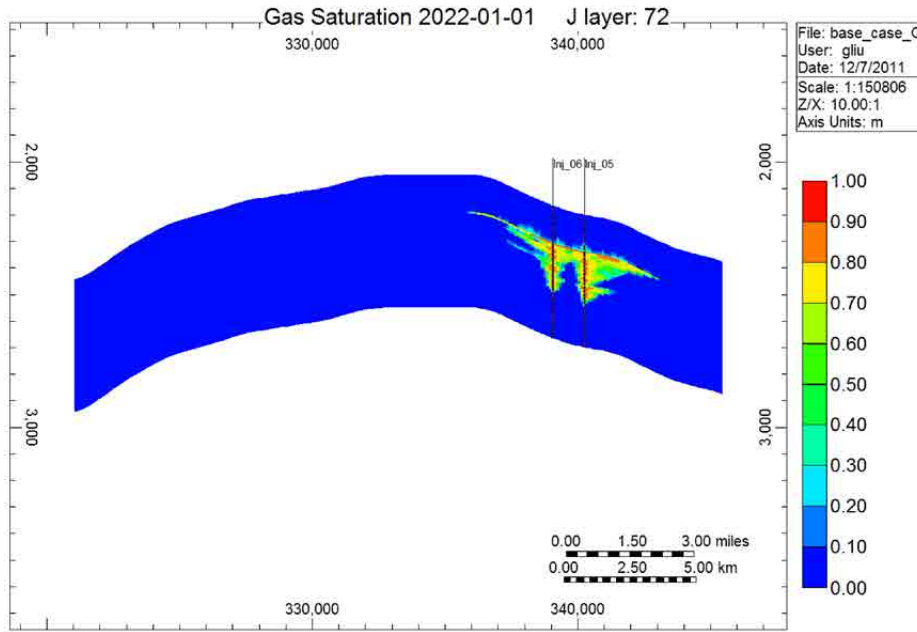


Figure E-93. Cross-sectional view of Case 8: CO₂ plume migration for 10 years from beginning of injection.

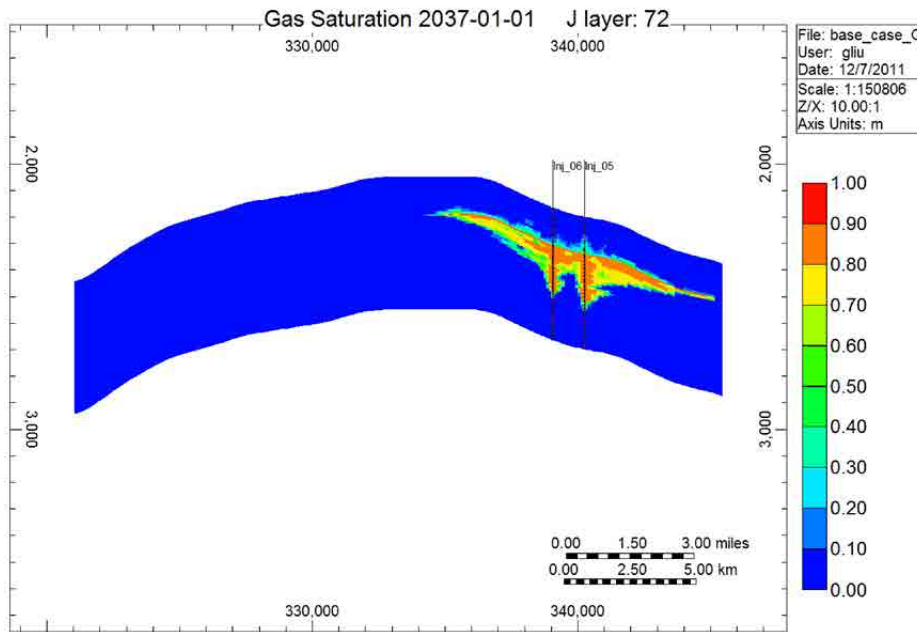


Figure E-94. Cross-sectional view of Case 8: CO₂ plume migration for 25 years from beginning of injection.

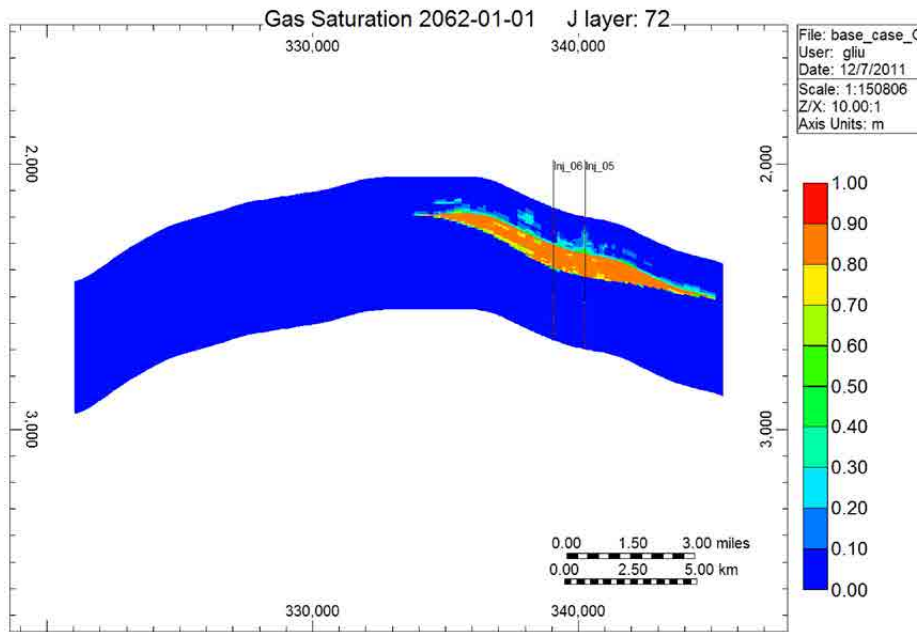


Figure E-95. Cross-sectional view of Case 8: CO₂ plume migration for 50 years from beginning of injection.

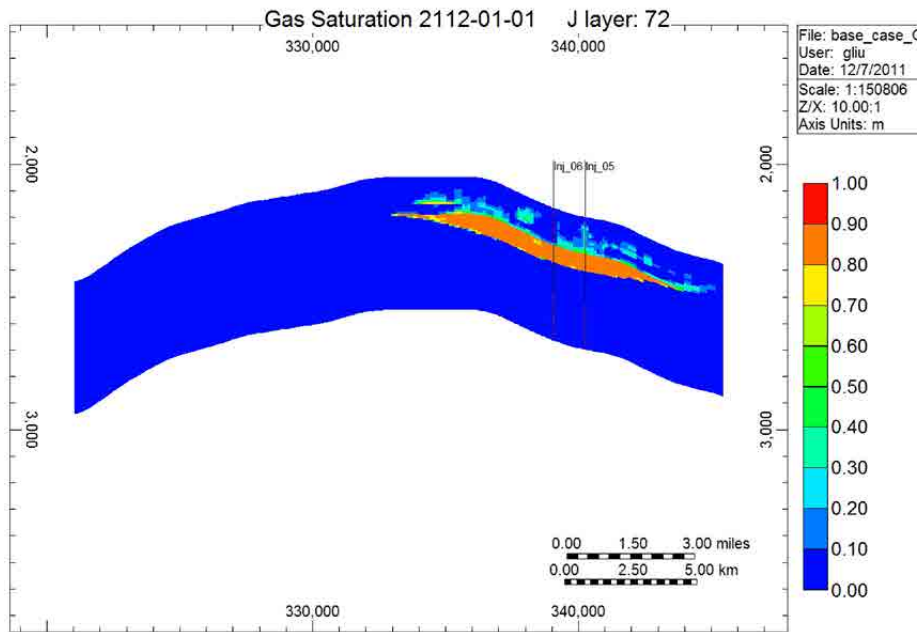


Figure E-96. Cross-sectional view of Case 8: CO₂ plume migration for 100 years from beginning of injection.

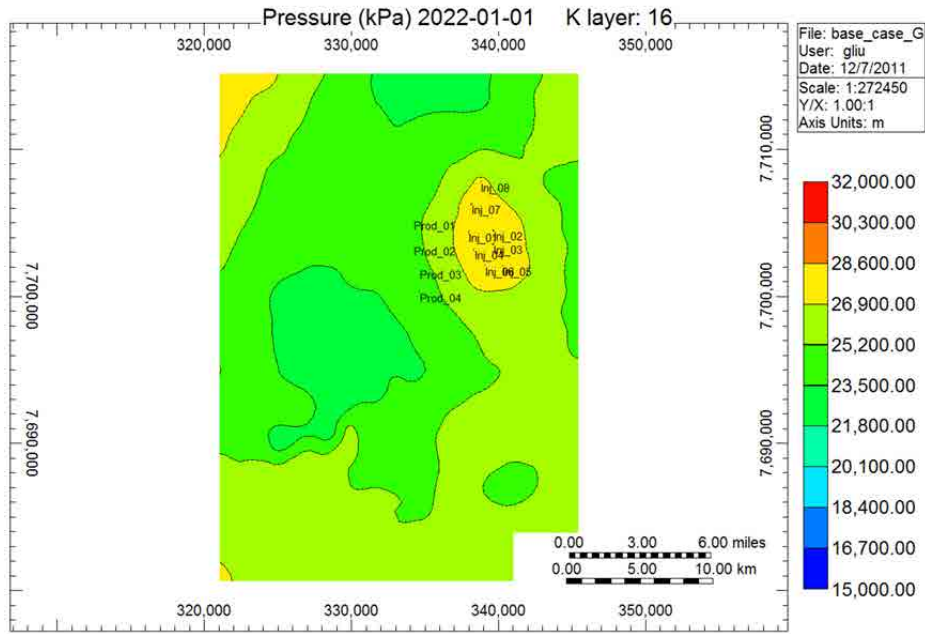


Figure E-97. Areal view of Case 8: pressure distributions for 10 years from beginning of injection.

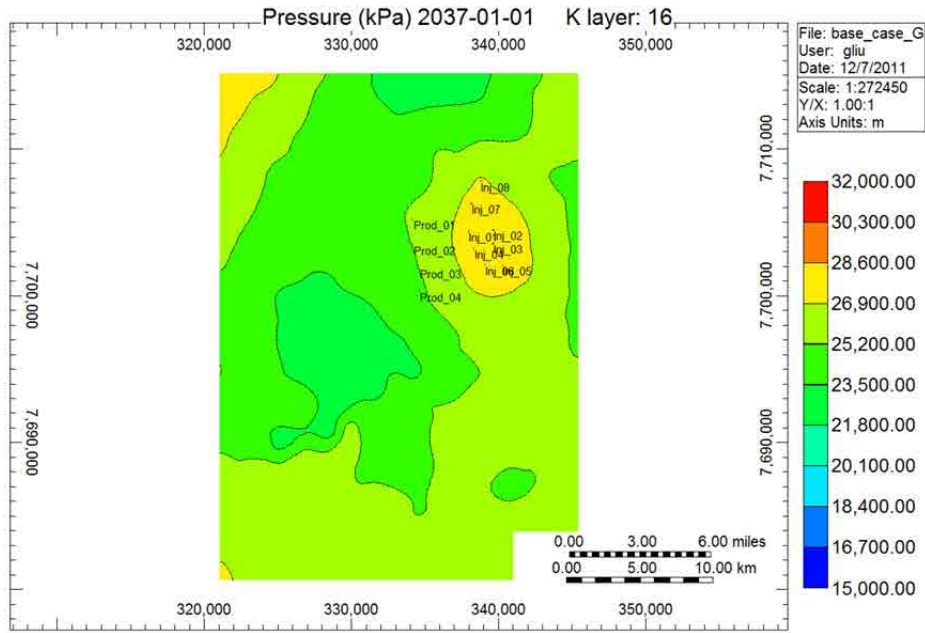


Figure E-98. Areal view of Case 8: pressure distributions for 25 years from beginning of injection.

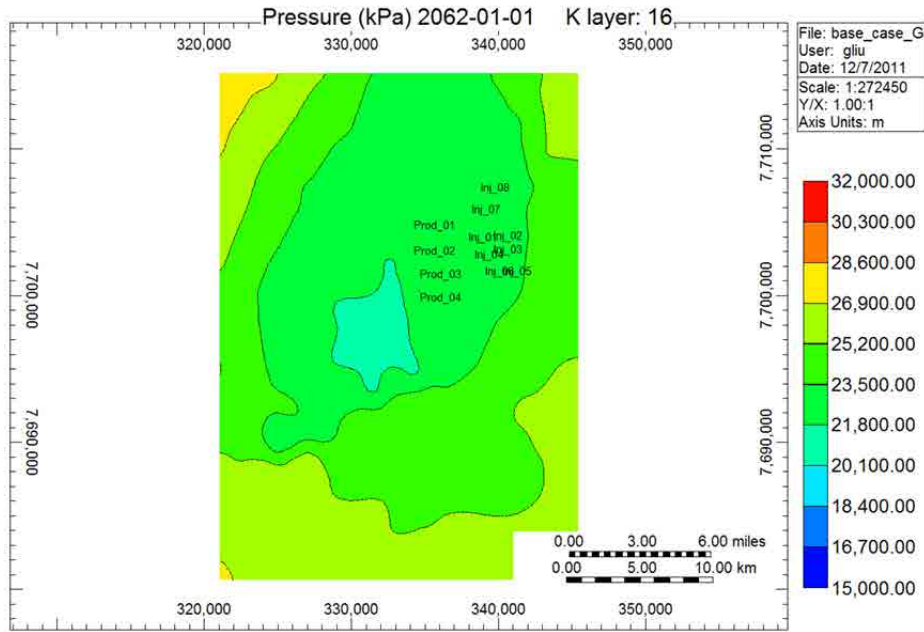


Figure E-99. Areal view of Case 8: pressure distributions for 50 years from beginning of injection.

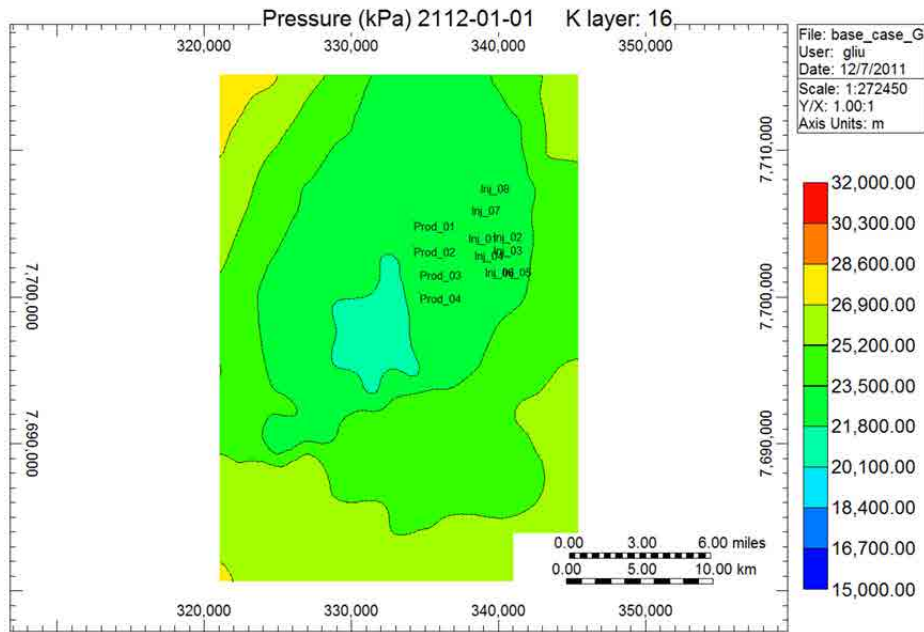


Figure E-100. Areal view of Case 8: pressure distributions for 100 years from beginning of injection.

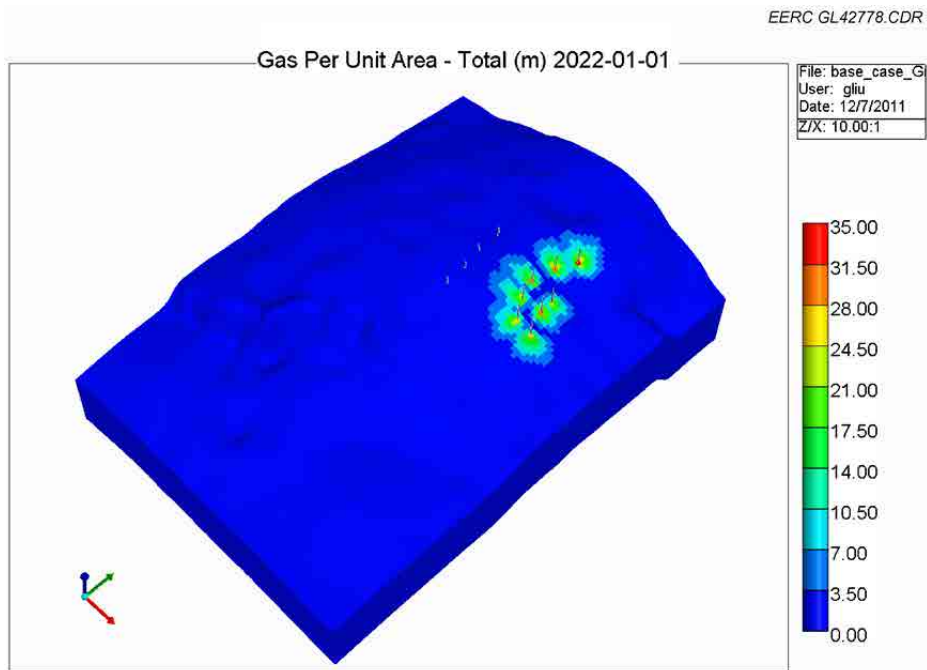


Figure E-101. 3-D view of Case 9: CO₂ plume migration for 10 years from beginning of injection.

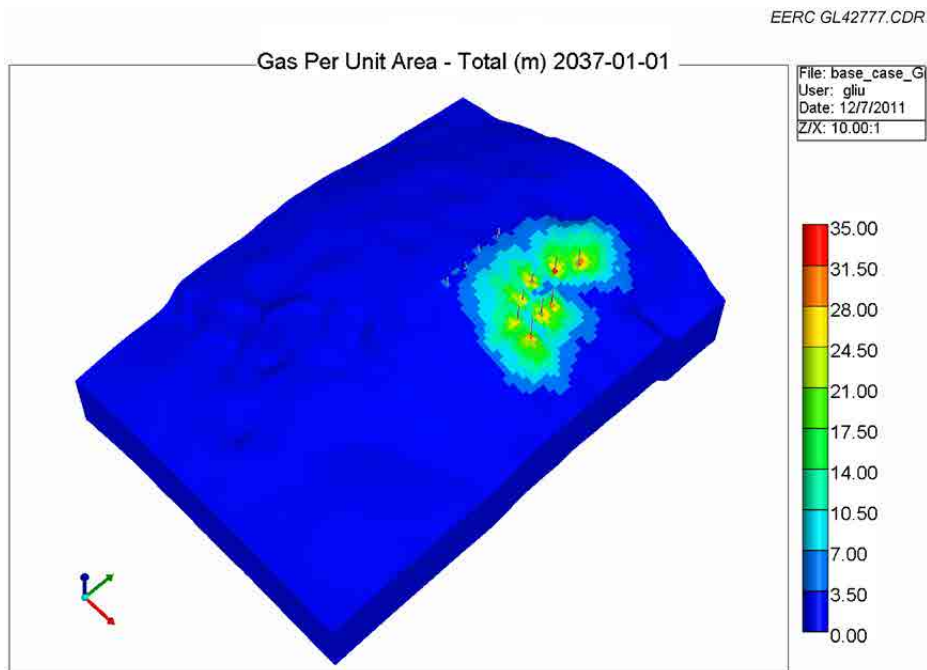


Figure E-102. 3-D view of Case 9: CO₂ plume migration for 25 years from beginning of injection.

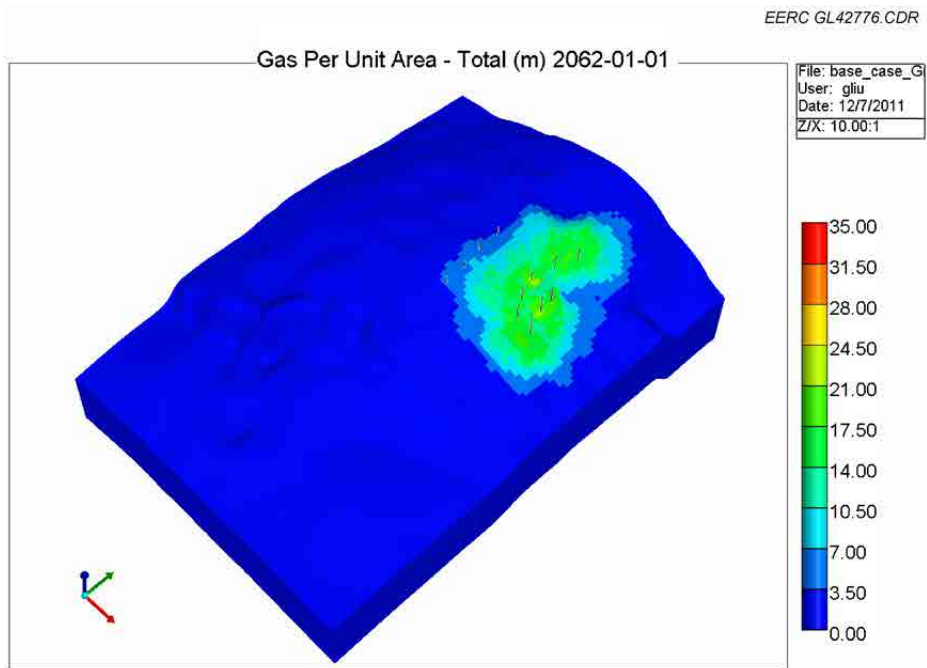


Figure E-103. 3-D view of Case 9: CO₂ plume migration for 50 years from beginning of injection.

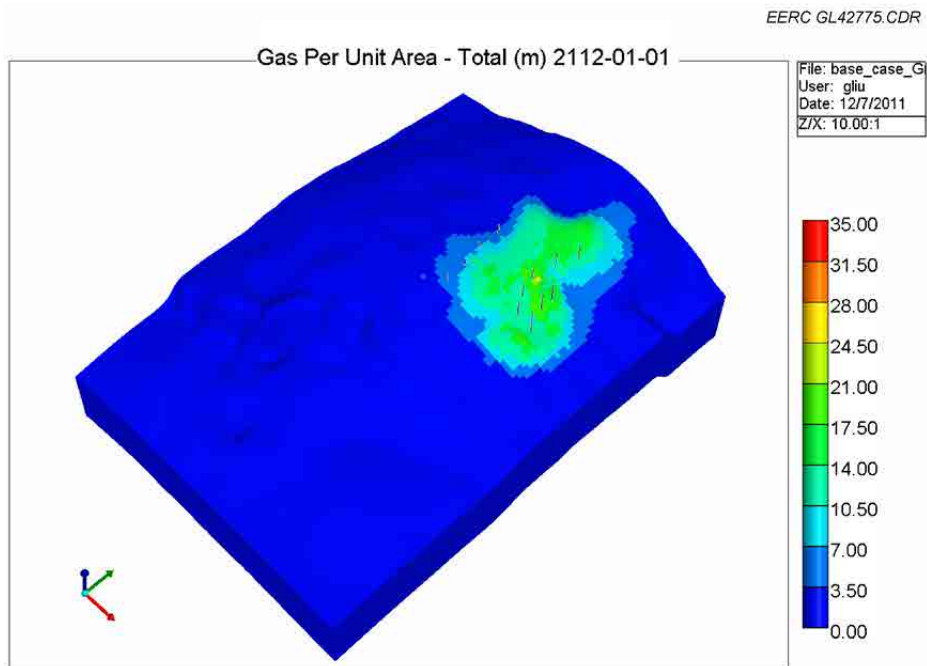


Figure E-104. 3-D view of Case 9: CO₂ plume migration for 100 years from beginning of injection.

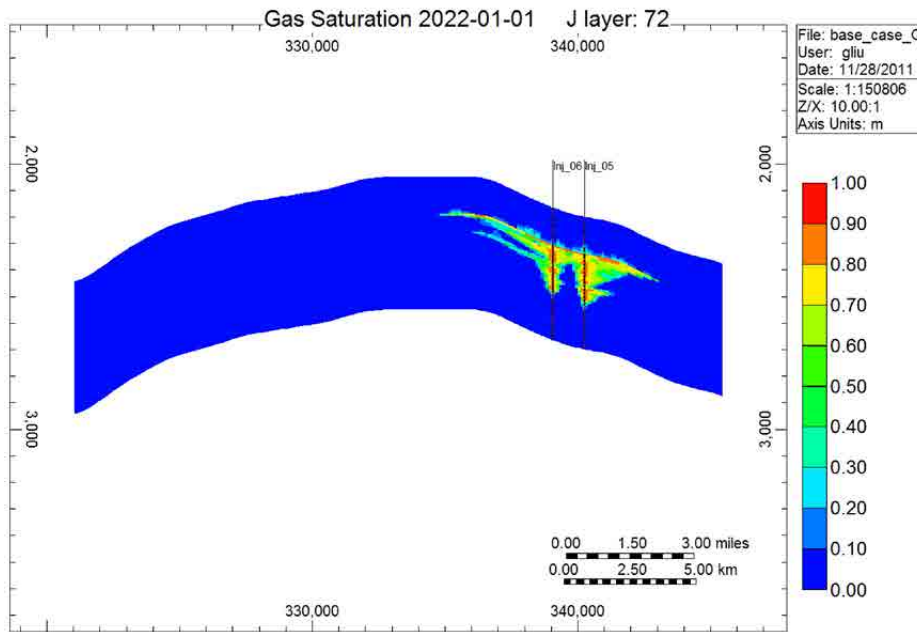


Figure E-105. Cross-sectional view of Case 9: CO₂ plume migration for 10 years from beginning of injection.

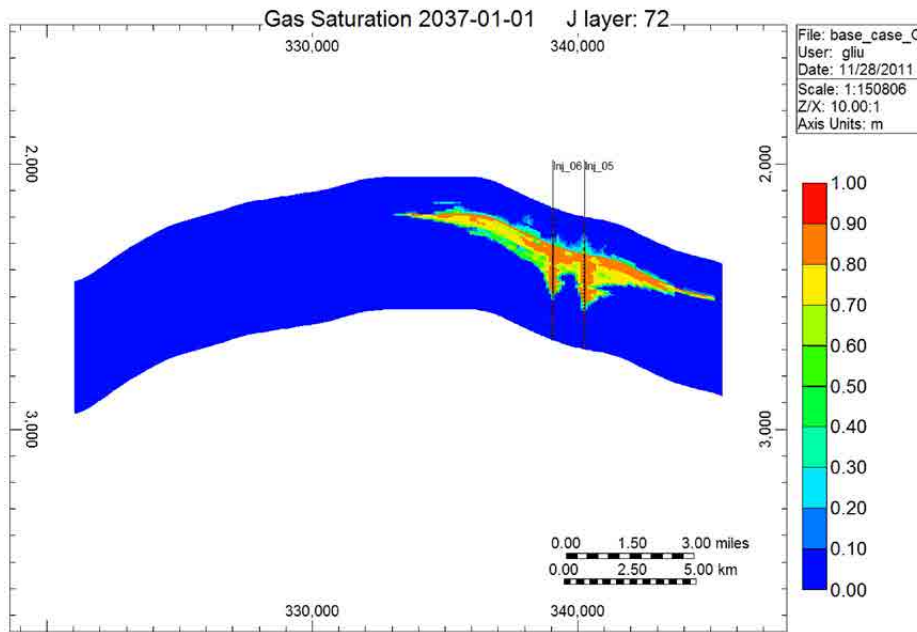


Figure E-106. Cross-sectional view of Case 9: CO₂ plume migration for 25 years from beginning of injection.

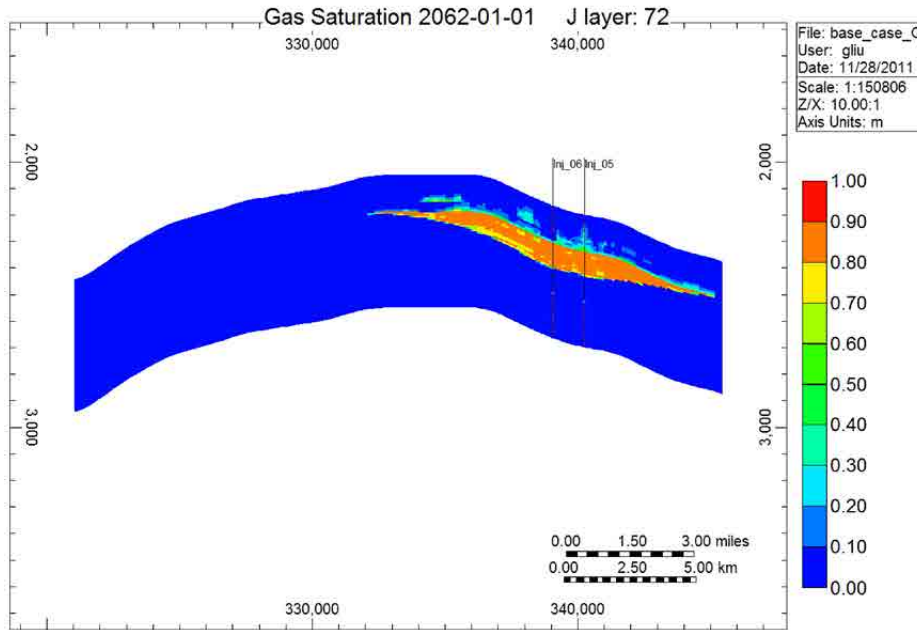


Figure E-107. Cross-sectional view of Case 9: CO₂ plume migration for 50 years from beginning of injection.

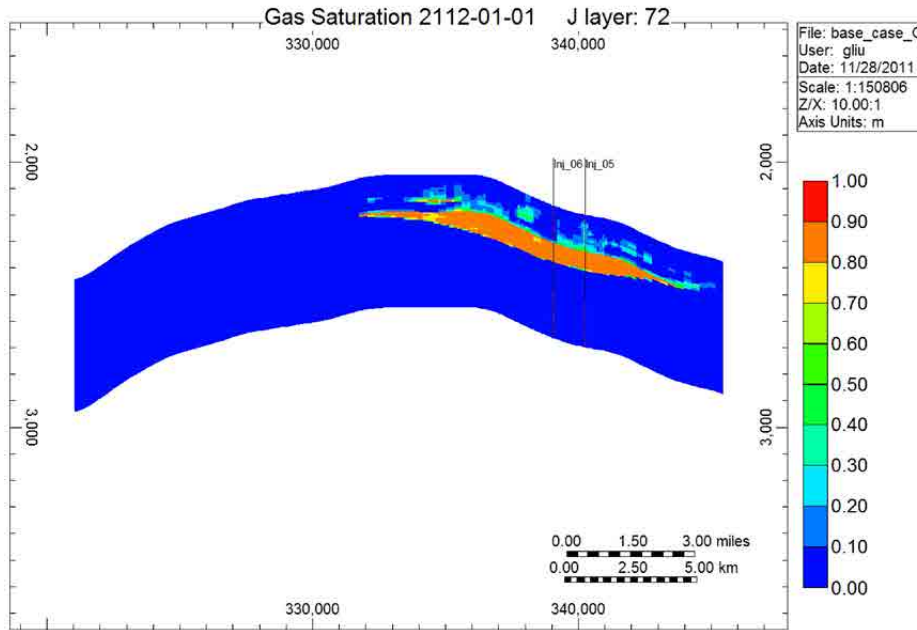


Figure E-108. Cross-sectional view of Case 9: CO₂ plume migration for 100 years from beginning of injection.

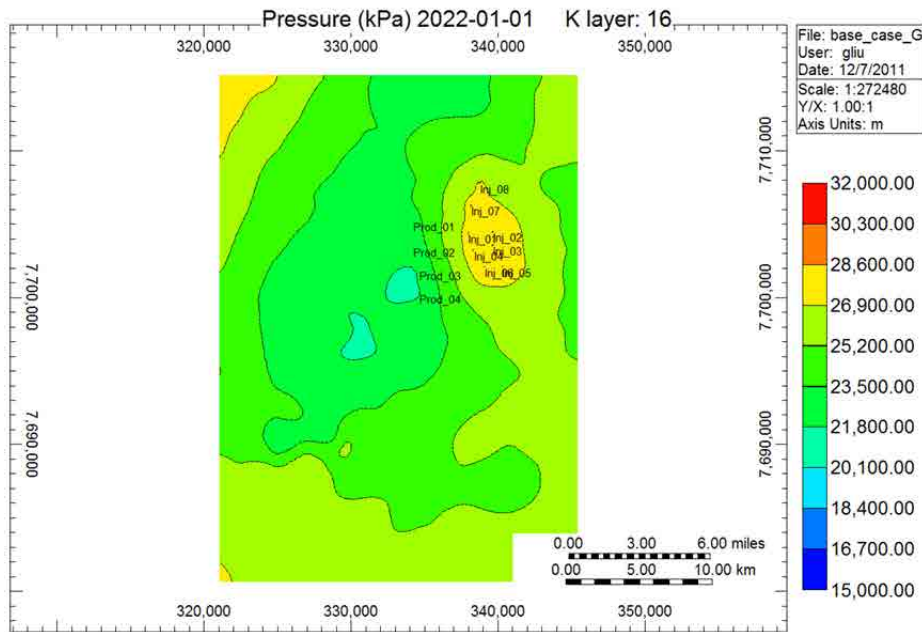


Figure E-109. Areal view of Case 9: pressure distributions for 10 years from beginning of injection.

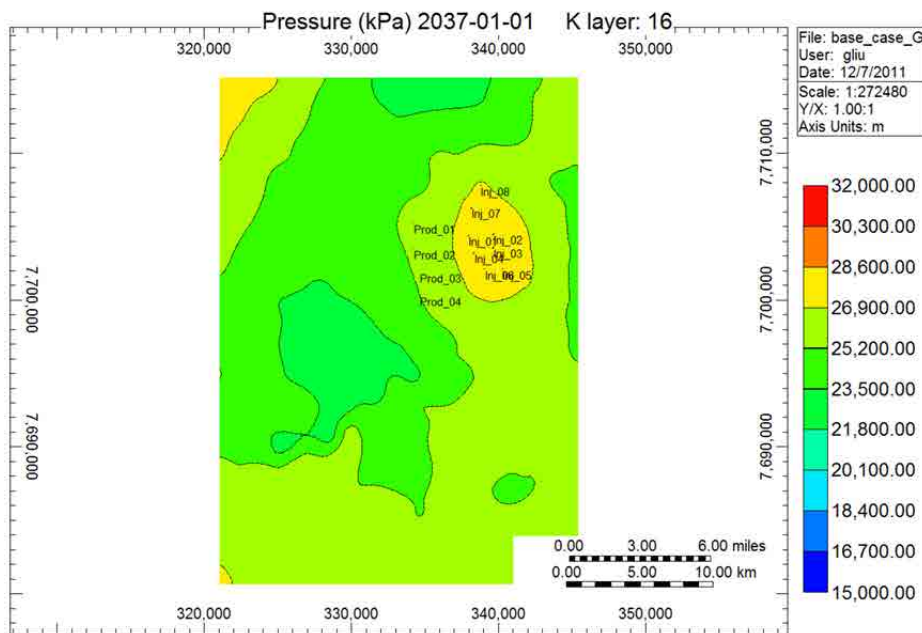


Figure E-110. Areal view of Case 9: pressure distributions for 25 years from beginning of injection.

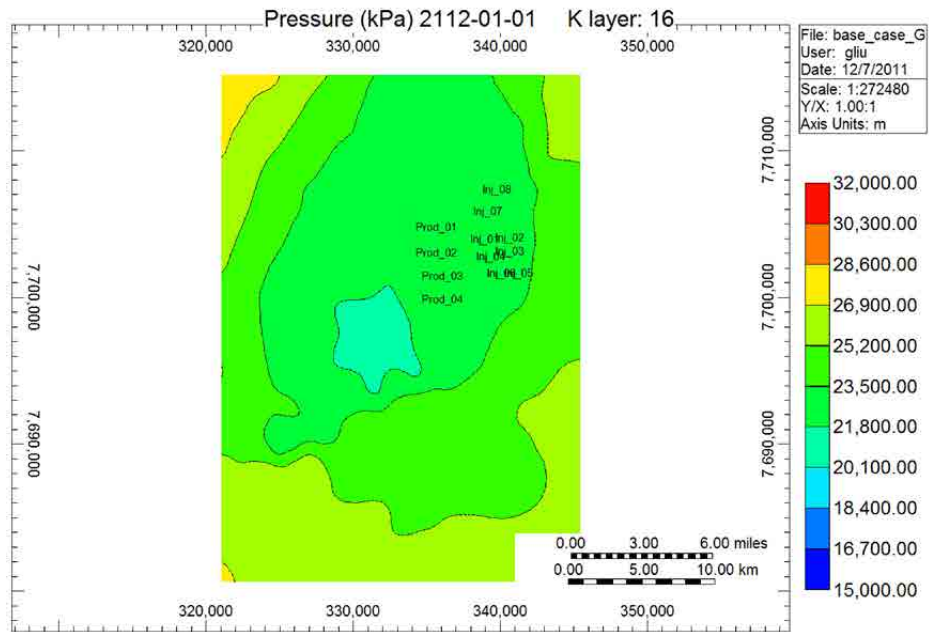


Figure E-111. Areal view of Case 9: pressure distributions for 50 years from beginning of injection.

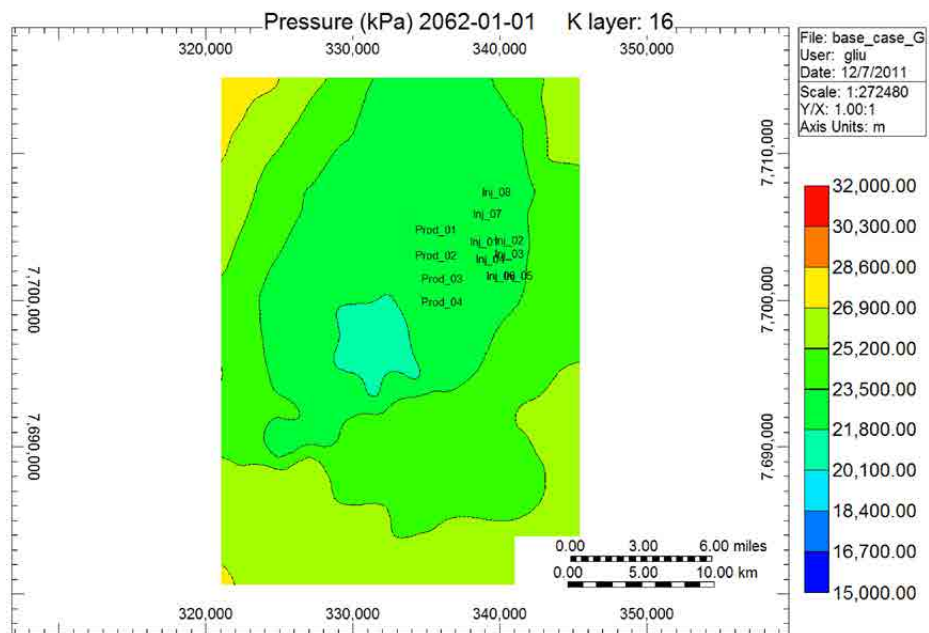


Figure E-112. Areal view of Case 9: pressure distributions for 100 years from beginning of injection.

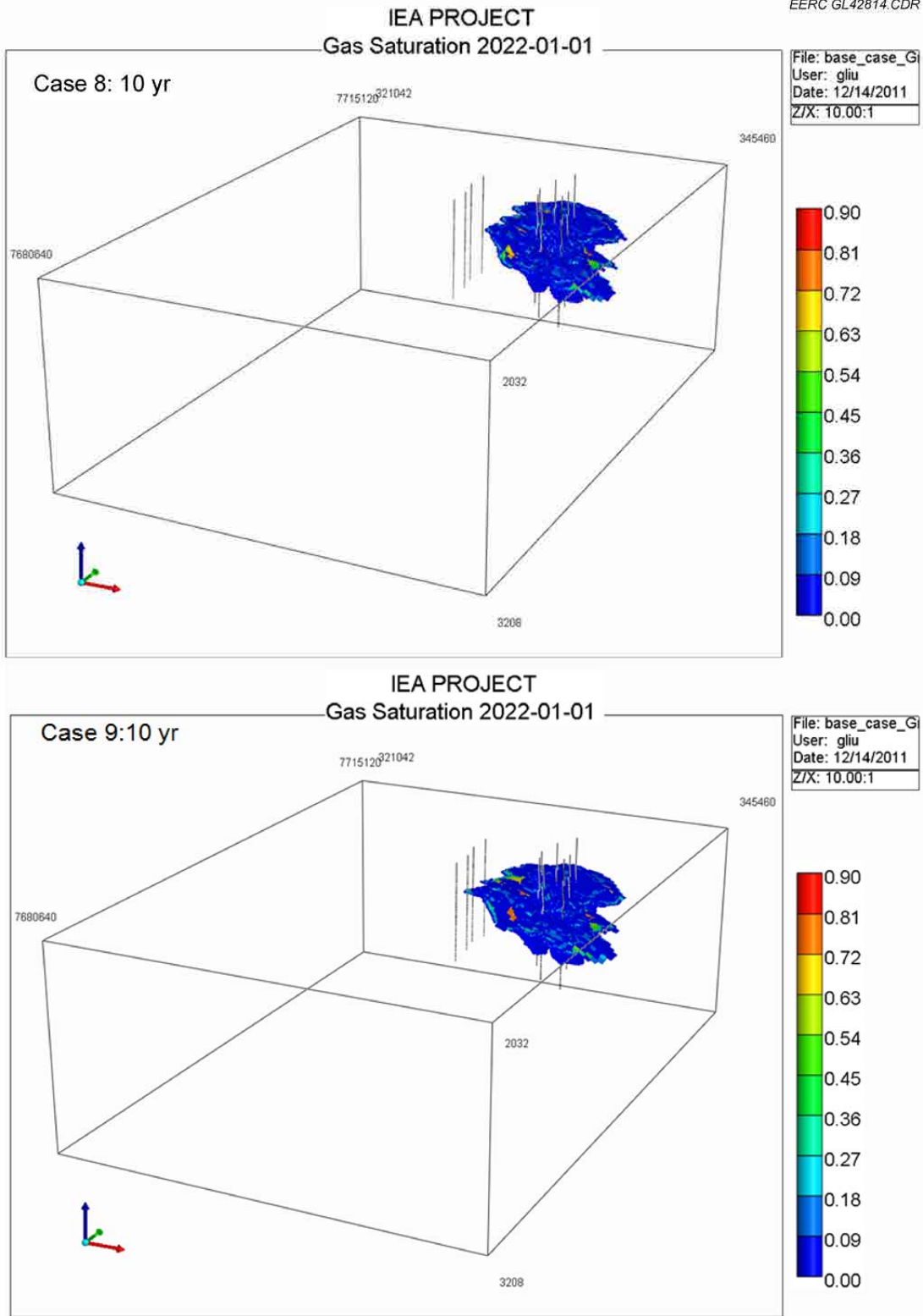


Figure E-113. 3-D view of CO₂ plume migration for 10 years from beginning of injection for Cases 8 and 9 (with and without water extraction).

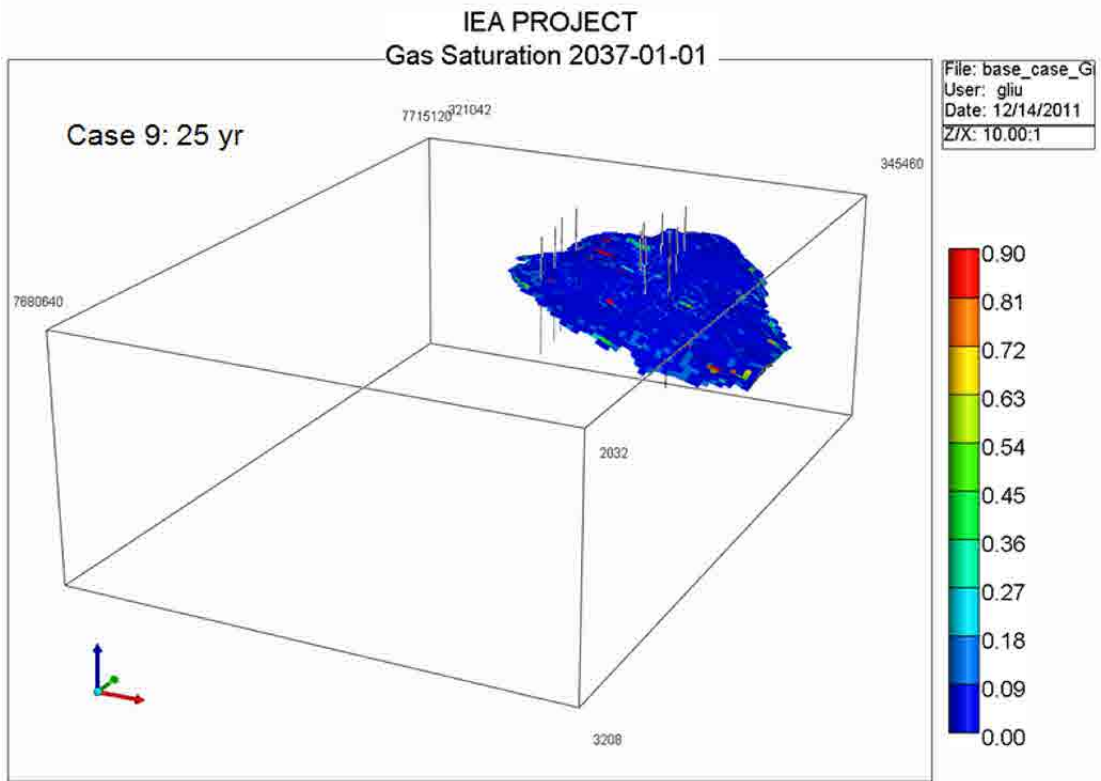
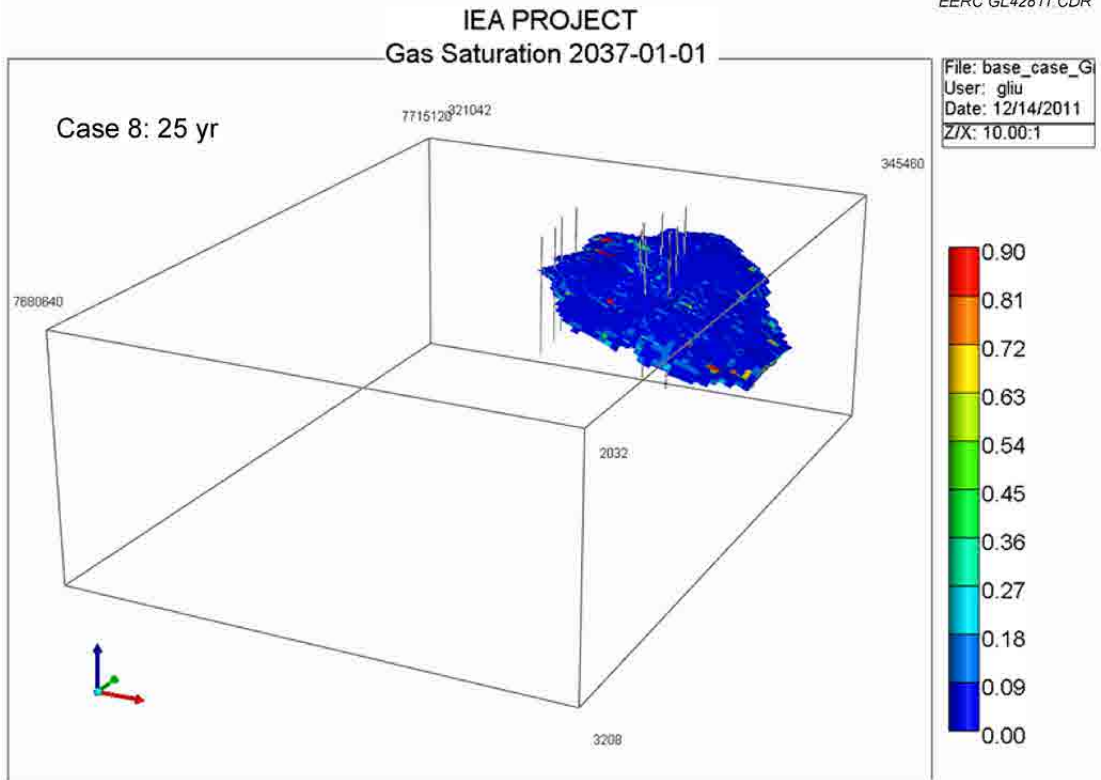


Figure E-114. 3-D view of CO₂ plume migration for 25 years from beginning of injection for Cases 8 and 9 (with and without water extraction).

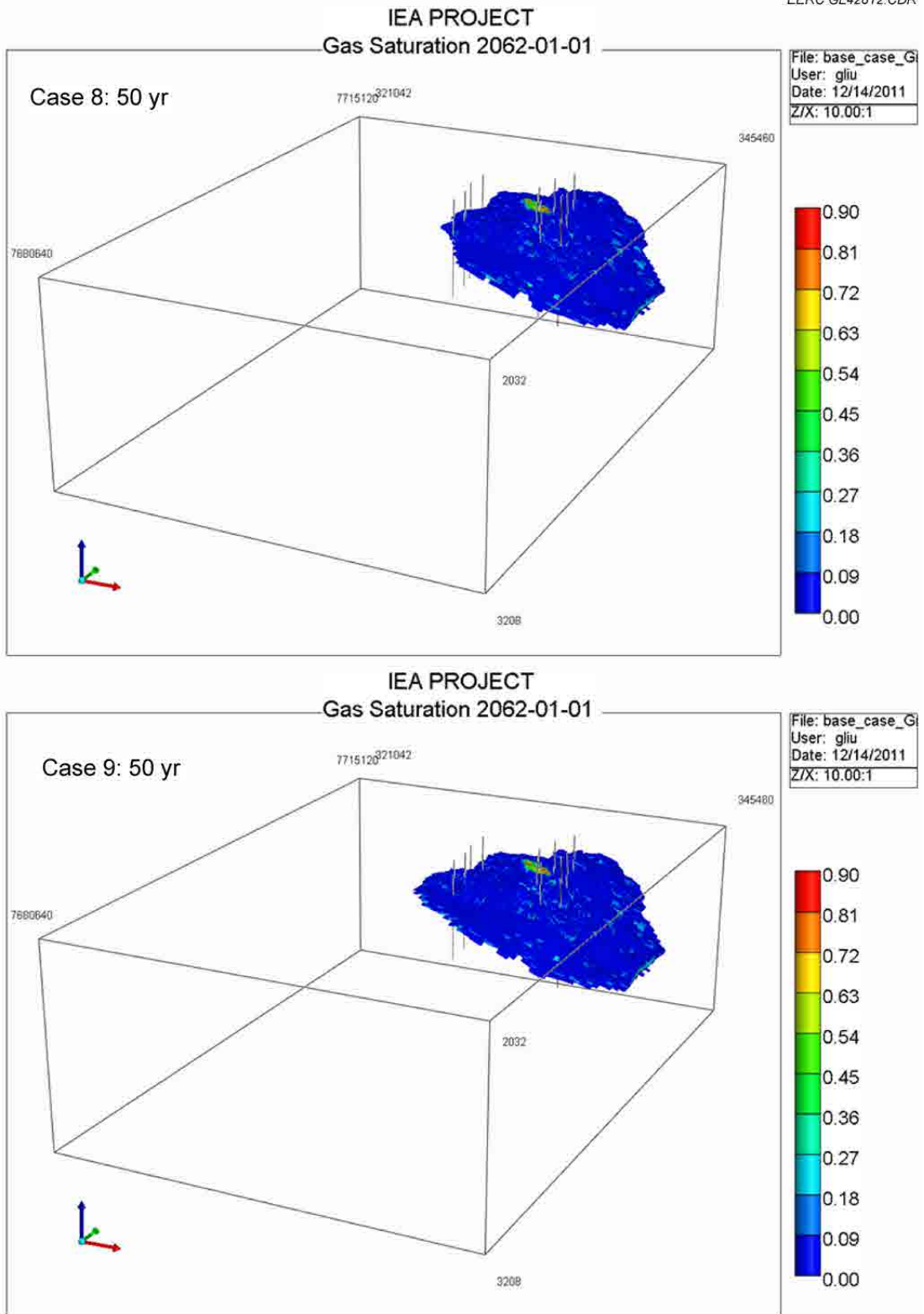


Figure E-115. 3-D view of CO₂ plume migration for 50 years from beginning of injection for Cases 8 and 9 (with and without water extraction).

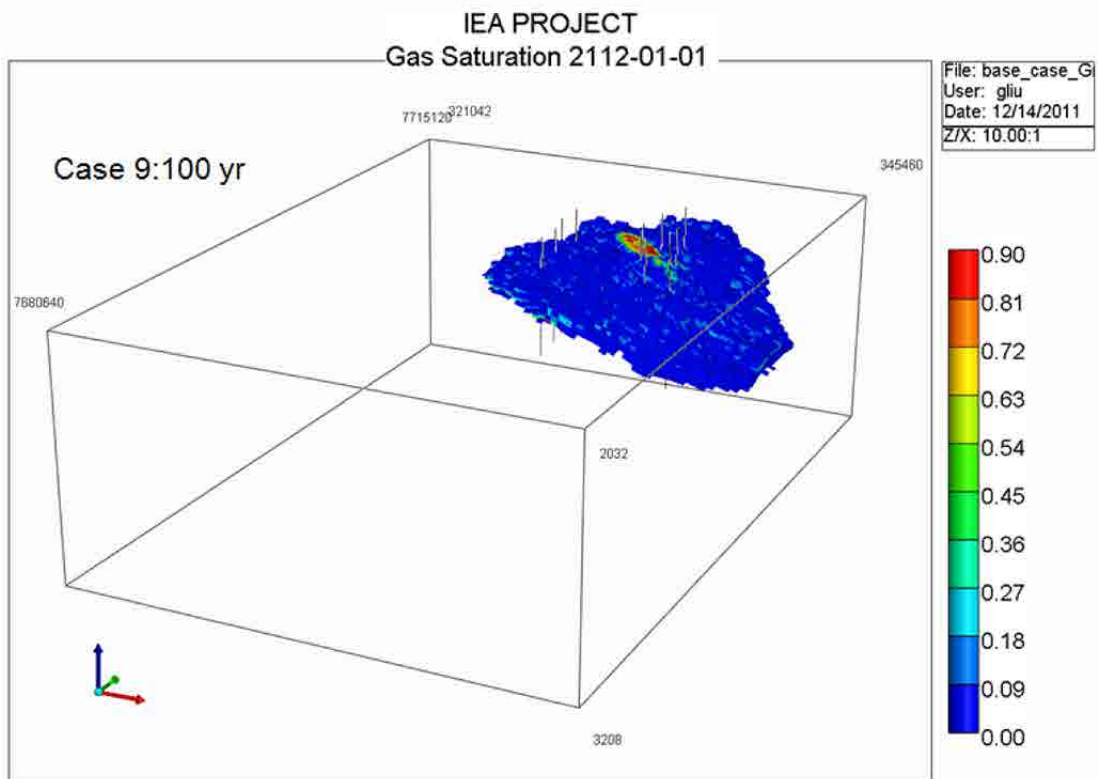
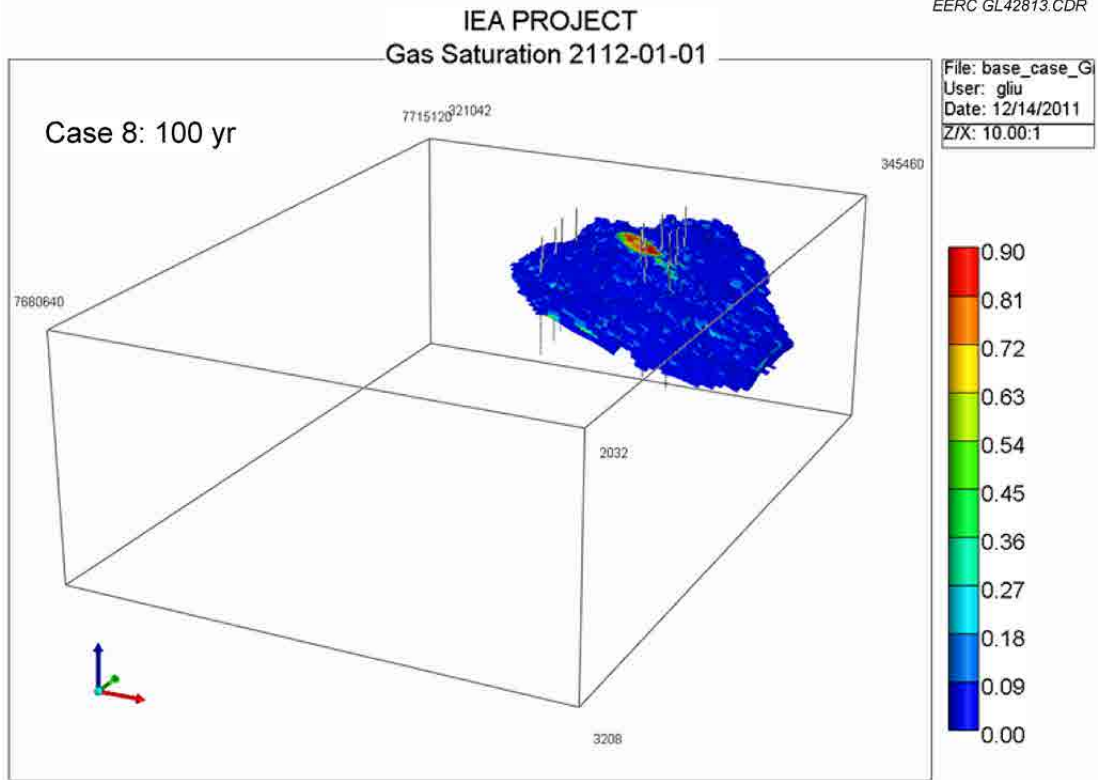


Figure E-116. 3-D view of CO₂ plume migration for 100 years from beginning of injection for Cases 8 and 9 (with and without water extraction).

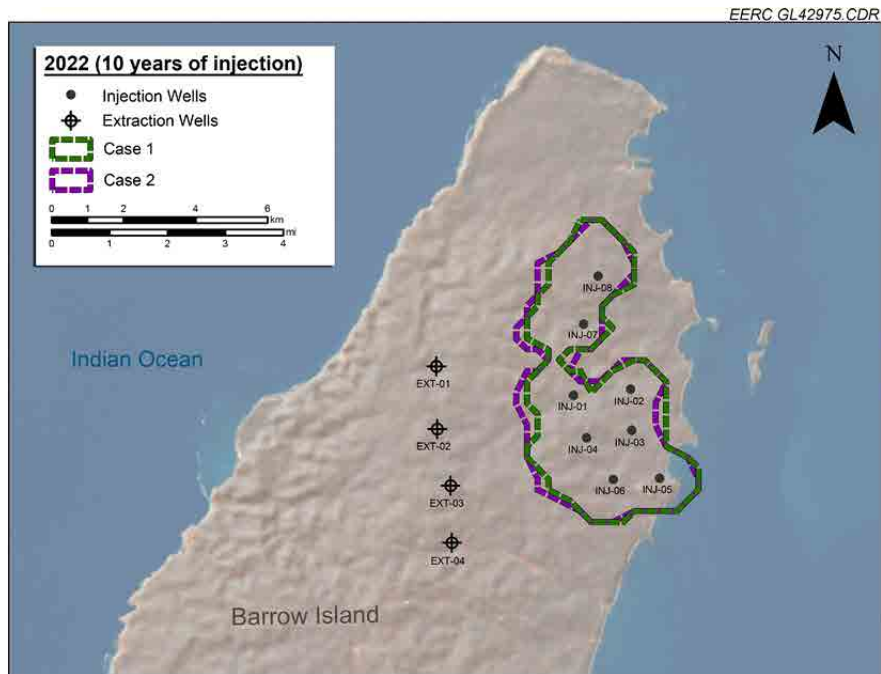


Figure E-117. Surface map view showing the plume extents generated by Cases 1 and 2 after 10 years.

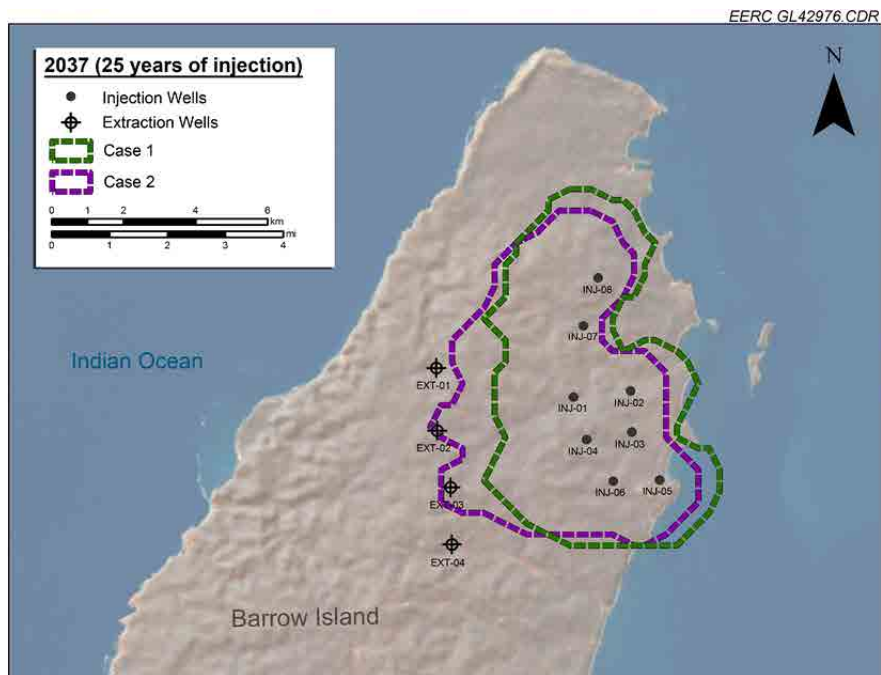


Figure E-118. Surface map view showing the plume extents generated by Cases 1 and 2 after 25 years.

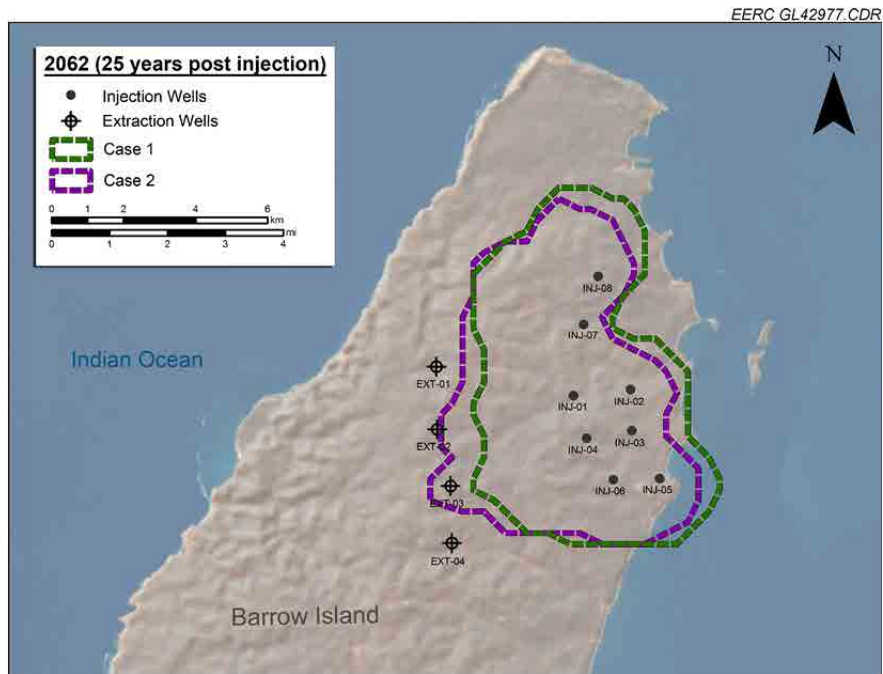


Figure E-119. Surface map view showing the plume extents generated by Cases 1 and 2 after 50 years.

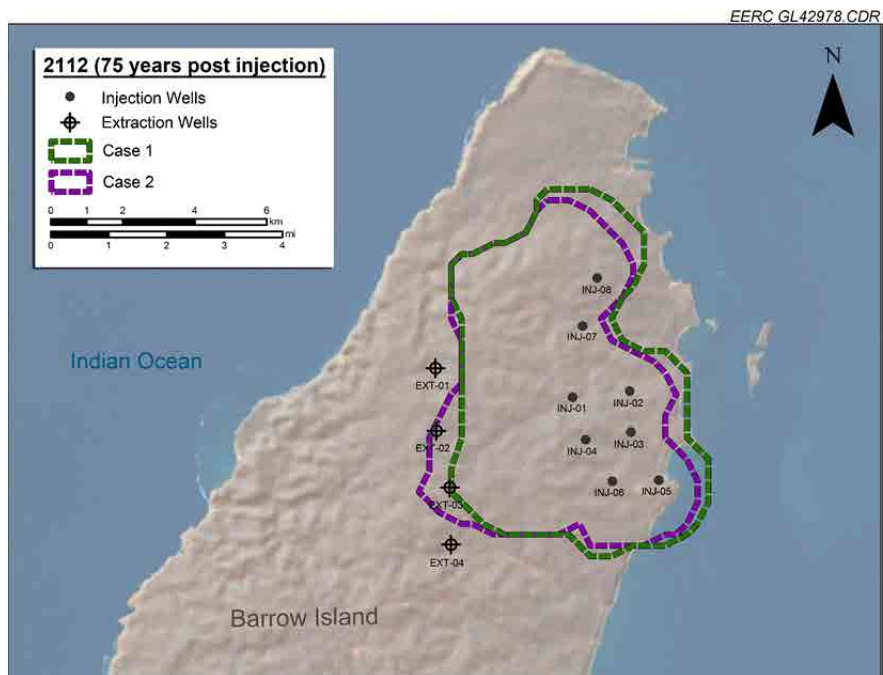


Figure E-120. Surface map view showing the plume extents generated by Cases 1 and 2 after 100 years.

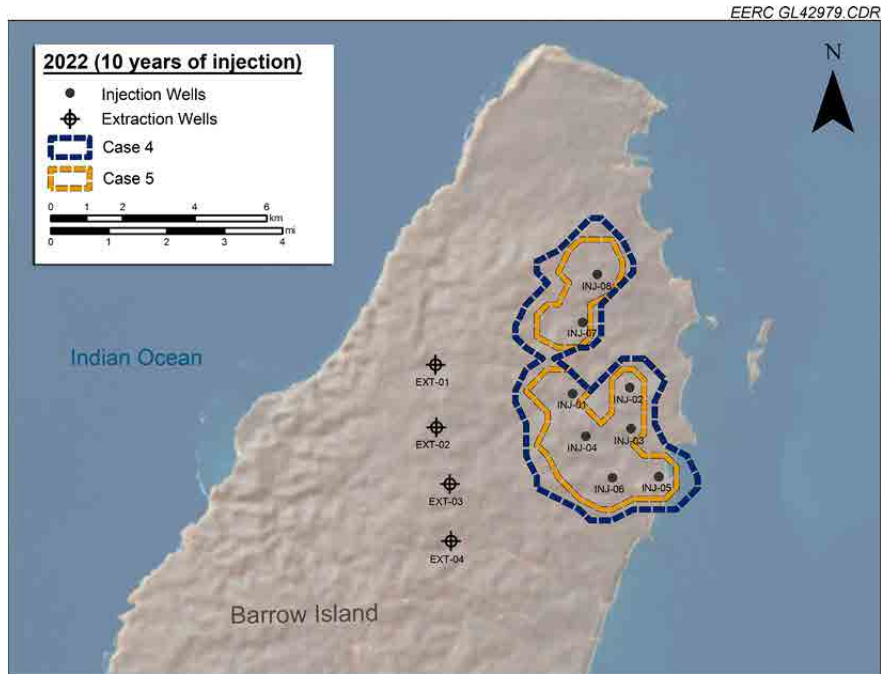


Figure E-121. Surface map view showing the plume extents generated by Cases 4 and 5 after 10 years.

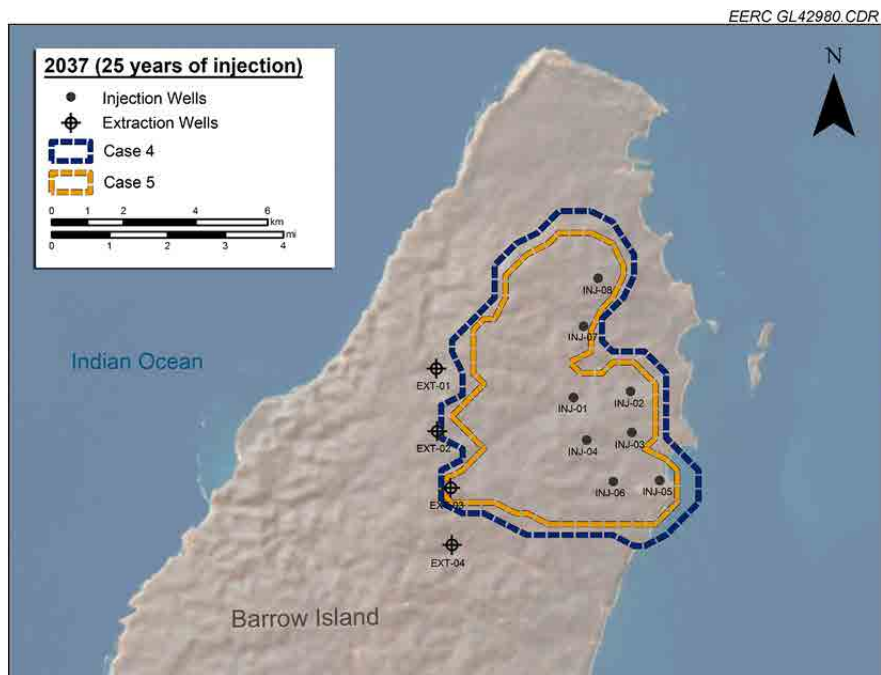


Figure E-122. Surface map view showing the plume extents generated by Cases 4 and 5 after 25 years.

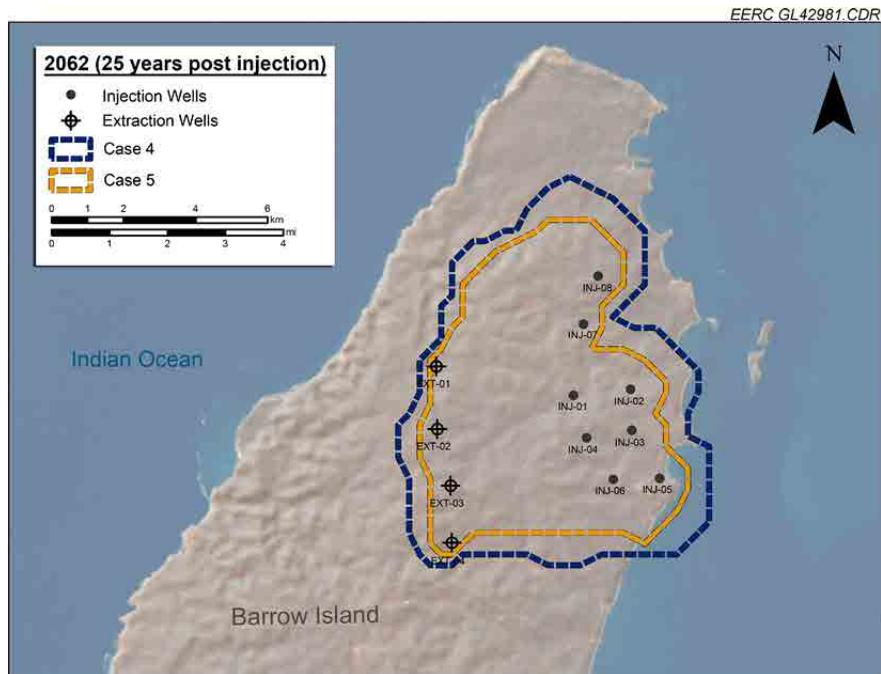


Figure E-123. Surface map view showing the plume extents generated by Cases 4 and 5 after 50 years.

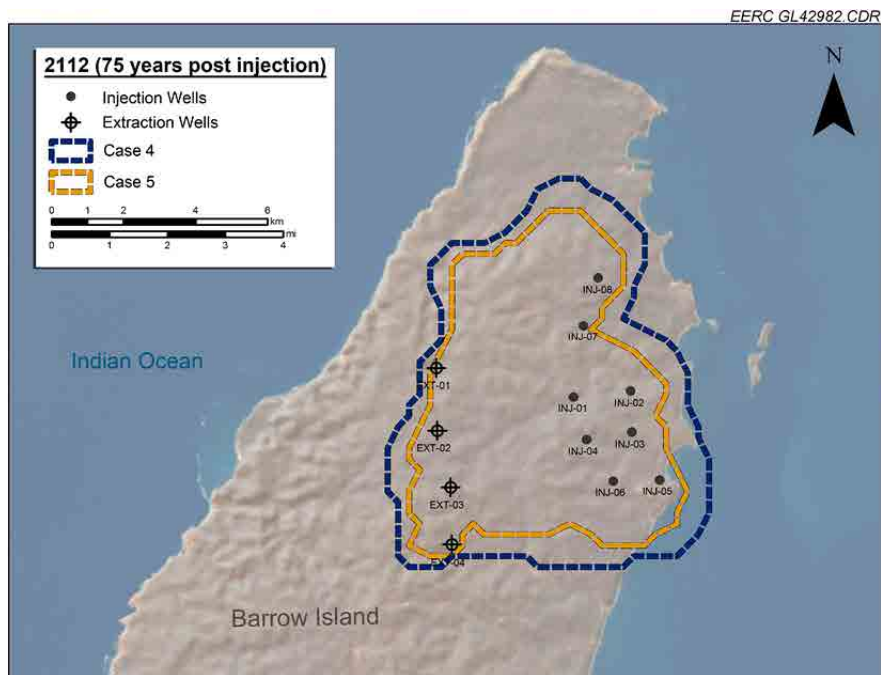


Figure E-124. Surface map view showing the plume extents generated by Cases 4 and 5 after 100 years.

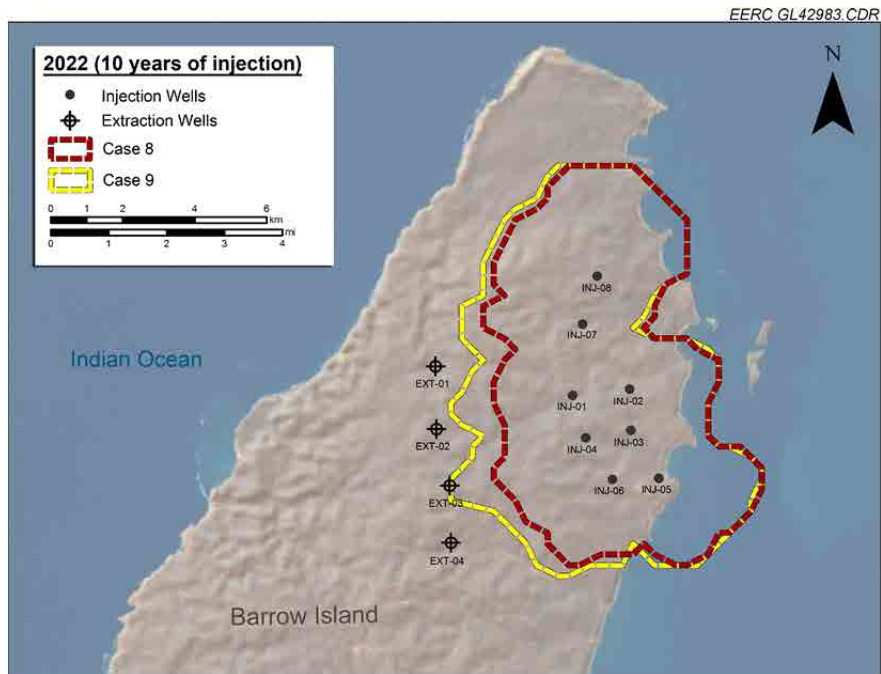


Figure E-125. Surface map view showing the plume extents generated by Cases 8 and 9 after 10 years.

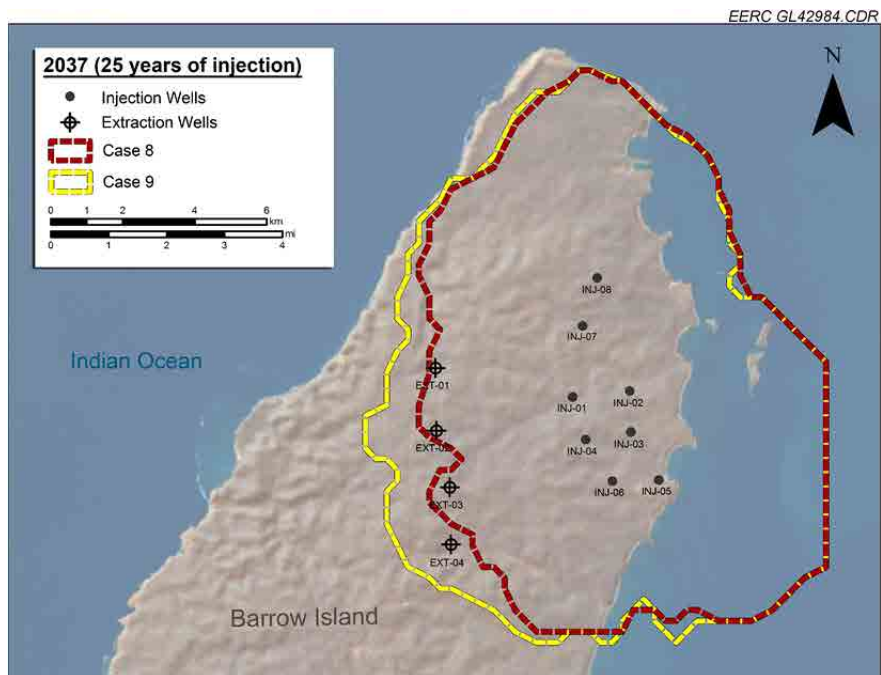


Figure E-126. Surface map view showing the plume extents generated by Cases 8 and 9 after 25 years.

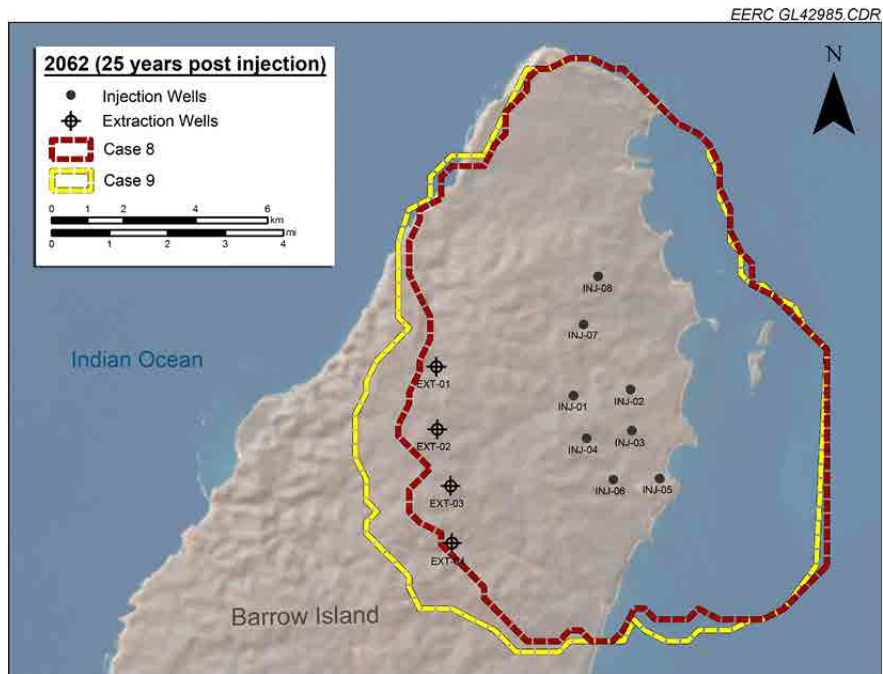


Figure E-127. Surface map view showing the plume extents generated by Cases 8 and 9 after 50 years.

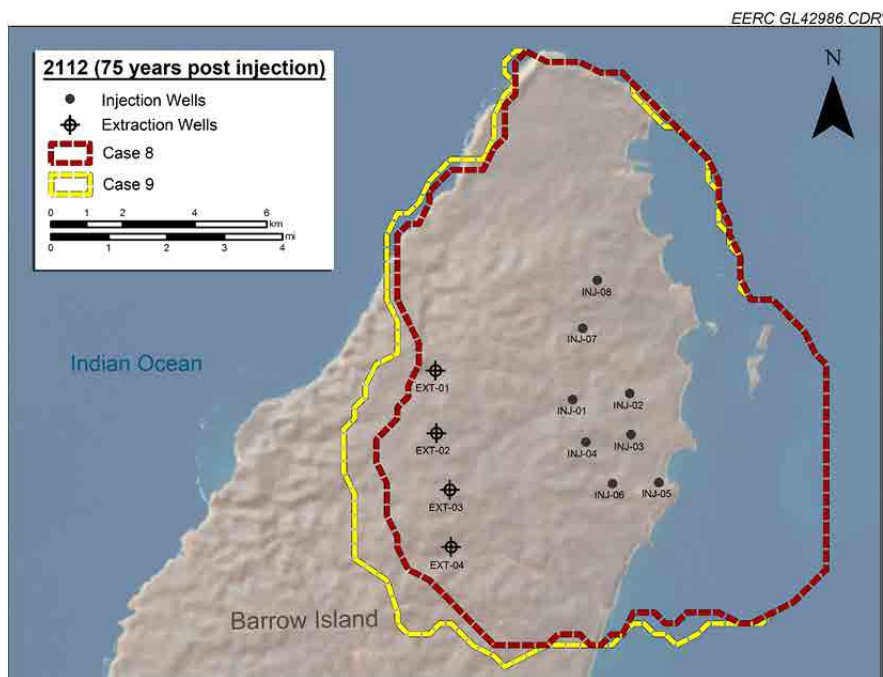


Figure E-128. Surface map view showing the plume extents generated by Cases 8 and 9 after 100 years.

APPENDIX F

TEAPOT DOME MODELING AND SIMULATIONS

TEAPOT DOME MODELING AND SIMULATIONS

As shown in Figure F-1 for the stratigraphic column of the Teapot Dome, the Dakota, Lakota, and Tensleep Formations are located below 1200 meters where pressure and temperature conditions are sufficient for CO₂ to be held in a supercritical state. In this study, the modeling and simulations for CO₂ storage and water extraction were focused on the Dakota and Lakota Formations because of favorable permeability and porosity conditions (Figures F-2 and F-3).

DYNAMIC SIMULATIONS

A total of seven scenarios were designed to address the relationships between CO₂ storage and water extraction with injection and production strategies that include vertical and horizontal water extraction as well as CO₂-saturated water injection with recycle from water extraction (Table F-1).

Cases 1 and 2 show the results of CO₂ injection without any water extraction with a single injector and two injector scenarios. Although an additional CO₂ injector was added in Case 2, the total injected CO₂ is less than twice the amount in Case 1, attributed to be a factor of well location. The well location of Case 1 was used as primary injector (Inj_02) for the remaining scenarios.

Case 3 replaced the second well location with a water extraction well, which aided injection and was able to increase the total injected CO₂ more than double the values of the base case. This was further optimized in Case 4, which utilized a horizontal well design for injection and extraction wells, which increased efficiency and storage capacity by a factor of 3.7 compared to Case 1. The horizontal injector–producer pair was also found to outperform two horizontal injection wells (Case 5).

Cases 6 and 7 were performed to analyze the efficiency of surface saturated water using recycled extracted fluid. Case 6 used one horizontal injector and one horizontal producer, which were found to be more efficient than the vertical injector and producer scenario in Case 7.

Detailed results of total injected CO₂, well rates and bottomhole pressures (BHPs), CO₂ plumes, and pressure distributions over time are shown in Figures F-4 through F-111 ordered by plots, 3-D view, areal view, and cross-sectional view.

REFERENCES

Curry, W.H., 1977, Teapot Dome—past, present, and future: American Association of Petroleum Geologists Bulletin, v. 61, no. 5.

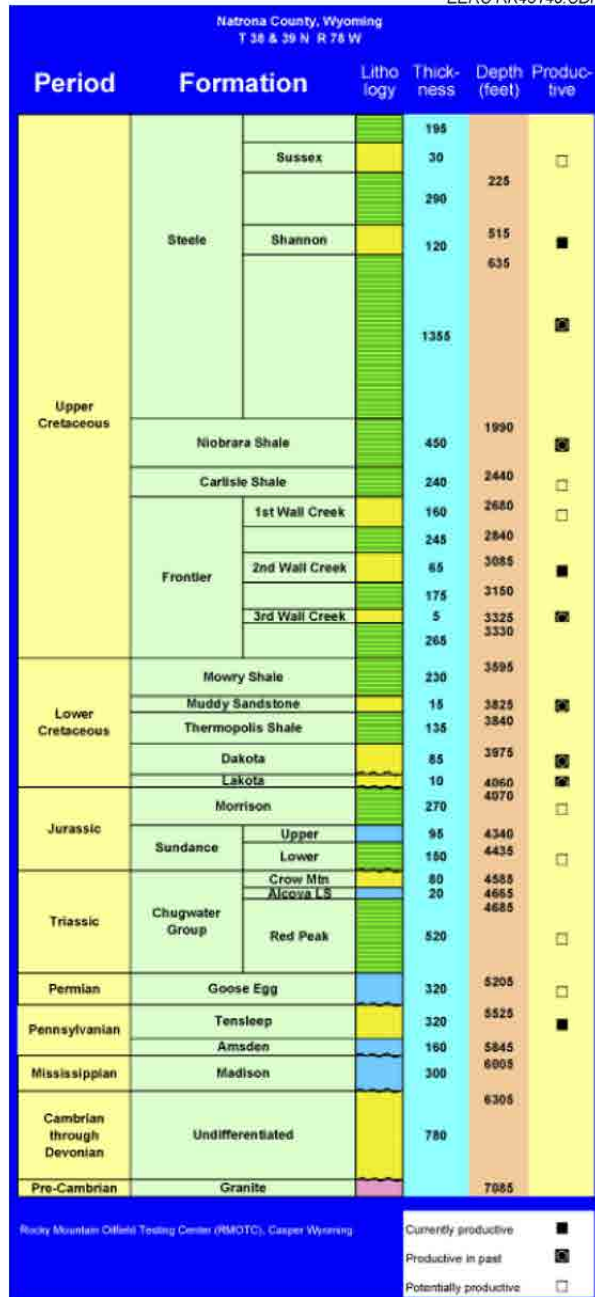


Figure F-1. Stratigraphic column of Teapot Dome (Curry, 1977).

Table F-1. Detailed Properties of the Simulation Cases Investigated

Variable	Unit	Case 1	Case 2	Case 3	Case 4	Case 5	Case 6 (surface dissolution)	Case 7 (surface dissolution)
Target Injection Rate/Well	Mt/year	2.0	2.0	2.0	2.0	2.0	2.4 solvent (moles/kg)	2.4 solvent (moles/kg)
Actual Injection Rate	kg/day	5.65E+05	8.37E+05	1.21E+06	2.09E+06	1.95E+06	2.35E+03	3.15E+02
Injection Period	Years	25	25	25	25	25	12.35	25
Cumulative Injected CO ₂	SC, ¹ tonnes	5.16E+06	7.64E+06	1.11E+07	1.91E+07	1.78E+07	5.64E+05	1.54E+05
Cumulative Injected CO ₂	RC, ² m ³	8.16E+06	1.23E+07	1.70E+07	2.85E+07	2.66E+07	N/A	N/A
Number of Injection Wells		1	2	1	1 (horizontal)	2 (horizontal)	1 (horizontal)	1
Extraction Wells Present		No	No	1	1 (horizontal)	No	1 (horizontal)	1
Extraction Well Location		N/A	N/A	EXT-01	EXT-01	N/S	EXT-01	EXT-01
Cumulative Extracted Water	RC, ² m ³	N/A	N/A	1.54E+07	1.77E+07	N/A	2.92E+07	1.49E+07
Average Daily Extraction Rate	SC, ¹ m ³ /day	N/A	N/A	1.66D+03	6.70E+03	N/A	6.35E+03	1.60E+03
Average Extraction Period	years	N/A	N/A	25	7.10	N/A	12.35	25.00
Highest Injection BHP	kPa	14,500	14,500 and 19,820	19,820	19,820	19,820 & 21,450	19,820	19,820
Lowest Production BHP	kPa	N/A	N/A	2,000	2000	N/A	2000	2000
Boundary Conditions		Semiclosed	Semiclosed	Semiclosed	Semiclosed	Semiclosed	Semiclosed	Semiclosed

¹ Standard conditions (25°C, 0.999 bar).

² Reservoir conditions (variable with depth, average of 255°C, 0.986 bar).

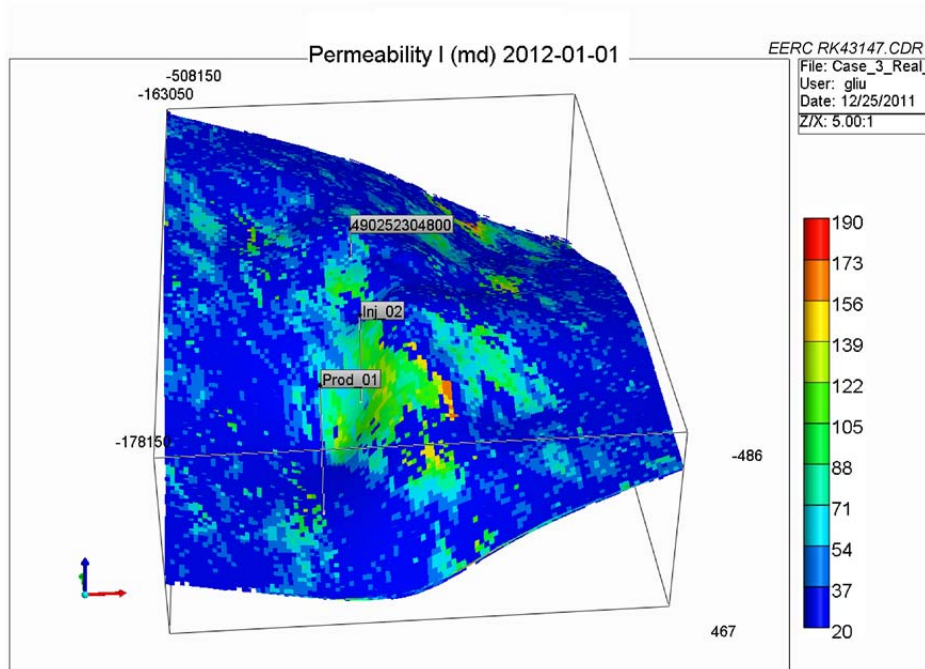


Figure F-2. Permeability of Dakota and Lakota Formations and well locations.

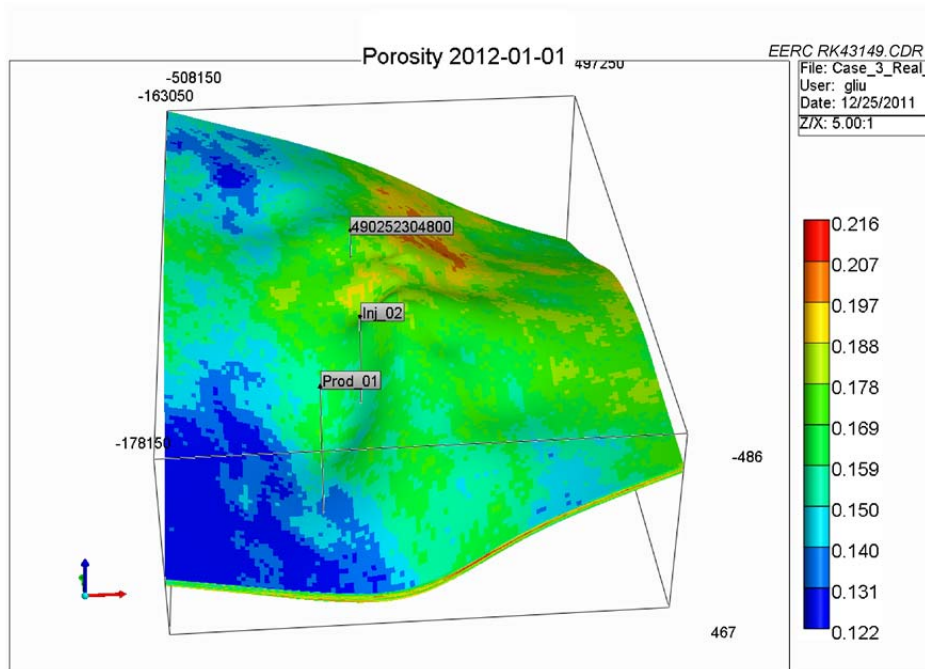


Figure F-3. Porosity of Dakota and Lakota Formations.

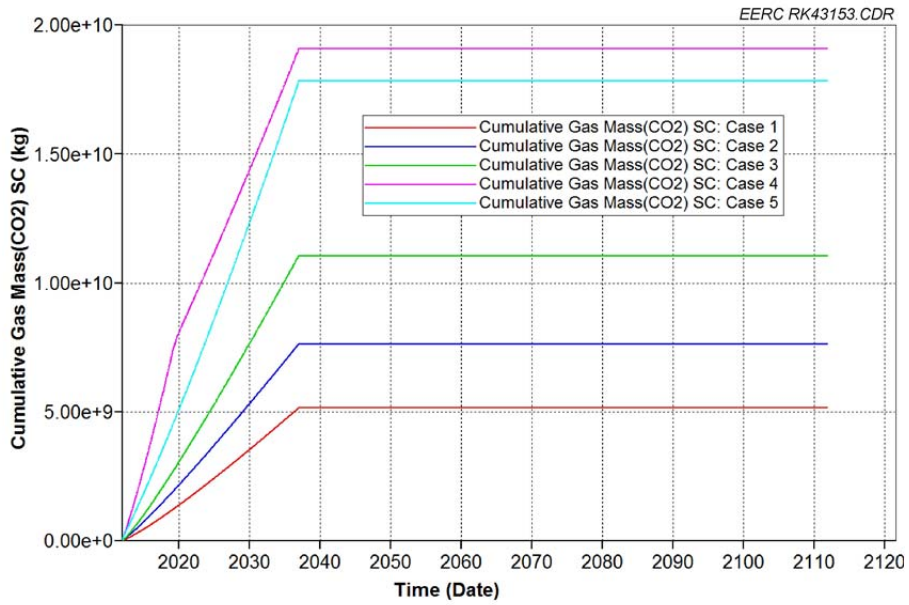


Figure F-4. Total injected CO₂ in Cases 1 to 5.

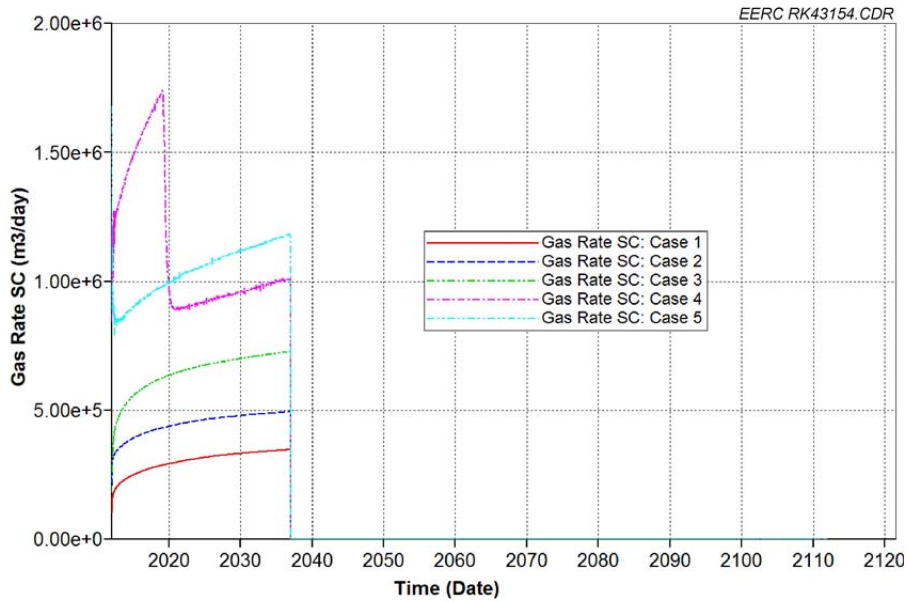


Figure F-5. CO₂ injection rate in Cases 1 to 5.

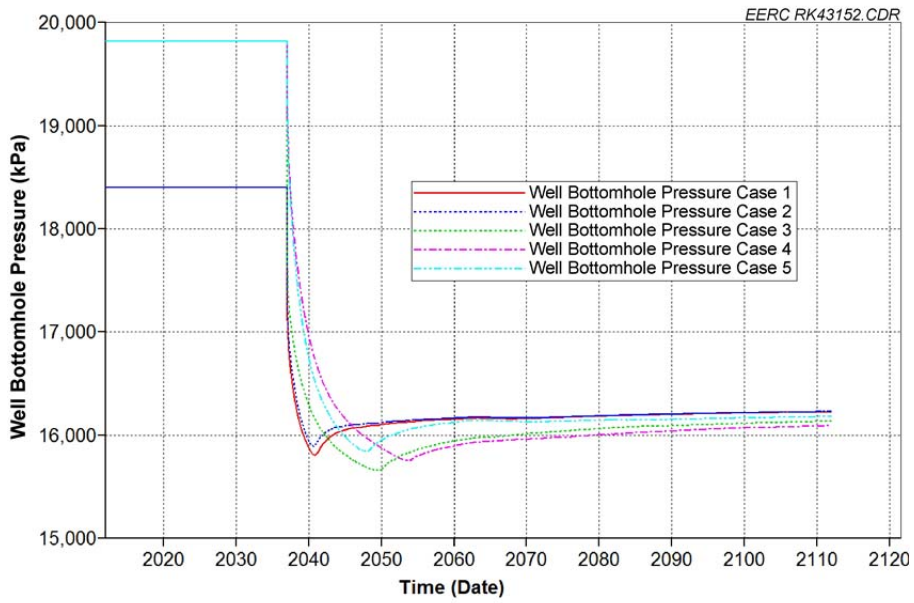


Figure F-6. BHPs of injection well in Cases 1 to 5.

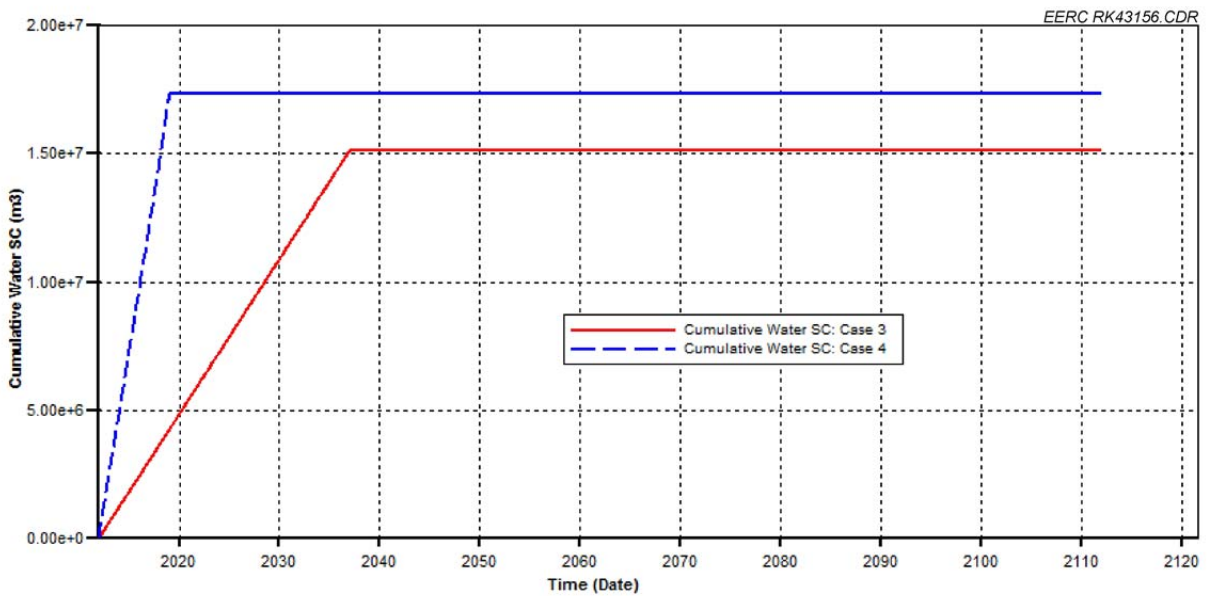


Figure F-7. Total produced water in Cases 3 and 4.

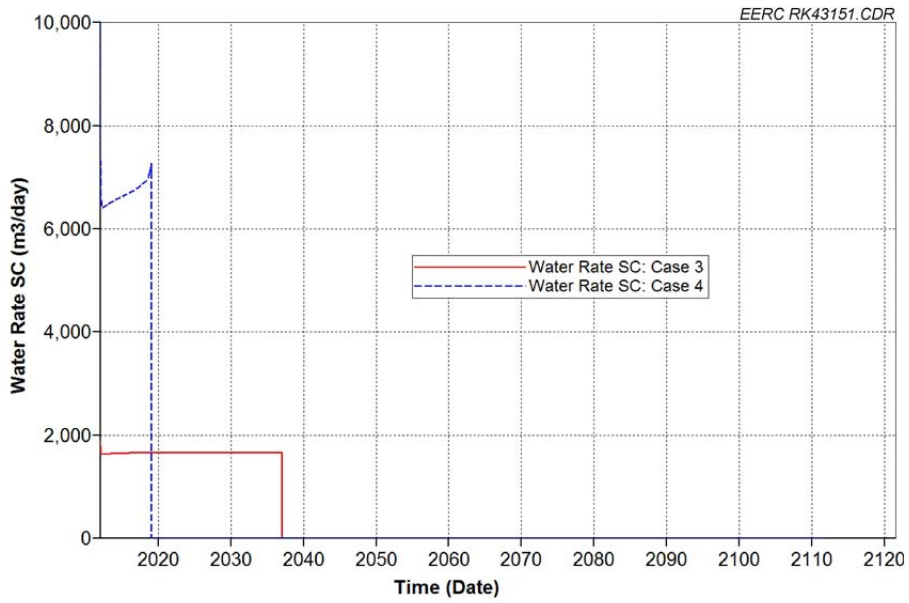


Figure F-8. Water production rate in Cases 3 and 4.

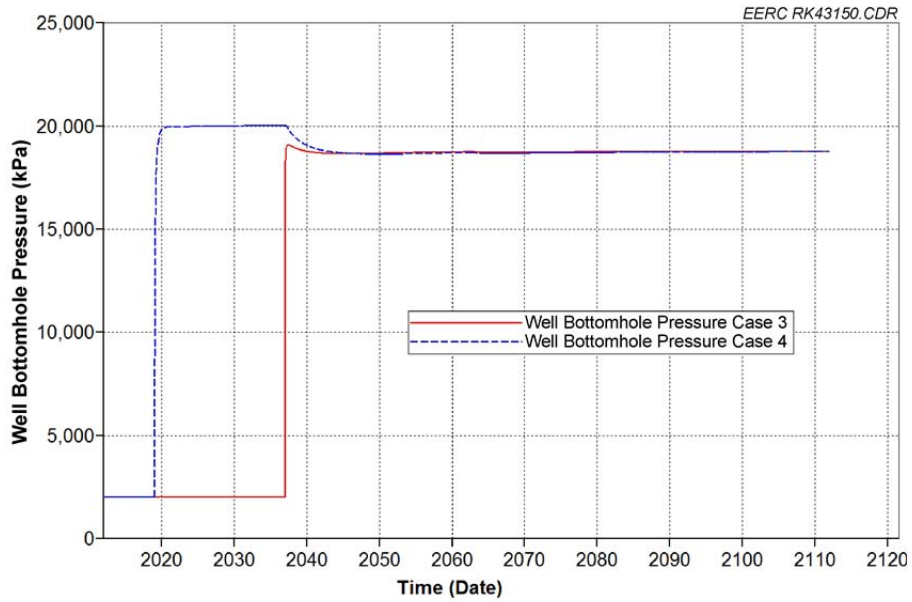


Figure F-9. BHPs of production well in Cases 3 to 4.

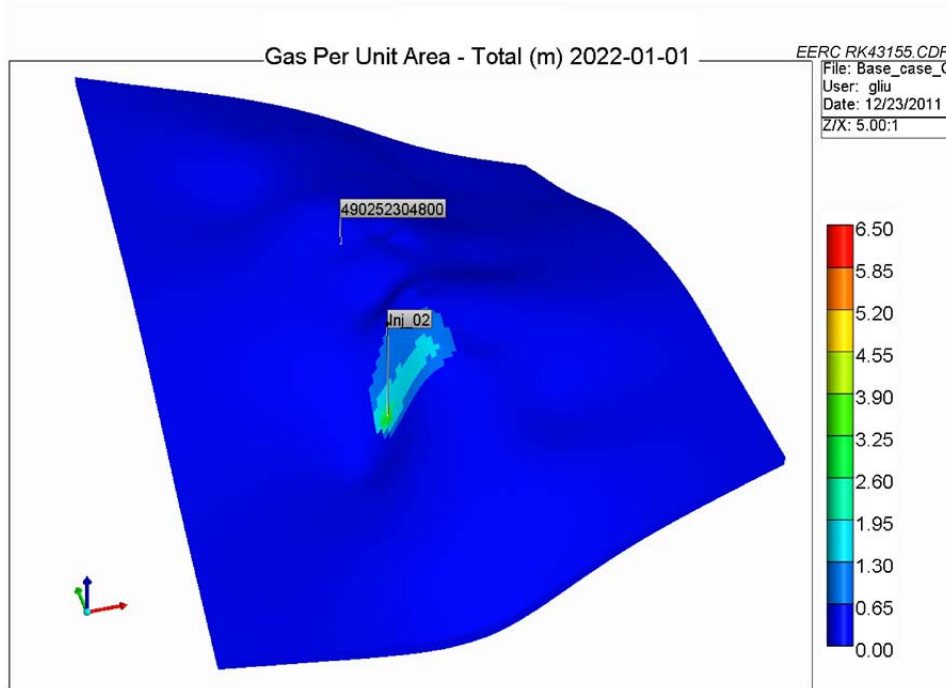


Figure F-10. 3-D view of Case 1: CO₂ plume migration for 10 years from beginning of injection.

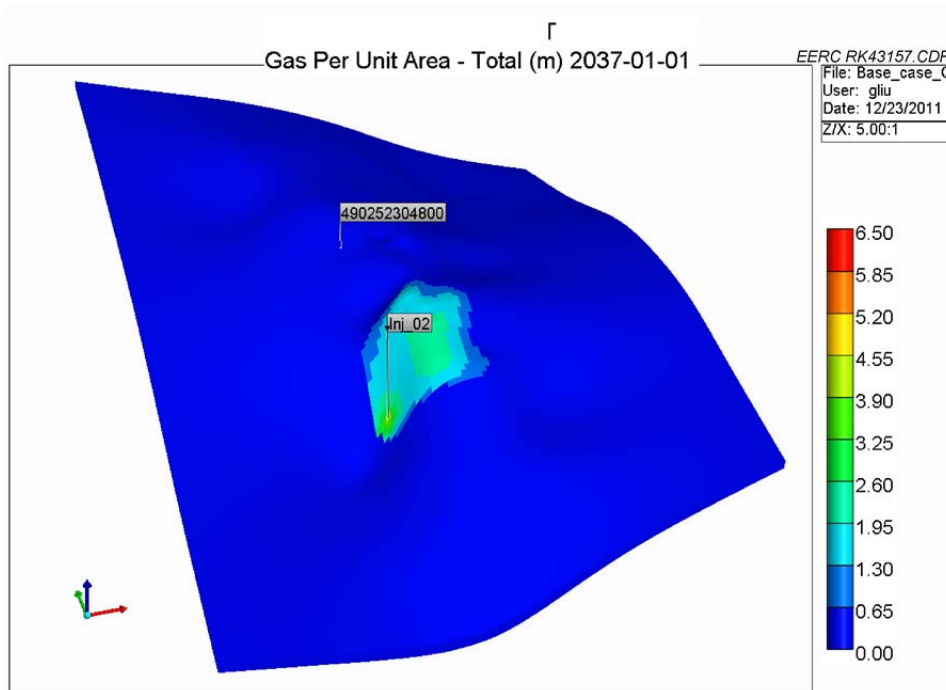


Figure F-11. 3-D view of Case 1: CO₂ plume migration for 25 years from beginning of injection.

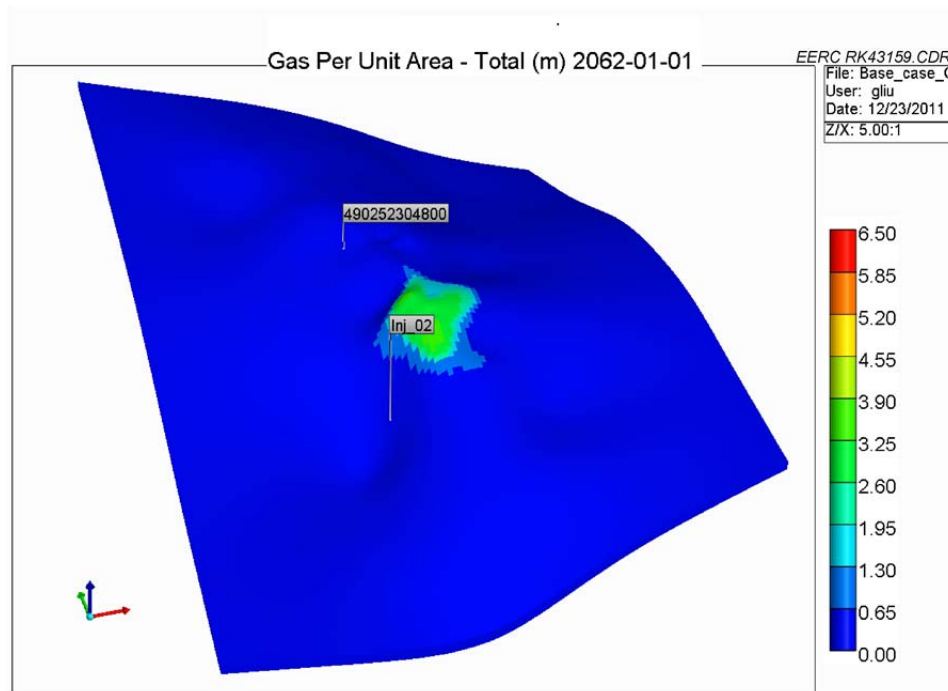


Figure F-12. 3-D view of Case 1: CO₂ plume migration for 50 years from beginning of injection.

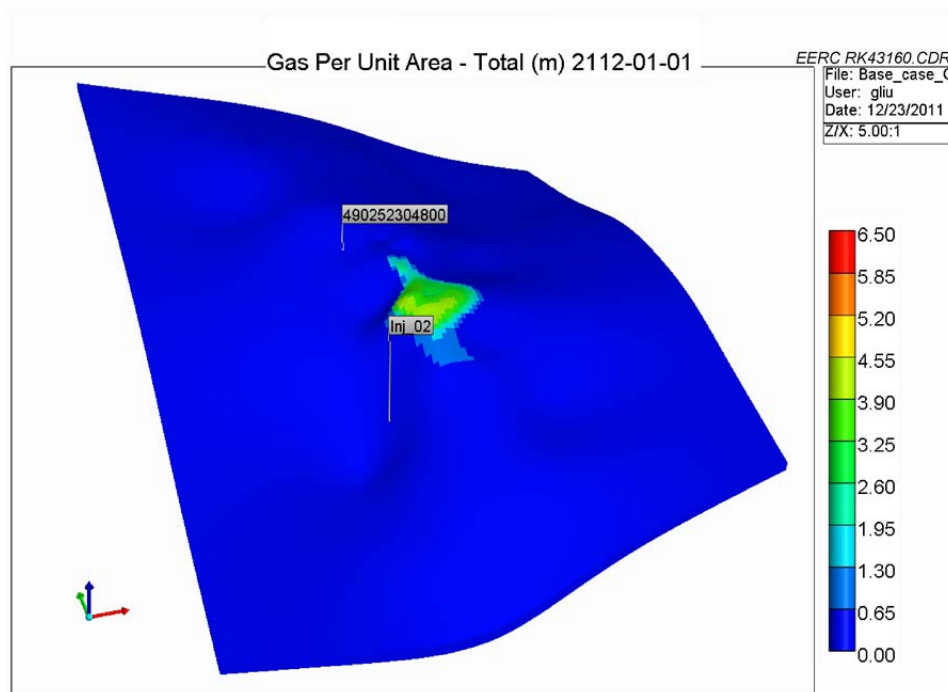


Figure F-13. 3-D view of Case 1: CO₂ plume migration for 100 years from beginning of injection.

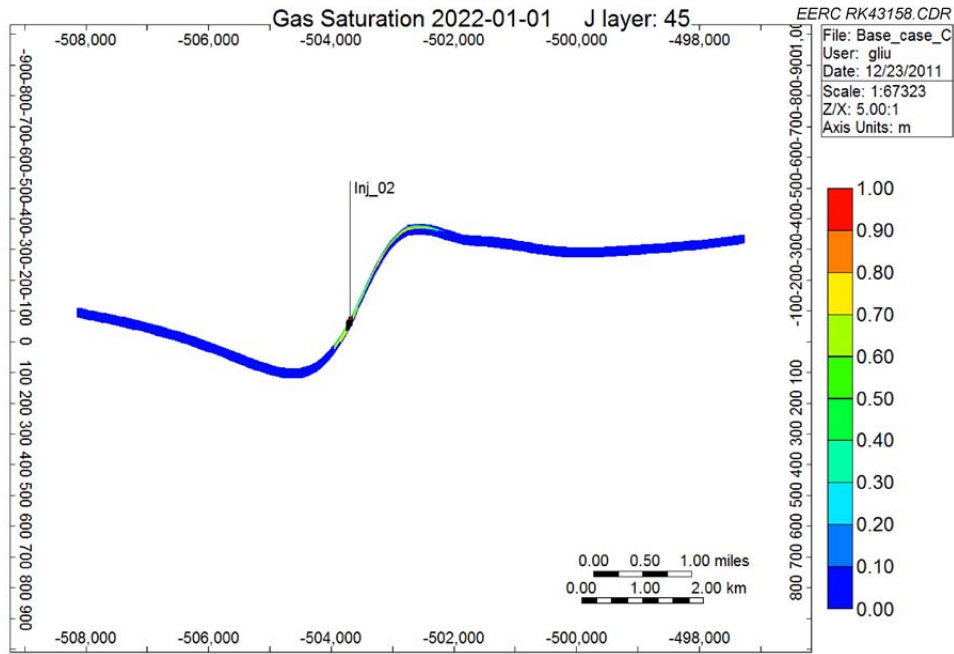


Figure F-14. Cross-sectional view of Case 1: CO₂ plume migration for 10 years from beginning of injection.

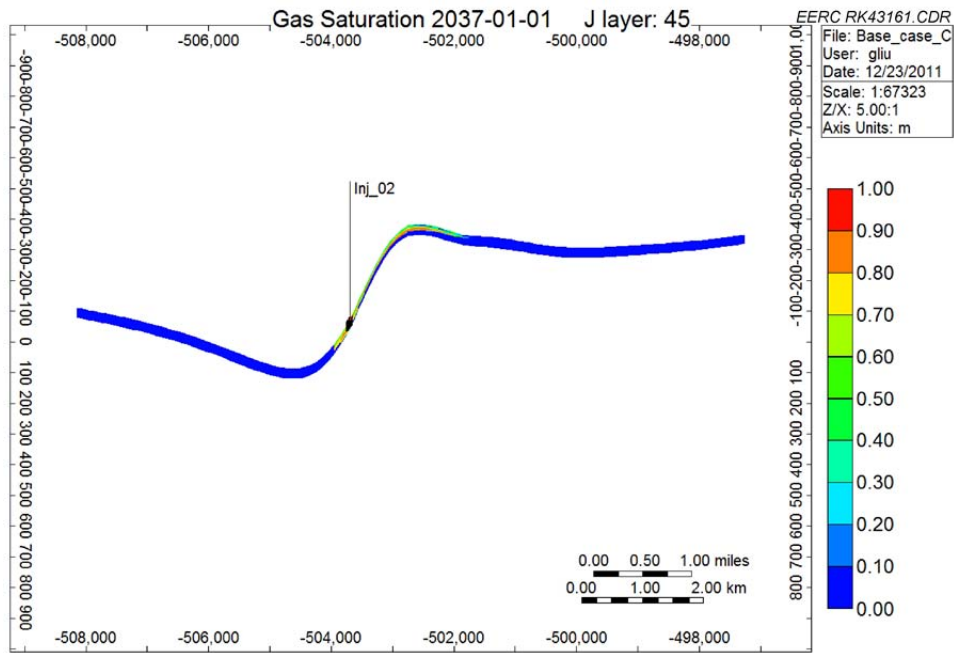


Figure F-15. Cross-sectional view of Case 1: CO₂ plume migration for 25 years from beginning of injection.

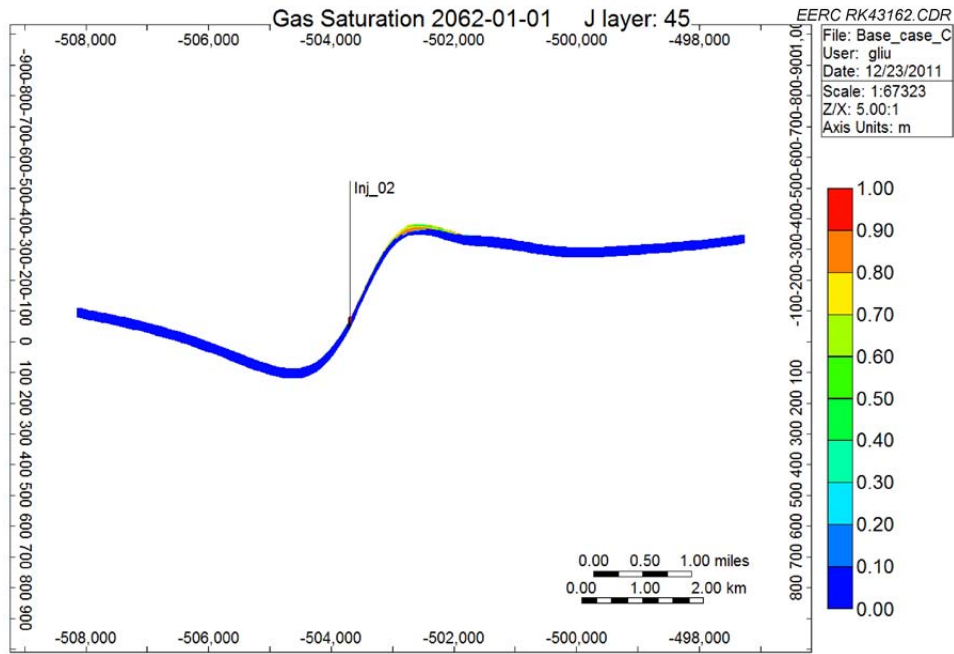


Figure F-16. Cross-sectional view of Case 1: CO₂ plume migration for 50 years from beginning of injection.

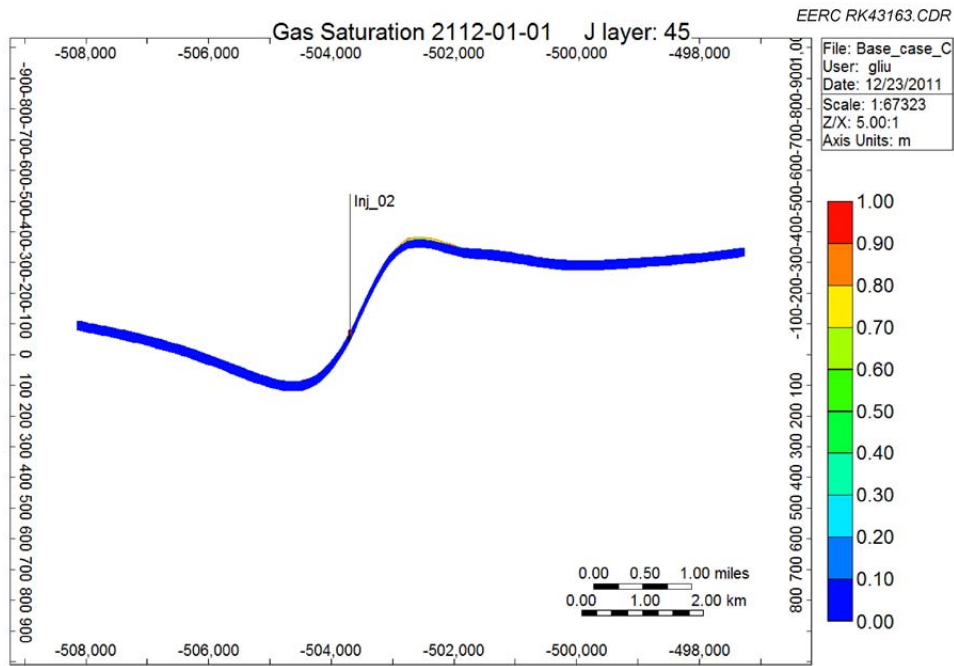


Figure F-17. Cross-sectional view of Case 1: CO₂ plume migration for 100 years from beginning of injection.

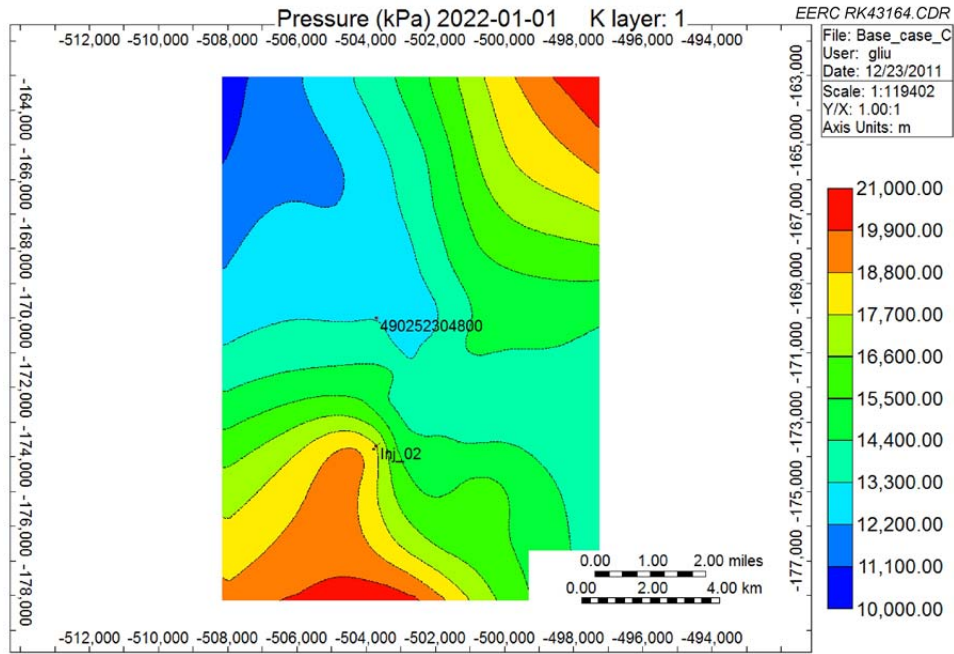


Figure F-18. Areal view of Case 1: pressure distributions for 10 years from beginning of injection.

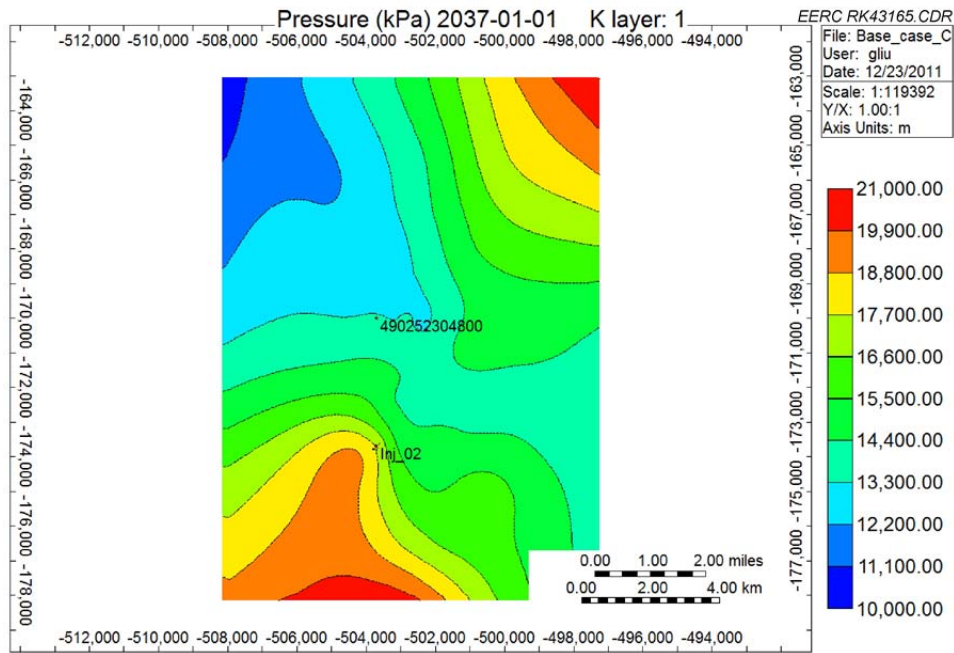


Figure F-19. Areal view of Case 1: pressure distributions for 25 years from beginning of injection.

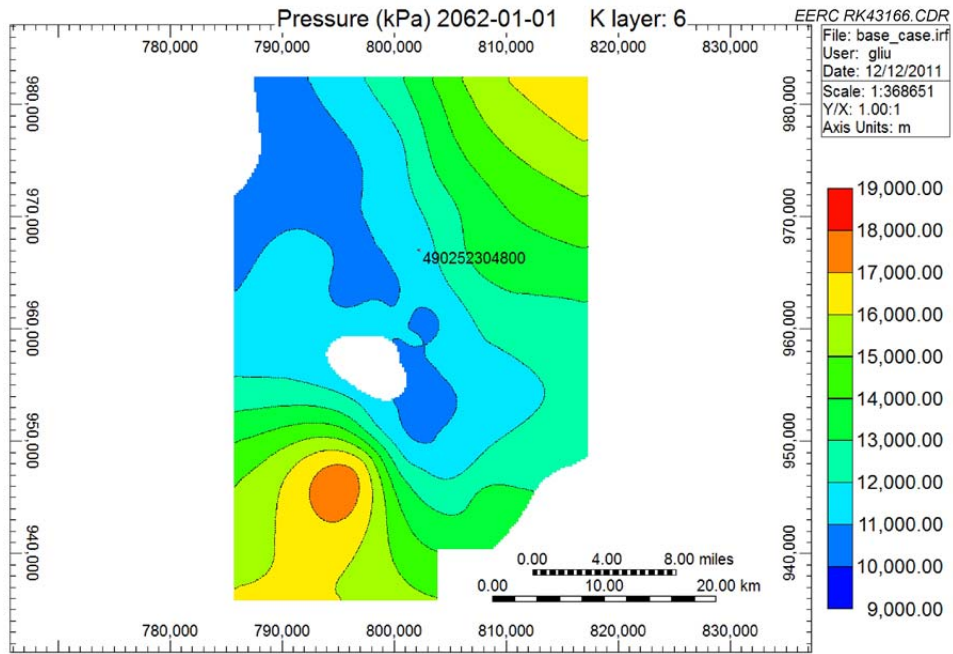


Figure F-20. Areal view of Case 1: pressure distributions for 50 years from beginning of injection.

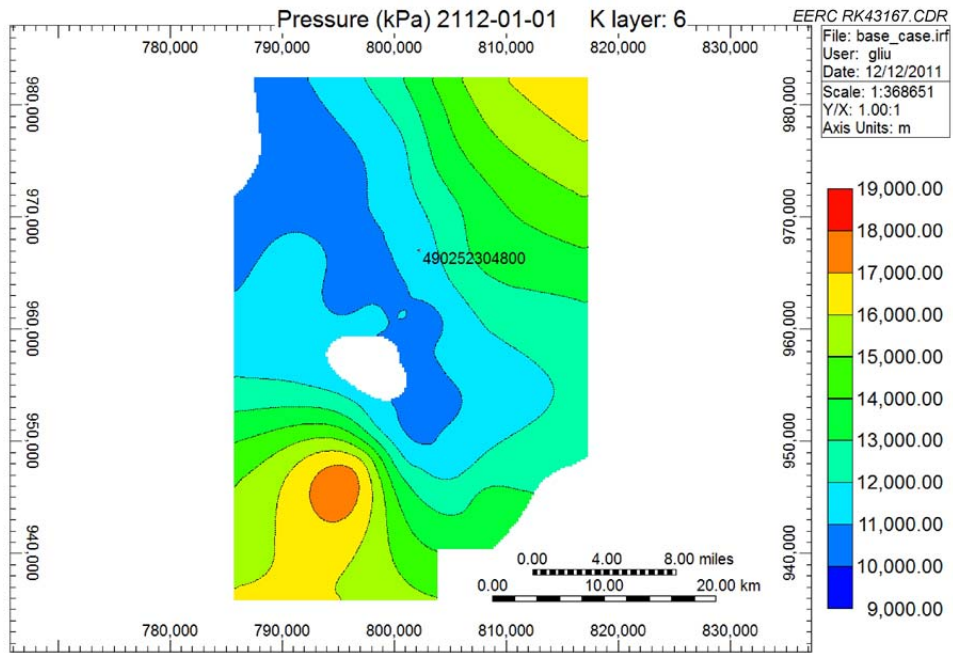


Figure F-21. Areal view of Case 1: pressure distributions for 100 years from beginning of injection.

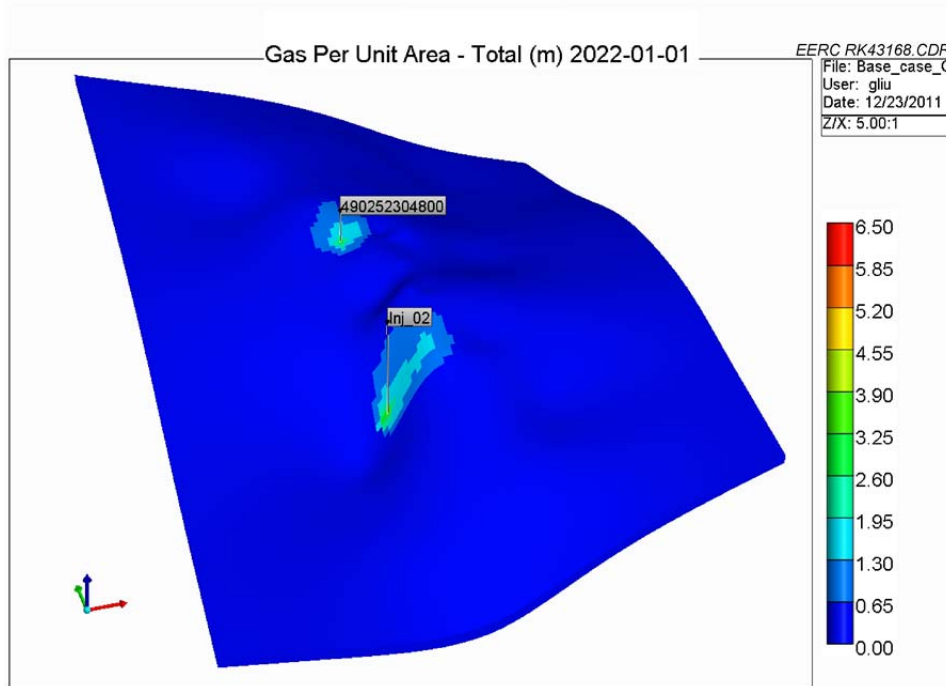


Figure F-22. 3-D view of Case 2: CO₂ plume migration for 10 years from beginning of injection.

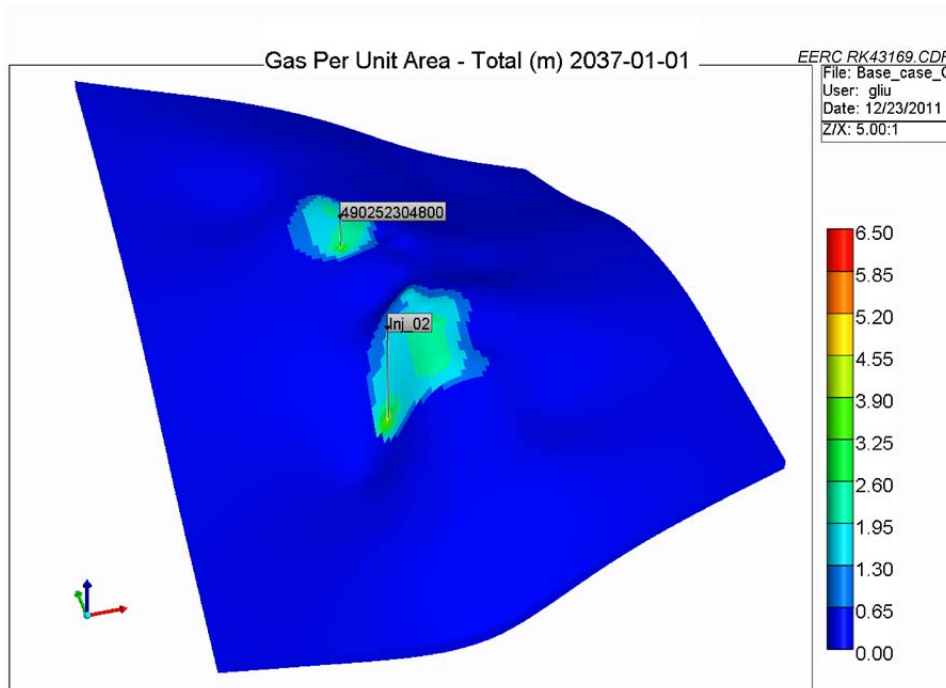


Figure F-23. 3-D view of Case 2: CO₂ plume migration for 25 years from beginning of injection.

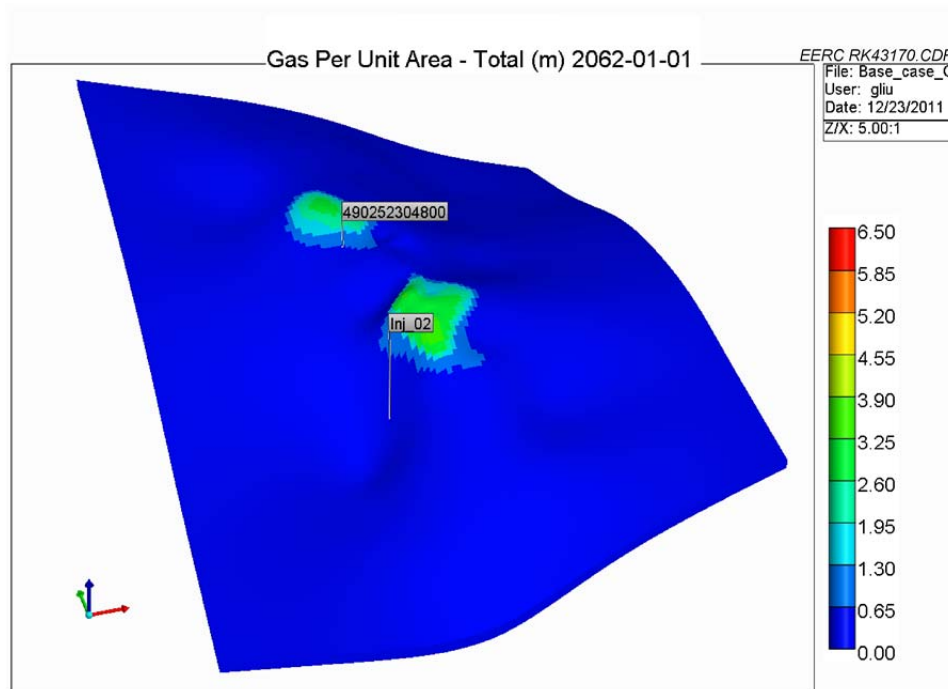


Figure F-24. 3-D view of Case 2: CO₂ plume migration for 50 years from beginning of injection.



Figure F-25. 3-D view of Case 2: CO₂ plume migration for 100 years from beginning of injection.

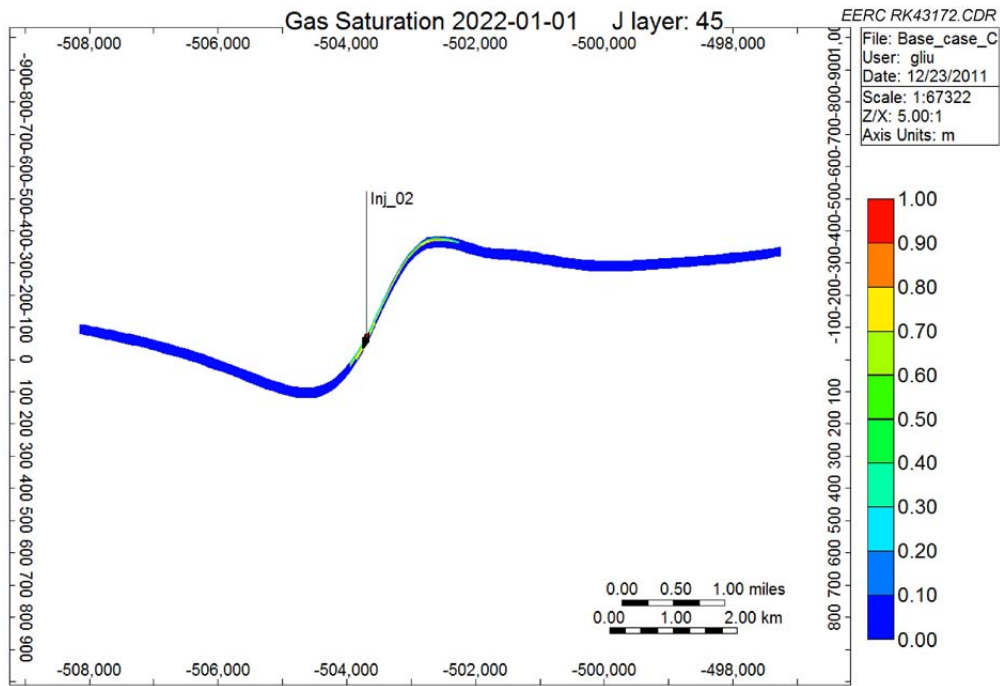


Figure F-26. Cross-sectional view of Case 2: CO₂ plume migration for 10 years from beginning of injection.

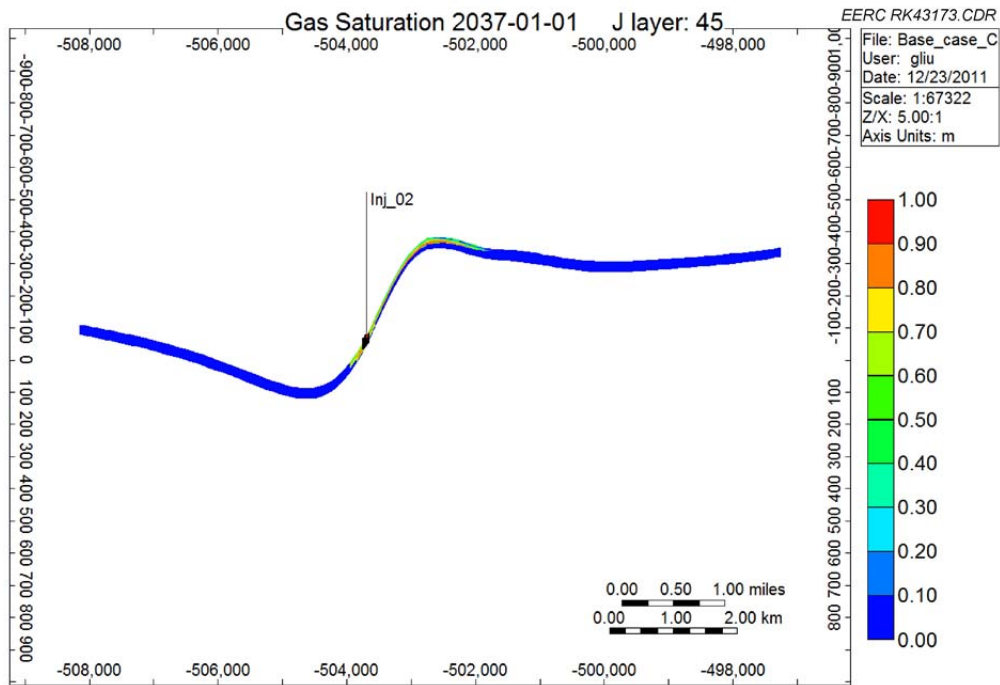


Figure F-27. Cross-sectional view of Case 2: CO₂ plume migration for 25 years from beginning of injection.

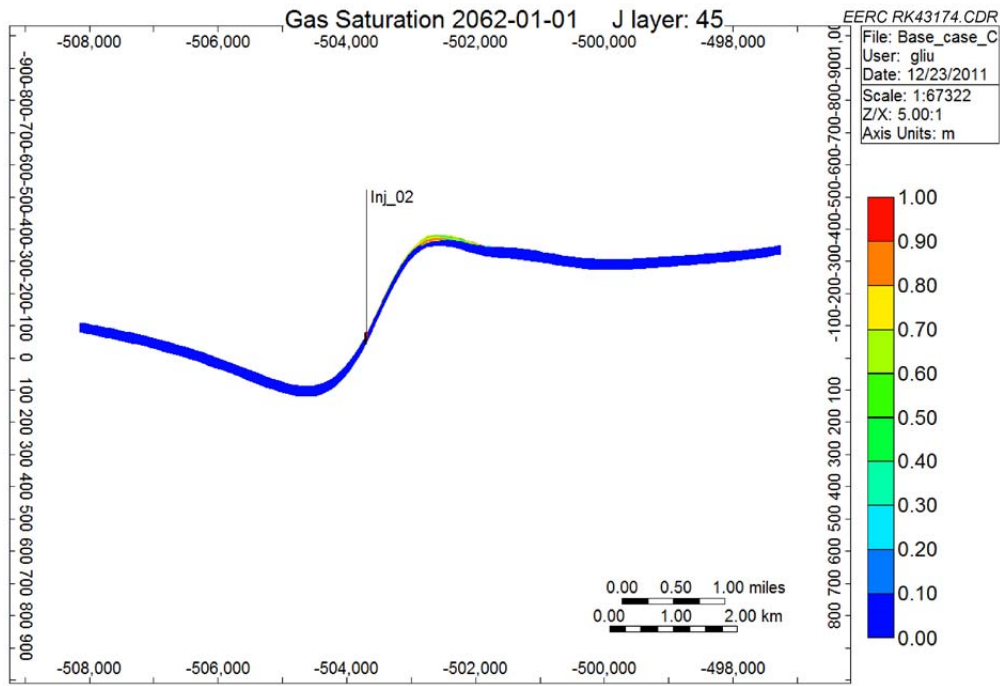


Figure F-28. Cross-sectional view of Case 2: CO₂ plume migration for 50 years from beginning of injection.

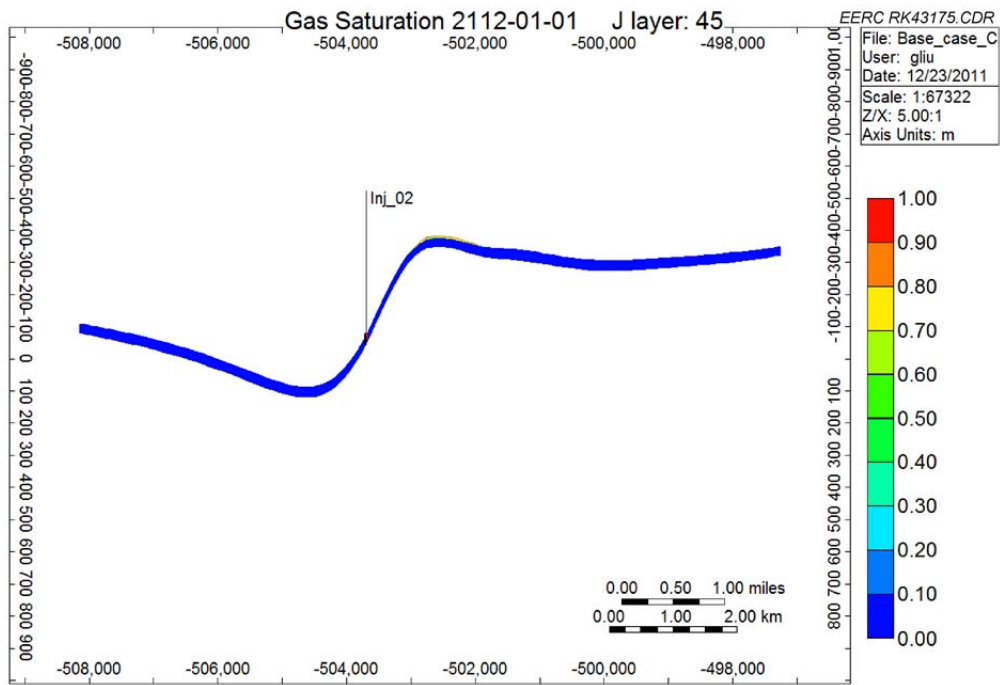


Figure F-29. Cross-sectional view of Case 2: CO₂ plume migration for 100 years from beginning of injection.

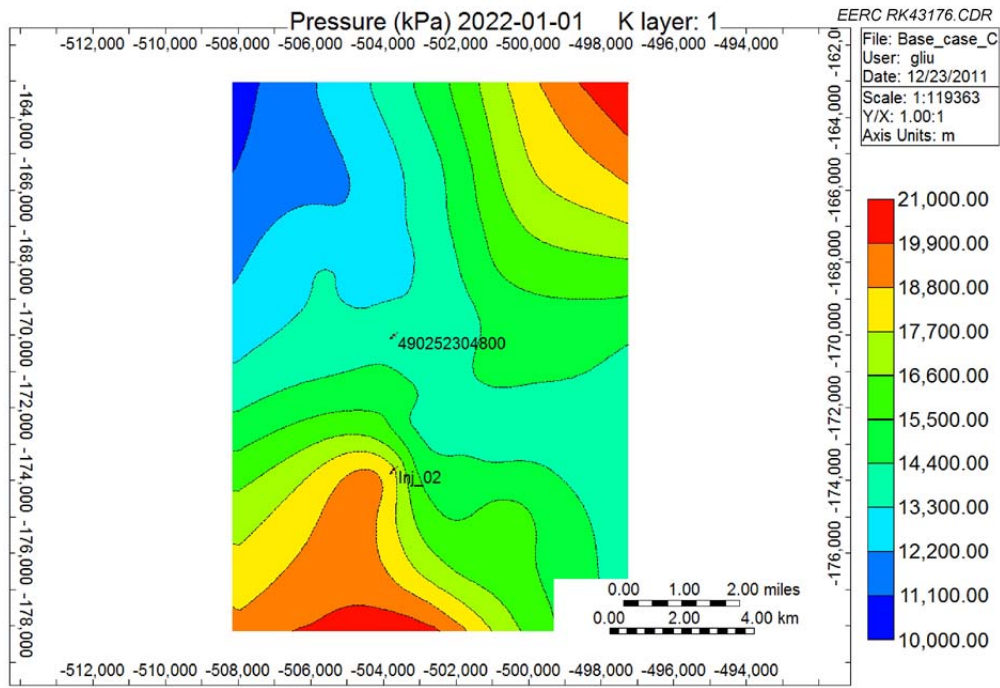


Figure F-30. Areal view of Case 2: pressure distributions for 10 years from beginning of injection.

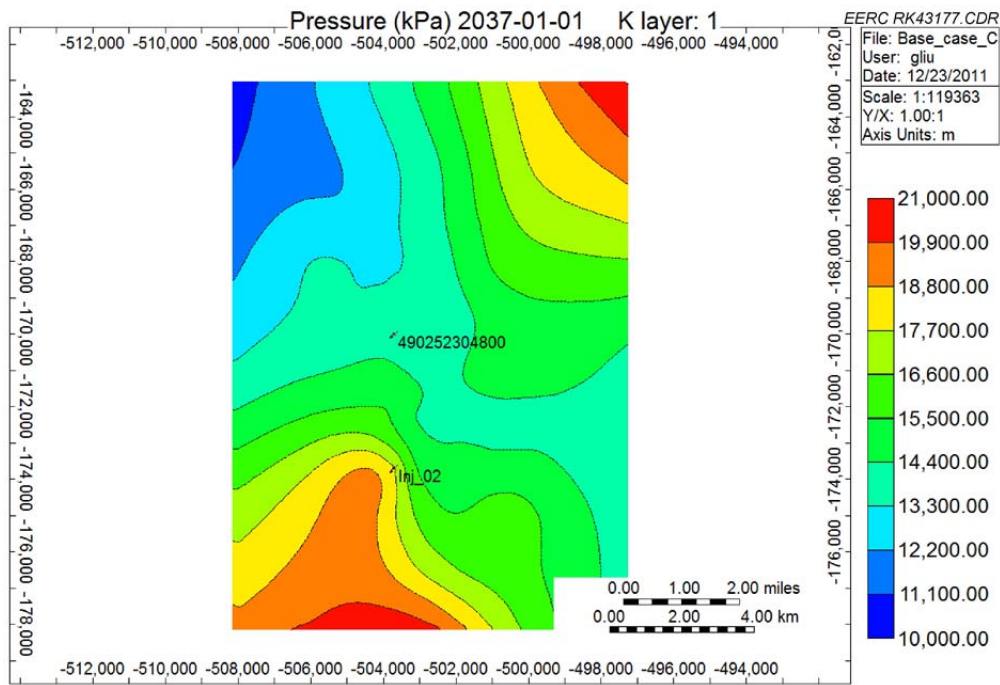


Figure F-31. Areal view of Case 2: pressure distributions for 25 years from beginning of injection.

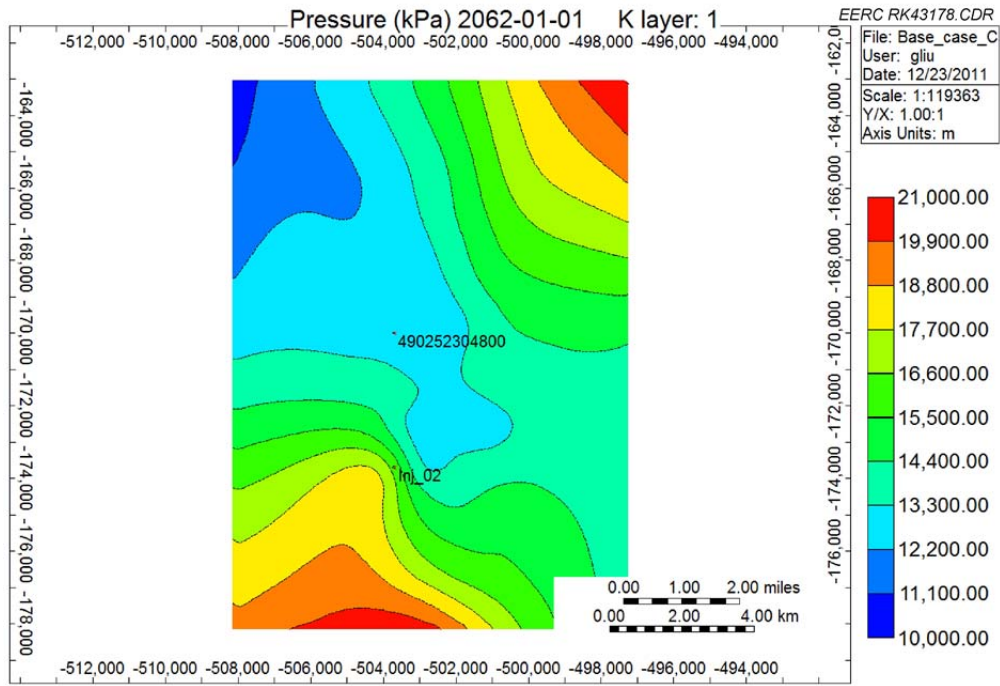


Figure F-32. Areal view of Case 2: pressure distributions for 50 years from beginning of injection.

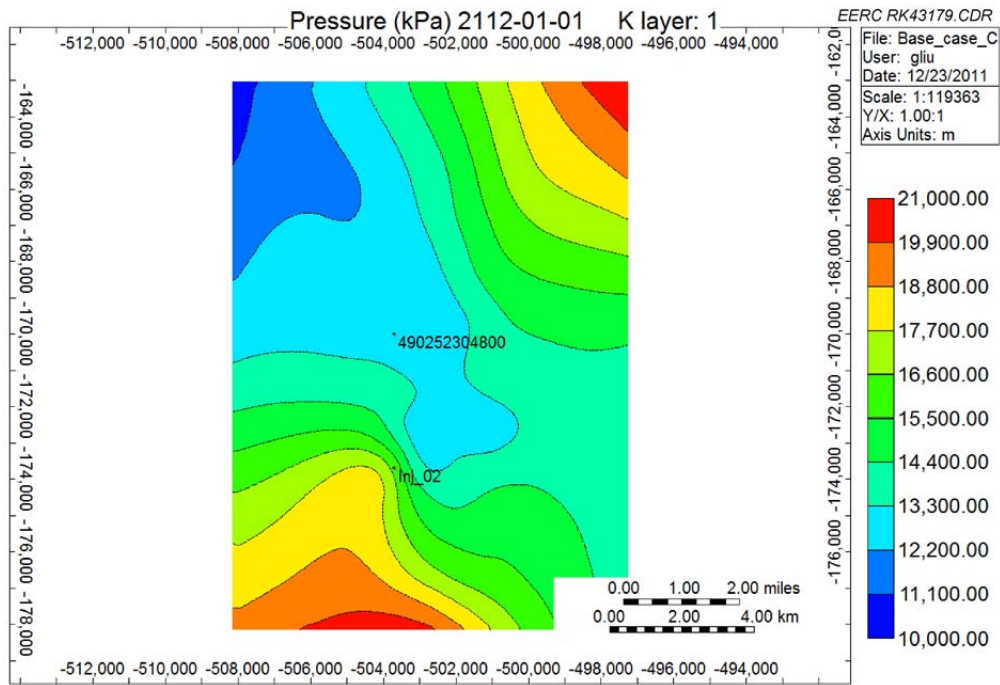


Figure F-33. Areal view of Case 2: pressure distributions for 100 years from beginning of injection.

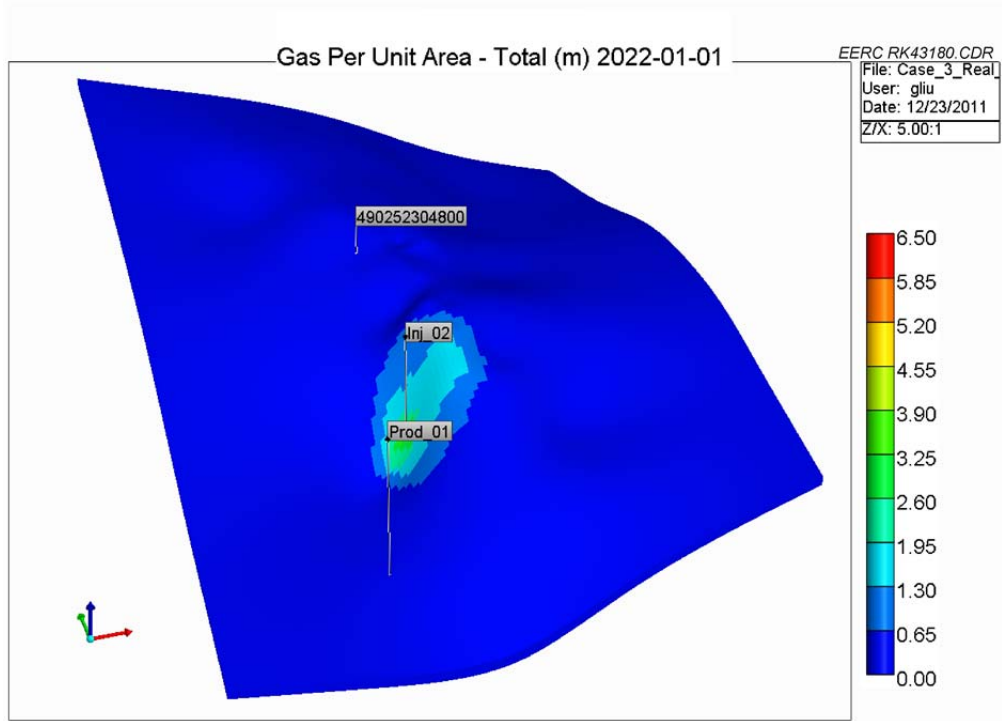


Figure F-34. 3-D view of Case 3: CO₂ plume migration for 10 years from beginning of injection.

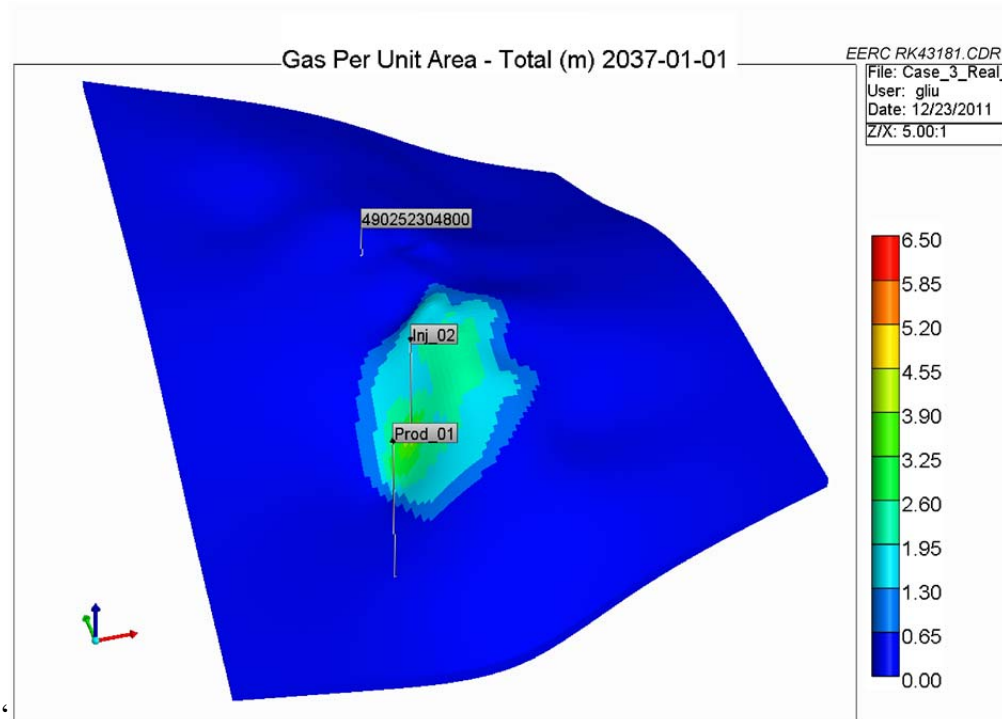


Figure F-35. 3-D view of Case 3: CO₂ plume migration for 25 years from beginning of injection.

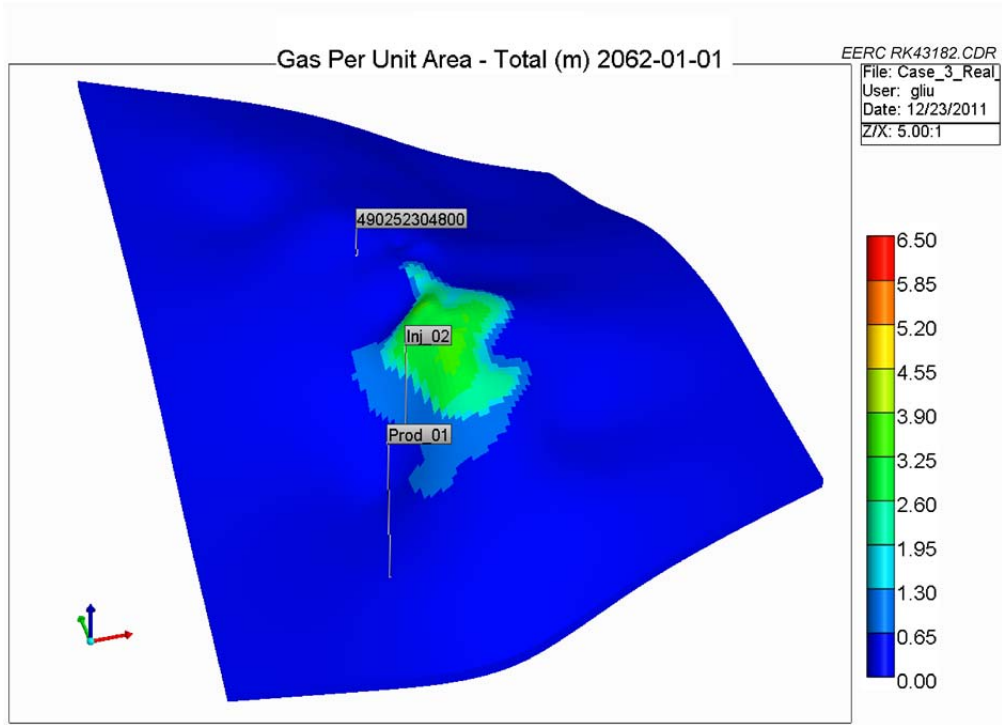


Figure F-36. 3-D view of Case 3: CO₂ plume migration for 50 years from beginning of injection.

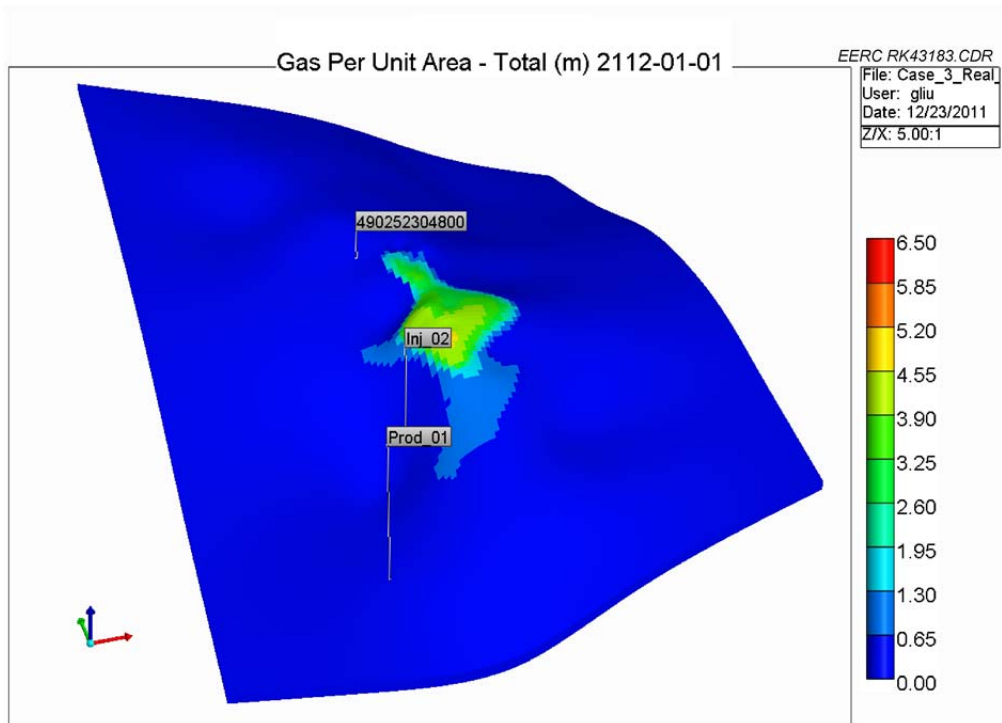


Figure F-37. 3-D view of Case 3: CO₂ plume migration for 100 years from beginning of injection.

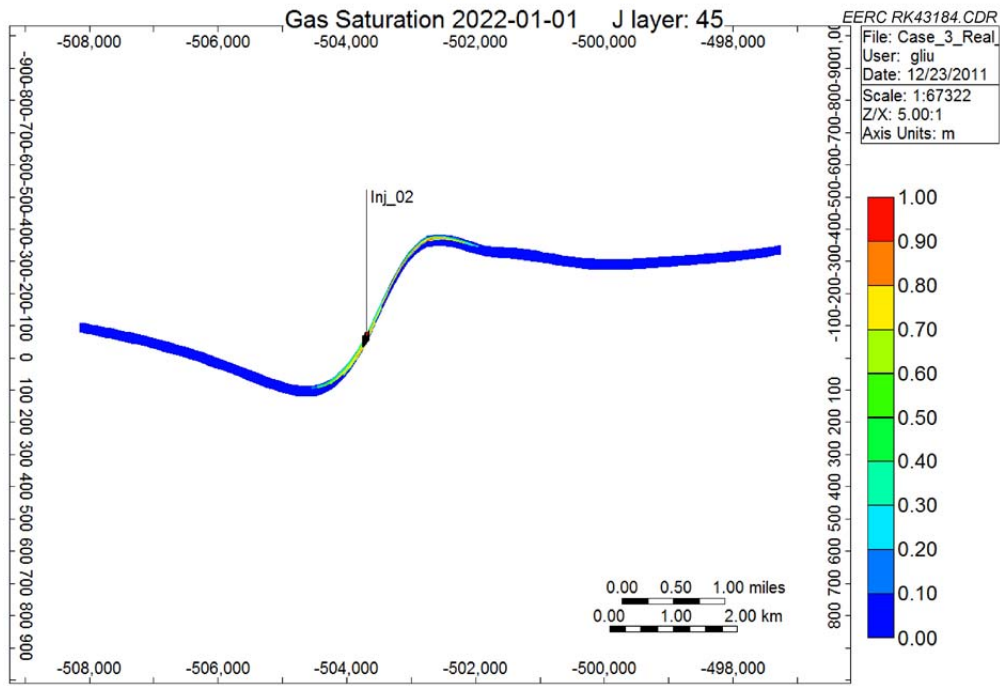


Figure F-38. Cross-sectional view of Case 3: CO₂ plume migration for 10 years from beginning of injection.

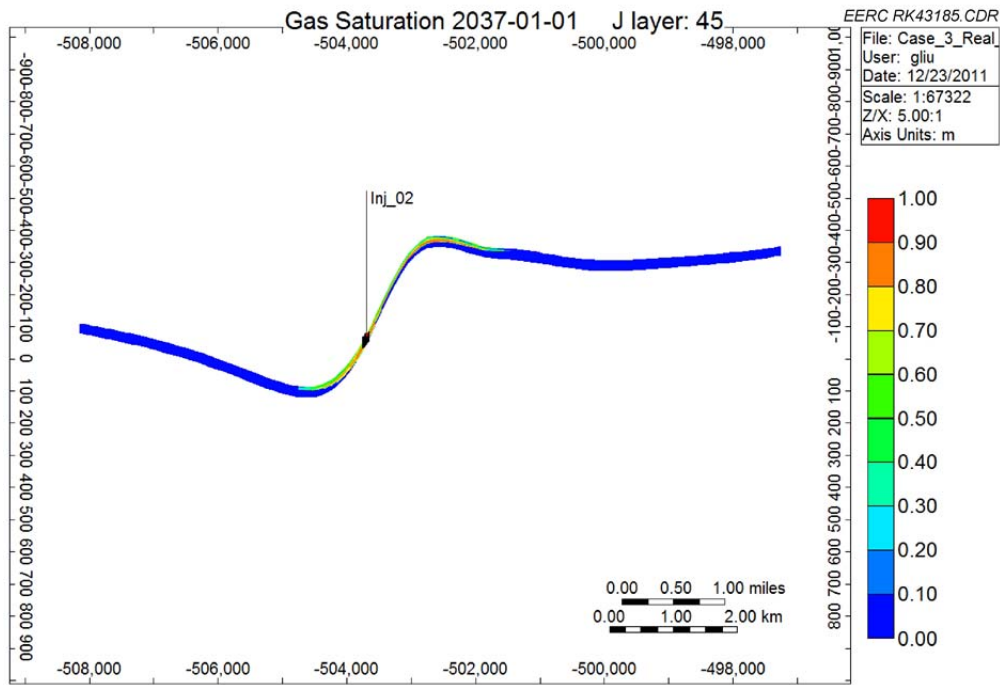


Figure F-39. Cross-sectional view of Case 3: CO₂ plume migration for 25 years from beginning of injection.

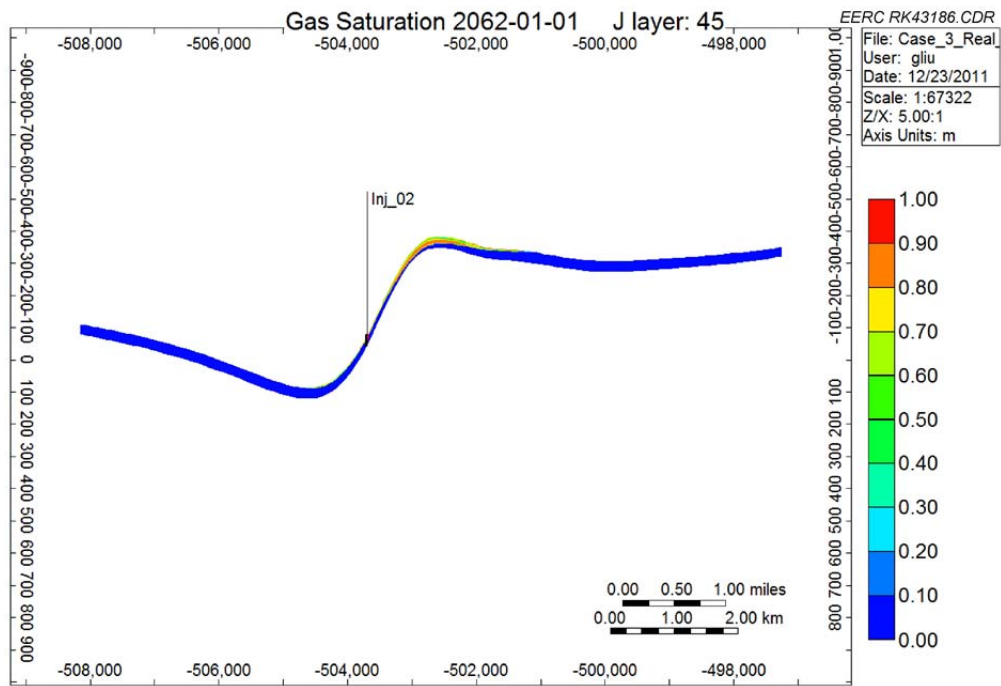


Figure F-40. Cross-sectional view of Case 3: CO₂ plume migration for 50 years from beginning of injection.

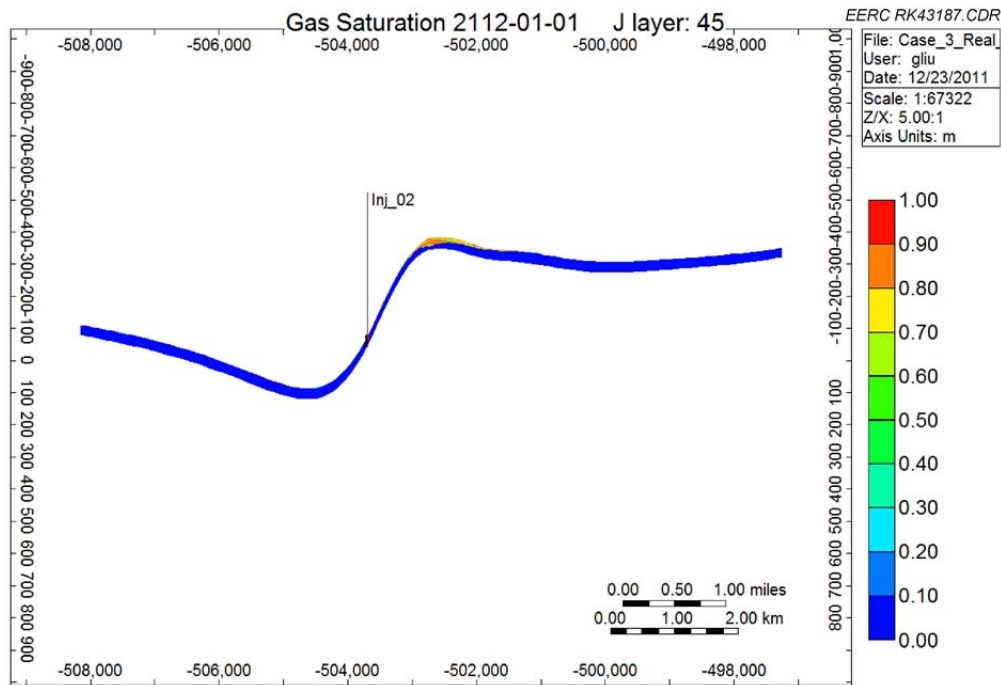


Figure F-41. Cross-sectional view of Case 3: CO₂ plume migration for 100 years from beginning of injection.

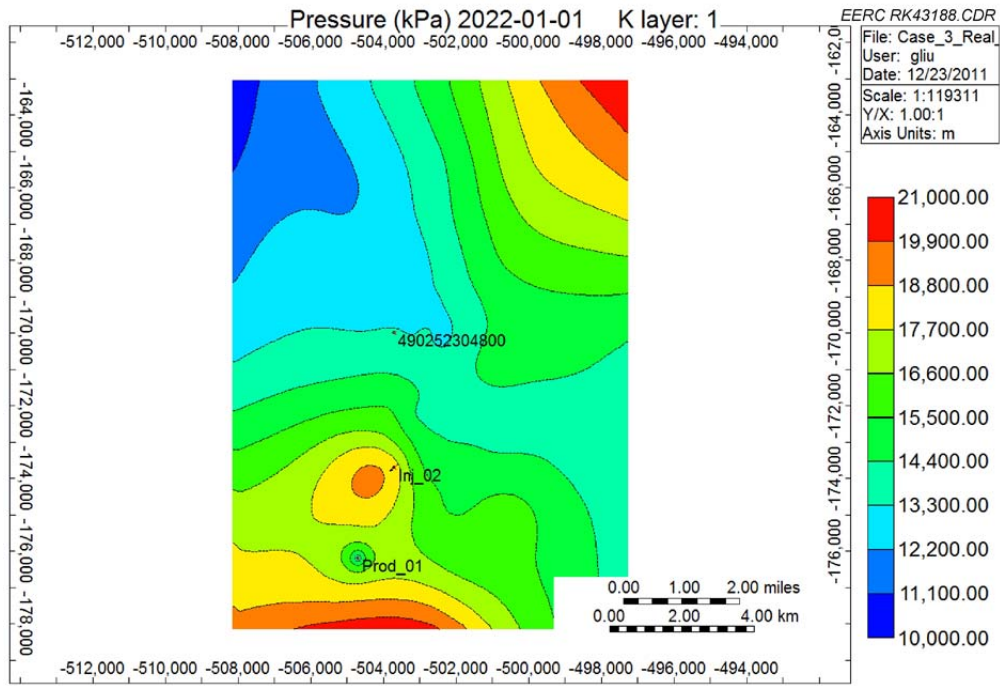


Figure F-42. Areal view of Case 3: pressure distributions for 10 years from beginning of injection.

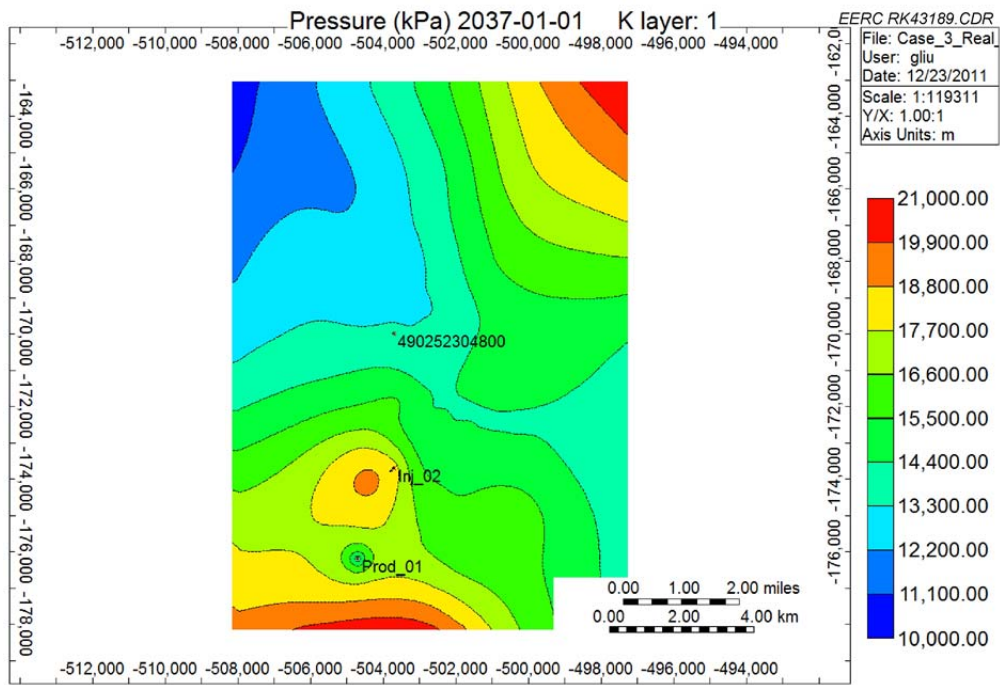


Figure F-43. Areal view of Case 3: pressure distributions for 25 years from beginning of injection.

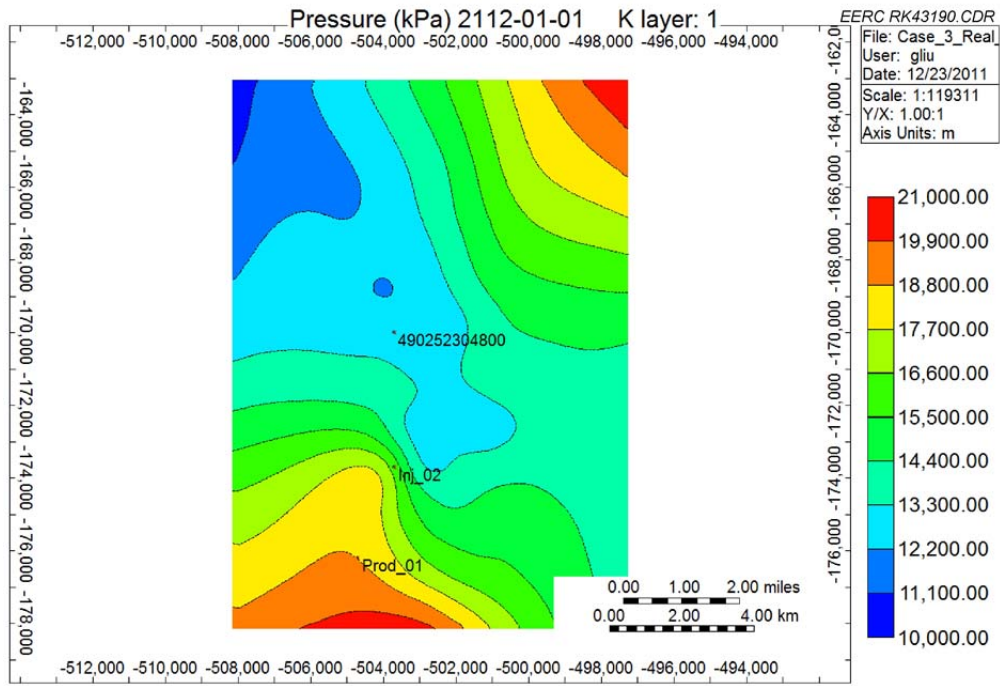


Figure F-44. Areal view of Case 3: pressure distributions for 50 years from beginning of injection.

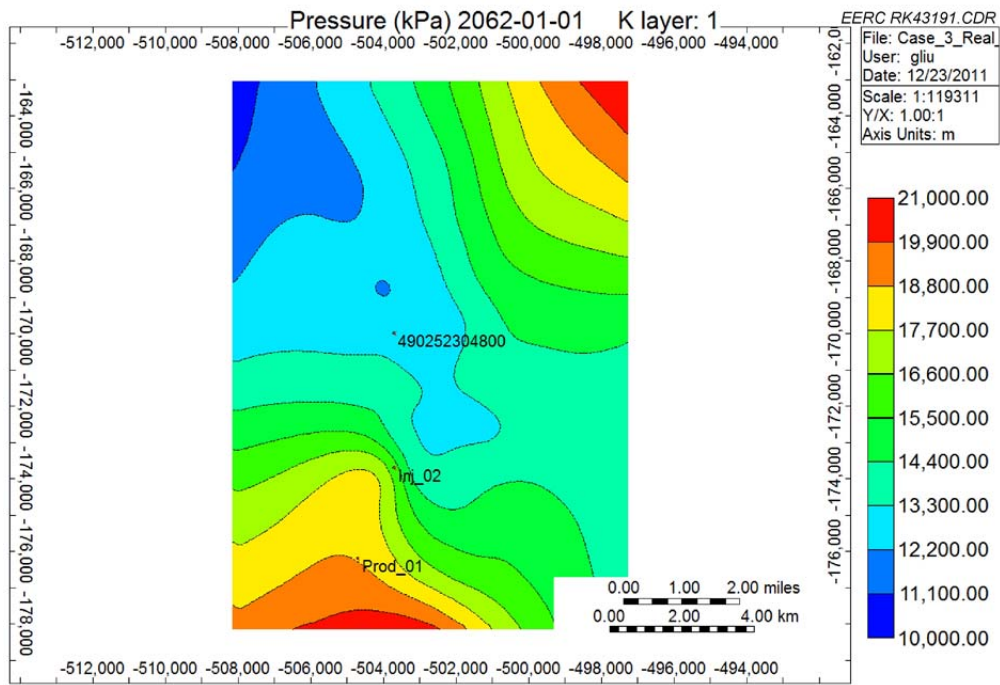


Figure F-45. Areal view of Case 3: pressure distributions for 100 years from beginning of injection.

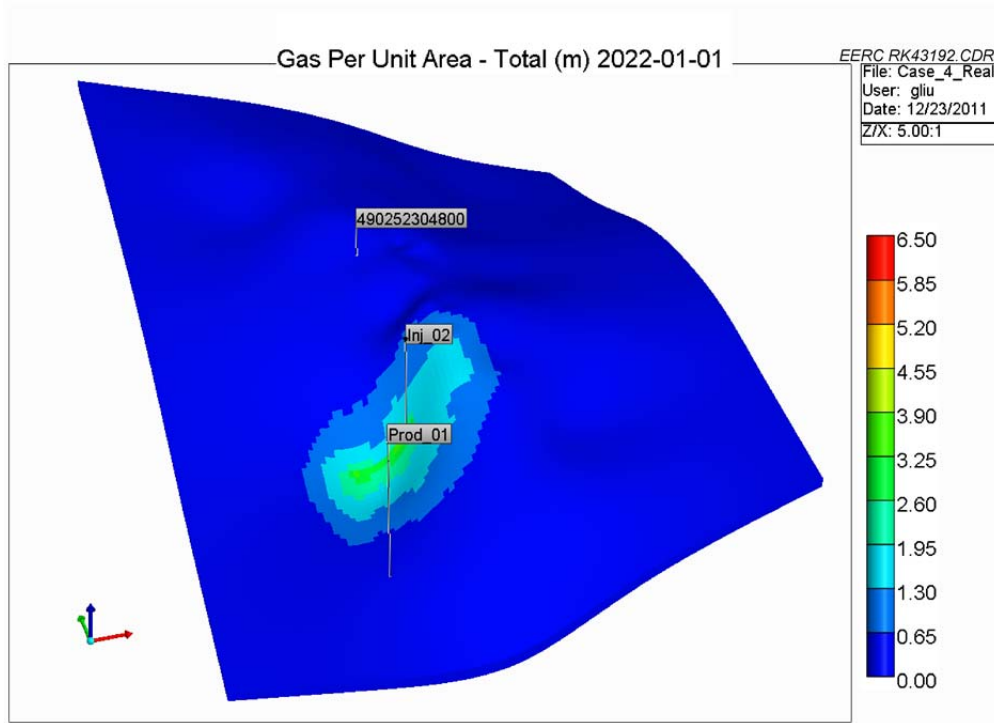


Figure F-46. 3-D view of Case 4: CO₂ plume migration for 10 years from beginning of injection.

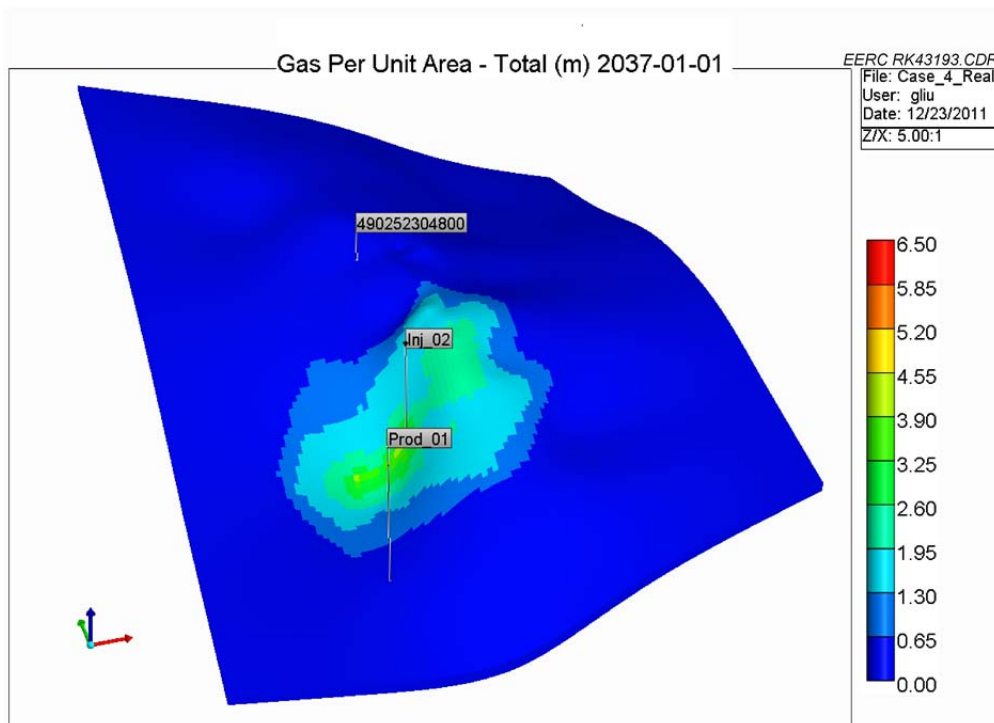


Figure F-47. 3-D view of Case 4: CO₂ plume migration for 25 years from beginning of injection.

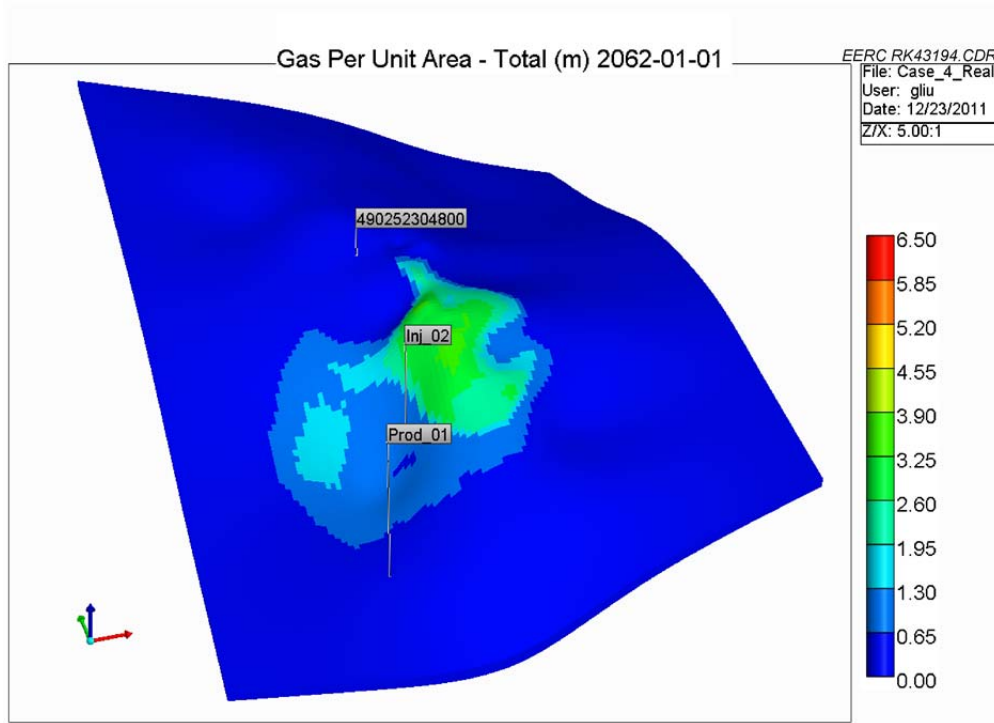


Figure F-48. 3-D view of Case 4: CO₂ plume migration for 50 years from beginning of injection.

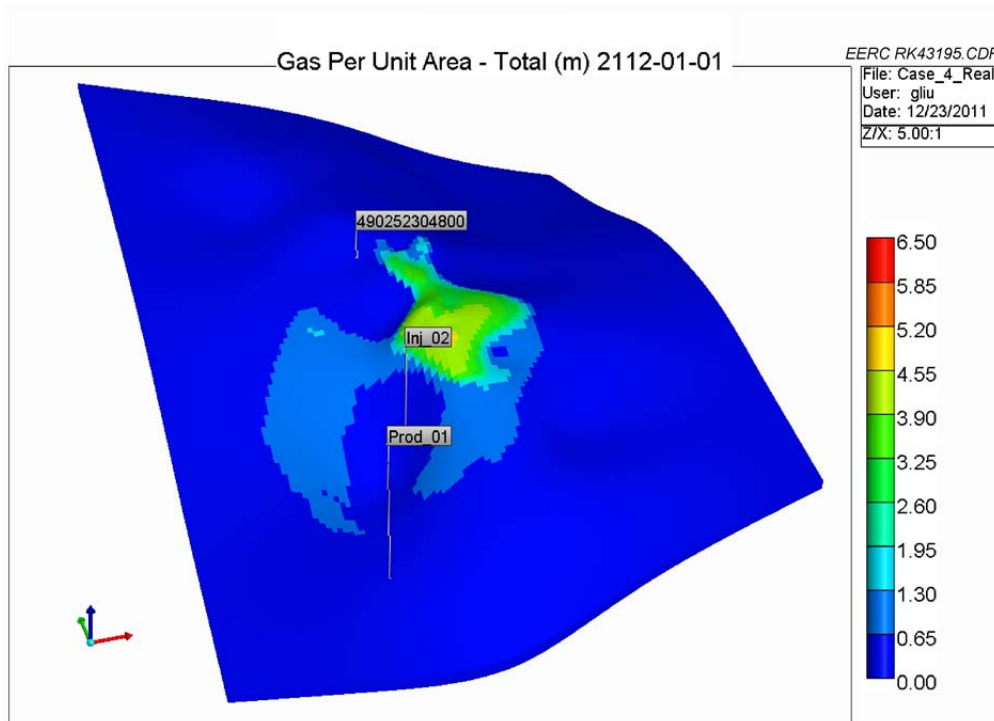


Figure F-49. 3-D view of Case 4: CO₂ plume migration for 100 years from beginning of injection.

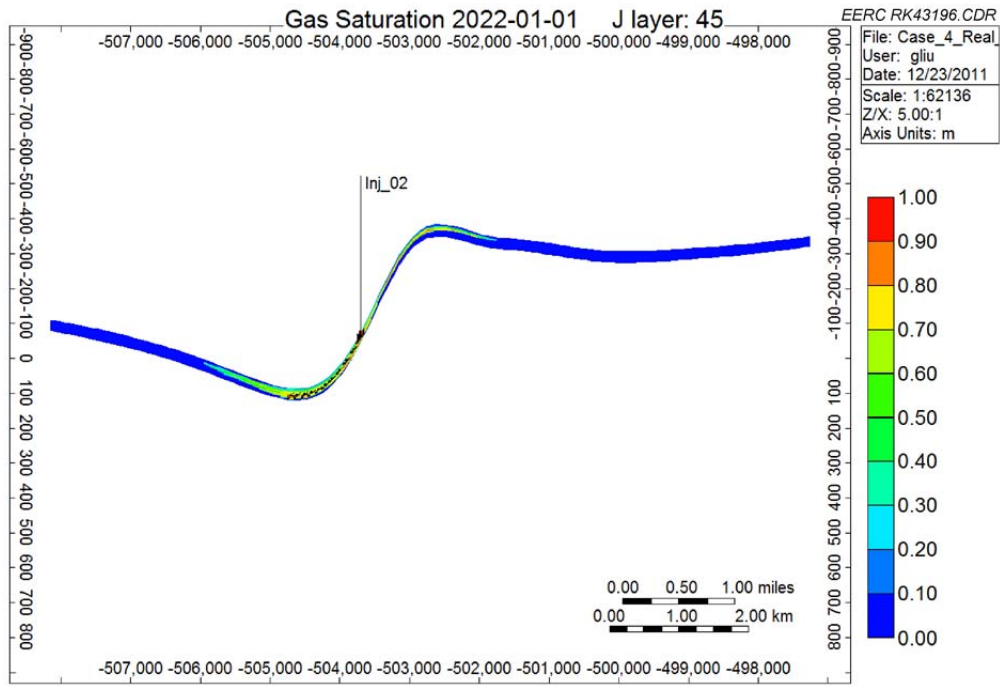


Figure F-50. Cross-sectional view of Case 4: CO₂ plume migration for 10 years from beginning of injection.

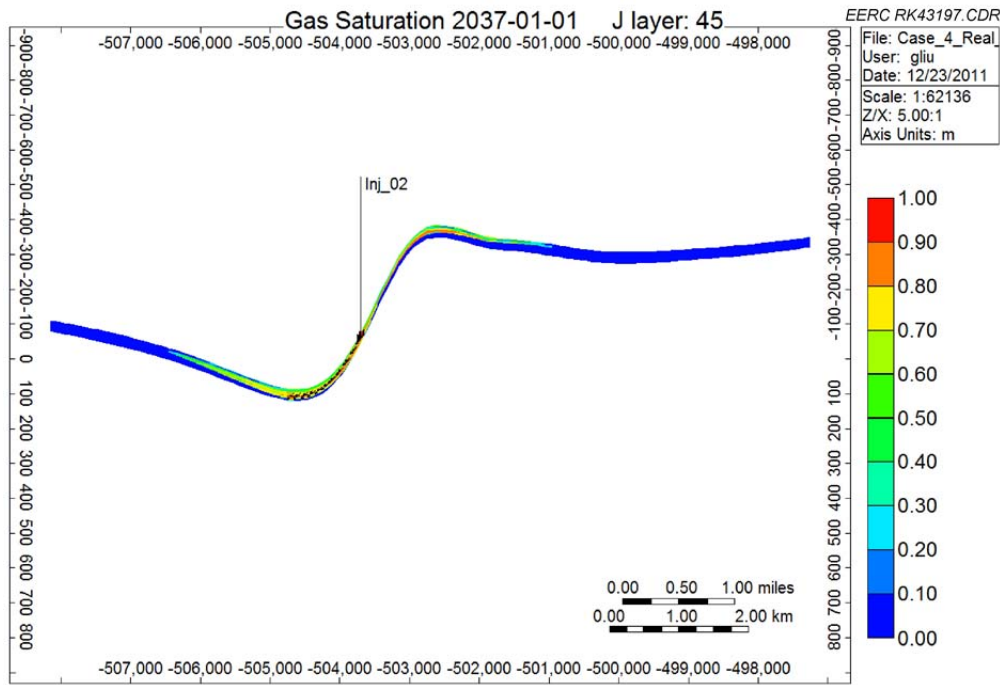


Figure F-51. Cross-sectional view of Case 4: CO₂ plume migration for 25 years from beginning of injection.

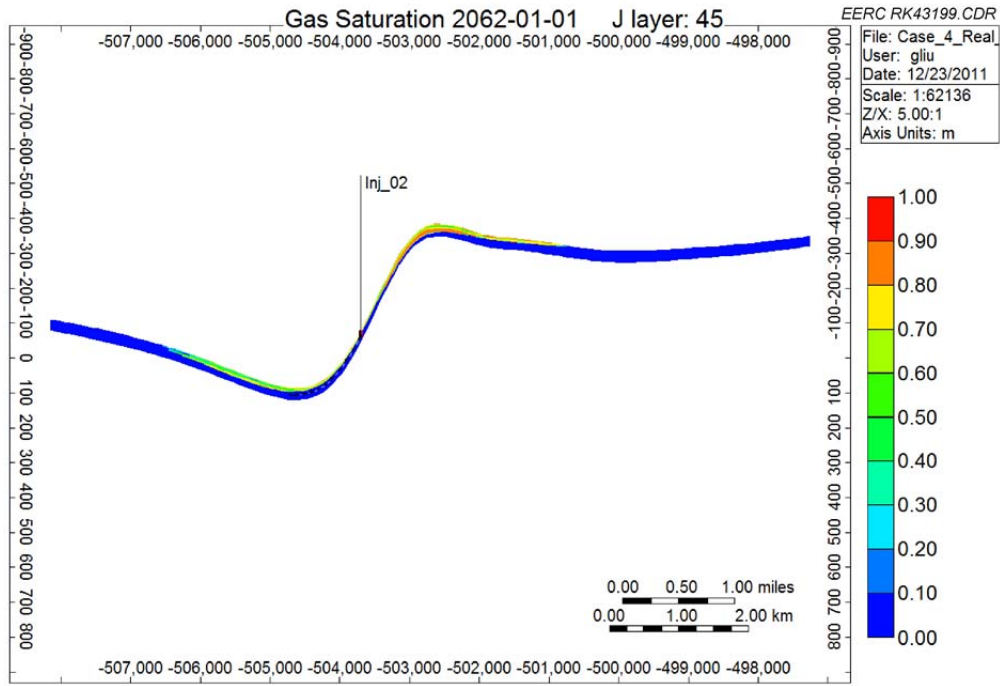


Figure F-52. Cross-sectional view of Case 4: CO₂ plume migration for 50 years from beginning of injection.

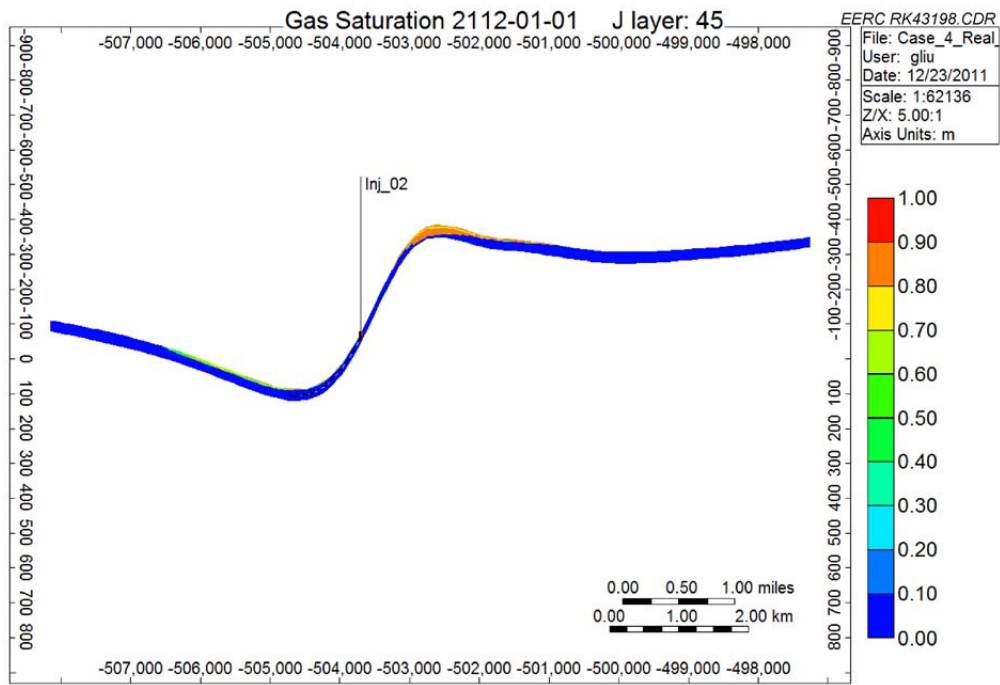


Figure F-53. Cross-sectional view of Case 4: CO₂ plume migration for 100 years from beginning of injection.

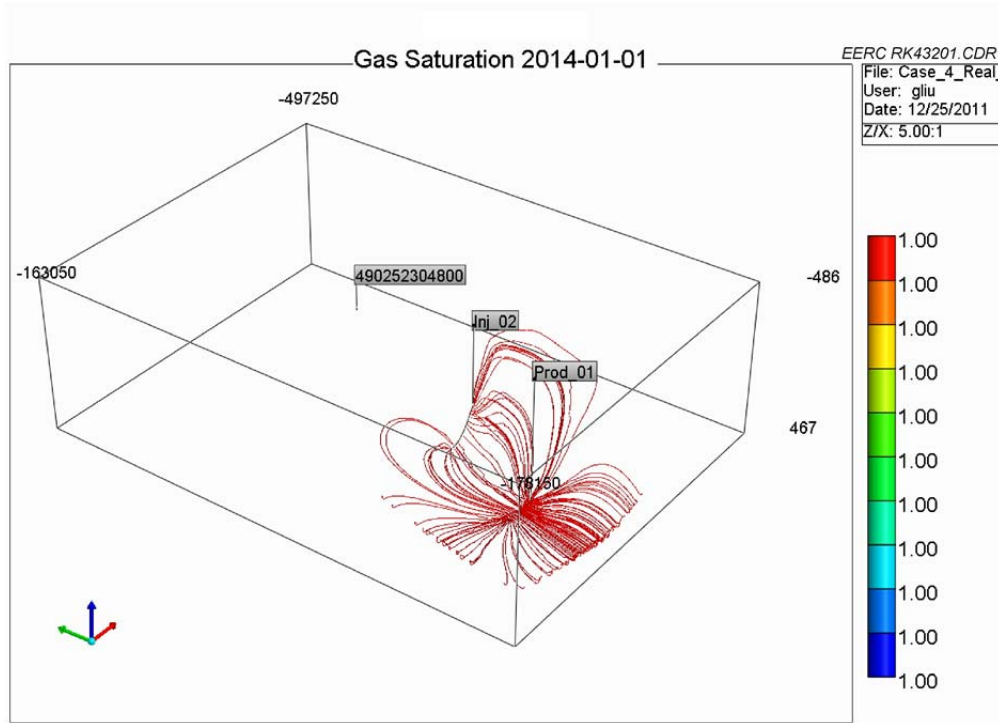


Figure F-54. Streamline demonstrations for horizontal injection and production wells used in Case 4: 2 years from beginning of injection of Case 8 (as an example).

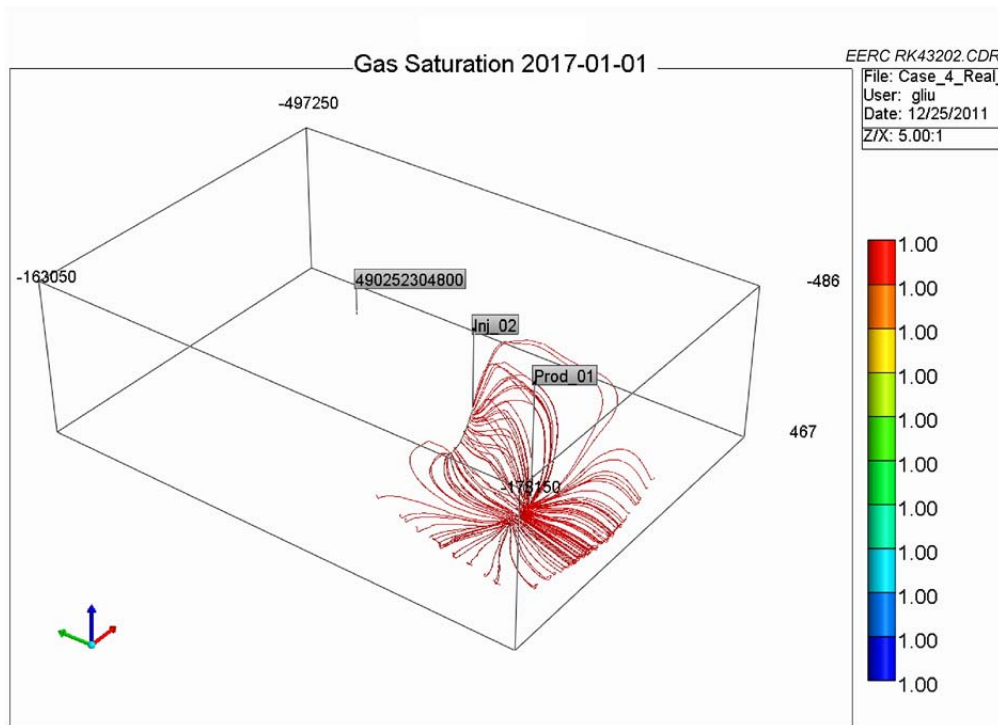


Figure F-55. Streamline demonstrations for horizontal injection and production wells used in Case 4: 5 years from beginning of injection of Case 8 (as an example).

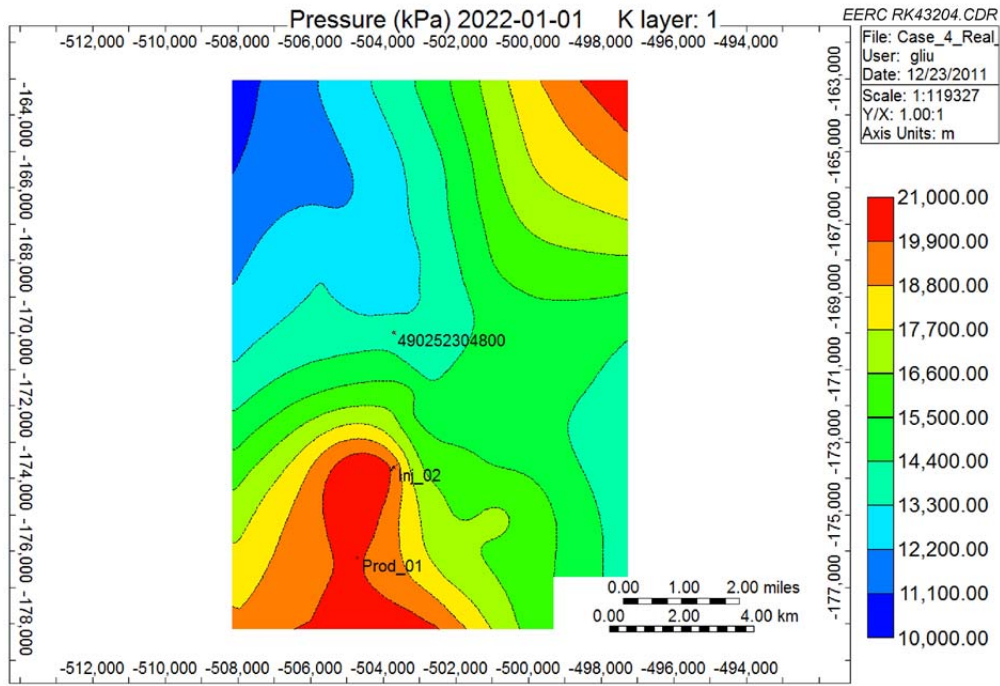


Figure F-56. Areal view of Case 4: Pressure distributions for 10 years from beginning of injection.

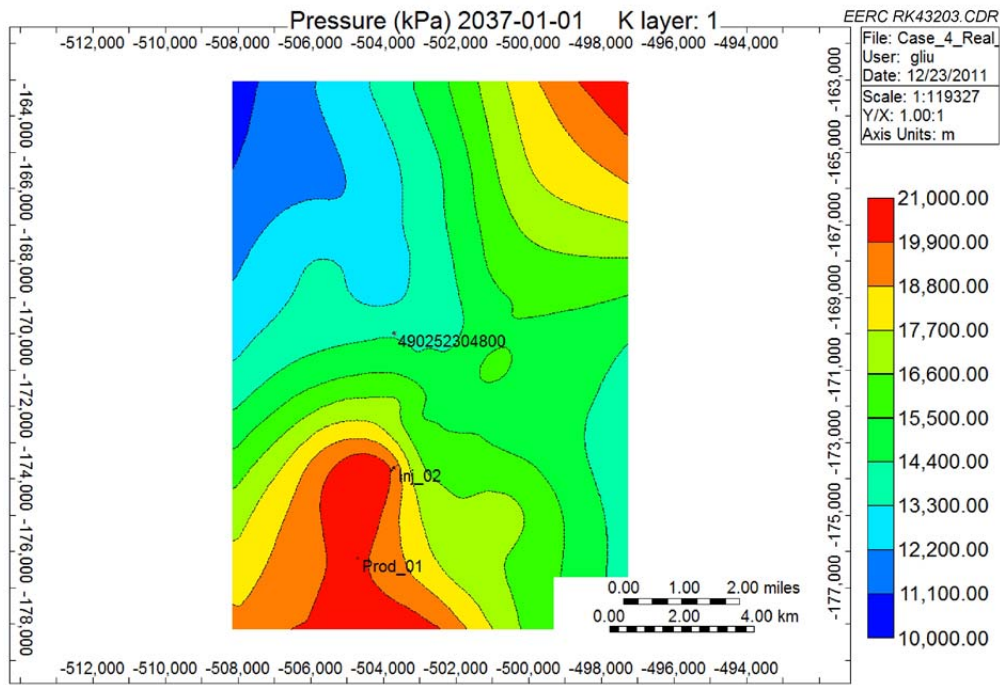


Figure F-57. Areal view of Case 4: Pressure distributions for 25 years from beginning of injection.

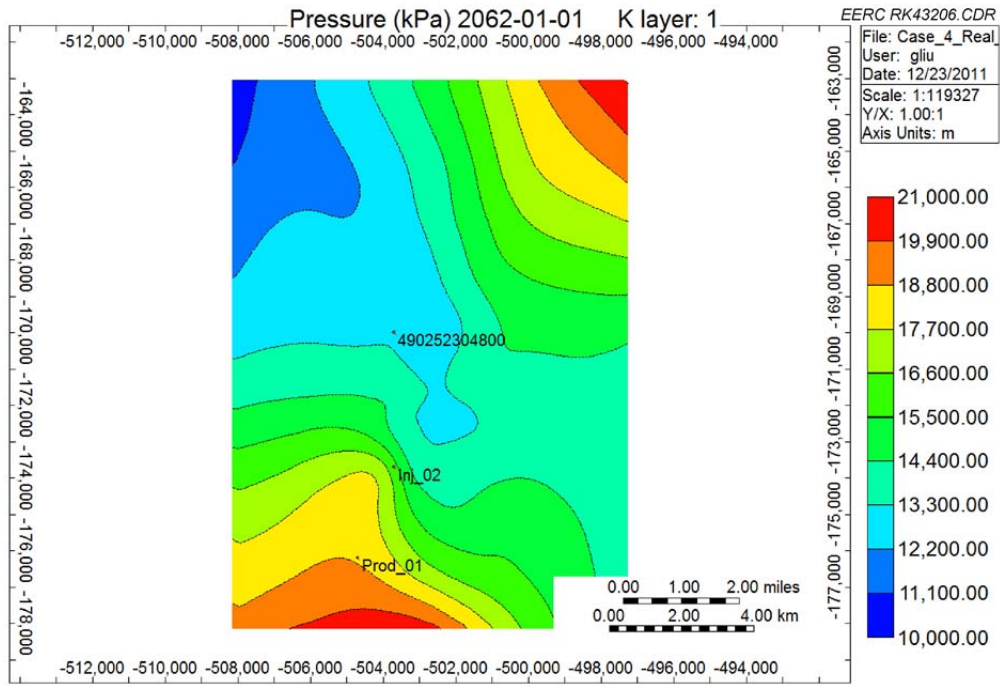


Figure F-58. Areal view of Case 4: pressure distributions for 50 years from beginning of injection.

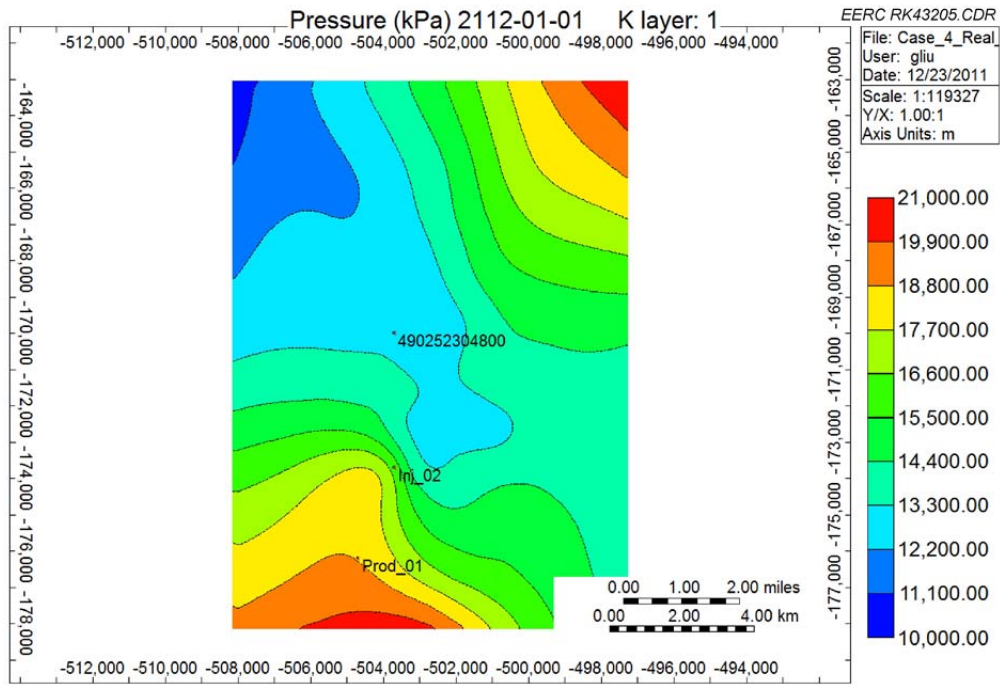


Figure F-59. Areal view of Case 4: pressure distributions for 100 years from beginning of injection.

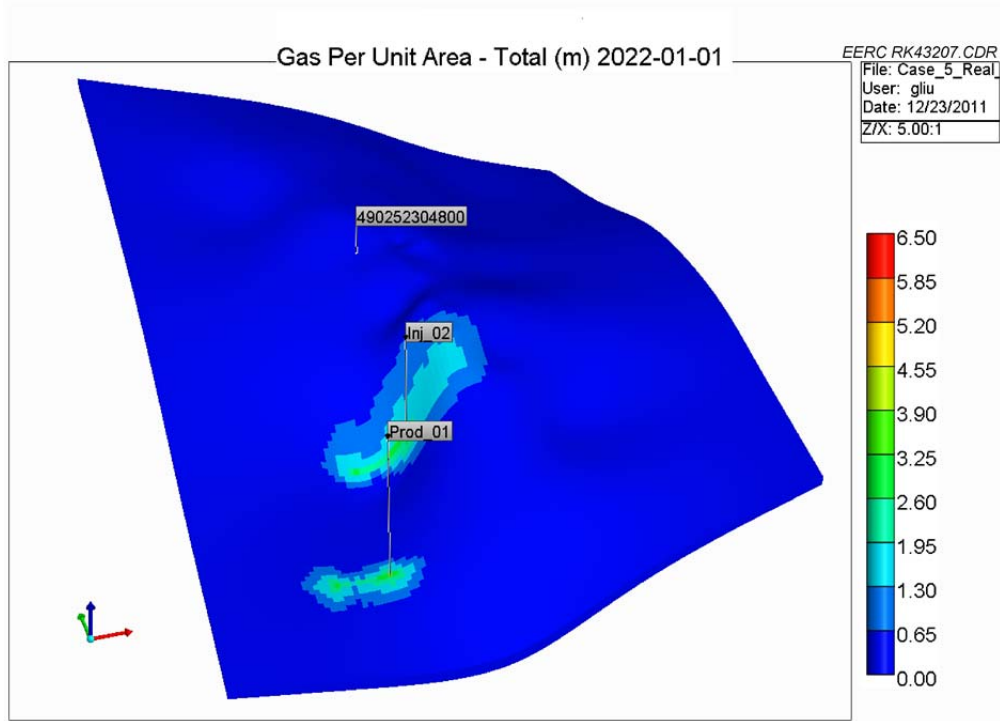


Figure F-60. 3-D view of Case 5: CO₂ plume migration for 10 years from beginning of injection.

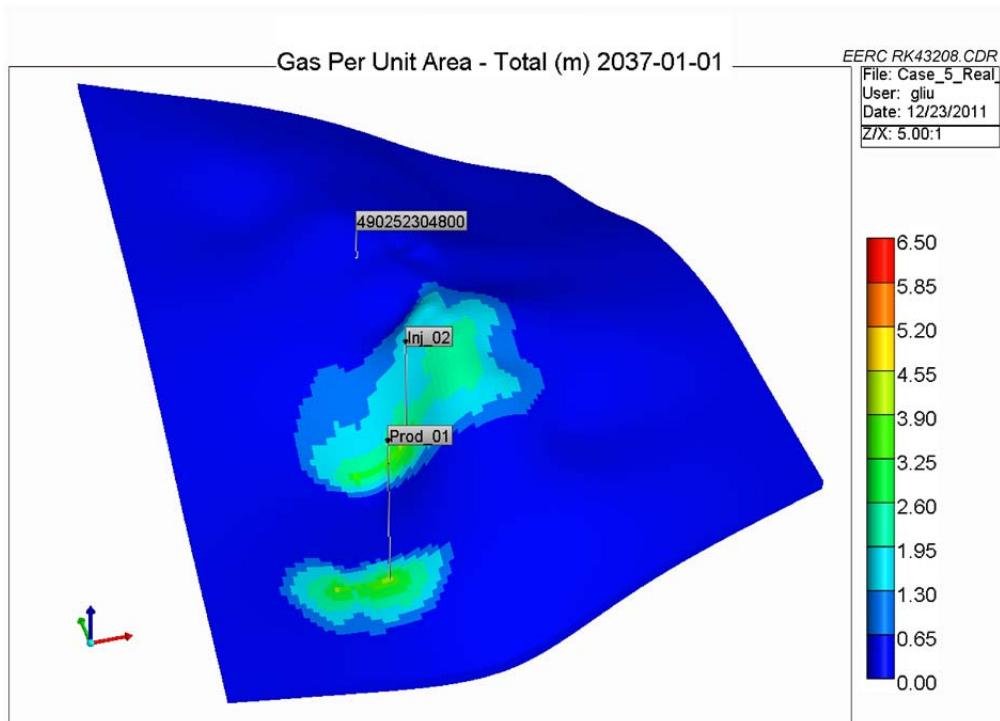


Figure F-61. 3-D view of Case 5: CO₂ plume migration for 25 years from beginning of injection.

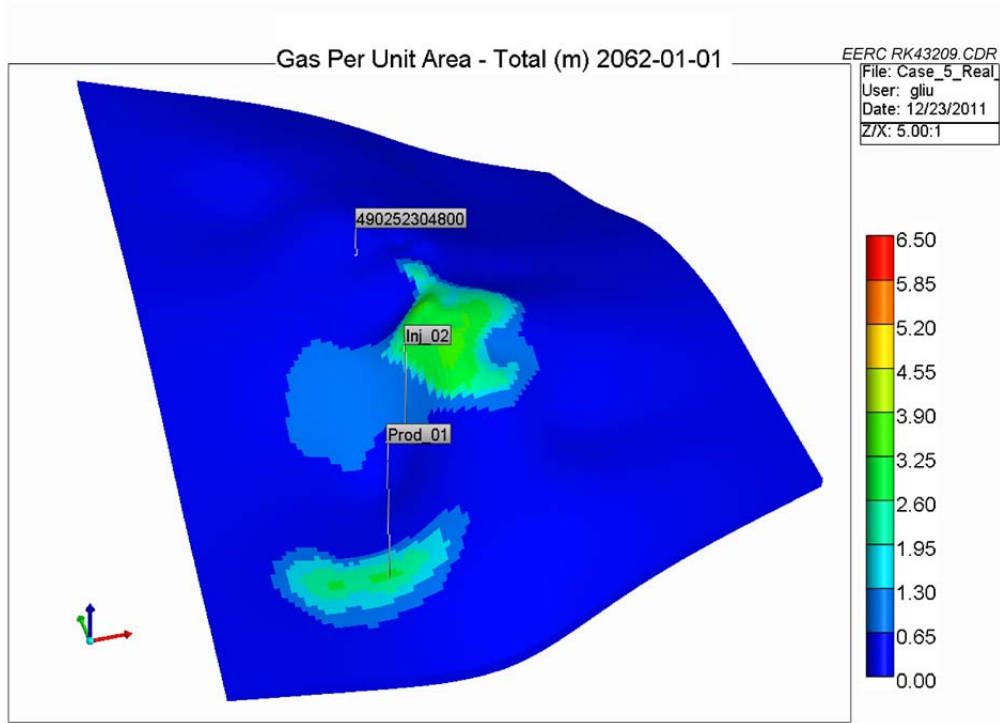


Figure F-62. 3-D view of Case 5: CO₂ plume migration for 50 years from beginning of injection.

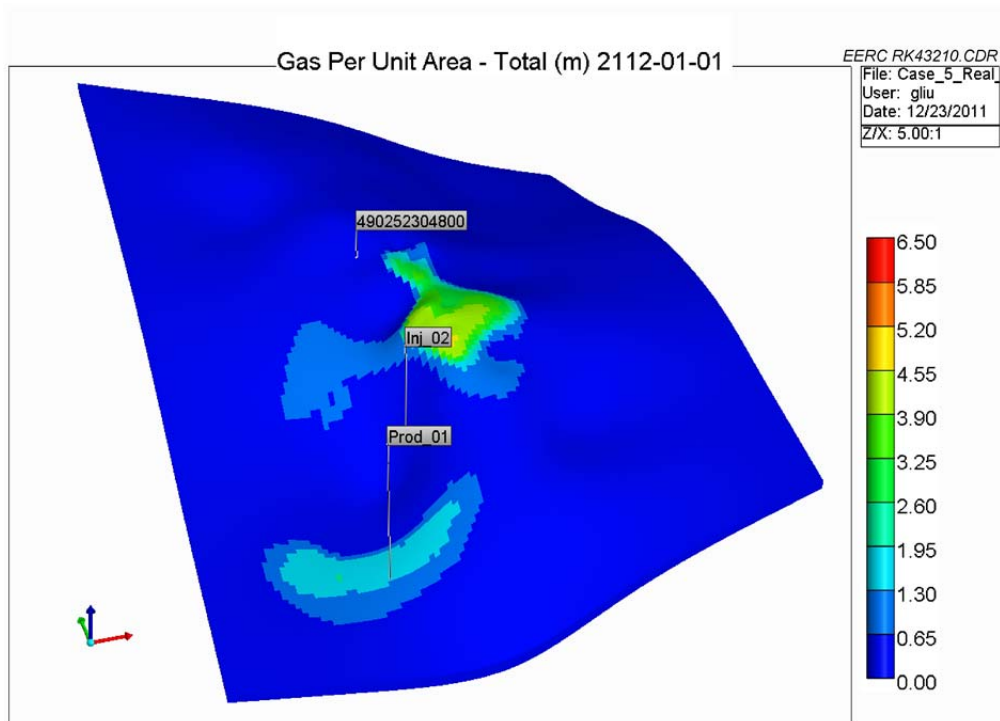


Figure F-63. 3-D view of Case 5: CO₂ plume migration for 100 years from beginning of injection.

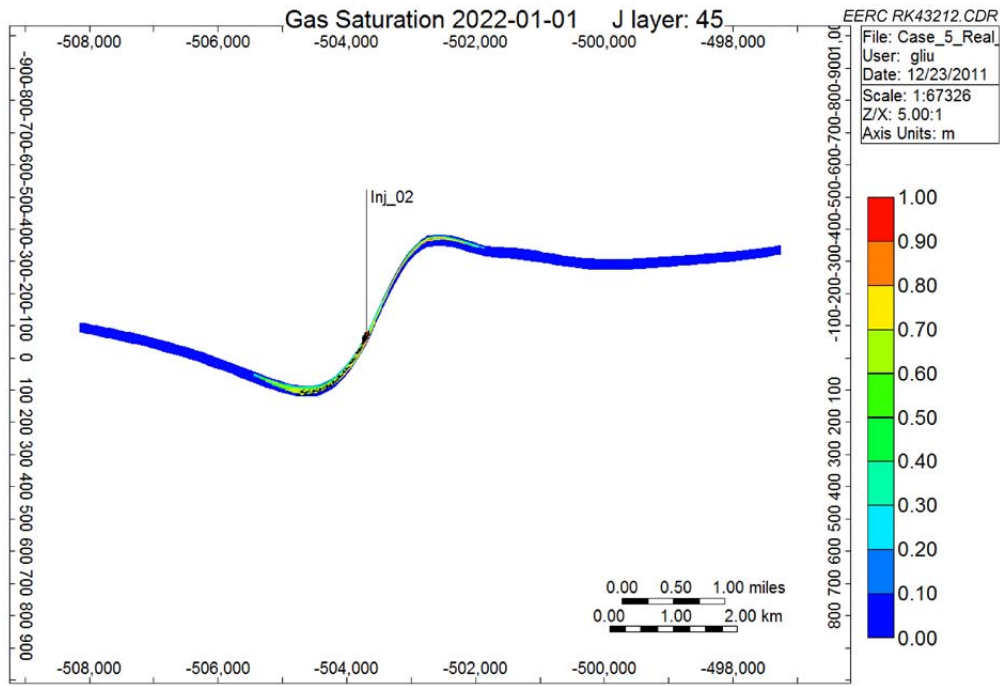


Figure F-64. Cross-sectional view of Case 5: CO₂ plume migration for 10 years from beginning of injection.

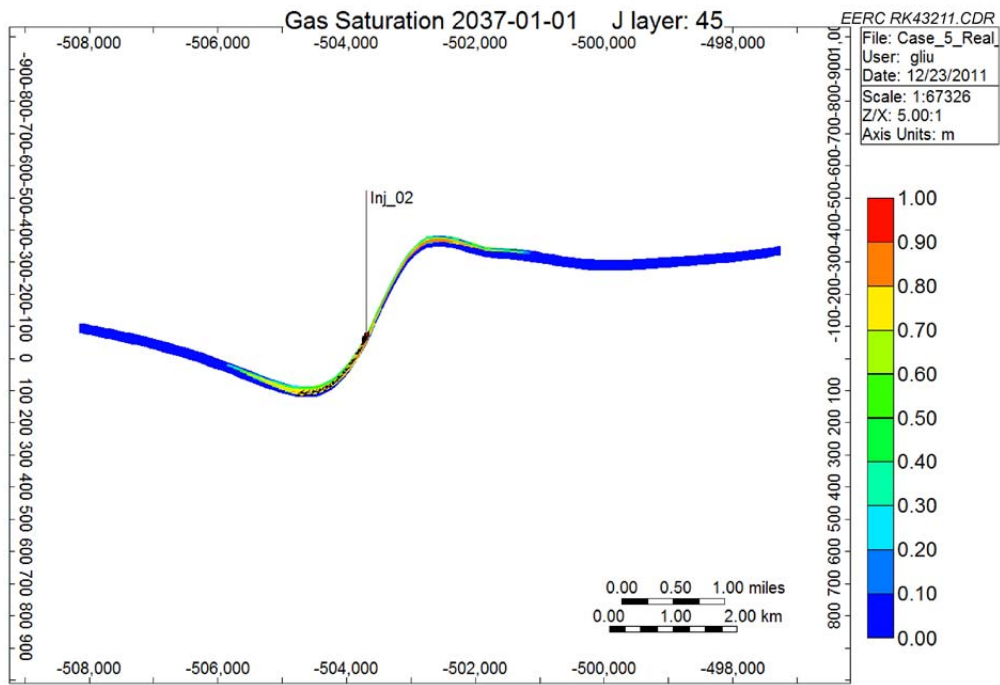


Figure F-65. Cross-sectional view of Case 5: CO₂ plume migration for 25 years from beginning of injection.

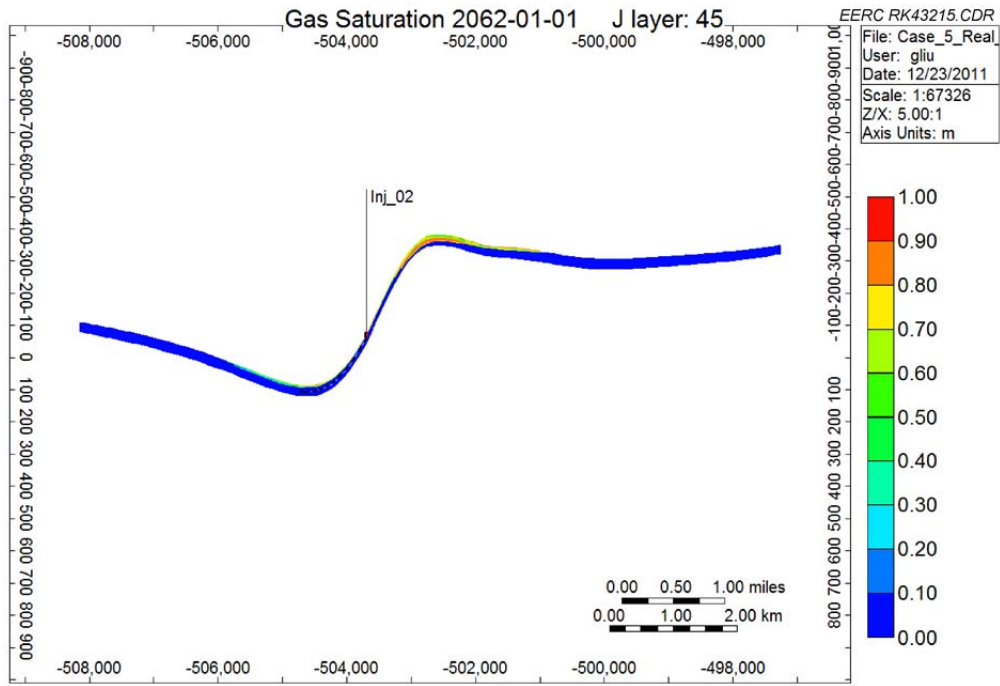


Figure F-66. Cross-sectional view of Case 5: CO₂ plume migration for 50 years from beginning of injection.

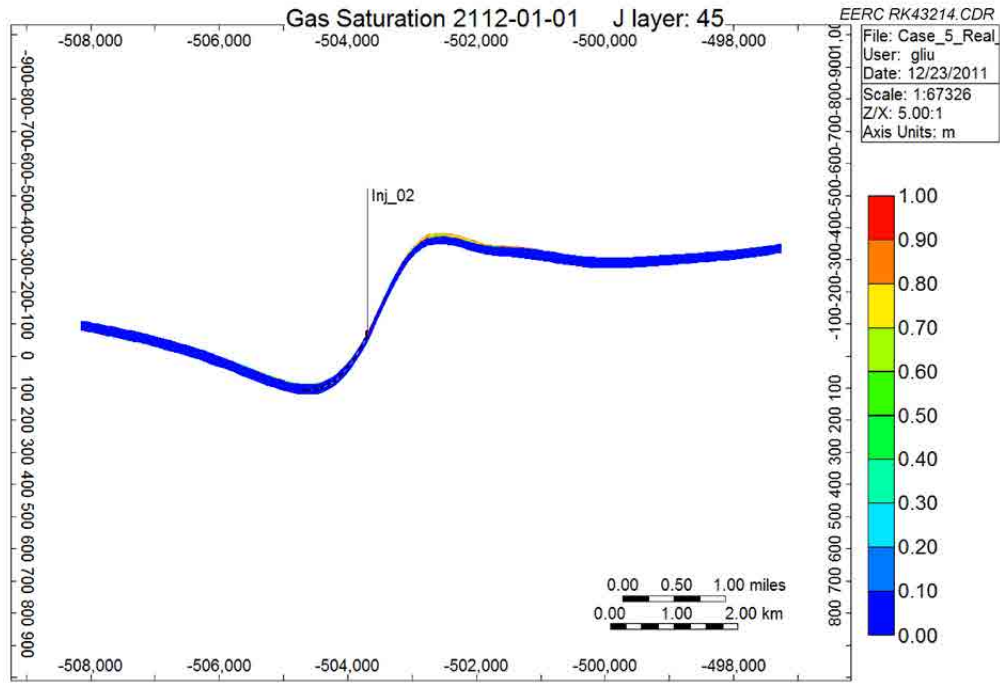


Figure F-67. Cross-sectional view of Case 5: CO₂ plume migration for 100 years from beginning of injection.

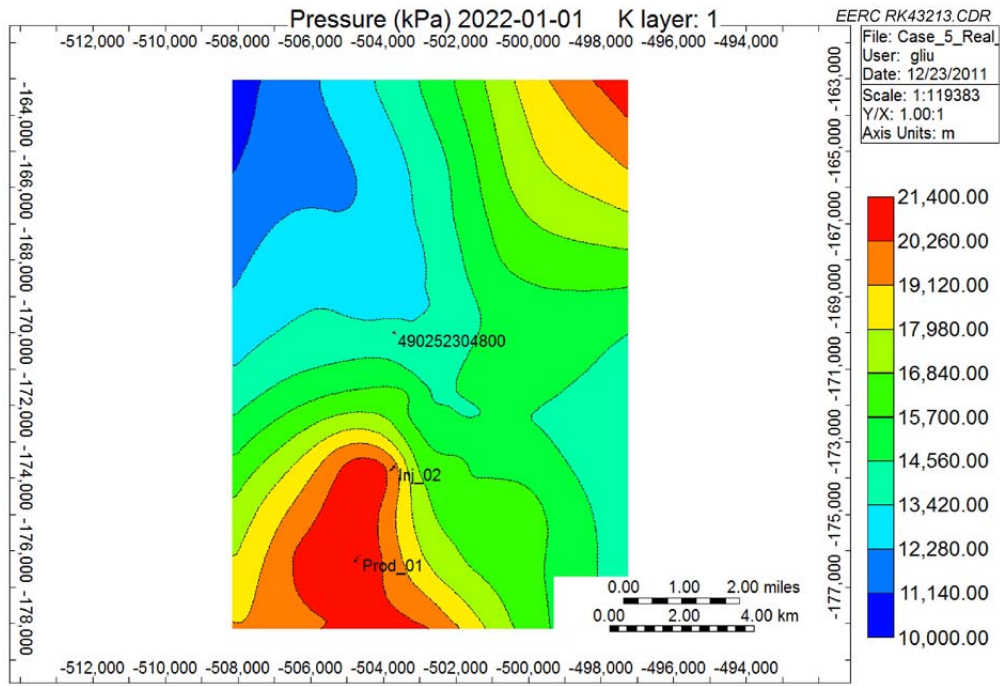


Figure F-68. Areal view of Case 5: pressure distributions for 10 years from beginning of injection.

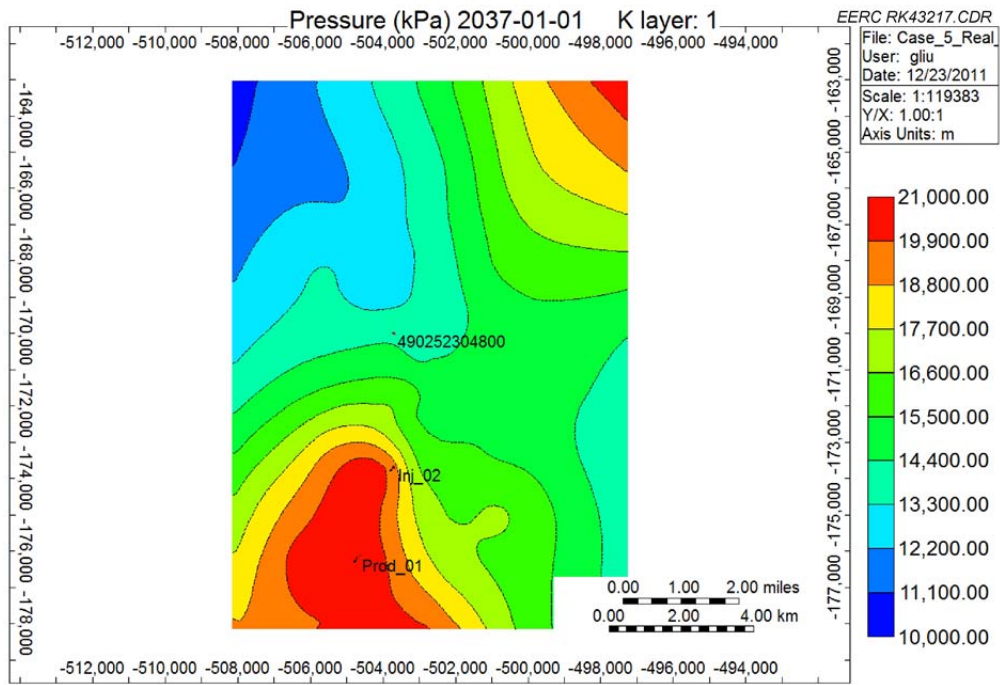


Figure F-69. Areal view of Case 5: pressure distributions for 25 years from beginning of injection.

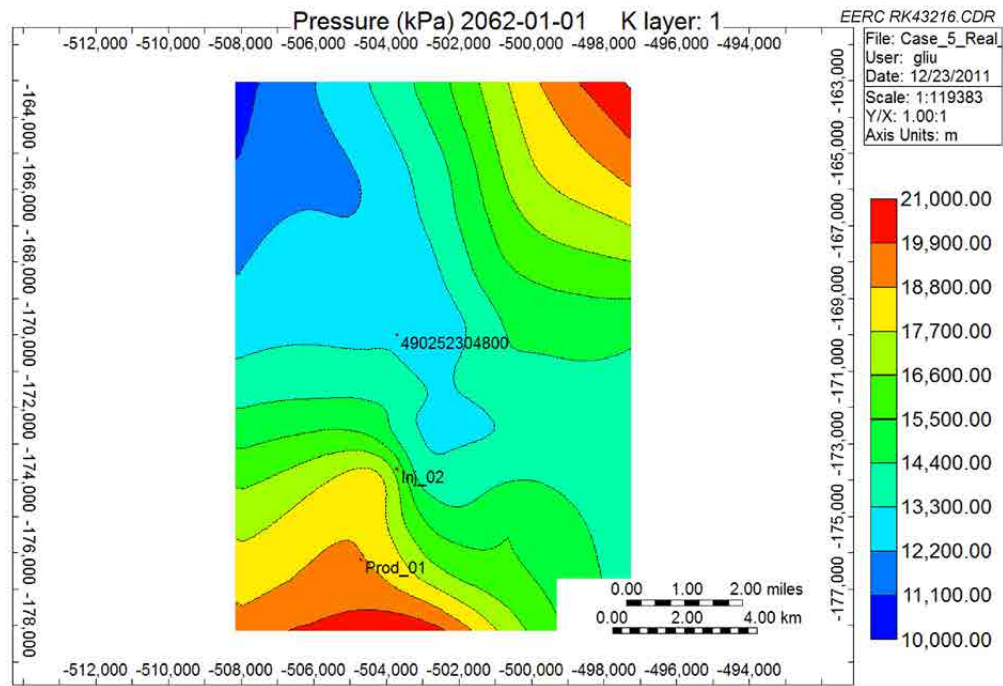


Figure F-70. Areal view of Case 5: pressure distributions for 50 years from beginning of injection.

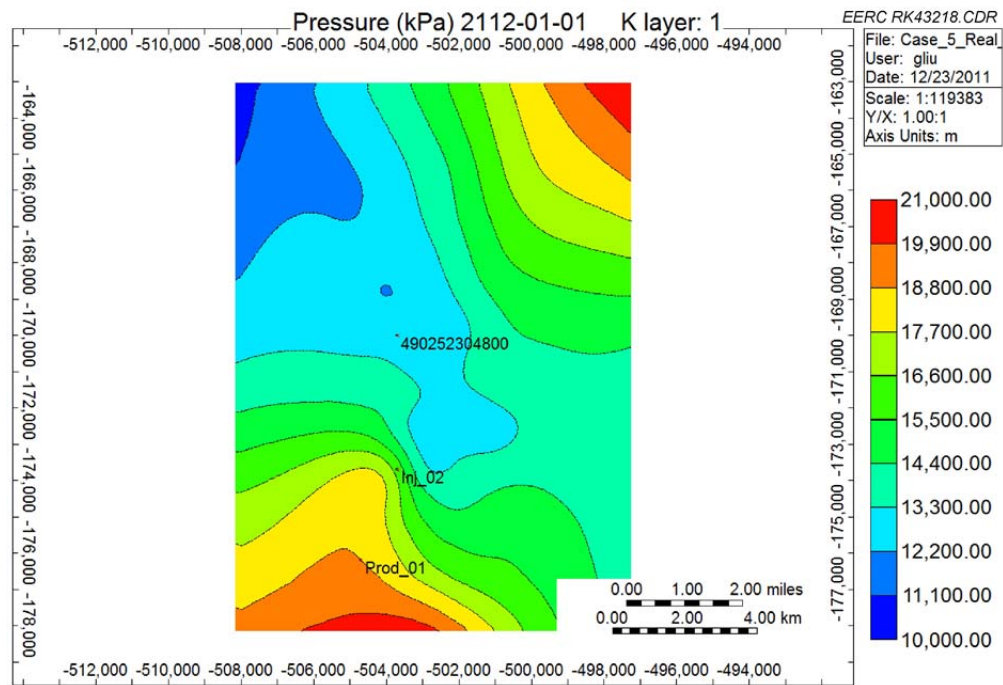


Figure F-71. Areal view of Case 5: pressure distributions for 100 years from beginning of injection.

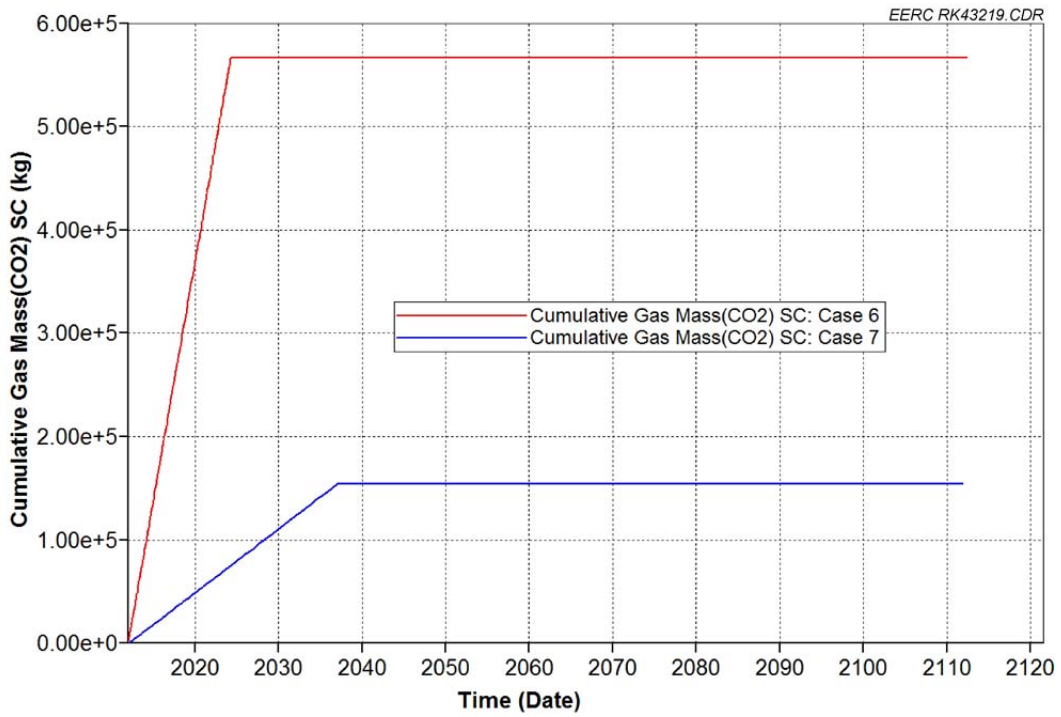


Figure F-72. Total injected CO₂ for Cases 6 and 7.

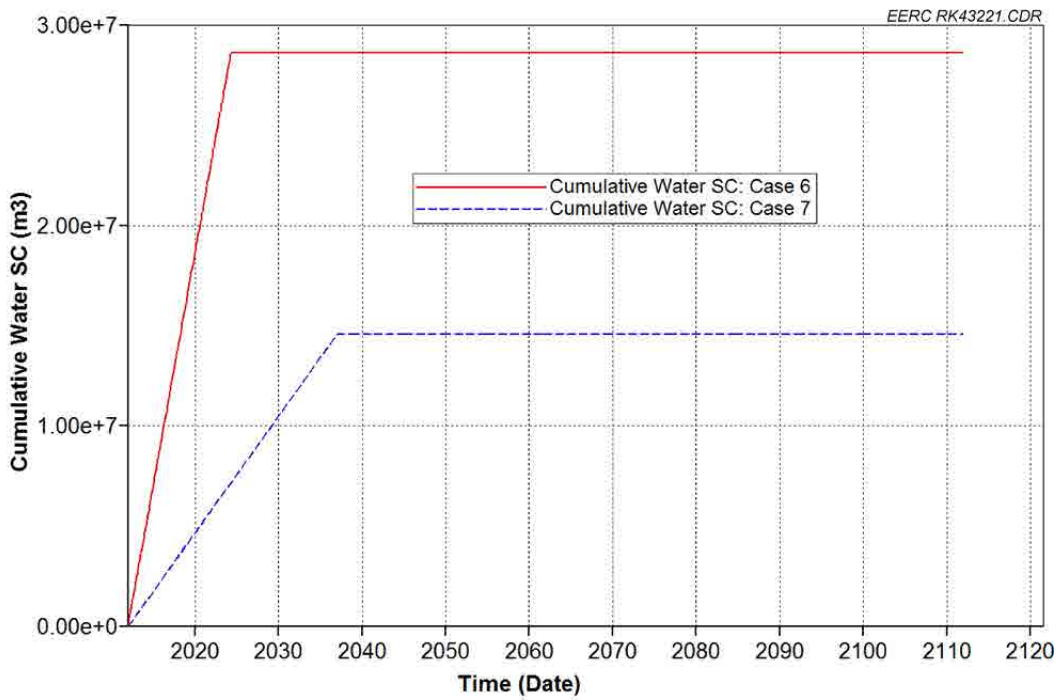


Figure F-73. Total produced water for Cases 6 and 7.

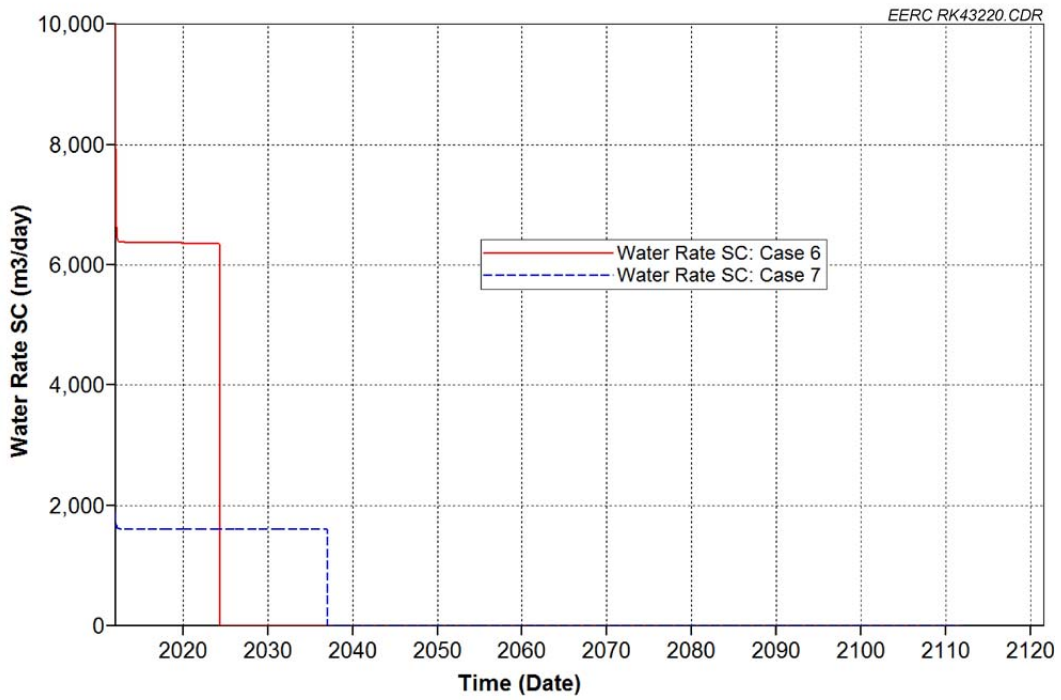


Figure F-74. Production rates for Cases 6 and 7.

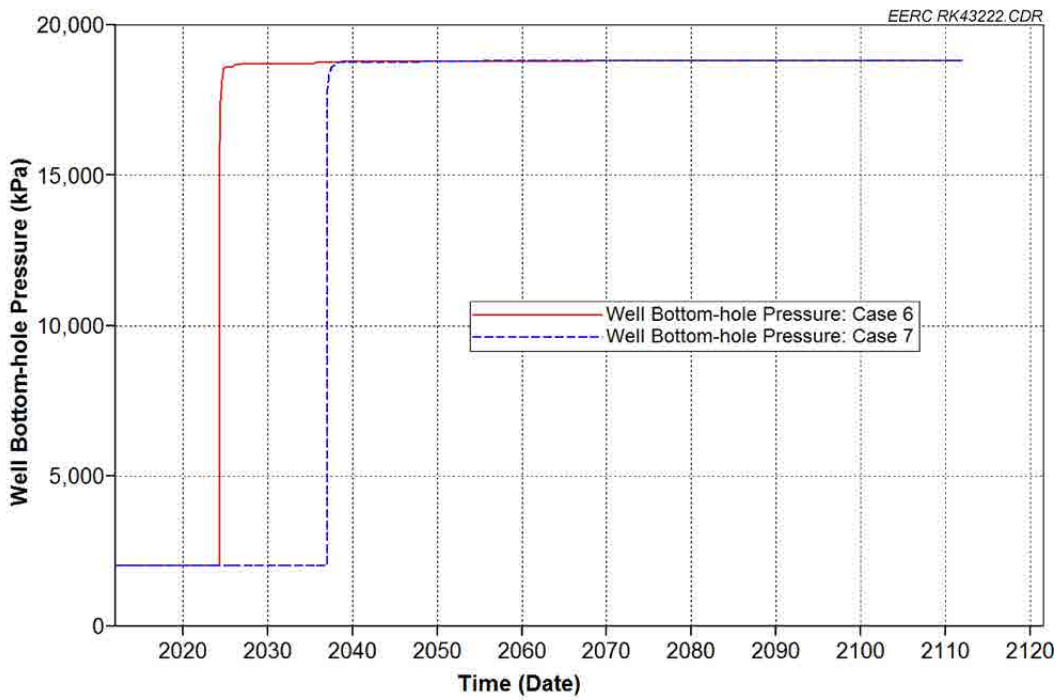


Figure F-75. BHPs of production wells for Cases 6 and 7.

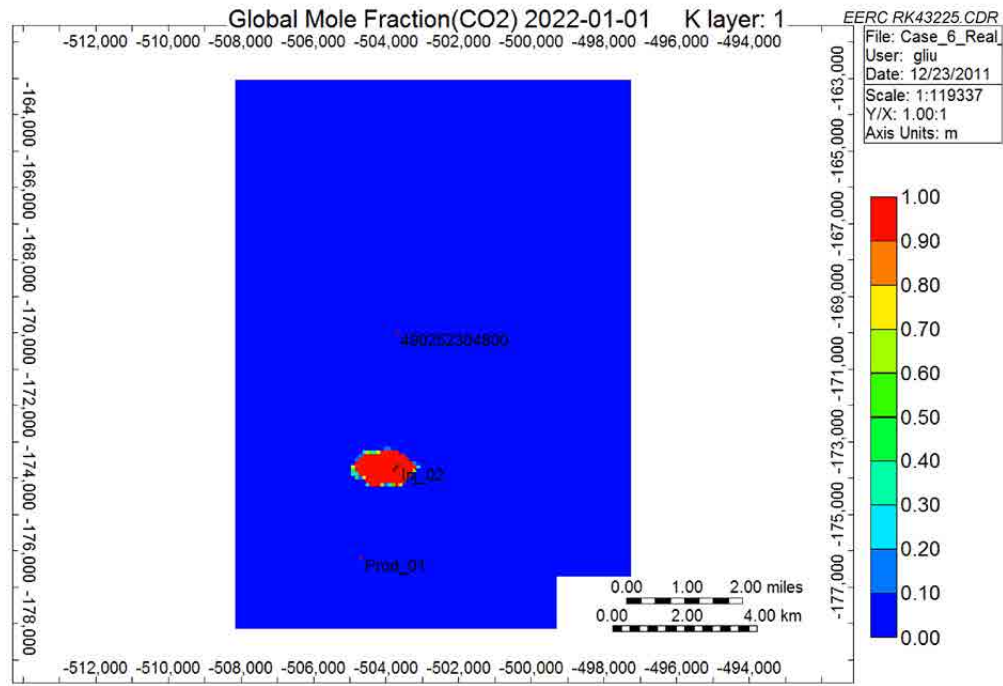


Figure F-76. 3-D view of Case 6: CO₂ plume migration for 10 years from beginning of injection.

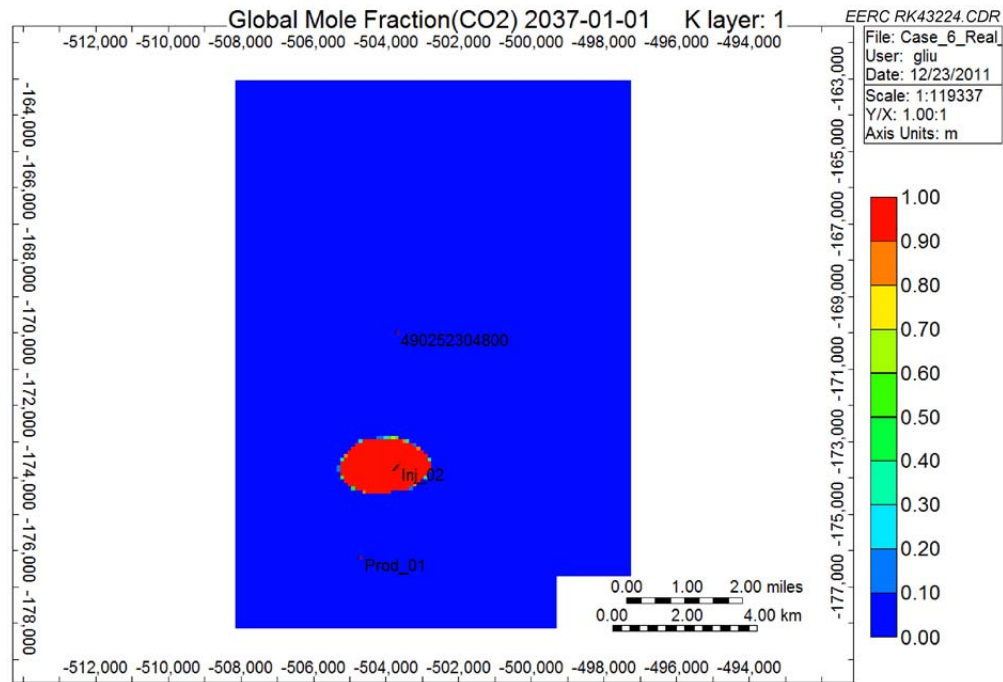


Figure F-77. 3-D view of Case 6: CO₂ plume migration for 25 years from beginning of injection.

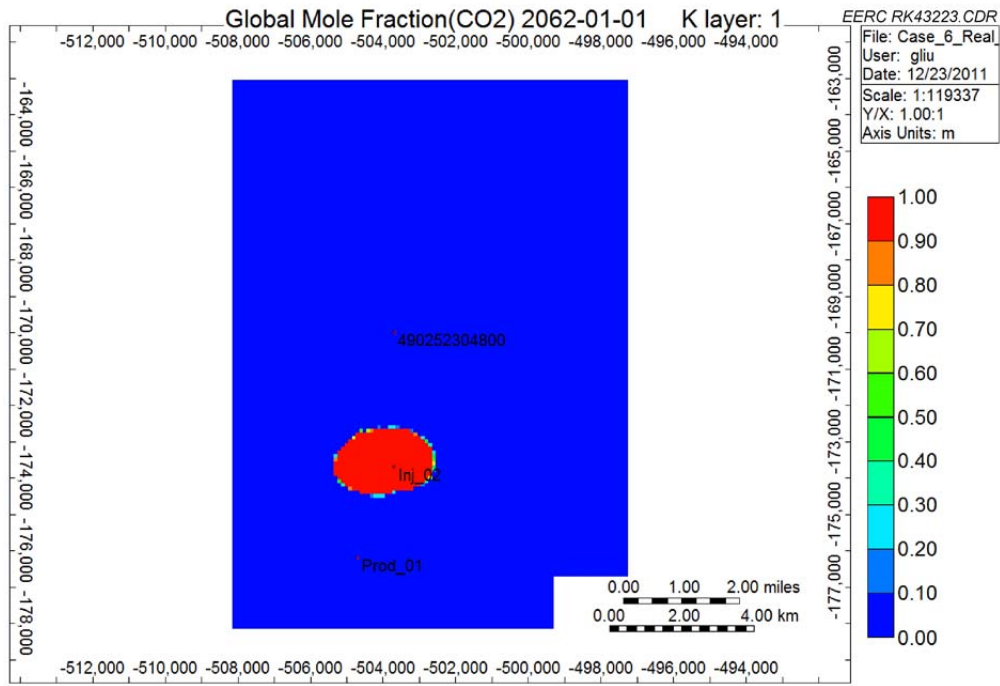


Figure F-78. 3-D view of Case 6: CO₂ plume migration for 50 years from beginning of injection.

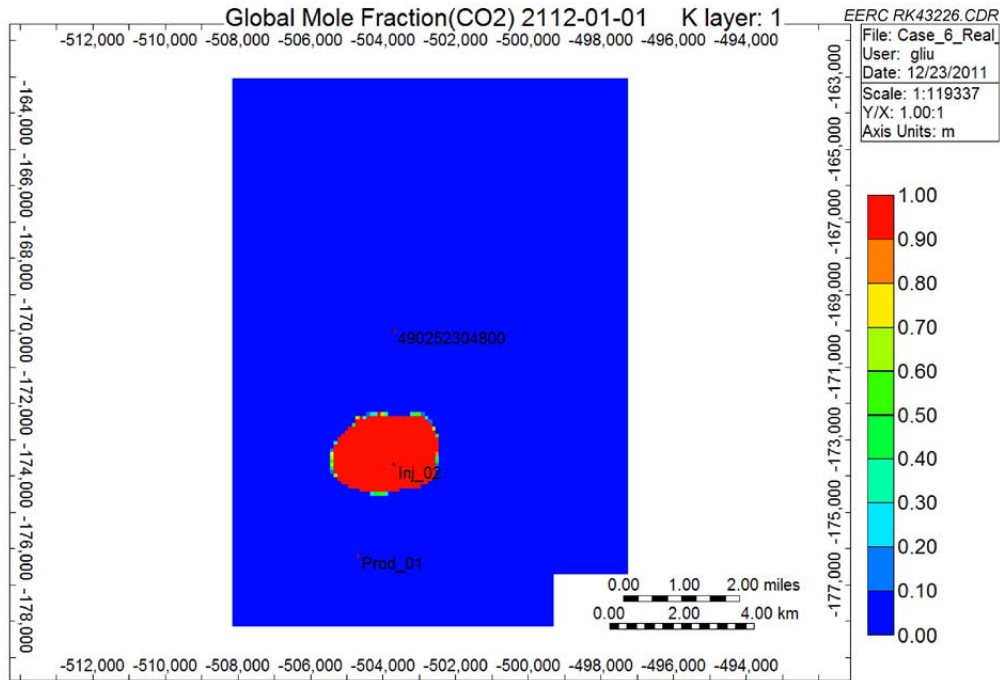


Figure F-79. 3-D view of Case 6: CO₂ plume migration for 100 years from beginning of injection.

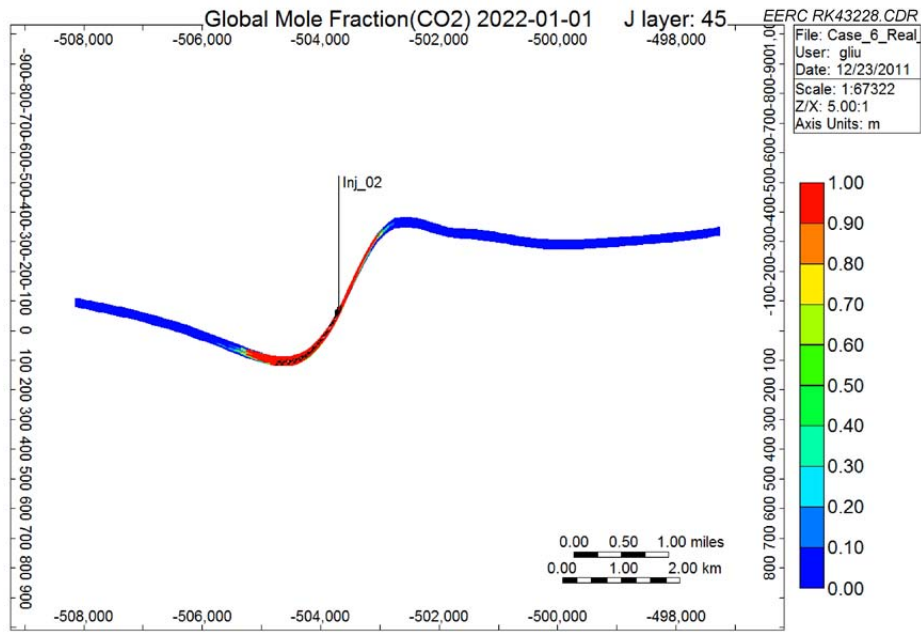


Figure F-80. Cross-sectional view of Case 6: CO₂ plume migration for 10 years from beginning of injection.

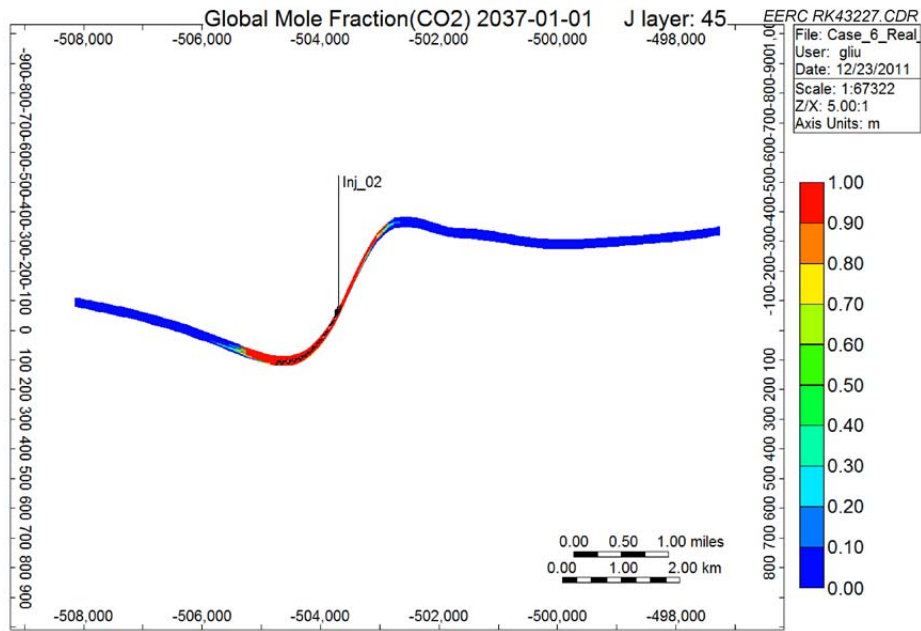


Figure F-81. Cross-sectional view of Case 6: CO₂ plume migration for 25 years from beginning of injection.

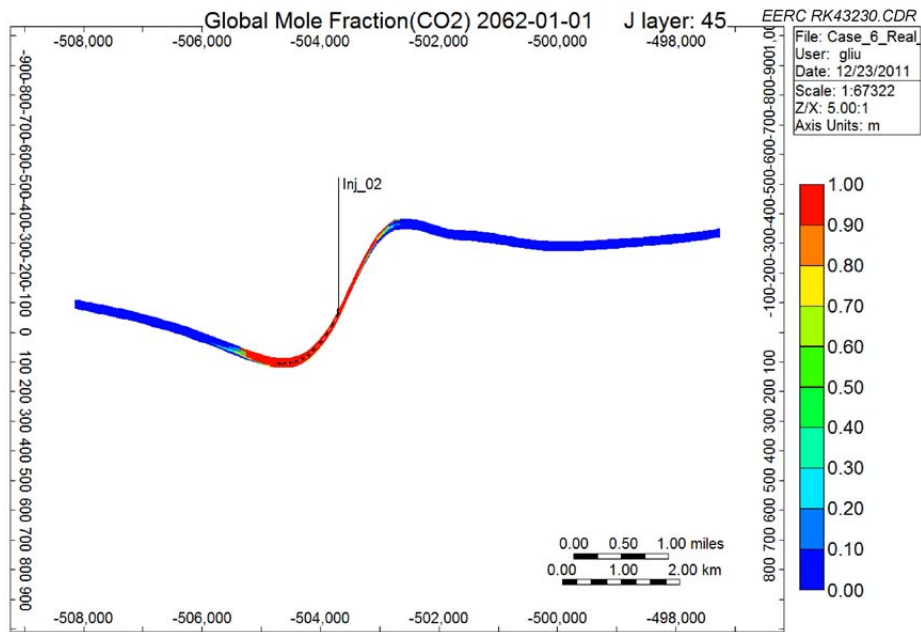


Figure F-82. Cross-sectional view of Case 6: CO₂ plume migration for 50 years from beginning of injection.

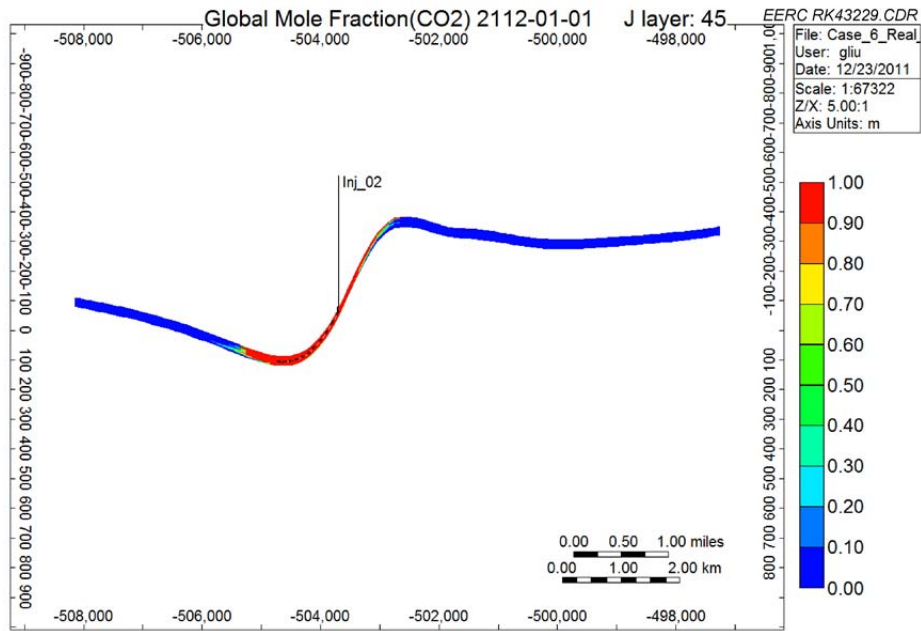


Figure F-83. Cross-sectional view of Case 6: CO₂ plume migration for 100 years from beginning of injection.

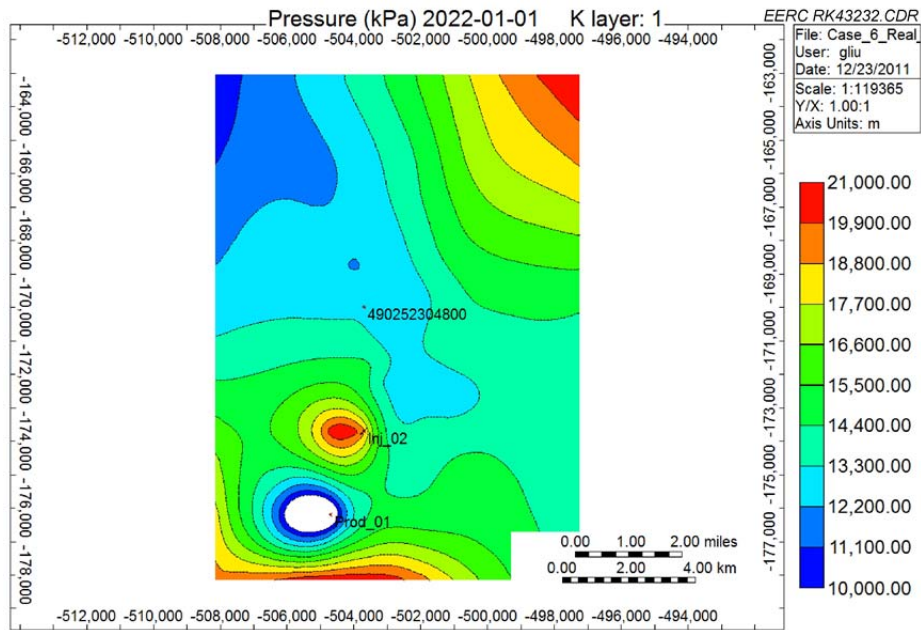


Figure F-84. Areal view of Case 6: pressure distributions for 10 years from beginning of injection.

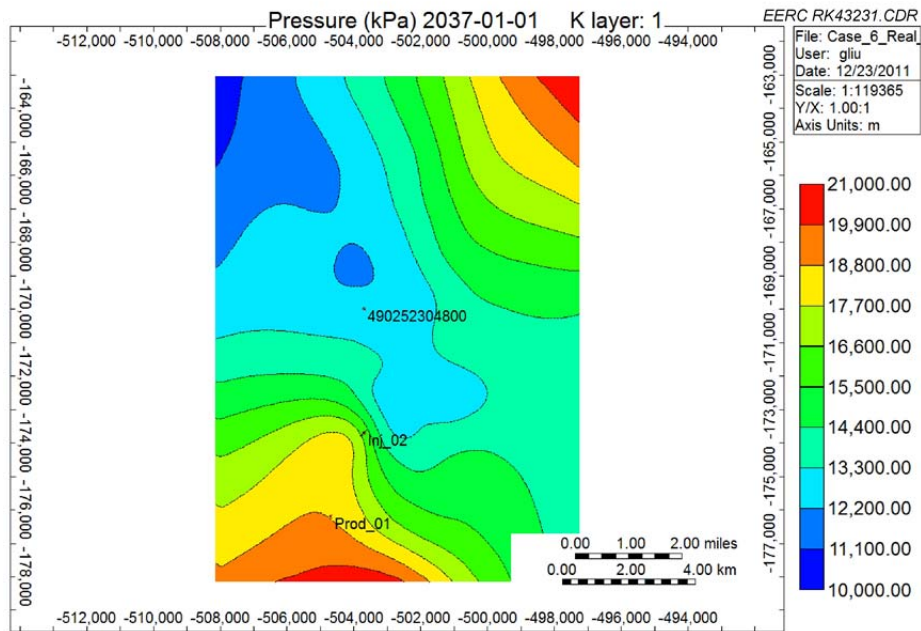


Figure F-85. Areal view of Case 6: pressure distributions for 25 years from beginning of injection.

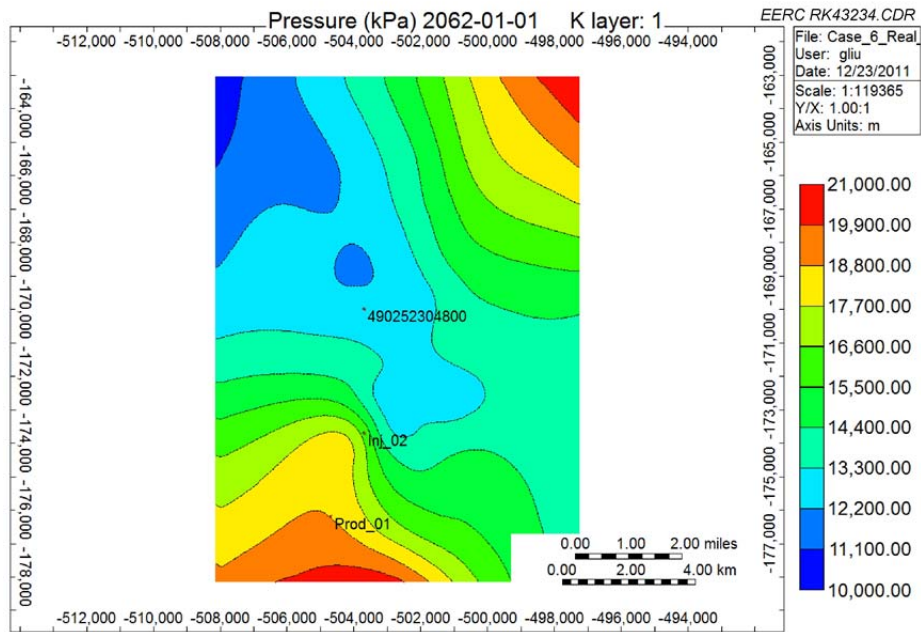


Figure F-86. Areal view of Case 6: pressure distributions for 50 years from beginning of injection.

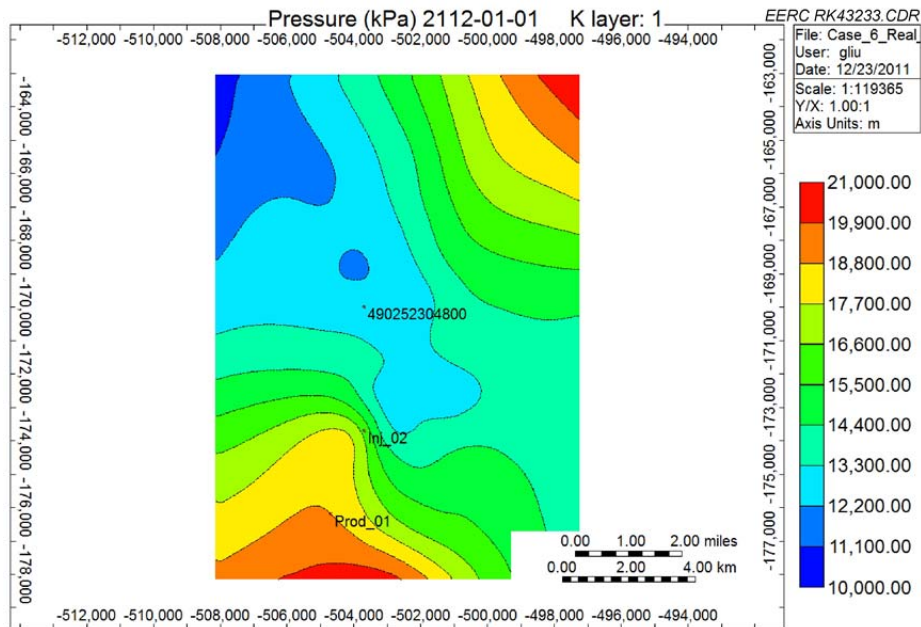


Figure F-87. Areal view of Case 6: pressure distributions for 100 years from beginning of injection.

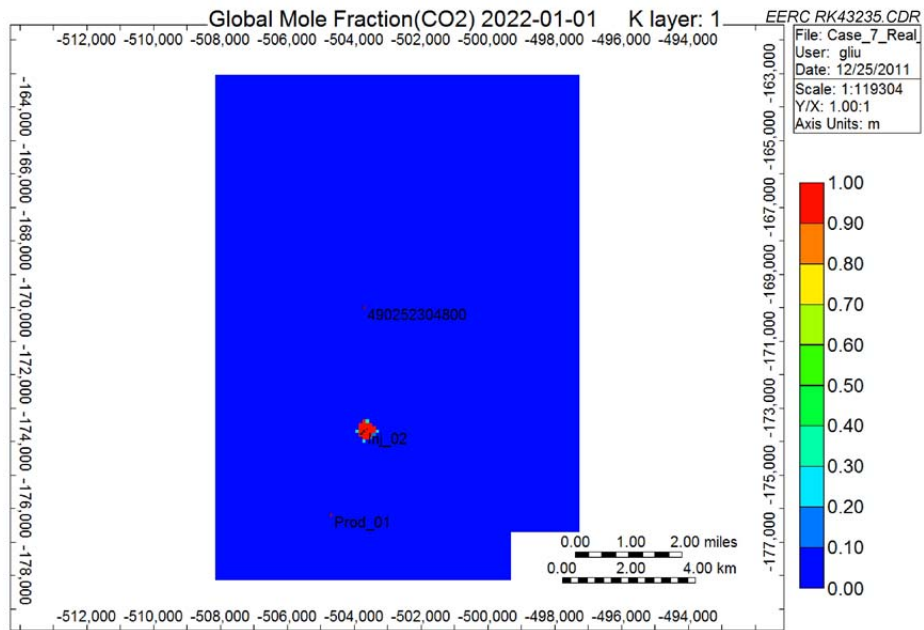


Figure F-88. 3-D view of Case 7: CO₂ plume migration for 10 years from beginning of injection.

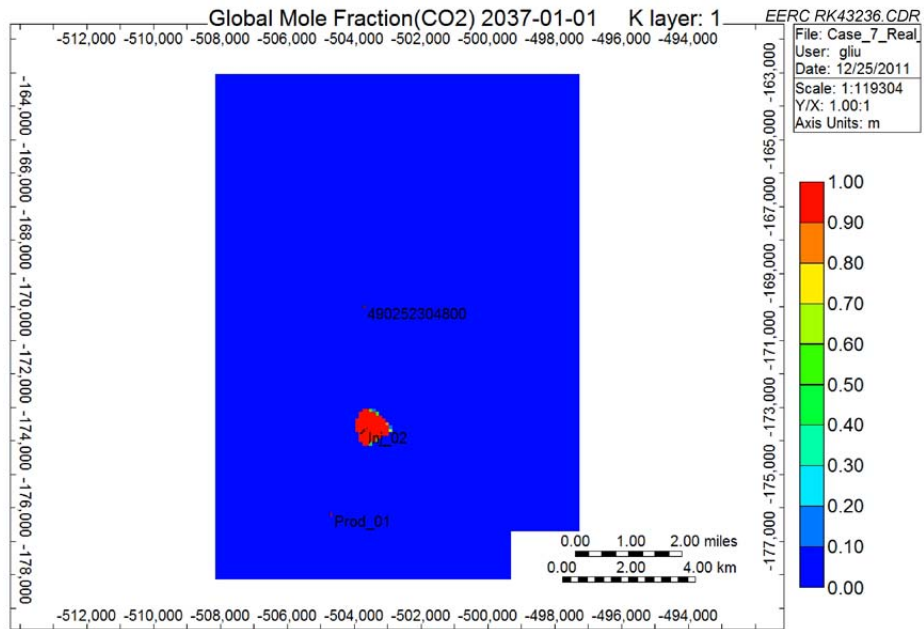


Figure F-89. 3-D view of Case 7: CO₂ plume migration for 25 years from beginning of injection.

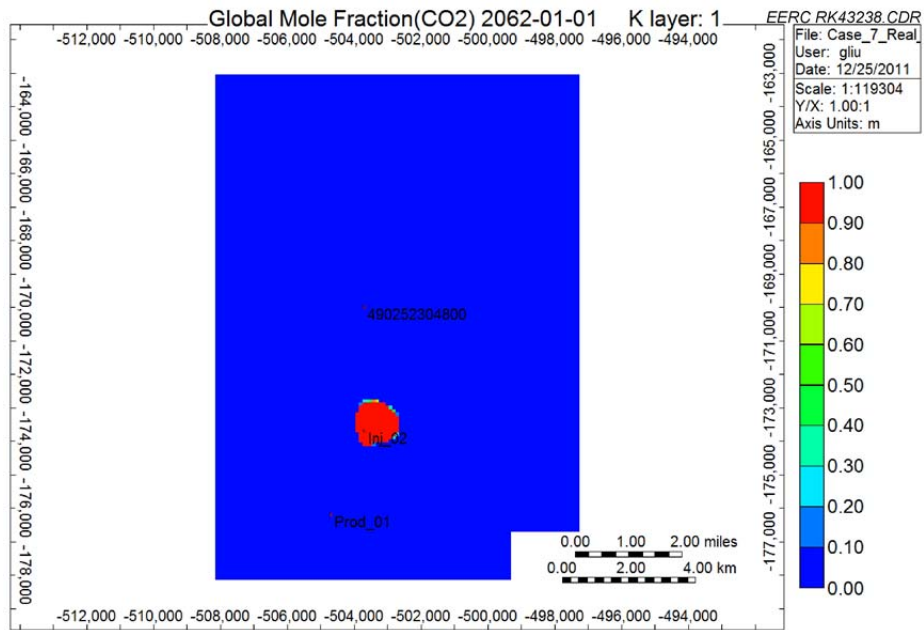


Figure F-90. 3-D view of Case 7: CO₂ plume migration for 50 years from beginning of injection.

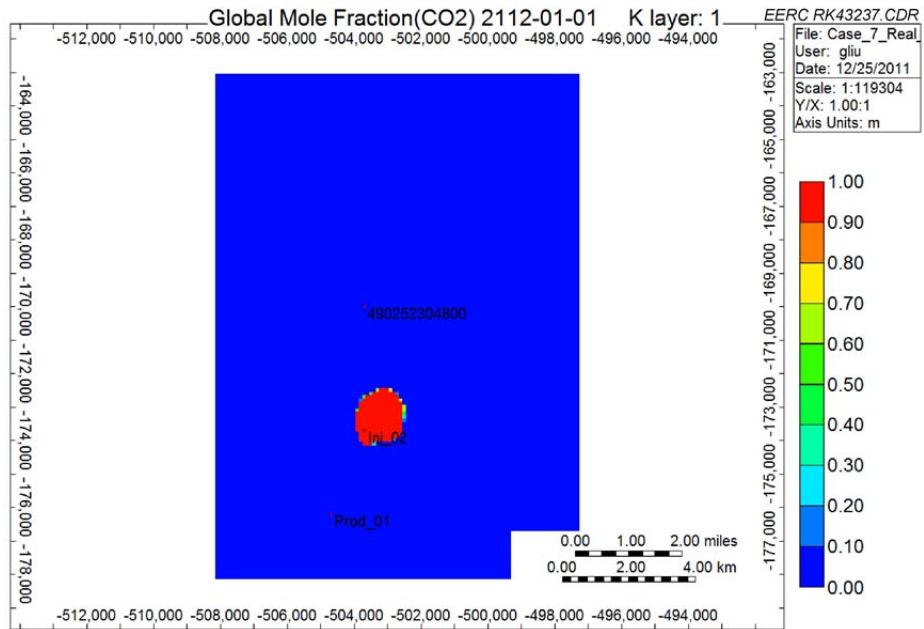


Figure F-91. 3-D view of Case 7: CO₂ plume migration for 100 years from beginning of injection.

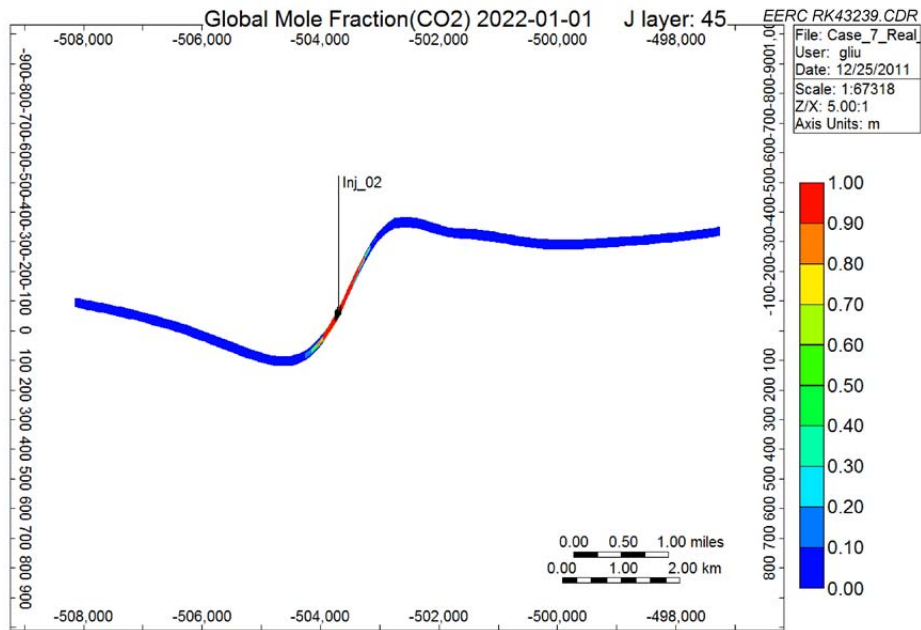


Figure F-92. Cross-sectional view of Case 7: CO₂ plume migration for 10 years from beginning of injection.

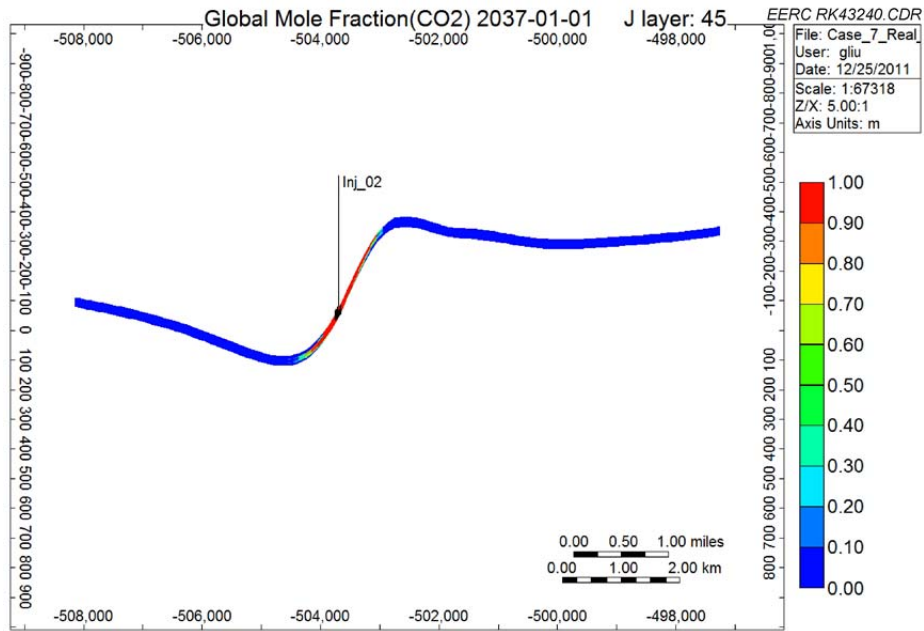


Figure F-93. Cross-sectional view of Case 7: CO₂ plume migration for 25 years from beginning of injection.

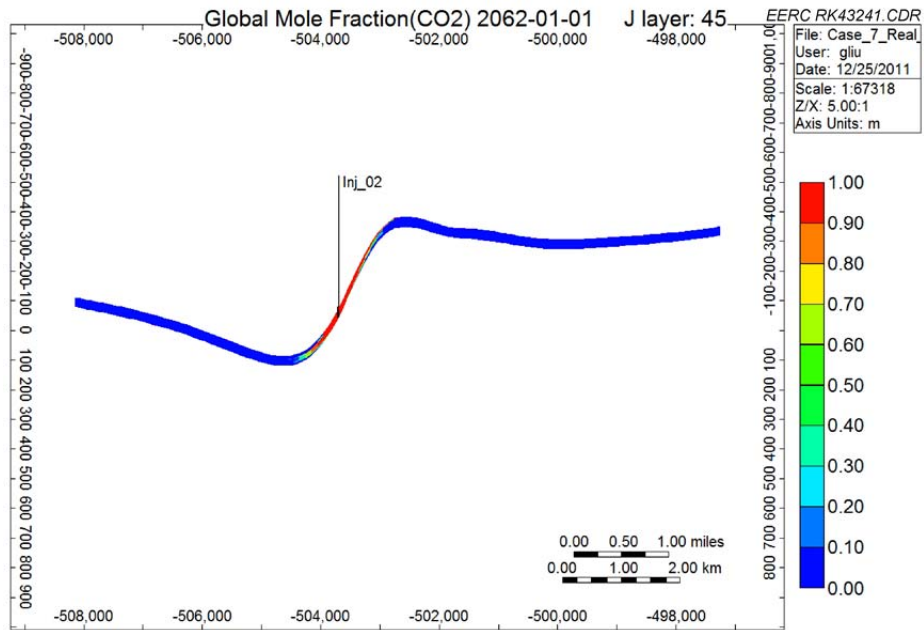


Figure F-94. Cross-sectional view of Case 7: CO₂ plume migration for 50 years from beginning of injection.

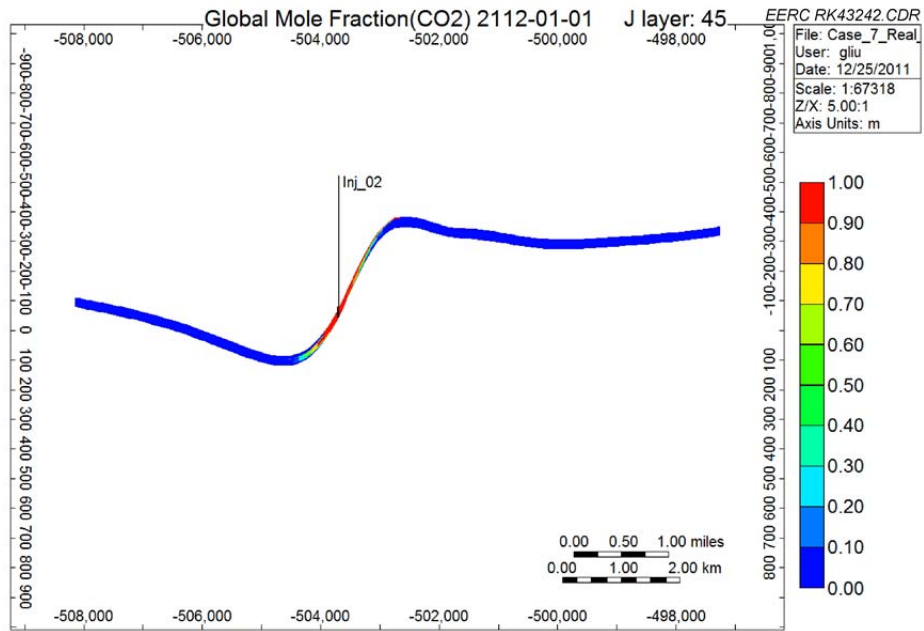


Figure F-95. Cross-sectional view of Case 7: CO₂ plume migration for 100 years from beginning of injection.

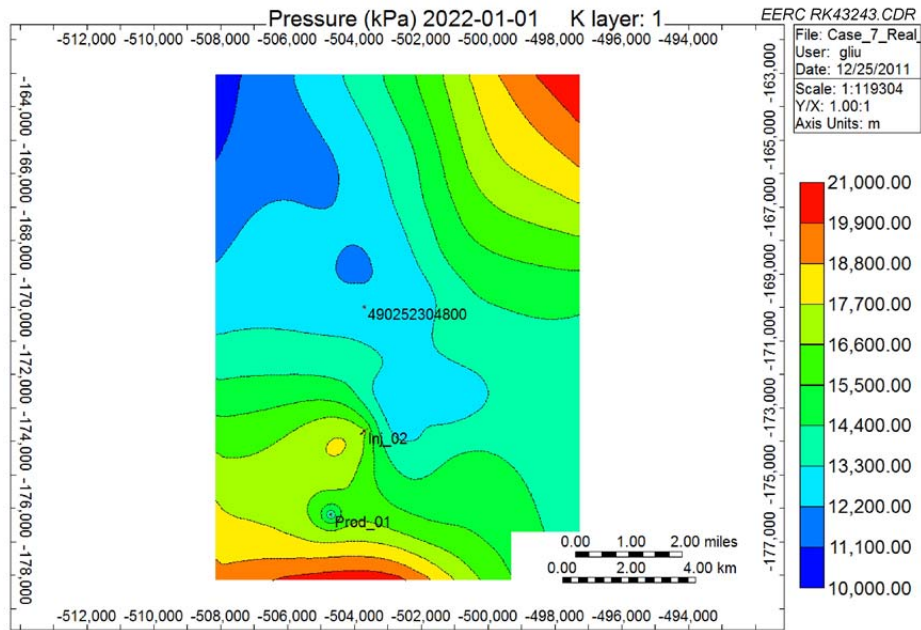


Figure F-96. Areal view of Case 7: pressure distributions for 10 years from beginning of injection.

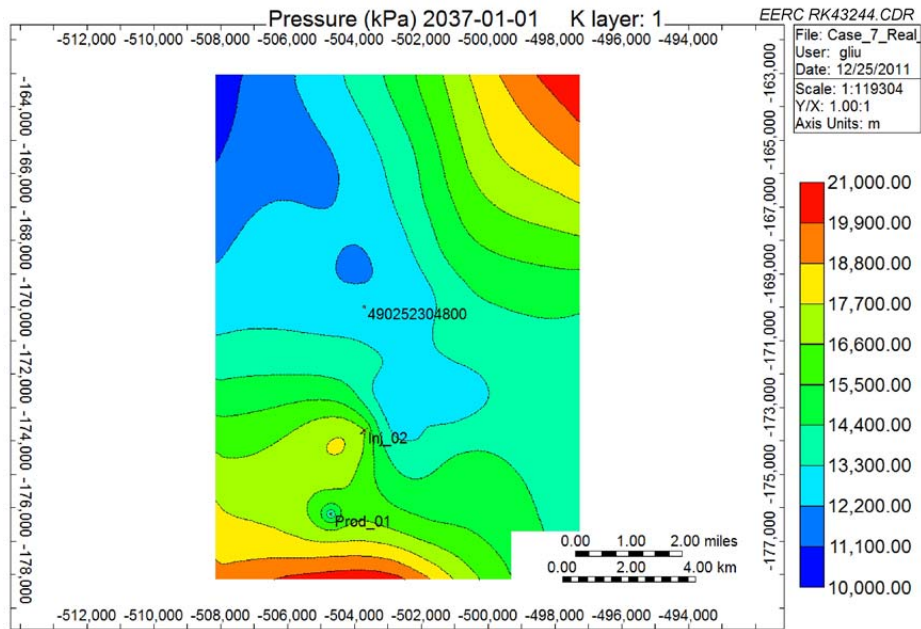


Figure F-97. Areal view of Case 7: pressure distributions for 25 years from beginning of injection.

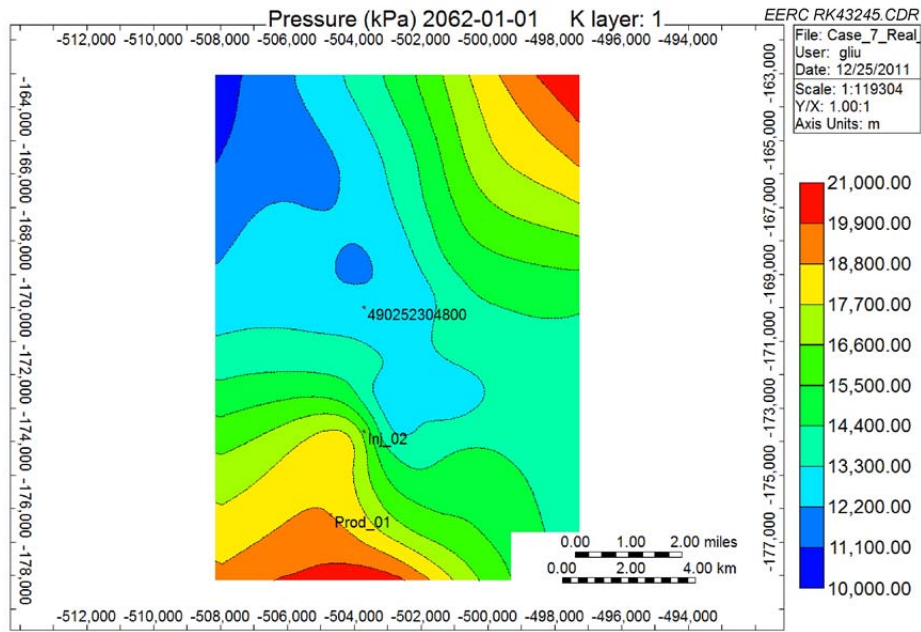


Figure F-98. Areal view of Case 7: pressure distributions for 50 years from beginning of injection.

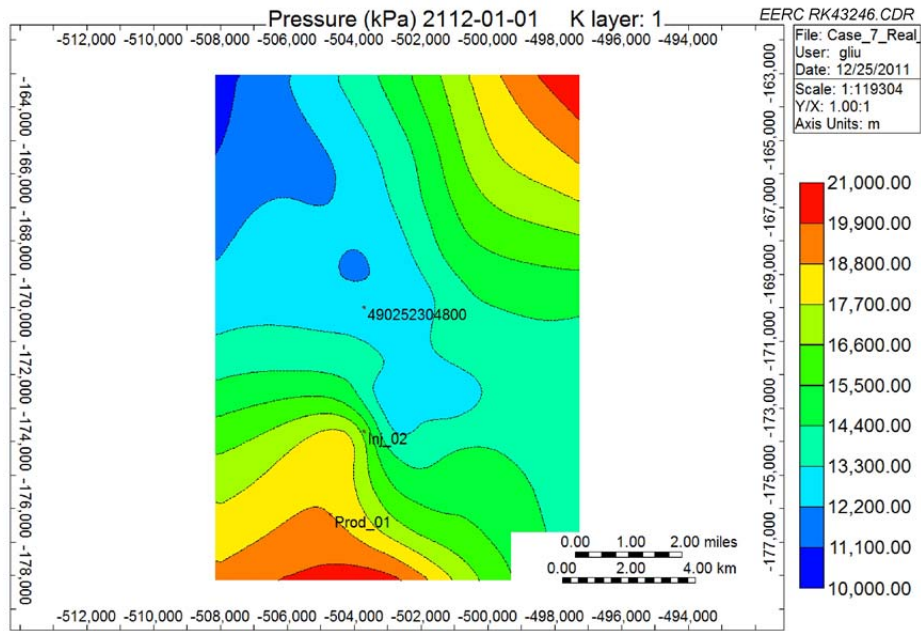


Figure F-99. Areal view of Case 7: pressure distributions for 100 years from beginning of injection.

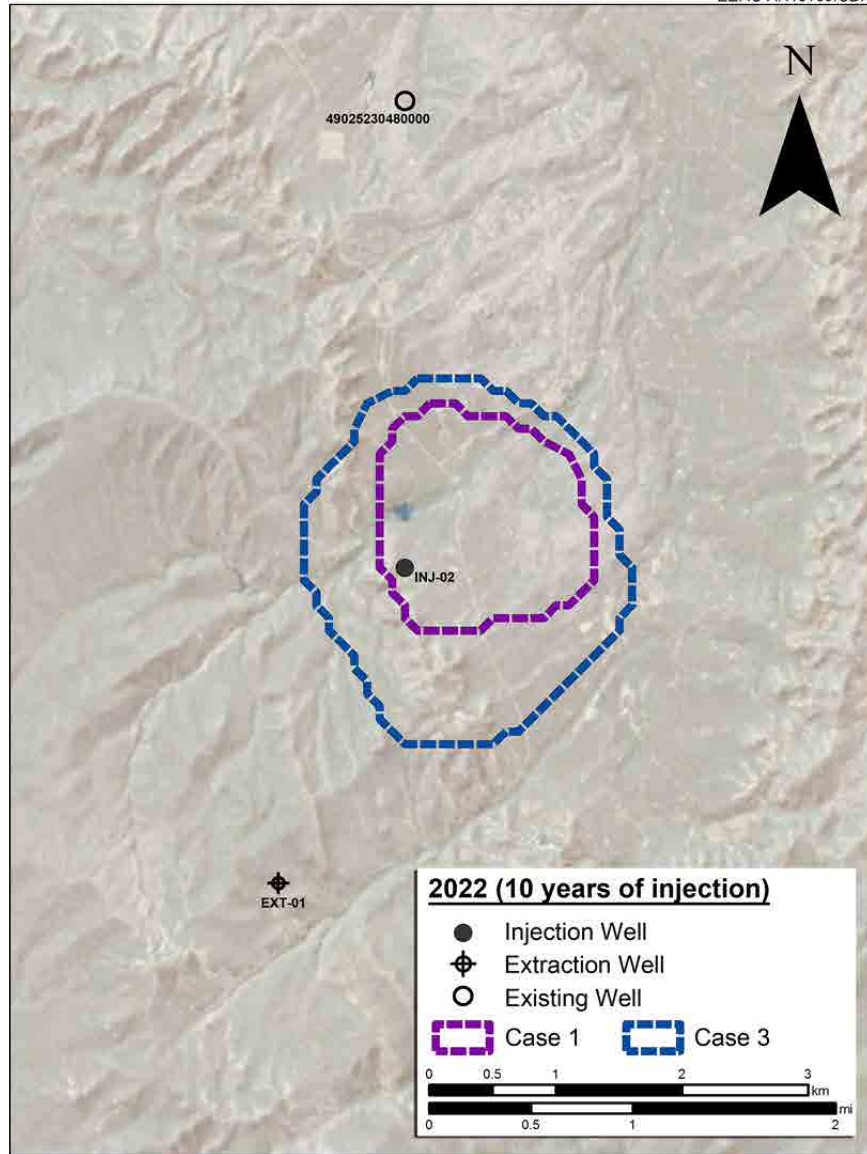


Figure F-100. Surface map view showing the plume extents generated by Cases 1 and 3 after 10 years.

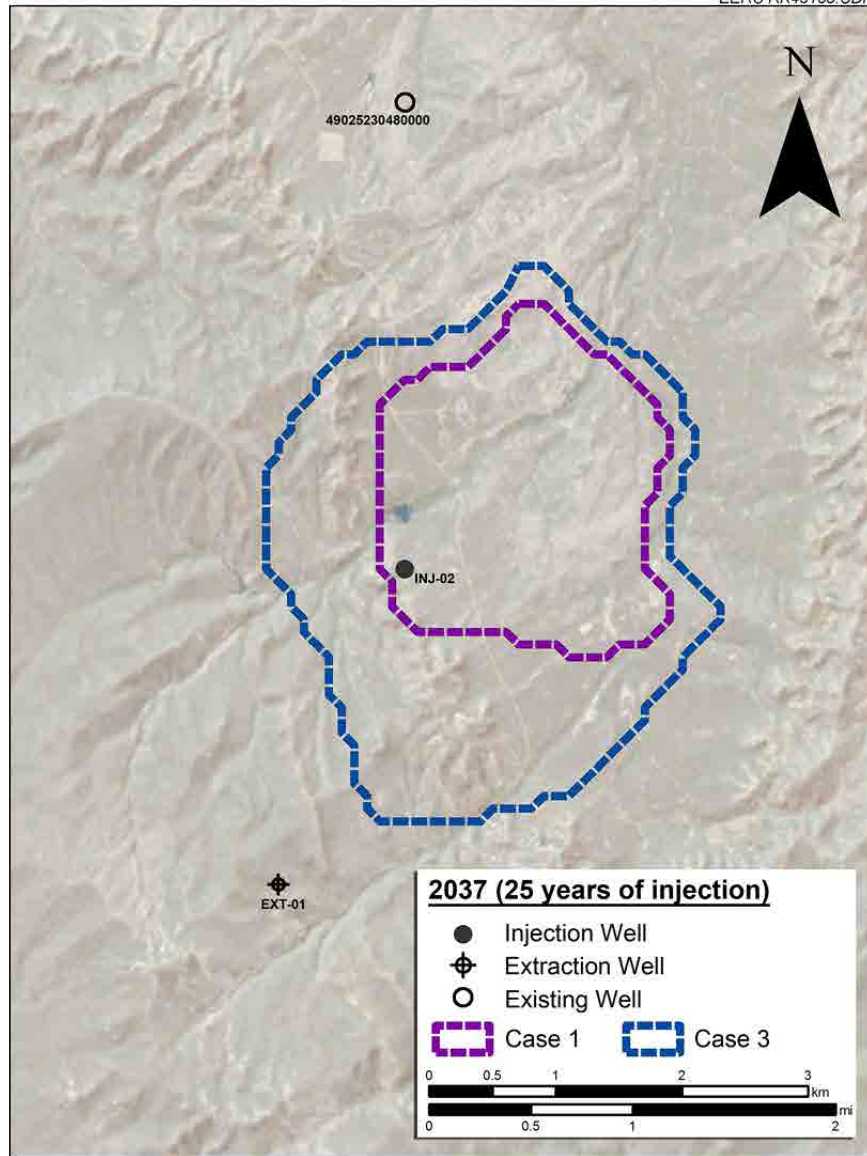


Figure F-101. Surface map view showing the plume extents generated by Cases 1 and 3 after 25 years.

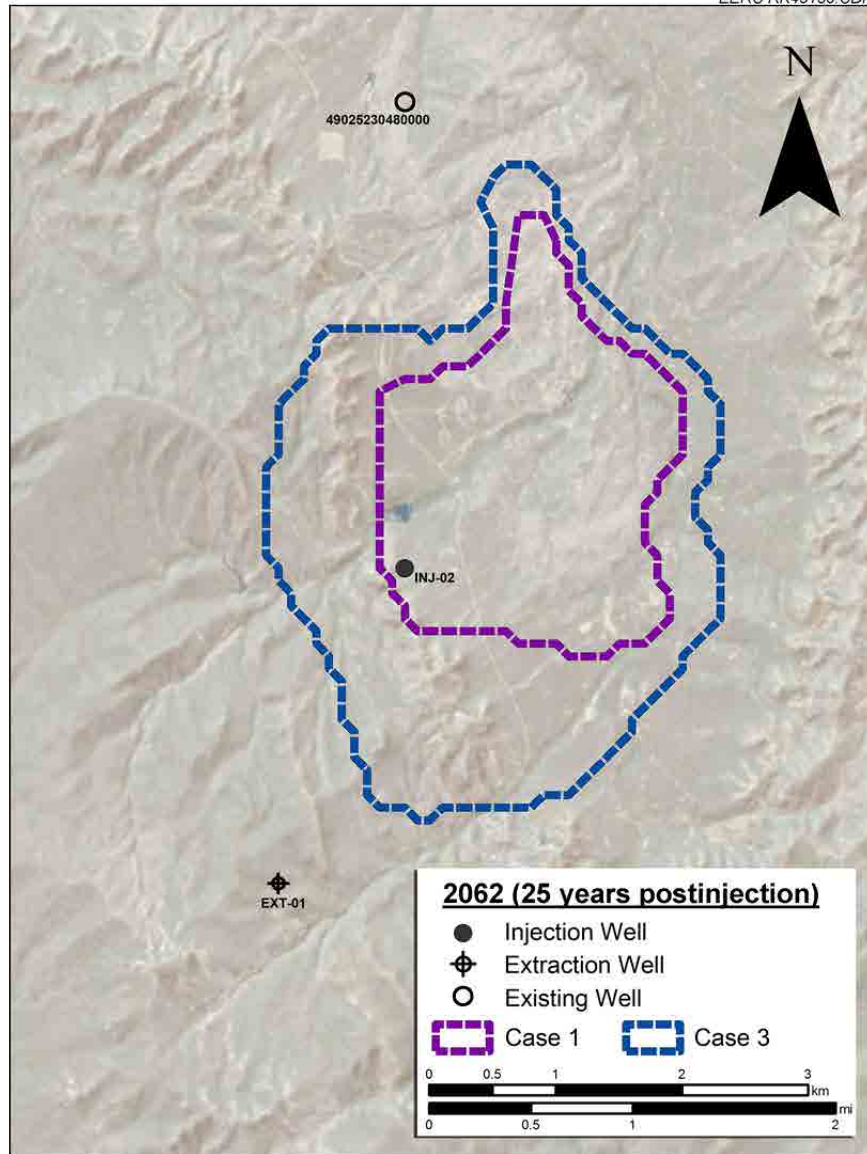


Figure F-102. Surface map view showing the plume extents generated by Cases 1 and 3 after 50 years.

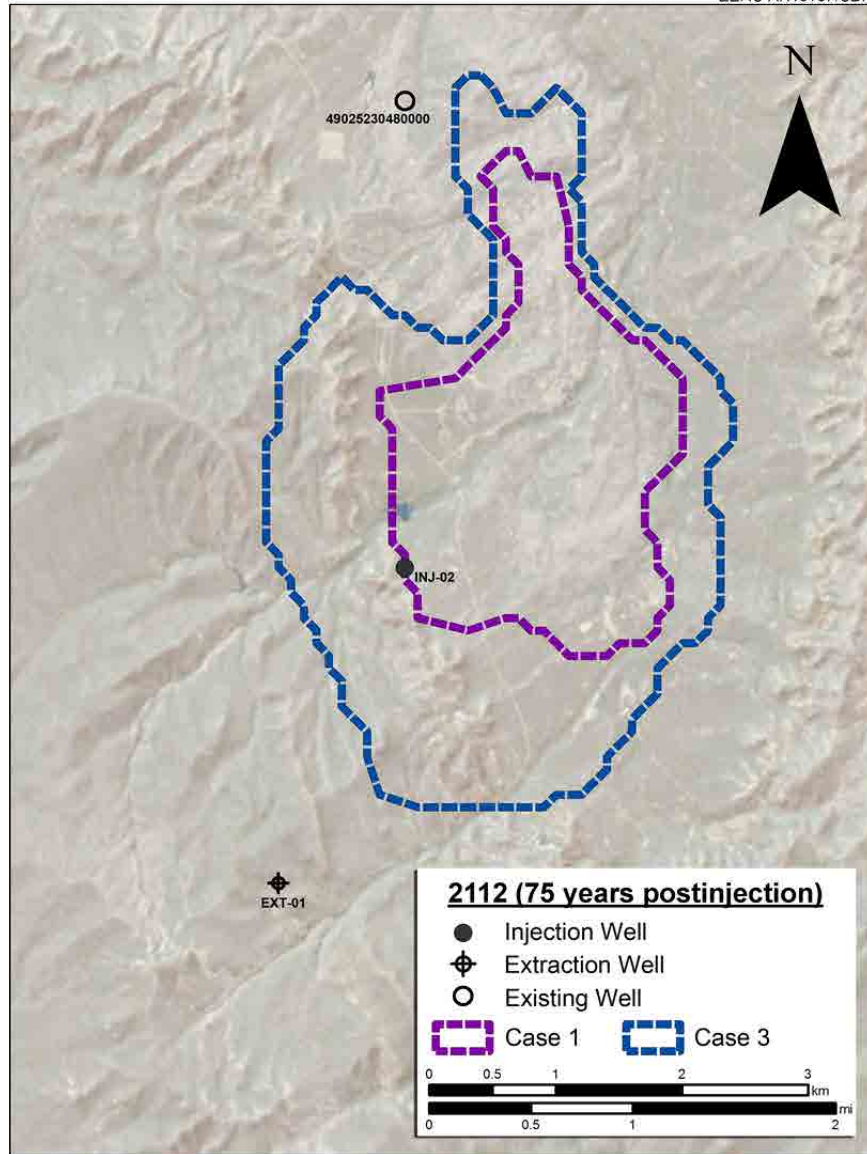


Figure F-103. Surface map view showing the plume extents generated by Cases 1 and 3 after 100 years.

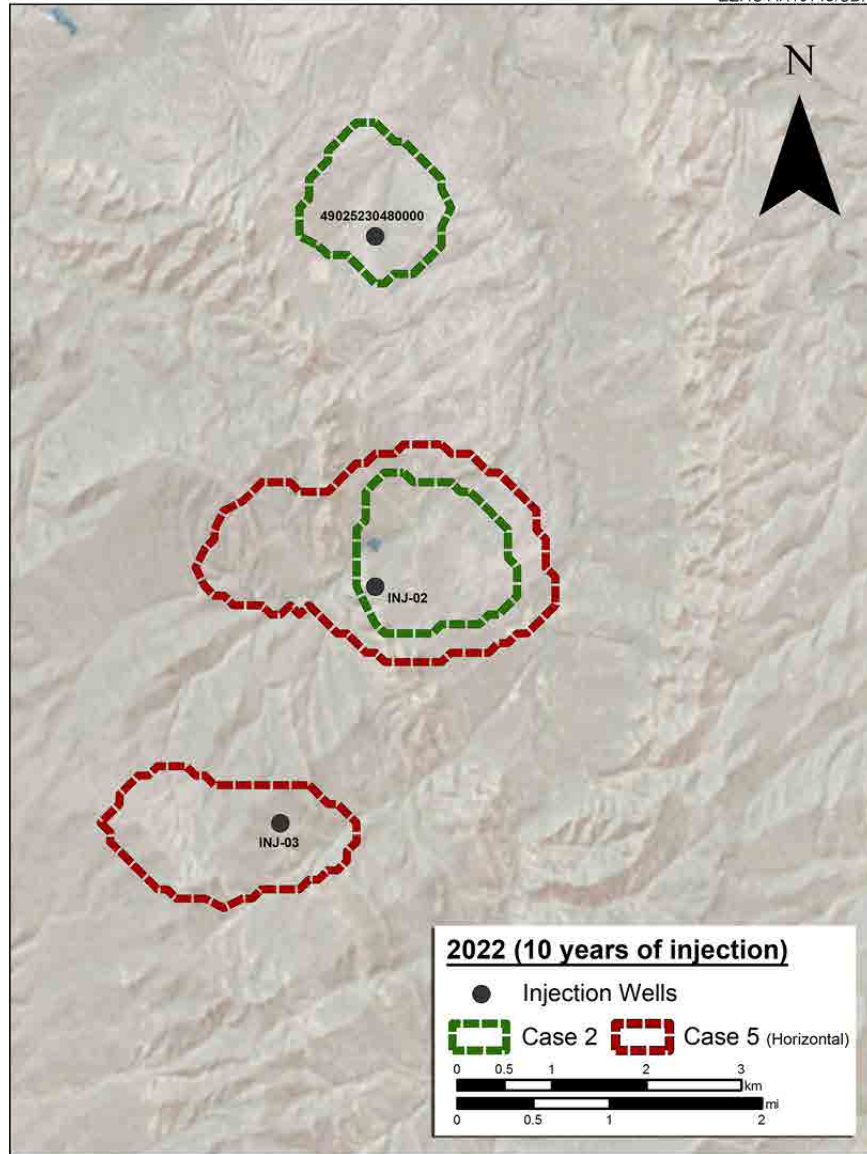


Figure F-104. Surface map view showing the plume extents generated by Cases 2 and 5 after 10 years.

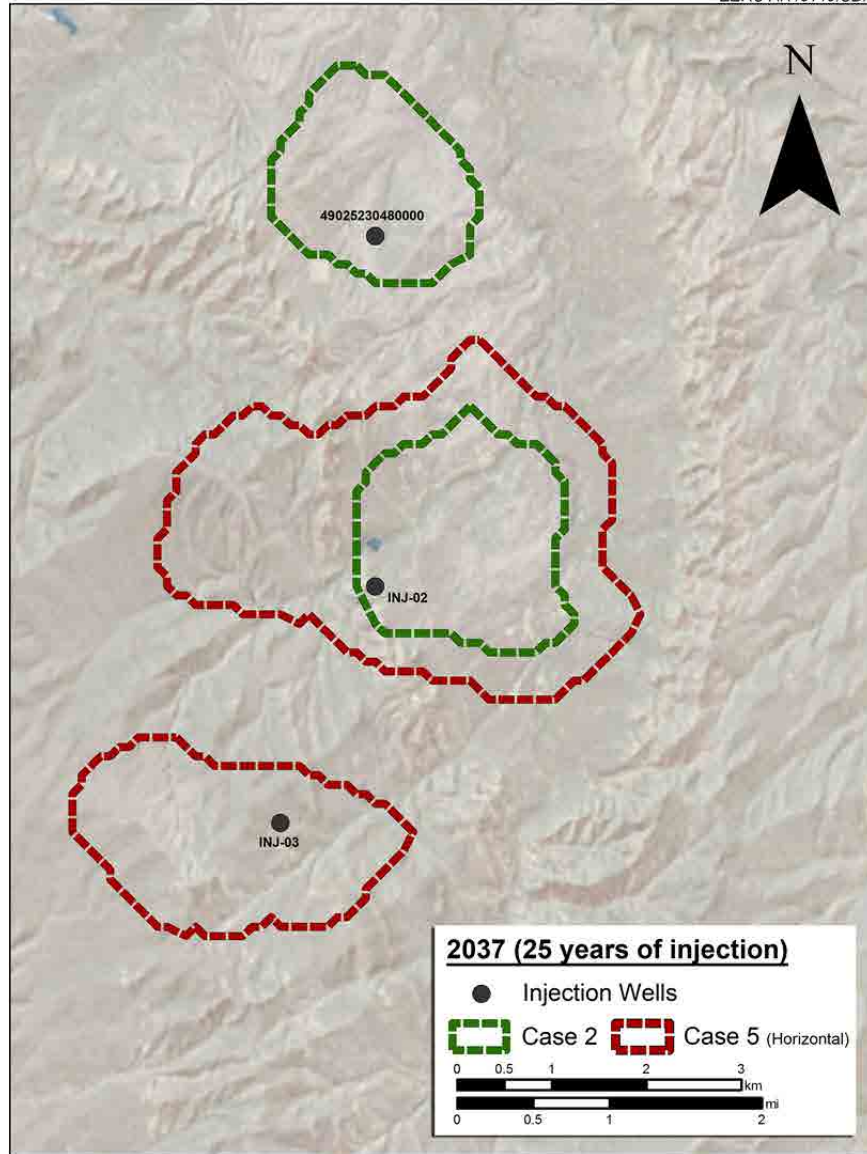


Figure F-105. Surface map view showing the plume extents generated by Cases 2 and 5 after 25 years.

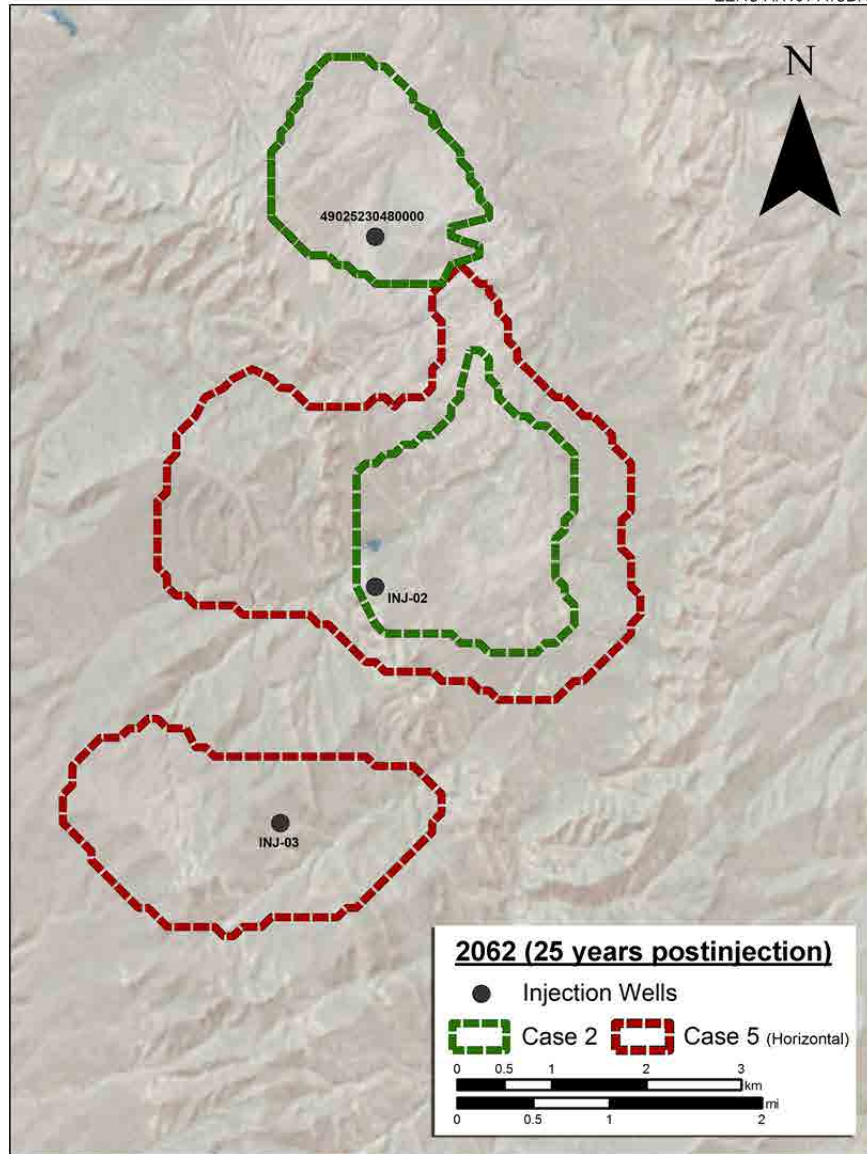


Figure F-106. Surface map view showing the plume extents generated by Cases 2 and 5 after 50 years.

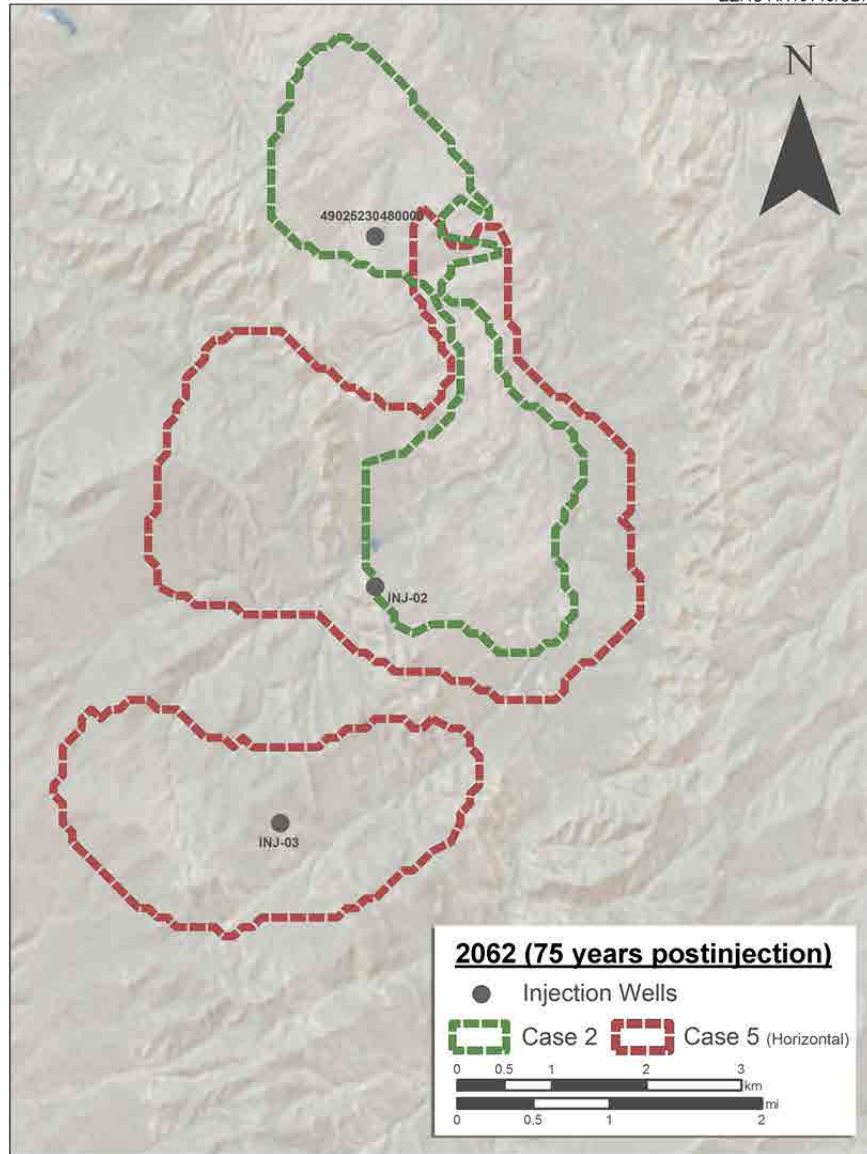


Figure F-107. Surface map view showing the plume extents generated by Cases 2 and 5 after 100 years.

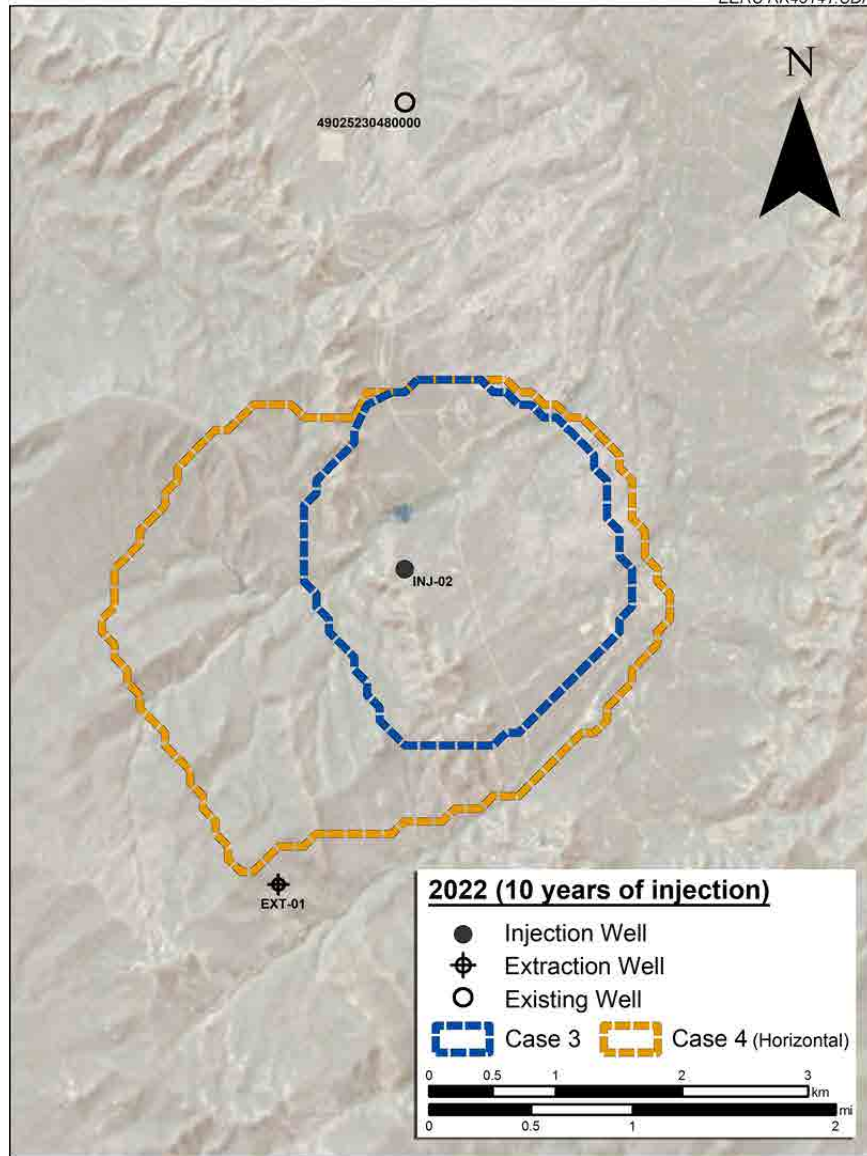


Figure F-108. Surface map view showing the plume extents generated by Cases 3 and 4 after 10 years.

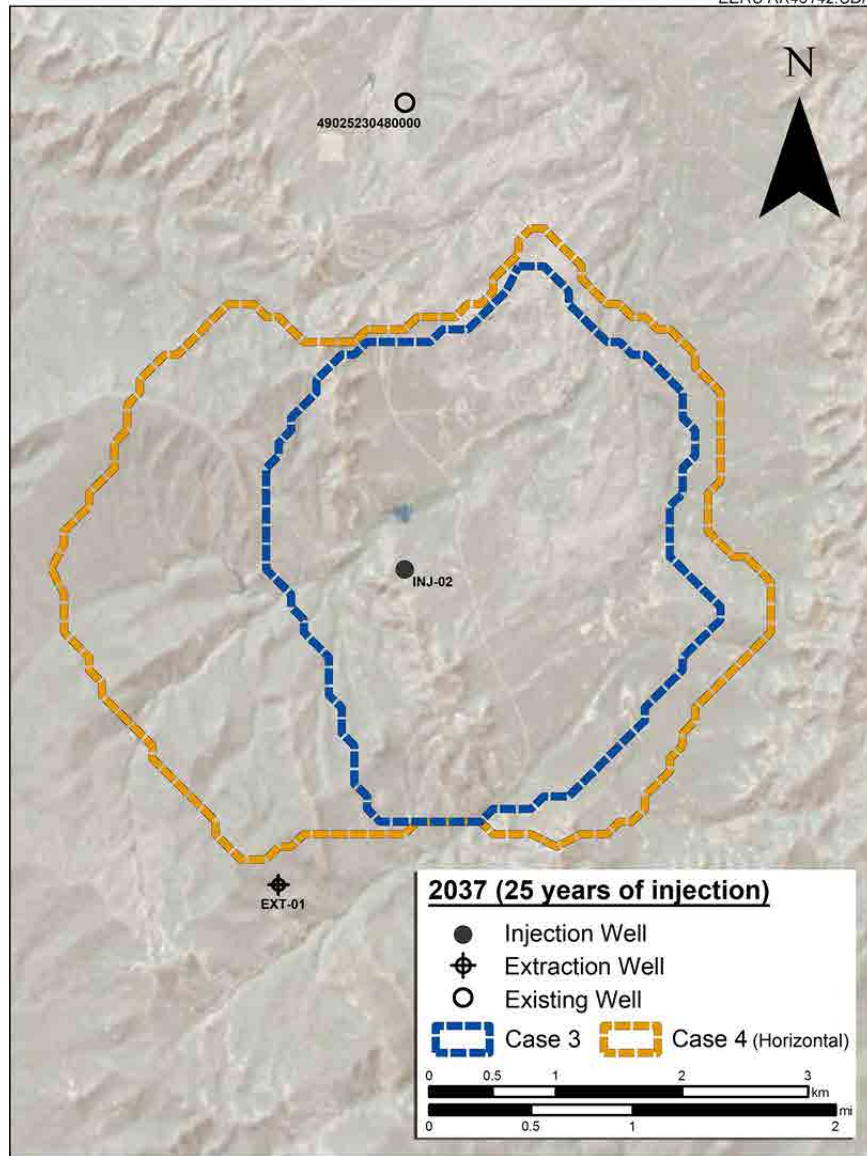


Figure F-109. Surface map view showing the plume extents generated by Cases 3 and 4 after 25 years.

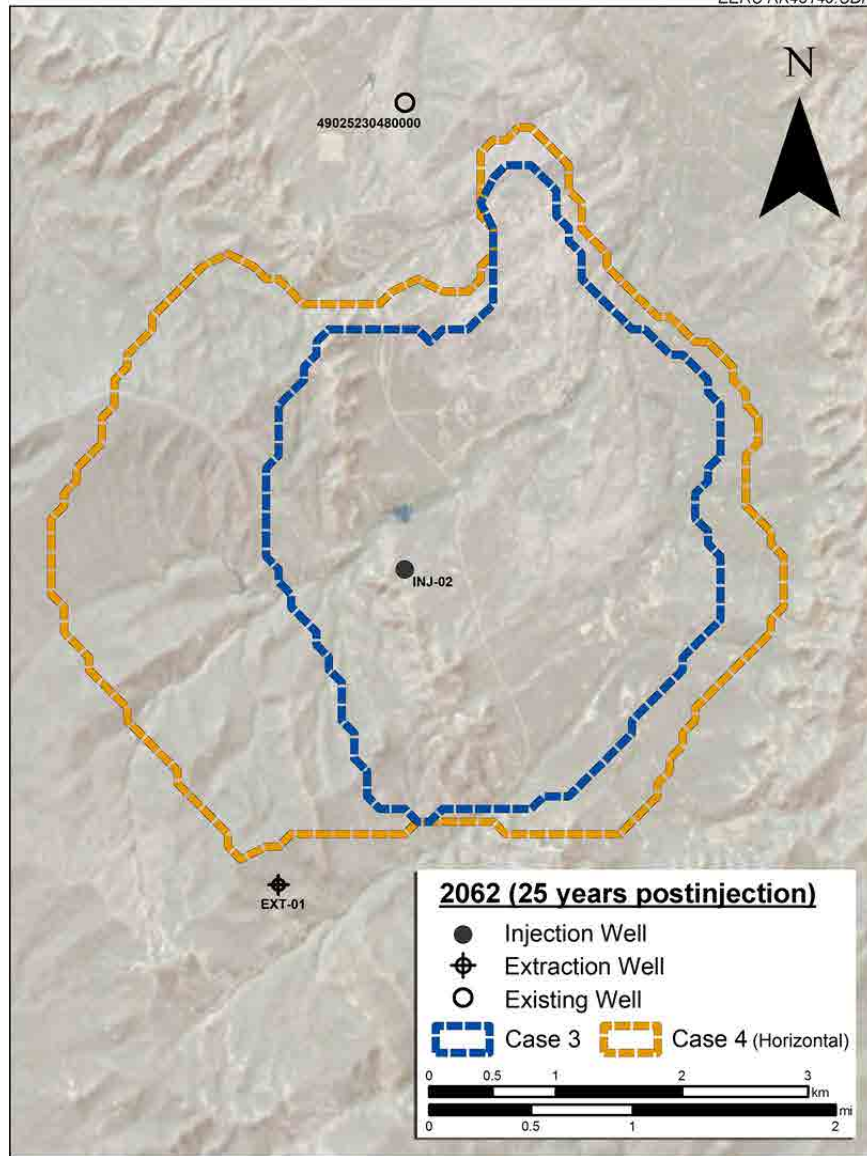


Figure F-110. Surface map view showing the plume extents generated by Cases 3 and 4 after 50 years.

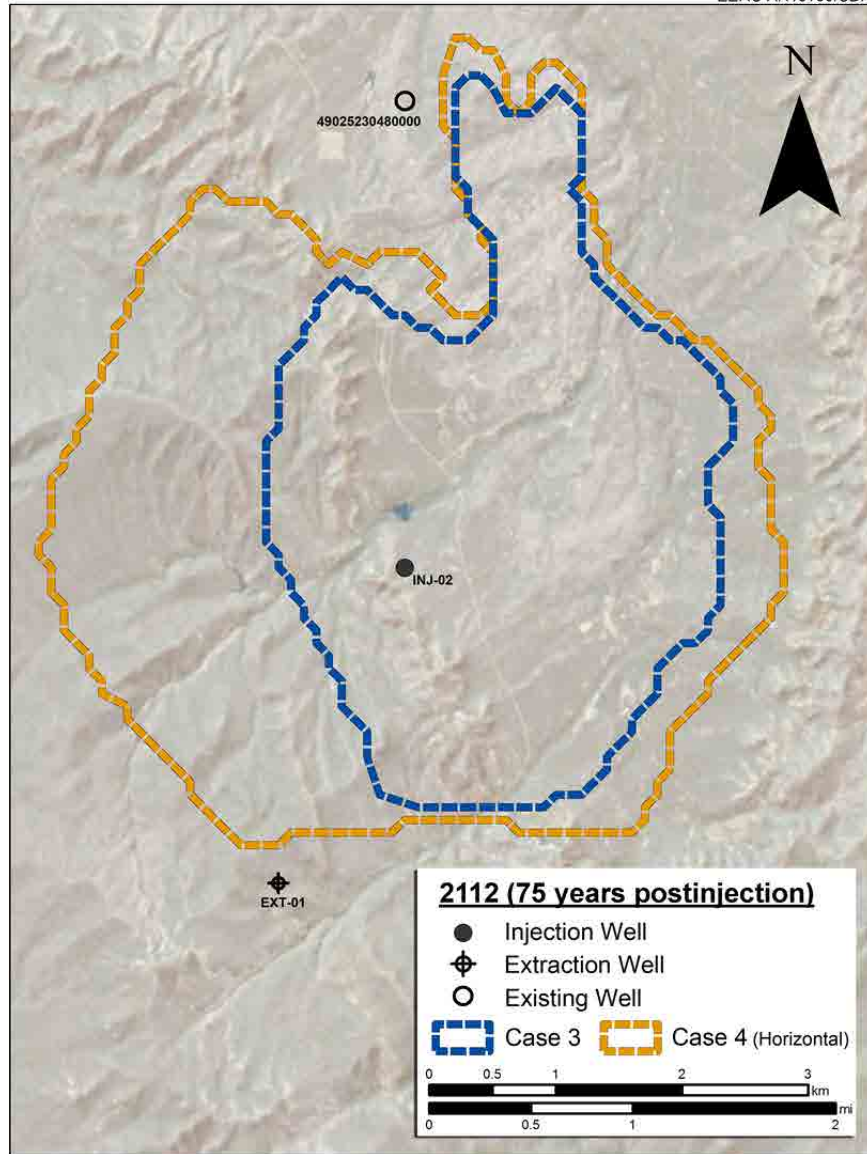


Figure F-111. Surface map view showing the plume extents generated by Cases 3 and 4 after 100 years.

APPENDIX G

SURFACE DISSOLUTION MODELING AND SIMULATIONS

SURFACE DISSOLUTION – EQUILIBRIUM MODELING

INTRODUCTION

Surface dissolution with reinjection of the CO₂-containing water has been proposed as a method for achieving geological CO₂ storage (Eke and others, 2011; Jain and Bryant, 2011; Burton and Bryant, 2009). This method involves extraction of formation water, dissolution of CO₂ into it within surface facilities, and reinjection of the solution into a geologic formation. The purported advantage of using the surface dissolution method is that it would result in an injected fluid which is denser than the native formation water, thus eliminating formation of a buoyant plume and reducing some of the risks associated with the injection of buoyant, free-phase CO₂. Surface dissolution might also be a technique for the stable storage of CO₂ in saline aquifers with formation pressures below the critical point of CO₂.

The ability to successfully use surface dissolution as a CO₂ storage approach will depend on many things, but a primary measure of the potential is the total solubility of inorganic carbon (i.e., CO₂, bicarbonate ions, carbonate ions) in the extracted water at the appropriate temperature and pressure conditions. Comparing the total inorganic carbon solubility to the density of pure-phase CO₂ under the same conditions provides an easy measure of the difference in storage capacity that might be obtained by following the alternative CO₂ storage approaches of injecting pure-phase CO₂ and surface dissolution.

Although the effective solubility of CO₂ can be higher than the density of pure-phase (i.e., gaseous) CO₂, this condition only occurs for some waters, only at lower temperatures and only at low pressures where the pure-phase CO₂ is a gas. At conditions relevant for the storage of CO₂ in deep saline formations, the density of pure-phase CO₂ will be higher than the effective density of dissolved CO₂. How much higher depends on the temperature and pressure considered and the chemical composition (e.g., salinity, pH, alkalinity) of the water. Also, this CO₂ solubility will always be much lower than can be calculated using available geochemical and aquatic chemistry software containing equilibrium thermodynamic models. This can provide an effective CO₂ density for the dissolved phase for comparison with the density of pure-phase CO₂ under storage reservoir conditions.

The potential effectiveness of using the CO₂ surface dissolution technique was evaluated by calculating the amount of CO₂ that could be dissolved into various waters over a range of temperatures and pressures. The CO₂ dissolution value at formation conditions is then compared to the amount of dense-phase CO₂, which would occupy the same volume under the same pressure and temperature conditions. An evaluation of the effect of CO₂ interaction with formation minerals is also provided.

The composition of the formation water is one of the critical inputs for calculation of CO₂ dissolution in water. Salinity of the water is a major contributor influencing the solubility of CO₂, but the chemical makeup of the water is also important. The pH and alkalinity (acid neutralizing capacity) of the water are very important because CO₂ behaves as an acid so high, pH and high-alkalinity waters will have higher capacities for CO₂ dissolution. The addition of

CO₂ to water can also change the scaling and corrosion potential of the water. The ability to accurately predict CO₂ solubility and other effects of CO₂ dissolution into a given water depends on the quality of the water analysis results available. Formation water samples used for measurement of water quality are altered from the original quality because changes in temperature and pressure experienced during sampling will allow the release of dissolved gases and precipitation of solids. If these changes are not accounted for, the resulting changes in pH, alkalinity, and other effects will alter predicted CO₂ solubility. Measurement errors experienced during analysis also need to be corrected before the water analysis results can be used. Common corrections are reconciliation of the charge balance, pH, and alkalinity.

Water reconciliation is an important step. In order to perform reconciliation for appropriate balancing charge, alkalinity, and pH values of examined water, it is necessary to perform several calculating steps. First, the water chemical properties that were measured at the surface conditions (normal atmospheric pressure and a temperature of 25°C) need to be recalculated at the reservoir pressure and temperature with equilibrium to formation minerals. Second, after the equilibrium calculation, minerals that have a saturation index different from zero need to be investigated, and an appropriate amount of selected minerals needs to be added in the mix along with the projected in situ gases for a second run of equilibrium calculations. This second step will determine the appropriate water chemistry and pH at the reservoir conditions.

Water Chemistry

Formation water analysis results were obtained for waters representative of those present in CO₂ storage reservoirs from each of the case study sites. The values used for the Ketzin site came from Würdemann and others (2010), those for Zama came from Talman and Perkins (2009), Trupp (2011) provided values for Gorgon, and values from Milliken (2007) were used for calculating CO₂ solubility for Teapot Dome (Table G-1). The water quality values for three of the four sites represent the storage reservoir used for the dynamic reservoir modeling simulations performed as part of the case studies. For Teapot Dome, the water chemistry use for these surface dissolution calculations were performed based on water chemistry from the Tensleep Formation rather than the Dakota Formation. The Tensleep Formation was originally intended to be the target storage reservoir for dynamic modeling simulations but was later replaced with the Dakota aquifer. It was retained for use here because the water is of a lower salinity, so it represents a higher solubility condition, thus expanding the range of solubility's studied.

Table G-1. Water Quality Parameters Used for Geochemical Modeling of Project Case Studies

	Gorgon		Ketzin		Zama		Teapot Dome	
	Surface ¹	Modeled Reservoir	Surface ²	Modeled Reservoir	Surface ³	Modeled Reservoir	Surface ⁴	Modeled Reservoir
pH (surface)	9.7	7.2	6.7	5.4	7.2	5.4	7.9	6.4
Element	mg/L	mg/L	mg/L	mg/L	mg/L	mg/L	mg/L	mg/L
Na	7400	7132	87,400	81,960	65,223	60,500	842	813
Ba	1.5	0.9						
K	8250	8094	412	396	314	296	90	87
Ca	34	16	2092	2426	9800	9860	368	362
Mg	22	12	814	823	2400	2341	34	28
Mn			1	1				
Fe	1	1	7	9			1	1
Li			2	2				
NH ₄			18	14				
Sr	2.2	1	1	1				
Si	10.3	10						
Mn	12	6						
Cl	11,771	11,390	134,000	127,200	100,000	109,100	1070	1050
Br			42	41			7	6
SO ₄	669	363	4	1040	1450	1373		
HCO ₃	6822	6310	88	47	810	912	148	234
CO ₃	2540	2840						
H ₂ SiO ₃			12	11	12	11	10	8
HBO ₂			36	24				
H ₂ S								
TDS ⁵ (sum of elements)	37,535	36,176	224,929	213,995	180,009	184,393	2570	2589
TDS	35,671	39,311	228,440	230,263	177,111	180,163	3200	3400

¹ Trupp (2011).

² Würdemann and others (2010).

³ Talman and Perkins (2009).

⁴ Milliken (2007).

⁵ Total dissolved solids.

Continued . . .

Table G-1. Water Quality Parameters Used for Geochemical Modeling of Project Case Studies (continued)

	Gorgon		Ketzin		Zama		Teapot Dome	
	Surface ¹	Modeled Reservoir	Surface ²	Modeled Reservoir	Surface ³	Modeled Reservoir	Surface ⁴	Modeled Reservoir
CO ₂ Dissolution (mol/L)	2.2	4	0.45	0.9	1.5	1.1	4	3
CO ₂ Dissolution (gl/L)	97	176	20	40	66	48	176	132
pH from CO ₂ Dissolution (low)	9.7	7.2	6.7	5.4	7.2	5.4	7.1	6.4
pH from CO ₂ Dissolution (High)	5.5	6.2	3.3	5.1	3.2	4.2	4.5	6.1
Sample Depth, m	1802		800		1300		2200	
Sample Temp., °C	180		35		71		95	
Sample Pressure, Mpa	19,800		6700		13,400			

¹ Trupp (2011).

² Würdemann and others (2010).

³ Talman and Perkins (2009).

⁴ Milliken (2007).

⁵ Total dissolved solids.

Evaluations of Water Chemistry

Reservoir Reactivity

Reservoir reactivity is a very important subject for carbon capture and storage (CCS) activities. The short-term reactions at the reservoir (especially dissolution) can affect the operations and productivity at the site, reservoir and, sometimes, in the field. For example, formation of deposits from mineral precipitation as a result of the CO₂ injection can significantly reduce the transitivity of the reservoir. Furthermore, the dissolution of anhydrite and/or other sulfur-bearing minerals can lead to production of the hydrogen sulfide and further souring of the formation. Long-term reactions can enhance or inhibit available reservoir pore space and help trap additional CO₂. Therefore, it is very important to consider the potential reactivity of the formation chosen for CCS activities.

The reactivity of minerals in the reservoir is a question of thermodynamic equilibrium. After the dissolution of the supercritical CO₂ into formation, the pH of water will drop, and the thermodynamic equilibrium is no longer maintained at this point. The minerals in the formation will react with the formation water and dissolved CO₂ in order to reach the new stable state. All minerals react at different rates (Figure G-1).

In order to further evaluate the reactivity of the reservoir in response to CO₂ injection, it is suggested to select the appropriate thermodynamic database for the PHREEQC (Truesdell and Jones, 1974) and Geochemist's Workbench (GWB) (Bethke and Yeakel, 2012) software. If the salinity of the formation water is lower than 150,000 mg/L, then the traditional Debye–Huckel activity model would be more appropriate for calculations (Truesdell and Jones, 1974). If the salinity of the formation water is high (total dissolved solids [TDS] is higher than 150,000 mg/L), the database based on the Pitzer (1979) coefficient model should be utilized instead (Parkhurst and Appelo, 1999). However, it is important to mention that the thermodynamic database based on the Pitzer formulation is missing the data on many minerals, elements, and gases (e.g., illite, pyrite, Al, H₂S, CH₄, etc.), and all calculations for high TDS waters should be verified with the Debye–Huckel activity model as well. The final CO₂ solubility values, which were calculated with the Debye–Huckel activity model, fall within acceptable error margin ($\pm 20\%$ accuracy); therefore, it was suggested to utilize the Debye–Huckel activity model for all calculations.

Gas Saturations Modeling

The gas dissolution into aqueous phase is controlled by the fugacity or chemical potential of the gas (Denbigh, 1971). However, this statement holds true only for the ambient low-pressure and -temperature environment. At the pressures and temperatures of interest, the partial pressure will consistently overestimate the fugacity. Therefore, it was suggested to utilize AQUALibrium (Carroll, 1998) software in order to calculate the solubility of pure gases in the assemblage and verify the calculations performed by the PHREEQC and GWB software.

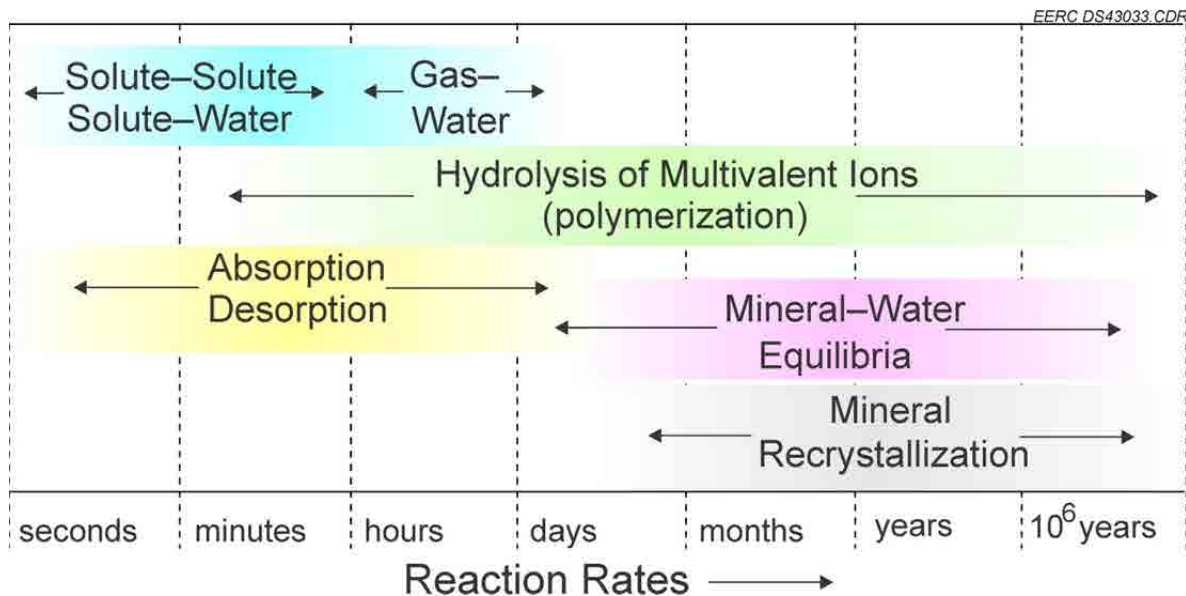


Figure G-1. Reaction rates for common reactions in aqueous systems (modified from Domenico and Schwartz, 1998).

Both, GWB and PHREEQC packages can utilize different approaches to calculate gas–formation water interactions (Parkhurst and Appelo, 1999; Bethke and Yeakel, 2012). It is possible to apply an “equilibrium gas phase” approach, where the gas phases are equilibrated at the constant pressure or at the fixed volume. Also, it is possible to treat the CO₂ as a reactant and dissolve an assigned amount of the gas through preassigned time intervals until the saturation point is reached. In this study, both approaches were evaluated with comparable results, and the first described scenario was selected as a primary calculation model.

CO₂ Dissolution Calculations

The equilibrium modeling was utilized as a method for the current set of calculations: the modeling components are assembled and the most “stable” thermodynamic state for the system is calculated at the infinite time conditions. Therefore, the calculated CO₂ dissolutions need to be considered as the maximum possible and the most optimistic scenario, especially where minerals are included in the run. For more precise calculations, kinetic modeling has to be utilized.

Mineral precipitation and scaling were calculated for surface CO₂ dissolution with consequent enriched water reinjection for CO₂ storage. This scenario is divided in two subroutines: 1) water is extracted from the reservoir and the pH, temperature, and pressure adjustments are modeled and 2) the CO₂ is dissolved in water and reinjected in the reservoir, where pH, pressure, and temperature are changing from surface to the reservoir conditions. Scaling and mineral precipitation rates were also included in this modeling.

RESULTS AND COMPARISONS

Ketzin

The amount of CO₂ that can be dissolved in Ketzin formation water is shown in Figure G-2 as a function of temperature for pressures ranging from 50 to 300 bars (absolute). As expected, the solubility of CO₂ increases with increasing pressure and decreases with increasing temperature. At the formation temperature and pressure of 40°C and 50 bar, respectively, the water has solubility for CO₂ of 0.45 mol/L. The range at this pressure over the temperatures indicated is 0.22 moles of CO₂ dissolved per liter at 170°C to 0.45 mol/L at 40°C. Once in the formation, the CO₂ will react over time with minerals, thus increasing the CO₂ storage capacity (Figure G-3). It may be possible to more closely match the formation storage capacity through the use of surface dissolution by performing it at higher pressures and lower temperatures than those present in the formation.

Figures G-4 and G-5 illustrate the pH of the water for the conditions tested. If CO₂ is injected directly into the formation, the formation water pH is buffered by the dissolution of minerals present in the reservoir, allowing for the greater average storage potential and greater storage potential at the reservoir pressure and temperature. The pH of the water during the surface CO₂ dissolution scenario is not buffered, and the pH slides toward much lower numbers. For instance, at pressure of 50 bars and temperature of 40°C, the pH value for surface CO₂ dissolution is 3.3, and the pH value for subsurface injection is 5.1. An acidic environment might pose a greater risk to equipment, such as pumps, pipes, and the wellbore itself.

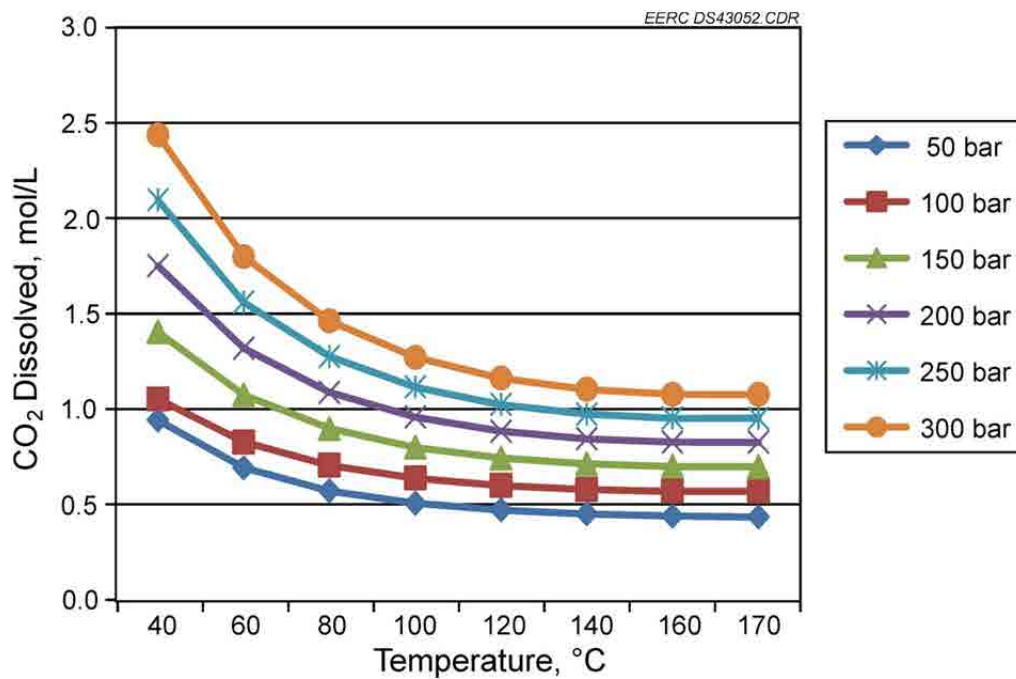


Figure G-2. CO₂ dissolution for Ketzin brine formation water with reservoir minerals.

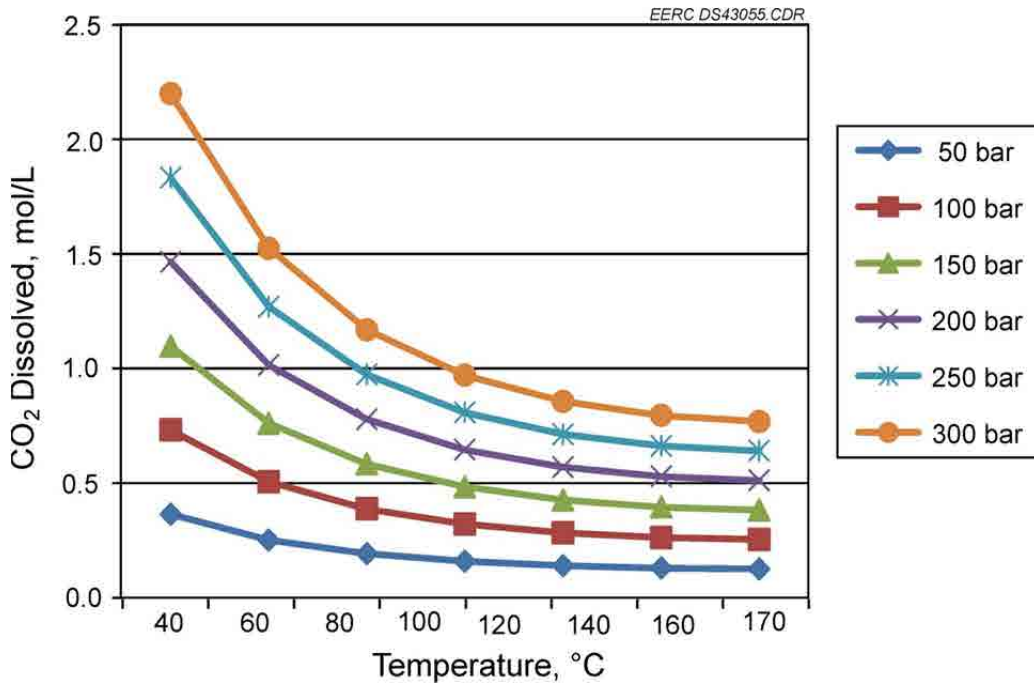


Figure G-3. CO₂ dissolution for Ketzin brine formation water without reservoir minerals.

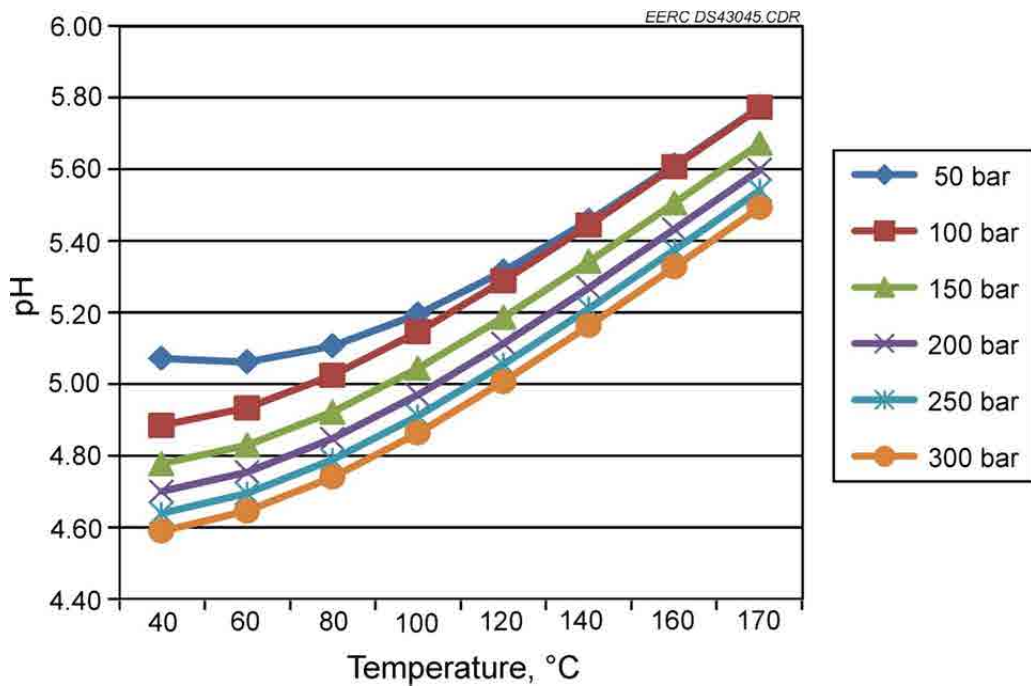


Figure G-4. Ketzin formation water pH with maximum dissolved CO₂ when reservoir minerals are included in the model.

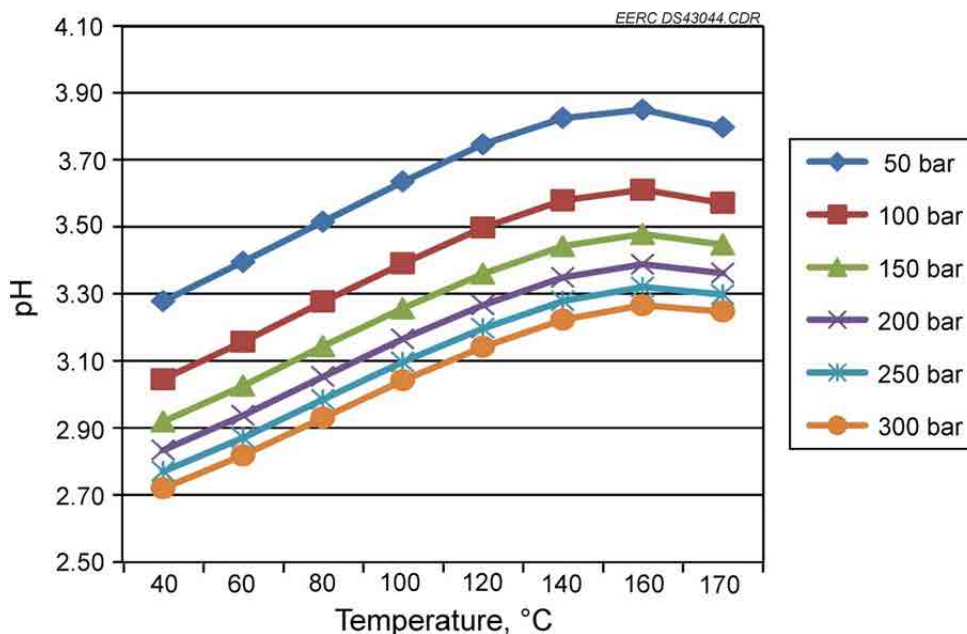


Figure G-5. Ketzin formation water pH with maximum dissolved CO₂ when reservoir minerals are not included in the model.

Zama

The amount of CO₂ that can be dissolved in the Zama site formation water is shown in Figure G-6 as a function of temperature for pressures ranging from 50 to 300 bars (absolute). As expected, the solubility of CO₂ increases with increasing pressure and decreases with increasing temperature. At the formation temperature and pressure of 60°C and 150 bar, respectively, the water has solubility for CO₂ of 1 mol/L. The range at this pressure over the temperatures indicated is 0.5 moles of CO₂ dissolved per L at 170°C to 1.35 mol/L at 40°C. Once in the formation, the CO₂ will react over time with minerals, thus increasing the CO₂ storage capacity. This is illustrated in Figure G-7. It may be possible to more closely match the formation storage capacity through the use of surface dissolution by performing it at higher pressures and lower temperatures than those present in the formation.

Figures G-8 and G-9 illustrate the pH of the water for the tested conditions. If CO₂ is injected directly into the formation, the formation water pH is buffered by the dissolution of minerals present in the reservoir, allowing for the greater average storage potential and greater storage potential at the reservoir pressure and temperature. The pH of the water during the surface CO₂ dissolution scenario is not buffered, and the pH slides toward much lower numbers. For instance, at pressure of 150 bars and temperature of 60°C, the pH value for surface CO₂ dissolution is 3.3 and the pH value for subsurface injection is 4.1. An acidic environment might pose a greater risk to equipment, such as pumps, pipes, and the wellbore itself.

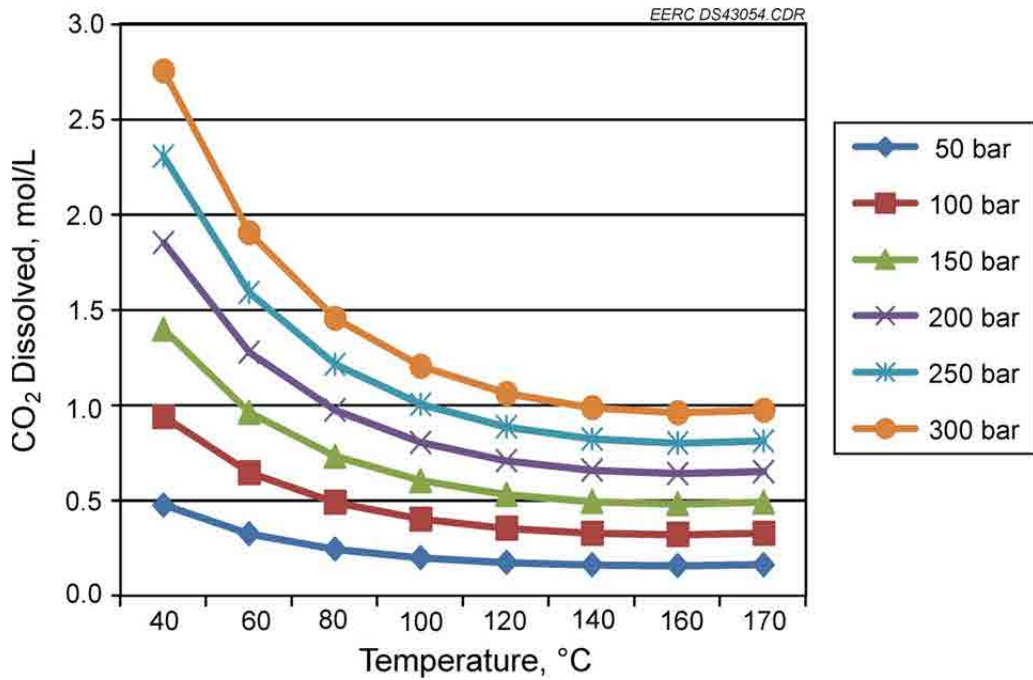


Figure G-6. CO₂ dissolution for Zama brine formation water with reservoir minerals.

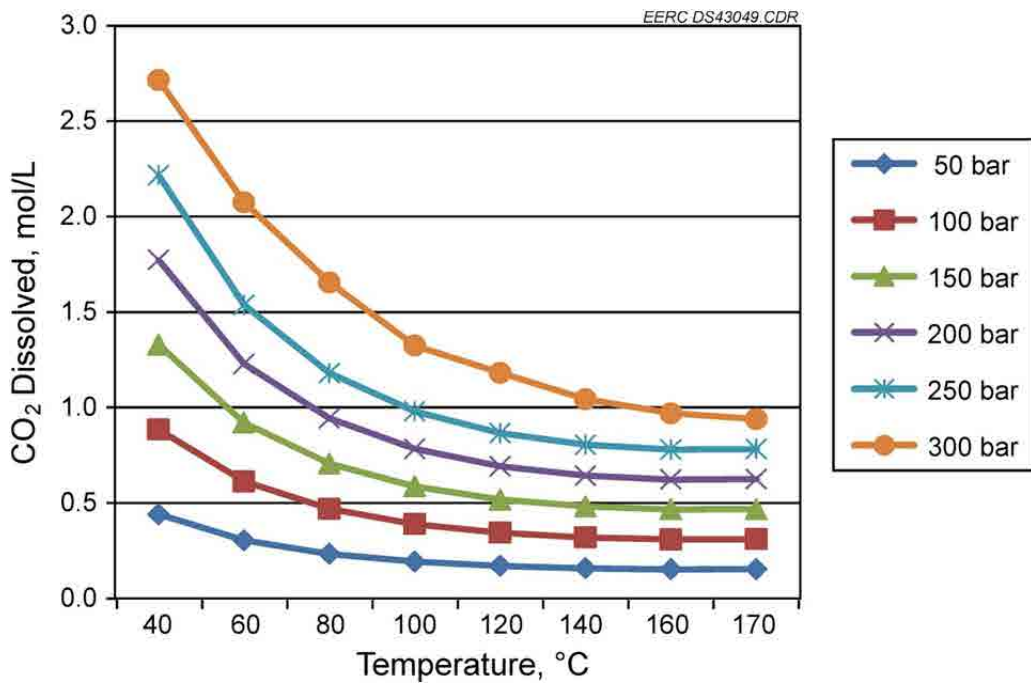


Figure G-7. CO₂ dissolution for Zama brine formation water without reservoir minerals.

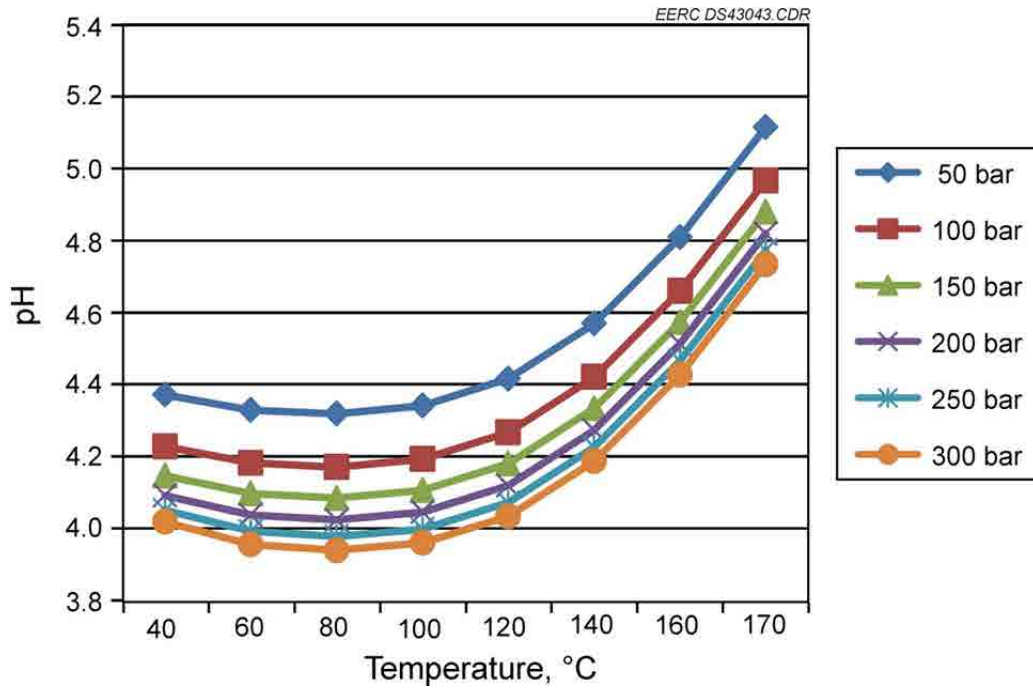


Figure G-8. Zama formation water pH with maximum dissolved CO₂ when reservoir minerals are included in the model.

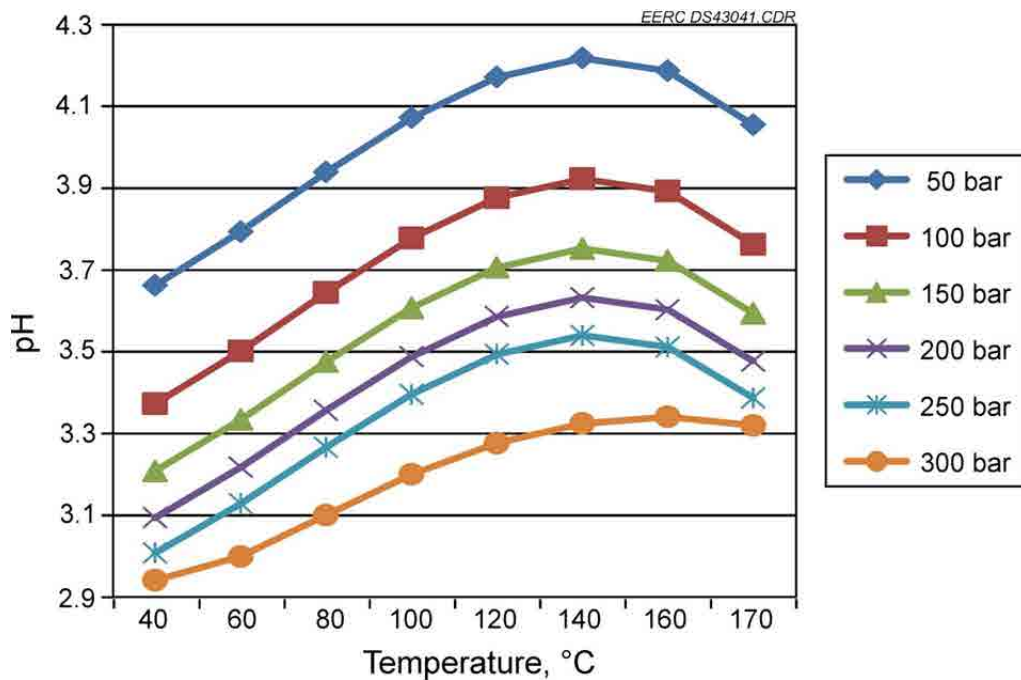


Figure G-9. Zama formation water pH with maximum dissolved CO₂ when reservoir minerals are not included in the model.

Gorgon HigG-Salinity Case

The amount of CO₂ that can be dissolved in Gorgon formation water (1802 m) is shown in Figure G-10 as a function of temperature for pressures ranging from 50 to 300 bars (absolute). As expected, the solubility of CO₂ increases with increasing pressure and decreases with increasing temperature. At the formation temperature and pressure of 120°C and 200 bar, respectively, the water has solubility for CO₂ of 2.2 mol/L. The range at this pressure over the temperatures indicated is 2 moles of CO₂ dissolved per liter at 170°C to 5.2 mol/L at 40°C. Once in the formation, the CO₂ will react over time with minerals, thus increasing the CO₂ storage capacity. This is illustrated in Figure G-10. It may be possible to more closely match the formation storage capacity through the use of surface dissolution by performing it at higher pressures and lower temperatures than those present in the formation. Assuming 3 mol/L is the desired storage capacity, we can see from Figure G-11 that this can be met by using dissolution conditions from 40°C and 150 bar (absolute) to approximately 95°C and 300 bar.

Figures G-12 and G-13 illustrate the pH of the water for the conditions tested. If CO₂ is injected directly into the formation, the formation water pH is buffered by the dissolution of minerals present in the reservoir, allowing for the greater average storage potential and greater storage potential at the reservoir pressure and temperature. The pH of the water during the surface CO₂ dissolution scenario is not buffered, and the pH slides toward much lower numbers. For instance, at pressure of 200 bars and temperature of 120°C, the pH value for surface CO₂ dissolution is 5 and the pH value for subsurface injection is 6.4. An acidic environment might pose a greater risk to equipment, such as pumps, pipes, and the wellbore itself.

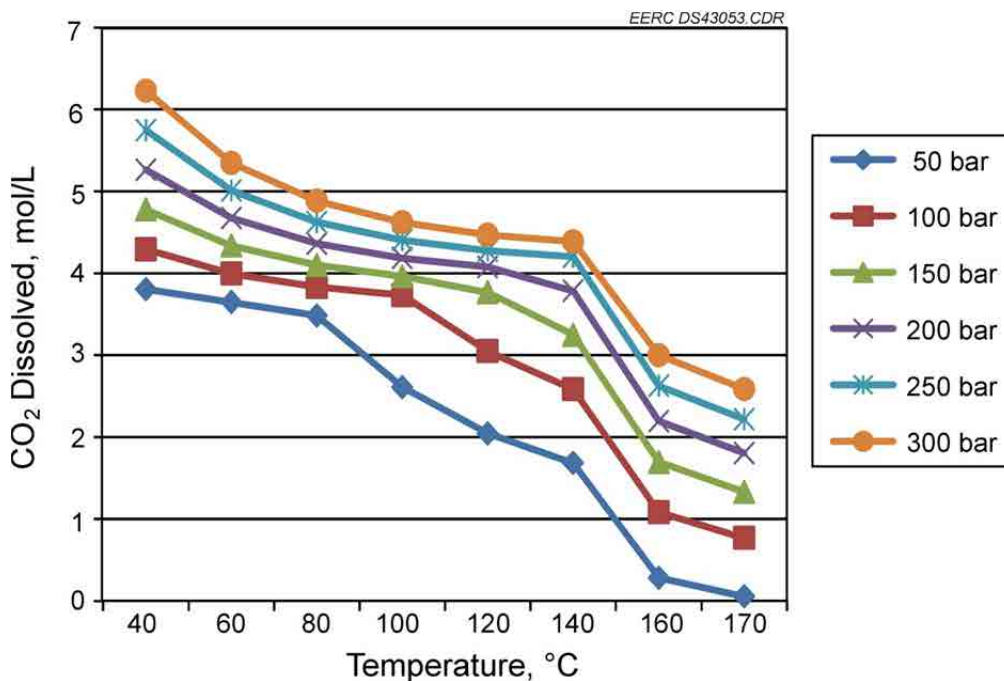


Figure G-10. CO₂ dissolution for Gorgon brine formation water with reservoir minerals.

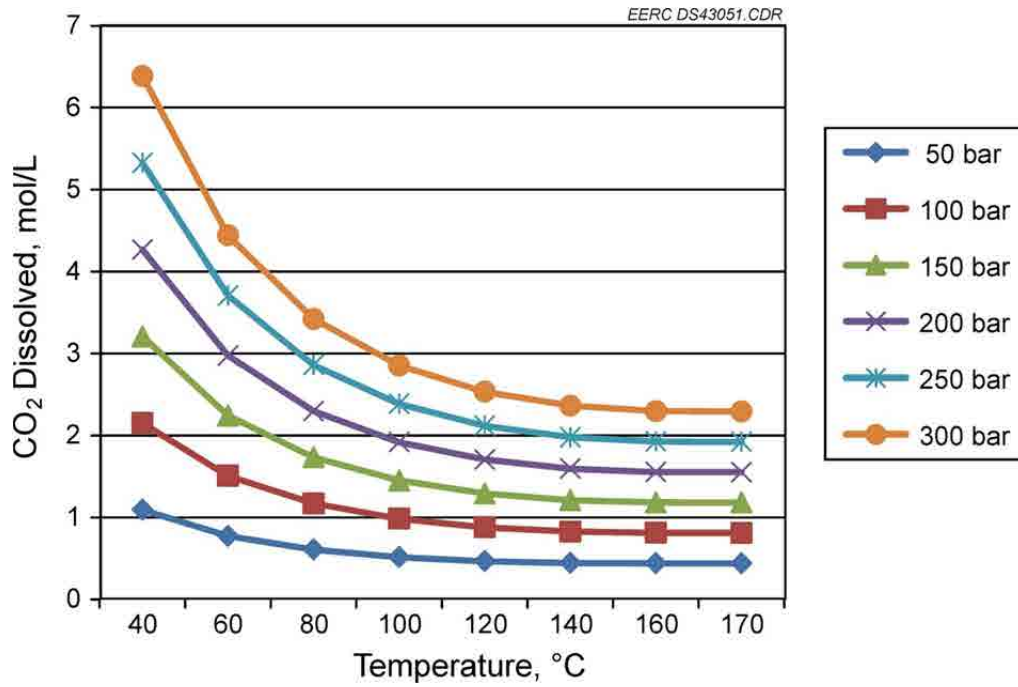


Figure G-11. CO₂ dissolution for Gorgon brine formation water without reservoir minerals.

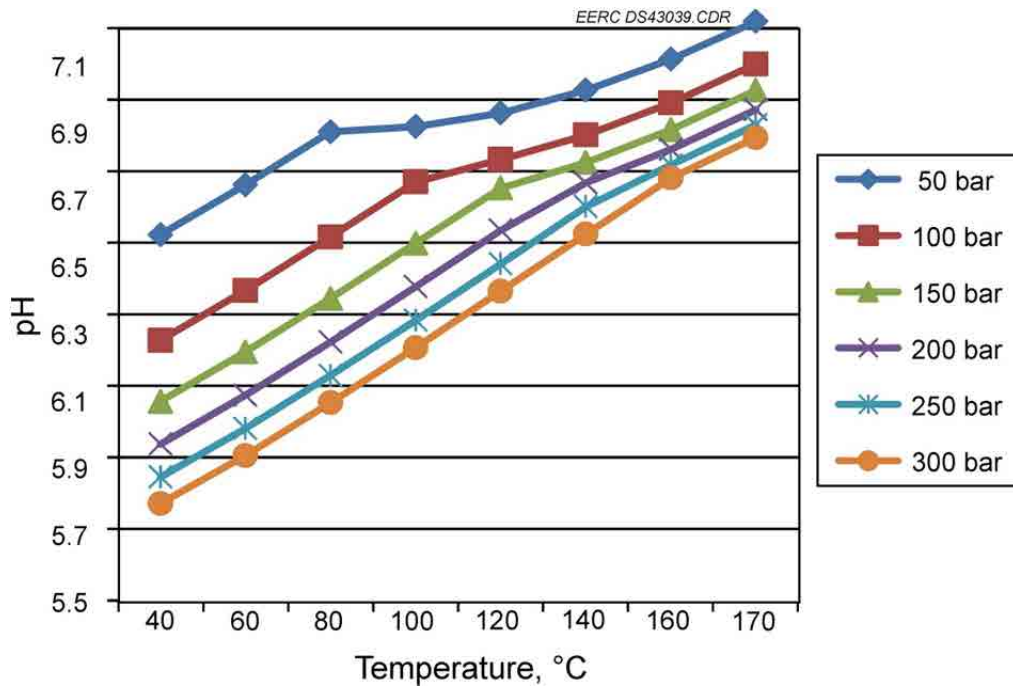


Figure G-12. Gorgon formation water pH with maximum dissolved CO₂ when reservoir minerals are included in the model.

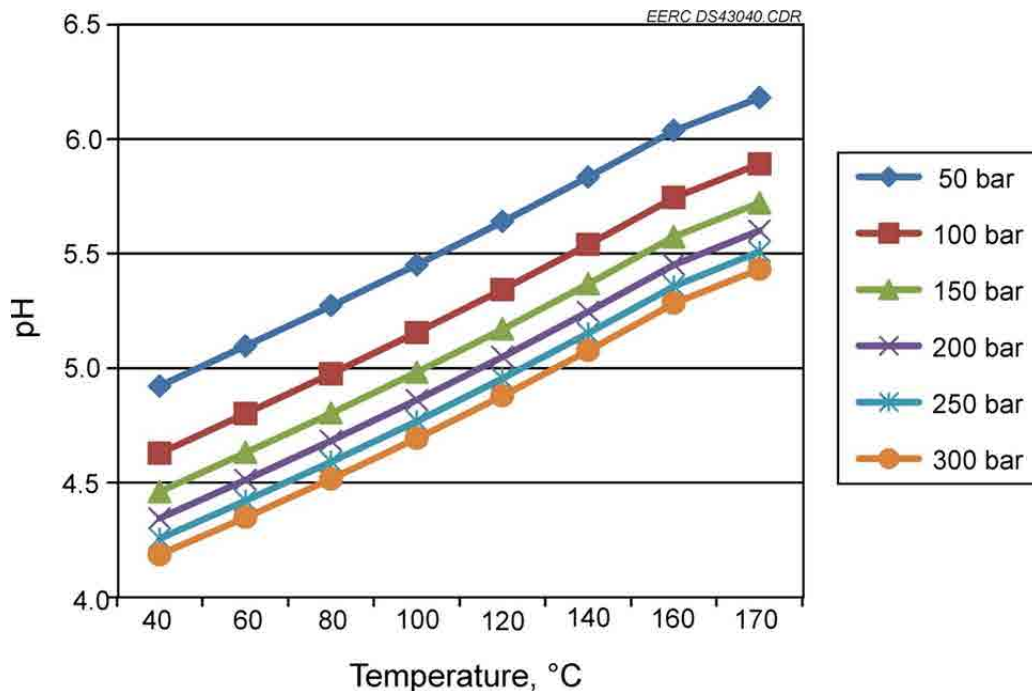


Figure G-13. Gorgon formation water pH with maximum dissolved CO₂ when reservoir minerals are not included in the model.

Gorgon Low-Salinity Case

The amount of CO₂ that can be dissolved in Gorgon formation water at a different depth interval (2243 m) is shown in Figure G-14 as a function of temperature for pressures ranging from 50 to 300 bars (absolute). As expected, the solubility of CO₂ increases with increasing pressure and decreases with increasing temperature. At the formation temperature and pressure of 170°C and 250 bar, respectively, the water has solubility for CO₂ of 2.65 mol/L. The range at this pressure over the temperatures indicated is 2 moles of CO₂ dissolved per liter at 170°C to 5.7 mol/L at 40°C. Once in the formation, the CO₂ will react over time with minerals, thus increasing the CO₂ storage capacity. This is illustrated in Figure G-15. It may be possible to more closely match the formation storage capacity through the use of surface dissolution by performing it at higher pressures and lower temperatures than those present in the formation. Assuming 3 mol/L is the desired storage capacity, we can see from Figure G-14 that this can be met by using dissolution conditions from 40°C and 150 bar (absolute) to approximately 95°C and 300 bar (absolute).

Figures G-16 and G-17 illustrate the pH of the water for the conditions tested. If CO₂ is injected directly into the formation, the formation water pH is buffered by the dissolution of minerals present in the reservoir, allowing for the greater average storage potential and greater storage potential at the reservoir pressure and temperature. The pH of the water during the surface CO₂ dissolution scenario is not buffered, and the pH slides toward much lower numbers.

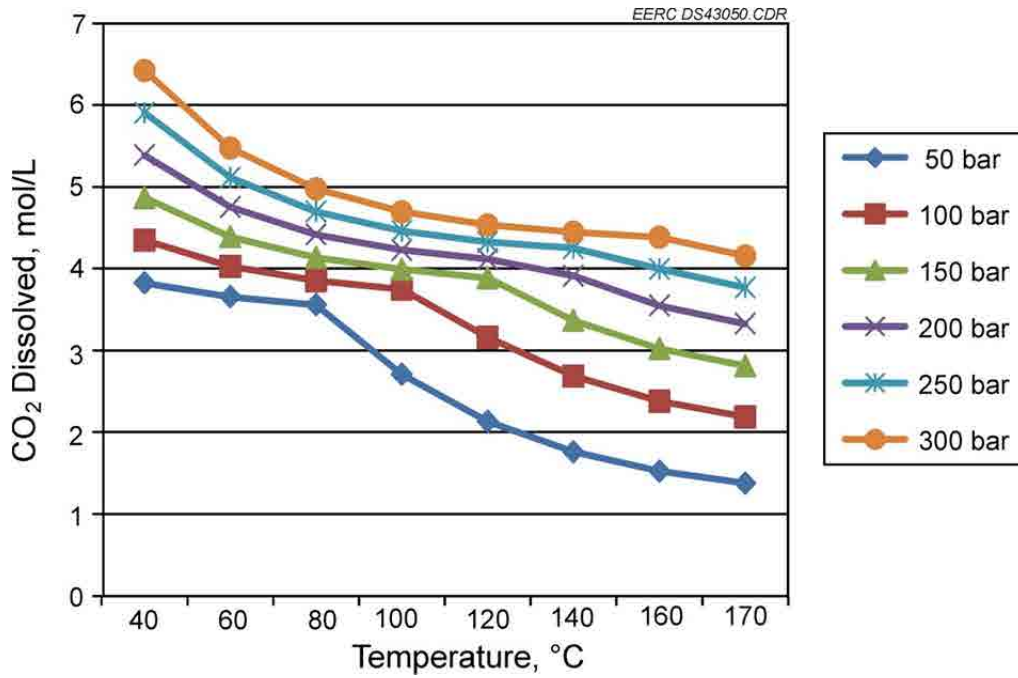


Figure G-14. CO₂ dissolution for Gorgon brine formation water with reservoir minerals.

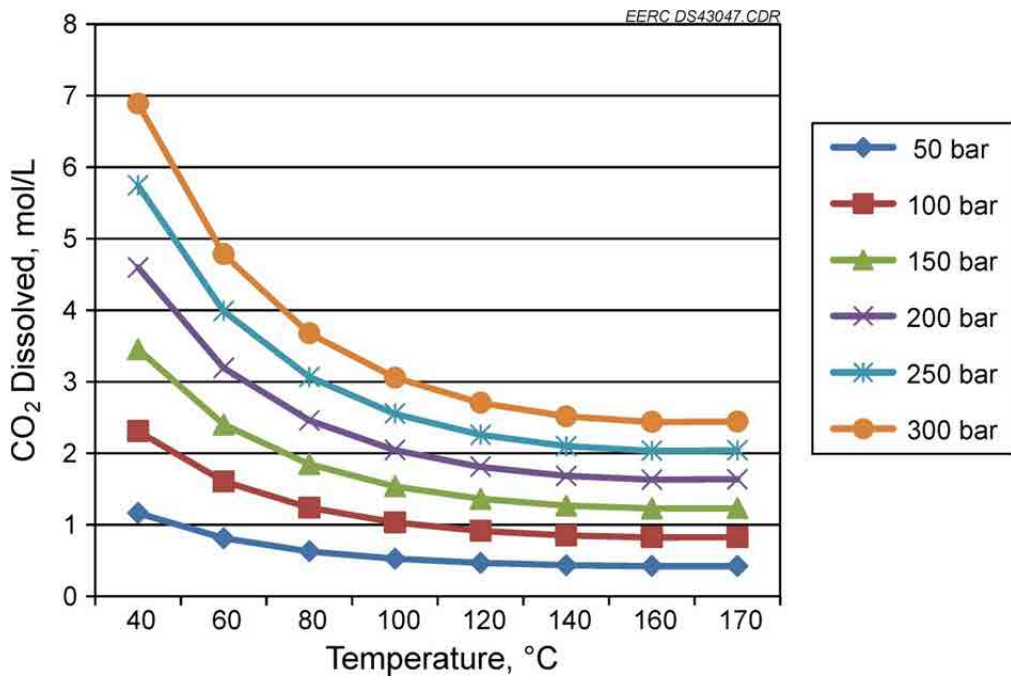


Figure G-15. CO₂ dissolution for Gorgon brine formation water without reservoir minerals.

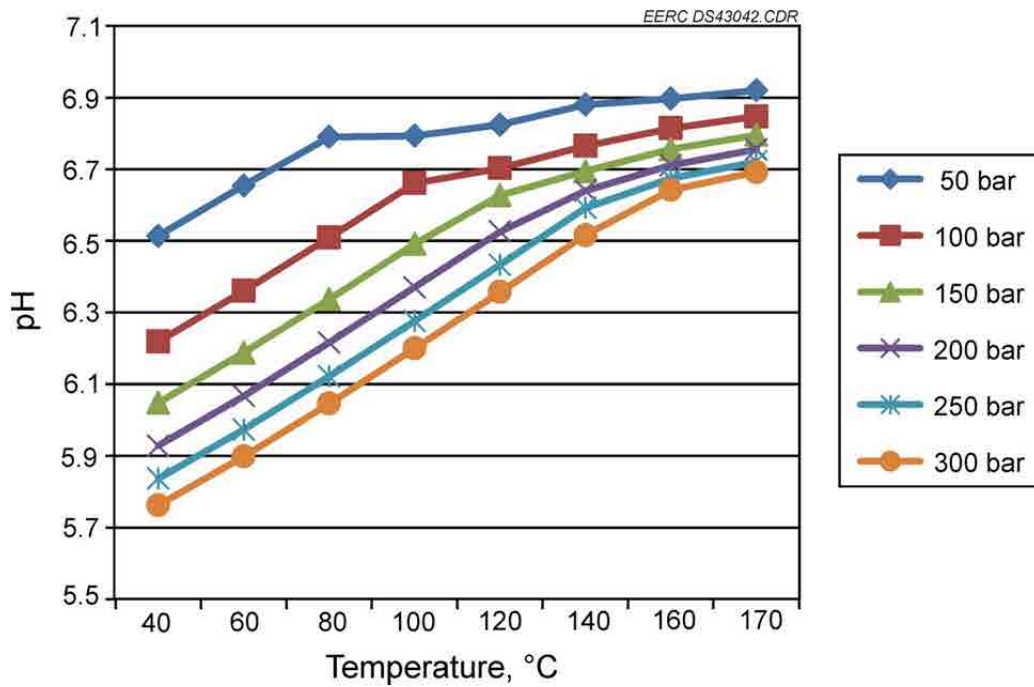


Figure G-16. Gorgon formation water pH with maximum dissolved CO₂ when reservoir minerals are included in the model.

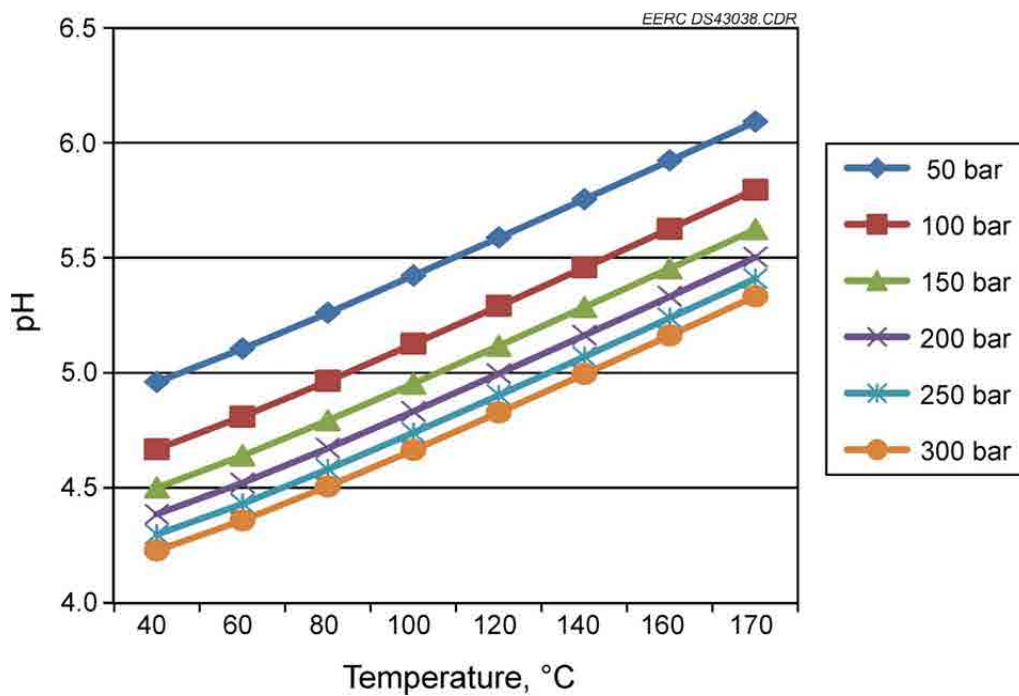


Figure G-17. Gorgon formation water pH with maximum dissolved CO₂ when reservoir minerals are not included in the model.

For instance, at pressure of 240 bars and temperature of 140°C, the pH value for surface CO₂ dissolution is 5.1, and the pH value for subsurface injection is 6.5. An acidic environment might pose a greater risk to equipment, such as pumps, pipes, and the wellbore itself.

Teapot Dome

The amount of CO₂ that can be dissolved in Teapot Dome water is shown in Figure G-18 as a function of temperature for pressures ranging from 50 to 300 bars (absolute). As expected, the solubility of CO₂ increases with increasing pressure and decreases with increasing temperature. At the formation temperature and pressure of 100°C and 200 bar, respectively, the water has solubility for CO₂ of 2.1 mol/L. The range at this pressure over the temperatures indicated is 1.7 moles of CO₂ dissolved per liter at 170°C to 4.8 mol/L at 40°C. Once in the formation, the CO₂ will react over time with minerals, thus increasing the CO₂ storage capacity (Figure G-19). It may be possible to more closely match the formation storage capacity through the use of surface dissolution by performing it at higher pressures and lower temperatures than those present in the formation.

Figures G-20 and G-21 illustrate the pH of the water for the conditions tested. If CO₂ is injected directly into the formation, the formation water pH is buffered by the dissolution of minerals present in the reservoir, allowing for the greater average storage potential and greater storage potential at the reservoir pressure and temperature. The pH of the water during the surface CO₂ dissolution scenario is not buffered, and the pH slides toward much lower numbers. For instance, at pressure of 200 bars and temperature of 100°C, the pH value for surface CO₂

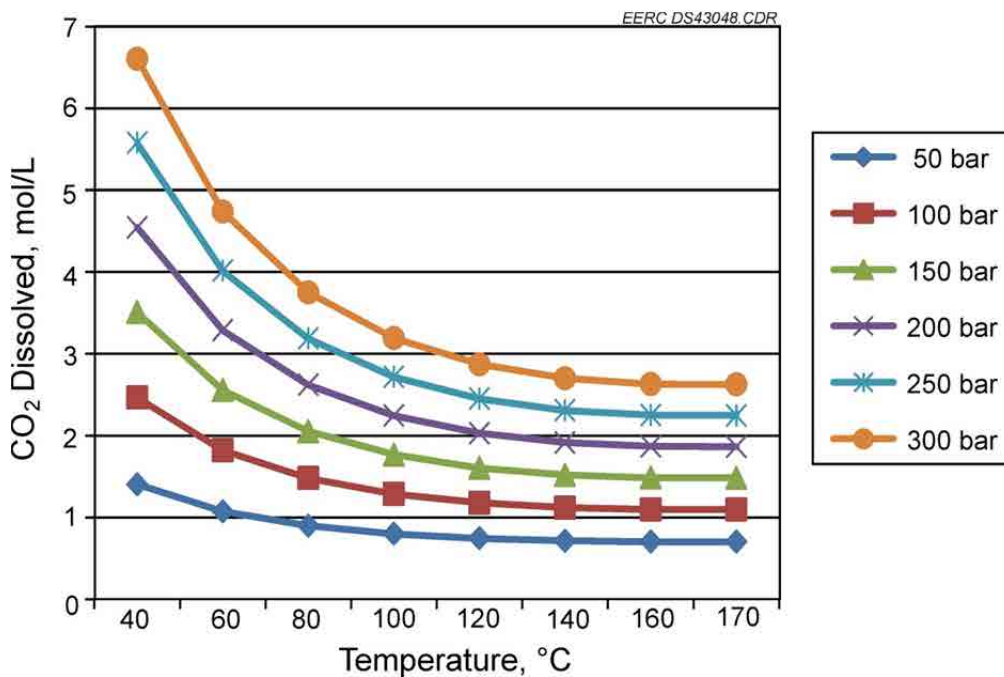


Figure G-18. CO₂ dissolution for Teapot Dome brine formation water with reservoir minerals.

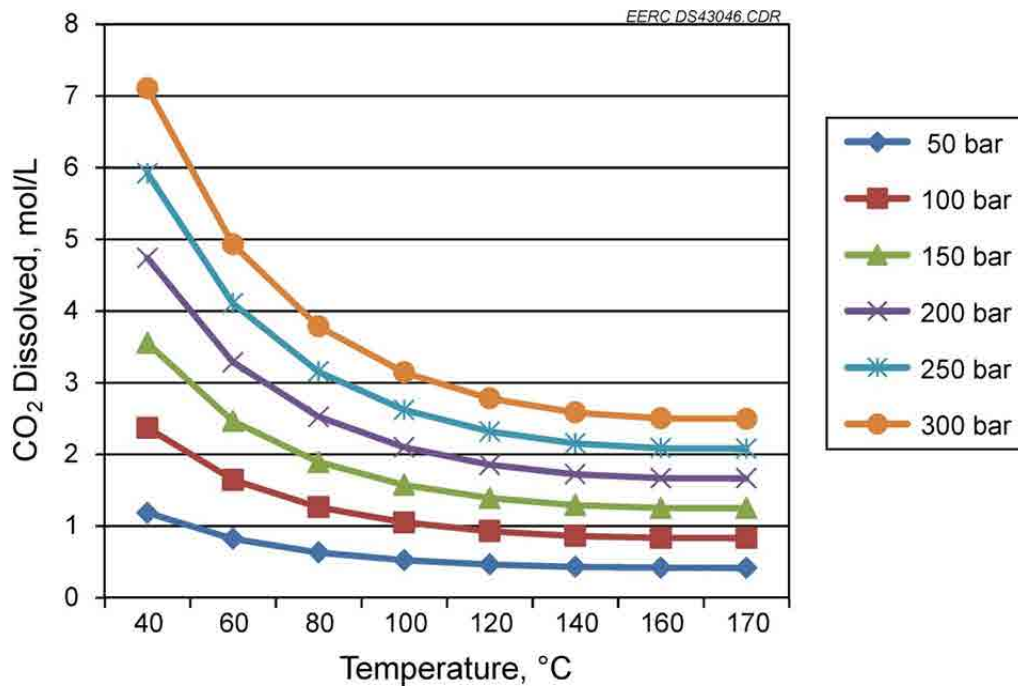


Figure G-19. CO₂ dissolution for Teapot Dome brine formation water without reservoir minerals.

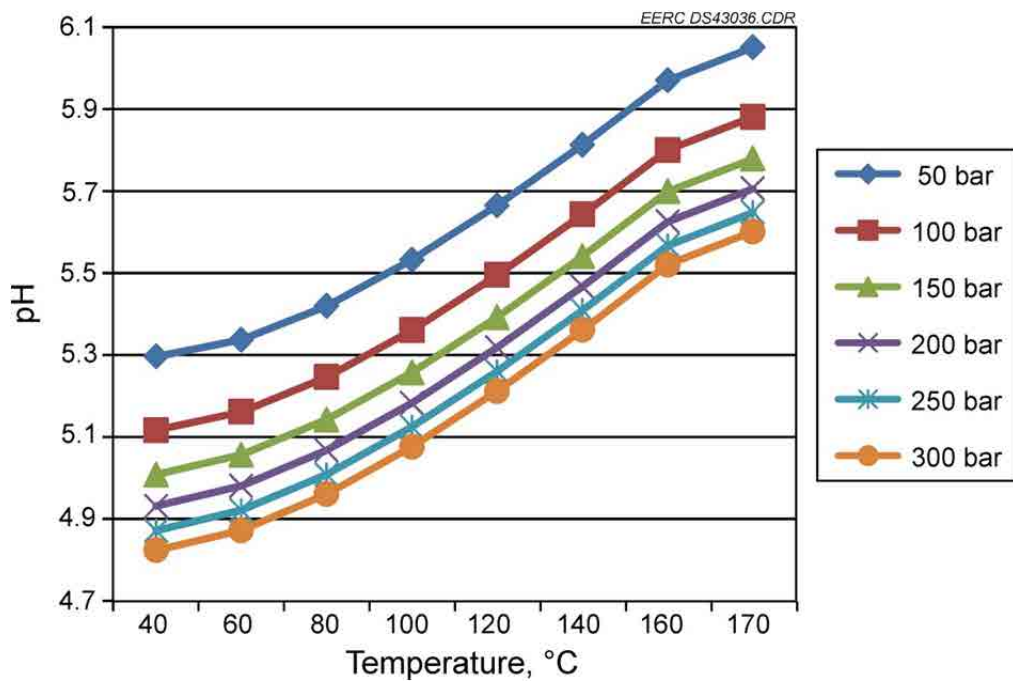


Figure G-20. Teapot Dome formation water pH with maximum dissolved CO₂ when reservoir minerals are included in the model.

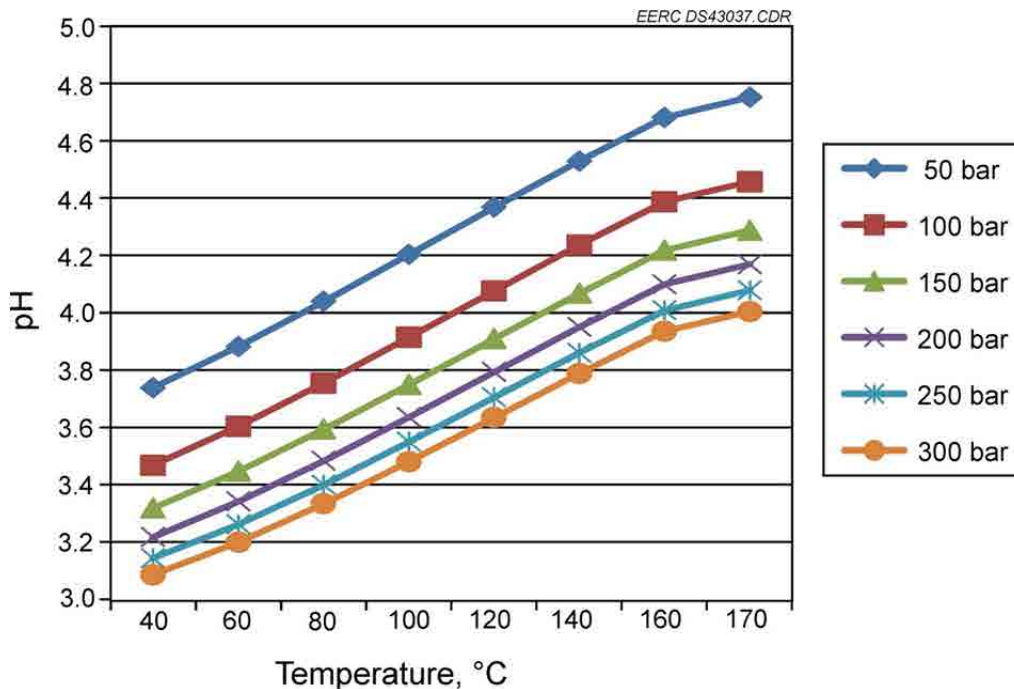


Figure G-21. Teapot Dome formation water pH with maximum dissolved CO₂ when reservoir minerals are not included in the model.

dissolution is 3.6 and the pH value for subsurface injection is 5.1. An acidic environment might pose a greater risk to equipment, such as pumps, pipes, and the wellbore itself.

OPERATIONAL CONCERNS

Operational concerns for surface dissolution are not trivial. Dissolution of CO₂ into water at high pressure would require the use of high-pressure equipment made of corrosion-resistant materials. These materials must be resistant to both wet CO₂ and high-salinity waters. Other operational concerns are associated with water production/extraction from the reservoir for on-surface dissolution. In the course of handling the water, it will be passed through a range of pressures and temperatures that will allow for the release of dissolved gases, the precipitation of dissolved solids, and the formation of scales. Scale and precipitate formation potentials were calculated for each water and are presented in Table G-2 along with the rest of the summarized CO₂ dissolution results. Only the low-salinity Teapot Dome water showed no potential for scale formation either in the production wellbore or in the formation. Scale formation in the production wellbore is an issue commonly of concern in oil and gas production and even in some water production wells. The most common approach used to overcome wellbore scale and corrosion problems is the use of chemical corrosion and scale inhibitors.

Table G-2 compares formation water parameters for four sites: Gorgon, Ketzin, Zama, and Teapot Dome. For Ketzin and Zama, the model estimates that mineral precipitation or scaling

Table G-2. Comparison of Water Parameters for Four Potential CO₂ Injection Sites

	Gorgon		Ketzin	Zama	Teapot Dome Inj 1 ¹
	High Salinity	Low Salinity			
Temperature Used for Surface Dissolution, °C	120	140	40	60	100
Pressure Used for Surface Dissolution, bar	200	250	50	150	200
CO ₂ Density ² at Limit Pressure, kg/m ³	390	429	116	562	461
pH (surface, 25°C, 1 atm)	9.7		6.7	7.2	7.93
pH (in reservoir)	7.2		5.4	5.4	6.4
pH (after dissolution without minerals)	5.2		3.3	3.3	3.6
pH (after dissolution with minerals)	6.4		5.2	4	5.1
TDS (formation)	39,311	7096	230,263	180,163	3400
TDS (surface, 25°C, 1 atm)	35,671		228,440	177,111	3200
Surface CO ₂ Dissolution, kg/m ³	79.6	92.4	16.0	8.33	92.2
Subsurface Dissolution, kg/m ³	181	187	41.4	8.55	98.7
Water Production, Mineral Precipitation, Wellbore Scaling Prediction					
Chrysotile, mg/L	80		None	None	None
Calcite/Strontionate/Dolomite, mg/L	2		1200	500	None
CaCl, mg/L	None		200	300	None
Water Injection, Mineral Precipitation, Wellbore Scaling Prediction					
Sulfate (anhydrite/gypsum), mg/L	None		500	500	None

¹ Injection Well 1 = Well 490252304800.² CO₂ density calculated using Styryjek and Vera, 1986.

might occur in the wellbore at certain pressure and temperature conditions. During the CO₂ dissolution in produced water at the surface, the precipitation of sulfate minerals and desalination might become a concern. In addition, highly saline waters/brines, such as those from Ketzin and Zama, are highly corrosive to wellbore steels, pipelines, and other equipment.

REFERENCES

- Bethke, C.M., and Yeakel, S., 2011, *Geochemist's workbench: reference manual: Aqueous Solutions*, LLC, Champaign, Illinois, www.gwb.com/gwb.htm (March 29, 2012).
- Burton, M., and Bryant, S.L., 2009, Eliminating buoyant migration of sequestered CO₂ through surface dissolution—implementation costs and technical challenges: *SPE Reserv. Eval. Eng.*, v. 12, p. 399–407.
- Carroll, J.J., 1998, *AQUAlibrium, Software for Phase Equilibria in Natural Gas–Water Systems*, www.telusplanet.net/public/jcarroll/ION.HTM (accessed September 2011).
- Denbigh, K., 1971, *The principles of chemical equilibrium*, (3rd Ed.): Cambridge University Press, 494 p.
- Domenico, P.A., and Schwartz, F.W., 1998, *Physical and chemical hydrogeology*: Wiley, v. 1, 528 p.
- Eke, P.E., Naylor, M., Haszeldine, S., and Curtis, A., 2011, CO₂/brine surface dissolution and injection—CO₂ storage enhancement: *SPE Proj Fac & Const*, v. 6, no. 1, p. 41–53.
- Jain, L., and Bryant, S.L., 2011, Optimal design of injection/extraction wells for the surface dissolution of CO₂ storage strategy: *Energy Procedia*, v. 4, p. 4299–4306.
- Milliken, M., 2007, Geothermal resources at Naval Petroleum Reserve-3 (NPR-3), Wyoming, *in* *Proceedings of the Thirty-Second Workshop on Geothermal Reservoir Engineering*: Stanford University, Stanford, California, January 22–24, 2007. <http://pete.stanford.edu/ERE/pdf/IGAstandard/SGW/2007/millike.pdf> (accessed October 2011).
- Parkhurst, D.L., and Appelo, C.A.J., 1999, *User's guide to PHREEQC (version 2) – a computer program for speciation, batcG-reaction, one-dimensional transport, and inverse geochemical calculations*: Water–Resources Investigations Report 99-4259, Denver, Colorado.
- Pitzer, K.S., 1979, Theory – Ion interaction approach, *in* Pytkowicz, R.M., ed., *Activity Coefficients in Electrolyte Solutions*, v. 1: Boca Raton, Florida, CRC Press, Inc., p. 157–208.
- Rosenbauer, R.J., Koksalan, T., and Palandri J.L., 2005, Experimental investigation of CO₂–brine–rock interactions at elevated temperature and pressure: Implications for CO₂ sequestration in deep-saline aquifers: *Fuel Processing Technology*, v. 86, p. 1581–1597.

- Stryjek, R., and Vera, J.H., 1986, PRSV: An improved Peng-Robinson equation of state for pure compounds and mixtures: *Canadian Journal of Chemical Engineering*, v. 64, no. 2, p. 323–333.
- Talman S., Perkins, E., and Jones, B., 2009, Detailed reservoir mineralogy for the Zama 08-33-115-6W6 well—petrographic and analytical results: Report for RPS Energy Canada, March.
- Truesdell, A.H., and Jones, B.F., 1974, WATEQ, A computer program for calculating chemical equilibria of natural waters: *Journal of Research, U.S. Geological Survey*, v. 2, p. 233–274. www.brr.cr.usgs.gov/projects/GWC_coupled/phreeqc (accessed September 2011).
- Trupp, M., 2011, personal communication to Energy & Environmental Research Center staff, July 17, 2011.
- Würdemann, H., Moller, F., Kuhn, M., Heidug, W., Christensen, N.P., Borm, G., and Schilling, F.R., 2010, CO₂SINK – From site characterisation and risk assessment to monitoring and verification: One year of operational experience with the field laboratory for CO₂ storage at Ketzin, Germany, Elsevier: *International Journal of Greenhouse Gas Control*, v. 4, p. 938–951.